Satoshi Obika · Mitsuo Sekine   *Editors*

Synthesis of Therapeutic Oligonucleotides

Springer

Synthesis of Therapeutic Oligonucleotides

Satoshi Obika • Mitsuo Sekine
Editors

Synthesis of Therapeutic Oligonucleotides

Springer

Editors
Satoshi Obika
Osaka University
Suita, Osaka, Japan

Mitsuo Sekine
Tokyo Institute of Technology
Yokohama, Kanagawa, Japan

Preface

Nucleic acids have been unambiguously recognized as potential resources for the development of new drugs to treat incurable genetic diseases, as well as functional materials for various applications in bioscience and biotechnology fields. In 2016, a new academic society, the Nucleic Acids Therapeutics Society of Japan, was inaugurated. This society was established based on a previous domestic organization, the Antisense Symposium. In addition, the Society of Nucleic Acids Chemistry was established in 2017 in Japan. During this time, organic chemistry of nucleic acids has gained importance in providing new drugs and materials. In Japan, we have a long history of nucleic acid chemistry studies. The first symposium on this subject was held at Osaka University in 1973 by the late Professor Morio Ikehara. Japan is unique in that large amounts of nucleic acids are produced as by-products of soy sauce and pulp. Therefore, many researchers working in biotechnology companies and universities have actively studied the utilization of such easily accessible natural products for a long period of time. As a result, Japan is one of the world's leading countries in nucleic acid chemistry research.

   This book contains the latest research from active researchers in the nucleic acid chemistry field in Japan. Part I reviews recent developments in chemical synthesis of DNA and RNA oligomers and includes practical applications such as large-scale synthesis of DNA and RNA fragments. Part II summarizes new strategies for the synthesis of oligonucleotides modified at the nucleobases, sugar moieties, and phosphodiester linkages; these changes have been developed to improve their original properties such as hybridization affinity for DNA and RNA, as well as resistance to nucleases. The topics discussed in this book would be beneficial to those who want to join nucleic acid chemistry research or to discover more effective nucleic acid drugs in the future. We hope that this book may provide an opportunity for researchers to gain new understanding and inspire new ideas in nucleic acid chemistry research that may eventually lead to novel concepts and techniques.

Suita, Japan   Satoshi Obika
Yokohama, Japan   Mitsuo Sekine
January 20, 2018

Contents

Part I
Synthesis of Natural Oligonucleotides

Non-protected Synthesis
of Oligonucleotides

Akihiro Ohkubo, Kohji Seio, and Mitsuo Sekine

Abstract Much attention has been paid to the development of effective methods for synthesizing modified oligonucleotides that have various functional groups. Recently, we have developed a selective phosphorylation toward the hydroxyl group (*O*-selective phosphorylation), which is named as the proton-block method. An activated phosphite method was also developed to synthesize modified DNA oligonucleotides having alkaline-labile functional groups. The DNA synthesis using the activated phosphite method, which involves a phosphite intermediate generated from the phosphoramidite building block, presents excellent chemoselectivity toward the hydroxyl groups on resins under solid-phase conditions. In addition, the *O*-selectivity of the phosphorylation with P–N bond cleavage using 6-nitro-HOBt is more than 99% in the RNA synthesis without base protection. In this review, we summarize the *O*-selective phosphorylation in DNA and RNA synthesis without base protection and the synthesis of modified oligonucleotides having alkaline-labile functional groups using these new methods.

Keywords *N*-unprotected DNA and RNA synthesis · *O*-selective phosphorylation · Modified oligonucleotides · P–N bond cleavage · Solid-phase synthesis · Silyl type linker

1   Introduction

During the recent two decades, a wide variety of modified oligonucleotides have been synthesized using nucleic acid chemistry [1]. These molecules have proved to be useful for gene therapy [2] and genetic diagnosis [3]. In order to further develop these techniques, there is a need to synthesize epoch-making artificial oligonucleotides that can result in the next generation DNA or RNA technology.

A. Ohkubo · K. Seio
Department of Life Science and Technology, Tokyo Institute of Technology, Midoriku, Yokohama, Japan

M. Sekine (✉)
Tokyo Institute of Technology, Yokohama, Kanagawa, Japan

Recently, modified oligonucleotides having base-labile functional groups have received much attention in the field of nucleic acid research. For example, aminoacyl tRNAs having an unnatural amino acid [4] and 2′-*O*-acyloxymethyl RNAs [5] are expected as the key molecules for protein engineering and down-regulation of gene expression. However, these compounds cannot be efficiently synthesized by using the standard methods of DNA/RNA synthesis because the base-labile ester functions are decomposed by treatment with ammonia in the final step in the solid-phase synthesis.

To overcome this problem, we started our original studies for developing new routes to synthesize the oligonucleotides having base-labile functional groups without base protection. When such strategies were employed, it was expected that *N*-phosphorylated branched oligonucleotides would be generated [6] because the exocyclic amino groups of cytosine and adenine bases are known to react with trivalent phosphorylating reagents. Therefore, we attempted to achieve the highly *O*-selective phosphorylation of the hydroxyl group in DNA and RNA synthesis without base protection [7].

In 1991, R. L. Letsinger first synthesized oligodeoxynucleotides using *N*-unprotected deoxynucleoside 3′-phosphoramidites via the phophoramidite method [8]. Two-step reactions were involved, including condensation and selective cleavage of the once-generated N–P bonds [9]. A year later, R. A. Jones reported the *H*-phosphonate method without base protection using *N*-unprotected deoxynucleoside 3′-H-phosphonate building blocks [10]. However, serious *N*-acylations on the base residues were observed when pivaloyl chloride was used as the condensing agent. In 1997, our research group improved the *H*-phosphonate approach using 2-(benzotriazol-1-yloxy)-1,1-dimethyl-2-pyrrolidin-1-yl-1,3,2-diazaphospholidinium hexafluorophosphate (BOMP) as the effective coupling agent which does not react with the base residues. A DNA 12 mer was thus obtained as shown by the main peak in the HPLC analysis [11]. A year later, Hayakawa and Kataoka reported a procedure for DNA fragments based on the phosphoramidite method without base protection, and a promoter of imidazolium triflate (IMT) was used to activate the deoxynucleoside-3′-phosphoramidite building blocks [12]. However, this method was not applied to the actual synthesis of DNA oligomers because ester exchange reactions might occur during the second treatment step in the condensation.

In this review, we describe our extensive studies on this subject after these precedent efforts.

2   Development of Proton-Block Strategy for the Synthesis of Oligonucleotides Without Base Protection

In the phosphoramidite method for synthesizing oligonucleotides, the chain elongation (phosphorylation) is carried out by activating phosphoramidite building blocks using acidic activators, such as 1*H*-tetrazole (p*K*a = 4.8) on polymer supports [8].

The pKa value of activators used in DNA/RNA synthesis varies from 4.5 to 7.0. On the other hand, the pK_{B+H} values of cytosine and adenine bases which have highly nucleophilic amino groups are 4.2 and 3.8, respectively. Therefore, cytosine and adenine can be protonated by using a certain activator having a pK_a value less than 3.8 during the condensation. The nucleophilicity of the resulting protonated amino groups can thus be greatly decreased (proton-block method, Fig. 1). Because the amino group of the guanine base shows the inherently low nucleophilicity, the phosphorylation on the base residue does not occur [9].

We examined extensively various compounds as the activators in terms of their pK_a values, solubility, hygroscopicity, and easiness in the activation of N-unprotected phosphoramidite monomers. As a result, 4-nitro-6-trifluoromethylbenzotriazol-1-ol (HO^{nt}Bt) [13], 5-nitrobenzimidazolium triflate (NBT), and triazolium triflate (TRT) were selected as the activators having pK_a values of 2.70, 2.76, and 2.85, respectively, which might meet the demand of this proton-block method (Fig. 2) [7a].

In order to evaluate the O-selectivity of the phosphorylation using these compounds as the activator, the synthesis of dimers (d[AT], d[CT], and d[GT]) were carried out. As shown in Fig. 3, 20 equivalents of N-unprotected phosphoramidite unit [7a] and 40 equivalents of an activator were added to the thymidine-loaded highly cross-linked polystyrene (HCP) resin in a mixture of acetonitrile and N-methylpyrrolidone (NMP). Because of the low solubility of these activators in acetonitrile and the risk of acid-promoted elimination of the DMTr group, NMP was used as the co-solvent. After the phosphorylation, oxidation, and deprotection of the DMTr group were successively carried out, the oligomers were released from the resin by treatment with 28% NH$_4$OH. The O-selectivity of the phosphorylation was evaluated by using HPLC.
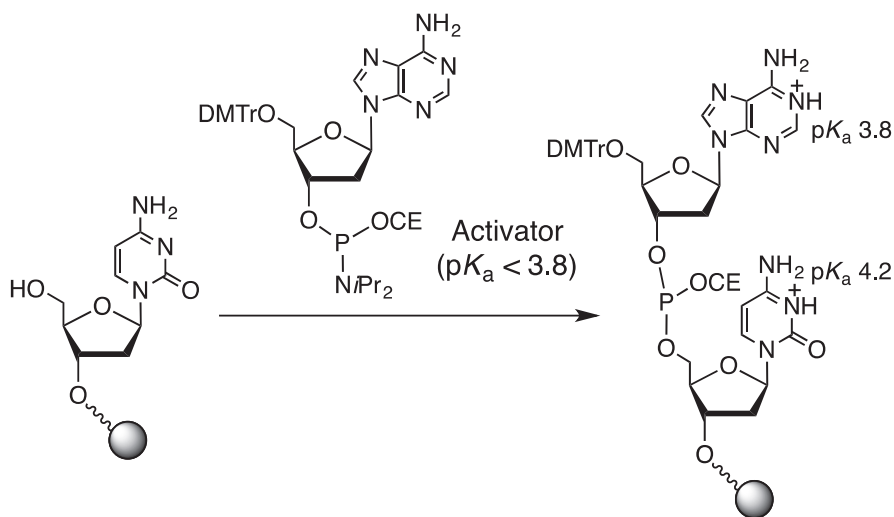
Fig. 1 Proton-block strategy for the synthesis of oligonucleotides without base protection
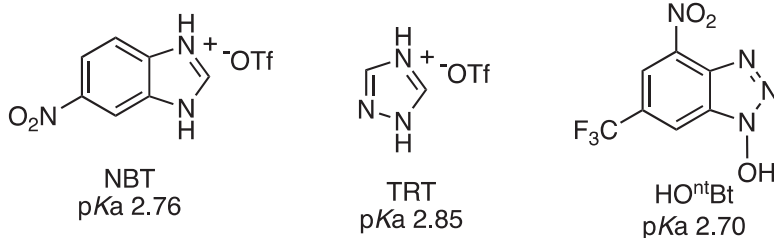
Fig. 2 Chemical structures of activators for the proton-block strategy
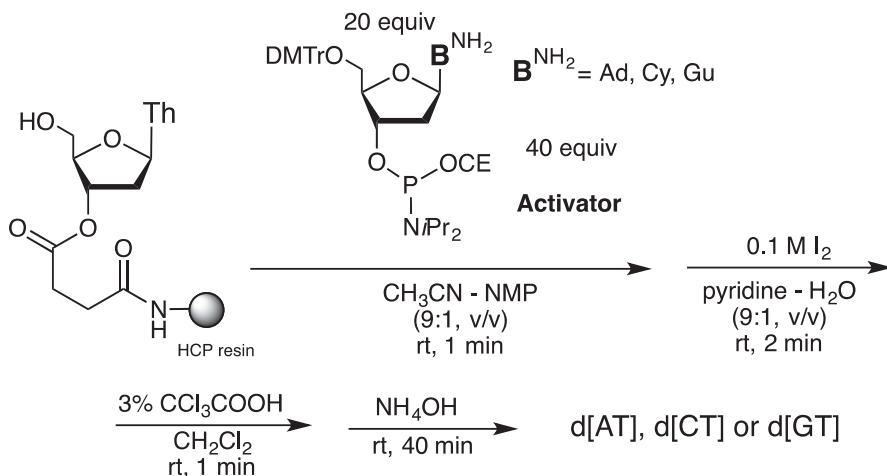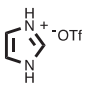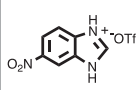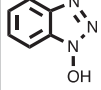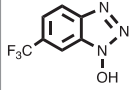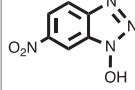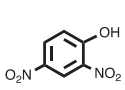
Fig. 3 Synthesis of d[AT], d[CT], and d[GT] using the *N*-unprotected phosphoramidite method

In the synthesis of d[AT] and d[CT] using imidazolium triflate (IMT, pK_a = 7.0) [12, 14], which was reported as the activator having the highest *O*-selectivity, the *O*-selectivities were 77.0% and 82.9%, respectively. In contrast, when HO^{nt}Bt, NBT, and TRT were used instead, the *O*-selectivities of the reactions were considerably improved.

In particular, NBT has the highest selectivity of 99% or more in dimer synthesis (Table 1).

For synthesizing trimers d[TXT] (X = A, C, and G) from the dimers obtained according to the above solid-phase synthesis, the *O*-selectivity of more than 99.8% can be achieved when NBT was used as the activator (Fig. 4). This strategy was applied to the synthesis of d[C$_6$T] and d[A$_6$T] in 21% and 25% yields, respectively (Fig. 5). In a similar manner, a DNA 12 mer of d[CAGTCAGTCAGT] was synthesized as the main product in 18% yield [7a]. However, the synthesis of these oligomers is accompanied by a series of minor peaks at later retention time in the anion-exchange HPLC. These minor peaks are assigned to a cluster of undesired *N*-branched oligomers. When IMT was used under similar conditions, these cluster peaks indicated the predominant products.

Table 1 The selectivity of condensation in the *N*-unprotected phosphoramidite method

	Ratio of the desired product					
Product	IMT	NBT	HOBt	HO^{tf}Bt	HO^{n}Bt	DNP
d[AT]	77.0	99.2	99.7	99.3	98.8	97.1
d[CT]	82.9	99.0	99.9	98.9	99.8	99.5
d[GT]	>99.9	>99.9	>99.9	>99.9	>99.9	>99.9
d[TAT]	90.5	>99.9	>99.9	99.1	97.5	99.6
d[TCT]	9.7	99.8	>99.9	98.7	97.2	99.4
d[TGT]	>99.9	>99.9	>99.9	>99.9	>99.9	>99.9
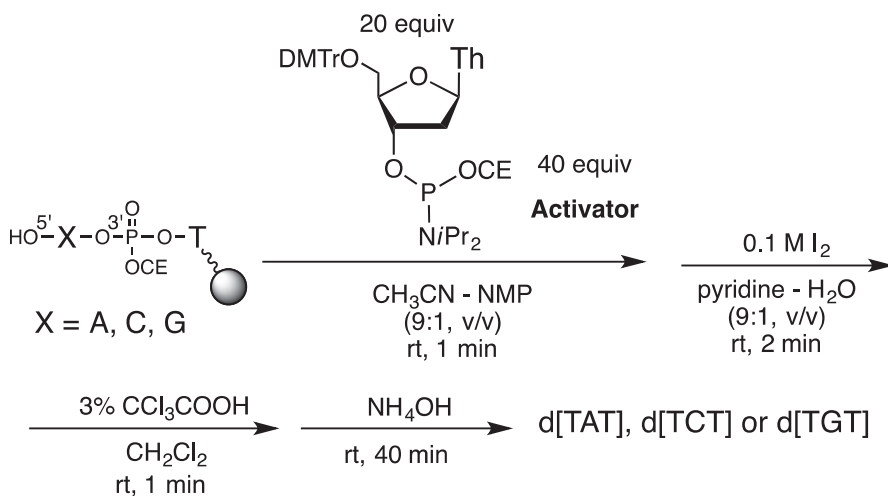
Fig. 4 Synthesis of d[TAT], d[TCT], and d[TGT] using the *N*-unprotected phosphoramidite method

3 Development of the Activated Phosphite Method Using *N*-Unprotected Phosphoramidites

Wada reported the *H*-phosphonate method for the synthesis of oligodeoxynucleotides using BOMP, a new type of phosphonium salt, as the condensing agent [11a]. The predominant *O*-selectivity observed in this method was explained by the strong MO interaction between the resulting trivalent phosphite triester intermediates and the 5′-terminal OH group in the growing DNA chain (Fig. 6).

Therefore, it can be speculated that the *O*-selectivity could be considerably improved if such a phosphite triester intermediate can be formed from the phosphoramidite building blocks.
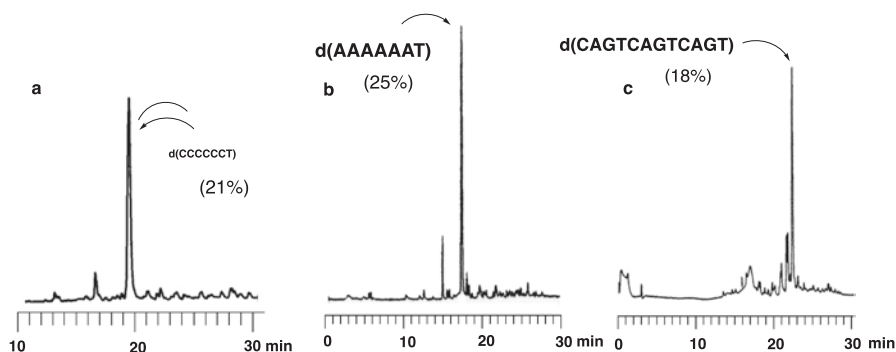
Fig. 5 The anion-exchange HPLC profiles of the crude mixtures in the synthesis of oligodeoxynucleotides
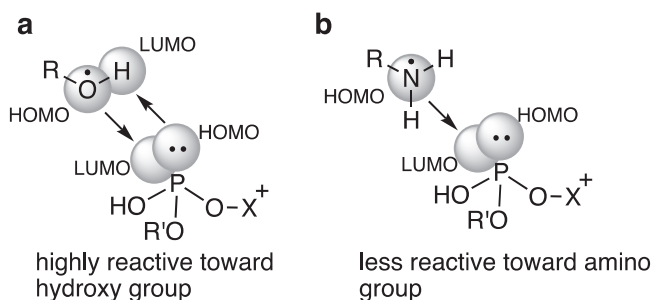
Fig. 6 The reaction selectivity in unprotected *H*-phosphonate method using BOMP

We examined a number of alcohol derivatives having acidic protons as the promoters (Fig. 7). The use of 1-hydroxybenzotriazole (HOBt, pK_a = 5.4) showed an excellent *O*-selectivity of more than 99.7% in the synthesis of d[XT] and d[TXT], as listed in Table 1 [7b]. d[CAGTCAGTCAGT] was synthesized in 36% yield. The HPLC analysis suggested that *N*-branched oligomers were negligibly formed in the synthesis.

More acidic reagents, such as 1-hydroxy-6-torifluoromethylbenzotriazole (HO^{tf}Bt, pKa = 4.3) and 1-hydroxy-6-nitrobenzotriazole (HO^{n}Bt, pKa = 3.5), decrease the *O*-selectivity. Interestingly, 2, 4-dinitrophenol (pKa = 4.1) still shows high *O*-selectivity [7c]. However, when this approach was employed using a DNA synthesizer, HO^{tf}Bt showed better results than HOBt. Using HO^{tf}Bt, α-d[TC*TTC*C*TTC*TTT] (61%, C*: 5-methyl-C), and d[CAGTCAGTCAGT] (32%) can be synthesized in satisfied yields [7c]. These oligomers were synthesized using the succinate linker on the highly cross-linked polystyrene (HCP) which was proved to be the best resin among the tested ones. However, this linker could be cleaved by ammonia. For synthesizing oligomers having base-labile functional groups, cleavable linkers under conditions rather than basic ones were required. Therefore, we used a silyl type of linker (Fig. 8a) [15].
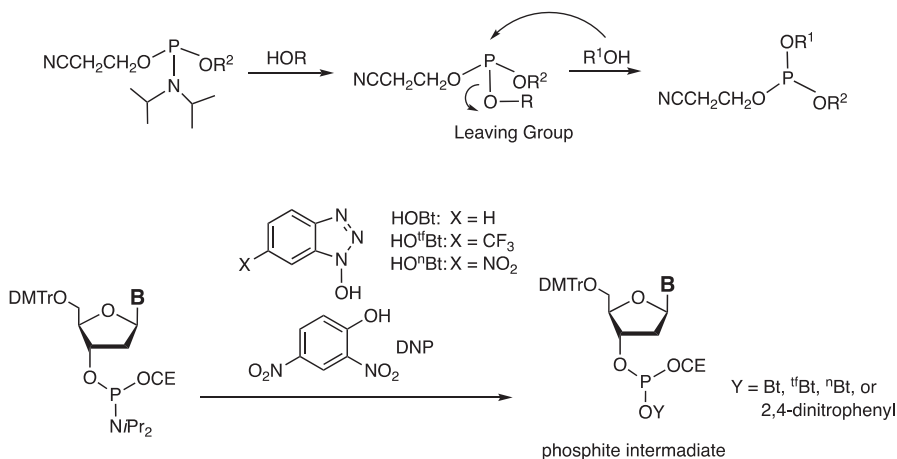
Fig. 7 Activated phosphite triester method
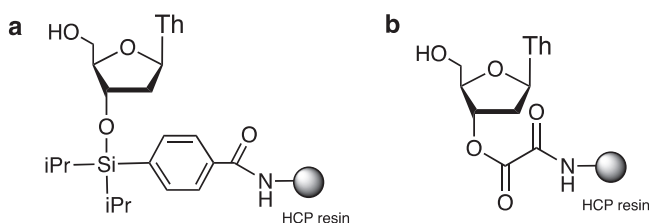
Fig. 8 Chemical structures of T-loaded HCP resins having silyl (**a**) and oxalyl (**b**) linkers

Thus, d[GC^{ac}ATCAGC^{ac}C^{ac}TCAT] having three C^{ac} bases (Fig. 10a) was synthesized in 33% yield using this linker which can be removed by treatment with Bu$_4$NF under neutral conditions (Fig. 9a) [7c]. Moreover, further improvement for the coupling conditions was conducted using the post-treatment of the P–N bonds on the base residues by BIT after every condensation. This improved procedure gave d[C$_5$T$_5$(CT)$_5$] in a high yield of 81%, indicated by the considerably simplified peak in HPLC (Fig. 9b). A long oligomer of d[T$_2$A$_5$T$_2$AT$_2$A$_3$T$_2$AT$_2$] was also obtained in a satisfactory yield (24%) using this improved procedure (Fig. 9c) [7c].

As one application of this method, we demonstrated the synthesis of oligodeoxynucleotides containing a dithymidine hydroxymethylphosphonate residue [Tp$_{(CH2OH)}$T] [16]. Such a residue was labile toward ammonia which was used for deprotecting the usual acyl protecting groups on the base residues. Ammonia, however, was sufficiently resistant under the conditions of 5% PrNH$_2$ in MeOH for 30 min, which was used for the cleavage of the base-labile oxalyl linker (Fig. 8b) [16]. Thus, d[pTxTpCpTxTpCpCpTxTpCpT], which contained many lipophilic species of the diastereomeric TxT units, was obtained using the oxalyl linker. This modified oligomer showed a strong triple strand formation with a hairpin DNA 34 mer [16] (Fig. 10).
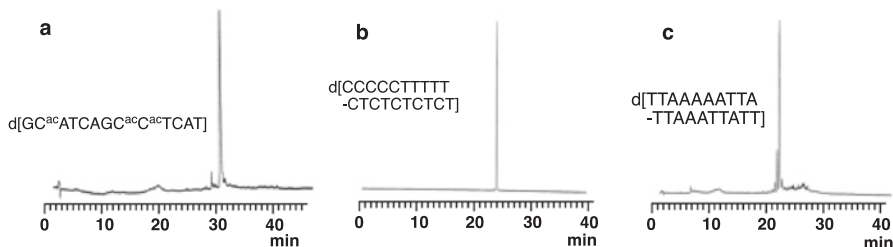
Fig. 9 The anion-exchange HPLC profiles of the crude mixtures in the synthesis of (**a**) d[GC^acATCAGC^acC^acTCAT], (**b**) d[C₅T₅CTCTCTCT], and (**c**) d[TTAAAAATTATTAAATTATT]
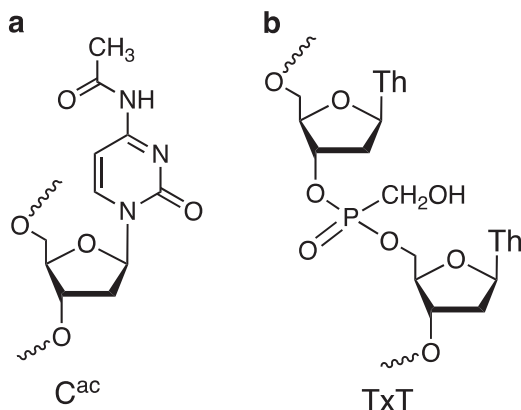
Fig. 10 Chemical structures of 2′-deoxy-*N*-acetylcytidine (**a**) and the hydroxymethylphosphonate (**b**) linkage

In place of the silyl linker (Fig. 8a) which is cleavable by Bu₄NF, we designed a new type of silyl linker containing a triazole ring, which can be formed by the reaction between the azido group and the acetylene group attached to the HCP resin, as shown in Fig. 11 [17].

The activated phosphite method is proved to be useful for synthesizing the oligodeoxynucleotides containing a cytosine N-oxide or an adenine N-oxide base. As the synthetic intermediates, the partially protected oligodeoxynucleotide derivatives, which incorporate the *N*-unprotected deoxyadenosine or deoxycytidine, can be produced on the HCP resin with the combination of *N*-protected and *N*-unprotected deoxynucleoside phosphoramidite units. Oxidation of these intermediates with mCPBA, followed by deprotection and cleavage of the linker, generates oligodeoxynucleotides having adenine-N-oxide or cytosine-N-oxide site specifically. The biological properties of DNA having such base-oxidized species were unknown at that time, although they can be formed via oxidation using hydrogen peroxide in cells. The synthesis of this type of oligomers was achieved using the *N*-unprotected deoxycytidine or deoxyadenosine phosphoramidite building block along with the
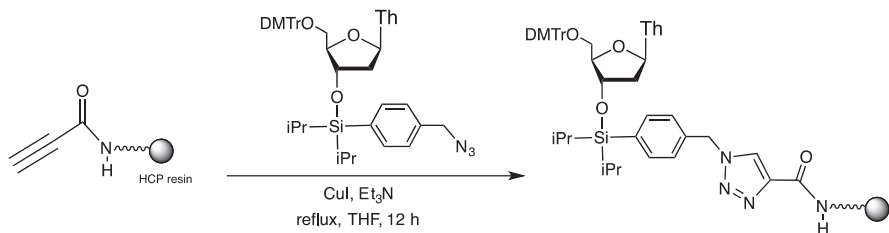
Fig. 11 A silyl type of linker constructed by Huisgen reaction
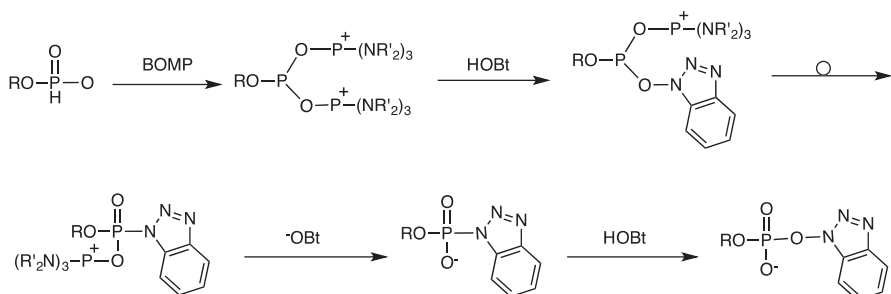
Fig. 12 Rearrangement of the phosphite intermediates in the *H*-phosphonate method

usual thymidine and (4-isopropylphenoxy)acetyldeoxyguanosine units. It is now clear that such modified oligomers can bind the complementary DNA strand correctly without the formation of mismatched base pairs [18].

4 Mechanism of the Activated Phosphite Method

In the *N*-unprotected phosphoramidite method, the reaction is considered to proceed via a phosphite triester intermediate. On the other hand, the intermediate, which is supposed as a plausible intermediate in the above-mentioned *H*-phosphonate method, is a kind of phosphite triester having a phosphonium cation (Fig. 12) [11a].

This intermediate is rapidly converted via an N–O rearrangement to give a phosphoramidate derivative, which might also react with the 5′-terminal HO group of the growing chain on the polymer support and give directly a five-valent phosphotriester. Therefore, there is a possibility that the phosphite intermediate in the activated phosphite method might be transferred to a phosphoramidate derivative (Fig. 13).

To confirm the presence of the rearrangement, we examined the synthesis of Tp(S)T using sulfurization in place of oxidation, as shown in Fig. 13. Consequently, the ratio of TpT/Tp(S)T was 4.9:95.1. When IMT was used, the ratio was decreased to 1.4:98.6 because of air oxidation. Therefore, the actual rearrangement in the phosphite triester method using HOBt was estimated to be a ratio of 3.5% [7c] (Fig. 14).
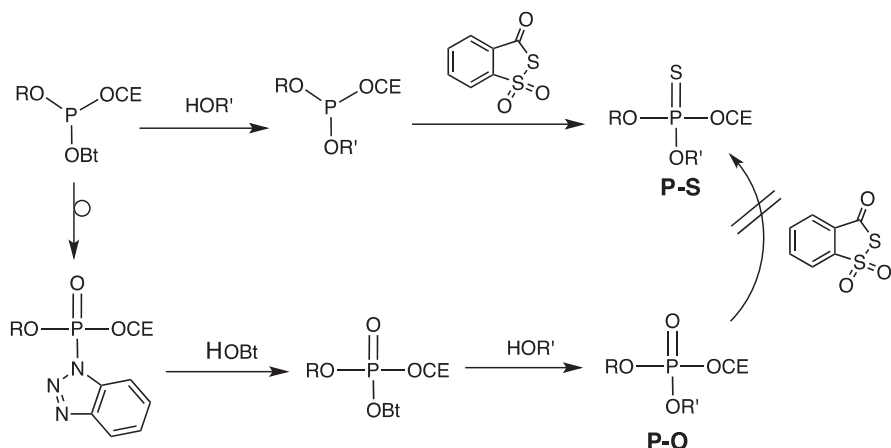
Fig. 13 Reaction mechanism of the phosphorylation in the activated phosphite method
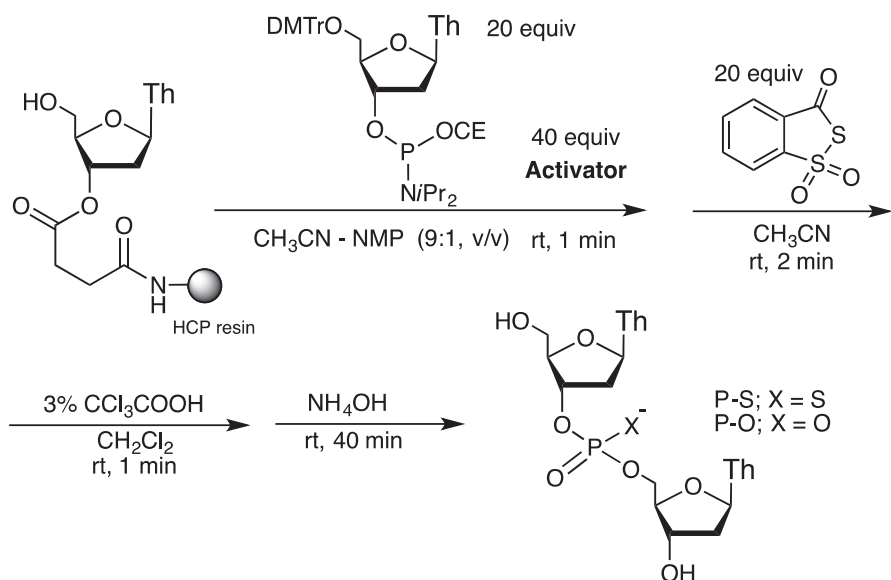
Fig. 14 Synthesis of the phosphorothioate TT dimer

5 Synthesis of RNA Oligomers Using the Activated Phosphite Method

For the synthesis of RNA, we applied our original procedure used for DNA synthesis to achieve this goal, using *N*-unprotected ribonucleotide building blocks. For this purpose, we examined the synthesis of AmpT and CmpT using

2′-*O*-methyladenosine and 2′-*O*-methylcytidine phosphoramidite units. It turned out that the efficiency of the condensation decreased greatly. Therefore, our efforts were focused on a condensation mode involving a two-step treatment initially introduced by R. L. Letsinger [9]. In this procedure, the post-treatment of the resulting *N*-branched species with a more acidic promoter was carried out after the condensation was finished, as shown in Fig. 15 [19]. In the first treatment, we employed a powerful activator, i.e., benzimidazolinium triflate (BIT) developed by Hayakawa. The resulting *N*-branched DNA oligomer species were treated using several HOBt derivatives as well as pyridine-HCl in the presence of aniline (Letsinger's choice). It was found that the use of HO^{n}Bt gave the best result, and the efficiency of the P–N bond cleavage remained at the level of more than 99%. Once the resulting phosphite ester derivative represented by ROP(OCe)(O^{n}Bt) could be converted to an inert five-valent species ROP(O)(OCe)(O^{n}Bt) via an inherent rearrangement as reported by us, we can obtain only the desired linear DNA chain at the final process.

According to this improved procedure, we also examined dimer synthesis using several kinds of 2′-O-masked adenosine and cytidine phosphoramidite building blocks. In all cases, the P–N bond cleavage was achieved in more than 99%, when the time for the second treatment was extended to 2 min. Using these conditions, we synthesized r[UUUUCUUUUU] as the almost single peak in HPLC. Starting from the C-loaded HCP resin having the silyl linker mentioned above, we also succeeded in synthesizing an RNA 25 mer of r[UAGAAGUG^{ac}CAUACUAG^{ac}UGAGUUUGC], where two base-labile *N*-acetylguanine bases were introduced into the oligomer. This synthesis was conducted in 14% yield [20].
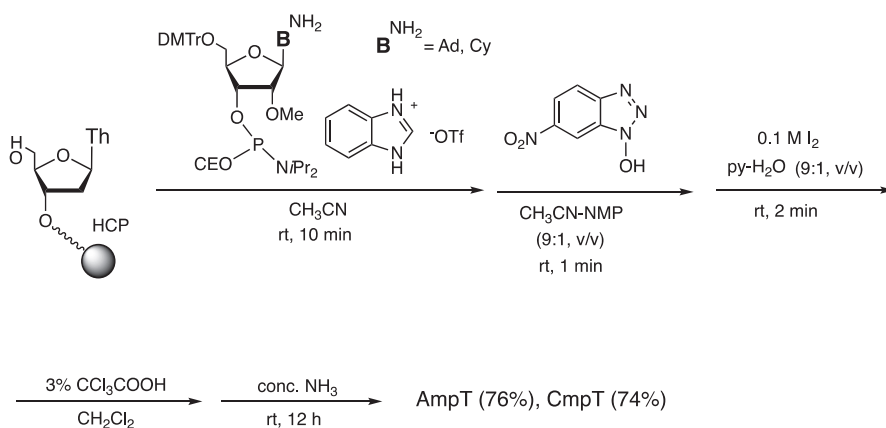
Fig. 15 Synthesis of the phosphorothioate TT dimer

6   Synthesis of Phosphoramidite Monomer Building Blocks

In the synthesis of oligonucleotides without base protection, N-unprotected mono-mer building blocks were required and therefore synthesized according to several methods. Since the selective 5′-*O*-dimethoxytritylation of deoxynucleosides has been reported by several research groups, direct 3′-*O*-phosphitylation of 5′-*O*-DMTr-deoxynucleosides has also been developed to obtain the *N*-unprotected monomer units. This process seems to be ideal, but some drawbacks occur in the two-step procedure. The selective 5′-*O*-dimethoxytritylation was not so good because simul-taneous 3′-*O*-dimethoxytritylation to some extent occurred. The purification of the desired product thus became a little challenging. Moreover, the yield of the 5′-*O*-DMTr-deoxyguanosine was not satisfied. From the practical viewpoint, we have developed an alternative to the usual method. On the basis of our own experi-ence that tervalent phosphoramidite derivatives were rather stable under basic con-ditions compared with the corresponding five-valent phosphoramidate derivatives, we found a simple treatment of the conventional deoxyribonucleoside phosphora-midite monomers using methylamine in THF [19, 21].

7   Conclusion

A number of methods for synthesizing DNA and RNA have been reported using the well-established phosphoramidite method up to date [8]. Under the restricted condi-tions of this standard method, it is difficult to synthesize oligonucleotides contain-ing base-labile functional groups. Usually, such base-labile functional groups have been introduced into DNA or RNA by post-modification using amino groups that can react with acylating agents containing the base-sensitive group. Our activated phosphite method now enables us to synthesize the base-labile modified oligonucle-otide derivatives in a more straightforward manner. Actually, the synthesis of oligo-nucleotides incorporating lipid structures using our original strategy has been reported [22].

References

1. (a) Manoharan M (2004) RNA interference and chemically modified small interfering RNAs. Curr Opin Chem Biol 8:570–579 (b) Singh Y, Murat P et al (2010) Recent developments in oligonucleotide conjugation. Chem Soc Rev 39:2054–2070. (c) Sharma VK, Sharma, RK et al (2014) Antisense oligonucleotides: modifications and clinical trials. Med Chem Commun 5:1454–1471
2. (a) Stein CA, Krieg AM (eds) (1998) Applied Antisense Oligonucleotide Technology, Wiley-Liss. (b) Crooke ST (ed) (2001) Antisense drug technology-principles, strategies and application, Marcel Dekker. (c) Prakash TP, Manoharan M et al (2000) Tetrahderon Lett

41:4855–4858; (d) Prakash TP, Kawasaki AM et al (2003) Org Lett 5:403. (e) Saneyoshi H, Seio K et al (2005) J Org Chem 70:10453

3. (a) Schena M, Shalon D et al (1995) Quantitative monitoring of gene expression patterns with complementary DNA microarray. Science 270:467–470. (b) Lockhart DJ, Dong H (1996) Expression monitoring by hybridization to high-density oligonucleotide arrays. Nat Biotechnol 14:16751680. (c) Kwiatkowski RW, Lyamichev V et al (1999) Clinical, genetic, and pharmacogenetic applications of the invader assay. Mol Diagn 4:353–364

4. (a) Robertson SA, Ellman JA et al (1991) A general and efficient Route for chemical aminoacylation of transfer RNAs. J Am Chem Soc 113,:2722–2729. b) Lodder M, Wang B et al (2005) The N-pentenoyl protecting group for aminoacyl-tRNAs. Methods 36:245–251

5. Parey N, Baraguey C et al (2005) First evaluation of acyloxymethyl or acylthiomethyl groups as biolabile 2′-O-protections of RNA. Org Lett 8:3869–3872

6. Wada T, Moriguchi T et al (1994) Synthesis and properties of N-phosphorylated ribonucleosides. J Am Chem Soc 116:9901–9911

7. (a) Sekine M, Ohkubo A et al (2003) Proton-block strategy for the synthesis of oligodeoxynucleotides without base protection, capping reaction, and P-N bond cleavage reaction. J Org Chem 68:5478–5492. (b) Ohkubo A, Seio K et al (2004) A new strategy for the synthesis of oligodeoxynucleotides directed towards perfect O-selective internucleotidic bond formation without base protection. Tetrahedron Lett 45:363–366. (c) Ohkubo A, Seio K et al (2004) O-Selectivity and utility of phosphorylation mediated by phosphite triester intermediates in the N-unprotected phosphoramidite method. J Am Chem Soc 126:10884–10896. (d) Ohkubo A, Kuwayama Y et al (2008) O-Selective condensation using P-N bond cleavage in RNA synthesis without base protection. Org Lett 10:2793–2796

8. (a) Beaucage SL, Caruthers MH (1981) Deoxynucleoside phosphoramidites-A new class of key intermediates for deoxypolynucleotide synthesis. Tetrahedron Lett 22:1859–1863; (b) Matteucci MD, Caruthers MH (1981) Synthesis of deoxyoligonucleotides on a polymer support. J Am Chem Soc 103:3185–3191; (c) McBride LJ, Caruthers MH (1983) An investigationof several deoxynucleoside phosphoramidites useful for synthesizing deoxyoligonucleotides. Tetrahedron Lett 24:245–248; (d) Beaucage SL Iyer RP (1992) Advances in the oligonucleotides bythe phosphoramidite approach. Tetrahedron 48:2223–2311

9. (a) Gryaznov SM, Letsinger RL (1991) Synthesis of oligonucleotides via monomers with unprotected bases. J Am Chem Soc 113:5876; (b) Gryaznov SM, Letsinger RL (1992) Selective O-phosphorylation with nucleoside phosphoramidite reagents. Nucleic Acids Res 20:1879–1882

10. Kung PP, Jones RA (1992) H-phosphonate DNA synthesis without amino protection. Tetrahedron Lett 33:5869–5872

11. (a) Wada T, Sato Y et al (1997) Chemical synthesis of oligodeoxyribonucleotides using N-unprotected H-phosphonate monomers and carbonium and phosphonium condensing reagents: O-selective phosphonylation and condensation. J Am Chem Soc 119:12710–12721. (b) Wad.a, T, Mochizuki A et al (1998) Functionalization of solid supports with N-unprotected deoxyribonucleosides. Tetrahedron Lett 39:5593–5596. (c) Wada T, Mochizuki A et al (1998) A convenient method for phosphorylation involving a facile oxidation of H-phosphonate monoesters via bis(trimethylsilyl) phosphites. Tetrahedron Lett 39:7123–7126. (d) Wada T, Honda F et al (1999) First synthesis of H-phosphonate oligonucleotides bearing N-unmodified bases. Tetrahedron Lett 40:915–918

12. (a) Hayakawa Y, Kataoka M (1998) Facile synthesis of oligodeoxyribonucleotides via the phosphoramidite method without nucleoside base protection. J Am Chem Soc 120:12395–12401. (b) Hayakawa Y, Kawai R (2001) Nucleotide synthesis via methods without nucleoside-base protection. Eur J Pharm Sci 13:5–16

13. Reese CB, Zhuo ZP (1993) Phosphotriester approach to the synthesis of oligonucleotides: a reappraisal. J Chem Soc Perkin Tran 1:2291–2301

14. Hayakawa Y, Kawai R et al (2001) Acid/azole complexes as highly effective promoters in the synthesis of DNA and RNA oligomers via the phosphoramidite method. J Am Chem Soc 123:8165–8176

15. Ohkubo A, Kasuya R et al (2008) Efficient synthesis of functionalized oligodeoxyribonucleotides with base-labile groups using a new silyl linker. Bioorg Med Chem 16:5345–5351

16. Ohkubo A, Aoki K et al (2005) Synthesis of oligodeoxyribonucleotides containing hydroxymethylphosphonate bonds in the phosphoramidite method and their hybridization properties. Tetrahedron Lett 46:8953–8957

17. Ohkubo A, Noma Y et al (2009) Introduction of 3′-terminal nucleosides having a silyl-type linker into polymer supports without base protection. J Org Chem 74:2817–2823

18. Tsunoda A, Ohkubo H et al (2008) Synthesis and properties of DNA oligomers containing 2′-deoxynucleoside N-oxide derivatives. J Org Chem 73:1217–1224

19. Ohkubo A, Kuwayama Y et al (2008) O-Selective condensation using P-N bond cleavage in RNA synthesis without base protection. Org Lett 10:2793–2796

20. Unpublished data

21. Ohkubo A, Sakamoto K et al (2005) Convenient synthesis of N-unprotected deoxynucleoside 3′-phosphoramidite building blocks by selective deacylation of N-acylated species and their facile conversion to other N-functionalized derivatives. Org Lett 7:5389–5392

22. Chillemi R, Greco V et al (2013) Oligonucleotides conjugated to natural lipids: synthesis of phosphatidyl-anchored antisense oligonucleotides. Bioconjug Chem 24:648–657

Various Coupling Agents in the Phosphoramidite Method for Oligonucleotide Synthesis

Masaki Tsukamoto and Yoshihiro Hayakawa

Abstract This review selects some representative coupling agents used for inter-nucleotide bond formation reactions in the phosphoramidite method, which is now the most widely employed method for the chemical synthesis of oligodeoxyribo-nucleotides and oligoribonucleotides, and it describes their utility, efficiency, and drawbacks. Moreover, the mechanism of the coupling of the nucleoside phosphora-midite and nucleoside promoted by the coupling agent is discussed in some cases. The selected coupling agents are 1*H*-tetrazole, 5-ethylthio-1*H*-tetrazole (ETT), 5-benzylthio-1*H*-tetrazole (BTT), 5-[3,5-bis(trifluoromethyl)phenyl]-1*H*-tetrazole (Activator 42), 4,5-dicyanoimidazole (DCI), certain carboxylic acids, and various acid/azole complexes such as benzimidazolium triflate (BIT) and saccharin 1-methylimidazole (SMI).

Keywords Synthesis of oligonucleotides · Phosphoramidite method ·
1*H*-Tetrazole · Acid/azole complexes · DNA oligomer · RNA oligomer

1 Introduction

In response to the recent progress in the life sciences, the importance of the chemical synthesis of DNA and RNA oligomers, i.e., oligonucleotides, has increased noticeably, because it is no exaggeration to say that research in the life sciences always uses chemically synthesized oligomers. In the chemical synthesis of oligonucleotides, a key stage is the construction of an internucleotide linkage [1–3]. Thus far, many methods have been reported for the formation of internucleotide bonds, such as the phosphodiester method developed by Khorana [4, 5], the

M. Tsukamoto (✉)
Graduate School of Information Science, Nagoya University, Nagoya, Japan
e-mail: tsukamoto@is.nagoya-u.ac.jp

Y. Hayakawa (✉)
Department of Applied Chemistry, Faculty of Engineering, Aichi Institute of Technology,
Toyota, Japan
e-mail: yoshi@aitech.ac.jp; yoshi@is.nagoya-u.ac.jp

phosphotriester method devised by Letsinger [6, 7] and Reese [2, 8], the phosphite method developed by Letsinger [9, 10], the phosphoramidite method devised by Caruthers [11–15], the *H*-phosphonate method as originally developed by Todd [16, 17], and the improved version devised by Froehler [18] and Stawinski [19]. Figure 1 outlines the modes of internucleotide bond formation in these methods.

Among the existing methods, the phosphoramidite method [1, 11–15] is the most widely employed at present, because this method has many advantages over the other methods. For example, nucleoside phosphoramidites, which are used as building blocks in the phosphoramidite method, are easily prepared and stable in storage. In addition, the phosphoramidite method generally enables higher speed and higher yield in internucleotide bond formation compared with the other methods. This factor is a great advantage in the synthesis of long oligonucleotides. Therefore, the phosphoramidite method has been applied not only to the synthesis of oligodeoxyribonucleotides but also to that of oligoribonucleotides and has enabled the production of a variety of biologically important substances, such as primers for the polymerase chain reaction, oligonucleotide probes, oligonucleotide medicines, and cyclic dinucleotides [20–30].

A typical reaction sequence in the solid-phase synthesis of a DNA oligomer via the phosphoramidite method is illustrated in Fig. 2 [3, 12–15]. First, the 5′-*O*-(4,4′-dimethoxytrityl) (DMTr) protecting group of a nucleoside is removed by an organic acid, such as dichloroacetic acid or trichloroacetic acid, to afford the nucleoside with a free 5′-hydroxy group (detritylation). Then, the product is reacted with a suitably protected deoxyribonucleoside phosphoramidite with the aid of a coupling agent (coupling). The 5′-hydroxy group that undergoes no reaction is capped with an acetyl group using acetic anhydride and pyridine (capping). The resulting phosphite triester is converted into the corresponding phosphate using a suitable oxidizing agent, such as iodine/H_2O/pyridine or *tert*-butyl hydroperoxide (TBHP)
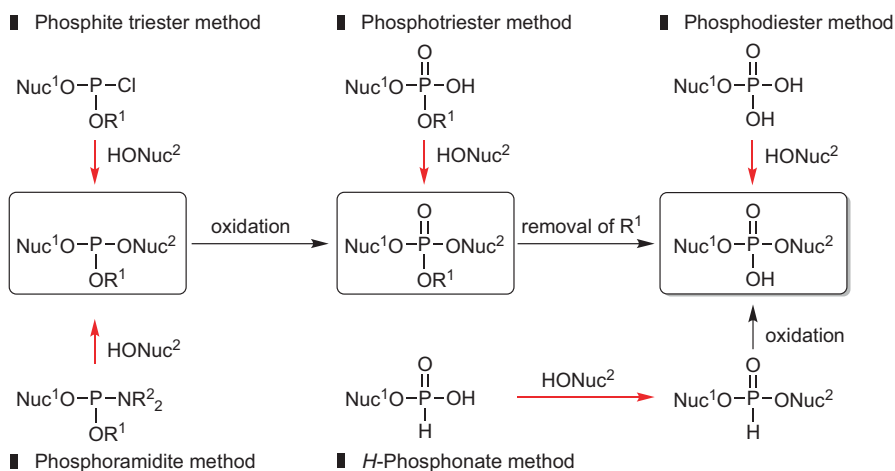
Fig. 1 Outline of representative methods of internucleotide bond formation, where the phosphate esters are shown in the acid form for simplicity
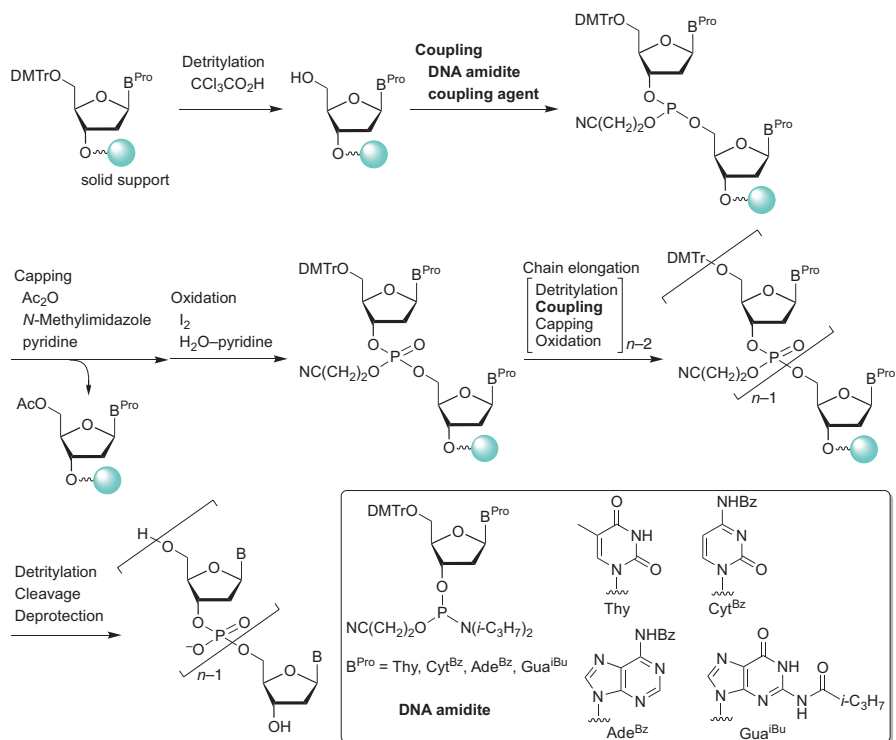
Fig. 2 Reaction sequence of solid-phase synthesis of oligodeoxyribonucleotides by the phosphoramidite method

[31] (oxidation). This four-step procedure, namely, detritylation, coupling, capping, and oxidation, is repeated until the nucleotide reaches the desired length (chain elongation). Finally, the fully protected oligonucleotide on the solid support is subsequently treated with an acid, which removes the 5′-O-DMTr protecting group, and with aqueous ammonia, which simultaneously detaches the product from the solid support and removes all the protecting groups to afford the target deprotected oligonucleotide.

The synthesis of oligoribonucleotides (RNA oligomers) is achieved in a similar manner. In the synthesis of ribonucleotides, protection of the 2′-hydroxy group is necessary. A 2′-O-tert-butyldimethylsilyl (TBDMS) group is most frequently employed for protection, as shown in Fig. 3 [3, 32, 33].

As mentioned above, the most important step in this pathway is the construction of the internucleotide linkage. In the phosphoramidite method, this is achieved on the basis of condensation of a nucleoside with a free 5′-hydroxy group and a nucleoside phosphoramidite assisted by an activator of the phosphoramidite, in other words, a coupling agent or promoter. Therefore, the invention of coupling agents with high efficiency is very important and a lot of effort has been devoted to research in this area so far. As a result, a number of coupling agents have been developed. Among these, this review selects several reagents with high utility and potential and

B^{Pro} = Ura, Cyt^{Ac}, Ade^{Bz}, Gua^{Ac}, etc.
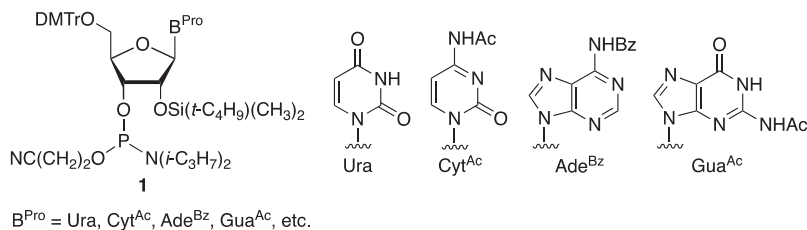
Fig. 3 Representative phosphoramidite building blocks for the synthesis of RNA derivatives

discusses the merits and demerits of these reagents, not merely in the solution-phase synthesis but also in the solid-phase synthesis of DNA and RNA oligomers [14, 32–38]. The selected coupling agents are 1*H*-tetrazole and its derivatives [5-ethylthio-1*H*-tetrazole (ETT), 5-benzylthio-1*H*-tetrazole (BTT), and 5-[3,5-bis (trifluoromethyl)phenyl]-1*H*-tetrazole (Activator 42)], 4,5-dicyanoimidazole (DCI), some carboxylic acids, and various acid/azole complexes [benzimidazolium triflate (BIT) and related compounds, and saccharin 1-methylimidazole (SMI)]. For some coupling agents, it is also discussed how the reagent activates the phosphoramidite and promotes the reaction.

Although there are two different types of phosphoramidite method, i.e., the method using nucleoside phosphoramidites with protected nucleobases (the *N*-protected method) and the method using nucleoside phosphoramidites with unprotected nucleobases (the *N*-unprotected method), this section only deals with examples of the *N*-protected method, because the *N*-unprotected method [39, 40] is reviewed in detail in the previous section.

2 Coupling Agents in the Phosphoramidite Method

2.1 *1*H-*Tetrazole and Its Derivatives*

2.1.1 1*H*-Tetrazole

1*H*-Tetrazole (TetH) [41] was the first phosphoramidite coupling agent to be invented. The historical background of this promoter has been described in several articles [12–15]. TetH displays high reactivity toward the phosphoramidites of all kinds of 2′-deoxyribonucleosides and generally accomplishes the condensation in a short period and in high yield. For example, a 1 μmol scale reaction of a deoxyribo-nucleoside *N,N*-diisopropylphosphoramidite and a deoxyribonucleoside with a free 5′-hydroxy group on a solid support is usually completed in 30 s (Fig. 2) to give the coupling product in >99% yield [42]. The reaction time varies depending on the scale of the reaction. On a larger scale, a longer reaction time is required for com-pletion. For example, a reaction time of 5 min is necessary for the reaction on a 160 μmol scale [43]. The method using TetH as the promoter has been applied to the production of DNA microarrays [15, 44, 45].

$$\text{HN} \underset{\underset{N}{\overset{N \cdot N}{\big\downarrow}}}{\Big\downarrow}$$

TetH

Because TetH is a rather strong acid, with a pK_a value comparable to that of acetic acid, TetH causes decomposition of the 5′-O-DMTr protecting group to a substantial extent. If this decomposition takes place during chain elongation of an oligonucleotide, it causes formation of oligomer by-products [(n+1)-mer, (n+2)-mer, etc.] that are longer than the desired length of the oligonucleotide (n-mer). This unwanted detritylation is suppressed by the addition of a basic compound, such as N-methylimidazole (NMI). The use of a mixed solution of 0.1 M NMI and 0.45 M TetH in acetonitrile is effective in decreasing the extent of unwanted detritylation and enables synthesis of 51 mer DNA on a 0.35 mmol scale in an average coupling yield of 98.3%, resulting in an overall yield of 41% [46].

The addition of NMI to TetH not only decreases the extent of unwanted detritylation but also accelerates the coupling reaction. The latter role of NMI is described in Sect. 2.4.

In comparison with the phosphoramidites of deoxyribonucleosides, those of ribonucleosides are generally less reactive, in particular in cases in which the protecting group on the 2′-hydroxy group is bulky, such as TBDMS (Fig. 3). The reactivity of TetH is not quite high enough to activate the less reactive ribonucleoside phosphoramidites. Thus, when TetH is used as the promoter in the coupling reaction using 2′-O-TBDMS-protected ribonucleoside phosphoramidites, the reaction sometimes requires rather a long time for completion. For example, the reaction of **1** (Fig. 3, B^{Pro} = Ura, Cyt^{Bz}, Ade^{Bz}, Gua^{iBu}) with the aid of TetH requires 12 min for completion, being achieved in 97–99% yield [47]; in this coupling reaction, prolongation of the reaction time does not improve the yield of the desired product but increases the formation of by-products [48]. Therefore, the more reactive TetH derivatives shown below have been invented and employed for the synthesis of RNA oligomers using ribonucleoside phosphoramidites as building blocks.

In order to invent more reactive promoters, it is helpful to know the mechanism of TetH-assisted condensation of nucleoside phosphoramidite and nucleoside. Therefore, here is a brief description of the mechanism that was proposed on the basis of kinetic and NMR studies of the condensation [49, 50]. As shown in Fig. 4, TetH initially acts as an acid that protonates the phosphoramidite **A** to form the ammonium species **B**. At the same time, the tetrazolide anion, Tet⁻, is formed. Subsequently, the resulting species **B** undergoes nucleophilic attack by Tet⁻ to give the phosphorotetrazolide **C**. Finally, nucleophilic substitution occurs between **C** and the nucleoside (Nuc²OH) to afford the coupling product, i.e., the phosphite triester **D**. In this process, the rate-determining step (RDS) is the reaction between **B** and Tet⁻ to form **C**. The formation of the intermediate **C** was actually confirmed by a ³¹P NMR study that monitored the reaction using 5′-O-DMTr-thymidine, 3′-[(methyl)-(N,N-dialkyl)]-phosphoramidites [49–52]. Thus, the elucidated mechanism suggests that a compound that has appropriate acidity and has a conjugate base with high nucleophilicity will act as an effective promoter. On the basis of this
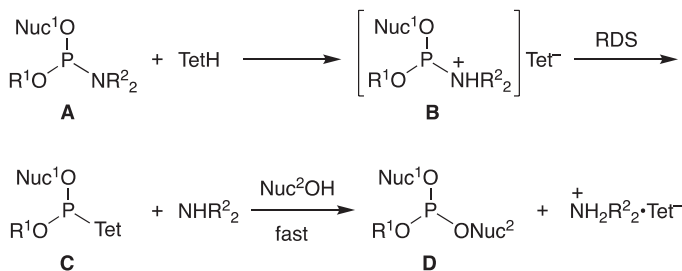
Fig. 4 Proposed mechanism of coupling reaction of a nucleoside phosphoramidite and a nucleoside promoted by TetH

consideration, several promoters have been developed that have higher reactivities than TetH. The compounds described in the following subsections are representative promoters with higher reactivities than TetH.

2.1.2   5-Ethylthio-1*H*-tetrazole

5-Ethylthio-1*H*-tetrazole (ETT), which is prepared from ethyl thiocyanate and sodium azide [53, 54], is a coupling agent with higher reactivity than TetH. This compound is now commercially available.

ETT
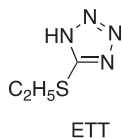
ETT accomplishes the coupling reaction with an average yield of 96.2–98.1% in the synthesis of DNA oligomers, such as 18 mers to 34 mers, on a TentaGel support on scales of 25 μmol–1 mmol [55]. The coupling yield is 1–2% higher than that in the case where TetH is used as the promoter.

The efficiency of ETT is also observed to be higher than that of TetH in the synthesis of RNA oligomers employing 2′-*O*-TBDMS-ribonucleoside phosphoramidites [Fig. 3, B^{Pro} = Ura, Cyt^{Ac}, Ade^{Pac}, Gua^{iPrPac} (Pac = phenoxyacetyl; iPrPac = 4-isopropylphenoxyacetyl)]. For example, in the synthesis of an oligoribonucleotide 36 mer on a 0.2 μmol scale, when ETT is used as a 0.25 M solution in acetonitrile, each coupling reaction in the chain elongation process is accomplished in 465 s (ca. 7.8 min) in an average coupling yield of 97.5% to provide the target oligonucleotide in an overall isolated yield of 45% [33]. On the other hand, when a 0.45 M solution of TetH in acetonitrile is used as the promoter for the coupling reaction, which is carried out for the same period as above, the synthesis gives the target product in an isolated yield of only 34%. The synthesis of RNA oligomers shorter than 36 mers on scales of 2.5–25 μmol with ETT as the promoter is also reported and, in this case, the coupling reaction is performed with an average yield of 97.5–99% [48].

ETT is also effective for the activation of ribonucleoside phosphoramidites with 2′-*O*-protecting groups other than the TBDMS group, such as the bis(2-acetoxyethoxy)methyl (ACE) orthoester [56], 2-cyanoethoxymethyl (CEM) [57], *tert*-butyldithiomethyl (DTM) [58], 2-(4-tolylsulfonyl)ethoxymethyl (TEM) [59], and levulinyl (Lv) [60] groups (Fig. 5) (for details of these protecting groups, see the literature [37]). Thus, ETT is advantageously employed as the promoter for the internucleotide bond forming reaction in the synthesis of oligoribonucleotides.

As well as TetH, ETT also leads to undesirable cleavage of the 5′-*O*-DMTr protecting group, which is more readily caused by ETT than by TetH. According to the results of control experiments shown in Table 1, the half-life of the 5′-*O*-DMTr protecting group is shorter in a solution of ETT compared with a solution of TetH [61]. The same phenomenon was observed for all kinds of nucleosides that were investigated. As mentioned above, this undesirable detritylation causes the formation of oligomer by-products that are longer than the desired length of the product. Therefore, when using ETT, we should carefully set the reaction conditions in order to prevent unwanted detritylation.

2.1.3   5-Benzylthio-1*H*-tetrazole

5-Benzylthio-1*H*-tetrazole (BTT) is an alternative TetH-related coupling agent with higher reactivity than TetH. This compound is prepared by the reaction of benzyl thiocyanate and sodium azide in the presence of ammonium chloride [62]. Also, this reagent is commercially available. Hygroscopicity is not observed in this compound. This reagent effectively activates various 2′-*O*-protected ribonucleoside phosphoramidites, in which the protecting groups are TBDMS [62], triisopropylsilyloxymethyl (TOM) [63], 2-cyanoethyl (CE) [64], CEM [65], pivaloyloxymethyl (PivOM) [66], 4-(*N*-dichloroacetyl-*N*-methylamino)benzyloxymethyl (4-DCA-MABOM) [67], etc. (Figs. 3 and 5) [37].

BTT
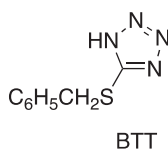
The efficiency of BTT toward 2′-*O*-TBDMS-protected ribonucleoside phosphoramidites is greater than those of not only TetH but also ETT [62]. The fact that this property of BTT is superior to that of TetH and ETT may arise from the acidity of BTT being higher than that of ETT or TetH.

In the solid-phase synthesis of 25 mer, 29 mer, and 42 mer RNA oligomers on a 1 μmol scale, in which a 0.25 M solution of BTT in acetonitrile and an eightfold excess of phosphoramidites are used to synthesize the solid-supported nucleotides, each coupling reaction is performed in 3 min with a yield of greater than 99% [62]. The synthesis of siRNA 21 mers is also carried out in a similar manner [68].
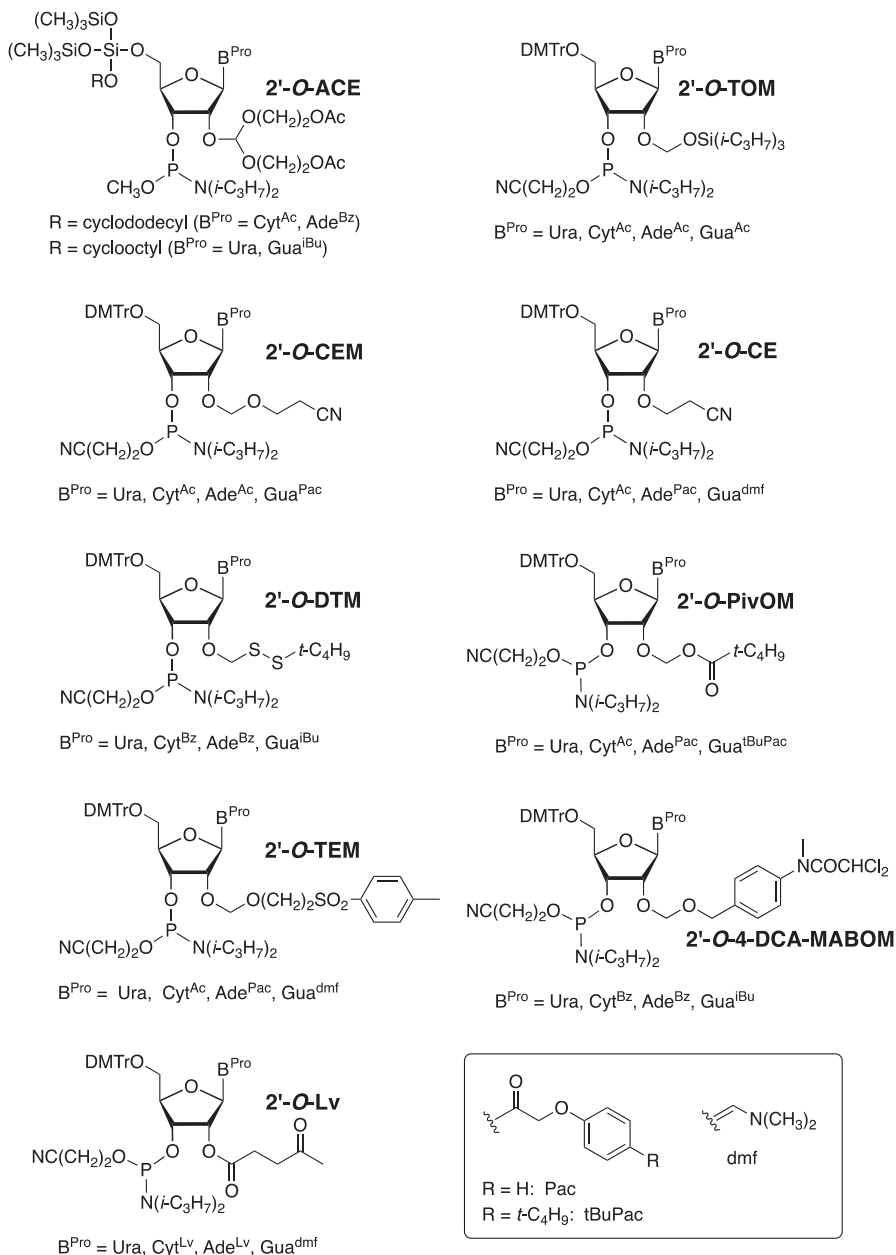
Fig. 5 Various 2′-O-protected ribonucleoside phosphoramidites that have been used so far

Table 1 Half-life of 5′-O-DMTr-protected nucleosides in a solution of TetH or ETT in acetonitrile at room temperature
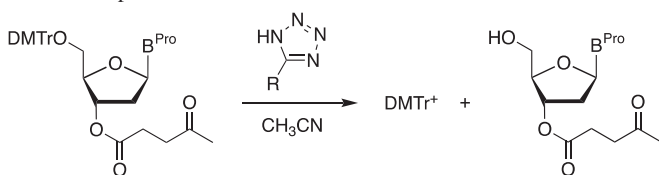
	Half-life ($t_{1/2}$) of the 5′-O-DMTr-protected nucleoside, h			
R in the tetrazole compound	B^{Pro} = Thy	B^{Pro} = Cyt^{Bz}	B^{Pro} = Ade^{Bz}	B^{Pro} = Gua^{iBu}
H	86	86	54	43
C_2H_5S	15	33	15	6.5

The reaction was carried out in a solution with a 0.1 M concentration of the 5′-O-DMTr-protected nucleoside and a 0.45 M concentration of the tetrazole promoter

BTT has a drawback of low solubility in acetonitrile, which is generally employed as the solvent for the coupling reaction. The concentration of a solution of BTT in acetonitrile that is easily prepared is 0.25 M. In such a low-concentration solution, the reaction is slow and requires a long time for completion. This situation is a major problem in the synthesis of long-chain oligonucleotides. The drawback is somewhat improved by the addition of a small amount of NMI in a similar way to the case using TetH, as described in Sect. 2.1.1. When NMI is added, it is possible to prepare a 0.3 M solution of BTT. In this more highly concentrated solution, the coupling efficiency increases somewhat compared with the case in a solution of lower concentration. The amount of NMI added strongly influences the yield of the coupling reaction. According to the results of the synthesis of an RNA 21 mer using 2′-O-TBDMS-protected nucleoside phosphoramidites on a 0.2 μmol scale, in which the coupling time is 2 min, the use of a 0.3 M BTT solution containing 0.5% NMI in acetonitrile gives the best result, producing the target oligomer in 56.9% yield [69]. The use of a higher concentration (for example, 2.5%) of the NMI solution rather decreases the yield of the product. Incidentally, in a synthesis using a 0.45 M solution of TetH in acetonitrile as the promoter for the construction of an internucleotide linkage, the desired product is obtained in a yield of only 3%.

In this reaction, NMI plays roles in not only preventing undesired detritylation but also promoting the coupling reaction; the latter role is discussed in Sect. 2.4 (Fig. 17) [46, 69].

BTT enables the synthesis of long-chain RNA oligomers, such as a 110 mer, using 2′-O-CEM-protected ribonucleoside phosphoramidites (Fig. 5). The synthesis is carried out on a 0.8 μmol scale using a 0.075 M solution of the phosphoramidite and a 0.25 M solution of BTT, where the coupling time is 2.5 min, to give the target oligomer in an overall yield of 5.5% [65].

2.1.4   5-[3,5-Bis(trifluoromethyl)phenyl]-1*H*-tetrazole (Activator 42)

5-[3,5-Bis(trifluoromethyl)phenyl]-1*H*-tetrazole, also known as Activator 42, is synthesized by the 1,3-dipolar cycloaddition of 3,5-bis(trifluoromethyl)benzonitrile and sodium azide assisted by zinc bromide (Fig. 6) [70]. This reagent is commercially available. This compound is highly soluble in acetonitrile (a 0.94 M solution is available), non-hygroscopic, and non-explosive.

Activator 42 is effective in the phosphoramidite reaction in both solution- and solid-phase syntheses. The reactivity of Activator 42 is higher than that of ETT in the solution phase. For example, Activator 42 completes the reaction shown in Fig. 7 three times faster than ETT.

Activator 42 enables the solid-phase synthesis of long-chain DNA oligomers up to 103 mer. The synthesis is achieved on a scale of 0.2–1.0 μmol using cyanoethyl phosphoramidites (Fig. 2, B^{Pro} = Thy, Cyt^{tBuPac}, Ade^{Bz}, Gua^{iBu}) and a 0.1 M solution of Activator 42 in acetonitrile. In this synthesis, the time required for the coupling reaction is 10–15 s. The average coupling yield in the synthesis of a 22 mer is higher than 99.0%. Activator 42 is also effective for the synthesis of RNA oligomers using 2′-*O*-TBDMS-protected phosphoramidites (Fig. 3, B^{Pro} = Ura, Cyt^{tBuPac}, Ade^{tBuPac}, Gua^{tBuPac}) [70].

The method using Activator 42 is applied in the synthesis of a three-way branched oligodeoxyribonucleotide 30 mer [71] and RNA sequences with the site-selective insertion of 5-carboxymethylaminomethyl-2-thiouridine [72].
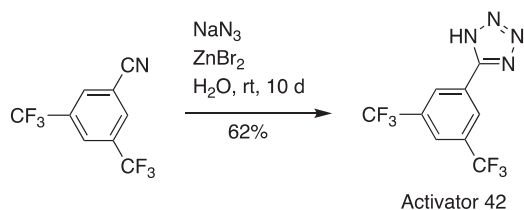
Fig. 6 Synthesis of 5-[3,5-bis(trifluoromethyl)phenyl]-1*H*-tetrazole (Activator 42)
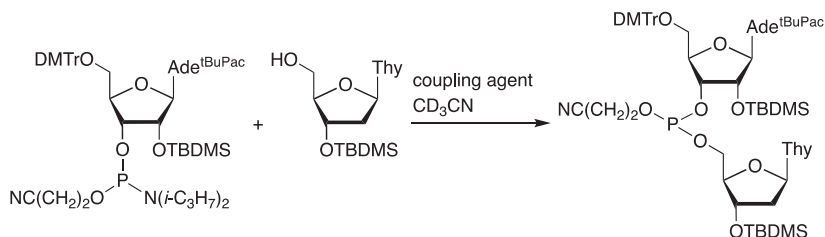
Fig. 7 Coupling reaction of a 2′-*O*-TBDMS-protected ribonucleoside phosphoramidite and a ribonucleoside with a free 5′-hydroxy group. tBuPac = 4-*tert*-butylphenoxyacetyl

Fig. 8 Synthesis of 4,5-dicyanoimidazole (DCI)
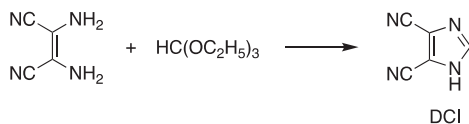
2.2 4,5-Dicyanoimidazole

4,5-Dicyanoimidazole (DCI), which is synthesized by the reaction of diaminomaleonitrile and ethyl orthoformate (Fig. 8), also acts as a useful coupling agent [73]. When compared with TetH, DCI is more reactive, less acidic, and more soluble in acetonitrile (its solubility in acetonitrile reaches 1.1 M [46]), and its conjugate base is more nucleophilic. Therefore, this coupling agent is sometimes used more advantageously than TetH or its derivatives described above.

DCI enables the synthesis of a 2′-fluoropyrimidine-ribopurine oligoribonucleotide 34 mer. The synthesis on a 1 mmol scale using 2 equiv. of 2′-O-TBDMS-protected nucleoside phosphoramidites or 2′-deoxy-2′-fluoronucleoside phosphoramidites and a 1 M solution of DCI in acetonitrile for the internucleotide bond formation reaction gives the desired product in 54% yield. In this synthesis, when a 0.45 M solution of TetH is used in place of the DCI solution, none of the desired oligomer is obtained [46]. A ribonucleotide 77 mer with the sequence of *Escherichia coli* tRNA[Asp] is similarly synthesized on a 1 μmol scale using DCI as the promoter for the construction of the internucleotide linkage [74]. DCI is also effective for the activation of ribonucleoside phosphoramidites such as **2** with a protecting group other than TBDMS on the 2′-hydroxy function. In fact, the method using DCI and **2** [R = 2-(2-nitrophenyl)propoxycarbonyl (NPPOC)] has enabled the preparation of poly rU and poly rA on a microarray [75].

R = DMTr, NPPOC
B^Pro = Ura, Cyt^Lv, Ade^Lv, Gua^dmf
2
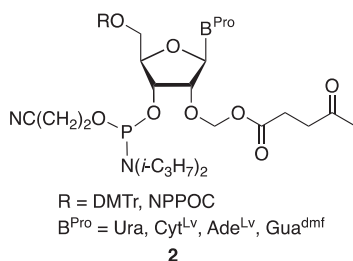
2.3 Carboxylic Acids

Although unfamiliar and little used so far, carboxylic acids have great potential as activating agents, because there are large number of analogs of carboxylic acids and thus the flexibility of choice is very high [76–78]. In addition, most carboxylic acids are commercially available at low cost.

The relationship between acidity and reactivity of carboxylic acids has been investigated and it has been found that, in general, stronger acids have higher reactivity. Among the carboxylic acids investigated so far, trichloroacetic acid (TCA) and 2,4-dinitrobenzoic acid (DNBA) have been the most effective. The order of reactivity of some representative carboxylic acids and TetH is as follows: TCA > trifluoroacetic acid (TFA) > dichloroacetic acid (DCA) > DNBA > TetH [78].

These coupling agents display good utility in both the solution-phase and solid-phase syntheses of deoxyribonucleotides (Fig. 9) [76–78]. In the solid-phase synthesis of a DNA 16 mer on a 0.2 μmol scale using cyanoethyl phosphoramidites as the building blocks and TCA as the activator, the coupling reaction proceeds for 15–30 s with an average coupling yield of 99% and thus affords the target compound in an overall yield of 88% [78]. A similar result is obtained by the use of DNBA (0.05 M), which completes the coupling reaction in 4 min, forming the internucleotide bond in 98–99% yield [76].

Carboxylic acid promoters also cause cleavage of the 5′-O-DMTr protecting groups of nucleosides to a substantial extent. For example, detritylation takes place at a rate of 0.2% in a 0.05 M solution of TCA in acetonitrile at room temperature during each coupling reaction. In a 0.05 M solution of DNBA in acetonitrile, the extent of the degradation of DMTr groups decreases to 0.01% [38, 76].

The mechanism of the condensation of a nucleoside and a nucleoside phosphoramidite promoted by DNBA has been elucidated on the basis of ^{31}P NMR spectral analysis. As shown in Fig. 10, first, the phosphoramidite undergoes protonation by DNBA, producing an N-protonated phosphoramidite and the carboxylate anion of
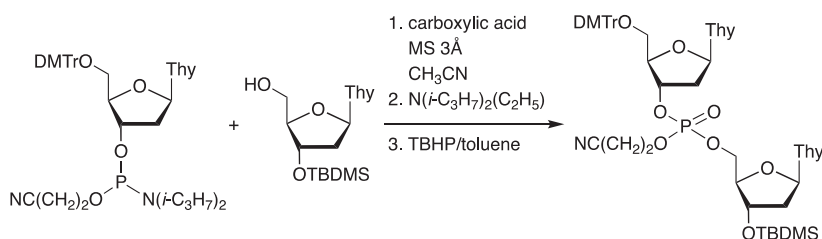
Fig. 9 Internucleotide bond formation reaction using a carboxylic acid as an activator of the phosphoramidite
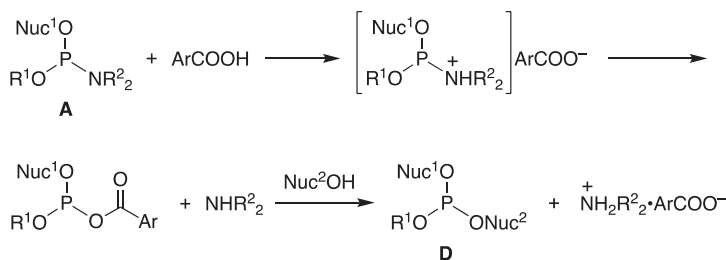
Fig. 10 Mechanism of 2,4-dinitrobenzoic acid-promoted condensation of a nucleoside and a nucleoside phosphoramidite. Ar = 2,4-dinitrophenyl

DNBA. Subsequently, these two products react to form a phosphorous/carboxylic mixed anhydride. Finally, this mixed anhydride reacts with a nucleoside with a free 5′-hydroxy group to afford the desired 3′-5′-linked dinucleoside phosphite [76, 78]. In this process, it is confirmed by the ^{31}P NMR spectrum that the mixed anhydride is present as the intermediate.

2.4 Acid/Azole Complexes

Salts of an acid with super-high acidity and an organic base with high nucleophilicity act as efficient activators of nucleoside phosphoramidites. Pyridinium tetrafluoroborate (PyTFB) is the first reported example of such a reagent [79]. Subsequently, a variety of salts of trifluoromethanesulfonic acid or perchloric acid and imidazole derivatives, namely, acid/azole complexes (HX/Az), have been developed. These include imidazolium trifluoromethanesulfonate (IMT), imidazolium perchlorate (IMP), 1-phenylimidazolium trifluoromethanesulfonate (*N*-PhIMT), benzimidazolium trifluoromethanesulfonate (BIT) [80, 81], saccharin 1-methylimidazole (SMI) [83, 84], and so on (Fig. 11). These acid/azole complexes, except for SMI, are readily obtained in high yields by mixing equal equivalents of the acid and the imidazole derivative in dichloromethane. SMI can be prepared from NMI and saccharin in acetonitrile. The acid/azole complexes, except for SMI, have high solubility in acetonitrile, which enables the preparation of a ≥0.4 M solution. The solubility of SMI seems to be slightly lower, but enables the preparation of a solution with a concentration of up to 0.25 M.

According to the results of control experiments (Fig. 12) [81], the reactivity of acid/azole complexes toward deoxyribonucleoside phosphoramidites is generally higher than that of other kinds of coupling agents, such as TetH, PyTFB, 2-bromo-4,5-dicyanoimidazole (BrDCI), and DCI. The relative reactivity of some representative promoters is summarized in Fig. 12 [81]. A similar tendency is observed towards a 2′-*O*-TBDMS-protected cyanoethyl phosphoramidite, as shown in Fig. 13 [64].

The acid/azole complex promoters can be applied in the synthesis of not only oligodeoxyribonucleotides but also oligoribonucleotides. For example, the solid-phase synthesis of a deoxyribonucleotide 20 mer using cyanoethyl phosphoramidites (Fig. 2, B^{Pro} = Thy, Cyt^{Ac}, Ade^{Pac}, Gua^{iPrPac}) and *N*-PhIMT as the promoter is achieved in an overall yield of 97.8% and therefore in an average coupling yield of 99.9%. *N*-PhIMT is also effective as promoter for the solid-phase synthesis of oligoribonucleotides using allyl phosphoramidites **5** (Fig. 14). Actually, a 20 mer is prepared in an overall yield of 78.8% and therefore in an average coupling yield of 98.8% [81].

The mechanism of the acid/azole salt-assisted coupling reaction has been studied by ^{31}P NMR spectral analysis of a model reaction using **3** as the nucleoside phosphoramidite, 3′-*O*-TBDMS-thymidine as the nucleoside with a free 5′-hydroxy group (Fig. 12), and IMP as the promoter. Figure 15 shows a pathway suggested by this study. First, the acid/azole complex (HX/Az) delivers a proton to the amidite **A**,
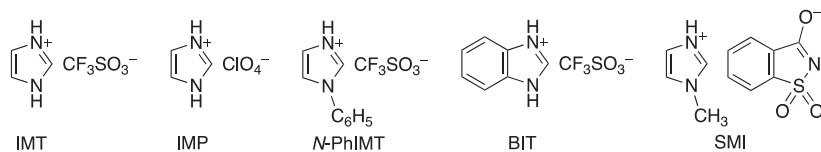
Fig. 11 Representative acid/azole complexes
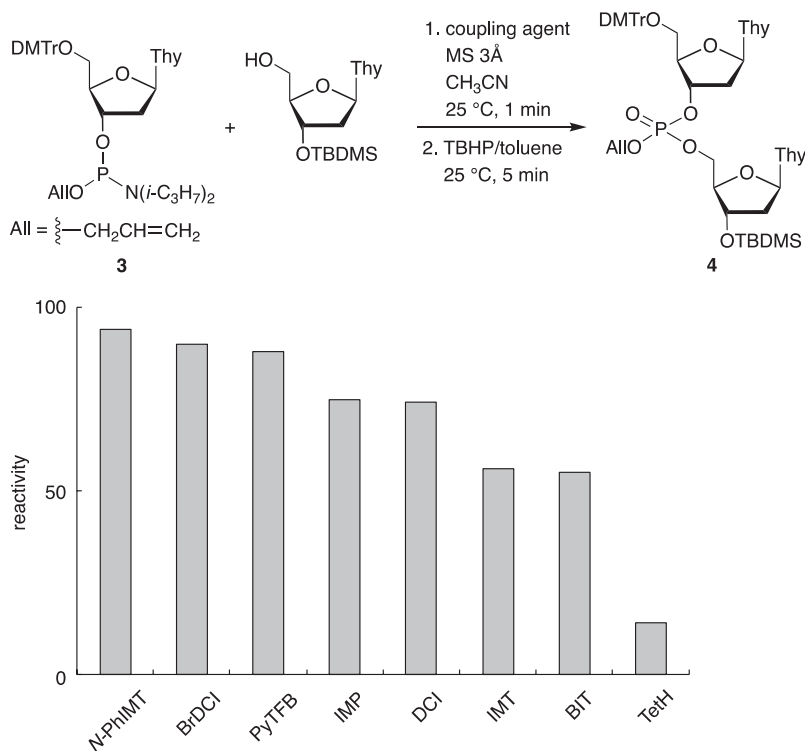
Fig. 12 Reactivity of some coupling agents estimated from the yield of the product **4** obtained by the reaction of the phosphoramidite **3** and 3′-*O*-TBDMS-thymidine for 5 min assisted by the promoter, followed by oxidation by TBHP

forming the *N*-protonated phosphoramidite species **E**. In this process, the free azole (Az) and the X⁻ anion (the conjugate base of HX) are also produced. Subsequently, Az attacks **E** in a nucleophilic manner to produce the phosphorazolide **F** with the release of diisopropylamine. Here the formation of **F** is confirmed by ^{31}P NMR analysis. Then, the reaction of **F** and the 5′-*O*-unprotected nucleoside (Nuc²OH) occurs to afford the phosphite triester **D**. In this process, it is suggested that the rate-determining reaction is the formation of the intermediate **F** [81].
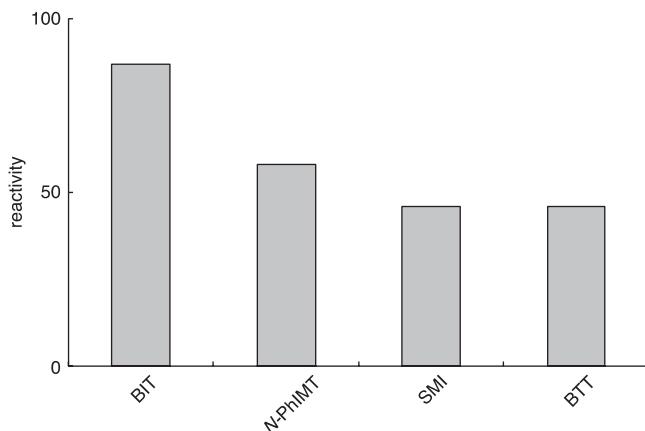
Fig. 13 Reactivity of some coupling agents estimated from the yield of the phosphite triester obtained by the reaction of a 2′-O-TBDMS-protected cyanoethyl phosphoramidite **1** (B^{Pro} = Ura) and 2′,3′-O,2-N-triacetylguanosine for 3 min
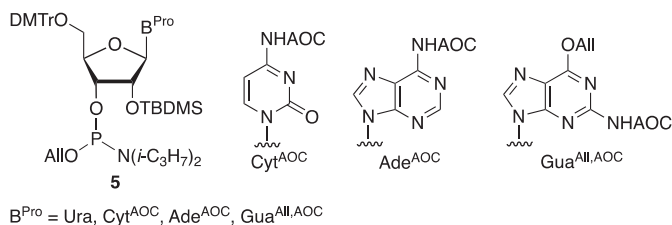
Fig. 14 Nucleoside phosphoramidite building blocks with allyl (All) and allyloxycarbonyl (AOC) protecting groups for the synthesis of RNA derivatives

Here, we would like to consider the reason why an acid/azole complex has higher reactivity than HX alone, such as TetH, in the condensation of a phosphoramidite and a nucleoside.

The reason may be clearly understood by comparing the mechanism of the reaction promoted by the HX/Az complex (Fig. 15) with that of the reaction promoted by HX (Fig. 16).

As mentioned above, in the reaction using HX alone as the promoter, the rate-determining step is nucleophilic substitution occurring between X^- and (Nuc^1O) $P(OR^1)(N^+HR^2_2)$ to form the intermediate $(Nuc^1O)P(OR^1)X$. Therefore, the rate of the reaction is roughly determined by the product of the concentrations of (Nuc^1O) $P(OR^1)(N^+HR^2_2)$ and X^- and the nucleophilicity of X^-. Accordingly, in order to obtain a high reaction rate, both concentrations, i.e., $[(Nuc^1O)P(OR^1)(N^+HR^2_2)]$ and $[X^-]$, should be high and the nucleophilicity of X^- should also be high. In other words, in order for HX to act as an excellent promoter, HX has to satisfy the follow-
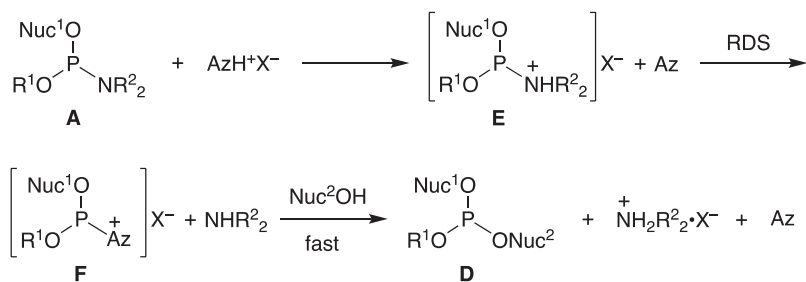
Fig. 15 Suggested mechanism of the coupling reaction of a nucleoside phosphoramidite and a nucleoside using an acid/azole complex as the promoter
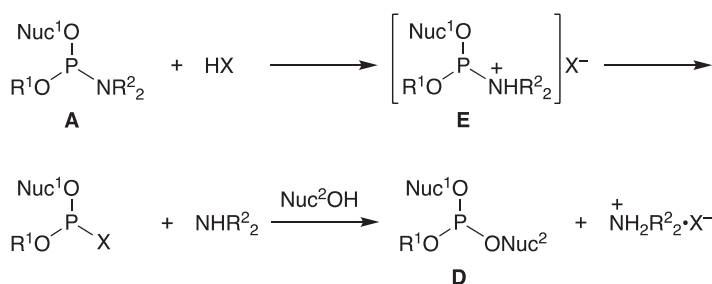
Fig. 16 Suggested mechanism of the coupling reaction of a nucleoside phosphoramidite and a nucleoside using an HX-type promoter

ing two requirements. One is that HX must be a strong acid and the other is that HX, after liberating H^+, must produce highly nucleophilic X^-. However, it is difficult for HX to satisfy these two requirements on its own, for the reasons explained below. The concentrations, $[(Nuc^1O)P(OR^1)(N^+HR^2_2)]$ and $[X^-]$, are affected by the acidity of HX, because both $(Nuc^1O)P(OR^1)(N^+HR^2_2)$ and X^- are generated by the delivery of H^+ from HX to the phosphoramidite (therefore $[(Nuc^1O)P(OR^1)(N^+HR^2_2)]$ and $[X^-]$ are theoretically equal). Thus, in order to obtain high concentrations of $(Nuc^1O)P(OR^1)(N^+HR^2_2)$ and X^-, HX should be a strong acid. However, when HX is a strong acid, the nucleophilicity of the conjugate base X^- inevitably decreases. Consequently, the reactivity of HX-type promoters is subject to limitations.

On the other hand, in the reaction promoted by an acid/azole complex HX/Az, the rate-determining step is the nucleophilic substitution of the azole Az, but not X^-, on $(Nuc^1O)P(OR^1)(N^+HR^2_2)$ to yield $(Nuc^1O)P(OR^1)Az^+$. Therefore, the rate of the reaction is determined by the strength of the nucleophilicity of Az, but not X^-, and the product of the concentrations of $(Nuc^1O)P(OR^1)(N^+HR^2_2)$ and Az, i.e., $[(Nuc^1O)P(OR^1)(N^+HR^2_2)]\cdot[Az]$. Here, the acidity of azolium salts is higher than or comparable to that of TetH [82] and the released azole from the azolium salt is more reactive than the tetrazolide anion toward the activated phosphoramidite [81]. In fact, this statement is supported by the *ab initio* calculation of proton dissociation ener-

gies (PDEs). This calculation indicates that acid/azole complexes, such as proton-ated compounds of imidazole, benzimidazole, and *N*-phenylimidazole, have PDEs in the range of ca. 234–240 kcal/mol, which are much lower than that of TetH (ca. 336 kcal/mol) [81]. Therefore, the reactants, $(Nuc^1O)P(OR^1)(N^+HR^2_2)$ and Az, are produced in higher concentrations in the reaction using the acid/azole complex than in the case using HX alone as the promoter.

It is of more importance that in the reaction promoted by the acid/azole complex, the species that acts as the nucleophile toward the intermediate $(Nuc^1O)P(OR^1)$ $(N^+HR^2_2)$ in the rate-determining step is Az, and not X^-, because the nucleophilicity of Az is higher than that of X^-. The nucleophilicity of most Az species is rather higher than that of the tetrazolide anion, Tet^-. This fact is experimentally confirmed by a competitive reaction using a mixture of one equivalent each of TetH, benzimid-azole, and diisopropylammonium tetrazolide $[N^+H_2(i\text{-}C_3H_7)_2 \cdot Tet^-]$ (Fig. 17). In this way, ^{31}P NMR monitoring has indicated that the phosphorobenzimidazolide **F′** is the sole product of this reaction and the phosphorotetrazolide is not formed at all [81].

As can be seen from the reaction mechanism, the acid/azole complex has the ability to both afford two rate-determining reactants, the protonated phosphorami-dite and the azole, in high concentrations and generate a nucleophile with high reactivity toward the protonated phosphoramidite species. As a result, the reactivity of the acid/azole complex becomes extremely high; in other words, higher than the reactivity of HX-type promoters.

SMI is an alternative acid/azole complex-type coupling agent. SMI acts as an activator for both deoxyribonucleoside and ribonucleoside phosphoramidites and is useful for the solid-phase synthesis of oligonucleotides on both CPG and rigid poly-styrene beads. According to reported results, the utility of this reagent is almost equal to that of TetH in the synthesis of DNA oligomers and better than that of ETT in the synthesis of RNA oligomers [83, 84].

On the basis of kinetic and spectral studies in acetonitrile, it is proposed that the coupling reaction promoted by SMI proceeds via the mechanism shown in Fig. 18. This reaction starts with protonation of the phosphoramidite by SMI to form $(Nuc^1O)P(OR^1)(N^+HR^2_2)$. Subsequently, this species reacts with the conjugate base of saccharin to give **G**. The production of **G** is confirmed by the ^{31}P NMR spectrum [85]. Finally, a substitution reaction occurs between **G** and the nucleoside with a
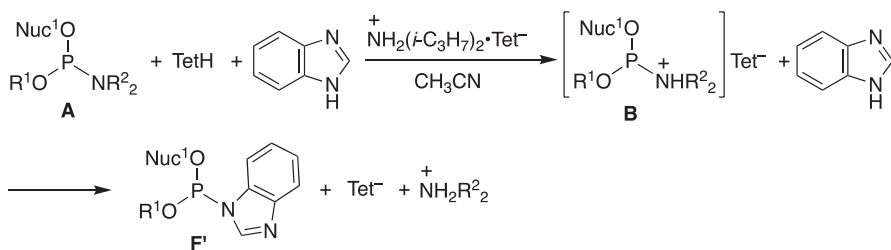
Fig. 17 Experiment to determine the difference in nucleophilicity between benzimidazole and the tetrazolide anion
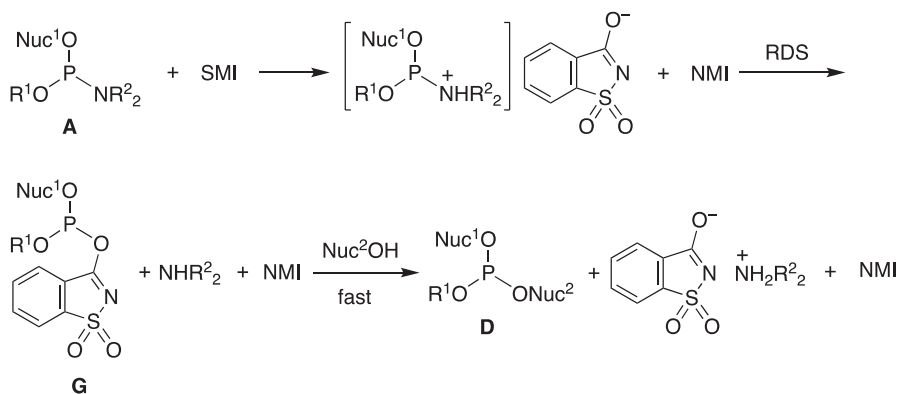
Fig. 18 Proposed mechanism of coupling reaction of a nucleoside phosphoramidite and a nucleoside promoted by SMI

free 5′-hydroxy group to afford a dinucleoside phosphite. Here, it is interesting that although SMI is an HX/Az complex similar to the above-mentioned BIT and IMP, the intermediates are different in the reaction promoted by SMI and in the reaction that uses BIT or IMP. The intermediate is **G** in the former reaction, but (Nuc^{1}O) P(OR^1)Az$^+$ in the latter reaction. The reason why such a difference is observed has not been well understood. In particular, in the reaction using SMI, the role of NMI is obscure. Because saccharin is a strong enough acid to cause detritylation of the 5′-protecting group of the phosphoramidite, NMI might play the role of a base that reduces the acidity of saccharin to prevent unwanted detritylation.

3 Conclusion

The chemical synthesis of DNA and RNA oligomers has so far played a major role and will continue to play a major role in the future in the life sciences that deal with nucleic acids. It is no exaggeration to say that there might not be the current significant progress in the life sciences without the chemical synthesis of nucleic acids. As mentioned in the Introduction, a variety of synthetic methods have been developed, such as the phosphodiester, phosphotriester, phosphite, phosphoramidite, and *H*-phosphonate methods. Among these, the phosphoramidite method is the most widely and frequently used at present.

In the phosphoramidite method, the key stage is the coupling reaction of a nucleoside 3′-phosphoramidite and a nucleoside with a free 5′-hydroxy group to form a dinucleoside phosphite with the assistance of a suitable coupling agent. Therefore, the invention of a useful coupling agent, in other words, an excellent activator of the phosphoramidite, is one of the most important factors in the phosphoramidite method. Ideally, the coupling agent should fulfill the following requirements [38, 70]: (1) easy and low-cost availability, (2) favorable properties for handling and

storage (being stable under usual conditions, non-explosive, nontoxic, and non-hygroscopic), (3) high solubility in acetonitrile, (4) high reactivity, giving high coupling yield, (5) low risk of decomposing the 5′-*O*-DMTr protecting group, (6) ability to be used in large-scale synthesis, and (7) ability to produce long-chain oligonucleotides in high yield. With the aim of the invention of such ideal promoters, extensive research has been carried out so far. As a result, a number of useful coupling agents have been developed, as described above. However, most of these do not perfectly fulfill all the requirements and are thus not ideal, although useful. For instance, TetH does not have sufficiently high reactivity, in particular toward ribonucleoside phosphoramidites, and sometimes does not provide a satisfactory yield in synthesis. ETT, BTT, and Activator 42 possess higher reactivity than TetH and are more useful than TetH for the synthesis of RNA oligomers, giving generally acceptable results. However, these promoters have a higher risk of cleaving the 5′-*O*-DMTr protecting group than TetH, because of their higher acidity. Carboxylic acids, such as TCA and DNBA, are an alternative class of promoters, but these promoters also have a rather high risk of decomposing the 5′-*O*-DMTr group. Acid/azole complexes may be the most effective coupling agents among the existing promoters, and some of these seem to be closest to the ideal promoter. However, the utility of most acid/azole complex reagents for large-scale synthesis has not been confirmed.

In conclusion, there are few coupling agents that perfectly satisfy all the requirements (1–7). Therefore, further efforts are necessary to invent the truly ideal coupling agent.

References

1. Beaucage SL, Iyer RP (1992) Advances in the synthesis of oligonucleotides by the phosphoramidite approach. Tetrahedron 48:2223–2311
2. Reese CB (2002) The chemical synthesis of oligo- and poly-nucleotides: a personal commentary. Tetrahedron 58:8893–8920
3. (2006) Chapter 4 synthesis of oligonucleotides. In: Blackburn GM, Gait MJ, Loakes D, Williams DM (eds) Nucleic acids in chemistry and biology, 3rd edn. The Royal Society of Chemistry, Cambridge, pp 143–166
4. Khorana HG (1968) Nucleic acid synthesis. Pure Appl Chem 17:349–381
5. Khorana HG (1968) Synthesis in the study of nucleic acids. Fourth Jubilee Lect Biochem J 109:709–725
6. Letsinger RL, Mahadevan V (1965) Oligonucleotide synthesis on a polymer support. J Am Chem Soc 87:3526–3527
7. Letsinger RL, Ogilvie KK (1967) Convenient method for stepwise synthesis of oligothymidylate derivatives in large-scale quantities. J Am Chem Soc 89:4801–4803
8. Reese CB (1978) The chemical synthesis of oligo- and poly-nucleotides by the phosphotriester approach. Tetrahedron 34:3143–3179
9. Letsinger RL, Finnan JL, Heavner GA, Lunsford WB (1975) Nucleotide chemistry. XX. Phosphite coupling procedure for generating internucleotide links. J Am Chem Soc 97:3278–3279
10. Letsinger RL, Lunsford WB (1976) Synthesis of thymidine oligonucleotides by phosphite triester intermediates. J Am Chem Soc 98:3655–3661

11. Beaucage SL, Caruthers MH (1981) Deoxynucleoside phosphoramidites–A new class of key intermediates for deoxypolynucleotide synthesis. Tetrahedron Lett 22:1859–1862

12. Caruthers MH (1985) Gene synthesis machines: DNA chemistry and its uses. Science 230:281–285

13. Caruthers MH (1991) Chemical synthesis of DNA and DNA analogs. Acc Chem Res 24:278–284

14. Beaucage SL, Caruthers MH (2001) Synthetic strategies and parameters involved in the synthesis of oligodeoxyribonucleotides according to the phosphoramidite method. In: Beaucage SL, Bergstrom DE, Glick GD, Jones RA (eds) Current protocols in nucleic acid chemistry. Wiley, New York, pp 3.3.1–3.3.20

15. Caruthers MH (2013) Chemical synthesis of DNA, RNA, and their analogues. Chem Int 35:8–11

16. Corby NS, Kenner GW, Todd AR (1952) 704. Nucleotides. Part XVI. Ribonucleoside-5′ phosphites. A new method for the preparation of mixed secondary phosphites. J Chem Soc:3669–3675

17. Hall RH, Todd A, Webb RF (1957) 644. Nucleotides. Part XLI. Mixed anhydrides as intermediates in the synthesis of dinucleoside phosphates. J Chem Soc:3291–3296

18. Froehler BC, Ng PG, Matteucci MD (1986) Synthesis of DNA via deoxynudeoside H-phosphonate intermediates. Nucleic Acids Res 14:5399–5407

19. Strömberg R, Stawinski J (2001) Synthesis of oligodeoxyribo- and oligoribonucleotides according to the *H*-phosphonate method. In: Beaucage SL, Bergstrom DE, Glick GD, Jones RA (eds) Current protocols in nucleic acid chemistry. Wiley, New York, pp 3.4.1–3.4.15

20. Sanghvi YS (2000) Large-scale oligonucleotide synthesis. Org Proc Res Dev 4:168–169

21. Dorsett Y, Tuschl T (2004) siRNAs: applications in functional genomics and potential as therapeutics. Nat Rev Drug Discov 3:318–329

22. (2006) Chapter 5 nucleic acids in biotechnology. In: Blackburn GM, Gait MJ, Loakes D, Williams DM (eds) Nucleic acids in chemistry and biology, 3rd edn. The Royal Society of Chemistry, Cambridge, pp 167–208

23. Keefe AD, Pai S, Ellington A (2010) Aptamers as therapeutics. Nat Rev Drug Discov 9:537–550

24. Hughes RA, Miklos AE, Ellington AD (2011) Gene synthesis: methods and applications. Methods Enzymol 498:277–309

25. Kosuri S, Church GM (2014) Large-scale de novo DNA synthesis: technologies and applications. Nat Meth 11:499–507

26. Dickey DD, Giangrande PH (2016) Oligonucleotide aptamers: a next-generation technology for the capture and detection of circulating tumor cells. Methods 97:94–103

27. Hyodo M, Hayakawa Y (2004) An improved method for synthesizing cyclic bis(3′–5′)diguanylic acid (c-di-GMP). Bull Chem Soc Jpn 77:2089–2093

28. Hyodo M, Sato Y, Hayakawa Y (2006) Synthesis of cyclic bis(3′-5′)diguanylic acid (c-di-GMP) analogs. Tetrahedron 62:3089–3094

29. Hyodo M, Hayakawa Y (2008) Synthesis, chemical properties and biological activities of cyclic bis(3′–5′)diguanylic acid (c-di-GMP) and its analogues. In: Modified nucleosides. Wiley-VCH, pp 343–363

30. Schwede F, Genieser H-G, Rentsch A (2017) The chemistry of the noncanonical cyclic dinucleotide 2′3′-cGAMP and its analogs. In: Seifert R (ed) Non-canonical cyclic nucleotides. Springer, Cham, pp 359–384

31. Hayakawa Y, Uchiyama M, Noyori R (1986) Nonaqueous oxidation of nucleoside phosphites to the phosphates. Tetrahedron Lett 27:4191–4194

32. Wincott FE (2001) Strategies for oligoribonucleotide synthesis according to the phosphoramidite method. In: Beaucage SL, Bergstrom DE, Glick GD, Jones RA (eds) Current protocols in nucleic acid chemistry. Wiley, New York, pp 3.5.1–3.5.12

33. Bellon L (2001) Oligoribonucleotides with 2′-*O*-(*tert*-butyldimethylsilyl) groups. In: Beaucage SL, Bergstrom DE, Glick GD, Jones RA (eds) Current protocols in nucleic acid chemistry. Wiley, New York, pp 3.6.1–3.6.13

34. Hayakawa Y (2001) Toward an ideal synthesis of oligonucleotides: development of a novel phosphoramidite method with high capability. Bull Chem Soc Jpn 74:1547–1565
35. Tsukamoto M, Hayakawa Y (2005) Strategies useful for the chemical synthesis of oligonucle-otides and related compounds. In: Atta-Ur-Rahman, Hayakawa Y (eds) Frontiers in organic chemistry, vol 1. Bentham, Hilversum, pp 3–40
36. (2007) The Glen report 19(2). http://www.glenresearch.com/GlenReports/GR19-2CONT.html
37. Höbartner C, Wachowius F (2010) Chemical synthesis of modified RNA. In: Mayer G (ed) The chemical biology of nucleic acids. Wiley, Chichester, pp 1–37
38. Wei X (2013) Coupling activators for the oligonucleotide synthesis via phosphoramidite approach. Tetrahedron 69:3615–3637
39. Ohkubo A, Seio K, Sekine M (2006) DNA synthesis without base protection using the phos-phoramidite approach. In: Beaucage SL, Bergstrom DE, Herdewijn P, Matsuda A (eds) Current protocols in nucleic acid chemistry. Wiley, Hoboken, pp 3.15.1–3.15.22
40. Hayakawa Y, Kawai R, Kataoka M (2001) Nucleotide synthesis via methods without nucleoside-base protection. Eur J Pharm Sci 13:5–16
41. Benson FR (1947) The chemistry of the tetrazoles. Chem Rev 41:1–61
42. (2010) The Glen report 22(1). http://www.glenresearch.com/GlenReports/GR22-1CONT.html
43. Wang Z, Olsen P, Ravikumar VT (2007) A novel universal linker for efficient synthesis of phosphorothioate oligonucleotides. Nucleosides Nucleotides Nucleic Acids 26:259–269
44. LeProust EM, Peck BJ, Spirin K, McCuen HB, Moore B, Namsaraev E, Caruthers MH (2010) Synthesis of high-quality libraries of long (150mer) oligonucleotides by a novel depurination controlled process. Nucleic Acids Res 38:2522–2540
45. Dellinger DJ, Monfregola L, Caruthers M, Roy M (2015) US Patent 0,315,227 A1
46. Vargeese C, Carter J, Yegge J, Krivjansky S, Settle A, Kropp E, Peterson K, Pieken W (1998) Efficient activation of nucleoside phosphoramidites with 4,5-dicyanoimidazole during oligo-nucleotide synthesis. Nucleic Acids Res 26:1046–1050
47. Scaringe SA, Francklyn C, Usman N (1990) Chemical synthesis of biologically active oligori-bonucleotides using β-cyanoethyl protected ribonucleoside phosphoramidites. Nucleic Acids Res 18:5433–5441
48. Wincott F, DiRenzo A, Shaffer C, Grimm S, Tracz D, Workman C, Sweedler D, Gonzalez C, Scaringe S, Usman N (1995) Synthesis, deprotection, analysis and purification of RNA and ribosomes. Nucleic Acids Res 23:2677–2684
49. Dahl BH, Nielsen J, Dahl O (1987) Mechanistic studies on the phosphoramidite coupling reac-tion in oligonucleotide synthesis. I. Evidence for nucleophilic catalysis by tetrazole and rate variations with the phosphorus substituents. Nucleic Acids Res 15:1729–1743
50. Berner S, Mühlegger K, Seliger H (1989) Studies on the role of tetrazole in the activation of phosphoramidites. Nucleic Acids Res 17:853–864
51. McBride LJ, Caruthers MH (1983) An investigation of several deoxynucleoside phosphorami-dites useful for synthesizing deoxyoligonucleotides. Tetrahedron Lett 24:245–248
52. Pon RT, Damha MJ, Ogilvie KK (1985) Modification of guanine bases by nucleoside phos-phoramidite reagents during the solid phase synthesis of oligonucleotides. Nucleic Acids Res 13:6447–6465
53. Lieber E, Enkoji T (1961) Synthesis and properties of 5-(substituted) mercaptotetrazoles. J Org Chem 26:4472–4479
54. LeBlanc BW, Jursic BS (1998) Preparation of 5-alkylthio and 5-arylthiotetrazoles from thio-cyanates using phase transfer catalysis. Synth Commun 28:3591–3599
55. Wright P, Lloyd D, Rapp W, Andrus A (1993) Large scale synthesis of oligonucleotides via phosphoramidite nucleosides and a high-loaded polystyrene support. Tetrahedron Lett 34:3373–3376
56. Scaringe SA, Wincott FE, Caruthers MH (1998) Novel RNA synthesis method using 5′-O-silyl-2′-O-orthoester protecting groups. J Am Chem Soc 120:11820–11821
57. Ohgi T, Masutomi Y, Ishiyama K, Kitagawa H, Shiba Y, Yano J (2005) A new RNA synthetic method with a 2′-O-(2-cyanoethoxymethyl) protecting group. Org Lett 7:3477–3480

58. Semenyuk A, Földesi A, Johansson T, Estmer-Nilsson C, Blomgren P, Brännvall M, Kirsebom LA, Kwiatkowski M (2006) Synthesis of RNA using 2′-*O*-DTM protection. J Am Chem Soc 128:12356–12357

59. Zhou C, Honcharenko D, Chattopadhyaya J (2007) 2-(4-Tolylsulfonyl)ethoxymethyl (TEM)-a new 2′-OH protecting group for solid-supported RNA synthesis. Org Biomol Chem 5:333–343

60. Lackey JG, Sabatino D, Damha MJ (2007) Solid-phase synthesis and on-column deprotection of RNA from 2′- (and 3′-) *O*-levulinated (Lv) ribonucleoside monomers. Org Lett 9:789–792

61. Krotz AH, Klopchin PG, Walker KL, Srivatsa GS, Cole DL, Ravikumar VT (1997) On the formation of longmers in phosphorothioate oligodeoxyribonucleotide synthesis. Tetrahedron Lett 38:3875–3878

62. Welz R, Müller S (2002) 5-(Benzylmercapto)-1*H*-tetrazole as activator for 2′-*O*-TBDMS phosphoramidite building blocks in RNA synthesis. Tetrahedron Lett 43:795–797

63. Wu X, Pitsch S (1998) Synthesis and pairing properties of oligoribonucleotide analogues containing a metal-binding site attached to β-D-allofuranosyl cytosine. Nucleic Acids Res 26:4315–4323

64. Saneyoshi H, Ando K, Seio K, Sekine M (2007) Chemical synthesis of RNA via 2′-*O*-cyanoethylated intermediates. Tetrahedron 63:11195–11203

65. Shiba Y, Masuda H, Watanabe N, Ego T, Takagaki K, Ishiyama K, Ohgi T, Yano J (2007) Chemical synthesis of a very long oligoribonucleotide with 2-cyanoethoxymethyl (CEM) as the 2′-*O*-protecting group: structural identification and biological activity of a synthetic 110mer precursor-microRNA candidate. Nucleic Acids Res 35:3287–3296

66. Lavergne T, Bertrand JR, Vasseur JJ, Debart F (2008) A base-labile group for 2′-OH protection of ribonucleosides: a major challenge for RNA synthesis. Chem Eur J 14:9135–9138

67. Cieślak J, Grajkowski A, Kauffman JS, Duff RJ, Beaucage SL (2008) The 4-(*N*-dichloroacetyl-*N*-methylamino)benzyloxymethyl group for 2′-hydroxyl protection of ribonucleosides in the solid-phase synthesis of oligoribonucleotides. J Org Chem 73:2774–2783

68. Gaglione M, Potenza N, Di Fabio G, Romanucci V, Mosca N, Russo A, Novellino E, Cosconati S, Messere A (2013) Tuning RNA interference by enhancing siRNA/PAZ recognition. ACS Med Chem Lett 4:75–78

69. Reddy KS (2008) US Patent 7,339,052 B2

70. Wolter A, Leuck M (2006) US Patent 0,247,431 A1

71. Utagawa E, Ohkubo A, Sekine M, Seio K (2007) Synthesis of branched oligonucleotides with three different Sequences using an oxidatively removable tritylthio group. J Org Chem 72:8259–8266

72. Leszczynska G, Pieta J, Wozniak K, Malkiewicz A (2014) Site-selected incorporation of 5-carboxymethylaminomethyl(-2-thio)uridine into RNA sequences by phosphoramidite chemistry. Org Biomol Chem 12:1052–1056

73. Woodward DW (1950) US Patent 2,534,331

74. Persson T, Kutzke U, Busch S, Held R, Hartmann RK (2001) Chemical synthesis and biological investigation of a 77-mer oligoribonucleotide with a sequence corresponding to *E. coli* tRNA[Asp]. Bioorg Med Chem 9:51–56

75. Lackey JG, Mitra D, Somoza MM, Cerrina F, Damha MJ (2009) Acetal levulinyl ester (ALE) groups for 2′-hydroxyl protection of ribonucleosides in the synthesis of oligoribonucleotides on glass and microarrays. J Am Chem Soc 131:8496–8502

76. Reddy MP, Farooqui F (1996) US Patent 5,574,146

77. Tsukamoto M, Nurminen EJ, Iwase T, Kataoka M, Hayakawa Y (2004) Internucleotide-linkage formation via the phosphoramidite method using a carboxylic acid as a promoter. Nucleic Acids Symp Ser 48:25–26

78. Hayakawa Y, Iwase T, Nurminen EJ, Tsukamoto M, Kataoka M (2005) Carboxylic acids as promoters for internucleotide-bond formation via condensation of a nucleoside phosphoramidite and a nucleoside: relationship between the acidity and the activity of the promoter. Tetrahedron 61:2203–2209

79. Brill WKD, Nielsen J, Caruthers MH (1991) Synthesis of deoxydinucleoside phosphorodithio-ates. J Am Chem Soc 113:3972–3980
80. Hayakawa Y, Kataoka M, Noyori R (1996) Benzimidazolium triflate as an efficient promoter for nucleotide synthesis via the phosphoramidite method. J Org Chem 61:7996–7997
81. Hayakawa Y, Kawai R, Hirata A, Sugimoto J-i, Kataoka M, Sakakura A, Hirose M, Noyori R (2001) Acid/azole complexes as highly effective promoters in the synthesis of DNA and RNA oligomers via the phosphoramidite method. J Am Chem Soc 123:8165–8176
82. Nurminen E, Lönnberg H (2004) Mechanisms of the substitution reactions of phosphorami-dites and their congeners. J Phys Org Chem 17:1–17
83. Sinha ND, Zedalis WE, Miranda GK (2003) WO Patent 004,512 A1
84. Sinha ND, Foster P, Kuchimanchi SN, Miranda G, Shaikh S, Michaud D (2007) Highly effec-tive non-explosive activators based on saccharin for the synthesis of oligonucleotides and phosphoramidites. Nucleosides Nucleotides Nucleic Acids 26:1615–1618
85. Russell MA, Laws AP, Atherton JH, Page MI (2008) The mechanism of the phosphoramidite synthesis of polynucleotides. Org Biomol Chem 6:3270–3275

Recent Development of Chemical Synthesis of RNA

Mitsuo Sekine

Abstract Recent studies on the chemical synthesis of RNA and related derivatives are reviewed. In particular, a variety of new 2′-hydroxyl protecting groups that are developed during the past decade are described and compared with the conventional ones from the organochemical point of view. Great improvements in the coupling efficiency and suppression of side reactions during RNA synthesis cycles are described in great detail. The methods and associated problems for constructing the key synthetic intermediates, i.e., 2′-*O*-protected ribonucleoside 3′-phosphoramidite building blocks, are also discussed.

Keywords Chemical synthesis of RNA · Automated synthesis · 2′-hydroxyl protecting group · Modified RNA · Solid-phase synthesis · Phosphoramidite approach · siRNA · Antisense RNA · Gene therapy

1 Introduction

During the past decade, potential functionalities of short-length RNAs are unveiled, such as small interfering RNA [1–6], micro RNA [7–10], short hairpin RNA [11, 12], and noncoding RNA (ncRNA) [13–17]. A series of new methods for the chemical synthesis of RNA are reported as well [18–23]. In the 1980s, a basic strategy for synthesizing DNA oligomers, i.e., the phosphoramidite approach, was established by Caruthers and Beaucage [24–26]. This approach is proven to be so reliable that it can be well applied to the automatic synthesis of DNA fragments using synthesizers. The present requirement in molecular biology also expands toward the stage of synthesizing oligodeoxynucleotides having more than 100 base length [27]. Recently, the full size of a naturally occurring genome of *Mycoplasma genitalium* has been successfully synthesized by using chemical and enzymatic strategies, and the custom synthesis of 50 mer-level DNA fragments and DNA ligations among the medium-size DNA fragments have been used [28]. On the other hand, the synthetic

M. Sekine (✉)
Tokyo Institute of Technology, Yokohama, Kanagawa, Japan

method of RNA is essentially based on the principle of DNA synthesis. The only difference between DNA and RNA chemical syntheses is the additional protection of the 2′-hydroxyl group of RNA. Such difference, however, makes RNA very challenging to be synthesized. The increased demand that long-length RNA oligomers have to be commercially supplied prompts several research groups to restart the study on the chemical synthesis of RNA using the latest organic chemistry. In this review, I summarize the recent papers focusing on the chemical synthesis of RNA, which appears like "Renaissance of RNA chemical synthesis."

2   Basic Principle of Solid-Phase Synthesis of DNA/RNA in Phosphoramidite Approach

The solid-phase method is unambiguously the best choice for the automated synthesis of DNA/RNA, which enables the continuous chain elongation using a repeated cycle of four-step reactions on insoluble polymer supports. As shown in Fig. 1, this synthetic cycle involves (1) detritylation, (2) condensation with a monomer, (3) oxidation of phosphite triester intermediates, and (4) capping reaction to avoid contamination of truncated sequences.

Attached to polymer support, the unmasked 5′-hydroxyl group of a 3′-terminal nucleoside is generated at the first step of detritylation. At the second step, the condensation of the 5′-hydroxyl group is conducted by using an activated nucleoside
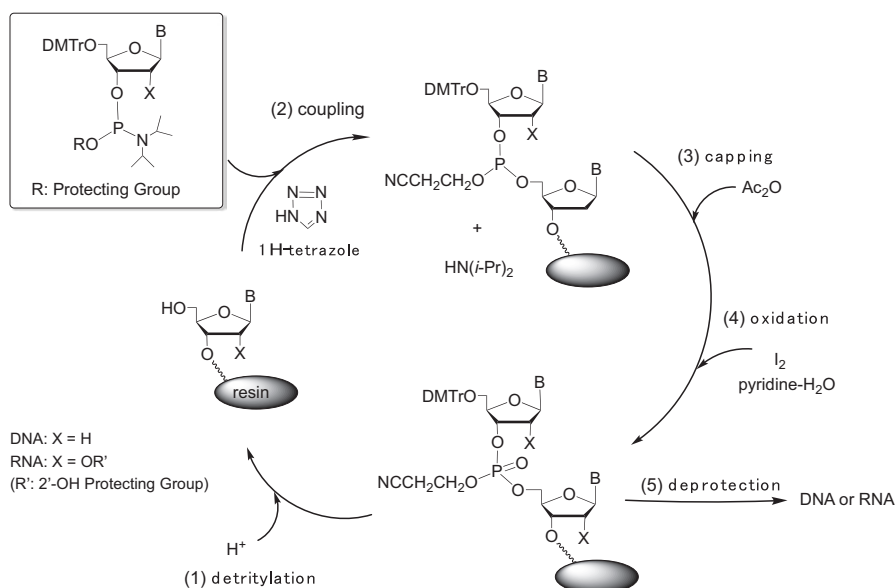
Fig. 1 Synthesis cycle of DNA and RNA

3′-phosphoramidite in the presence of an activator of the P–N bond of the amidite. At the third step, the unreacted 5′-hydroxyl group is masked by the acetylation to avoid further condensation from this site. At the last step, oxidation of the phosphite triester is performed using I_2. After the synthetic cycle is finished, the growing chain is released using ammonia for the cleavage of the linker between the oligomer and its support. Meanwhile, the base protecting groups of acyl type and the phosphate protecting groups of cyanoethyl type are removed. The resulting oligonucleotide masked by a DMTr group [29] at the 5′-terminal site is purified by C18 cartridge column and adsorbed on the cartridge. Finally, the DMTr group is removed by treatment with an acid from the cartridge. The desired oligomer is obtained by elution using aqueous acetonitrile and further purified by HPLC. The base-labile protecting groups, such as phenoxyacetyl [30], acetyl, and 4-*tert*-butylphenoxyacetyl [31], are used for protecting the base parts to decrease the total time required for the full deprotection. The most standard activator is 1*H*-tetrazole in the usual case [28]. More effective activators also have been developed, such as benzylthio-1*H*-tetrazole [32], ethylthio-1*H*-tetrazole [33], 4,5-dicyanoimidazole [34], 5-[3,5-bis(trifluoromethyl)phenyl]-1*H*-tetrazole [35], and benzimidazolium triflate [36].

3 Current RNA Synthesis Using TBDMS as 2′-Hydroxyl Protecting Group

Currently, the use of the *tert*-butyldimethylsilyl (TBDMS) group as the 2′-hydroxyl protecting group is the widely reported method for synthesizing RNA. The TBDMS group was first developed by Ogilvie [37]. The synthesis of the appropriate *N*-protected 5′-*O*-(4,4′-dimethoxytrityl)-2′-*O*-TBDMS-ribonucleoside derivatives was reported via the controlled reactions between *N*-protected 5′-*O*-(4,4′-dimethoxytrityl)ribonucleoside derivatives and *t*-butyldimethylsilyl chloride in the presence of silver nitrate. Fortunately, the 2′-*O*-TBDMS product can be separated from the 3′-*O*-TBDMS product by silica gel column chromatography because the former is eluted faster than the latter. We used this synthetic protocol to synthesize more practically ribonucleoside monomer of 3′-phosphoramidite building blocks than the monomer units previously used [38–40].

The TBDMS group is well known to be removed by treatment with 1 M Bu$_4$NF in THF [41]. The additional protection of the 2′-hydroxyl group using the TBDMS group in RNA synthesis requires the sufficient stability of this protecting group upon the necessary ammonia treatment for removing the base protecting groups at the last stage [39]. The cleavage of the 3′–5′ phosphodiester bond might occur when the 2′-*O*-TBDMS group is partially eliminated from the *N*-protected RNA species. The once generated 2′-OH group might attack the phosphorus atom, leading to the formation of a 2′,3′-cyclic phosphate ring as well as the break of the phosphorus atom and the downstream 5′-oxygen [42]. To avoid this side reaction, Usman found the optimized conditions that can suppress the elimination of the TBDMS group by
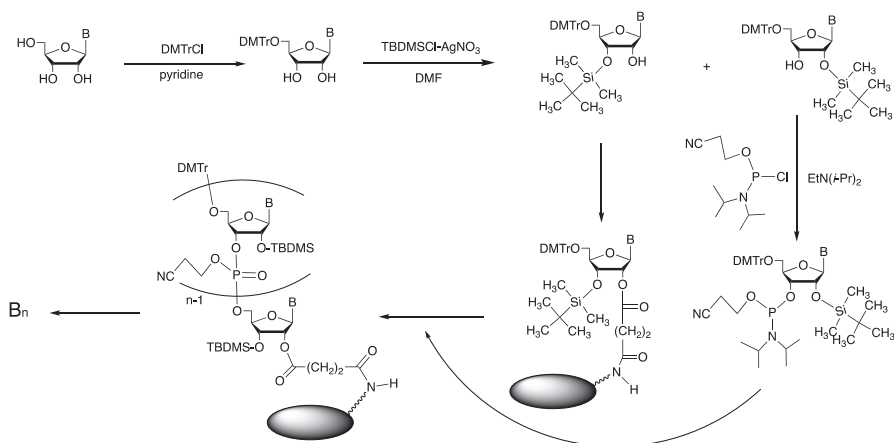
Fig. 2 RNA synthesis using the TBDMS group

the use of ammonia in EtOH [39]. In recent years, to avoid the complete phospho-diester linkage break, more base-labile *N*-protecting groups, such as phenoxyacetyl and acetyl, have been used to accelerate the deprotection of the *N*-protecting group under these conditions. Thus, oligoribonucleotides have been supplied to users by custom synthesis companies (Fig. 2).

4   RNA Synthesis Using Acid-Labile 2′-Hydroxyl Protecting Groups

As the 2′-hydroxyl protecting groups, acid-labile tetrahydrofuran-2-yl [43, 44] and tetrahydropyran-2-yl [45, 46] are also available. However, the selection of the DMTr group as the 5′-protecting group limits such acetal type of protecting groups because the delicate selective deprotection of the DMTr group is needed for further chain elongation without damaging the THP and THF groups. Via using these protecting groups, moderate-length RNA oligomers are synthesized, such as the 24 RNA fragments of Hop-Stunt viroid reported by us [43]. Other methods using a levulinyl group as the hydradine-labile 5′-protecting group are also reported in the phosphoramidite approach [47] (Fig. 3).

As an acid-labile 2′-OH protecting group, Reese reported that Cpep was removed at pH 3.8. Cpep became more stable at pH 0.5 because of the electron-withdrawing effect of the completely protonated amino group on the 2′-oxygen [48]. The inherent property of this protecting group greatly varies its stability at different pH values, allowing the use of the DMTr group as the 5′-hydroxyl group. This kind of pH-dependent removable protecting groups has extensively been developed by Reese [49, 50]. Among them, the Cpep group is a more suitable protecting group, which has the largest difference in stability between removal of the DMTr group
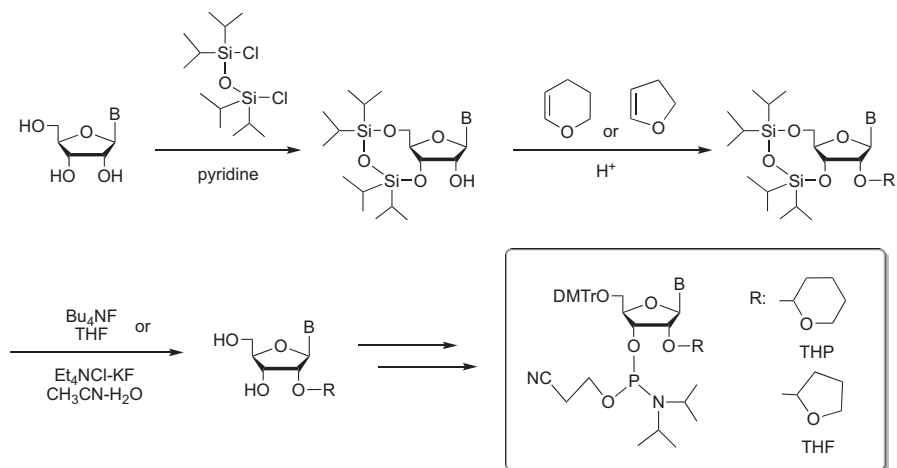
Fig. 3 RNA synthesis using acid-labile THP and THF protecting groups
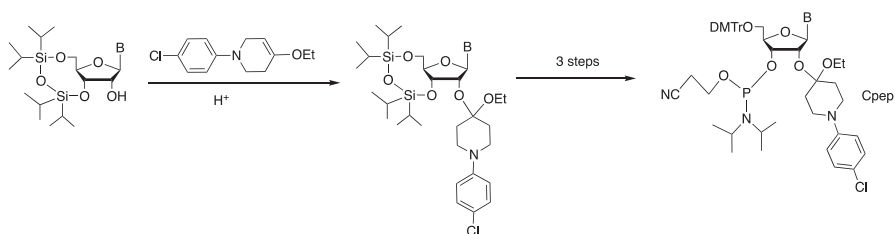
Fig. 4 RNA synthesis using the pH-dependent removable Cpep group

and final deprotection involving the 2′-OH protecting group. The tertiary carbon of the Cpep group is the only drawback as far as the condensation efficiency is concerned because the steric bulkiness around the 2′-protecting group directly affects the condensation (Fig. 4).

In 1998, Caruthers reported a new type of RNA monomer building blocks, which have a silicate SIL group as the 5′-hydroxyl protecting group and an orthoacetal-type group of bis(2-acetoxyethoxy)methyl (ACE) as the 2′-hydroxyl protecting group [51]. The former can be removed by 1.1 M HF and 1.6 M Et₃N in DMF for 90 s. The ACE group can be removed by a two-step reaction. The first step was the deacylation required for removing the base protecting groups. During the deacylation, the acetyl groups of the ACE group were simultaneously removed. The resulting 2′-O-bis(2-hydroxyethoxy)methyl orthoester, which can be removed at pH 3.0 at 55 °C for 10 min, is ten times more acid-labile than the ACE orthoester. Because the orthoester was hydrolyzed, the formyl group attached to the 2′-oxygen is completely removed via changing the pH of the acidic solution to 7.7–8.0, followed by keeping it at 55 °C for 10 min.
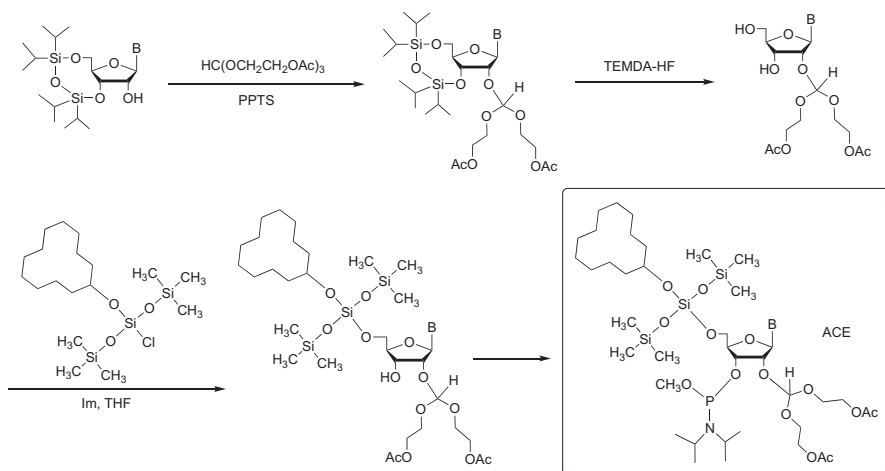
Fig. 5 RNA synthesis using the ACE group capable of a two-step procedure

The new combination of the two protecting groups enables us to synthesize oligoribonucleotides without using any acidic conditions, such as 1% trifluoroacetic acid or 3% trichloroacetic acid in CH_2Cl_2. The acidic condition is usually required for removing the conventional DMTr group in the standard RNA synthesis. However, this method is limited to the use of the methyl group for protecting the phosphate protecting group. The methyl group can be removed by treatment with 1 M disodium 2-carbamoyl-2-cyanoethylene-1,1-dithiolate in DMF for 30 min [52]. The conditions used for this approach involve (1) coupling: 30 equiv. of ethylthio-1*H*-tetrazole, 15 equiv. of phosphoramidite, 90 s and (2) capping: *N*-methylimidazole-acetic anhydride, 30 s; oxidation: 3 M *t*-BuOH/toluene, 40 s. The coupling yields were achieved with an efficacy of more than 99% within 90 s. The synthesis cycle required 11.5 min on polystyrene supports loaded with an appropriate nucleoside (5–7 µmol/g) via a succinate linkage. The RNA monomer building blocks are now commercially available. Using this method, an RNA 36 mer of UCUCCAUCUGAUGAGGCCGAAAGGCCGAAAAUCCCC is synthesized (Fig. 5).

5   RNA Synthesis Using 2′-Protecting Groups Having an Acetal Skeleton

5.1   *(2-Nitrobenzyl)oxymethyl (NBOM) Group*

In 1992, Gough reported a method for synthesizing RNA using 2-*O*-(2-nitrobenzyloxymethyl)-protected monomer building blocks [53–55]. The monomer units were synthesized using the reaction between 2′,3′-*O*-(dibutylstannylene)ribonucleoside derivatives and 2-nitrobenzyl chloromethyl ether. For example, this reaction starting from uridine finally gave the 2′-*O*-(2-nitrobenzyloxymethyl)
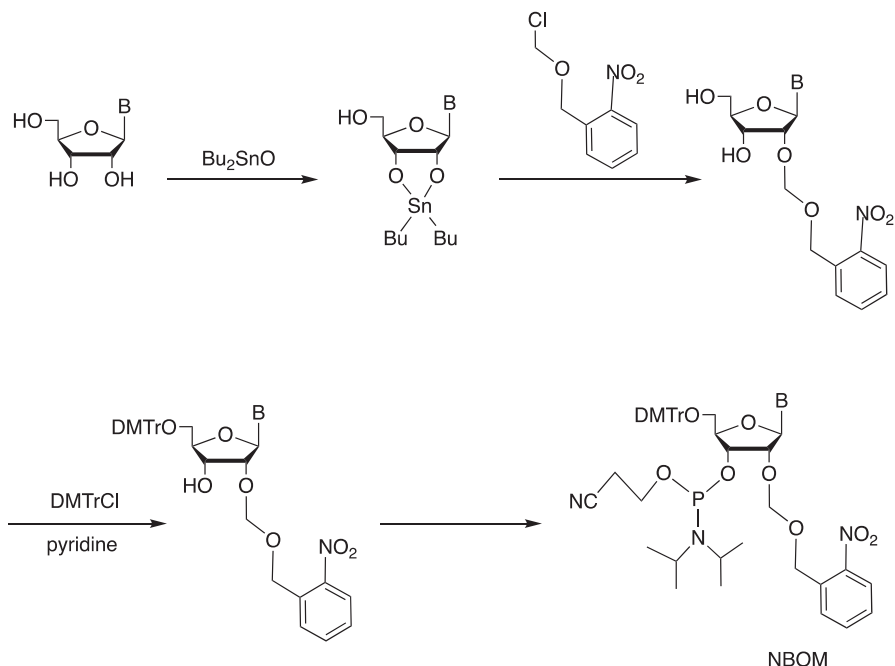
Fig. 6 RNA synthesis using the photo-labile NBOM group

uridine (2′-*O*-NBOM-uridine) in 39% yield, after the extensive separation from the 3′-*O*-NBOM regioisomer. The synthesis of RNA 33 mer having an average coupling efficiency of >98% was achieved using a universal support [56], to which the 3′–5′ reversed uridine linker was attached. The use of the NBOM group enabled us to eliminate completely all of the base protecting groups by treatment with ammonia at 50 °C for 24 h. At the last stage, UV light irradiation in aqueous *t*-BuOH at pH 3.7 for 4.5 h resulted in the complete deprotection and gave the desired RNA [53]. The chemistry developed by Gough was also applied to the synthesis of enantiomeric RNA [57] (Fig. 6).

Interestingly, Gough also reported that the 4-nitrobenzyloxymethyl group, where the position on the phenyl group was shifted to the 4-position, can be removed by treatment with TBAF in THF for 24 h, when U_{12} was synthesized using a similar uridine building block that was prepared via the reaction of 2′,3′-*O*-(dibutylstannylene) uridine with 4-nitrobenzyloxymethyl chloride [58].

5.2 2-(Trimethylsilyl)ethoxymethyl (SEM) Group

In 1994, the first example of the acetal type of the protecting group (R-OCH₂OR′, where R = ribose residue and = alkyl or aryl) was reported by Usman [59]. The oligoribonucleotide synthesis was achieved using the 2-(trimethylsilyl)
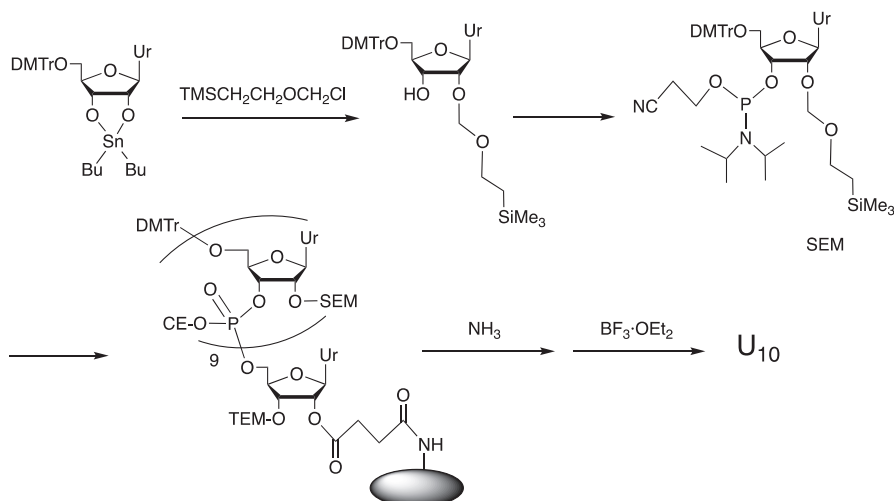
Fig. 7 RNA synthesis using the 2-(trimethylsilyl)ethoxymethyl (SEM) group

ethoxymethyl (SEM) group as a new 2′-OH protecting group. This protecting group was introduced into the 2′-hydroxyl group or uridine via the reaction between its 2′,3′-O-dibutylstannylated derivative and SEM-Cl. The decauridylate was synthesized using the uridine phosphoramidite building block. The removal of the SEM group was carried out by treatment with $BF_3 \cdot OEt_2$ in CH_3CN for 15–30 min to give $(Up)_9U$ in 74% yield. However, further studies on the SEM group are not reported (Fig. 7).

6 RNA Synthesis Using the Triisopropylsilyloxymethyl (Tom) Group

In 1999, Pitsch reported an innovative 2′-protecting group, i.e., triisopropylsilyloxymethyl (Tom) [60, 62]. This new protecting group can be uniquely and quickly removed by treatment with 1 M Bu_4NF in THF. High yield synthesis of RNA can be achieved because of the low hindered bulkiness of the Tom group. As far as the protecting group is concerned, the Tom group has a methylene group and an oxygen atom on the second and third positions, respectively, from the 2′-oxygen of the ribose residue. This atom arrangement allows more available space around the 3′-phosphoramidite site as the coupling site. The coupling efficiency thus increases compared with that of the 2′-O-TBDMS building blocks.

The key intermediates of 2′-O-TOM-ribonucleoside derivatives were prepared by reacting 5′-O-DMTr-ribonucleoside derivatives with Bu_2SnCl_2/i-Pr_2NEt in 1,2-dichloroethane at 25 °C for 1 h, followed by 1.1–1.3 equiv. of TOM-Cl at 80 °C for 20 min. Associated with the base moieties, the side reactions were observed only

to a small extent of less than 5%, when the acetyl group was used for protecting the base residues of C, A, and G [60]. The acetyl group is proved to be removed within 1 h using 10 M MeNH$_2$ in EtOH-H$_2$O (1:1, v/v) at 25 °C. Thus, four kinds of 5′-O-DMTr-2′-O-TOM-ribonucleoside derivatives were obtained in 40–60% yields.

The TOM group can be removed from 2′-O-TOM-ribonucleoside derivatives by treating with 1 M Bu$_4$NF·3H$_2$O in THF within 5 min. The removal of the Tom group was not influenced by the addition of water to the original 1 M THF solution of Bu$_4$NF. It is a sharp contrast to the deactivation of this reagent when it is used for removal of the 2′-O-TBDMS group. Therefore, co-solvents such as DMSO, DMF, and 1-methylpyrrolidine-2-one can be used for the insoluble protected oligonucleotide intermediates. For the solid-phase synthesis of RNA, a new type of heptanedioate linker between RNA and Controlled pore glass (CPG) was developed. Coupling yields of >99% were observed from the beginning, independent of the sequence length. The synthetic cycle involves (1) 4% dichloroacetic acid/1,2-dichloroethane; (2) coupling: 0.1 M phosphoramidite, 0.25 M BTT/CH$_3$CN (2.5 and 7 min for 1.5 and 10 μmol scales, respectively); (3) capping: a 1:1 mixture of Ac$_2$O/2,6-lutidine/THF (1:1:8, v/v/v) and 16% 1-methyl-1*H*-imidazole/THF (1 and 3 min); and (4) oxidation: I$_2$/H$_2$O/py/THF (3:2:20:75, v/v/v/v; 0.7 and 2.5 min).

Pitsch showed that the Tom method gave an average coupling yield of 99.4%. The average coupling yields were estimated to be 99.5% and 99.7% for synthesizing 2′-OMe-RNA and DNA, respectively, using the corresponding phosphoramidite units under identical conditions. Via this method, an RNA 84 mer was successfully synthesized. Pitsch's method was successfully applied to the synthesis of modified oligoribonucleotides, which contained a variety of functional groups tethered to the 6′-O-position of β-D-allofuranosylcytosine [63, 64], oligodeoxynucleotides containing a cytidine derivative with various functional groups at the 2′-position via an acetal type of tether [65], and aminoacylated tRNA [66]. The Tom chemistry was also successfully applied to synthesize oligoribonucleotides containing ^{15}N-labeled C, A, and G [67] and nucleobase analogs [68] (Fig. 8).

The breakthrough of this C–O–Si atom arrangement was achieved by employing the reagent of ClCH$_2$OSi(*i*Pr)$_3$ that was easily obtained by the reaction of MeSCH$_2$OSi(*i*Pr)$_3$ with SO$_2$Cl$_2$.

7 Cyanoethoxy-1-Methylethyl (CEE) and Cyanoethoxymethyl (CEM) Groups

A similar atom arrangement of C–O–C in the previous protection mode of the 1-cyanoethoxy-1-methylethyl (CEE) group was reported by Wada [69]. However, CEE is a branched structure at the acetal carbon, as shown in Fig. 9. During the extensive screening of the 2′-OH protecting groups for RNA synthesis, Pfleiderer first described that the CEE group can be introduced into the 2′-OH group via the acid-catalyzed addition of 2-cyanoethyl vinyl ether and be removed by treatment
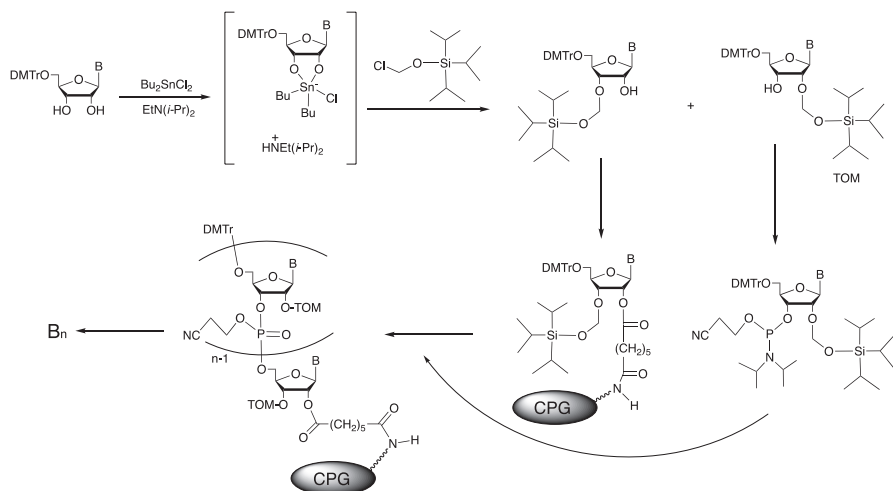
Fig. 8 RNA synthesis using the triisopropylsilyloxymethyl (Tom) group
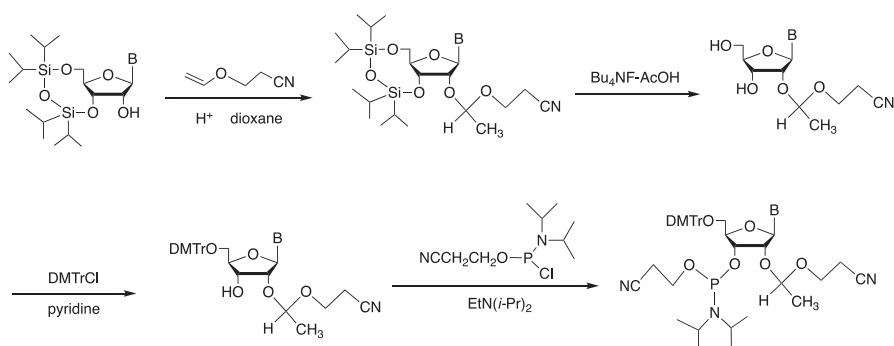
Fig. 9 RNA synthesis using the 1-(2-cyanoethyl)-1-methylethyl (CEE) group

with 1 M Bu$_4$NF in THF [70]. The CEE group can be introduced into the 2′-hydroxyl group via the addition reaction in the presence of an acid like the THP group. Wada reported the detailed chemical properties of the CEE group of 5′-*O*-DMTr-2′-*O*-CEE-uridine. This group was quickly removed within 1 min by the action of 0.5 M TBAF in THF. However, it became stable for Et$_3$N·3HF or 25% ammonia, and 0.5 M DBU/CH$_3$CN cleaved the CEE group slowly with $t_{1/2}$ = 240 min.

Yano and Ohgi reported a simple protecting group, i.e., cyanoethoxymethyl (CEM), as a new 2′-hydroxyl protecting group in RNA synthesis [71, 72]. This choice, which resulted in more effective coupling, can synthesize an RNA 115 mer. Basically, the introduction of the CEM group in the 2′-hydroxyl group of ribonucleosides was carried out via the reaction of 5′-*O*-DMTr-ribonucleoside derivatives with ClCH$_2$OCH$_2$CH$_2$CN in the presence of Bu$_2$SnCl$_2$ and *i*-Pr$_2$Net. The latter reagent was generated by the reaction of MeSCH$_2$OCH$_2$CH$_2$CN with SO$_2$Cl$_2$ [71] (Fig. 10).
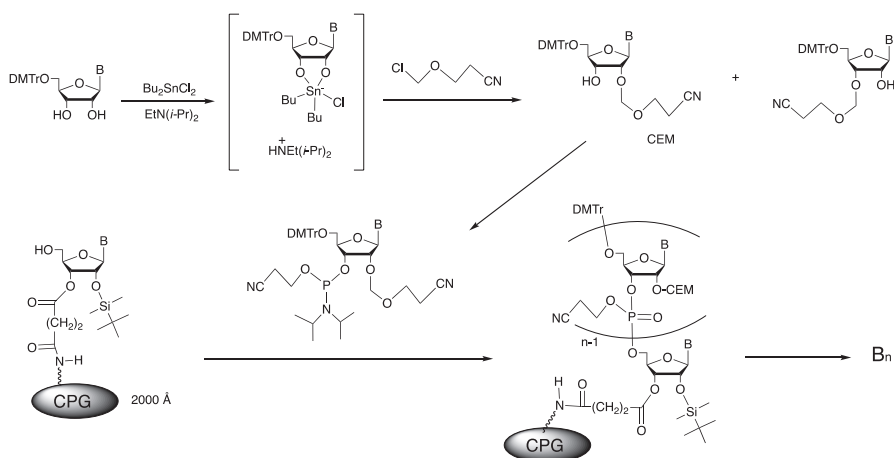
Fig. 10 RNA synthesis using the 2-cyanoethoxymethyl (CEM) group

5-Ethylthio-1*H*-tetrazole was used as the activator, and the coupling time was 150 s for oligoribonucletide synthesis. It was reported that the loss of the CEM group was less than 5% when ammonia was used for deprotecting the base protecting groups. The CEM group was torelent to Et$_3$N·3HF, but can be removed by treatment with 1 M TBAF in THF for several hours. During the removal of the CEM group by the successive treatments using 1 M TBAF and ammonia, formation of cyanoethyl adducts was observed. To prevent this side reaction, 10% *n*-propylamine and 1% bis(2-mercaptoethyl) ether in 1 M TBAF in THF were found to generate the desired fully deprotected adduct-free product. Under these improved conditions, an RNA 55 mer having high purity was synthesized. This method is comparable in efficiency with DNA synthesis, and the coupling yields are greater than 99% at each step.

Later, Ohgi and Yano reported the successful synthesis of the longest oligoribonucleotide so far using CEM chemistry [72]. For this synthesis, they established a new route to synthesize the 2′-*O*-CEM-ribonucleoside derivatives via the reaction between 3′,5′-*O*-(1,1,3,3-tetraisopropyldisiloxane-1,3-diyl) ribonucleoside derivatives and 2-cyanoethyl methylthiomethyl ether in the presence of *N*-iodosuccinimide and triflic acid in THF at −45 °C. The yield of adenosine was low. Therefore, the 2′-*O*-methylthiomethyladenosine derivative was allowed to react with 2-cyanoethanol under similar reaction conditions. The condensation was carried out using BMT, which gave the cleanest results among the tested activators, including 4,5-dicyanoimidazole, benzimidazolium triflate, and 1*H*-tetrazole. CPG having a pore size of 2000 Å also improved the results. The final choice of the conditions was (1) detritylation: 4% trichloroacetic acid in CH$_2$Cl$_2$; (2) coupling: 0.075 M phosphoramidite, 0.25 M BMT in CH$_3$CN; (3) capping: 0.1 M Pac$_2$O in THF + 6.5% 2-dimethylaminopyridine, 2% *N*-methylimidazole, and 10% 2,6-utidine in THF; (4) oxidation: 0.1 M I$_2$ in THF/pyridine/water (7:1:2, v/v/v); and (5) 0.1 M Pac$_2$O in THF + 6.5% 2-dimethylaminopyridine, 2% *N*-methylimidazole, and 10% 2,6-utidine

in THF. In this synthetic cycle, an additional capping step at the last step was added to the usual cycle. The reason was not described in their paper, and the compete capping reaction results in a clear HPLC pattern of the crude RNA.

In this study, 2-(*N,N*-dimethylamino)pyridine (2-DMAP) was used as the catalyst in place of the usual reagent 4-(*N,N*-dimethylamino)pyridine (4-DMAP). The purpose was to avoid the displacement on the phosphorylated species formed during the condensation using the usual catalyst, giving rise to a pyridinium salt which might be converted to an amino group to ultimately form the oligoribonucleotide containing 2,6-diaminopurine base moieties. The full deprotection was conducted via a four-step procedure. The CEM group of the phosphate group was removed by treatment with 50% Et$_3$N in acetonitrile. The base protecting groups were removed by treatment with 0.5 M TBAF in DMSO containing 0.5% nitromethane as an acrylonitrile scavenger at room temperature for 5 h. The successive treatment with TBAF gave the DMTr-on RNA, which, in turn, was separated by reversed-phase column chromatography and finally treated with 80% acetic acid to give the desired RNA 100 mer in an excellent yield (Fig. 11).

In this method, 5-benzylthio-1*H*-tetrazole (BTT) was used as the activator for condensation in 150 s. Thus, an RNA 110 mer was successfully synthesized. This is the longest sequence achieved to date for the chemical synthesis of RNA. A trace amount of 2,6-diaminopurineriboside was detected after enzymatic degradation of the oligomer, which was formed via the reaction of an 6-*O*-(4-DMAP)-adduct with ammonia at the final deprotecton step. In this study, 0.5 M Bu$_4$NF in the presence of 0.5% nitromethane was used to avoid the Michael addition of the once generated acrylonitrile, after deprotection of the cyanoethyl group from the phosphotriester linkage to the base residues. The addition efficacy of nitromethane was originally reported by Wada. Yano reported that the elimination of the CEM group occurred in less than 5% during the treatment using conc. NH$_4$OH-EtOH (3:1, v/v) at 40 °C.

After Yano reported the use of the CEM group as the 2′-*O*-protecting group, several research groups have recently developed this acetal structure as the skeleton of the protecting group, changing the terminal alkyl group that can be removed by Bu$_4$NF or other reagents such as DTT and hydradine.
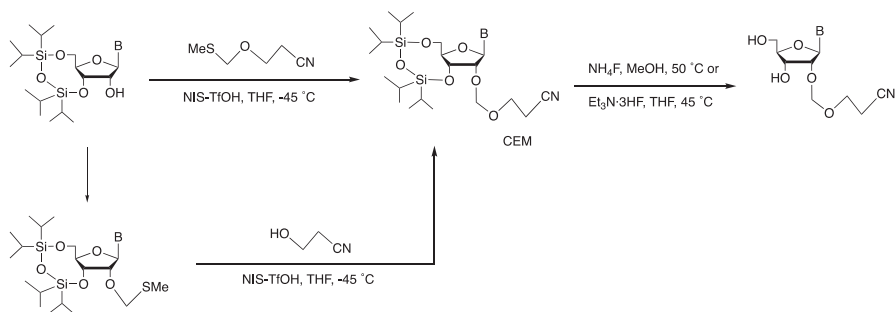
Fig. 11 RNA synthesis using the CEM group
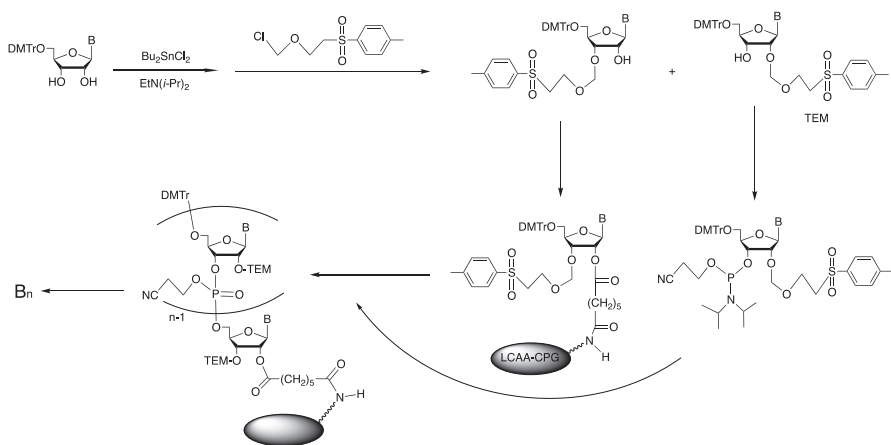
Fig. 12 RNA synthesis using the 4-methylphenylsulfonylethoxymethy (TEM) group

8 RNA Synthesis Using 4-Methylphenylsulfonylethoxymethyl (TEM) Group

Chattopadhyaya reported that 4-methylphenylsulfonylethoxymethy (TEM) can be removed by treatment with 1M TBAF in THF [72]. $ClCH_2OCH_2CH_2SO_2C_6H_4\text{-}CH_3$ was used as the introducing reagent of this protecting group. The $2'$-O-TEM-ribonucleoside derivatives were prepared by a procedure similar to that described by Pitsch using $2',3'$-O-stannylyne intermediates (Fig. 12).

ETT was confirmed to be the best activator in that study. The coupling time was set as 120 s to give the optimized yield. The TEM group was designed as a more stable protecting group toward ammonia than the CEM group, which was eliminated to less than 5% during the deprotection of the base protecting groups. Basically, the TEM group has properties similar to those of the CEM group. The deprotection of the TEM group, however, was acommplized in 5 min using 1 M TBAF in THF. Chattopadhyaya reported that, when the same deprotection procedure as the CEM strategy was employed, satisfied results were not obtained, mainly because a vinyl sulfon derivative formed after the elimination of the TEM group was too reactive toward the nucleobase moieties.

The best choice to avoid such side reactions was the use of 1 M TBAF in THF having 10% n-propylamine and 1% bis(2-mercaptoethyl) ether. Therefore, several oligoribonucleotides were synthesized under these conditions. The detailed side reactions of the base moieties having vinyl sulfone were reported by the same research group [73].

9 RNA Synthesis Using *tert*-Butyldithiomethyl (DTM) Group

On the other hand, Kwiatkowski created another type of O,S-acetal protecting group, which can be uniquely removed by DTT via reduction of the disulfide bond [74].
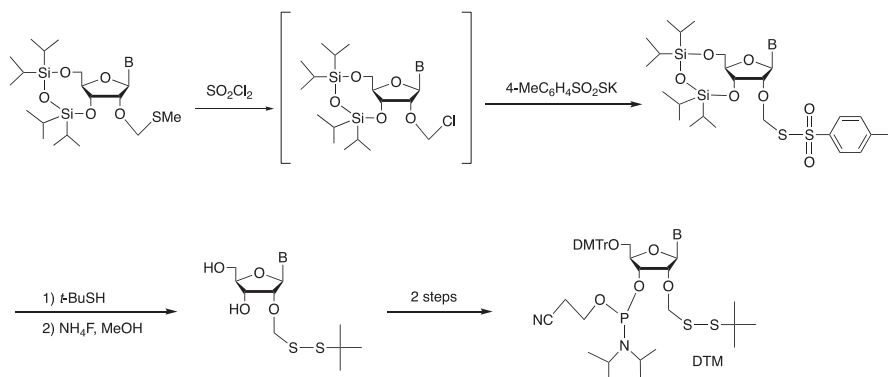
Fig. 13 RNA synthesis using the *t*-butyldithiomethyl (DTM) group

   The construction of RNA monomer building blocks was carried out as shown in Fig. 13. The methylthiomethyl ether was converted to a chloromethyl ether intermediate, which, in turn, was allowed to react with *p*-MePhSO$_2$SK to give the the O,S-acetal derivatives. The in situ reaction of these products with *t*-BuSH gave the desired disulfide products in good yields. Fortunately, this disulfide bond has been proven to be stable upon the 3′-phosphitylation. The building blocks can thus be isolated without decomposition. It is interesting that the phosphoramidite residue can exist in the presence of the disulfide bond in the neighboring site of the same molecule. However, the guanosine building block protected by an isobutyryl group on the base was gradually decomposed upon dissoving it in acetonitrile, and other ribonucleoside phosphoramidite derivatives were stable. Protection of the 6-*O*-position of guanosine using the diphenylcarbamoyl (DPC) protecting group stabilized the phosphoramidite. The intermediate having a structure of HSCH$_2$O-R (R = ribose moiety) was found to be unexpectedly stable at relatively low pH regions, which, however, was removed in 7 min upon treatment at pH 8.8 °C at 55 °C. For long sequences, 1.5 h was required at the same pH and temperature. At the oxidation step of the synthetic cycle, a 0.1 M I$_2$ solution cleaved partially the S–S bond. This problem can be overcome using a dilute 0.02 M I$_2$ solution. By this method, several siRNA 21 mers containing a TT sequence at their 3′-end were successfully synthesized.

10   RNA Synthesis Using [[2-(Methylthio)phenyl]thio]methyl (MPTM) Group

In our previous study, [[2-(methylthio)phenyl]thio]methyl (MPTM) was developed as the 2′-*O*-protecting group [75, 76] in the phosphotriester approach using the phenylthio group as the phosphate protecting group [77]. This *O,S*-acetal type of the protecting group can be removed by treatment with HgCl$_2$ under neutral conditions. The MPTM group was very stable under acidic and basic conditions. Such intemediate having an Sn–S bond would be utilized in modifying RNA with a variety of functional groups (Fig. 14).
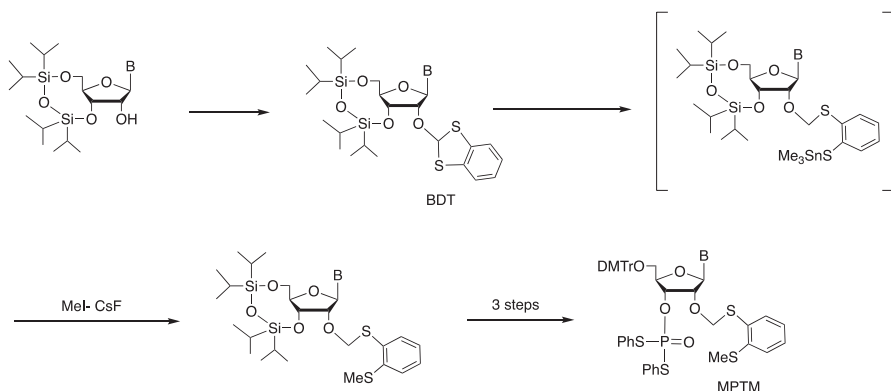
Fig. 14 RNA synthesis using [[(2-methylthio)phenyl]oxy]methyl (MPTM) group

11   RNA Synthesis Using (*N*-Dichloroacetyl-*N*-methyl) aminobenzyloxylmethyl (DCMABOM) Group

Beucage et al. have recently reported a variety of thermo-labile protecting groups in nucleic acid synthesis. In their contineous studies, a new type of a thermo-labile (*N*-dichloroacetyl-*N*-methyl)aminobenzyloxylmethyl (DCMABOM) group was reported, whose removal is possible via a two-step procedure [78]. When this protecting group is introduced into the 2′-hydroxyl group of RNA, it can be removed by treatment with ammonia, followed by thermolysis of the resulting *N*-methylbenzyloxymethyl group in 0.1 M acetic acid at 90 °C for 15–40 min. The ammonia treatment at the first step generated a 4-aminobenzyloxymethyl group, which was, in turn, removed via 1,6-elimination to give the 2′-hydroxyl group. For the synthesis of monomer building blocks, the NIS mediated the reaction between 2′-*O*-methylthiomethylribonucleoside derivatives and the corresponding benzyl alcohol. However, the synthesis of the purine nucleoside derivatives faced a reproducibility issue. An alternative method for the synthesis of the purin ribonucleoside building unit was employed. The reaction of 5′-*O*-DMTr-ribonucleoside derivatives stannylated with 4-(*N*-dichloroacethyl-*N*-methyl)aminobenzyloxymethyl chloride was involved to give the 2′-*O*-DCMABOM-substituted product (Fig. 15).

An RNA 20 mer was synthesized by this protection method. The enzymatic assay suggested that the amout of RNA fragments containing (2′→5′)-internucleotidic phosphodiester linkages was negligible. It is neccessay to improve the 2′-*O*-protection of ribonucleoside purines using this group because the yield for introducing this protecitng group into the 2′-hydroxyl group is low. In connection to this study, Gough et al. also reported RNA synthesis using 4-nitrobenzyloxymethyl (NBOM) as the 2′-protecting group [79]. This NBOM group can be reduced to an amino group by treatment with TiCl₃ at pH 6.0 at 25 °C for 1 h. However, this conversion cannot be applied to the synthesis of RNA having four canonical ribonucleosides (Fig. 16).
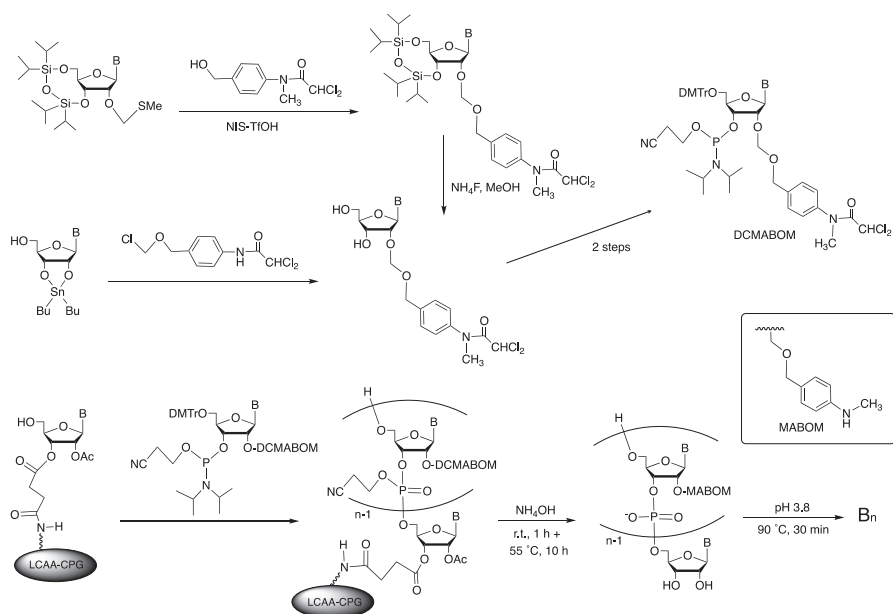
Fig. 15 RNA synthesis using the 4-(*N*-dichloroacetyl-*N*-methyl)aminobenzyloxymethyl group
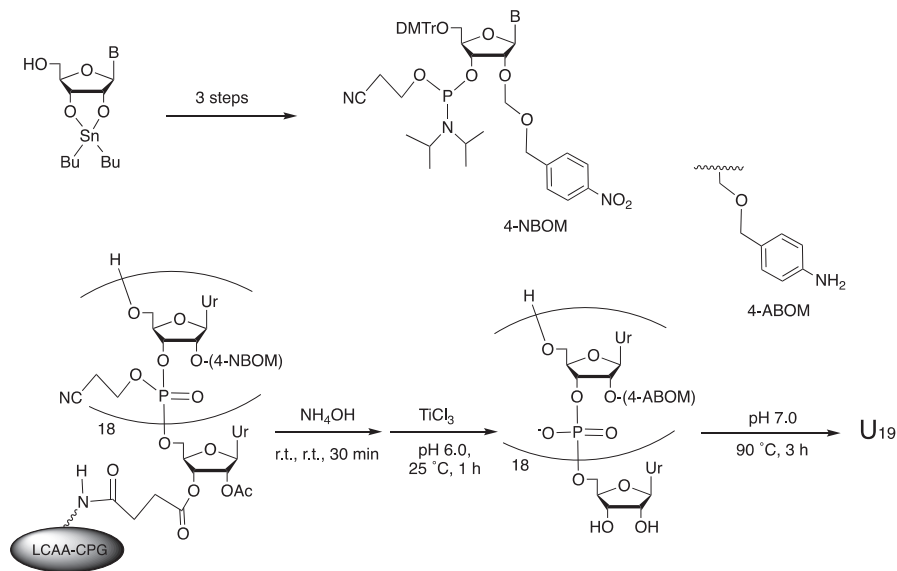
Fig. 16 RNA synthesis using the 4-NBOM group

12 RNA Synthesis Using the Acetal Levulinyl Ester (ALE) Group

As a new acetal-type of the protecting group, Damha developed levulinyloxymethyl (ALE) [80], which has a levulinyl group removable upon treatment with hydradine in pyridine-acetica acid (3:2, v/v). The levulinyl group itself has been used as the 2′-*O*-protecting group by Pon [81]. However, great care has to be exercised in purifying these building blocks in order to avoid contamination with the isomeric 3′-*O*-Lev 2′-phosphoramidites. The 2′-*O*-acyl group tends to easily migrate to the 2′-hydroxyl group because of its neighboring participation effect. On the contrary, protecting groups of the acetal-type cannot migrate between the 2′- and 3′-hydroxyl groups. The levulinyloxymethyl (LVOM) thus designed acquires a hydradine-labile property like this class of protecting groups as mentioned before.

This group could be introduced into the 2′-hydroxyl group using activation of the methylthiomethyl group with SO_2Cl_2, followed by alkylation of the resulting chloromethyl ether intermediates with $NaOC(O)CH_2CH_2C(O)CH_3$ in the presence of a crown ether. For the guanosine derivative, the second step reaction was carried out with NaOLev in the presence of 4-chlorostyrene. This modification avoided the side reaction on the guanine moiety to give the desired 2′-*O*-ALE–guanosine derivative in good yield. In this synthesis, tedious transformation of the FMOC group introduced into the base parts of the Lev group was required because this study was directed toward microarray fabrications.

The phosphoramidite building blocks having the 5′-*O*-DMTr group were used to construct dT_9-rN-dT_5 (rN) U, C, A, and G on a Q-CPG solid support. These oligomers were obtained by successive treatments with Et_3N-CH_3CN (3:2, vv/) for 1 h, 0.5 M hydradine in pyridine–acetic acid (3:2, v/v) for 1 h, and 1 M TBAF in THF for 16 h.

During this work, Damha compared the coupling efficiencies of the previous RNA monomer building blocks with ALE units under the same coupling conditions for 1 and 10 min. The coupling efficiency for 1 min was increased on the order of 2′-*O*-ALE (99.7%) > 2′-*O*-TOM (96.3%) > 2′-*O*-TBDMS (94.7%; 2′-*O*-ACE was not evaluated). For 10 min coupling, the order was 2′-*O*-ACE (99.0%) > 2′-*O*-ALE (98.7%) > 2′-*O*-TOM (98.1%) 2′-*O*-TBDMS (98.4%).

For constructing RNA microarrays on glass, 5′-*O*-(2-(2-nitrophenyl) propoxycarbonyl)-2′-*O*-ALE-3′-phosphoramidite derivatives were synthesized and used. The 2-(2-nitrophenyl)propoxycarbonyl group was removed by photo irradiation at 360 nm. The combination of this 5′-*O*-protecting group with the ALE group selectively removed all of the protecting groups on the base and phosphate moieties by treating with hydradine and Et_3N while keeping the Q linker inert. Thus, unprotected RNA oligomers could be generated as RNA microarray chips on a glass plate (Fig. 17).
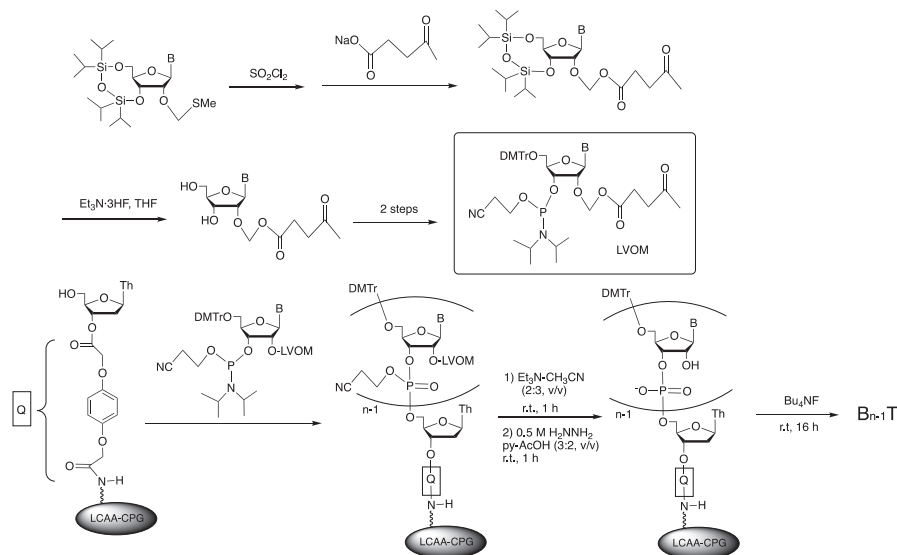
Fig. 17 RNA synthesis using the levulinyloxymethyl (LVOM) group

13 RNA Synthesis Using the Cyanoethyl (CE) Group

We have studied 2′-*O*-modified RNAs as drugs for gene therapy. During our study, we found that 2′-*O*-cyanoethylated RNA oligomers exhibited great enzyme resistance and higher hybridization affinity for the complementary DNA or RNA strands than the unmodified ones [82]. Later, the cyanoethyl group introduced into the 2′-hydroxyl group was found to be removed by treatment with 1 M TBAF to give RNA oligomers [83].

The synthesis of monomer building blocks involves Michael reaction of appropriately protected 3′,5′-*O*-(1,1,3,3-tetraisopropyldisiloxane-1,3-diyl)ribonucleosides with acrylonitrile in *t*-BuOH in the presence of Cs_2CO_3. Under these mild conditions, the cyanoethyl group can be introduced into the 2′-hydroxyl group in high yield. However, full protection of the base residues in the case of cytosine, adenine, and guanine was required. A multi-step protection–deprotection procedure had to be used in the synthesis of each monomer building block. Quite recently, we have improved this long-step procedure because we found the selective *O*-cyanoethylation of 3′,5′-*O*-(1,1,3,3-tetraisopropyldisiloxane-1,3-diyl)ribonucleosides without using base protecting groups. This innovative finding could make our strategy a more promising tool for RNA synthesis in the near future (Fig. 18).

In the previous papers concerning ribonucleoside and oligoribonucleosides modified with CEM and CEE groups, these acetal protecting groups having a cyanoethyl substitute on the acetal function could be removed by the action of TBAF. This is rationalized in terms of the higher p*K*a value (10.5) [60] of the hydroxyl group of hemiacetal compounds than that (p*K*a 15–16) of alcohols. Therefore, we first
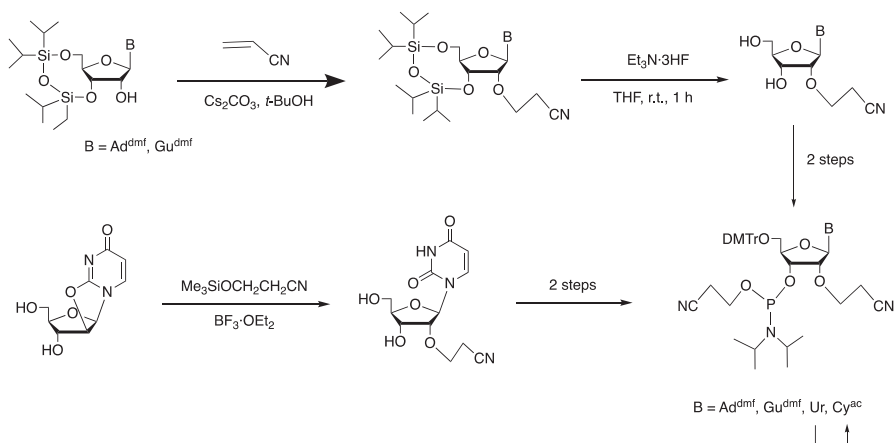
Fig. 18 RNA synthesis using the 2-cyanoethyl (CE) group

expected that the leaving group activity of the ribosyl 2′-OH group was poor because the pKa values of the 2′-OH group of ribonucleosides were reported to be higher (12.14–12.86) [84] by two orders than the pKa (10.5) value of hemiacetals. To our surprise, however, the cyanoethyl group was completely removed in 10 min when 2′-O-cyanoethyluridine was treated with 1 M TBAF in THF. The use of 1 M TBAF-AcOH in THF or Et$_3$N·3HF was not effective. On the other hand, the decyanoethylation proceeded very slowly (70% cleavage in 24 h) when Uce was treated with 0.5 M DBU in CH$_3$CN. The use of excess ammonia resulted in the complete decyanoethylation of Uce in 50 min. The rates of the decyanoethylation from the ribonucleoside derivatives varied: Ace (8 min) > Gce (9 min) > Cce (24 min) > Uce (48 min). The decyanoethylation of UcepU proceeded with a t$_{1/2}$ of 36 min, which was considerabley delayed compared with that (10 min) of Uce.

Because ammonia treatment was required for removal of the base protecting groups, the partial deblocking of the 2′-O-cyanoethyl group was incompatible under the standard conditions used for RNA synthesis. However, we found that the addition of ammonium acetate to the ammonia solution improved the stability of the 2′-O-cyanoethyl group without the influence of deblocking the acyl protecting groups on the base moieties. The use of conc. NH$_4$OH-NH$_4$OAc (10:1, w/w) detarded the decyanoethylation (10% in 12 h) that was considerably improved compared with that (100% in 12 h) of only conc. NH$_4$OH. Actually, the use of conc. NH$_4$OH-NH$_4$OAc (10:1, w/w) at room temperature for 1.5 h for full deprotection of protected oligomers on CPG successfully gave 2′-O-cyanoethylated derivatives without chain cleavage. Thus, for example, 2′-O-cyanoethyl RNA 12 mer (GceAceCceUce)$_4$ was obtained. This 2′-O-cyanoethyl RNA oligomer proved to have high hybridization affinity for the complementary DNA and RNA strands. In addition, its enzyme resistance toward nucleases was greatly improved. Simple treatment of 2′-O-cyanoethylated RNA oligomers with 1 M TBAF gave 2′-O-unmasked RNA oligomers. Thus, the 21 nt antisense sequence of mirR-
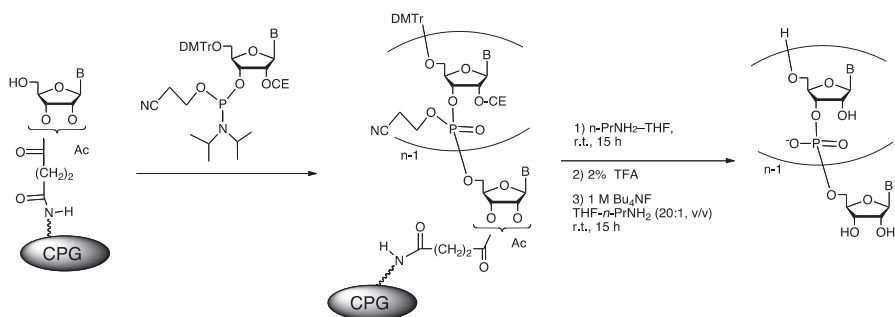
Fig. 19 RNA synthesis using the Ce group

bantam, GCUUUCAAAAUGAUCUCACUG, was synthesized via this new method. Because the cyanoethyl group seems to be the smallest among the protecting groups mentioned above, the condensation rate was also remarkably improved. At least, this choice was better than the TBDMS strategy (Fig. 19).

14 RNA Synthesis Without Using Base Protection

Quite recently, we have developed a new method for the synthesis of RNA using *N*-unprotected monomer building blocks [75]. Several papers concerning the synthesis of DNA without using the base protecting groups have been reported to date [75–78]. Among them, the most reliable method proved to be based on the way a combined reagent of BIT and HOBT was used as the activator of the P–N bond of N-unprotected monomer phosphoramidite units, as reported by us. Using this reagent, we succeeded in synthesizing an RNA–DNA chimeric 21 mer of 2′-OMe-[CCUACAGAGAACUGCGGUU]-TT. In this approach, the TBDMS group was used as the 2′-hydroxyl protecting group. *O*-selective phosphorylation was achieved at the coupling step by the following mechanism. Even when the N-free base moieties are phosphorylated by the activated phosphoramidite units, HOBT serves as the reagent that can cleave the P–N bond on the base moieties to give the N-free species again. HOBt was the best choice of reagent for this P–N bond cleavage reaction. The *O*-selectivity in condensation was more than 99%. Actually, oligoribonucleotides can be obtained as sufficiently pure materials by this method (Fig. 20).

15 Recent Studies on RNA Chemical Synthesis

Although many new approaches to RNA synthesis as described above have been reported, some research groups still have been finding more ideal methods. One of them is an alternative approach reported by Markiewicz who used aroyloxymethyl
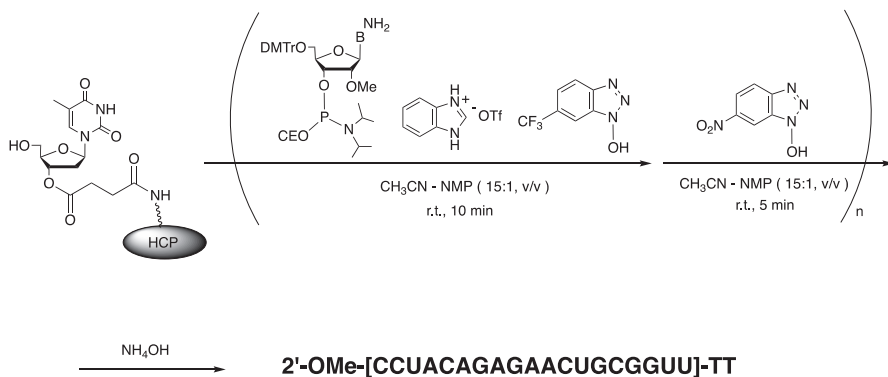
Fig. 20 RNA synthesis using *N*-unprotected monomer building blocks

groups as the 2′-base-labile protecting group [84]. Kataoka reported the use of *N*-unprotected monomer units of 5′-*O*-tBDMS-2′-*O*-acetylribonucleoside 3′-O-*H*-phosphonates in the liquid-phase *H*-phosphonate method using polyethyrene glycol support [85]. However, this method involves several serious problems which could be overcome because it is well known that the use of pivaloyl chloride as a condensing reagent resulted in great acylation on the unprotected nucleobases. Recently, Chiba has reported a straightforward method for synthesizing oligoribonucleotide blocks using a Cbz-type alkyl-chain-soluble support attached to the 3′-OH group of 3′-terminal nucleosides without chromatographic purification [86]. Lastly, the use of cyanoethoxy(methoxy)methyl (-CH$_2$OCH$_2$OCH$_2$CH$_2$CN) as a new type of 2′-O-protecting group which was developed by Aoki et al. is interesting. This unique protecting group can be used as a less hindered protecting group [87].

16 Summary and Perspectives

In the current synthesis of RNA, several methods have been utilized by custom synthesis companies which supply oligoribonucleotides with moderate nucleotide length up to 50 mer as sufficiently pure products. At present, long RNA oligomers which have more than 100 nt can be synthesized. With an increase of the RNA length demanded by researchers in molecular biology, organic chemists should search for more effective methods for the synthesis of 200 mer-level RNA oligomers. For this purpose, the choice of a more suitable 2′-hydroxyl protecting group is inevitable and essential. Although a lot of new methods have recently been developed, more sophisticated approaches should be created by finding out the optimized conditions at each step and new protection modes.

References

1. Fire A, Xu S, Montgomery MK et al (1998) Potent and specific genetic interference by double-stranded RNA in *Caenorhabditis elegans*. Nature 391:806–811
2. Elbashir SM, Harborth J, Lendeckel W et al (2001) Duplexes of 21-nucleotide RNAs mediate RNA interference in cultured mammalian cells. Nature 411:494–498
3. Manoharan M (2002) Oligonucleotide conjugates as potential antisense drugs with improved uptake, biodistribution, targeted delivery, and mechanism of action. Antisense Nucleic Acid Drug Dev 12:103–128
4. Amarzguioui M, Lundberg P, Cantin E et al (2006) Rational design and in vitro and in vivo delivery of Dicer substrate siRNA. Nat Protoc 1:508–517
5. Ozcan G, Ozpolat B, Coleman RL, Sood AK, Lopez-Berestein G (2015) Preclinical and clinical development of siRNA-based therapeutics. Adv Drug Deliv Rev 87:108–119
6. Behlke MA (2008) Chemical modification of siRNAs for in vivo use. Oligonucleotides 18:305–319
7. Lewis BP, Burge CB, Bartel DP (2005) Conserved seed pairing, often flanked by adenosines, indicates that thousands of human genes are microRNA targets. Cell 120:15–20
8. Esau CC, Monia BP (2007) Therapeutic potential for microRNAs. Adv Drug Deliv Rev 59:101–114
9. Chua JH, Armugam A, Jeyaseelan K (2009) MicroRNAs: biogenesis, function and applications. Curr Opin Mol Ther 11:189–199
10. Liao W, Dong J, Peh HY, Tan LH, Lim KS, Li L, Wong WF (2017) Oligonucleotide therapy for obstructive and restrictive respiratory diseases. Molecules 22:139
11. Siolas D, Lerner C, Burchard J et al (2005) Synthetic shRNAs as potent RNAi triggers. Nat Biotechnol 23:227–231
12. Ge Q, Dallas A, Ilves H et al (2010) Effects of chemical modification on the potency, serum stability, and immunostimulatory properties of short shRNAs. RNA 16:118–130
13. Waterston RH, Lindblad-Toh K, Birney E et al (2002) Initial sequencing and comparative analysis of the mouse genome. Nature 420:520–562
14. Storz G, Altuvia S, Wassarman KM (2005) An abundance of RNA regulators. Annu Rev Biochem 74:199–217
15. Eddy SR (2001) Non-coding RNA genes and the modern RNA world. Nat Rev Genet 2:919–929
16. Vogel J (2009) A rough guide to the non-coding RNA world of salmonella. Mol Microbiol 71:1–11
17. Mehler MF, Mattick JS (2007) Noncoding RNAs and RNA editing in brain development, functional diversification, and neurological disease. Physiol Rev 87:799–823
18. Watts JK, Deleavey GF, Damha MJ (2008) Chemically modified siRNA: tools and applications. Drug Discov Today 13:842–855
19. Beaucage SL (2008) Solid-phase synthesis of siRNA oligonucleotides. Curr Opin Drug Discov Dev 11:203–216
20. Lönnberg H (2009) Solid-phase synthesis of oligonucleotide conjugates useful for delivery and targeting of potential nucleic acid therapeutics. Bioconjug Chem 20:1065–1094
21. Reese CB (2002) The chemical synthesis of oligo- and poly-nucleotides: a personal commentary. Tetrahedron 58:8893–8920
22. Reese CB (2005) Oligo- and poly-nucleotides: 50 years of chemical synthesis. Org Biomol Chem 3:3851–3868
23. Beaucage SL, Reese C (2009) Recent advances in the chemical synthesis of RNA. In: Beaucage SL, Bergstrom DE, Glick GD et al (eds) Current protocols in nucleic acid chemistry. Wiley, New York, pp 2.16.1–2.2.31
24. Beaucage SL, Caruthers MH (2000) In: Beaucage SL, Bergstrom DE, Glick GD et al (eds) Current protocols in nucleic acid chemistry, vol I. Wiley, New York, pp 3.3.1–3.3.20

25. Beaucage SL, Iyer RP (1993) The synthesis of modified oligonucleotides by the phosphoramidite approach and their applications. Tetrahedron 49:6123–6194
26. Beaucage SL, Iyer RP (1992) Advances in the synthesis of oligonucleotides by the phosphoramidite approach. Tetrahedron 48:2223–2311
27. Bornscheuer U (2010) The first artificial cell-A revolutionary step in synthetic biology? Angew Chem Int Ed 49:5228–5230
28. Gibson DG (2008) Complete chemical synthesis, assembly, and cloning of a mycoplasma genitalium genome. Science 319:1215–1220
29. Smith M, Rammer DH, Goldberg IH et al (1962) Polynucleotides. XIV. Specific synthesis of the C3′-C5′ internucleotide linkage. Synthesis of uridylyl(3′→5′)-uridine and uridylyl-(3′→5′)-adenosine. J Am Chem Soc 84:430–440
30. Schulhof JC, Molko DS, Teoule R (1987) The final deprotection step in oligonucleotide synthesis is reduced to a mild and rapid ammonia treatment by using labile base-protecting groups. Nucleic Acids Res 15:397–416
31. Sinha ND, Davis P, Usman N et al (1993) Labile exocyclic amino protection of nucleosides in DNA, RNA and oligonucleotide analog synthesis facilitating *N*-deacylation, minimizing depruination and chain degradation. Biochimie 75:13–23
32. Welz R, Müller S (2002) 5-(Benzylmercapto)-1*H*-tetrazole as activator for 2′-*O*-TBDMS phosphoramidite building blocks in RNA synthesis. Tetrahedron Lett 43:795–797
33. Sproat B, Colonna F, Mullah B et al (1995) An efficient method for the isolation and purification of ligoribonucleotides. Nucleosides Nucleotides 14:255–273
34. Vargeese C, Carter J, Yegge J et al (1998) Efficient activation of nucleoside phosphoramidites with 4,5-dicyanoimidazole during oligonucleotide synthesis. Nucleic Acids Res 26:1046–1050
35. Leuck M, Wolter A, Stumpe A (2008) U.S. Pat. Appl. Publ., US 20080064867 A1 20080313. Activator 42 is commercially available from Proligo Co. Ltd. For its recent use see: Utagawa E, Ohkubo A, Sekine M et al (2007) Synthesis of branched oligonucleotides with three different sequences using an oxidatively removable tritylthio group. J Org Chem 72:8259–8266
36. Hayakawa Y, Kataoka M, Noyori R (1996) Benzimidazolium triflate as an efficient promoter for nucleotide synthesis via the phosphoramidite method. J Org Chem 61:7996–7997
37. Hakimelahi H, Proba ZA, Ogilvie KK (1982) New catalyst and procedures for the dimethoxytritylation and selective silylation of ribonucleosides. Can J Chem 60:1106–1113
38. Ogilvie KK, Damha MJ, Usman N et al (1987) Developments in the chemical synthesis of naturally occurring DNA and RNA sequences with normal and unusual linkages. Pure Appl Chem 59:325–330
39. Usman N, Ogilvie KK, Jiang MY et al (1987) The automated chemical synthesis of long oligoribunucleotides using 2′-*O*-silylated ribonucleoside 3′-*O*-phosphoramidites on a controlled-pore glass support: synthesis of a 43-nucleotide sequence similar to the 3′-half molecule of an *Escherichia coli* formylmethionine tRNA. J Am Chem Soc 109:7845–7854
40. Ogilvie KK, Usman N, Nicoghosian K (1988) Total chemical synthesis of a 77-nucleotide-long RNA sequence having methionine-acceptance activity. Proc Natl Acad Sci U S A 85:5764–5768
41. Corey EJ, Venkateswarlu A (1972) Protection of hydroxyl groups as *tert*-butyldimethylsilyl derivatives. J Am Chem Soc 94:6190–6191
42. Nagai H, Fujiwara T, Fujii M et al (1989) Reinvestigation of deoxyribonucleoside phosphorothioites–synthesis and properties of deoxyribonucleoside-3′-dimethyl phosphites. Nucleic Acids Res 17:8581–8593
43. Tanimura H, Maeda M, Fukazawa T et al (1989) Chemical synthesis of the 24 RNA fragments corresponding to hop stunt viroid. Nucleic Acids Res 17:8135–8147
44. Tanimura H, Fukazawa T, Sekine M et al (1988) The practical synthesisof RNA fragments in the solid phase approach. Tetrahedron Lett 29:577–578
45. Iwai S, Ohtsuka E (1988) Synthesis of oligoribonucleotifes by the phosphoramidite approach using 5′-levullinyl and 2′-tetrahydrofuranyl protection. Tetrahedron Lett 29:5383–5386

46. Iwai S, Ohtsuka E (1988) 5′-Levulinyl and 2′-tetrahydrofurany protection for the synthesis of oligoribonucleotides by the phosphoramidite approach. Nucleic Acids Res 16:9443–9456

47. Van der Marel GA, Wille G, van Boom JH (1982) Solid-phase synthesis of the RNA fragment: rAAGAAGAAGAAGA. Recueil Trav Chim Pays-Bas 101:241–246

48. Lloyd W, Reese C, Song Q et al (2000) Some observations relating to the use of 1-aryl-4-alkoxypiperidin-4-yl groups for the protection of the 2′-hydroxy functions in the chemical synthesis of oligoribonucleotides. J Chem Soc Perkin Trans I:165–176

49. Reese C, Thompson EA (1988) A new synthesis of 1-arylpiperidin-4-ols. J Chem Soc Perkin Trans I:2881–2885

50. Capaldi DC, Reese CB (1994) Use of the 1-(2-fluorophenyl)-4-methoxypiperidin-4-yl (Fpmp) and related protecting groups in oligoribonucleotide synthesis: stability of internucleotide linkages to aqueous acid. Nucleic Acids Res 22:2209–2216

51. Scaringe SA, Wincott FE, Caruthers MH (1998) Novel RNA synthesis method using 5′-O-silyl-2′-O-orthoester protecting groups. J Am Chem Soc 120:11820–11821

52. Dahl BJ, Bjergarde K, Henriksen L et al (1990) A highly reactive, odorless substitute for thiophenol triethylamine as a deprotection reagent in the synthesis of oligonucleotides and their analogs. Acta Chem Scand 44:639–641

53. Schwartz WE, Breaker RR, Asteriadis GT et al (1992) Rapid synthesis of oligoribonucleotides using 2′-O-(ortho-nitrobenzyloxymethyl)-protected monomers. Bioorg Med Chem Lett 2:1019–1024

54. Miller TJ, Schwartz ME, Gough GR (2000) 2′-Hydroxyl-protecting groups that are either photochemically labile or sensitive to fluoride ions. In: Beaucage SL, Bergstrom DE, Glick GD et al (eds) Current protocols in nucleic acid chemistry. Wiley, New York, pp 2.5.1–2.5.36

55. Miller TJ, Schwartz ME, Gough GR (2000) Synthesis of oligoribonucleotides using the 2-nitrobenzyloxymethyl group for 2′-hydroxyl protection. In: Beaucage SL, Bergstrom DE, Glick GD et al (eds) Current protocols in nucleic acid chemistry. Wiley, New York, pp 3.7.1–3.7.8

56. DeBear JS, Hayes JA, Koleck MP et al (1987) A universal glass support for oligonucleotide synthesis. Nucleoside Nucleotides 6:821–830

57. Pitsch S (1997) An efficient synthesis of enantiomeric ribonucleic acids from D-glucose. Helv Chim Acta 80:2286–2314

58. Pitsch S, Weiss PA, Wu X et al (1999) Fast and reliable automated synthesis of RNA and partially 2′-O-protected precursors ('caged RNA') based on two novel, orthogonal 2′-O-protecting groups. Helv Chim Acta 82:1753–1761

59. Wincott FE, Usman N (1994) 2′-(Trimethylsilyl)ethoxymethyl protection of the 2′-hydroxyl group in oligoribonucleotide synthesis. Tetrahedron Lett 35:6827–6830

60. Pitsch S, Weiss PA, Jenny L et al (2001) Reliable chemical synthesis of oligoribonucleotides (RNA) with 2′-O-[(triisopropylsilyl)oxy]methyl(2′-O-tom)-protected phosphoramidites. Helv Chim Acta 84:3773–3794

60. Pitsch S, Weiss PA (2001) Chemical synthesis of RNA sequences with 2′-O-[(triisopropylsilyl)oxy]methyl-protected ribonucleoside phosphoramidites. In: Beaucage SL, Bergstrom DE, Glick GD et al (eds) Current protocols in nucleic acid chemistry. Wiley, New York, pp 3.8.1–3.8.15

61. Wu X, Pitsch S (1999) Functionalization of the sugar moiety of oligoribonucleotides on solid support. Bioconjug Chem 10:921–924

62. Wu X, Pitsch S (1998) Synthesis and pairring properties of oligoribonucleotide analogues containing a metal-binding site attached to β-D-allofuranosyl cytosine. Nucleic Acids Res 26:4315–4323

63. Wu X, Pitsch S (2000) Synthesis of 5′-C- and 2′-O-(bromoalkyl)-substituted ribonucleoside phosphoramidites for the post-synthetic functionalization of oligonucleotides on solid support. Helv Chim Acta 83:1127–1144

64. Stutz A, Höbartner C, Pitsch S (2000) Novel fluoride-labile mucleobase-protecting groups for the synthesis of 3′(2′)-O-aminoacylated RNA sequences. Helv Chim Acta 83:2477–2483

65. Wenter P, Pitsch S (2003) Synthesis of selectively ^{15}N-labeled 2′-O-[[triisopropylsilyl]oxy] methyl] (=tom)-protected ribonucleoside phosphoramidites and their incorporation into a bistable 32 mer RNA sequence. 86:3955–3974

66. Porcher S, Pitsch S (2005) Synthesis of 2′-O-[(triisopropylsilyl)oxy]methyl (=tom)-protected ribonucleoside phosphoramidites containing various nucleobase analogues. Helv Chim Acta 88:2683–2703

67. Umemoto T, Wada T (2004) Oligoribonucleotide synthesis by the use of 1-(2-cyanoethoxy) ethyl (CEE) as a 2′-hydroxy protecting group. Tetrahedron Lett 45:9529–9531

68. Matysiak S, Fitznar HP, Schnell R et al (1998) Nucleosides – part LXIII – acetals as new 2′-O-protecting functions for the synthesis of oligoribonucleotides: synthesis of uridine building blocks and evaluation of their relative acid stability. Helv Chim Acta 81:1545–1566

69. Ohgi T, Masutomi Y, Ishiyama K (2005) A new RNA synthetic Method with a 2′-O-(2-cyanoethoxyemthyl) protecting group. Org Lett 7:3477–3480

70. Zhou C, Honcharenko D, Chattopadhyaya J (2007) 2-(4-Tolylsulfonyl)ethoxymethyl (TEM)–a new 2′-OH protecting group for solid-supported RNA synthesis. Org Biomol Chem 5:333–343

71. Zhou C, Pathmasire W, Honchararenko D et al (2007) High-quality oligo-RNA synthesis using the new 2′-O-TEM protecting group by selectively quenching the addition of p-tolyl vinyl sulphone to exocyclic amino functions. Can J Chem 85:293–301

72. Semenyuk A, Foldesi A, Johansson T et al (2006) Synthesis of RNA using 2′-O-DTM protection. J Am Chem Soc 128:12356–12357

73. Sekine M, Nakanishi T (1991) Oligoribonucleotide synthesis by use of [[2-(methylthio)phenyl]thio]methyl (MPTM) group as the 2′-hydroxyl protecting groups. Chem Lett:121–124

74. Sekine M, Nakanishi T (1989) [[2-(Methylthil)phenyl]thio]methyl (MPTM): a new protecting group of hydroxyl groups caable of conversion to a methyl group. J Org Chem 54:5998–6000

75. Sekine M, Hata T (1999) Chemical synthesis of oligonucleotides by use of phenylthio group. Curr Org Chem 3:25–66

76. Cieslak J, Kauffman JS, Kolodziejski MJ et al (2007) Assessment of 4-nitrogenated benzyloxymethyl groups for 2′-hydroxyl protection in solid-phase RNA synthesis. Org Lett 9:671–674

77. Lackey JG, Mitra D, Somoza MM et al (2009) Acetal levulinyl ester (ALE) groups for 2′-hydroxyl protection of ribonucleosides in the synthesis of oligoribonucleotides on glass and microarrays. J Am Chem Soc 131:8496–8502

78. Gough GR, Miller TJ, Mantick NA (1996) p-Nitrobenzyloxymethyl: a new fluoride-removable protecting group for ribboneoside 2′-hydroxyls. Tetrahedron Lett 37:981–982

79. Pon RT, Yu S (1997) Hydroquinone-O,O′-diacetic acid ('Q-linker') as a replacement for succinyl and oxalyl linker arms in solid phase oligonucleotide synthesis. Nucleic Acids Res 25:3629–3635

80. Saneyoshi H, Seio K, Sekine M (2005) A general method for the synthesis of 2′-O-cyanoethylated oligoribonucleotides having promising hybridization affinity for DNA and RNA and enhanced nuclease resistance. J Org Chem 70:10453–10460

81. Saneyoshi H, Ando K, Seio K et al (2007) Chemical synthesis of RNA via 2′-O-cyanoethylated intermediates. Tetrahedron 63:11195–11203

82. Velikyan I, Acharya S, Trifonova A et al (2001) The pK(a)'s of 2′-hydroxyl group in nucleosides and nucleotides. J Am Chem Soc 123:2893–2894

83. Markiewicz W T, Tos-Marciniak A et al WO2014148928 A1

84. Kataoka M. (2014) JP WO2014/017615 A

85. Matsuno Y, Takao S, Kim S, Chiba K (2016) Synthetic method for oligonucleotide block by using alkyl-chain-soluble support. Org Lett 18:800–803

86. Aoki E, Suzuki H, Itoh A. (2013) WO/2013/027843

RNA Synthesis Using the CEM Group

Hidetoshi Kitagawa

Abstract We have developed a solid-phase synthesis of RNA oligomers with 2-cyanoethoxymethyl (CEM) as the 2′-hydroxyl protecting group. The method allows the synthesis of RNA oligomers with high efficiency and high purity. In this section, we describe the synthesis of CEM amidites and RNA synthesis by using CEM amidites. The advantages of the CEM group include its low steric hindrance, leading to a high coupling yield, and its ease of removal under mild conditions without any decomposition of the RNA oligomers.

Keywords 2-cyanoethoxymethyl · CEM · TBAF · 2′-hydroxyl protecting group · RNA · Solid-phase synthesis · Phosphoramidite · SiRNA

1 Introduction

On the research of RNA synthesis, it has been important to select a suitable protecting group for the 2′-position. This protecting group must be stable throughout the solid-phase synthesis, and must be readily removable under mild conditions. The *t*-butyldimethylsilyl (TBDMS) group [1] is one of the most popular 2′-hydroxyl-protecting group for ribonucleosides whose phosphoramidites are commercially available. 2′-*O*-TBDMS protection gives RNA of reasonable purity in reasonable yield. Furthermore, 2′-*O*-TBDMS ribonucleoside phosphoramidites require relatively long coupling times and do not produce the highest coupling yields [1, 2]. To resolve these problems, more-powerful activators or less bulky 2′-hydroxyl-protecting groups have been reported [3–6]. Although these solutions represent major improvements in the synthesis of RNA oligonucleotides [7], there is still room for improvement in their practical application.

We developed CEM phosphoramidites as the solution of the issue [8–10]. I would like to describe here about CEM chemistry and its experimental detail.

H. Kitagawa (✉)
Nippon Shinyaku Co., Ltd., Tsukuba, Ibaraki, Japan
e-mail: h.kitagawa@po.nippon-shinyaku.co.jp

2 Synthesis of CEM Amidites

CEM amidites are synthesized from the corresponding nucleoside derivatives (**1a–e**) and CEM reagent. CEM reagent (cyanoethyl methyl thiomethyl ether, CEM-SMe) is prepared by treating a solution of 2-cyanoethanol in dimethyl sulfoxide (DMSO) with acetic anhydride and acetic acid (Fig. 1).

Alkylation of **1a–e** with CEM-SMe proceeds in 80–90% yield to give **2a–e**. Diols **3a–e** can be easily obtained from the deprotection of **2a–e** and the crystallization from the reaction mixture directly. Then, the protection of 5′-OH group and the phosphitylation of 3′-OH group give the CEM amidites **5a–e** (Fig. 2).
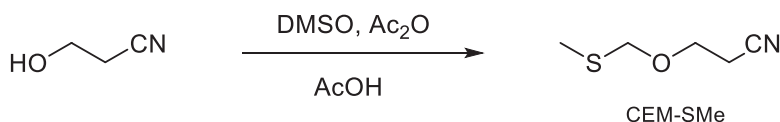
Fig. 1 Preparation of CEM-SMe
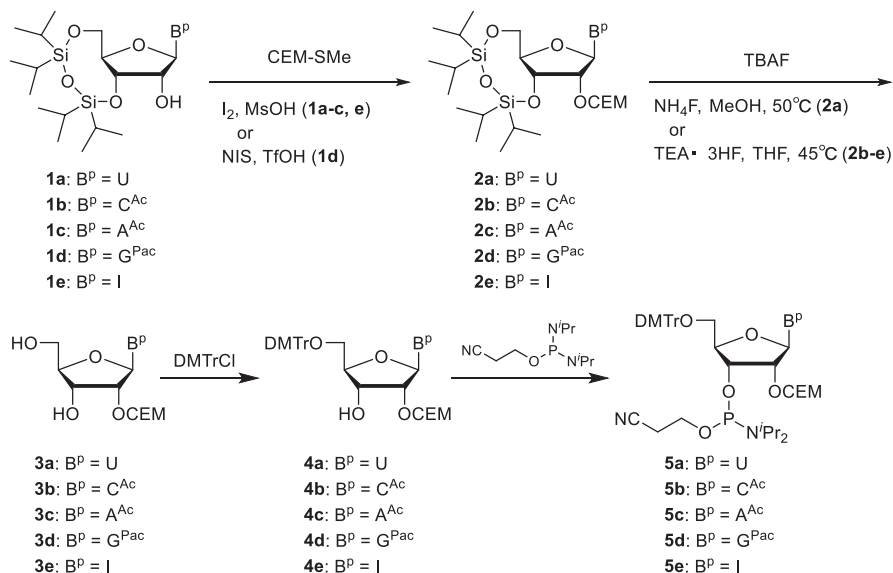
Fig. 2 Synthesis of CEM amidites
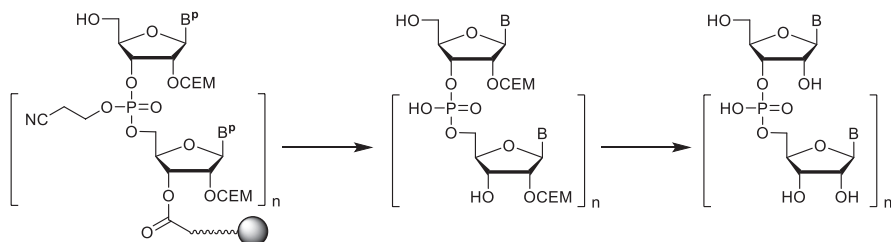
Fig. 3 Synthesis of RNA

3 Synthesis of RNA

For oligomer synthesis with CEM amidites, controlled-pore glass (CPG) is used as the solid support and 5-ethyl-1*H*-tetrazole as the activating agent with a coupling time of 150 s. Unlike CPG, polystyrene resins swell during the synthetic cycle, so that although they can be used for the synthesis of shorter oligomers, in our experience they are unsuitable for the synthesis of longer oligomers (>80 nt) (Fig. 3).

4 Experimental Section

4.1 Preparation of CEM-SMe

Acetic anhydride (324 mL) and acetic acid (231 mL) were added into 3-hydroxypropionitrile (32 g, 450 mmol) in DMSO (450 mL) at room temperature. After stirring for 24 h, an aq. NaHCO$_3$ suspension (990 g in 4.5 L) was dropped slowly into the reaction mixture for 1 h. Then the mixture was stirred for 1 h. The mixture was extracted with AcOEt, dried with Na$_2$SO$_4$, and evaporated off to give crude oil. The desired product (CEM-SMe) was obtained by the distillation of the oil (38 g, 64% yield, b.p. 82–84 °C/2 mmHg).

^{1}H NMR (CDCl$_3$): δ 2.18 (*s*, 3H), 2.66 (*t*, 2H, *J* = 6.3 Hz), 3.77 (*t*, 2H, *J* = 6.3 Hz), 4.69 (s, 2H).

4.2 Synthesis of U-CEM Phosphoramidite (5a.)

4.2.1 3′,5′-*O*-(Tetraisopropyldisiloxane-1,3-diyl)-2′-*O*-(2-cyanoethoxymethyl)uridine (2a.)

3′,5′-*O*-(Tetraisopropyldisiloxane-1,3-diyl) uridine (1a, 50.6 g, 104 mmol) was coevaporated with toluene twice (2 × 150 mL) and dried in vacuo for 1 h. The residue was dissolved in dry THF (100 mL) under Ar and cooled to 0 °C. To the

solution, MeSO$_3$H (0.76 mL, 0.1 eq.) was added dropwise over a 3-min period. After 10 min, I$_2$ (158 g, 6 eq.) was added quickly and the mixture stirred for 10 min. Then 2-cyaonoethyl methylthiomethyl ether (16.4 g, 1.2 eq.) was added dropwise over a 10-min period and the mixture stirred at 0 °C. After 30 min, the reaction was analyzed by HPLC and it was confirmed that the reaction was complete. After a further 15 min the reaction mixture, kept at 0 °C, was added dropwise to an ice-cooled mixture of sat. aq. NaHCO$_3$ (500 mL), sat. aq. Na$_2$S$_2$O$_3$ (500 mL), and AcOEt (100 mL) with vigorous stirring and confirmation of the disappearance of the brown color of I$_2$. (This treatment requires about 40 min. The pH of the aqueous phase was confirmed to be basic with pH paper during treatment). The mixture was then extracted with AcOEt (700 mL) and the aqueous layer re-extracted with AcOEt (500 mL). The organic layers were combined and washed with H$_2$O (1000 mL), then with sat. aq. NaCl (500 mL), dried over MgSO$_4$, and concentrated to afford the residue (**2a**, 70.8 g).

^{1}H NMR(500 MHz, CDCl$_3$): δ 0.97–1.12(*m*, 28H); 2.68–2.73(*m*, 2H); 3.78–3.86(*m*, 1H); 3.96–4.05(*m*, 2H); 4.12–4.30(*m*, 4H); 5.0–5.04(*m*, 2H); 5.70(*d*, 1H, *J* = 8.2 Hz); 5.75(*s*, 1H); 7.90(*d*, 1H, *J* = 8.2 Hz); 9.62(*br.s*, 1H). ^{13}C NMR (125 MHz, CDCl$_3$): δ 12.8, 13.0, 13.4, 18.7, 59.2, 62.7, 68.1, 77.8, 81.7, 89.1, 94.4, 101.8, 118.0, 139.1, 150.2, 163.5.

4.2.2 2′-*O*-(2-Cyanoethoxymethyl)uridine (3a.)

To the residue (**2a**, 70.8 g) obtained as described above in dry MeOH (300 mL), NH$_4$F (11.6 g, 3.0 eq.) was added and the mixture heated at 50 °C for 7.5 h under Ar. After the deprotection was judged to be sufficient by HPLC monitoring, the solvent was evaporated off. After the addition of CH$_3$CN (400 mL), the resulting precipitate was filtered and washed with CH$_3$CN (100 mL). (The precipitate changed from powder form to crystal form after washing with CH$_3$CN.) The filtrate was extracted with hexane (2 × 500 mL) and the hexane phase was removed. After the CH$_3$CN phase was concentrated, the residue was dissolved in EtOH (170 mL), which was crystallized with the assistance of ultrasonic waves. The resulting crystals were filtered and dried to give **3a** (21.5 g; 63% yield; 2 steps; HPLC purity, >99%). mp 124.5 °C.

^{1}H-NMR(500 MHz, DMSO-d_6): δ 2.72–2.76(*m*, 2H); 3.55–3.71(*m*, 4H); 3.87(s, 1H); 4.10–4.16(*m*, 2H); 4.76(*s*, 2H); 5.15–5.17(*m*, 1H); 5.25(*d*, 1H, *J* = 4.6 Hz); 5.64(*d*, 1H, *J* = 8.1 Hz); 5.87(*d*, 1H, *J* = 4.6 Hz); 7.93(d, 1H, *J* = 8.1 Hz); 11.35(*bs*, 1H). ^{13}C NMR (125 MHz, DMSO-d_6): δ 18.0, 60.3, 62.4, 68.5, 78.3, 85.0, 86.3, 93.8, 101.9, 119.0, 140.3, 150.6, 163.0. Anal. Calcd for C$_{13}$H$_{17}$N$_3$O$_7$: C, 47.71; H, 5.24; N, 12.84. Found: C, 47.57; H, 5.21; N, 12.64.

4.2.3   5′-*O*-(4,4′-Dimethoxytrityl)-2′-*O*-(2-xyanoethoxymethyl)uridine (4a.)

3a (33.8 g, 103 mmol) was coevaporated with dry pyridine and dried in vacuo for 1 h. The residue was dissolved in dry pyridine (600 mL) under Ar, to which 4,4′-dimethoxytrityl chloride (40 g, 118 mmol) was added, and the mixture was stirred at room temperature for 2.5 h. After the consumption of the starting material was judged to be sufficient by TLC, the mixture was evaporated at 40 °C, diluted with CH_2Cl_2, and partitioned between sat. aq. $NaHCO_3$ and CH_2Cl_2. The organic layer was washed with H_2O, dried over Na_2SO_4, and then concentrated at 40 °C. The residue was purified by column chromatography on silica gel to give **4a** (50.8 g, 78% yield).

Silica gel chromatography: hexane/AcOEt/acetone +0.05% (v/v) pyridine, 2/1/1 (v/v/v) → 1.5/1/1 (v/v/v).

^{1}H NMR(500 MHz, $CDCl_3$): δ 2.47(*d*, 1H, *J* = 7.8 Hz); 2.69(*t*, 2H, *J* = 6.3 Hz); 3.55(*dd*, 1H, *J* = 11.3, 2.2 Hz); 3.62(*dd*, 1H, *J* = 11.3, 2.2 Hz); 3.83(s, 6H); 3.87(*t*, 2H, *J* = 6.3 Hz); 4.07–4.08(*m*, 1H); 4.32(*dd*, 1H, *J* = 5.3,1.9 Hz); 4.54(*q*, 1H, *J* = 5.3 Hz); 4.94,5.11(2*d*, 2H, *J* = 6.9 Hz); 5.32(*d*, 1H, *J* = 8.2 Hz); 6.00(*d*, 1H, *J* = 1.9 Hz); 6.85–6.88(*m*, 4H); 7.29–7.41(*m*, 9H); 8.02(*d*, 1H, *J* = 8.2 Hz); 8.53(*bs*, 1H). ^{13}C NMR (125 MHz, $CDCl_3$): δ 19.0, 55.3, 61.3, 63.5, 68.9, 80.0, 83.2, 87.3, 88.0, 95.0, 102.3, 113.4, 117.8, 127.2, 128.1, 128.2, 130.1, 130.2, 135.0, 135.2, 139.8, 144.3, 150.0, 158.7, 158.8, 162.5. Anal. Calcd for $C_{34}H_{35}N_3O_9(+1/2H_2O)$: C, 63.94; H, 5.68; N, 6.58. Found: C, 63.97; H, 5.67; N, 6.64.

4.2.4   5′-*O*-(4,4′-Dimethoxytrityl)-2′-*O*-(2-cyanoethoxymethyl)uridine 3′-*O*-(2-Cyanoethyl *N, N*-diisopropylphosphoramidite) (5a.)

The mixture of **4a** (48.0 g, 76.2 mmol) and diisopropylamine tetrazolide (14.6 g, 85.0 mmol) was suspended in dry CH_3CN (400 mL) under Ar. To the mixture, bis(*N,N*-diisopropylamino)(cyanoethoxy)phosphine (25.6 g, 84.8 mmol) in CH_3CN (100 mL) was added and heated at 40 °C for 2.0 h. After the consumption of the starting material was judged to be sufficient by TLC, the reaction mixture was evaporated at 40 °C and diluted with CH_2Cl_2, then transferred directly to the top of silica gel and purified to give the corresponding product **5a** (51.9 g, 82% yield).

Silica gel chromatography: hexane/AcOEt +0.05% (v/v) pyridine, 1/1 (v/v) → 1/1.5 (v/v) → 1/2 (v/v).

UV (CH_3CN): λ (ε) = 237 (19700), 263 (sh, 10,100), 282 (sh, 3700). ^{31}P NMR (202 MHz, $CDCl_3$): δ 151.8, 153.4. Anal. Calcd for $C_{43}H_{52}N_5O_{10}P(+H_2O)$: C, 60.91; H, 6.42; N, 8.26. Found: C, 60.94; H, 6.13; N, 8.39.

4.3   Synthesis of C-CEM Phosphoramidite (5b.)

4.3.1   4-*N*-Acetyl-3′, 5′-*O*-(tetraisopropyldisiloxane-1,3-diyl)-2′-*O*-(2-cyanoethoxymethyl)cytidine (2b.)

4-*N*-Acetyl-3′,5′-*O*-(tetraisopropyldisiloxane-1,3-diyl)cytidine   (**1b**,   70   g, 132.6 mmol) was dried in vacuo, dissolved in dry THF (132 mL) under Ar, and cooled to 0 °C. After 15 min, MeSO$_3$H (10.3 mL, 159.2 mmol, 1.2 eq.) was added dropwise to the solution over a 10-min period and stirred for 15 min. I$_2$ (201 g, 795 mmol, 6 eq.) was added quickly and then stirred for 15 min. To the mixture, 2-cyaonoethyl methylthiomethyl ether (24.48 mL, 1.5 eq.) was added dropwise over 10 min and stirred at 0 °C. After 15 min, the reaction mixture was analyzed by HPLC. After a further 15 min, the reaction mixture, kept at 0 °C, was added dropwise to an ice-cooled mixture of sat. aq. NaHCO$_3$ (800 mL), sat. aq. Na$_2$S$_2$O$_3$ (700 mL), and AcOEt (100 mL) with vigorous stirring and confirmation of the disappearance of brown color of I$_2$ (≈40 min). The pH of the aqueous phase was confirmed to be basic with pH paper during treatment. The mixture was then extracted with AcOEt (400 mL) and the aqueous layer re-extracted with AcOEt (2 × 400 mL). The organic layers were combined, washed with H$_2$O (500 mL) and sat. aq. NaCl (500 mL), dried over MgSO$_4$, and concentrated to afford the residue (**2b**, 101.7 g).

^{1}H NMR(500 MHz, CDCl$_3$): δ 0.90–1.11(*m*, 28H); 2.28(*s*, 3H); 2.62–2.79(*m*, 2H); 3.78–3.89(*m*, 1H); 3.96–4.04(*m*, 2H); 4.19–4.23(*m*, 3H); 4.30(*d*, 1H, *J* = 13.6 Hz); 5.00(*d*, 1H, *J* = 6.8 Hz); 5.09(*d*, 1H, *J* = 6.8 Hz); 5.77(*s*, 1H); 7.44(*d*, 1H, *J* = 7.5 Hz); 8.30(*d*, 1H, *J* = 7.5 Hz); 10.13(*s*, 1H). ^{13}C NMR (125 MHz, CDCl$_3$): δ 12.5, 12.8, 13.0, 13.3, 16.8, 16.9, 17.0, 17.2, 17.3, 17.4, 18.6, 24.9, 59.2, 62.6, 67.8, 77.5, 81.8, 90.0, 94.3, 96.2, 117.9, 144.0, 154.7, 162.8, 170.4. Anal. Calcd for C$_{27}$H$_{46}$N$_4$O$_8$Si$_2$(+1/2H$_2$O): C, 52.27; H, 7.64; N, 9.04. Found: C, 52.27; H, 7.41; N, 8.95.

4.3.2   4-*N*-Acetyl-2′-*O*-(2-cyanoethoxymethyl)cytidine (3b.)

The reaction described above was carried out again. The combined oily residue (**2b**, 206 g, 267.9 mmol) was dissolved in dry THF (600 mL), TEA/3HF (52.4 mL, 1.2 eq.) was added under Ar, and the mixture was heated at 45 °C for 2 h. After the reaction mixture was cooled to 0 °C, the resulting precipitate was filtered, washed with dry THF (2 × 500 mL), and dried to give **3b** (84.6 g; 86% yield; two steps; HPLC purity, 97%). mp 177.0 °C.

^{1}H NMR(500 MHz, D$_2$O): δ 2.13(*s*, 3H); 2.66–2.71(*m*, 2H); 3.72–3.78(*m*, 3H); 3.90(*dd*, 1H, 13.0, 2.6 Hz); 4.06–4.11(*m*, 1H); 4.20(*dd*, 1H, *J* = 7.1,5.2 Hz); 4.29(*dd*, 1H, *J* = 5.1,2.9 Hz); 4.83(*d*, 1H, *J* = 7.2 Hz); 4.94(*d*, 1H, *J* = 7.2 Hz); 5.95(*d*, 1H, *J* = 2.9 Hz); 7.25(*d*, 1H, *J* = 7.6 Hz); 8.25(*d*, 1H, *J* = 7.6 Hz). ^{13}C NMR (125 MHz, DMSO-*d$_6$*): δ 17.9, 24.3, 59.3, 62.3, 67.4, 78.7, 84.1, 88.7, 93.5, 95.2, 119.1, 144.9, 154.5, 162.4, 171.0. Anal. Calcd for C$_{15}$H$_{20}$N$_4$O$_7$(+1/2H$_2$O): C, 47.74; H, 5.61; N, 14.85. Found: C, 47.45; H, 5.47; N, 14.50.

4.3.3 4-*N*-Acetyl-5′-*O*- (4,4′-dimethoxytrityl) -2′ -*O*- (2-cyanoethoxymethyl)cytidine (4b.)

3b (27 g, 73 mmol) was coevaporated with dry pyridine and dried in vacuo for 30 min. The residue was dissolved in dry THF (250 mL) and dry pyridine (250 mL) under Ar. To the solution, molecular sieves 4A (40 g) was added and the mixture stirred for 30 min. To the mixture, 4,4′-dimethoxytrityl chloride was added at room temperature with stirring in three portions (12 g, 12 g, 13.3 g; total, 37.3 g; 110 mmol) at 1 h intervals and the mixture was stirred for further hour after the last addition. After the consumption of the starting material was judged to be sufficient by TLC, MeOH (5 mL) was added and the mixture stirred for 5 min. The reaction mixture was filtered through celite and washed with AcOEt. The filtrate was evaporated at 40 °C and partitioned between AcOEt and sat. aq. $NaHCO_3$. The organic layer was washed with sat. aq. NaCl, dried over Na_2SO_4, and concentrated at 40 °C. The residue was purified by column chromatography on silica gel to give **4b** (43.6 g, 88% yield).

Silica gel chromatography: hexane/AcOEt/acetone +0.05% (v/v) pyridine, 1/1/1 (v/v/v) → 0/1/1 (v/v/v).

^{1}H NMR(500 MHz, CDCl$_3$): δ 2.19(*s*, 3H); 2.56(*d*, 1H, *J* = 8.8 Hz); 2.65(*t*, 2H, *J* = 6.2 Hz); 3.55(*dd*, 1H, *J* = 10.5, 2.5 Hz); 3.63(*dd*, 1H, *J* = 10.5, 2.5 Hz); 3.82(*s*, 6H); 3.86(*t*, 2H, *J* = 6.2 Hz); 4.09–4.14(*m*, 1H); 4.28(*d*, 1H, *J* = 5.1 Hz); 4.44–4.49(*m*, 1H); 4.97,5.24(2*d*, 2H, *J* = 6.9 Hz); 5.96(*s*, 1H); 6.86–6.88(*m*, 4H); 7.09(*d*, 1H, *J* = 6.9 Hz); 7.26–7.42(*m*, 9H); 8.48(*d*, 1H, *J* = 6.9 Hz); 8.59(*bs*, 1H). ^{13}C NMR (125 MHz, CDCl$_3$): δ 19.0, 25.0, 55.3, 60.8, 63.4, 68.0, 79.9, 83.0, 87.2, 89.7, 84.9, 96.4, 113.4, 118.0, 127.2, 128.0, 128.2, 130.1, 135.2, 135.5, 144.3, 144.7, 155.0, 158.7, 158.8, 162.3, 169.7. Anal. Calcd for $C_{36}H_{38}N_4O_9(+1/2H_2O)$: C, 63.61; H, 5.78; N, 8.24. Found: C, 63.21; H, 5.77; N, 7.99.

4.3.4 4-*N*-Acetyl-5′-*O*-(4,4′-dimethoxytrityl)-2′-*O*-(2-cyanoethoxymethyl) cytidine 3′-*O*-(2-cyanoethyl *N, N*-diisopropylphosphoramidite) (5b.)

The mixture of **4b** (43.6 g, 65 mmol) and diisopropylamine tetrazolide (12.2 g, 71.5 mmol) was suspended in dry CH$_3$CN (250 mL) under Ar. To the mixture, bis(*N,N*-diisopropylamino)(cyanoethoxy)phosphine (21.5 g, 71.5 mmol) was added and the mixture heated at 40 °C for 2.5 h. After the consumption of the starting material was judged to be sufficient by TLC, the reaction mixture was evaporated at 40 °C and diluted with CH$_2$Cl$_2$, then transferred directly to the top of the silica gel column, purified, and concentrated at 40 °C. The residue was dissolved in AcOEt and precipitated by adding dropwise to hexane. The resulting precipitate was filtered and dried to give the corresponding product **5b** (44.4 g, 75% yield).

Silica gel chromatography: hexane/AcOiPr/acetone +0.05% (v/v) pyridine, 2/1/1 (v/v/v). After removal of the phosphite reagent, the eluent was changed as follows: hexane/AcOEt/acetone +0.05% (v/v) pyridine, 1/1/1 (v/v/v) → 1/2/2 (v/v/v).

UV (CH$_3$CN): λ (ε) = 237 (27400), 277 (6120), 283 (6660), 304 (7630). ^{31}P NMR (202 MHz, CDCl$_3$): δ 151.6, 153.7. Anal. Calcd for C$_{45}$H$_{55}$N$_6$O$_{10}$P(+H$_2$O): C, 60.80; H, 6.46; N, 9.45. Found: C, 60.87; H, 6.08; N, 9.49.

4.4 Synthesis of A-CEM Phosphoramidite (5c.)

4.4.1 6-*N*-Acetyl-3′,5′-*O*-(tetraisopropyldisiloxane-1,3-diyl)-2′-*O*-(2-cyanoethoxymethyl)adenosine (2c.)

6-*N*-Acetyl-3′,5′-*O*-(tetraisopropyldisiloxane-1,3-diyl) adenosine (**1c**, 60.0 g, 108.7 mmol) was coevaporated with toluene twice (2 × 100 mL) and dried in vacuo for 1 h. The residue was dissolved in dry THF (108 mL) under Ar and cooled to 0 °C. To the solution, MeSO$_3$H (1.04 g, 0.1 eq.) was added dropwise. After 10 min, I$_2$ (165.6 g, 6 eq.) was added quickly and stirred for 15 min. To the mixture, 2-cyaonoethyl methylthiomethyl ether (21.3 g, 1.5 eq.) was added and stirred at 0 °C for 2 h. The reaction mixture kept at 0 °C was added dropwise to the ice cooled mixture of sat. aq. NaHCO$_3$ (500 mL), sat. aq. Na$_2$S$_2$O$_3$ (500 mL), and AcOEt (200 mL) with vigorous stirring and confirmation of the disappearance of brown color of I$_2$ ($\approx$40 min). The mixture was then extracted with AcOEt. The organic layer was washed with sat. aq. NaHCO$_3$ and sat. aq. NaCl, dried over MgSO$_4$, and concentrated to afford the residue.

^{1}H NMR(500 MHz, CDCl$_3$): δ 0.98–1.11(*m*, 28H); 2.62(*s*, 3H); 2.69(*td*, 2H, *J* = 6.5, 1.5 Hz); 3.81–3.89(*m*, 1H); 4.02–4.09(*m*, 2H); 4.17(*d*, 1H, *J* = 9.4 Hz); 4.28(*d*, 1H, *J* = 13.4 Hz); 4.50(*d*, 1H, *J* = 4.5 Hz); 4.67(*dd*, 1H, *J* = 8.8, 4.5 Hz); 5.02(*d*, 1H, *J* = 7.0 Hz); 5.08(*d*, 1H, *J* = 7.0 Hz); 6.10(*s*, 1H); 8.34(*s*, 1H); 8.66(*s*, 1H); 8.67(*s*, 1H). ^{13}C NMR (125 MHz, CDCl$_3$): δ 12.6, 12.8, 13.3, 16.8, 16.9, 17.0, 17.1, 17.2, 17.4, 18.8, 25.6, 59.6, 62.9, 68.8, 78.2, 81.5, 88.7, 94.8, 117.5, 122.3, 140.7, 149.1, 150.1, 152.3, 170.3. Anal. Calcd for C$_{28}$H$_{46}$N$_6$O$_7$Si$_2$: C, 52.97; H, 7.30; N,13.24. Found: C, 52.68; H, 7.30; N, 13.10.

4.4.2 6-*N*-Acetyl-2′-*O*-(2-cyanoethoxymethyl)adenosine (3c.)

The reaction described above was carried out three times. The combined oily residue (**2c**, 181.27 g, 328.5 mmol) was dissolved in dry THF (650 mL), TEA·3HF (63.5 g, 1.2 eq.) was added under Ar, and the mixture was heated at 45 °C for 3 h. The resulting precipitate was cooled to 0 °C, filtered, washed with dry THF (200 mL), 10% MeOH/AcOEt solution (MeOH/AcOEt, 1:9; 2 × 200 mL), and dried to give **3c** (85.9 g; 66.6% yield; two steps; HPLC purity, 98.8%). mp 167.0 °C.

^{1}H NMR(500 MHz, DMSO-*d$_6$*): δ 2.25(*s*, 3H); 2.53–2.68(*m*, 2H); 3.41–3.46(*m*, 1H); 3.56–3.64(*m*, 2H); 3.69–3.73(*m*, 1H); 4.00–4.01(*m*, 1H); 4.36–4.37(*m*, 1H); 4.72–4.78(*m*, 3H); 5.20(*bt*, 2H, *J* = 5.5 Hz); 5.41(*d*, 1H, *J* = 5.2 Hz); 6.17(*d*, 1H, *J* = 5.7 Hz); 8.66(*s*, 1H); 8.72(*s*, 1H); 10.72(*s*, 1H). ^{13}C NMR (125 MHz, DMSO-*d$_6$*):

δ 17.8, 24.3, 61.0, 62.3, 69.1, 78.6, 86.0, 86.1, 94.1, 118.9, 123.6, 142.6, 149.6, 151.5, 151.7, 168.8. Anal. Calcd for $C_{16}H_{20}N_6O_6$: C, 48.98; H, 5.14; N, 21.42. Found: C, 48.72; H, 5.06; N, 21.06.

4.4.3   6-*N*-Acetyl-5′-*O*-(4,4′-dimethoxytrityl)-2′-*O*-(2-cyanoethoxymethyl)adenosine (4c.)

3c (27.2 g, 70 mmol) was coevaporated with dry pyridine (100 mL) and dried in vacuo for 1 h. The residue was dissolved in dry pyridine (300 mL) under Ar, 4,4′-dimethoxytrityl chloride (33.3 g, 98 mmol) was added at 0 °C, and the mixture was stirred at room temperature for 3 h. After the consumption of the starting material was judged to be sufficient by TLC, the mixture was concentrated at 40 °C, diluted with CH_2Cl_2, and partitioned between CH_2Cl_2 and water. The organic layer was washed with sat. aq. $NaHCO_3$, dried over Na_2SO_4, and concentrated at 35 °C. The residue was purified by column chromatography on silica gel to give **4c** (43.6 g, 91% yield).

Silica gel chromatography: hexane/AcOEt/acetone +0.05% (v/v) pyridine, 1/1/1 (v/v/v) → 1/2/2 (v/v/v).

^{1}H NMR(500 MHz, CDCl$_3$): δ 2.51(*t*, 2H, *J* = 6.2 Hz); 2.58(*d*, 1H, *J* = 5.5 Hz); 2.61(*s*, 3H); 3.45(*dd*, 1H, *J* = 10.7,4.0 Hz); 3.54(*dd*, 1H, *J* = 10.7,3.2 Hz); 3.62–3.79(*m*, 2H); 3.79(*s*, 6H); 4.25(*bq*, 1H, *J* = 4.6 Hz); 4.59(*q*, 1H, *J* = 5.2 Hz); 4.87–4.94(*m*, 3H); 6.23(d, 1H, *J* = 4.4 Hz); 6.80–6.83(*m*, 4H); 7.22–7.32(*m*, 7H); 7.40–7.43(*m*, 2H); 8.20(s, 1H); 8.61(*bs*, 1H); 8.62(*s*, 1H). ^{13}C NMR (125 MHz, CDCl$_3$): δ 18.8, 25.7, 55.3, 63.0, 63.5, 70.5, 80.1, 84.1, 86.8, 87.1, 95.7, 113.3, 117.5, 122.1, 127.0, 127.9, 128.2, 129.1, 130.1, 135.5, 141.7, 144.4, 149.3, 150.9, 152.5, 158.6, 170.5. Anal. Calcd for $C_{37}H_{38}N_6O_8$(+H_2O): C, 62.35; H, 5.65; N, 11.79. Found: C, 62.77; H, 5.56; N, 11.55.

4.4.4   6-*N*-Acetyl-5′-*O*-(4,4′-dimethoxytrityl)-2′-*O*-(2-cyanoethoxymethyl) adenosine 3′-*O*-(2-Cyanoethyl *N, N*-diisopropylphosphoramidite) (5c.)

The mixture of **4c** (43.0 g, 61.9 mmol) and diisopropylammonium tetrazolide (11.8 g, 68.9 mmol) was suspended in dry CH_3CN (400 mL) under Ar. To the mixture, bis(*N,N*-diisopropylamino)(cyanoethoxy)phosphine (20.5 g, 68.0 mmol) was added and heated at 40 °C for 2.5 h. After the consumption of the starting material was judged to be sufficient by TLC, the reaction mixture was evaporated at 40 °C and diluted with CH_2Cl_2, then transferred directly to the top of the silica gel column and purified to give the corresponding product **5c** (52.5 g, 95% yield).

Silica gel chromatography: AcOEt/acetone +0.05% (v/v) pyridine, 5/1 (v/v).

UV (CH$_3$CN): λ (ε) = 237 (18100), 241 (sh, 16,400), 271 (16,700). ^{31}P NMR (202 MHz, CDCl$_3$): δ 152.7, 152.8. Anal. Calcd for $C_{46}H_{55}N_8O_9P$(+1/2H_2O): C,61.11; H, 6.24; N, 12.40. Found: C, 61.12; H, 6.04; N, 12.48.

4.5　Synthesis of CEM-G Phosphoramidite (5d.)

4.5.1　2N-Phenoxyacetyl-3′,5′-O-(tetraisopropyldisiloxane-1,3-diyl)-2′-O-(2-cyanoethoxymethyl)guanosine (2d.)

2N-Phenoxyacetyl-3′,5′-O-(tetraisopropyldisiloxane-1,3-diyl) guanosine (**1d**, 100 g, 152 mmol) and 2-cyaonoethyl methylthiomethyl ether (29.8 g, 1.5 eq.) were dissolved in dry THF (300 mL) under Ar. To the solution, CF_3SO_3H (21.1 mL, 1.5 eq.) was added slowly dropwise at $-45\ °C$ over 10 min. Then, N-iodosuccinimide (51.1 g, 1.5 eq.) was added and stirred for 30 min. To the reaction mixture, triethylamine (35 mL, 1.65 eq.) was added dropwise. The mixture cooled at $-45\ °C$ was poured into the ice cooled mixture of sat. aq. $NaHCO_3$ (500 mL), sat. aq. $Na_2S_2O_3$ (500 mL), and AcOEt (500 mL) with vigorous stirring followed by extraction with AcOEt. The aqueous layer was extracted with AcOEt again. The combined organic layer was washed with sat. aq. $Na_2S_2O_3$, sat. aq. $NaHCO_3$, sat. aq. NaCl, dried over $MgSO_4$, and concentrated to give the residue (**2d**, 122.46 g).

　^{1}H NMR(500 MHz, $CDCl_3$): δ 0.99–1.11(m, 28H); 2.59–2.77(m, 2H); 3.82–4.05(m, 3H); 4.15(d, 1H, J = 9.3 Hz); 4.25–4.35(m, 2H); 4.52–4.56(dd, 1H, J = 9.3,4.3 Hz); 5.00,5.07(2d, 2H, J = 7.2 Hz); 5.95(s, 1H) 6.99–7.12(m, 3H); 7.35–7.40(m, 2H); 8.09(s, 1H); 9.38(bs, 1H); 11.85(bs, 1H). ^{13}C NMR (125 MHz, $CDCl_3$): δ 12.6, 12.8, 12.9, 13.3, 16.8, 16.9, 17.1, 17.2, 17.4, 18.9, 59.5, 63.0, 67.1, 68.7, 79.3, 81.5, 87.8, 94.8, 114.8, 117.6, 122.3, 122.8, 129.9, 136.7, 146.4, 146.7, 155.3, 156.6, 169.8. Anal. Calcd for $C_{34}H_{50}N_6O_9Si_2(+1/2H_2O)$: C, 54.31; H, 6.84; N, 11.18. Found: C, 54.23; H, 6.72; N, 11.22.

4.5.2　2N-Phenoxyacetyl-2′-O-(2-cyanoethoxymethyl)guanosine (3d.)

The residue obtained as described above (**2d**, 118 g) was dissolved in dry THF (300 mL). To the solution, TEA·3HF (23.5 g, 1.0 eq.) was added under Ar and heated at 35 °C for 2 h. The reaction mixture was cooled to 0 °C, H_2O (60 mL) was added, and the mixture was stirred for 1 h. To this mixture, Et_2O (900 mL) was added. After stirring at room temperature for 30 min, the resulting precipitate was filtered, washed with cold EtOH (2 × 300 mL), Et_2O (300 mL), and dried to give **3d** (58.8 g; 80.5% yield; two steps; HPLC purity, 97.1%). mp 112.7 °C.

　^{1}H NMR(500 MHz, DMSO-d_6): δ 2.59–2.66(m, 2H); 3.41–3.63(m, 4H); 3.98(m, 1H); 4.32(m, 1H); 4.58–4.62(t, 1H, J = 5.3 Hz); 4.71–4.78(dd, 2H, J = 13.1, 6.8 Hz); 4.87(s, 2H); 5.12(s, 1H) 5.37(s, 1H); 5.97(d, 1H, J = 6.1 Hz) 6.96–6.99(m, 3H); 7.28–7.34(m, 2H); 8.30(s, 1H); 11.78(bs, 2H). ^{13}C NMR (125 MHz, DMSO-d_6): δ 17.8, 61.0, 62.3, 66.3, 69.1, 78.7, 85.0, 86.1, 93.9, 114.4, 114.5, 119.0, 120.3, 121.3, 129.5, 137.8, 147.6, 148.5, 154.9, 157.6, 171.0.

4.5.3 2N-Phenoxyacetyl -5′-O- (4,4′-dimethoxytrityl) -2′ -O- (2-cyanoethoxymethyl)guanosine (4d.)

3d (27.5 g, 55 mmol) was coevaporated with dry pyridine and dried in vacuo for 30 min. The residue was dissolved in dry THF (270 mL) and dry pyridine (270 mL) under Ar. To the solution, molecular sieves 4A (28 g) was added and stirred for 10 min. To the mixture, 4,4′-dimethoxytrityl chloride was added at room temperature with stirring in three portions (9 g, 9 g, 9.9 g; total, 27.9 g; 82 mmol) at intervals of 1 h and the mixture was stirred for a further hour after the last addition. After the consumption of the starting material was judged to be sufficient by TLC, MeOH (10 mL) was added and stirred for 2 min. The reaction mixture was filtered through celite and washed with CH_2Cl_2. The filtrate was evaporated at 40 °C and partitioned between sat. aq. $NaHCO_3$ and CH_2Cl_2. The organic layer was washed with sat. aq. NaCl, dried over Na_2SO_4, and then concentrated at 40 °C. The residue was purified by column chromatography on silica gel to give **4d** (43 g, 97% yield).

Silica gel chromatography: $CH_2Cl_2/CH_3CN/MeOH$ +0.05% (v/v) pyridine, 300/100/8 (v/v/v).

^{1}H NMR(500 MHz, $CDCl_3$): δ 1.92(s, 3H); 2.47–2.51(m, 2H); 2.68(bs, 1H); 3.30(dd, 1H, 10.7, 3.8 Hz); 3.47(dd, 1H, 10.7, 3.8 Hz); 3.55–3.60(m, 1H); 3.65–3.70(m, 1H); 3.74,3.75($2s$, 6H); 4.22–4.23(m, 1H); 4.55–4.58(m, 1H); 4.78,4.83($2d$, 2H, J = 7.0 Hz); 5.01(t, 1H, J = 5.1 Hz); 5.99(d, 1H, J = 5.1 Hz); 6.76–6.79(m, 4H); 7.17–7.44(m, 9H); 7.88(s, 1H); 8.36(bs, 1H); 12.06(bs, 1H). ^{13}C NMR (125 MHz, $CDCl_3$): δ 18.9, 55.3, 63.3, 63.5, 67.0, 70.7, 79.8, 84.3, 85.6, 86.9, 95.3, 113.3, 114.9, 117.5, 122.1, 123.0, 127.1, 128.0, 128.1, 130.0, 130.1, 135.4, 135.5, 137.5, 144.4, 146.5, 148.0, 155.3, 156.4, 158.7, 169.6. Anal. Calcd for $C_{43}H_{42}N_6O_{10}$(+1/2H_2O): C, 63.60; H, 5.33; N, 10.35. Found: C, 63.62; H, 5.22; N, 10.47.

4.5.4 2N-Phenoxyacetyl-5′-O-(4,4′-dimethoxytrityl)-2′-O-(2-cyanoethoxymethyl)guanosine 3′-O-(2-Cyanoethyl N, N-diisopropylphosphoramidite) (5d.)

The mixture of **4d** (43 g, 54 mmol) and diisopropylammonium tetrazolide (10.1 g, 59 mmol) was suspended in dry CH_3CN (215 mL) under Ar. To the mixture, bis(N,N-diisopropylamino)(cyanoethoxy)phosphine (32.4 g, 107 mmol) was added and heated at 40 °C for 5 h. and stirred at room temperature for 16 h. After the consumption of the starting material was judged to be sufficient by TLC, the reaction mixture was evaporated at 40 °C and diluted with CH_2Cl_2, transferred directly to the top of the silica gel column and purified, then concentrated at 40 °C. The residue was dissolved in AcOEt, and added dropwise to hexane. The resulting precipitation was filtered and dried to give the corresponding product **5d** (37.9 g, 70% yield).

Silica gel chromatography: AcOEt/CH_3CN + 0.05% (v/v) pyridine, 40/1 (v/v).

UV (CH_3CN): λ (ε) = 238 (27700), 257 (sh, 18,300), 274 (sh, 13,800), 284 (sh, 10,100). ^{31}P NMR (202 MHz, $CDCl_3$): δ 152.7, 152.8. Anal. Calcd for $C_{52}H_{59}N_8O_{11}P$(+H_2O): C,61.17; H, 6.02; N, 10.97. Found: C, 61.20; H, 5.68; N, 10.94.

4.6 Synthesis of CEM-I Phosphoramidite (5e.)

4.6.1 3′,5′-O-(Tetraisopropyldisiloxane-1,3-Diyl)-2′-O-(2-cyanoethoxymethyl)inosine (2e.)

3′,5′-O-(tetraisopropyldisiloxane-1,3-diyl) inosine (**1e**, 51.0 g, 100 mmol) was dissolved into dry THF (200 mL). $MeSO_3H$ (13.0 mL, 200 mmol) was added slowly dropwise at 0 °C. Then, 2-cyaonoethyl methylthiomethyl ether (19.7 g, 150 mmol) and iodine (152 g, 600 mmol) were added and stirred for 30 min. The reaction mixture was poured into the mixture of sat. aq. $NaHCO_3$ – sat. aq. $Na_2S_2O_3$ (1/2). The aqueous layer was extracted with AcOEt. The combined organic layer was washed with the mixture of sat. aq. $NaHCO_3$ – sat. aq. $Na_2S_2O_3$ (1/1), washed with sat. aq. NaCl, dried over Na_2SO_4, and concentrated to give the precipitate (**2e**, 94.3 g).

ESI-MS: 594 (m+H), 616 (m+Na). Anal. Calcd for $C_{26}H_{43}N_5O_7Si_2$ (+0.3H_2O): C, 52.11; H, 7.33; N, 11.69. Found: C, 52.43; H, 7.37; N, 11.31.

4.6.2 2′-O-(2-Cyanoethoxymethyl)inosine (3e.)

2e (94.3 g, 100 mmol, the precipitate above) was dissolved in dry THF (200 mL). To the solution, TEA·3HF (19.6 g, 120 mmol) was added under Ar and heated at 45 °C for 3 h. The reaction mixture was cooled to 0 °C. After removal of the supernatant, the mixture concentrated to give **3e** (36.8 g, crude).

ESI-MS: 350 (m-H). Anal. Calcd for $C_{14}H_{17}N_5O_6$ (H_2O): C, 45.53; H, 5.19; N, 18.96. Found: C, 45.57; H, 4.39; N, 19.12.

4.6.3 5′-O- (4,4′-Dimethoxytrityl) -2′ -O-(2-cyanoethoxymethyl)inosine (4e.)

3e (25.5 g, 69 mmol, crude) was dissolved in dry THF (200 mL) and dry pyridine (200 mL) under Ar. To the mixture, 4,4′-dimethoxytrityl chloride (31.6 g, 93.3 mmol) was added at room temperature. After stirring over night, MeOH (20 mL) was added to the mixture. The reaction mixture was stirred for 10 min and evaporated off. The residue was dissolved in AcOEt (500 mL). The organic layer was washed with aq. $NaHCO_3$, washed with sat. aq. NaCl, dried over Na_2SO_4, and then evaporated off. The residue was dissolved in AcOEt (150 mL) and cooled to 0 °C to give the precipitate. The precipitate was filtered off and dried in vacuo to give **4e** (30.1 g, 67% yield from **1e**).

ESI-MS: 652 (m-H). Anal. Calcd for $C_{35}H_{35}N_5O_8$ (+0.2H_2O): C, 63.96; H, 5.43; N, 10.65. Found: C, 63.62; H, 5.01; N, 10.43.

4.6.4   5′-*O*-(4,4′-Dimethoxytrityl)-2′-*O*-(2-cyanoethoxymethyl)inosine 3′-*O*-(2-Cyanoethyl *N, N*-diisopropylphosphoramidite) (5e.)

The mixture of **4e** (51.6 g, 78.9 mmol), diisopropylamine tetrazolide (17.6 g, 102.6 mmol), and molecular sieves 4A (20 g) were suspended in dry CH_3CN (416 mL) under Ar. To the mixture, bis(*N,N*-diisopropylamino)(cyanoethoxy)phosphine (30.9 g, 102.6 mmol) was added and heated at 40 °C for 7 h. The reaction mixture was cooled to 0 °C, filtered off, and then evaporated off to give the residue. The residue was purified by column chromatography on silica gel to give **5e** (55.5 g, 82% yield).

^{31}P NMR (202 MHz, $CDCl_3$): δ 152.6, 152.8.

Notes:

1. After dimethoxytritylation, the compounds should be treated while keeping the temperature below 45 °C in order to avoid detritylation.
2. When purification is carried out by column chromatography on silica gel, pyridine (0.05%) should be included in the eluent in order to avoid detritylation.
3. One of the main purposes of the column chromatography after the reaction **4 → 5** is to remove an impurity derived from the phosphite reagent, that cannot be monitored by HPLC.
4. When the column chromatography was carried out after the reaction **4 → 5**, the presence of an impurity derived from the phosphite reagent was checked by TLC monitoring, in which the TLC plate was heated with a heat gun after dipping it in 0.7% ninhydrin/EtOH solution.
5. Ahydrous condition is important in the reaction **1a-c, e → 2a-c, e**. The presense of H_2O make the following byproduct below.
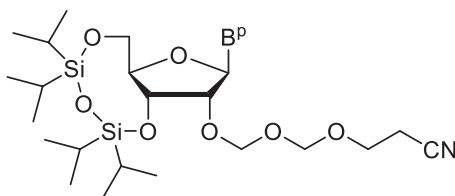
4.7   *Synthesis of Oligoribonucleotide*

CPG, functionalized with the appropriate first nucleoside, was placed in an empty 1-μmol synthesis column fitted with a filter. The column was installed in the synthesizer (Applied Biosystems, Expedite 8909). The reagents and solvents, shown in Table 1, were loaded into the synthesizer: 0.05 M CEM-amidite in CH_3CN (eight equiv.), Activator, Capping solutions A and B, Oxidizing solution, and Deblocking solution. Solid phase synthesis was performed automatically on the synthesizer

Table 1 Reagents

Deblocking solution	3% trichloroacetic acid (TCA) in CH_2Cl_2
Activator	0.25 M 5-benzylthio-1*H*-tetrazole (BMT) in CH_3CN
Capping solutions A	0.2 M phenoxyacetic anhydride (Pac_2O) in THF
Capping solutions B	10% *N*-methylimidazole (NMI), 10% 2,6-lutidine in THF
Oxidizing solution	0.1 M I_2 in 7:1:2 (v/v/v) THF/pyridine/H_2O

Table 2 Synthetic conditions for a 1-µmol-scale synthesis

Step	Operation	Reagent	Time (s)
1	Deblocking	Deblocking solution	60
2	Coupling	0.05 M amidite in CH_3CN + Activator	150
3	Capping	Capping solution A + Capping solution B	30
4	Oxidation	Oxidizing solution	10
5	Capping	Capping solution A + Capping solution B	120

according the synthetic cycle shown in Table 2. 5′ end of the RNA was detritylated on the synthesizer. This detritylation step should be omitted when the RNA is purified with the DMTr group attached. The column was removed from the synthesizer, and dried in vacuo.

4.8   Cleavage and Deprotection

The CPG from the synthesis column was transferred to a 5-mL screw-cap vial. EtOH (0.5 mL) and 28% aqueous ammonia (1.5 mL) was added to the vial and cap it tightly. The mixture was heated for 2 h. in a 40 °C water bath. The CPG was removed from the suspension by using a 2.1-cm-diameter Kiriyama funnel fitted with filter paper, collecting the filtrate in a 30-mL round-bottom flask. The CPG was washed with water (1 mL) and then MeOH (5 mL). The filtrate in the 30-mL round-bottom flask was evaporated off to give an oily residue. The residue was dried in vacuo for at least 15 min to completely remove residual water. The residue was dissolved in DMSO (0.5 mL). CH_3NO_2 (5 µL) was added into the solution. The volume of CH_3NO_2 is 1% of the volume of TBAF solution added in the next step. 1 M TBAF solution (0.5 mL) was added into the solution and stir at 30 °C for 1 h. Twenty equivalents of TBAF per CEM group are required. For a 50-mer synthesized on a 1-µmol scale, 1000 µmol TBAF are required (50 CEM × 20 µmol TBAF/CEM), or 1.0 mL of 1 M TBAF solution. TBAF solution should not be added before adding the CH_3NO_2. For longer RNAs (>25 nt), a longer deprotection time (2–8 h) is needed. The solution was cooled to 0 °C, then 1 M Tris-Cl (0.5 mL) was added. The mixture was stirred for 15 min at 0 °C. The volume of 1 M Tris-Cl is equal to that

of the TBAF solution used. The mixture was poured into EtOH (10 mL) in a 15-mL centrifuge tube. The tube was centrifuged at 3000 rpm, 0 °C, for 5 min, and the ethanolic supernatant decanted off. The precipitate was dried in vacuo for at least 30 min to completely remove the EtOH. The residue was purified by reversed-phase or anion-exchange HPLC.

References

1. Usman N, Ogilvie KK, Jiang M-Y, Cedergren RJ (1987) The automated chemical synthesis of long oligoribonucleotides using 2′-O-silylated ribonucleotides 3′-O-phosphoramidites on a controlled-pore glass support: synthesis of a 43-nucleotide sequence similar to the 3′-half molecule of an *Escherichia coli* formylmethionine tRNA. J Am Chem Soc 109:7845–7854
2. Gough GR, Miller TJ, Mantick NA (1996) p-Nitrobenzyloxymethyl: a new fluoride-removable protecting group for ribonucleoside 2′-hydroxyls. Tetrahedron Lett 37:981–982
3. Welz R, Müller S (2002) 5-(benzylmercapto)-1H-tetrazole as activator for 2′-O-TBDMS phosphoramidite building blocks in RNA synthesis. Tetrahedron Lett 43:795–797
4. Scaringe SA, Wincott FE, Caruthers MH (1998) Novel RNA synthesis method using 5′-O-silyl-2′-O-orthoester protecting groups. J Am Chem Soc 120:11820–11821
5. Pitsch S, Weiss PA, Jenny L, Stutz A, Wu X (2001) Reliable chemical synthesis of oligoribonucleotides (RNA) with 2′-O-[(triisopropylsilyl)oxy]methyl (2′-O-tom)-protected phosphoramidites. Helv Chim Acta 84:3773–3795
6. Semenyuk A, Földesi A, Johansson T, Estmer-Nilsson C, Blomgren P, Brännvall M, Kirsebom LA, Kwiatkowski M (2006) Synthesis of RNA using 2′-O-DTM protection. J Am Chem Soc 128:12356–12357
7. Micura R (2002) Small interfering RNAs and their chemical synthesis. Angew Chem Int Ed 41:2265–2269
8. Ohgi T, Masutomi Y, Ishiyama K, Kitagawa H, Shiba Y, Yano J (2005) A new RNA synthetic method with a 2′-O-(2-cyanoethoxymethyl) protecting group (CEM). Org Lett 7:3477–3480
9. Shiba Y, Masuda H, Watanabe N, Ego T, Takagaki K, Ishiyama K, Ohgi T, Yano J (2007) Chemical synthesis of a very long oligoribonucleotide with 2-cyanoethoxymethyl (CEM) as the 2′-O-protecting group: structural identification and biological activity of a synthetic 110 mer precursor-microRNA candidate. Nucleic Acid Res 35:3287–3296
10. Nagata S, Hamasaki T, Uetake K, Masuda H, Takagaki K, Oka N, Wada T, Ohgi T, Yano J (2010) Synthesis and biological activity of artificial mRNA prepared with novel phosphorylating reagents. Nucleic Acid Res 38:7845–7857

Liquid-Phase Synthesis of Oligonucleotides

Satoshi Katayama and Kunihiro Hirai

Abstract This review will summarize recent progress of liquid-phase oligonucleotide synthesis and also briefly introduce the challenge to develop a process that applies our original liquid-phase synthesis technology for practical use.

Recent progress in various types of oligonucleotide therapeutics, such as antisense, aptamer, siRNA and miRNA, has led to growing demand for economical and/or large scale production. Conventionally-known solid-phase synthesis which has been only a method of choice over the past few decades rapidly supplies oligonucleotides in high quality but in a limited quantity. Major issues of solid-phase synthesis that need to be addressed are scale-up and manufacturing cost. The former is attributable to the dedicated synthesizer's capacity and the latter associate with heterogeneous reactions: use of expensive resins and excess amidite reagents.

Liquid-phase approaches may overcome these limitations. Behind the progress of solid-phase synthesis, researchers have investigated unique liquid-phase approaches. Among them, several methods utilizing soluble supports instead of solid resins are combining the advantage of solid-phase synthesis and liquid-phase synthesis, and expected to have possibility of industry applicable methods.

Keywords Liquid-phase oligonucleotide synthesis · Solution-phase · Large scale production · Soluble supports · Scale-up · AJIPHASE®

1 Introduction

For several decades, oligonucleotides have been known to have important diagnostics and therapeutic applications [1]. Recently, chemically modified oligonucleotide [2] such as 2′-*O*-methoxyethyl gapmers [3], 2′,4′-locked nucleic acids [4], and phosphodiamidate morpholino oligomers [5], have emerged as potential drugs that work through the antisense or exon skipping mechanisms. In 2013, the FDA

S. Katayama (✉) · K. Hirai
Bio-Functional Molecular Chemistry Group, Research Institute for Bioscience Products & Fine Chemicals, Ajinomoto Co. Inc., Kawasaki-ku, Kawasaki-shi, Japan
e-mail: satoshi_katayama@ajinomoto.com

approved the antisense drug Kynamro® [6] and several other oligonucleotide pipe-lines are currently in the late stage of human clinical trials. Currently, oligonucle-otides are produced using automated solid-phase synthesis involving phosphoramidite chemistry [7], and the development of an economical large-scale oligonucleotide synthesis has been an important issue for pharmaceutical companies and contract manufacturers. Solid-phase methods produce oligonucleotides of high quality up to the kilogram scale; however, for widespread use to be practical, further scaling-up is required. In its current form, solid-phase synthesis is difficult to scale-up due to the cost of the resins and the need for relatively large excesses of expensive reagents. Purification is also important because oligonucleotides for pharmaceutical applica-tions must be extremely pure.

A solution-phase approach to oligonucleotide synthesis is likely to overcome these limitations. The scalability of the process would be unlimited in much the same way as conventional organic synthesis, and the amount of reagent required may be reduced by conducting the reactions in homogeneous solutions. Numerous papers have been published that use solution-phase phosphotriester chemistry [8], *H*-phosphonate chemistry [9], or modified versions of these. One of the most impressive examples of *H*-phosphonate chemistry is the synthesis of the 20-mer antisense oligonucleotide Viravene® [9]. The highlight of the synthesis is the use of a convergent synthetic approach involving trimer oligonucleotide blocks to make the process economical; however, the major drawback of the method is that it requires laborious column chromatography purification after each condensation step. During the synthesis of long oligomers, their solubility can also hamper dis-solution of the reaction mixture.

The 'liquid-phase method' combines the advantages of the solution-phase and solid-phase methods and lacks the disadvantages described above. The concept was first demonstrated for the synthesis of peptides [10] and replaces the solid-support with soluble anchor molecules such as poly(ethylene glycol) (PEG) chains or other organic tags. The method allows homogeneous reactions to be carried out using stoichiometric amounts of the reagents, and easy dissolution and isolation are possible.

We have been developing a new liquid-phase method for oligonucleotide synthe-sis that uses AJIPHASE®—our method previously developed for peptide manufac-ture. In this paper, we review recent publications that describe the use of liquid-phase methods to synthesize oligonucleotide synthesis. In addition, we briefly introduce preliminary results concerning oligonucleotide synthesis using AJIPHASE®.

2 PEG-Based Liquid-Phase Synthesis

Replacing solid-phase resins with soluble polymers is the most straightforward way to carry out liquid-phase synthesis. Several approaches have been reported using, for example, cellulose acetate [11], β-cyclodextrin [12], and PEG. The most impor-tant PEG-based example may be the pioneering work by Bonora et al. involving the

highly efficient liquid-phase (HELP) method [13]. Importantly, the synthesis is performed in a homogeneous solution so it requires a smaller excess of reagents than solid-phase methods, growing intermediates can be isolated by precipitation and filtration, a large amount of oligonucleotide can be obtained from only one run, and the synthesis is easily monitored by non-destructive spectrophotometric methods.

The first oligonucleotide syntheses conducted using the PEG-based liquid-phase approach made use of well-known phosphotriester chemistry [14]. One method employed a protected phosphotriester as the building block. The condensation step was optimized using mesitylenesulfonylnitrotriazole (MSNT) as an activating agent, *N*-methylimidazole as catalyst, and anhydrous pyridine as solvent. The coupling yield ranged from 90% to 95%, used a threefold excess of nucleotide and the reaction time was 60 min. Another method used less-expensive protected nucleosides as the building block. They were phosphorylated in situ with the bi-functional reagent 2-chlorophenyl-*O*,*O*-bis(1-benzotriazolyl) phosphate, and after the activation step, the mixture was left to react for 60 min. Both of the above protocols were used to synthesize 8-mer DNA with moderate yields and quality.

Phosphoramidite chemistry [15] and *H*-phosphonate chemistry [16] have also been used in conjunction with the PEG-supported liquid-phase strategy. The phosphoramidite HELP method ("HELP Plus") was a clear improvement on the earlier HELP method in terms of reaction time, yield, and length of oligomers produced. Phosphoramidite synthons are widely used in solid-phase methods, but the HELP Plus method was the first liquid-phase method to use them. The synthesis of 20-mer DNA was achieved using the larger 12,000 Da PEG monoethylether as support. Phosphorothioate (PS) derivatives are widely recognized as important compounds for antisense therapeutics and 20-mer PS DNA has been prepared using the "HELP S" method [17]. Replacing the oxidation reaction with a sulfurization allowed the preparation of a fully sulfurized target compound in high yield. The use of *H*-phosphonate nucleotides allows the HELP Plus method to be even more economically efficient than other liquid-phase methods as they are as reactive, more stable, and less expensive than phosphoramidite nucleotides. Additionally, it is not necessary to perform an oxidation after each coupling step; a single oxidation of the final product is sufficient. However, in a preliminary study of the procedure, it was found that, unfortunately, the succinate bonds between PEG and oligonucleotide and the internucleotide *H*-phosphinate diester were unstable during the synthesis.

Currently, the most important PEG-supported liquid-phase synthesis may be the large-scale synthesis of phosphorothioate oligonucleotides using the blockmer strategy [18]. The synthons are fully protected 3′-5′ phosphorothioate dinucleotides, with a phosphoramidite group at the 3′ position, as a reacting moiety for coupling with the 5′-hydroxyl of the growing oligonucleotide chain (Fig. 1). The advantages of blockmers are that they reduce the level of n−1 deletion sequences and increase the yield by reducing the number of precipitation and filtration steps. The synthesis of a fully thiolated 15-mer was performed using a 10,000 Da methoxyl PEG support. The overall yield was 58% and the average yield of a single step was 92.5%. The lower average yield observed can be attributed to a reduced recovery of the growing chain toward the end of the synthesis. Chromatographic purification
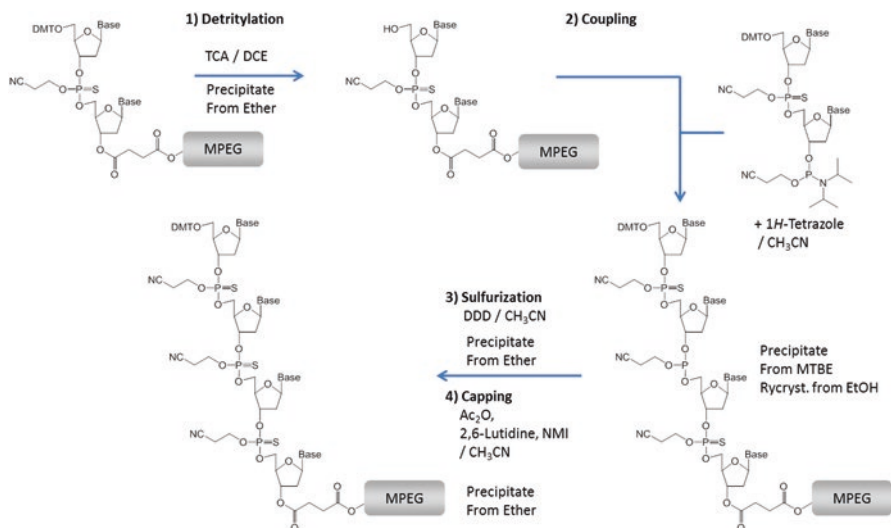
Fig. 1 Liquid-phase synthesis of oligonucleotides using the blockmer strategy and methoxyl poly(ethylene glycol) (MPEG). *Abbreviations*: *DCE* 1,2-dichloroethane, *DDD* diethyldithiodicarbonate, *DMT* bis-(4-methoxyphenyl)phenylmethyl, *MTBE* methyl *tert*-butyl ether, *NMI N*-methyl imidazole, *TCA* trichloroacetic acid

has been attempted using both reverse phase and strong anion-exchange HPLC. The purity of the crude material was 43.6% and the purity of the final material was 96.5%. This purity may not be high enough for pharmaceutical applications.

The utilization of PEG-supports in liquid-phase synthesis appears to be particularly convenient for commercially relevant large-scale syntheses. Because all of the chemical reactions are performed in solution, the scaling up of the process is simple. The use of phosphoramidite reagents offers the best reaction time, coupling yield, and oligonucleotide length; however, further improvement of the process is necessary to obtain higher purity compounds in an economical way.

3 Non-polymeric Anchor-Assisted Synthesis

3.1 Ionic Liquid Tag-Assisted Synthesis

The limitations of soluble polymer supports include low loading capacity and limited solubility when using longer sequences. To overcome these limitations, non-polymeric supports can be used (Fig. 2). For example, ionic liquid-based supports have been used by Donga et al. to synthesize tetrameric DNA and the pentaribonucleotide AGAUC using phosphoramidite chemistry [19]. Although the ionic-tag method solves the solubility problems that are encountered when using polymer-based methods, it is limited due to sluggish 5′-detritylation of the first nucleoside.
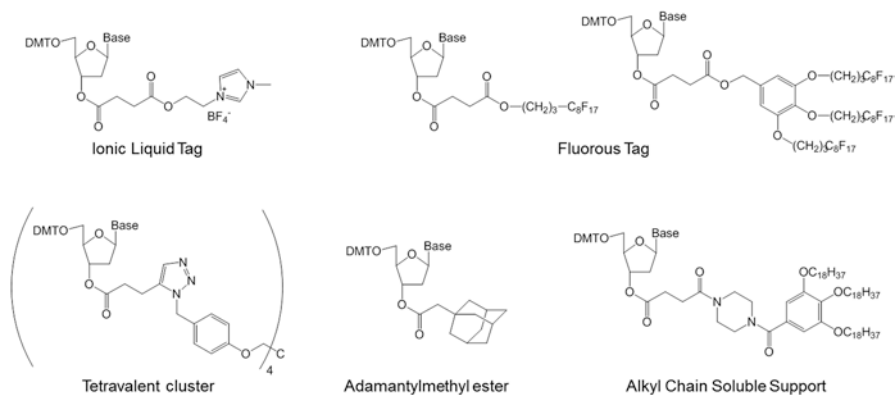
Fig. 2 Examples of non-polymeric soluble support molecules. *Abbreviation*: *DMT* bis-(4-methoxyphenyl)phenylmethyl

3.2   Fluorous Tag-Assisted Synthesis

Fluorous tags are used to simplify the separation and purification of intermediates in the synthesis of biopolymers because they enable the growing oligonucleotides to be purified by liquid-liquid extraction or solid-liquid extraction procedures and take advantage of the affinity of fluorous supports with fluorous solvents or silica gel. Wada et al. used fluorous supports derived from benzyl molecules with fluorine-bearing hydrocarbon groups for preparation of oligonucleotides [20]. They reported stereospecific synthesis of dinucleotides using thymidine derivatives bearing a simple perfluoroalkyl tag at the 3′ end and diastereopure 3′-oxazaphospholidine nucleoside monomers.

Other approaches include the use of a fluorous dimethoxytrityl protecting group at the 5′-hydroxy group of phosphoramidite monomers [21], or the use of fluorous silyl groups [22] at the 5′-end of the growing chain. Target oligonucleotides could be easily isolated from failed (n−1) and truncated sequences using liquid-liquid extraction, simple precipitation, or solid-phase extraction techniques. Fluorous affinity purification is a powerful tool that is especially useful for the isolation of long oligonucleotides, and extraction or precipitation approaches may be suitable for large-scale production.

3.3   Tetravalent Cluster Approach

Tetravalent cluster approaches combine phosphoramidite chemistry and triester chemistry for the synthesis of short oligonucleotides [23]. Over the course of the synthesis, the growing oligonucleotides—which are tetrahedrally branched from a pentaerythritol-derived core—are precipitated from methanol. The advantages of

this type of approach include good atom economy and easy analysis due to the small size and radially symmetric structure. However, further optimization is needed to avoid side reactions and improve the yield.

3.4 Adamntylmethylester Synthesis

On a very large scale, liquid-liquid extraction would be the method of choice for isolating the growing oligonucleotides and avoid time-consuming precipitations. An adamantylmethylester-based synthesis using adamantine acetic acid supports allows an extractive work-up approach to be used. However, several side reactions such as loss of cyanoethyl protecting groups on internucleotides or the loss of the benzoyl group from cytosine or adenosine bases were found to occur [24].

3.5 Alkyl Chain-Assisted Synthesis

Gallic acid derivatives with long alkyl chains have also been used in liquid-phase synthesis of biopolymers. Recently, the method was used in conjunction with phosphoramidite chemistry for the synthesis of a 21-mer RNA with a 3′-TT overhang region [25]. Although the yield and purity were high (98% average, 78% purity by HPLC after cleavage), the need for many purification steps (60 steps for a 21-mer oligonucleotide) makes the method unsuitable for industrial use.

As discussed in Sect. 5, the AJIPHASE® liquid-phase synthetic procedure also uses soluble, long alkyl chains. Our aim was to develop a method suitable for production of oligonucleotides at in quantities larger than 1 kg and a one-isolation-per-cycle procedure has been successfully developed.

4 Other Approaches

4.1 Product Anchored Sequential Synthesis (PASS) Method

PASS is a method that combines features of solid-phase and solution-phase techniques and may enable up scaling and isolation of the target compound from failure sequences (Fig. 3). Dimethoxytrityl resin (DMT) PASS is an interesting example of this approach [26]. This process consists of three steps per cycle: (1) coupling of a 3′-O-protected oligonucleotide substrate with DMT resin-bound monomer; (2) release of the n + 1 oligonucleotide from the DMT resin using acid treatment; (3) isolation of desired growing chain by simple aqueous/organic extraction. The PASS process allows facile removal of reagents, does not create highly homologous impurities such as n − 1 oligonucleotides, and uses a recyclable DMT resin. The problems encountered when using this method in conjunction with phosphoramidite
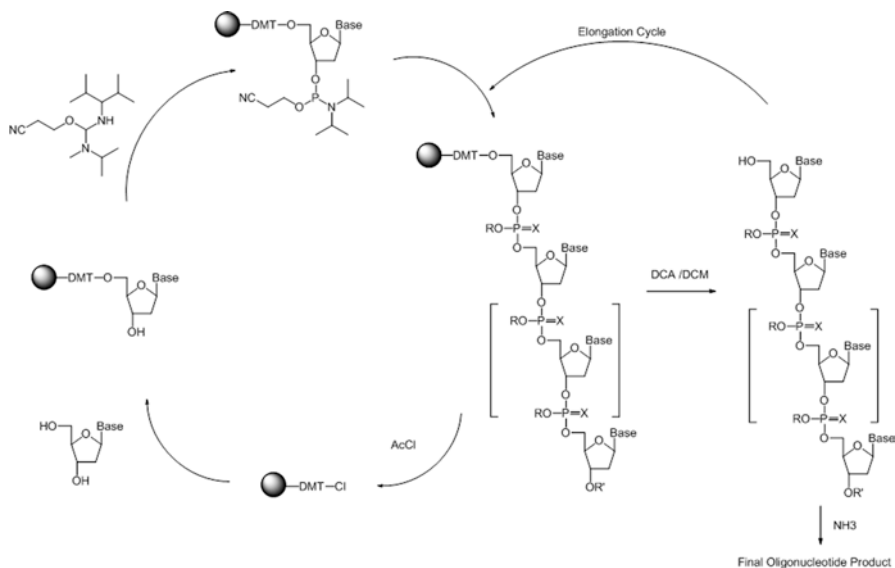
Fig. 3 Scheme showing the product anchored sequential synthesis (PASS) method. *Abbreviations*: *Ac* acetyl, *DCA* dichloroacetic acid, *DCM* dichloromethane, *DMT* bis-(4-methoxyphenyl) phenylmethyl

chemistry are the instability of CE groups during the synthesis and the insolubility of the growing protected oligonucleotides in process solvents. Alternative phosphate-protecting groups such as the more stable 4-nitrophenylethyl group or the more soluble N^3-benzyl-thymidine were adopted with limited success.

4.2 Solution-Phase Synthesis Using Polymer-Supported Reagents

Polymer-bound reagents can be used to promote chemical transformations of oligonucleotides in solution [27]. Solid-supported reagents reduce or even eliminate purification steps since they can simply be removed from the reaction mixture by filtration. Several polymer-bound reagents have been designed for use in oligonucleotide synthesis: poly(4-vinylpyridinium *p*-toluenesulfonate) can be used instead of tetrazole to activate phosphoramidite monomers, periodate immobilized on the anion-exchange resin Amberlyst A-26 can be used for oxidation, polymer-supported tetrathionate can be used for sulfurization, and *H*-phosphonate chemistry can be carried out with solid-supported acyl chloride and phosphoryl chloride. Although the synthesis of a hexaoligonuleotide using a convergent strategy with activation by polymer-bound acyl chloride was effective for short oligonucleotides, oxidation after each coupling was required due to the instability of the *H*-phosphonate diester linkage of 5′- detritylated intermediates.

5   AJIPHASE® for Oligonucleotide Synthesis

Current liquid-phase oligonucleotide synthesis methods using soluble polymers or non-polymeric support molecules allow homogeneous reactions to be carried out with smaller excesses of expensive monomers and easy separation of growing intermediates. However, to our knowledge, there has been no report of its use to commercially manufacture therapeutic oligonucleotides on an industrial-scale, presumably due to the laborious nature of the process. Even though precipitation can be used to isolate growing oligonucleotides, as shown in Table 1, for a method that required three isolations per monomer, even with a 99% yield per step, the final yield for a 21-mer oligonucleotide would only be 55%. If only one isolation is needed per step, the final yield would be 82%.

We have adapted our successful liquid-phase peptide synthesis protocol AJIPHASE® [28] to phosphoramidite chemistry [29]. Anchor molecules such as benzyl or diphenylmethyl alcohol (or amine) with long alkyl chains are used instead of resins (Fig. 4) and the anchored oligonucleotides can be easily precipitated from polar solvents. In order to develop a more scalable, practical method we developed the "one-isolation-per-cycle" process. A typical reaction cycle is shown in Fig. 5 and begins with removal of the DMT group from starting material **1** using organic acid in dichloromethane to give **2**. The reaction is then neutralized to prevent premature removal of the 5′-DMT group of the next phosphoramidite monomer **3**. As DMT deprotection is reversible, scavenging the DMT cation is necessary. Investigation into DMT scavengers found that alcohols such as MeOH or EtOH, silanes such as Et_3SiH, pyrrole derivatives, and indole derivatives are all effective. Alcohols should be avoided because they react with phosphoramidite, and due to the irreversibility of the reaction, pyrrole or indole derivatives should be chosen. Once the solution is neutralized and the DMT cation is scavenged, the next coupling reaction can be carried out by adding the next activated phosphoramidite monomer. Any activators for solid-phase synthesis can be used, but in some cases, activation is not necessary because the organic salt generated by the acid and base used for DMT removal and neutralization can serve as the activating agent. Coupling normally proceeds efficiently with a slight excess of phosphoramidite **3** (1.5–2.0 equivalents) within 1 h. After completion of the coupling, iodine in wet pyridine for oxidation of P(III) to P(IV)—or alternatively a sulfurization reagent—can be added directly to the reaction mixture. After about 1 h, product **5** is precipitated from a polar solvent such as methanol or acetonitrile.

Starting from 5′-DMT-thymidine attached to the soluble anchor molecule, corresponding phosphoramidite monomers were used to prepare a 20-mer DNA using

Table 1 Difference in yield for a 21-mer oligonucleotide when isolations are conducted after each reaction (i.e. three times per cycle) or after each cycle

	Average yield of each isolation	No. isolations	Final yield
Isolation after each reaction	99%	60 steps	55%
Isolation after each cycle	99%	20 Steps	82%
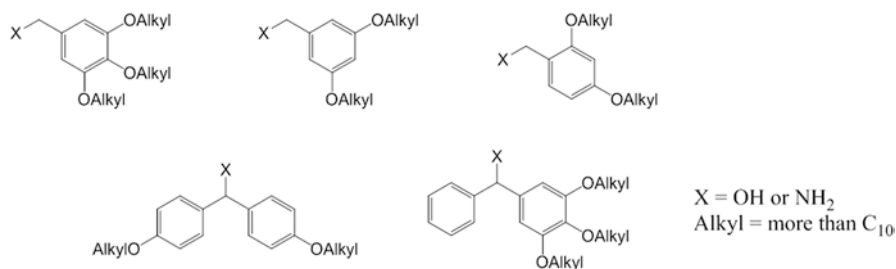
Fig. 4 Examples of the soluble supports used for the AJIPHASE® protocol
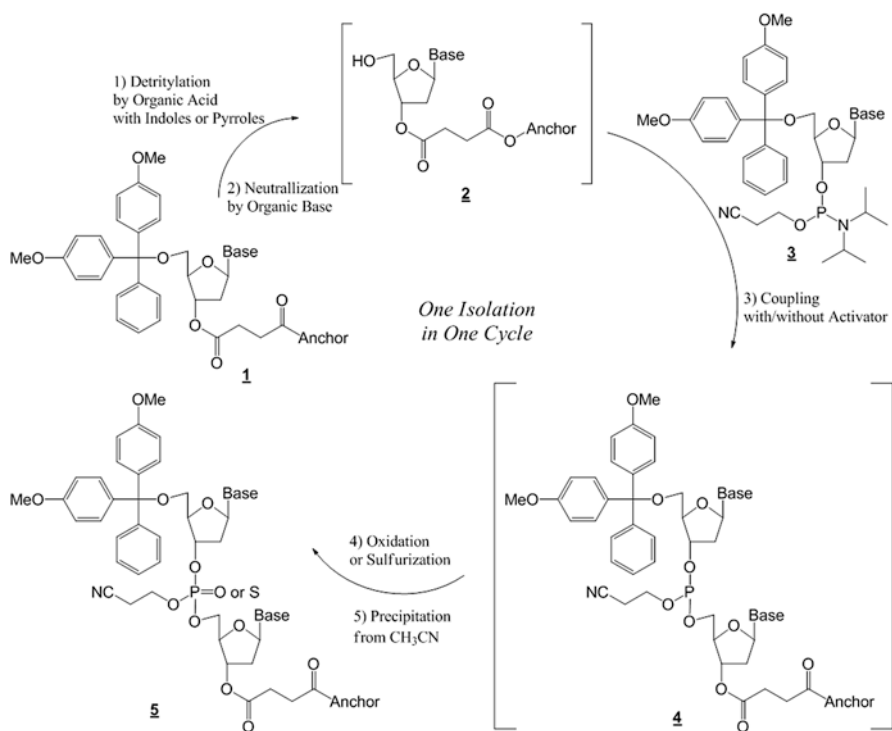
Fig. 5 Typical synthetic cycle of AJIPHASE® protocol for oligonucleotide syntheses

the above method. The growing oligonucleotides were easily precipitated and separated after each cycle and the fully protected, anchored 20-mer DNA was isolated after 19 synthetic cycles. The yield by weight was 60% (average yield of each cycle was about 98%). The protecting groups and the support molecule were removed by treating with aqueous ammonia. After washing and releasing on a Sep-Pak cartridge, the target compound was obtained in pure form (Figs. 6 and 7). Currently, further scaling-up and process optimization are in progress and the results will be reported elsewhere.
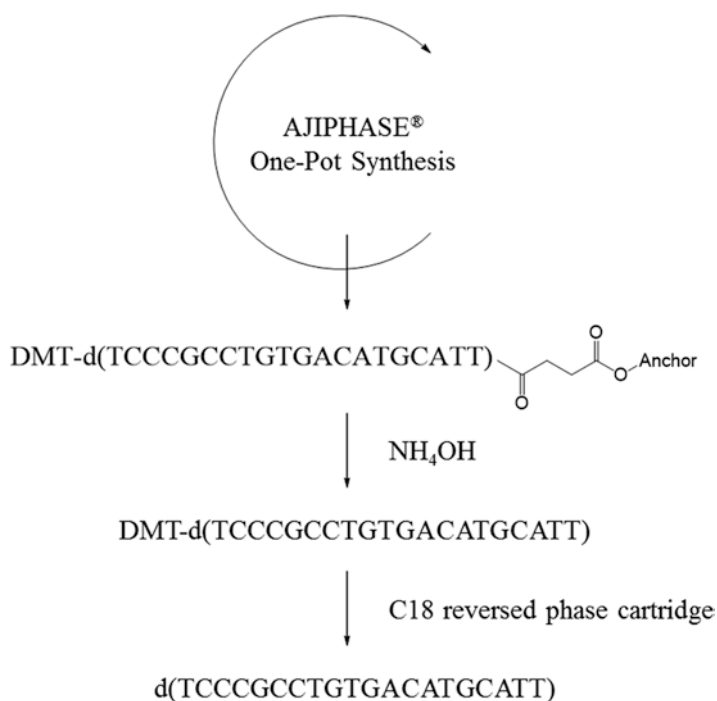
Fig. 6 Over view of the synthesis of 20-mer DNA using the AJIPHASE® protocol
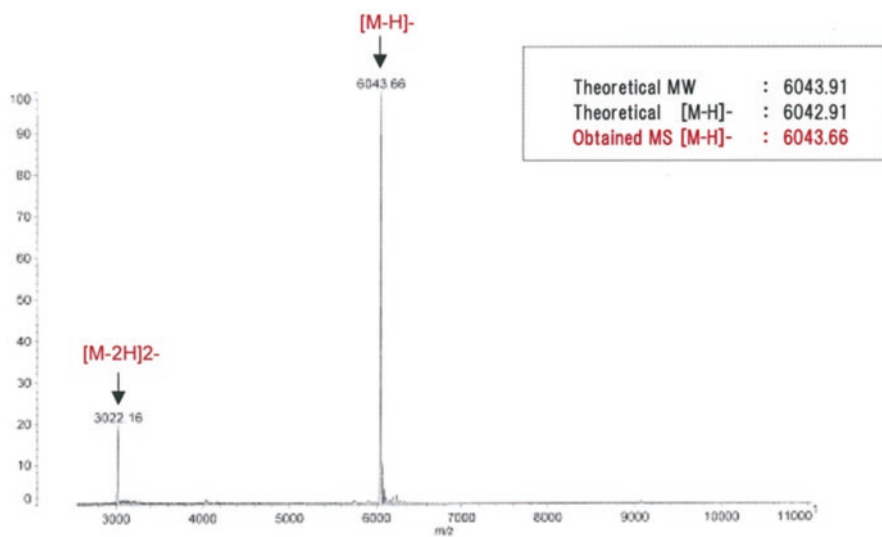
Fig. 7 Time-of-flight mass spectrum of pure 20-mer DNA prepared using the AJIPHASE® protocol

6   Conclusion

Cost-effective, large-scale preparation of oligonucleotides must be achieved if clinical application of oligonucleotides is to be realized. We believe that "liquid-phase" methods are a promising and AJIPHASE® process is the most practical one among the "liquid-phase" methods though there is still room for improvement. More effective preparation methods can be devised based on a better understanding of phosphoramidite chemistry in solution and an ability to control side reactions or impurities. We hope to establish a practical large scale manufacturing process for oligonucleotides to enable the spread of oligonucleotide therapeutics near future.

13th July, 2016

References

1. Freier SM, Watt AT (2001) Basic principles of antisense drug discovery. In: Crooke ST (ed) Antisense drug technology: principles, strategies, and applications, 2nd edn. Marcel Dekker, New York
2. a) Sharma VK, Sharma RK, Singh SK (2014) Antisense oligonucleotides: modifications and clinical trials. Med Chem Commun 5:1454–1471; b) Sharma VK, Rungta P, Prasad AK (2014) Nucleic acid therapeutics: basic concepts and recent developments. RCS Adv 4:16618–16631
3. Geary RS, Khatsenko O, Bunker K et al (2001) Absolute bioavailability of 2′-O-(2-methoxyethyl)-modified antisense oligonucleotides following intraduodenal instillation in rats. J Pharmacol Exp Ther 296:898–904
4. a) Campbell MA, Wengel J (2011) Locked vs. unlocked nucleic acids (LNA vs. UNA): contrasting structures work towards common therapeutic goals. Chem Soc Rev 40:5680–5689; b) Kaur H, Babu BR, Maiti S (2007) Perspectives on chemistry and therapeutic applications of Locked Nucleic Acid (LNA) Chem Rev 107:4672–4697; c) Obika S (2004) Development of bridged nucleic acid analogues for antigene technology. Chem Pharm Bull 52:1399–1404
5. Summerton J, Weller D (1997) Morpholino antisense oligomers: design, preparation, and properties. Antisense Nucleic Acid Drug Dev 7:187–195
6. a) Geary RS, Baker BF, Crooke ST (2015) Clinical and preclinical pharmacokinetics and pharmacodynamics of mipomersen (Kynamro®): a second-generation antisense oligonucleotide inhibitor of apolipoprotein B. Clin Pharmacokinet 54:133–146; b) Hair P, Cameron F, McKeage K (2013) Mipomersen sodium: first global approval. Drugs 73:487–493
7. Sanghvi YS, Schulte M (2004) Therapeutic oligonucleotides: the state-of-the-art in purification technologies. Curr Opin Drug Discov Devel 6:765–776
8. Reese CB (1978) The chemical synthesis of oligo- and poly-nucleotides by the phosphotriester approach. Tetrahedron 34:3143–3179
9. a) Reese CB, Song Q (1997) A new approach to the synthesis of oligonucleotides and their phosphorothioate analogues in solution. Bioorg Med Chem Lett 7:2787–2792; b) Reese CB, Song Q (1999) The H-phosphonate approach to the solution phase synthesis of linear and cyclic oligoribonucleotides. Nucl Acids Res 27:963–971; c) Reese CB, Song Q (1999) The H-phosphonate approach to the synthesis of oligonucleotides and their phosphorothioate analogues in solution. J Chem Soc Perkin Trans 1 1477–1486; d) Reese CB, Yan H (2002) Solution phase synthesis of ISIS 2922 (Vitravene) by the modified H-phosphonate approach. J Chem Soc Perkin Trans 1:2619–2633
10. Bayer E, Mutter M (1972) Liquid phase synthesis of peptide. Nature 237:512–513

11. Kamaike K, Hasegawa Y, Masuda I et al (1990) Oligonucleotide synthesis in terms of a novel type of polymer-support: a cellulose acetate functionalized with 4-(2-hydroxyethylsulfonyl) dihydrocinnamoyl substituent. Tetrahedron 46:163–184

12. Gimenez A, Kungurtsev V, Virta P et al (2012) Acetylated and methylated β-cyclodextrins as viable soluble supports for the synthesis of short 2′-oligodeoxyribo-nucleotides in solution. Molecules 17:12012–12120

13. a) Bonora GM (1987) Gazzetta Chim Ital 117:379–380; b) Bonora GM (1995) Polyethylene glycol. Appl Biochem Biotechnol 54:3–17

14. a) Bonora GM, Scremin CL, Colonna FP et al (1990) Nucleic Acids Res 18:3155–3159; b) Colonna FP, Scremin CL, Bonora GM (1991) Large scale H.E.L.P. synthesis of oligode-oxynucleotides by the hydroxybenzotriazole phosphotriester approach. Tetrahedron Lett 32:3251–3254; c) Bonora GM, Scremin CL, Colonna FP et al (1991) Nucleosides Nucleotides 10:269–273

15. Bonora GM, Biancotto G, Maffini M et al (1993) Large scale, liquid phase synthesis of oligo-nucleotides by the phosphoramidite approach. Nucleic Acids Res 21:1213–1217

16. Zaramella S, Bonora GM (1995) The application of *H*-phosphonate chemistry in the HELP synthesis of oligonucleotides. Nucleosides Nucleotides 14:809–813

17. a) Scremin CL, Bonora GM (1993) Liquid phase synthesis of phosphorothioate oligonu-cleotides on polyethylene glycol support. Tetrahedron Lett 34:4663–4666; b) Bonora GM, Zaramella S, Ravikumar V (2001) Large-scale solution synthesis of phosphorothioate oligo-nucleotides: a comparison of the phosphoroamidite and phosphotriester dimeric approaches. Croat Chim Acta 74:779–786

18. Bonora GM, Rossin R, Zaramella S et al (2000) A liquid-phase process suitable for large-scale synthesis of phosphorothioate opligonucleotides. Org Proc Res Dev 4:225–231

19. a) Donga RA, Khaliq-Uz-Zaman SM, Chan TH et al (2006) A novel approach to oligonucle-otide synthesis using an imidazolium ion tag as a soluble support. J Org Chem 71:7907–7910; b) Donga RA, Hassler M, Chan TH et al (2007) Oligonucleotide synthesis using ionic liquids as soluble supports. Nucleosides Nucleotides Nucleic Acids 26:1287–1293; c) Donga RA, Chan TH, Damha MJ (2007) Ion-tagged synthesis of an oligoribonucleotide pentamer—the continuing versatility of TBDMS chemistry. Can J Chem 85:274–282

20. a) Wada T (2013) Methods for the synthesis of functionalized nucleic acids. International Patent WO 2005/070859 A1, 24 Jan 2013; b) Oka N, Murakami R, Kondo T et al (2013) Stereocontrolled synthesis of dinucleoside phosphorothioates using a fluorous tag. J Fluorine Chem 150:85–91

21. a) Pearson WH, Berry DA, Stoy P et al (2005) Fluorous affinity purification of oligonucle-otides. J Org Chem 70:7114–7122; b) Berry DA, Pearson WH (2006) Fluorous oligonucle-otide reagents and affinity purification of oligonucleotides acids. International Patent WO 2006/081035 A2, 3 Aug 2006; c) Dandapani S (2006) Recent applications of fluorous separa-tion methods in organic and bioorganic chemistry. QSAR Comb Sci 8:681–688

22. a) Mishra R, Mishra S, Misra K (2006) Synthesis and application of fluorous-tagged oligo-nucleotides. Chemistry Lett 35:1184–1185; b) Tripathi S, Misra K, Sanghvi YS (2005) Group for 5′-hydroxyl protection of oligonucleosides. Org Prep Proc Int 37:257–263

23. a) Biernat J, Wolter A, Köster H (1983) Purification orientated synthesis of oligodeoxynucle-otides in solution. Tetrahedron Lett 24:751–754; b) Wörl R, Köster H (1999) Synthesis of new liquid phase carriers for use in large scale oligonucleotide synthesis in solution. Tetrahedron 55:2941–2956; c) Kungurtsev V, Laakkonen J, Molina AG et al (2013) Solution-phase synthe-sis of short oligo-2-deoxyribonucleotides by using clustered nucleosides as a soluble support. Eur J Org Chem:6687–6693; d) Kungurtsev V, Virta P, Lönnberg H (2013) Synthesis of short oligodeoxyribonucleotides by phosphotriester chemistry on a precipitative tetrapodal support. Eur J Org Chem 7886:7890

24. de Koning MC, Ghisaidoobe ABT, Duynstee HI et al (2006) Simple and efficient solution-phase synthesis of oligonucleotides using extractive work-up. Org Proc Res Dev 10:1238–1245

25. a) Chiba K, Kin S, Soichiro T et al (2010) Hydrophobic group-linked nucleoside, hydrophobic group-linked nucleoside solution and method of synthesizing hydrophobic group-linked oligonucleotide. Japanese Patent JP 2010-275254, 9 Dec 2010; b) Kim S, Matsumoto M (2013) Oligonucleotide synthesis method using highly dispersible liquid-phase support. International Patent WO 2013/179412 A1, 5 Dec 2013; c) Kim S, Matsumoto M, Chiba K (2013) Liquid-phase RNA synthesis by using alkyl-chain-soluble support. Chem Eur J 19:8615–8620; d) Shoji T, Kim S, Chiba K (2014) Synthesis of conjugated oligonucleotide in solution phase using alkyl-chain-soluble support. Chem Lett 43:1251–1253

26. Mihaichuk JC, Hurley TB, Vagle KE (2000) The dimethoxytrityl resin product anchored sequential synthesis method (DMT PASS): a conceptually novel approach to oligonucleotide synthesis. Org Proc Res Dev 4:214–224

27. a) Dueymes C, Schönberger A, Adamo I et al (2005) High-yield solution-phase synthesis of di- and trinucleotide blocks assisted by polymer-supported reagents. Org Lett 7:3485–3488; b) Adamo I, Dueymes C, Schönberger A et al (2006) Solution-phase synthesis of phosphorothioate oligonucleotides using a solid-supported acyl chloride with H-phosphonate chemistry. Eur J Org Chem 436–448; c) Adamo I, Dueymes C, Schönberger A et al (2004) Method for preparing oligonucleotides. International Patent WO2004/013154 12 Feb 2004; d) Mohe N, Heinonen P, Sanghvi Y-S et al (2005) A solid supported reagent for internucleoside H-phosphonate linkage formation. Nucleosides Nucleotides Nucleic Acids 24:897–899

28. a) Takahashi D (2009) Method for production of peptide. International Patent WO 2009014176, 29 Jan 2009; b) Takahashi D (2009) Method for selective removal of dibenzofulvene derivative. International Patent WO 2009014177 29 Jan 2009; c) Takahashi D (2010) Fluorene compound. International Patent WO 2010104169, 16 Sep 2010; d) Takahashi D (2010) Diphenylmethane compound. International Patent WO 20100249374, 30 Sep 2010; e) Takahashi D (2011) Benzyl compound. International Patent WO 2011078295, 30 Jun 2011; f) Takahashi D, Yano T, Fukui T (2012) Novel diphenylmethyl-derived amide protecting group for efficient liquid-phase peptide synthesis: AJIPHASE. Org Lett 14:4514–4517; g) Takahashi D, Yamamoto T (2012) Development of an efficient liquid-phase peptide synthesis protocol using a novel fluorene-derived anchor support compound with Fmoc chemistry; AJIPHASE®. Tetrahedron Lett 53:1936–1939; h) Takahashi D (2012) Aromatic compound containing specific branch. International Patent WO 2012029794 Mar 8 2012; i) Takahashi D (2012) Method for producing peptide. International Patent WO 2012165545, 6 Dec 2012; j) Takahashi D (2012) Method for producing peptide. International Patent WO 2012165546, 6 Dec 2012; k) Takahashi D (2013) Method for removing Fmoc group. International Patent WO 2013089241, 20 Jun 2013

29. a) Hirai K, Katayama S (2012) Method for producing oligonucleotide. International Patent WO 2012157723, 22 Nov 2012; b) Hirai K, Katayama S, Torii T et al (2013) Base-protected oligonucleotide. International Patent WO 2013122236, 22 Aug 2013

Large-Scale Oligonucleotide Manufacturing

Eduardo Paredes and Tatsuya Konishi

Abstract In the past decades, synthetic oligonucleotides have been explored for therapeutic purposes and seven oligonucleotide drugs have been successfully approved by FDA with many oligonucleotides, approximately 100, are in clinical trials worldwide. The increase in demand for a large quantity of oligonucleotide material for therapeutic applications has led to more cost-effective manufacturing technologies. Synthetic oligonucleotide quality has been improved by using raw materials with the highest possible purity. At the same time, yields and throughput have been increased significantly by the introduction of high loaded polymer supports like NittoPhase™ and by continuous development and optimization of oligonucleotide manufacturing processes that allow oligonucleotide manufacturers to access to a wide variety of oligonucleotide modifications. However, large scale oligonucleotide manufacturing is still not straight forward. In this chapter, considerations on large scale manufacturing equipment and a small scale modeling approach for scaling up each of the manufacturing processes are described.

Keywords Large scale · Oligonucleotide synthesis · Manufacturing process · Chromatography · Cleavage & deprotection · Solid support

1 Manufacturing Process for Therapeutic Oligonucleotides

The oligonucleotide manufacturing process consists of five major steps, (1) synthesis, (2) cleavage and deprotection (C&D), (3) purification, (4) desalting and concentration and (5) lyophilization, as shown in Fig. 1. Additional steps can be added depending on the type of oligonucleotide being manufactured. Each manufacturing steps requires specifically designed equipment and associated in-process-controls to

E. Paredes (✉)
Nitto Avecia, Cincinnati, OH, USA
e-mail: eduardo.paredes@avecia.com

T. Konishi
Nitto Denko Corporation, Osaki, Miyagi, Japan
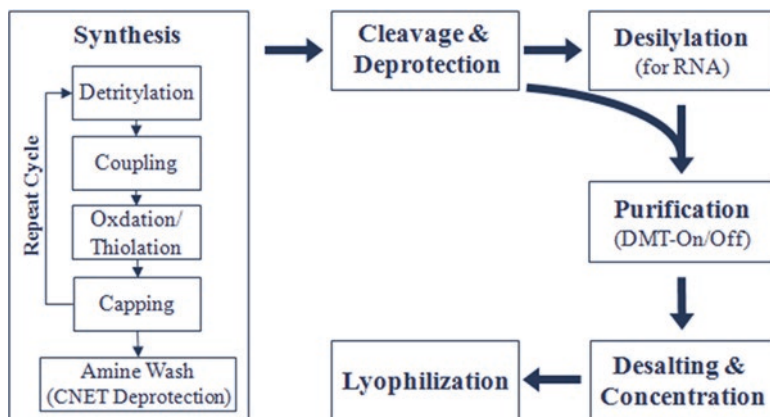
Fig. 1 Oligonucleotide manufacturing process steps

ensure batch reliability and quality. The most complex step is the synthesis step which requires sophisticated equipment and specialized software.

1.1 Oligonucleotide Synthesis

Solid phase synthesis has been employed for the manufacture of oligonucleotides from micrograms for research use, to multiple kilograms per batch in support of advanced clinical trials or commercial supply. During solid phase synthesis, phosphoramidite monomers are added sequentially onto a solid support to generate the desired full-length oligonucleotide. Each cycle of base addition consist of four chemical reactions, detritylation, coupling, oxidation/thiolation and capping. The manufacture of an oligonucleotide 20 bases long generally requires about 80 iterative reactions. Following synthesis, the C&D step releases the oligonucleotide from the solid-support and removes the protecting groups from bases and phosphates. This step can be performed in batch mode where the entirety of the solid-support manufactured is reacted with C&D solution in a reactor. The crude material generated is then purified generally using chromatographic purification to isolate full-length oligonucleotides from their related impurities. Finally, isolation through desalting and further lyophilization yields pure oligonucleotide solid material.

1.1.1 Solid Support

Silica-based controlled pore glass (CPG) has been widely used in solid phase oligonucleotide synthesis. CPG support is mechanically and chemically stable to the solvents used during oligonucleotide synthesis. Typically, CPG support with a pore size of 500 Å is used for oligonucleotide synthesis up to 30 bases long and a pore

diameter of 1000 Å for up to 50 bases [1]. The lengths of therapeutic oligonucleotides are generally under 50 bases long, hence CPG support with 500 Å or 1000 Å pore size satisfies this need. Two thousand Ångström pore size supports and other long-mer supports are available. Disadvantages of glass supports, however, include the instability towards basic conditions used during C&D which can lead to formation of impurities and low loading capacity.

To mitigate CPG's disadvantages, high-loaded porous polystyrene supports with loadings of 200 μmol nucleoside per gram of support were developed by Pharmacia Biotech (now part of GE Healthcare). Another high loading solid support (NittoPhase) that was developed by Nitto Denko in collaboration with IONIS Pharmaceuticals (IONIS) is being sold by Kinovate Life Sciences (part of Nitto Denko). IONIS developed a new polystyrene based high loaded support, which recently was made available commercially by GE Healthcare under the name Primer Support 5G (350 μmol/g). Latest developments have led to a support called NittoPhase HL with loadings of 350 μmol nucleoside per gram is the most widely used in large scale oligonucleotide synthesis. Common types of solid supports used in therapeutic oligonucleotide manufacturing are summarized in Fig. 2 (Table 1).

Traditionally, a nucleoside succinate is allowed to react with an amino or hydroxyl functionalized support to manufacture a nucleoside loaded support [2]. The succinate linkage created is stable to conditions and reagents used during solid phase synthesis. At the end of the synthesis, during basic C&D conditions the succinate linkage is hydrolyzed, releasing the oligonucleotide chain from the support. Other more base labile linkers have been developed such as oxalate [3] and Q-linker [4], however the succinate linkage is the most widely used in large scale oligonucleotide synthesis.
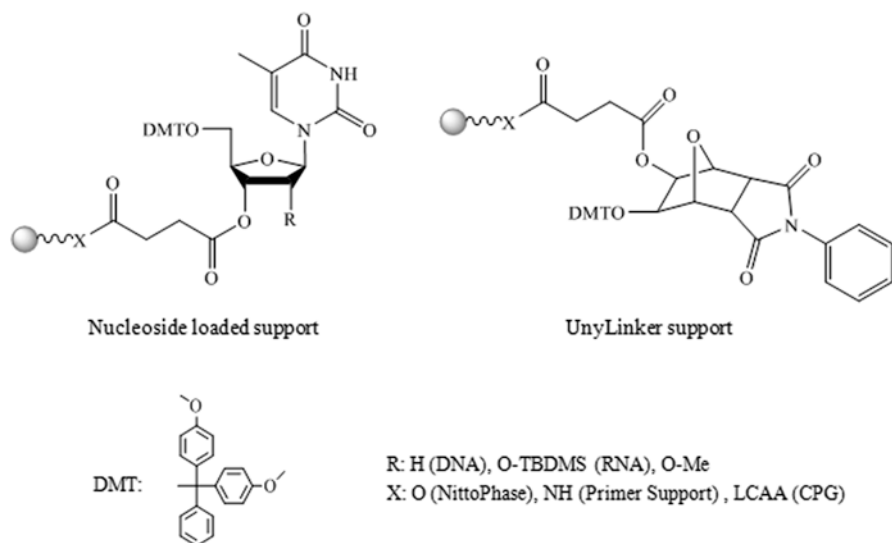
Fig. 2 Common type of solid support used in oligonucleotide manufacturing

Table 1 Common type of solid support used in therapeutic oligonucleotide manufacturing

Solid support	Linker/loadings	Supplier
NittoPhase HL	Nucleoside or UnyLinker/350 umol/g	Kinovate Life Sciences (Part of Nitto Denko)
Primer support 5G	Nucleoside or UnyLinker/350 umol/g	GE Healthcare
CPG	Nucleoside UnyLinker, 70–90 umol/g	Prime Synthesis or Chemgenes,

CPG supports require a spacer in between the nucleoside succinate and the support to ensure good coupling efficiencies. Thereby, CPG support is derivatized with a long chain alkyl amine (LCAA) [5] or other similar linkers [1a, 6], before attaching the nucleoside succinate.

Polystyrene supports require no additional linker. The nucleoside succinate is directly attached to the support.

Solid supports without pre-loaded nucleosides are, termed universal support. These supports have several advantages over nucleoside loaded supports. They do not suffer from loss of base protecting groups that could occur during manufacture or storage of nucleotide loaded support. Loss of base protecting groups can lead to formation of impurities such as branchmers and depurinated species [7]. Additionally, same universal support can be used for a synthesis of oligonucleotides with a wide variety of chemistries. Many different universal supports have been developed in the past decades [8]. Today the most widely used universal supports is UnyLinker [9] (Fig. 2). However, the manufacturing conditions for the use of Unylinker need to be optimized to ensure its full removal.

1.1.2   Synthesizer

There are many commercially available oligonucleotide synthesizers that are used for small scale and research grade oligonucleotide synthesis. Among equipment manufacturers, only GE Healthcare Life Sciences (GE) has synthesizers ranging from the μmol scale (ÄKTA oligopilot plus 10/100) to 1000 mmol or higher scale (OligoProcess). OligoProcess systems are generally custom built and can be tailored to meet the end user's needs. The advantage of GE systems is that they are all employ the same 'flow-through column' technology and are controlled by the UNICORN software. This allows for seamless scale-up from the ÄKTA oligopilot plus. For mid-scale production runs (10–50 mmol) GE has the OP400 system which bridges the gap between the ÄKTA oligopilot plus and OligoProcess system.

There are other players in the large scale oligonucleotide equipment like LEWA and ASAHI KASEI. These companies have traditionally occupied the chromatography and downstream processing space but are capable of building custom synthesizers by using their existing pump and valve technologies.

1.2   Oligonucleotide Cleavage and Deprotection

Oligonucleotide deprotection involves three steps: removal of a cyanoethyl (CNET) protecting group from the phosphate backbone, cleavage of the oligonucleotide chain from the support, and base deprotection. This process is generally carried out in batch mode where the entirety of the solid support is incubated with C&D reagents (Table 2).

Following deprotection, the spent solid support is filtered and crude oligonucleotide solution recovered. Depending on the C&D reagents and the type of oligonucleotide being processed, an amine wash may be performed at the end of synthesis and prior to the C&D to remove the phosphate protecting groups while the oligonucleotide is still attached to the solid support that can prevent the formation of the CNET adduct [10, 11]. The C&D step involves soaking the oligonucleotide attached support in the reagent and shaking the mixture using temperature controlled orbital shaker.

For certain production applications, the batch size might require larger than commercially available shakers, and even if available, such a process may not be performed safely. In such instances, an on-column cleavage and deprotection strategy can be used. In this strategy, the oligonucleotide attached support is not unpacked from the column housing following synthesis. A customized heated-reservoir/reactor and pump system is used to deliver the C&D reagents into the column. The solution is then re-circulated until the process is complete. The solution containing the deprotected oligonucleotide is then recovered and further processed as desired. Figure 3 shows an on-column cleavage and deprotection schematic.

For RNAs, the TBDMS (tert-butyldimethylsilyl, 2′ hydroxyl protecting group) must be removed prior to further processing. This is typically achieved by treating the crude RNA oligonucleotide still carrying the TBDMS groups from the C&D step with a fluoride source as described in Table 3. This reaction is carried out in jacketed reactors with overhead mechanical stirrers. As this step involves heating, cooling and tight pH control, the system used must have both an efficient heat transfer and mixing capability for scalable and reproducible operations.

Table 2 Typical reagents used for oligonucleotide C&D

Reagent	Incubation temperature (°C)	Incubation time (h)
Ammonium hydroxide	r.t – 65	10–24
NH4OH/EtOH(3:1)	r.t – 65	10–24
AMA-Ammonium hydroxide: Methylamine (1:1)	r.t – 50	1–5
Methylamine	r.t – 50	0.5–3
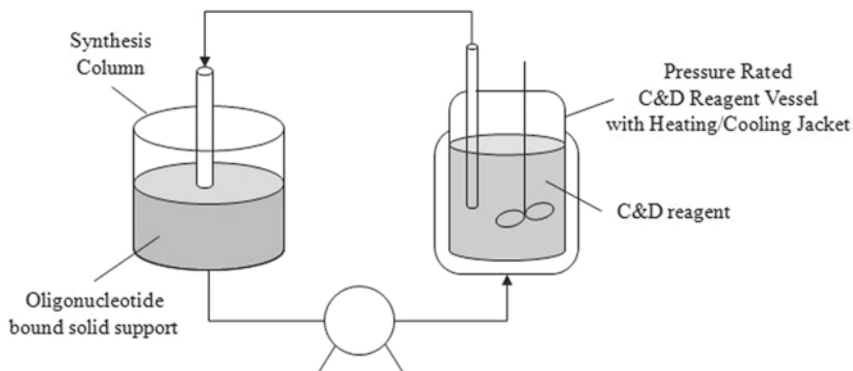
Fig. 3 On-column cleavage and deprotection schematic

Table 3 Typical reagents used for desylilation

Reagent	Incubation temperature (°C)	Incubation time (h)
TBAF in THF[a]	r.t.	9–17
TEA · 3HF	40–65	1.5–3

[a]Require anhydrous condition

1.3 Oligonucleotide Chromatography

The purification of oligonucleotide crude solutions is generally achieved by chromatographic methods [12]. The choice of chromatographic type and its associated set-ups heavily relies on the expected oligonucleotide use. Although oligonucleotide primers require little to no purification, therapeutic oligonucleotides require extensive chromatographic purification to ensure that a high quality API is manufactured. Table 4 summarizes the most widely used modes available for oligonucleotide purification. Taking advantage of the internucleotide phosphodiester (PO) and phosphorothioate (PS) linkage, anion exchanged and ion-paired reversed phase (IP-RP) chromatographic purifications on HPLC equipment are widely used for the purification of therapeutic oligonucleotide.

   The use of the anion exchange technique [12a, d, g, 13] ensures that fine separation between oligonucleotides and their closely related impurities (n−1, n−2 and n+1, n+2), and even PO impurities for phosphorothioates are discriminated. Additionally, as the elution is generally performed with sodium salts, the process in turn ensures that synthesis and C&D related counter ions are removed and the purified oligonucleotide is isolated in its desired sodium form. On the other hand, the use of IP-RP approaches ensures that not only charge-based residues, but also charge-neutral lipophilic impurities are discriminated [14]. However, as IP-RP chromatography requires the use of a counter ion, generally triethylamine, an

Table 4 Chromatographic purification of oligonucleotides

Purification mode	Resin	Company	Particle size (μm)	Exchange ligand
Anion exchange	Q Sepharose FF	GE Healthcare	45–165	Quaternary amine
	Q Sepharose HP	GE Healthcare	34	Quaternary amine
	Source 15Q/30Q	GE Healthcare	15/30	Quaternary amine
	TSKgel SuperQ-5PW	Tosoh Bioscience	20/30	Quaternary amine
	TOYOPearl GigaCap Q-650S	Tosoh Bioscience	35	Quaternary amine
	Oligo-Wax	Phenomenex	10	Quaternary amine
Reversed phase	Oligo-RP	Phenomenex	10	C18
	Triart C18	YMC	10–20	C18
	Source 15/30 RPC	GE Healthcare	15/30	Matrix surface
	Oligo R3	Thermo Fisher Scientific	30	C18
	TSKgel Phenyl-5PW	Tosoh Bioscience	10–20	Phenyl
	PRP-C18	Hamilton Company	10	C18

additional salt-exchange step is required to yield the purified oligonucleotide in its sodium form.

Alternative considerations for purification resin choice are re-usability, safe pH range, operational back-pressure, purification loading and recovery. Resin re-usability plays a big part of fixed purification systems that would handle heavy purification schedule workloads. This factor is mostly determined by the resin type and attachment chemistry. Polymeric supports like styrene and methacrylate are generally accepted as more re-usable when compared to silica supports. Safe pH range is a consideration when strict GLP practices are in place, which require heavy cleaning schedules, for which the trend generally follows re-usability. Operational back pressure is generally a consideration in semi-prep HPLC systems that can have prohibitive pressure limits. For this consideration, smaller-sized beads are generally observed to exhibit higher operating pressures. Further, disparate choice of purification support nature to selected eluents (i.e. aqueous buffers on silica based resins) also exhibit high operational back pressure. Purification loading and recovery are important considerations. Generally, IP-RP resins have lower loading limits and exhibit lower recoveries than their anion exchange counterparts. Given all the considerations, purification resin choice is highly sequence and application dependent with additional considerations like available equipment set-ups playing an important part in the final decision.

Unlike oligonucleotide synthesis which requires highly specialized equipment which may not be readily available especially at large scales, chromatography systems are more accessible since these systems have wider applications ranging from biopharmaceuticals to small molecules. The key to efficient therapeutic grade oligonucleotide purifications therefore lies mostly on the stationary phase, eluent and conditions used. Equally important is the purification column and column packing strategy employed. Nonetheless, for purification equipment designed for

oligonucleotides, GE is among the industry leaders with the ÄKTA purification platforms which complement their synthesizers. Just like in synthesis, GE provides systems from the research scale (ÄKTApurifier/pure) to large volume manufacturing (BioProcess/ÄKTAprocess). The ÄKTApurifier and BioProcess have been discontinued and replaced with AKTApure and ÄKTAprocess respectively. The ÄKTAprocess can deliver flow rates up to 2000 L/h. Whereas the UNICORN software makes processes developed on GE's purification platforms easy to scale up and transfer, the systems suffer from both their low pressure and low temperature rating and are not amenable for processes which require high pressure and sufficient denaturing temperature conditions. Similarly to the equipment, GE's purification columns are generally designed for low pressure applications at temperatures below 40 °C.

For high pressure and temperature purification equipment, ASAHI KASEI, LEWA and Novasep are amongst the major players. For purification columns Load and Lock stainless columns (Agilent and Agar Machining) have high-pressure Dynamic Axial Compression (DAC) packing which provides improved bed stability and higher loading. They can also be jacketed for use at higher temperatures.

1.4   Oligonucleotide Ultrafiltration and Diafiltration

Following purification, the most widely accepted choice for therapeutic oligonucleotide isolation at manufacturing scales is the use of tangential flow filtration (TFF). This approach employs an appropriately sized filter membrane (membranes available from Pall or Millipore) and uses a pump to circulate the sample through the TFF set-up making the process more efficient (Fig. 4). For TFF, a sample placed in a feed vessel is fed against the membrane holder which houses an appropriately sized membrane filter. Given a feed pressure higher than the osmotic pressure of the solution, the salt solution passes through the membrane's pores while the oligonucleotide is diverted back to the feed vessel. As the solution concentrates, concerted addition of buffer or purified water effectively desalts the solution. The main drawback of this approach is the requirement of a large solution volume due to the system void volume.

The UF/DF approach used depends on the manufacturing scale and the expected application. For 500 µmol scales and above, a TFF system as shown in Fig. 4 is recommended. TFF systems are the easiest to set up and are readily amenable to scale up. All that is needed is membrane holder, two pumps, pressure gauges, tubing with fittings and a sample reservoir. The ease of setting these up allows the end user a lot of flexibility. Membrane holders and accessories can be obtained from key manufacturers like EMD Millipore, PALL or Sartorius.

GE's ÄKTA crossflow is available for fully automated small scale TFF systems. The attendant UNICORN software allows for instant in process control (IPC) and process log. For pilot and manufacturing scale applications, GE's UniFlux system is
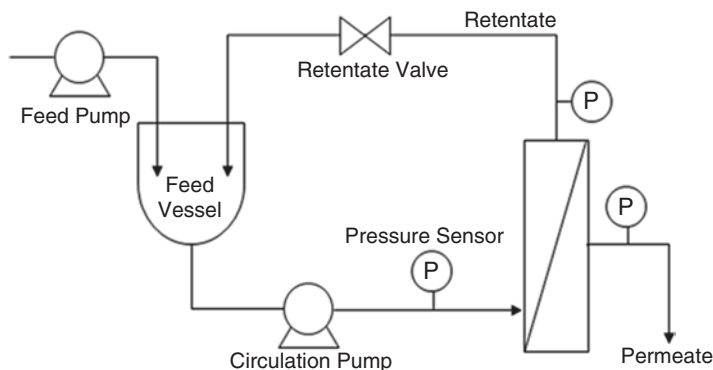
Fig. 4 Tangential flow filtration systems

available in sizes of 10, 30, 120 and 400 LPM. Fully automated large scale TFF skids like the Allegro series are also available from PALL. EMD Millipore also recently launched the fully automated Mobius® FlexReady Solutions. SARTOFLOW Smart is a modular and flexible small scale benchtop system is available from Sartorius. A versatile system, this machine can be switched from a TFF to Chromatography skid with minimum component changes. Sartorius also offers additional mid-scale instruments for semi-prep applications. There are several other manufacturers of TFF systems for applications beyond oligonucleotides purification and desalting.

1.5   Oligonucleotide Lyophilization

Since the pH of double distilled water is about 5.5, oligonucleotides in aqueous solutions will slowly undergo acid-catalyzed depurination over time. At the same time, there is a considerable risk of contamination from micro-organisms which might lead to degradation. Therefore, for long-term storage and easier handling, purified oligonucleotides are typically lyophilized (freeze dried) to powder in the final manufacturing step. As briefly discussed earlier in this report, during the TFF step of large scale manufacture, the desalted oligonucleotide API is concentrated to a predetermined concentration. This concentration, usually a range, is a controlled process parameter to ensure that upon lyophilization, a product with a consistent morphology is obtained.

Lyophilization is performed using a freezer dryer, which is a machine consisting of a sample chamber, a condenser and a vacuum pump. The oligonucleotide API is frozen and lyophilized to obtain the final product in powder form via sublimation. Common bench top freeze dryers are manufactured by Labconco while pilot and production freeze dryers include VirTis Genesis and Hull.

There are four main steps in the lyophilization process namely sample preparation, freezing, primary drying and secondary drying. In the sample preparation step, the desalted oligonucleotide API solution is filtered through a 0.2 μm filter to remove any incidental in process particulates from the drug product. The filtered solution is then transferred into vials for small scale batches, or into freeze drying trays or containers. These containers, like Gore LyoGuard® trays, are specially made with optimal volume capacity and fitted with membranes that allow for water removal without product spills or contamination.

The container or tray with the product is then placed inside the sample chamber shelf and frozen, usually at −40 °C. The rate of freezing depends on the temperature the shelf, the amount of product in each tray and the height of the solution in each tray. These factors alongside the concentration of the oligonucleotide will in turn impact the drying rate and the morphology of the product obtained. It is therefore critical that these factors be put into consideration when developing the lyophilization recipe. During this step, the frozen water exists in the product solution in two forms, (a) water free (unbound) from the oligonucleotide solid, (b) water trapped within the solid product.

After the freezing step, the primary drying step kicks in. In this step, the condenser temperature is lowered to a temperature much lower than that of the lyophilization chamber, usually less than −70 °C. The chamber pressure is then lowered by pulling the vacuum. These set of conditions result in a phase change from solid to gas i.e. the free water frozen water sublimes to vapor which is then instantaneously trapped in the −70 °C condenser and turned back to ice. Since the sublimation process is accompanied by a decrease in product temperature, the chamber shelves are heated to keep the resultant product cake at constant temperature. It is typical to monitor both the shelf and product temperatures during this process. When both temperatures reach equilibrium, it is an indication that the primary drying step is complete.

After the completion of the primary drying step, no 'free water' left in the product. But the trapped water is still within the solid product. Since this water is more difficult to remove, the shelf temperature is increased gradually, usually to 25 ± 5 °C at the same or lower pressures used for primary drying.

2   Small-Scale Modeling for Oligonucleotide Manufacturing

The precarious relationship between production-scale manufacturing and small-scale modeling approaches requires diligent scrutiny. Lowered yield, changes in impurity profile, and process deviations are amongst the most common critical scale-up issues that are attributed to improper small-scale models. Therefore, any work to ensure reliable scale-up manufactures needs to focus around critical processing steps and establish scalable operating parameters. This section will cover several case studies where appropriate small-scale models were developed to ensure reliable manufactures.

2.1 Case Study 1 (Synthesis)

One of the most complex manufacturing operations to model given the sheer number of critical operating parameters is solid-phase synthesis. Although each step during synthesis has a scalable critical parameter worth discussion, this review will focus on the most critical and one of the easiest parameters to model during synthesis process development work: synthesis support bed height. This parameter is critical as it bridges the relationship between scalable process flow rates and reagent contact time. The experience discussed is based mainly on a case study centered on the relationship between bed height and detritylation-dependent depurination.

For the study, the synthesis of a fully-phosphorothioated 18-mer oligodeoxynucleotide was performed at three different bed heights keeping all other parameters constant (Table 5). As mentioned earlier, performing the syntheses in this manner would lead to a positively linear relationship between bed height and reagent contact time. Although for most reagents, this is generally not an issue, extending the contact time of the detritylation reagent with oligodeoxynucleotides, which are sensitive to acid-based depurination and further strand cleavage during C&D, would lead to lower FLP (Full Length Product) purity (Fig. 5).

The first three experiments in the experimental set demonstrate this fact where the synthesis at 9 cm bed height results in higher levels of pre-peak impurities as compared to the synthesis at 2 cm bed height. To demonstrate that this is generally not attributed to other reagents' contact time and is mainly due to detritylation-dependent depurination during extended detritylation contact times, performing an additional two syntheses at the short 2 cm bed height but using reagent flow rates for detritylation reagent that mimic the higher bed height also causes the crude material quality to drop. Therefore, the relationship between reagent flow rates and synthesis support housing proportions needs to be scrutinized on the basis of critical reagent contact times to ensure reliable scale-up manufactures.

Table 5 Influence of detritylation bed height and flow rate on depurination [15]

Synthesis scale	Column bed height	Column volume (CV)	Detritylation flow rate	Detritylation contact time	FLP purity
mmol	cm	mL	cm/h (mL/min)	min/CV	%
0.25	2	6.3	400 (21)	0.30	87
1.69	4.5	43.8	400 (65)	0.68	83
3.37	9	87.5	400 (65)	1.35	78
0.25	2	6.3	200 (10)	0.60	83
0.25	2	6.3	65 (3.5)	1.85	77
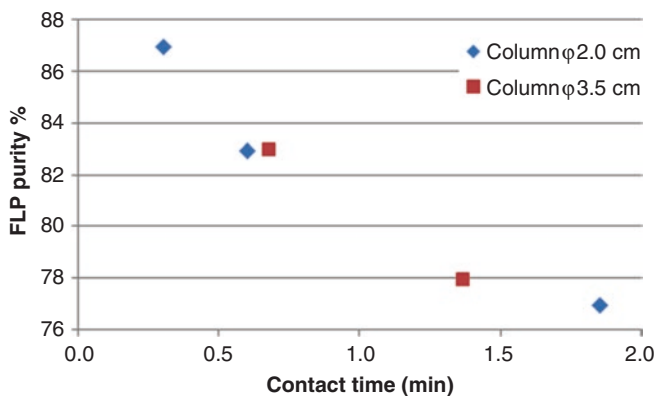
Fig. 5 Influence of detritylation contact time on FLP content in the crude [15]. Increased bed height leads to increased detrit contact time when using the same linear flow rate. Increased detrit contact time leads to lowere FLP content in the curude by acid-induced depurination and subsequent degradation of an 18-mer PS DNA during basic cleavage and deprotection step

2.2 Case Study 2 (C&D)

As C&D processes are generally performed in basic media at elevated temperatures, the most critical and challenging parameter to model during process development work is heat transfer. Although a solution in a small vessel might reach the desired internal temperature in a fraction of an hour, larger vessels require significant more heat to be transferred to reach the optimal internal deprotection temperatures. As this process is heavily influenced by vessel proportions, materials of construction, and even heating element characteristics, developing a small-scale model for C&D is deceptively simple. In some instances, after determining ramp-up rates, simply adjusting incubation time at large scale is sufficient to ensure reliable manufactures. However, as ramp-up rates for larger scales are generally harder to determine and as the large scale equipment is significantly different from lab scale heating elements, the process can be challenging. This process is complicated further in the case of oligoribonucleotides. In addition to C&D considerations, following oligonucleotide removal from the solid support and base deprotection, the removal of the requisite 2′-OH protecting groups needs to be carried out in an acidic media with an organic co-solvent. As the reaction pH is being adjusted from ~11 to ~5, a large exothermic reaction needs to be controlled. Additionally, as both the 2′-protected ON and several reagent byproducts precipitates during this transition, precise heat control is critical to ensure reliable manufactures. Therefore diligent alignment of heating/cooling capabilities needs to be established. In the next case study, a set of three C&D reactions are presented (Fig. 6). In the first experiment, the crude material for a 24-mer oligonucleotide conjugate with 2′-OH, 2′-OMe, and 2′-F modifications that underwent C&D using an appropriate heating scale-down model is presented (small scale model in Fig. 6). Attempting a similar reaction at manufacturing scale
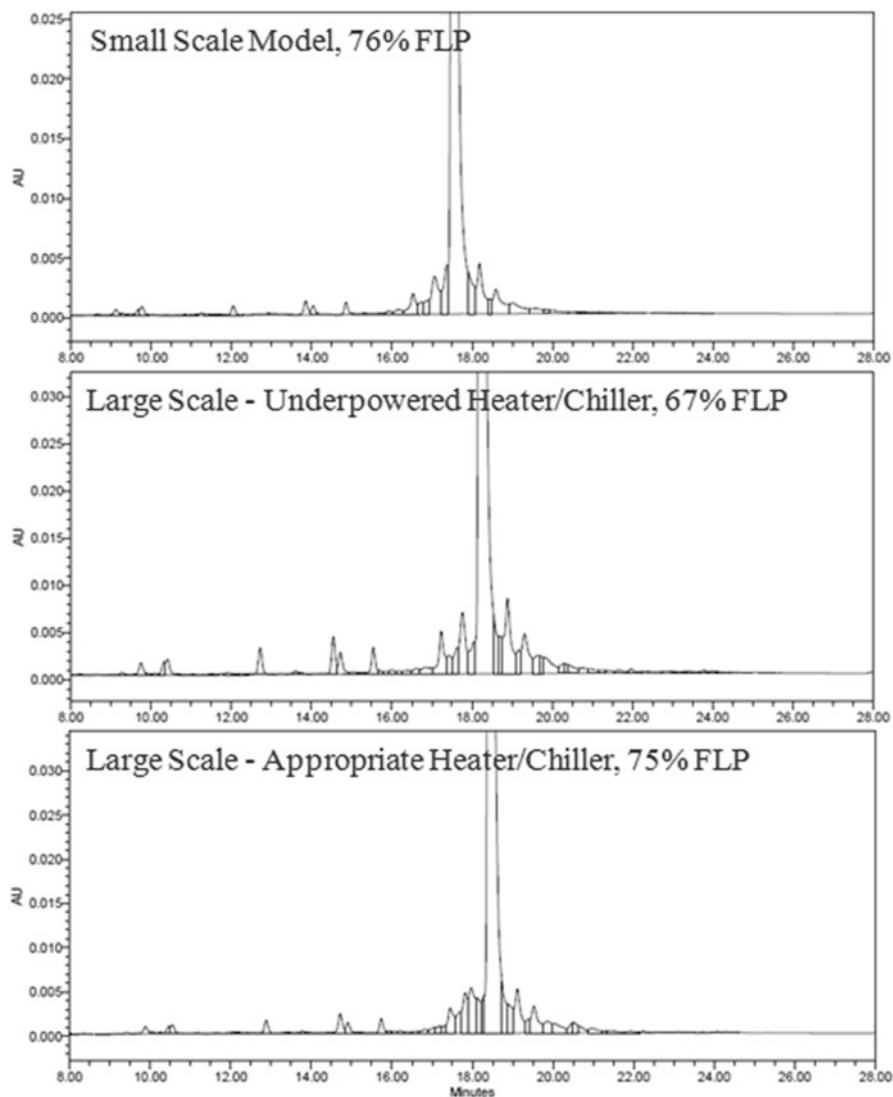
Fig. 6 Influence of C&D heat transfer on crude quality [15]

using equipment set up with non-model heating/cooling characteristics, generates a significantly lower quality crude material. As the heat generated is uncontrolled and the ramp-up/down rates are slower, significant oligonucleotide damage is evident from the impurity profile (underpowered heater/chiller in Fig. 6). Finally, ensuring that the heating/cooling capabilities of the large-scale equipment are in line with the small-scale model ensures a reliable manufacture.

2.3   Case Study 3 (Purification)

Another process operation where large scale-equipment is easily misaligned is oligonucleotide purification. For this process operation, myriad parameters need to be taken into account to ensure a successful manufacture. Although column packing methodologies, column conditioning, incoming crude matrix, loading/elution flow rates, eluent preparation, operating backpressure, amongst others, are important to a successful purification, one of the most challenging parameter to align is purification temperature. Given that heat transfer differs widely between scales and equipment set-ups and that temperature might even vary within the equipment itself (between eluent tanks, pump system, eluent heaters, column inlet, column outlet, and even fractionation temperature) it is critical to ensure that not only the purification temperature wherever measured but the actual heating and cooling rates at every step are being modeled. The following case study presents the heated purification of a 21-mer RNA mix-mer lipophilic conjugate. From Fig. 7, it is clear that high temperature is necessary to denature the RNA during purification. Any attempts at purifying this material at temperatures lower than 30 °C resulted in low quality fractions. However, there is a balance between denaturation for purification and heat-generated degradation. For this material, it was found that purification at 40–50 °C resulted in high quality fractions. However, further addition of 5 °C of heat resulted in lower quality fractions again mostly due to degradation. Further it was found that the time spent at temperature within the heating elements before interaction with the column was also critical thus implicating ramp-up rates. Overall, tight temperature control and maintaining heat transfer rates during purification amongst other critical for a smooth scale-up of heated purification.
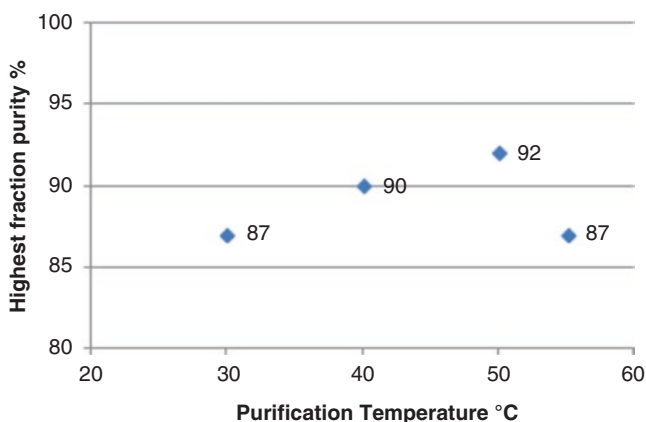
Fig. 7 RNA purifications are highly sensitive to purification temperature. Crude purity ~80%, Column 2.5 cm diameter ×30 cm bed height, crude loading ~25 mg/ml-media, flow rate 200 cm/h, eluent A Sodium phosphate/acetonitrile, eluent B Sodium phosphate/acetonitrile +1 M NaBr

Overall, diligent scrutiny and control over scalable parameters and diligent manufacturing equipment modeling provide a route for reliable large-scale manufactures. Careful attention to system proportions, void volumes, heat transfer, equipment loading, sample concentration, amongst other critical operating parameters ensure that any process development activities are useful in predicting large-scale manufactures. Through this responsible process development approach, batch reliability and oligonucleotide quality can be maximized and maintained.

References

1. (a) Katzhendler J, Cohen S, Rahamim E, Weisz M, Ringel I, Deutsch J (1989) The effect of spacer, linkage and solid support on the synthesis of oligonucleotides. Tetrahedron 45:2777–2792; (b) Kozlov IA, Dang M, Sikes K, Kotseroglou T, Barker DL, Zhao C (2005) Significant improvement of quality for long oligonucleotides by using controlled pore glass with large pores. Nucleosides Nucleotides Nucleic Acids 24(5–7):1037–1041
2. Yip KF, Tsou KC (1971) A new polymer-support method for the synthesis of ribooligonucleotide. J Am Chem Soc 93:3272–3276
3. Alul RH, Singman CN, Zhang GR, Letsinger RL (1991) Oxalyl-CPG: a labile support for synthesis of sensitive oligonucleotide derivatives. Nucleic Acids Res 19(7):1527–1532
4. (a) Pon RT, Yu S (1997) Hydroquinone-O,O′-diacetic acid ('Q-linker') as a replacement for succinyl and oxalyl linker arms in solid phase oligonucleotide synthesis. Nucleic Acids Res 25(18):3629–3635; (b) Pon RT, Yu S (1997) Hydroquinone-O,O′-diacetic acid as a more labile replacement for succinc acid linkers in solid-phase oligonucleotide synthesis. Tetrahedron Lett 38(19):3327–3330
5. Gough GR, Brunden MJ, Gilham PT (1983) 2′(3′)-O-benzoyluridine 5′ linked to glass: an all-purpose support for solid phase synthesis of oligodeoxyribonucleotides. Tetrahedron Lett 24(48):5321–5324
6. Vargeese C, Wang W (2007) Methods and reagents for oligonucleotide synthesis. US7205399, 04/17/2007
7. Kurata C, Bradley K, Gaus H, Luu N, Cedillo I, Ravikumar VT, Van Sooy K, McArdle JV, Capaldi DC (2006) Characterization of high molecular weight impurities in synthetic phosphorothioate oligonucleotides. Bioorg Med Chem Lett 16(3):607–614
8. (a) Nelson PS, Muthini S, Vierra M, Acosta L, Smith TH (1997) Rainbow universal CPG: a versatile solid support for oligonucleotide synthesis. Biotechniques 22(4):752–756; (b) Lyttle MH, Dick DJ, Hudson D, Cook RM (1999) A phosphate bound universal linker for DNA synthesis. Nucleosides Nucleotides 18:1809–1824; (c) Schcuer-Larsen C, Rosenbohm C, Jøgensen TJD, Wengel J (1997) Introduction of a universal solid support for oligonucleotide synthesis. Nucleosides Nucleotides 16:67–80; (d) Scott S, Hardy P, Sheppard RC, McLean MJ (1994) A universal support for oligonucleotide synthesis. In: Epton R (ed) Innovations and perspectives in solid phase synthesis. 3rd international symposium. mayflower worldwide. pp 115–124; (e) Kumar P, Dhawan G, Chandra R, Gupta KC (2002) Polyamine-assisted rapid and clean cleavage of oligonucleotides from cis-diol bearing universal support. Nucleic Acids Res 30(23):e130; (f) Kumar P, Mahajan S, Gupta KC (2004) Universal reusable polymer support for oligonucleotide synthesis. J Org Chem 69(19):6482–6485; (g) Anderson E, Brown T, Picken D (2003) Novel photocleavable universal support for oligonucleotide synthesis. Nucleosides Nucleotides Nucleic Acids 22(5–8):1403–1406; (h) Anderson KM, Jaquinod L, Jensen MA, Ngo N, Davis RW (2007) A novel catechol-based universal support for oligonucleotide synthesis. J Org Chem 72(26):9875–80; (i) Morvan F, Meyer A, Vasseur JJ (2007) A universal and recyclable solid support for oligonucleotide synthesis. Curr Protoc Nucleic Acid Chem. Chapter 3, Unit 3.16

9. (a) Guzaev AP, Manoharan M (2003) A conformationally preorganized universal solid support for efficient oligonucleotide synthesis. J Am Chem Soc 125(9):2380–2381; (b) Ravikumar VT, Kumar RK, Olsen P, Moor MN, Carty RL, Andrade M, Gorman D, Zhu X, Cedillo I, Wang Z, Mendez L, Scozzari AN, Aguirre G, Somanathan R, Bernees S (2008) UnyLinker: an efficient and scaleable synthesis of oligonucleotides utilizing a universal linker molecule: a novel approach to enhance the purity of drugs. Org Process Res Dev 12:399–410

10. Capaldi DC, Gaus H, Krotz AH, Arnold J, Carty RL, Moore MN, Scozzari AN, Lowery K, Cole DL, Ravikumar VT (2003) Synthesis of high-quality antisense drugs. Addition of acrylonitrile to phosphorothioate oligonucleotides: adduct characterization and avoidance. Org Process Res Dev 7(6):832–838

11. Eritja R, Robles J, Avino A, Albericio F, Pedroso E (1992) A synthetic procedure for the preparation of oligonucleotides without using ammonia and its application for the synthesis of oligonucleotides containing O-4-alkyl thymidines. Tetrahedron 48:4171–4182

12. (a) Noll B, Seiffert S, Hertel F, Debelak H, Hadwiger P, Vornlocher HP, Roehl I (2011) Purification of small interfering RNA using nondenaturing anion-exchange chromatography. Nucleic Acid Ther XXX; (b) Gjerde DT, Hoang L, Hornby D (2009) RNA purification and analysis: sample preparation, extraction, chromatography. Wiley-VCH, Weinheim, p xi. 195 p; (c) Vargeese C (2006) Deprotection and purification of oligonucleotides and their derivatives. US6989442; (d) Shanagar J (2005) Purification of a synthetic oligonucleotide by anion exchange chromatography: method optimisation and scale-up. J Biochem Biophys Methods 64(3):216–225; (e) Deshmukh RR, Eriksson KO, Moore P, Cole DL, Sanghvi YS (2001) A case study: oligonucleotide purification from gram to hundred gram scale. Nucleosides Nucleotides Nucleic Acids 20(4–7):567–576; (f) Andrus A, Kuimelis RG (2001) Overview of purification and analysis of synthetic nucleic acids. Curr Protoc Nucleic Acid Chem. Chapter 10, Unit 10.3; (g) Deshmukh RR, Cole DL, Sanghvi YS (2000) Purification of antisense oligonucleotides. Methods Enzymol 313:203–226; (h) Wincott F, DiRenzo A, Shaffer C, Grimm S, Tracz D, Workman C, Sweedler D, Gonzalez C, Scaringe S, Usman N (1995) Synthesis, deprotection, analysis and purification of RNA and ribozymes. Nucleic Acids Res 23(14):2677–2684

13. (a) Bergot BJ, Egan W (1992) Separation of synthetic phosphorothioate oligodeoxynucleotides from their oxygenated (phosphodiester) defect species by strong-anion-exchange high-performance liquid chromatography. J Chromatogr A 599:35–42; (b) Deshmukh RR, Miller JE, De Leon P, Leich WE II, Cole DL, Sanghvi YS (2000), Process development for purification of therapeutic antisense oligonucleotides by anion-exchange chromatography. Org Process Res Dev 4:205–213; (c) Metelev V, Agrawal S (1992) Ion-exchange high-performance liquid chromatography analysis of oligodeoxyribonucleotide phosphorothioates. Anal Biochem 200(2):342–346; (d) Banerjee A, Bose HS, Roy KB (1991) Fast and simple anion-exchange chromatography for large-scale purification of self-complementary oligonucleotides. Biotechniques 11(5):650–656; (e) Cohn WE (1950) The anion-exchange separation of ribonucleotides. J Am Chem Soc 72:1471–1478

14. (a) Cramer H, Finn KJ, Herzberg E (2011) Purity analysis and impurities determination by reversed-phase HPLC. In: Bonilla J, Srivatsa GS (eds) Handbook of analysis of oligonucleotides and related products. CRC Press, Boca Raton, pp 1–46; (b) McCarthy SM, Gilar M, Gebler J (2009) Reversed-phase ion-pair liquid chromatography analysis and purification of small interfering RNA. Anal Biochem 390(2):181–188; (c) Lei B, Li S, Xi L, Li J, Liu H, Yao X (2009) Novel approaches for retention time prediction of oligonucleotides in ion-pair reversed-phase high-performance liquid chromatography. J Chromatogr A 1216(20):4434–4439; (d) McCarthy SM, Warren WJ, Dubey A, Gilar M (2008) Ion-pairing systems for reversed-phase chromatoraphy separation of oligonucleotides. In: TIDES Conference, Las Vegas, NV; (e) Kirkland JJ (2004) Development of some stationary phases for reversed-phase high-performance liquid chromatography. J Chromatogr A 1060(1–2):9–21; (f) Azarani A, Hecker KH (2001) RNA analysis by ion-pair reversed-phase high performance liquid chromatography. Nucleic Acids Res 29(2):E7

15. Cramer H (2015). In: Development of small scale models to predict large scale manufacturing results, Euro TIDES, Berlin, Berlin

Part II
Synthesis and Properties of Artificial Oligonucleotides

Nucleosides and Oligonucleotides Incorporating 2-Thiothymine or 2-Thiouracil Derivatives as Modified Nucleobases

Kohji Seio and Mitsuo Sekine

Abstract Nucleosides containing 2-thiothymine and 2-thiouracil as base moieties have been incorporated into oligonucleotides to enhance their hybridization affinity and base discrimination ability. For the incorporation of these thio-bases into oligonucleotides, efficient methods for the synthesis of thio-modified nucleosides and the incorporation of the thio-nucleosides into oligonucleotides under solid-phase conditions are necessary. In this chapter, the physicochemical properties of thio-modified bases and the methods for the syntheses of 2-thiouridine and 2-thiothymidine are described. In addition, the solid-phase synthesis of oligonucleotides incorporating these thio-nucleosides is described.

Keywords Sulfur · 2-Thiouracil · 2-Thiothymine · Hydrogen bond · London dispersion force

Abbreviations

Ura	Uracil
s^2Ura	2-Thiouracil
Thy	Thymine
s^2Thy	2-Thiothymine
U	Uridine
s^2U	2-Thiouridine
T	Thymidine

K. Seio (✉)
Department of Life Science and Technology, Tokyo Institute of Technology, Tokyo, Japan
e-mail: seio.k.aa@m.titech.ac.jp

M. Sekine
Tokyo Institute of Technology, Yokohama, Kanagawa, Japan

s^{2}T   2-Thiothymidine
rT   Ribothymidine
rs^{2}T   2-Thioribothymidine
Bz   Benzoyl
Tol   Toluoyl
DMTr   4,4′-dimethoxytrityl

1 Purposes of the Thio Modification of Uracil and Thymine

Several examples of the modification of nucleobases with sulfur atoms have been reported in the literature. Usually, the carbonyl oxygens are replaced by sulfur atoms leading to new nucleobases possessing thiocarbonyl groups. Especially, 2-thiouracil (s^{2}Ura) and 2-thiothymine (s^{2}Thy) have been widely studied (Fig. 1). Owing to the physicochemical properties of sulfur atom which are different from oxygen atom, oligonucleotides including thio-modified nucleobases show useful properties such as higher affinity to complementary DNAs or RNAs, and improved base pairing selectivity.

In this chapter, the properties of s^{2}Ura, s^{2}Thy, and related nucleosides are discussed on the basis of the physicochemical properties of sulfur. In addition, the synthesis and properties of oligonucleotides incorporating these modified building blocks are also described.

Uracil (Ura)   2-Thiouracil (s^{2}Ura)   Thymine (Thy)   2-Thiothymine (s^{2}Thy)

2-Thiouridine (s^{2}U)   2-Thiothymidine (s^{2}T)   2-Thioribothymidine (rs^{2}T)
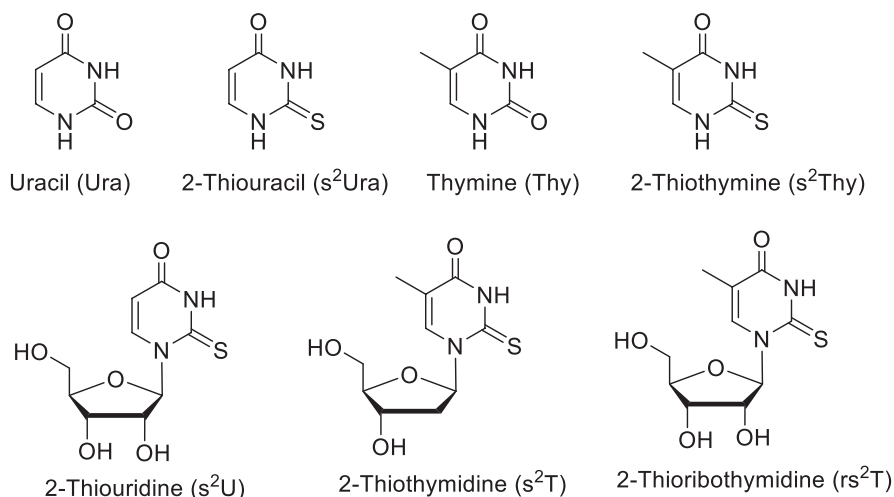
Fig. 1 Structures of thio-modified nucleobases and nucleosides

2 Physicochemical Similarities and Differences Between Oxygen and Sulfur

In this section, the basic physicochemical properties of oxygen and sulfur are summarized to help understanding the effects of the thio-modification on the properties of oligonucleotides.

Oxygen and sulfur are group 16 elements positioned in the second and third row of the periodic table, respectively. In most oxygen-containing organic molecules, the oxygen atoms can be replaced by sulfur atoms. For example, most hydroxy, ether, and carbonyl groups can be replaced with sulfhydryl, thioether, and thiocarbonyl groups, respectively.

Despite such structural similarities, there are several physicochemical differences between oxygen and sulfur that can affect the physicochemical properties of thio-modified nucleobases, nucleosides, and oligonucleotides.

2.1 Atom Sizes

The ground state electron configuration of oxygen and sulfur is $1s^2 2s^2 2p^4$ and $1s^2 2s^2 2p^6 3s^2 3p^4$, respectively. Since the outer shell electron orbitals of sulfur are 3s and 3p, which are larger than the 2s and 2p orbitals of oxygen, the atomic radius of sulfur is larger than that of oxygen.

Several estimated indexes are used to compare the atom sizes of oxygen and sulfur. The Van der Waals radii, frequently used for discussing the size of atoms, are 1.52 and 1.80 Å for oxygen and sulfur [8], respectively. This index suggests that the radius of sulfur is 1.2–1.3 times larger than that of oxygen.

The difference in the electron configuration between oxygen and sulfur also affects the length of the chemical bonds containing one of these two atoms. The typical bond lengths were reported to be 1.4 Å for a C–O single bond, 1.8 Å for a C-S single bond, 1.2 Å for a C=O double bond, and 1.6 Å for a C=S double bond [15]. Approximately, the bond between carbon and sulfur is supposed to be 0.4 Å longer than the corresponding carbon-oxygen bond. The space filling models of the thio-modified nucleobases optimized at HF 6-31G**level of calculations is shown in Fig. 2. As it can be seen, the thio-modification changes the steric bulkiness at the
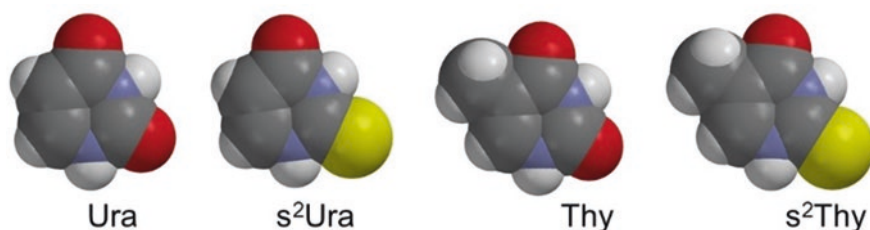

Fig. 2 Space filling models of thio-modified nucleobases

minor groove side of the nucleobase, which influences various physicochemical properties of thio-modified nucleobases, nucleosides, and oligonucleotides.

2.2 Electronic Properties

The electronegativity of atoms is a parameter used to predict the distribution of electrons in a molecule. The Pauling's electronegativity [2] is 3.44 and 2.58 for oxygen and sulfur, respectively, suggesting that oxygen is more negatively charged than sulfur. Besides the "static" distribution of electrons, there is another important factor, namely the polarizability (α, $\times 10^{-24}$ cm^3), which is an index that relates to the deformation of the electron cloud around the nucleus when an atom is placed in an outer electric field. The polarizability affects the molecular interactions between nucleobases, such as the London dispersion force [33]. The α values of oxygen and sulfur are 0.80 and 2.90, respectively [15]. Thus, the electron cloud of sulfur is more deformable than that of oxygen.

The consequence of these basic electronic properties is that the oxygen of the carbonyl group bears more negative charges than the sulfur of the thiocarbonyl group. It is expected that the carbonyl group can effectively interact with the surrounding polar functional groups through dipole-dipole or electrostatic interactions. On the contrary, the large atomic surface and large polarizability of the thiocarbonyl group indicate that the interaction between sulfur and the nearby atoms through the London dispersion force is more effective than that between oxygen and nearby atoms.

3 Physicochemical Properties of 2-Thiouracil and 2-Thiothymine

2-Thiouracil and 2-thiothymine are derivatives of uracil (Ura) and thymine (Thy), respectively, in which the carbonyl group at the 2-position is replaced by a thiocarbonyl group. It should be noted that these bases exist in nature as modified nucleobases in transfer RNAs [18]. Nucleobases, nucleosides, and oligonucleotides have several properties that make these modifications potentially useful for the development of nucleic acid drugs.

3.1 Intrinsic Hydrogen Bonding Ability of s²Ura and s²Thy

Quantum chemical calculations have been carried out for a Watson-Crick base pair composed of 2-thiouracil and adenine, in order to clarify the hydrogen bonding stability of this base pair. Šponer et al. reported a study at the MP2/6-31G*(0.25)

level of calculations showing that the base pairing energy of adenine (Ade) and Thy was −11.8 kcal/mol, whereas that of Ade and s²Ura was −12.1 kcal/mol (Fig. 3a, b, [31]). These results suggest that the thio-modification at the two-position of the pyrimidine ring has only a small effect, equal to 0–0.3 kcal/mol, on the strength of the Watson-Crick base pair with A, probably because the 2-thio group does not participate in the base pairing.

Similar calculations were also carried for the Wobble base pairs of guanine (Gua) and Ura, and Gua and s²Ura. The data of these MP2 level calculations showed that the hydrogen bond energy between Gua and Ura was −12.7 kcal/mol, while that of Gua and s²Ura was −12.1 kcal/mol (Fig. 3c, d, [32]). It should be noted that although the 2-thio group is involved in the hydrogen bonding in the Wobble base pair, the energy difference between unmodified and thio-modified base pairs is as large as 0.6 kcal/mol. Šponer also reported higher level calculations, which corresponded to the RI-MP2/aug-cc-pVTZ level denoted as aDZ→aTz (Fig. 3c, d in parenthesis, [32]) and that the energy of Gua-Ura and Gua-s²Ura was −15.8 and −14.6 kcal/mol, respectively. In this case, the energy difference increased to 1.2 kcal/mol.

These results indicate that despite the widespread opinion of the weak hydrogen bonding ability of sulfur, the thiocarbonyl group of s²Ura does not greatly destabilize the base pair with Gua. The hydrogen bond ability of sulfur is also suggested by recent studies on hydrogen bonded complexes between small molecules [6] and amino acid residues in proteins [5]. The hydrogen bond ability of sulfur, which is comparable to that of oxygen, may be due to the fact that the London dispersion interaction between sulfur and proton, which is stronger than that with oxygen,
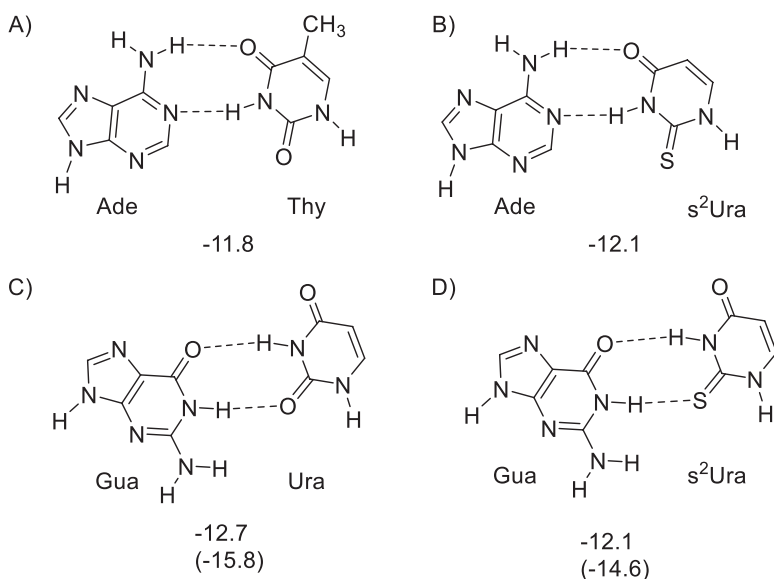
Fig. 3 Hydrogen bond energies (kcal/mol) of (**a**, **b**) Watson-Crick and (**c**, **d**) Wobble base pairs. The values are reported from [31]. The values in parenthesis are cited from [32]

compensates for the electrostatic interaction between sulfur and proton, which is weaker than that between oxygen and proton [31].

A recent study suggested that in the base pairing under aqueous conditions, another factor, i.e., the desolvation penalty, should be considered. The desolvation penalty is the energy associated with the breakage of the hydrogen bonds between water molecules and each of two nucleobases upon formation of a pair of two nucleobases. When s²Ura and Ura are compared, s²Ura is less hydrated than Ura. Therefore, the dehydration penalty is smaller in the process of formation of the s²Ura-A pair than the Ura-A pair, and the s²Ura-A pair becomes more stable than Ura-A [14].

3.2 Stacking Interactions of s²Ura

Quantum chemical calculations at the MP2 level have also been carried out for the stacked dimers of two free s²Ura or Ura bases. In these calculations, the two bases have a parallel arrangement and can freely rotate to search for the most stable conformation. In the case of the most stable geometry of the s²Ura-s²Ura pair, the two bases are perpendicular and the stacking interaction energy is −8.08 kcal/mol [30], which is smaller than that of Ura-Ura, which is about −6 kcal/mol for a similar geometry (Šponer 1996). Thus, it is expected that the enhanced London dispersion attraction of sulfur contributes to the stabilization of the stacked pair.

In the B-type duplex geometry (Fig. 4a), the 2-thiocarbonyl group of s₂T stacks on the 3′-downstream nucleobase, and it is expected to stabilize the helical conformation. Recently, Masaki et al. carried out systematic molecular dynamics and experimental analyses on the stability of a 2′-modified RNA duplex containing s²Ura. The structure suggests that the 2-thio group of s²Ura also effectively stacks on the 3′-downstream nucleobase, stabilizing the A-type duplex structure (Fig. 4b, [16]).
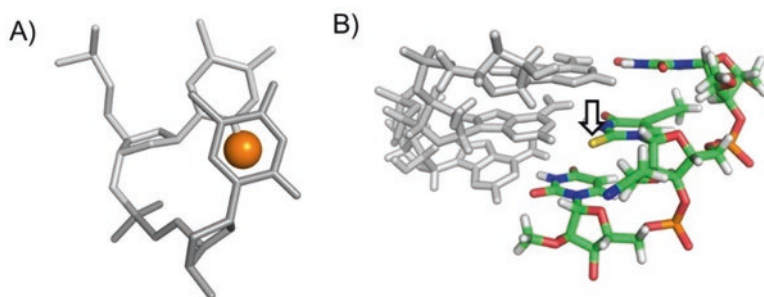
Fig. 4 Interaction of the 2-thio carbonyl group in (**a**) standard B-type helix geometry and (**b**) A-type duplex incorporating a 2′-(2-cyanoethyl)-5-propinyl-2-thiouridine residue [16]. The thiocarbonyl group is indicated by an arrow

3.3 'Rigid' Sugar Conformation of 2-Thiouridine (s^2U) and 2-Thiothymidine (s^2T) Derivatives

The 2-thio modification of uridine or ribothymidine affects their sugar conformation. The conformational properties of a nucleoside can be modeled as an equilibrium between N-type (C3′-*endo*) and S-type (C2′-*endo*) conformations, and indexed by the population of either conformer (Fig. 5). In the case of ribothymidine, the population of the N-type conformer (%N) is 52%, while the %N of 2-thioribothymidine is 73% [38]. Thus, it is clear that the 2-thio modification of ribothymidine stabilizes the N conformer. It should also be noted that in the case of deoxynucleosides, the %N of thymidine and 2-thiothymidine, which are 36 and 41%, respectively, differs only by 5%. Thus, this implies that the 2′-hydroxy group also plays an important role. The effect of the 2-thiocarbonyl group is schematically explained in Fig. 5. In the S-type conformation, the thiocarbonyl and the 2′-hydroxyl groups are in close proximity, and a steric repulsion occurs between them. On the contrary, in the N-type conformation both the nucleobase and the 2′-hydroxy group are in a pseudo-axial position, and the steric repulsion does not occur. In addition to such steric effects, a recent theoretical study [39] suggested the importance of the orbital interactions involving C=S bonds and C2-N3 bond, and distant electrostatic interactions between the S atom and H2′. Thus, the N-type conformation of the thio-modified nucleosides is thought to be stabilized by these steric and electronic interactions.

3.4 Conformational Properties of Single Stranded Oligonucleotides Incorporating 2-Thiouridine

The above properties of thio-modified nucleobases and nucleosides are retained after the nucleoside residues are incorporated into single stranded oligonucleotides.

For example, many studies revealed that a single stranded oligoribonucleotide incorporating 2-thiouridine tends to form a helical structure even in the absence of a counterstrand. As an example, Kumar et al. investigated the conformation of an

Fig. 5 Conformation equilibrium of the ribose moiety of a nucleoside illustrated using ribothymidine and 2-thioribothymidine. The population (%) is reported from [38]

N-type (C3'-endo)
52%(X = O)
73%(X = S)

S-type (C2'-endo)
48%(X = O)
27%(X = S)
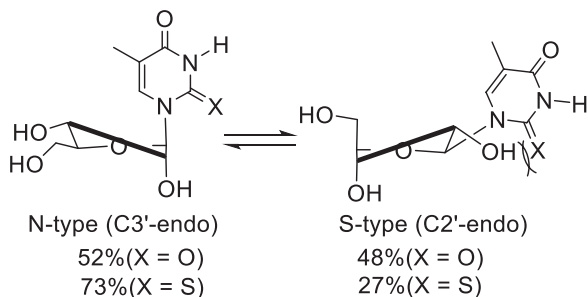
RNA pentamer whose sequence was 5′-G[s²U]UUC-3′ by using circular dichroism spectroscopy, and found that this sequence maintained a helical conformation in which s²U and upper and lower bases stacked at both 30 and 10 °C, whereas the natural type pentamer 5′-GUUUC-3′ partially melted at 30 °C (Kumar et al. 1997). In view of the sugar conformation described in 2-3, the stabilization of the N-type sugar conformation was also observed for dinucleotides incorporating s²U [1, 29]. These properties can be explained by the strong stacking effects of s²Ura and the rigid conformation of s²U. It should be noted that the rigid conformation of single stranded oligonucleotides incorporating s²U is an important factor to explain the hybridization properties of the thio-modified oligonucleotides described in the next section.

3.5 Hybridization Ability of Oligonucleotides Incorporating 2-Thiouridine Derivatives

It has been reported that oligonucleotides incorporating s²U and its 2′-O-substituted derivative formed a more stable duplex with a complementary strand compared to the duplex without thio-modification. Two mechanisms are possible by which the thio-modification stabilizes the duplex. The first is the strong stacking effect of the thiocarbonyl group, which works effectively in the helical structure, as described in Fig. 4. The second is the so called "pre-organization" effect that stabilizes the duplex from an entropic point of view. In general, the formation of a duplex from two single stranded oligonucleotides is an entropically unfavorable process because the entropy of the flexible single stranded state is larger than that of the rigid duplex state [7]. Either of these effects is expected to contribute to the higher hybridization ability of 2-thio-modified oligonucleotides.

For example, Kumar et al. reported that 5′-G[s²U]UUC-3′ and the complementary 2′-O-methyl RNA formed a duplex whose T_m value was 30.7 °C, whereas the T_m value of the duplex incorporating U instead of s²U was 19.0 °C (Kumar et al. 1997). Thus, this clearly suggested that s²U stabilized the duplex. Thermodynamic analyses revealed that the stabilization originated from the enthalpic ($\Delta H°$) term, which decreased from −43.22 to −46.46 kcal/mol owing to the thio-modification. In contrast, the entropic term ($\Delta S°$) which also decreased from −148.2 to −152.8 eu upon the thio-modification contributed to the destabilization of the duplex. As a whole, the duplex was stabilized by −2.8 kcal/mol in terms of the Gibbs free energy ($\Delta G°$) owing to the thio-modification. Therefore, in this case, the thermodynamic parameters suggested that the strong stacking of s²Ura, which decreased the $\Delta H°$, contributed to the duplex stabilization.

On the contrary, another comparative study on the duplexes formed by thio-modified-RNA/RNA and RNA/RNA, whose sequences were 5′-UAGC[s²U]CC-3′/3′-AUCGAGG-5′ and 5′-UAGCUCC-3′/3′-AUCGAGG-5′, respectively, revealed that the $\Delta H°$ of the thio-modified duplex was larger than that of the unmod-

ified duplex by 2.2 kcal/mol, whereas the $\Delta S°$ increased by 9 eu owing to the thio-modification. Thus, in this case, the $\Delta S°$ term, which originated from the conformational rigidity of s^2U, contributed more to the duplex stabilization due to the thio-modification. Therefore, these thermodynamic studies indicate that various physicochemical properties of s^2U such as the strong stacking ability of the nucleobase and the conformational rigidity can contribute to the increased duplex stability. It was also suggested that the contribution of each term differed depending on the oligonucleotides' sequence, the position of s^2U in the oligonucleotides, and the backbone structure.

However, it should be noted that irrespective of such mechanistic complexity, the incorporation of s^2U or its derivatives including 2′-*O*-substituted, 5-substituted, and 2′,5-disubstituted s^2U derivatives [16] contributed to the stabilization of most sequences and structural contexts such as RNA/RNA (Kumar et al. 1997; [29]), RNA/2′-*O*-substituted-RNA [21, 23], RNA/DNA [29], and DNA/DNA duplexes [11].

3.6   Base Discrimination of 2-Thiouridine Derivatives in a Duplex

The incorporation of s^2U and its derivatives is promising for the development of nucleic acid drugs not only because of the duplex stabilization effects discussed above, but also for the high base discrimination ability especially to recognize A over G. It is well known that U and G can form Wobble-type base pairs in nucleic acid duplexes, and a duplex containing U-G pairs is relatively stable [36]. Thus, it is important to develop uridine analogues that selectively form base pairs with G.

Shohda et al. reported the T_m values of a duplex between 2′-*O*-methyl-RNA containing a s^2U, whose sequence was 5′-CGUU[s^2U]UUGC-3′, and the complementary RNA strand 3′-GCAA[X]AACG-5′ where X = A or G. As a result, the duplex where X = A showed a T_m value of 42.2 °C, whereas when X = G the T_m value decreased to 26.5 °C, which is 15.7 °C lower than the above duplex containing the s^2U-A pair [29]. In contrast, the 2′-*O*-methyl-RNA having the same sequence except for the replacement of s^2U with U showed much poorer discrimination, giving T_m values of 36.7 and 32.8 °C for X = A and G, respectively. These data clearly suggested that s^2U had higher base pairing selectivity than U towards A over G. It should be noted that the selectivity was confirmed for the duplex formed by replacing the complementary RNA with DNA.

Detailed thermodynamic studies were carried out for an RNA-RNA duplex incorporating s^2U-A or s^2U-G base pair [34]. In the cases of duplexes whose sequences were 5′-GAG[s^2U]GAG-3′/3′-CUC[X]CUC-5′ and 5′-AUGAC[s^2U]-3′/3′-UACUG[X]-5′, where X = A or G, the T_m of the duplex containing the s^2U-A pair was higher than that of the duplex containing the s^2U-G pair by 15.9 °C, which corresponded to a Gibbs free energy difference of 3.4 kcal/mol.

3.7 Application of 2-Thiouridine Derivatives as Nucleic Acid Drugs

It has long been proposed that the duplex stabilizing and base discrimination properties are useful for the development of antisense or other nucleic acid drugs [10, 34].

As an example, Masaki et al. synthesized 30 mer 2′-O-methyl-RNAs whose sequences were 5′-CXCCAACAGCAAAGAAGAXGGCAXXXCXAG-3′, where X is U, s^{2}U, or s^{2}T [17]. This sequence is named as the mB30 sequence and it is designed to bind to the dystrophin pre-mRNA and induce skipping of exon 51 to cure the out-of-frame shift of exon 52 depleted *mdx* mouse [3]. As a result, the oligonucleotides having X = s^{2}T or s^{2}U showed higher affinity to complementary RNA than the oligonucleotide X = U. However, in vivo experiments using the *mdx* mice suggested that the order of the exon skipping efficiencies was X = s^{2}T > U > s^{2}U. Thus, it was suggested that the in vivo activities of the thio-modified oligonucleotides were affected by the methyl group at the five position.

Another example of thio-modified antisense oligonucleotides was reported by Østergaard et al. [24], who introduced s^{2}T in the DNA region of gapmer oligonucleotides and reported the modulation of RNase-H cleavage sites and the improvement of the allele specificity.

4 Chemical Synthesis of 2-Thiouridine Derivatives and Their Incorporation into Oligonucleotides

Various derivatives of 2-thiouridine have been reported in the literature. In general, two synthetic routes are available for the preparation of 2-thiouridine; one consists in connecting a ribose or deoxyribose derivative with a 2-thiouracil derivative by glycosylation, and the other is based on the direct thionation of a uridine derivative.

4.1 Synthesis of 2-Thiouridine and 2-Thiothymidine by Glycosylation

2-Thiouridine can be synthesized by using per-acylated ribose and a silylated base according to the Vorbrüggen procedure [13, 37]. The resulting 2-thiouridine derivative can be converted to the corresponding 3′-phosphoramidite according to a standard procedure (Fig. 6a).

2-Thiodeoxyuridine and 2-thiothymidine can be synthesized as shown in Fig. 6b starting from α-1-chloro-2-deoxy-3,5-di-toluoylribose and silylated 2-thiouracil or 2-thiothymine, respectively [26]. The same method is applicable to the synthesis of various 5-substituted 2-thiodeoxyuridine derivatives [27].

A)

R = H , CH$_3$. etc

B)

R = H , CH$_3$. etc
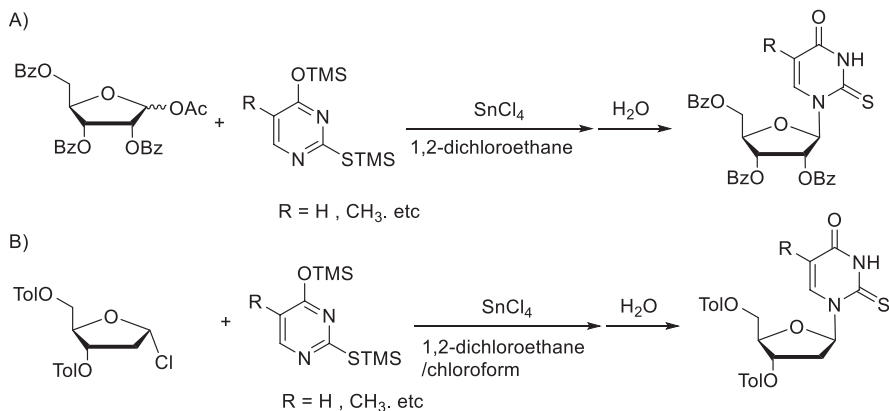
Fig. 6 Synthetic routes towards 2-thiomodified nucleosides via glycosylation

4.2 Synthesis of 2-Thiouridine Derivatives Form Uridine Derivatives

Another approach for the synthesis of 2-thiouridine derivatives is the direct conversion of the carbonyl group at the 2-position of uridine derivatives into a thio-carbonyl group. As shown in Fig. 7a, Ueda and Shibuya reported the conversion of 2,3-*O*-isopropylidene-2,5′-anhydrouridine **1** into 2,3-*O*-isopropylidene-2-thiouridine derivative **2** by treatment with liquid H$_2$S [35]. A similar approach by using 2,5′-anhydrouridine **3** was also reported [9]. This protocol was modified and used for the synthesis of 2′-*O*-(2-methoxyethyl) or 2′-fluoro-2-thioribothymidine (Rajeev et al. 2003). In this report, 5′-*O*-mesyl-ribothymidine **4** was converted to the cyclo derivative **5** and then converted *in situ* to the ethoxy derivative **6**. After protection of the 5′-hydroxy group, the ethoxy group was substituted by H$_2$S to give 2-thio compound **7**.

Another route for the synthesis of 2-thiouridine was also reported as shown in Fig. 8 [21]. In this reaction, uridine derivative **8** in which the hydroxy and 4-*O* moieties were protected with TBDMS and 2,6-dimethylphenyl groups, respectively, was used. Subsequent treatment of **8** with the Lawesson's reagent gave the desired 2-thionated compound **9** in 94% yield. The 2,6-dimethylphenyl group was removed by treatment with *syn-o*-nitrobenzaldoxime in the presence of 1,1,3,3-tetramethylguanidine. Importantly, this approach can be utilized for more complex base and sugar modified nucleosides (Fig. 9), for example in the thionation of uridine derivatives having 2′-*O*-methyl (**9**), allyl (**10**), and 2-methoxyethyl (**11**) groups. In addition, Masaki et al. [16] reported the synthesis of a 2-cyanoethyl derivative [25] as sugar modified nucleoside (**12**). In addition, as base modified nucleosides, the thionation by the Lawesson's reagent was compatible with 5-methyl (**13**), 5-bromo (**14**), or 5-propynyl (**15**) groups [16].
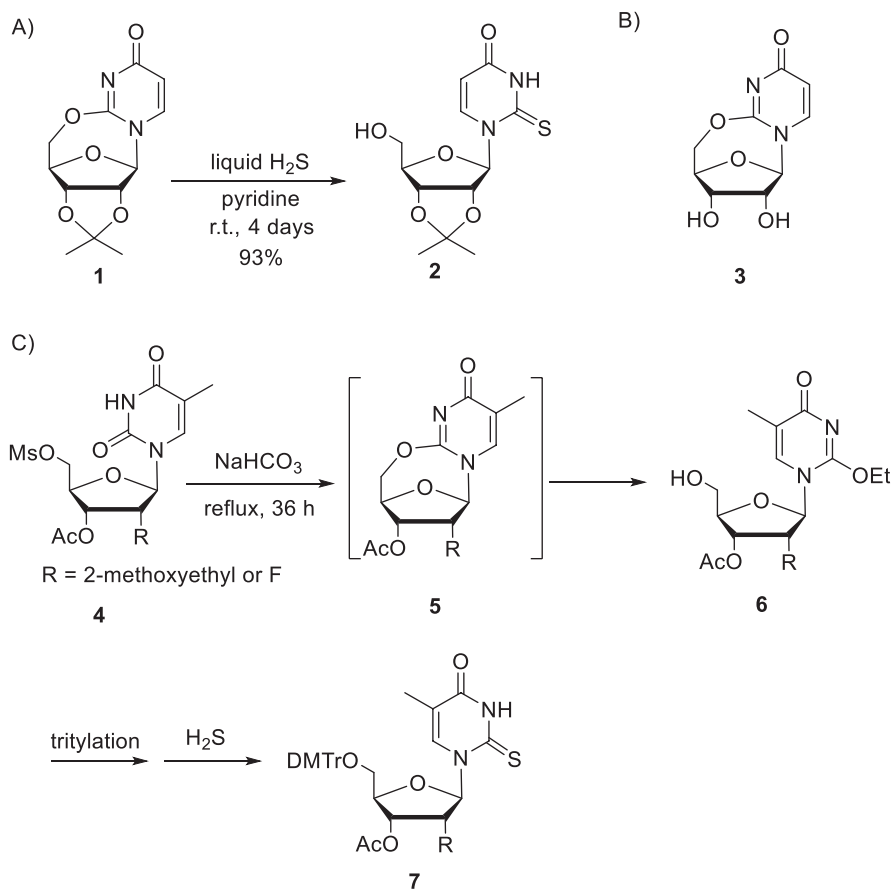
Fig. 7 Synthesis of 2-thiouridine from cyclonucleosides and C) and Lawesson's reagent
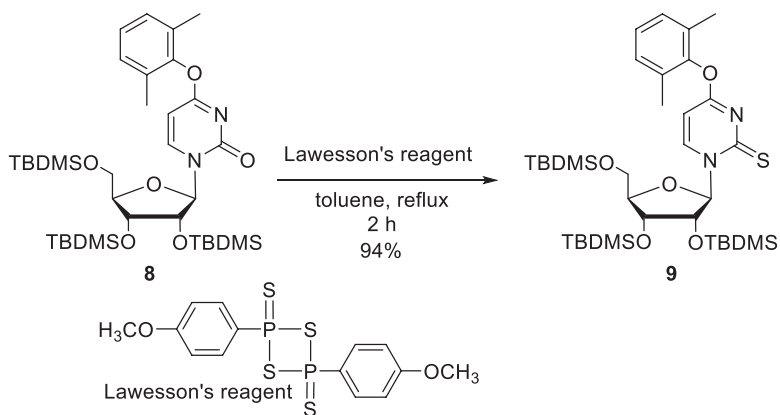
Fig. 8 Synthesis of a 2-thiouridine derivative using the Lawesson's reagent
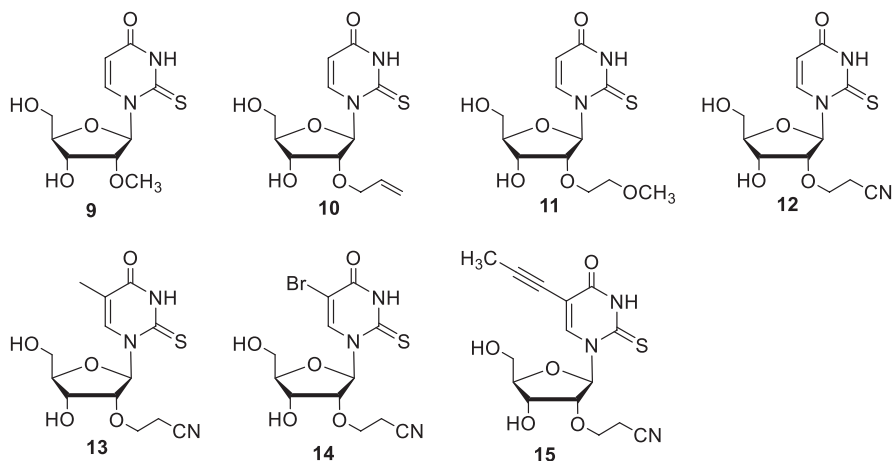
Fig. 9 Thio-modified nucleosides synthesized by the procedure of [21]

4.3 Synthesis of the Phosphoramidites of 2-Thiothymidine and 2-Thiouridine Derivatives and Their Use in Oligonucleotide Synthesis

2-Thiothymidine and 2-thiouridine derivatives can be incorporated into oligonucleotides using either base-protected (**16**) or unprotected (**17**) phosphoramidites. The phosphoramidites can be synthesized from the corresponding base-protected or unprotected nucleosides using the conventional 2-cyanoethyl *N,N*-diisopropylchlorophosphoramidite [28] or 2-cyanoethyl *N,N,N',N'*-tetraisopropylphosphorodiamidite [20] as phosphitylating agents.

To prepare the base protected phosphoramidites, the toluoyl group was used to protect the *N*3 or *O*4 positions of 2-thiothymidine **16** [11]. The use of the benzoyl group for the protection of 2-thiouridine derivatives was reported to be unsuccessful because of its instability during the tritylation step [29]. By using the base protected phosphoramidite, the oligonucleotides can be synthesized according to the standard phosphoramidite DNA/RNA synthesis protocol (Fig. 10).

When base unprotected phosphoramidites were used, the oxidation step during the standard phosphoramidite DNA/RNA synthesis protocol could be problematic. It has been reported that the 2-thio groups of 2-thiouridine derivatives are susceptible to oxidizing agents such as hydrogen peroxide, percarboxylic acids [4], and 0.1 M iodine in pyridine-H_2O (9:1, v/v) [22]. Under these conditions 2-thiouridine derivatives such as **18** are converted to 4-pyrimidone **19** or uridine **20** derivatives.

In order to avoid such side reactions during oligonucleotide synthesis, Kumar et al. employed 10% *tert*-butyl hydroperoxide in acetonitrile for 6 min for the oxidation step in the phosphoramidite DNA/RNA synthesis protocol [12]. Moreover,
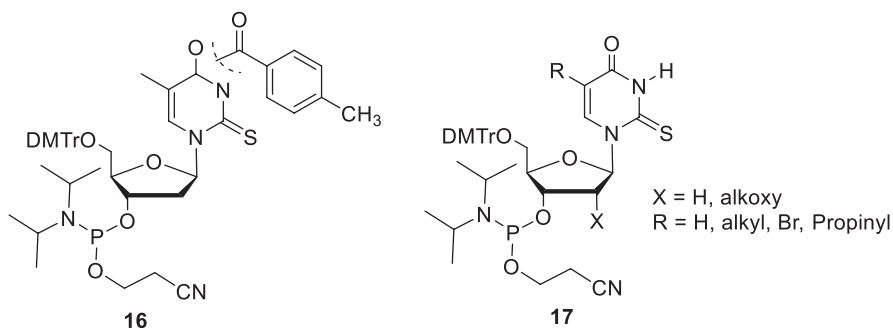
Fig. 10 Structure of base-protected phosphoramidite of s²T (**16**) and general structures of base-unprotected thio-modified phosphoramidites (**17**)
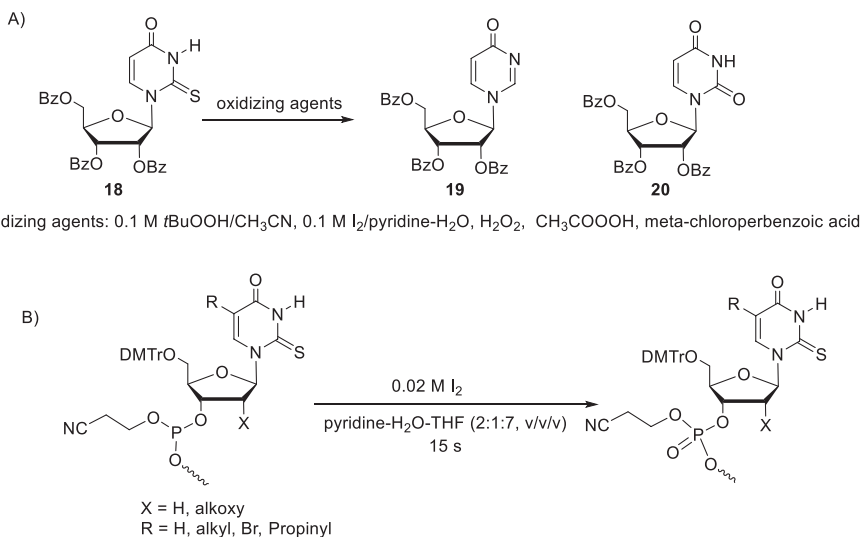
Fig. 11 (**a**) Desulfurization of the 2-thiocarbonyl group and (**b**) oxidation protocol using 0.02 M I₂

Okamoto et al. reported that the oxidation by 0.02 M I₂ [19] in pyridine-H₂O-THF (2:1:7, v/v/v) for 15 s was more suitable for the synthesis of oligodeoxynucleotide incorporating one to five 2′-*O*-methyl-2-thiouridine residues. By using such conditions, oligonucleotides incorporating various 2-thiouridine derivatives having substituents at the 2′- and/or the five-positions have been successfully synthesized [16, 17] (Fig. 11).

References

1. Agris PF, Sierzputowska-Gracz H, Smith W, Malkiewicz A, Sochacka E, Nawrot B (1992) Thiolation of uridine carbon-2 restricts the motional maintain genome integrity. J Am Chem Soc 114:2652–2656

2. Allred AL (1961) Electronegativity values from thermochemical data. J Inorg Nucl Chem 17:215–221

3. Aoki Y, Nakamura A, Yokota T, Saito T, Okazawa H, Nagata T, Takeda S (2010) In-frame dystrophin following exon 51-skipping improves muscle pathology and function in the exon 52-deficient mdx mouse. Mol Ther 18:1995–2005

4. Bartos P, Ebenryter-Olbinska K, Sochacka E, Nawrot B (2015) The influence of the C5 substituent on the 2-thiouridine desulfuration pathway and the conformational analysis of the resulting 4-pyrimidinone products. Bioorg Med Chem 23:5587–5594

5. Biswal HS, Wategaonkar S (2009) Nature of the N−H⋯S hydrogen bond. J Phys Chem A 113:12763–12773

6. Biswal HS, Wategaonkar S (2010) O-H⋯O versus O-H⋯S hydrogen bonding. 3. IR-UV double resonance study of hydrogen bonded complexes of p-cresol with diethyl ether and its sulfur analog. J Phys Chem A 114:5947–5973

7. Bloomfield VA, Crothers DM, Tinoco I Jr (2000) Nucleic acids: structures, properties, and functions, University Science Books Sausalito, Turner DH, p 259 Chapter 8: Conformational changes

8. Bondi A (1964) van der Waals Volumes and Radii. J Phys Chem 68:441–451

9. Chen LC, Su TL, Pankiewicz KW, Watanabe KA (1989) Synthesis of 2,5′-anhydro-2-thiouridine and its conversion to 3′-O-acetyl-2,2′-anhydro- 5′-chloro-5′-deoxy-2-thiouridine. Studies directed toward the synthesis of 2′-deoxy-2′-substituted arabino nucleosides. Nucleosides Nucleotides Nucleic Acids 8:1179–1188

10. Diop-Frimpong B, Prakash TP, Rajeev KG, Manoharan M, Egli M (2015) Stabilizing contributions of sulfur-modified nucleotides: crystal structure of a DNA duplex with 2'-O-[2-(methoxy)ethyl]-2-thiothymidines. Nucleic Acids Res 33:5297–5307

11. Kuimelis RG, Nambiar KP (1994) Synthesis of oligodeoxynucleotides containing 2-thiopyrimidine residues—a new protection scheme. Nucleic Acids Res 22:1429–1436

12. Kumar RK, Davis DR (1995) Synthesis of oligoribonucleotides containing 2-thiouridine: incorporation of 2-thiouridine phosphoramidite without base protection. J Org Chem 60:7726–7727

13. Kumar RK, Davis DR (1997) Synthesis and studies on the effect of 2-thiouridine and 4-thiouridine on sugar conformation and RNA duplex stability. Nucleic Acids Res 25:1272–1280

14. Larsen AT, Fahrenbach AC, Sheng J, Pian J, Szostak JW (2015) Thermodynamic insights into 2-thiouridine-enhanced RNA hybridization. Nucleic Acids Res 43:7675–7687

15. Lide DR (ed) (2004) CRC handbook of chemistry and physics, 84th edn. CRC Press LLC, Boca Raton

16. Masaki Y, Miyasaka R, Hirai K, Tsunoda H, Ohkubo A, Seio K, Sekine M (2012) Prediction of the stability of modified RNA duplexes based on deformability analysis: oligoribonucleotide derivatives modified with 2′-O-cyanoethyl-5-propynyl-2-thiouridine as a promising component. Chem Commn 48:7313–7315

17. Masaki Y, Inde T, Nagata T, Tanihata J, Kanamori T, Seio K, Takeda S, Sekine M (2015) Enhancement of exon skipping in mdx52 mice by 2′-O-methyl-2-thioribothymidine incorporation into phosphorothioate oligonucleotides. Med Chem Commun 6:630–633

18. Motorin Y, Helm M (2010) tRNA stabilization by modified nucleotides. Biochemist 49:4934–4944

19. Mullah B, Andrus A (1995) Oxidative conversion of N-dimethylformamidine nucleosides to N-cyano nucleosides. Tetrahedron Lett 36:4373–4376

20. Nielsen J, Dahl O (1987) Improved synthesis of (Pr$^i_2$ N$_2$) POCH$_2$CH$_2$CN. Nucleic Acids Res 15:3626

21. Okamoto I, Shohda K, Seio K, Sekine M (2003) A new route to 2'-O-Alkyl-2-thiouridine derivatives via 4-O-protection of the uracil base and hybridization properties of oligonucle-otides incorporating tThese modified nucleoside derivatives. J Org Chem 68:9971–9982

22. Okamoto I, Seio K, Sekine M (2006) Improved synthesis of oligonucleotides containing 2-thiouridine derivatives by use of diluted iodine solution. Tetrahedron Lett 47:583–585

23. Okamoto I, Seio K, Sekine M (2008) Study of the base discrimination ability of DNA and 2'-O-methylated RNA oligomers containing 2-thiouracil bases towards complementary RNA or DNA strands and their application to single base mismatch detection. Bioorg Med Chem 16:6034–6041

24. Østergaard ME, Kumar P, Nichols J, Watt A, Sharma PK, Nielsen P, Seth PP (2015) Allele-selective inhibition of mutant Huntingtin with 2-Thio- and C5- Triazolylphenyl-deoxythymidine-modified antisense oligonucleotides. Nucleic Acid Ther 25:266–274

25. Saneyoshi H, Seio K, Sekine M (2005) A general method for the synthesis of 2'-O-cyanoethylated oligoribonucleotides having promising hybridization affinity for DNA and RNA and enhanced nuclease resistance. J Org Chem 70:10453–10460

26. Shigeta S, Mori S, Kira T, Takahashi K, Kodama E, Konno K, Nagata T, Kato H, Wakayama T, Koike N, Saneyoshi M (1999) Antiherpesvirus activities and cytotoxicities of 2-thiopyrimidine nucleoside analogues in vitro. Antivir Chem Chemother 10:195–209

27. Shigeta S, Mori S, Watanabe F, Takahashi K, Nagata T, Wakayama T, Saneyoshi M (2002) Synthesis and antiherpesvirus activities of 5-alkyl-2-thiopyrimidine nucleoside analogues. Antivir Chem Chemother 13:67–82

28. Shinha ND, Biernat J, Köster H (1983) β -Cyanoethyl N,N-dialkylamino/N-morpholinomonochloro phosphoamidites, new phosphitylating agents facilitating ease of deprotection and work-up of synthesized oligonucleotides. Tetrahedron Lett 24:5843–5846

29. Shohda K, Okamoto I, Wada T, Seio K, Sekine M (2000) Synthesis and properties of 2'-O-methyl-2-thiouridine and oligoribonucleotides containing 2'-O-methyl-2-thiouridine. Bioorg Med Chem Lett 10:1795–1798

30. Šponer J, Leszczynski J, Hobza P (1997) Thioguanine and thiouracil: hydrogen-bonding and stacking properties. J Phys Chem A 101:9489–9495

31. Šponer J, Leszczynski J, Hobza P (2001) Electronic properties, hydrogen bonding, stacking, and cation binding of DNA and RNA bases. Biopolymers 61:3–31

32. Šponer J, Jurečka P, Hobza P (2004) Accurate interaction energies of hydrogen-bonded nucleic acid base pairs. J Am Chem Soc 126:10142–10151

33. Stone AJ (1996) The theory of intermolecular forces. Oxford University press, Oxford

34. Testa SM, Disney MD, Turner DH, Kierzek R (1999) Thermodynamics of RNA−RNA duplexes with 2- or 4-thiouridines: implications for antisense design and targeting a group I intron. Biochemistry 38:16655–16662

35. Ueda T, Shibuya S (1970) Synthesis of sulfur-bridged uracil anhydronucleosides. Chem Pharm Bull 18:1076–1078

36. Varani G, McClain W (2000) The G x U wobble base pair. A fundamental building block of RNA structure crucial to RNA function in diverse biological systems. EMBO Rep 1:18–23

37. Vorbruggen H, Strehlke P (1973) Eine einfache synthese von 2-thiopyrimidin-nucleosiden. Chem Ber 106:3039–3061

38. Yamamoto Y, Yokoyama S, Miyazawa T, Watanabe K, Higuchi S (1983) NMR analyses on the molecular mechanism of the conformational rigidity of 2-thioribothymidine, a modified nucleoside in extreme thermophile tRNAs. FEBS Lett 157:95–99

39. Zhang R, Eriksson LA (2010) Theoretical study on conformational preferences of ribose in 2-thiouridine—the role of the 2'OH group. Phys Chem Chem Phys 12:3690–3697

Site-Specific Modification of Nucleobases in Oligonucleotides

Yoshiyuki Hari

Abstract Site-specific modification of oligonucleotides is a powerful approach for synthesis of oligonucleotides containing various derivatives of nucleobases, sugars, and phosphate backbones. By using this method, the structure of a modified moiety can be effectively screened to find artificial oligonucleotides having desired functions. In fact, many studies using a variety of site-specific modification methods have been reported to date. In this chapter, the site-specific modifications focusing on nucleobases within oligonucleotides are summarized. Moreover, as an experimental example of site-specific modification of an oligonucleotide, the preparation of *N*,*N*-disubstituted cytosine derivatives using reaction of 4-triazolylpyrimidin-2-one nucleobase with various secondary amines is demonstrated.

Keywords Site-specific modification · Oligonucleotide · Nucleobase · Post-synthetic modification

1 Introduction

Since oligonucleotides can be applied in various fields such as medicine, genetic diagnosis and life science research, the development of novel, modified functional oligonucleotides has attracted attention. In general, the process of development is as follows: (i) design of the target nucleoside or molecule, (ii) synthesis of the building block for oligonucleotide synthesis, (iii) synthesis of the desired oligonucleotide using an automated DNA synthesizer, and (iv) functional evaluation of the oligonucleotide. The process must often be repeated many times to obtain a functional oligonucleotide, which is practically difficult because of enormous amount of time required, particularly for synthesis (Fig. 1a). In contrast, site-specific chemical modification of oligonucleotides is a powerful and attractive strategy, which allows synthesis of a number of oligonucleotides modified at a specific position from a single oligonucleotide bearing a reactive site (Fig. 1b). This approach can

Y. Hari (✉)
Faculty of Pharmaceutical Sciences, Tokushima Bunri University, Tokushima, Japan
e-mail: hari@ph.bunri-u.ac.jp

131
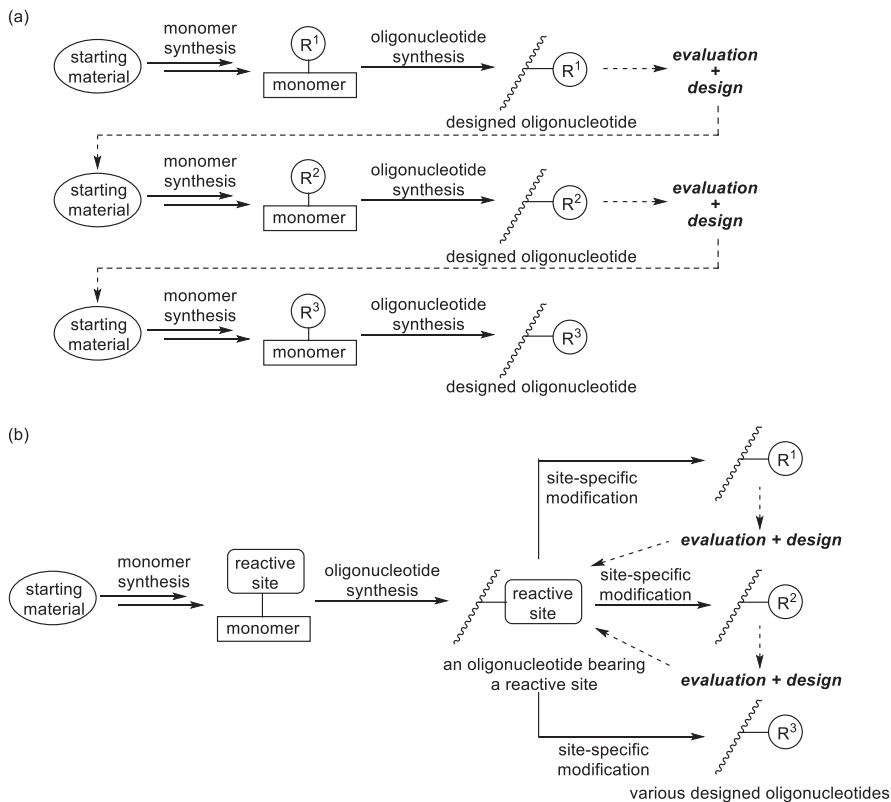
Fig. 1 Process of developing functional oligonucleotides: (**a**) General approach and (**b**) site-specific modification of an oligonucleotide
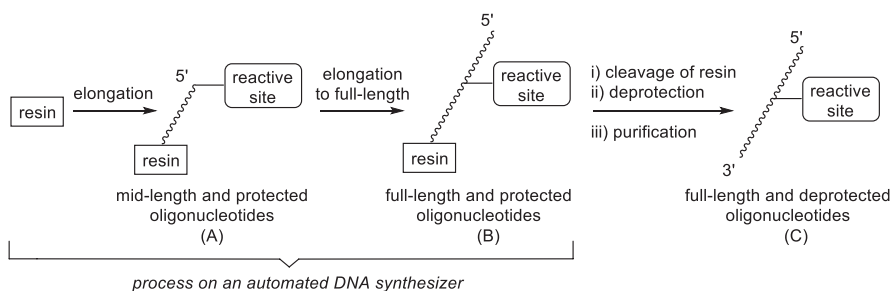
Fig. 2 Synthesis of oligonucleotides and possible timings of modification

streamline the process of finding the optimal structure for an oligonucleotide with desired function.

The site-specific modifications of oligonucleotides are generally conducted at any phase of (A)–(C), as shown in Fig. 2. Phase (A) is in the interim of elongation

of oligonucleotide by an automated DNA synthesizer, wherein protected and resin-attached oligonucleotides bearing the reactive site at the 5′-terminus are produced. Phase (B) is after complete elongation and results in full-length oligonucleotides containing protecting groups, resin, and the reactive site. Phase (C) is after deprotection, cleavage from the resin, and purification, wherein protection- and resin-free oligonucleotides bearing the reactive site are isolated.

To date, the site-specific modifications of oligonucleotides have been performed on various positions (e.g., nucleobase moiety, sugar moiety, phosphate linkage, and 5′- or 3′-terminus) [1–5]. Among them, modifications of nucleobases are interesting due to their applications, not only in attachment to functional molecules like fluorescent compounds, but also in improvement of functional nucleobases (e.g., increasing the recognition ability of target base in the formation of nucleic acid complexes). Thus, this chapter mainly focuses on the site-specific modifications of nucleobase moieties, and introduces previous reports, including a detailed experimental procedure.

2   Modifications at the 2- or 4-Positions of Pyrimidine Nucleobases

It was reported by Sung that protected oligonucleotides including 4-(1,2,4-triazol-1-yl)pyrimidin-2-ones as nucleobase precursors, prepared by liquid-phase synthesis using phosphotriester method, could be converted into cytosine analogs or uracil analogs. For instance, conversion of 4-(1,2,4-triazol-1-yl)pyrimidin-2-one into *N,N*-dimethylcytosine by treatment with dimethylamine (Fig. 3a) [6, 7]. Afterwards, this conversion was widely applied to oligonucleotides that were prepared by
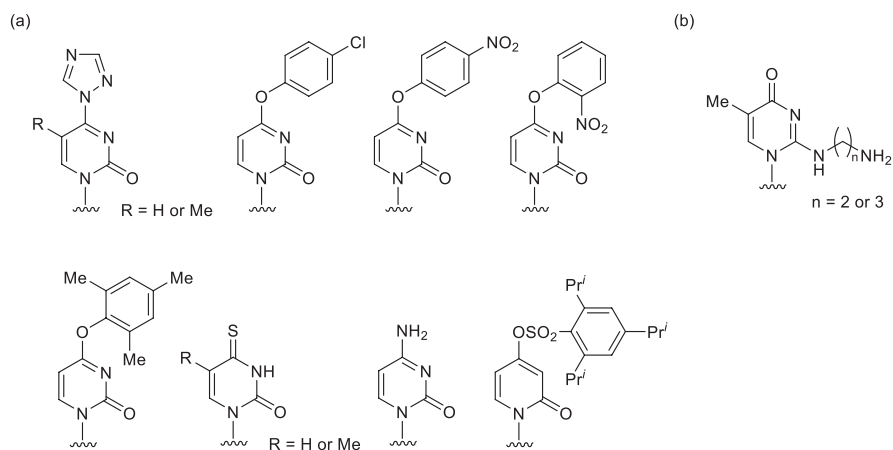
Fig. 3 Structures of pyrimidine-nucleobase precursors for modifications at the 4-position (**a**) and at the 2-position (**b**)

solid-phase synthesis using phosphoramidite method. In general, because of the high reactivity of triazolylated nucleobases against nucleophilic reagents, the conversion of triazolylated nucleobase precursors is conducted on protected oligonucleotides attached to the resin. For example, oligonucleotides containing 5-methyl-N^4,N^4-ethanocytosine for hybridization triggered cross-linking [8, 9], diazirine-linked cytosines for photo cross-linking [10], and N-substituted cytosines for targeting of double-stranded DNA [11–13] have been synthesized. Moreover, 4-thiothymine or O^4-alkylthymines have also been prepared [14–16]. In the case of a short trinucleotide prepared using H-phosphonate method, on-resin conversion of 4-triazolylated 5-methylpyrimidin-2-one into a 4-guanidino analog by guanidine treatment was achieved by Pedroso et al. [17]. 4-(Chlorophenoxy)pyrimidin-2-one can also be used instead of triazolylated pyrimidin-2-one for the preparation of various N^4-substituted cytosines by amine treatment (Fig. 3a) [18]. Moreover, Komatsu et al. reported on-resin conversion of 4-(p-nitrophenoxy)pyrimidin-2-one into 4-thiouracil or O^4-methyluracil [19]. 4-(o-Nitrophenoxy)pyrimidin-2-one was also used for the preparation of 4-thiouracil [20].

Unlike a labile triazolylated nucleobase precursor, 4-(2,4,6-trimethylphenoxy) pyrimidin-2-one is intact under mild ammonolysis conditions (Fig. 3a). Therefore, by use of phoshoramidites bearing facilely removable base-protecting groups [21], protecting group- and resin-free oligonucleotides including 4-(2,4,6-trimethylphenoxy)pyrimidin-2-one can be synthesized. Consequently, conversion at the final step makes possible and treatment with ammonia and primary amines solution at high temperature (55 °C or 65 °C) produces oligonucleotides containing the corresponding cytosines [22–24].

4-Thiopyrimidin-2-one nucleobases, i.e., 4-thiouracil and 4-thiothymine, within oligonucleotides can be used as convertible nucleobases to form S^4-alkyl and S^4-alkylthio derivatives by using alkyl iodides and N-(alkylthio)phthalimides or S-alkyl methanethiosulfonate in sodium phosphate buffer (pH 8.0) containing DMF as a co-solvent (Fig. 3a) [25–27]. The treatment with ammonia results in a substitution reaction, producing the corresponding amine derivative (5-methylcytosine from 4-thiothymine) [28].

Bisulfite-catalyzed transamination reaction of an oligonucleotide using alkylamines can convert natural cytosines in the oligonucleotide into the corresponding N^4-alkylated cytosines (Fig. 3a) [29]. Only cytosines within single-stranded region are converted while cytosines pairing with guanines in the double-stranded region are intact. Because no conversion of 5-methylcytosines occurs in this transamination reaction, only the cytosines in oligonucleotides including 5-methylcytosines can be transformed into various N^4-alkylated cytosines [30]. By means of this transamination, Miller's group found that an N^4-(3-acetamidopropyl)cytosine nucleobase in an oligonucleotide selectively interacted with a CG base pair in double-stranded DNA during triplex formation [31].

Taniguchi and Sasaki et al. reported on-resin conversion of the primary amino group in N^2-(aminoalkyl)-5-methylisocytosines into the guanidino and ureido groups for exploring a nucleobase that recognizes a CG interrupting site in antiparallel triplexes (Fig. 3b) [32]. The on-resin derivatization was achieved by

Fmoc-selective deprotection of fully protected and resin-attached oligonucleotides containing N^2-(Fmoc-protected aminoalkyl)-5-methylisocytosine followed by treatment with 1H-pyrazole-1-carboxamidine or trimethylsilylisocyanate. On-resin guanidinylation of the primary amino group by 1H-pyrazole-1-carboxamidine is also reported by Manoharan et al. [33] and Seidman et al. [11].

On-resin modification for the synthesis of N^4,N^4-disubstituted 3-deazacytosines is achieved using 4-(2,4,6-triisopropylphenylsulfonyloxy)pyridine-2-one as a precursor (Fig. 3a). This modification was used in the development of oligonucleotides for sequence-selective targeting of double-stranded DNA [34].

3 Modifications at the 2- or 6-Positions of Purine Nucleobases

Site-specific modifications for synthesis of oligonucleotides bearing various purine nucleobase analogs, such as N^6-substituted adenines, and N^2-substituted guanines, are well known. In general, after preparation of fully protected and resin-attached oligonucleotides bearing the purine analogs with leaving groups in an automated DNA synthesizer, treatment of the oligonucleotides with appropriate nucleophiles leads to oligonucleotides containing the desired nucleobase analogs. For example, polycyclic aromatic hydrocarbon adducts at the N^6-position of adenine can be synthesized from 6-fluoropurine [35], and not only 6-chloro analogs like 6-chloropurine [36, 37] and 6-chloro-2-methylthiopurine [38], but also 6-(4-chlorophenoxy)purine [18] are usable for the conversion into the 6-(substituted amino)purine congeners (Fig. 4a). For base-protected and resin-attached oligonucleotides that were elongated and oxidized using H-phosphonate method, 6-(pentafluorophenoxy)-2-trifluoroacetamidopurine nucleobase was transformed into the 6-(substituted amino)purine derivatives (Fig. 4a) [39].
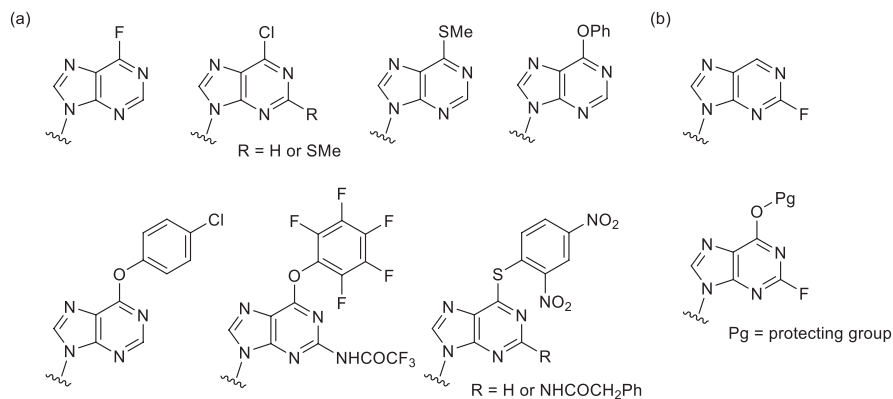
Fig. 4 Structures of purine-nucleobase precursors for modifications at the 6-position (**a**) and at the 2-position (**b**)

Meanwhile, 6-(2,4-dinitrophenylthio)purine [40] and its 2-phenylacetamido congener [16, 41] can be transformed into the corresponding 6-mercapto, 6-amino, 6-methylamino, 6-methoxy and 6-hydroxy analogs by treatment with 2-mercaptoethanol/ammonia, ammonia, methylamine, methanol/DBU, sodium hydroxide, respectively (Fig. 4a). The 2,4-dinitrophenylthio group acts as a good leaving group, and the substitution reactions with various nucleophiles proceed at room temperature. However, 6-mercapto analogs might be produced by attack of a nucleophile on the carbon at the 1-position of 2,4-dinitrophenyl group, instead of the carbon at the 6-position of the purine moiety. Concerning 6-methylthiopurine (Fig. 4a), oxidation of the methylthio moiety with magnesium salt of monoperoxyphthalic acid (MMPP) or mCPBA, followed by treatment with amines or aqueous sodium hydroxide, yields the desired oligonucleotides including N^6-substituted adenines or inosine [38, 42]. This conversion can be performed both for fully protected and resin-attached oligonucleotides and for free oligonucleotides [42]. Oxidation of a methylthio moiety within free oligonucleotides would prefer a milder oxidizing reagent, MMPP, to mCPBA.

Since 6-phenoxypurine is stable to mild ammonia treatment, the use of phosphoramidites bearing facilely removable base-protecting groups [21] allows synthesis of protection- and resin-free oligonucleotides containing 6-phenoxypurine nucleobase (Fig. 4a) [43]. After that, 6-phenoxypurine can be transformed into the corresponding N^6-substituted adenine by treatment with amines, and oligonucleotides capable of forming cross-linkage of disulfide were found.

Oligonucleotides containing N^2-substituted guanines can be synthesized by conversion of 2-fluoroinosine [36] and its O^6-protected congeners [10, 18, 37, 44, 45] by various amines such as aminoalcohols, polyamines and diazirine-linked amines (Fig. 4b).

4   Other Modifications in Nucleobase Units

5-Alkoxycarbonylpyrimidin-2-ones are promising substrates for modifications at the 5-position of pyrimidine nucleobases (Fig. 5). For example, for fully protected and resin-attached oligonucleotides, 5-methoxycarbonyl- [46, 47] or 5-trifluoroethoxycarbonyl-uracils [48] can be transformed by amine treatment into the corresponding 5-(N-substituted carbamoyl)uracils. For purified and deprotected oligonucleotides containing 5-(aminoalkylcarbamoyl)uracil prepared using this method,
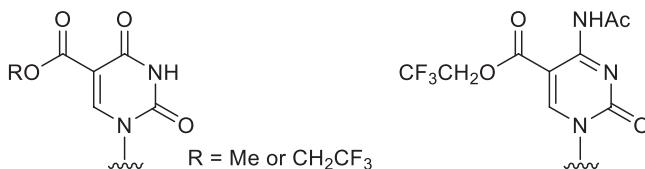

Fig. 5   Structures of 5-alkoxycarbonylpyrimidin-2-ones for modifications at the five-position

introduction of functional groups into terminal amino groups was achieved by Matsuda et al. [49]. They also reported modifications for oligonucleotides with an amino-linker at the 1′-position of the sugar [50]. The trifluoroethoxycarbonyl group can also be used for site-specific modifications, such as substitution at five-position of cytosine nucleobase [51]. The modification on alkoxycarbonyl groups by treatment with nucleophiles, such as amines, has been applied to nucleic acids with alkoxycarbonyl-modified sugar moieties [52, 53]. On the other hand, in the case of using uracil containing *N*-hydroxysuccinimide-ester unit at the five-position, the desired amide formation is achieved by amine treatment immediately after incorporation of the uracil into an oligonucleotide in an automated DNA synthesizer. Seeberger et al. used this method for installing carbohydrates into oligonucleotides [54]. Kahl and Greenberg succeeded in the on-resin amide-formation from amino or carboxyl groups linked to the five-position of uracil [55].

The Sonogashira-coupling reaction is used for site-specific modification of oligonucleotides. Coupling of 5-iodouracil unit within fully protected and resin-attached oligonucleotides with terminal alkynes in the presence of a palladium catalyst, a cupper catalyst, and an amine base is often carried out, and oligonucleotides containing various 5-substituted uracil units can be synthesized [56–61]. Direct coupling reaction with a 5-iodouracil unit in the middle of oligonucleotides has a low efficiency [56], and in that case, it is possible to synthesize the desired oligonucleotides containing an alkyne unit by a multi-step operation. The steps are as follows: (i) elongation to a longer chain with the 5-iodouracil unit by an automated DNA synthesizer (timing of (A) shown in Fig. 2); (ii) removal of the resin linked to the oligonucleotide before deprotection of the 5′-DMTr group; (iii) Sonogashira-coupling reaction on the CPG resin under anhydrous conditions; (iv) washing of the resin, followed by drying with an inert gas; (v) reinstallation of the resin on the synthesizer; and (vi) resumption of elongation of oligonucleotide by the synthesizer [56–58]. This procedure is also applicable to Sonogashira-coupling reaction with other nucleobase units, such as N^4-protected 5-iodocytosine, N^6-protected 8-bromoadenine, and N^2-protected 8-bromoguanine [59]. On the other hand, 4-iodobenzyloxy unit in the middle of oligonucleotides gave Sonogashira-coupling products, using fully elongated and on-resin oligonucleotides with all protecting groups, including the 5′-DMTr group. By this modification, Filichev and Pedersen found twisted intercalating nucleic acids stabilizing Hoogsteen-type nucleic acid complexes [62].

Unlike in the Sonogashira-coupling reaction, the reaction of 5-iodouracil nucleobase in the middle of protected oligonucleotides linked to the resin with sodium azide proceeds to yield the 5-azido congener, producing the fluorescent-labeled uracil derivative by successive copper-catalyzed azide–alkyne cycloaddition (CuAAC) reaction [63]. Moreover, on-resin Stille coupling of 5-iodouracil or 2-iodoadenine within protected RNA oligonucleotides can be achieved [64]. For Suzuki-Miyaura cross-coupling reaction, 5-iodouracil [65–67] and 8-bromoguanine [68] within free oligonucleotides without protecting groups and resin are usable. Meanwhile, 5-ethynyluracil nucleobase of 5′- or 3′-terminus of protected oligonucleotides linked on ArgoPore resin is a good substrate for copper-catalyzed oxidative acetylenic coupling with molecules, including terminal acetylene [69].
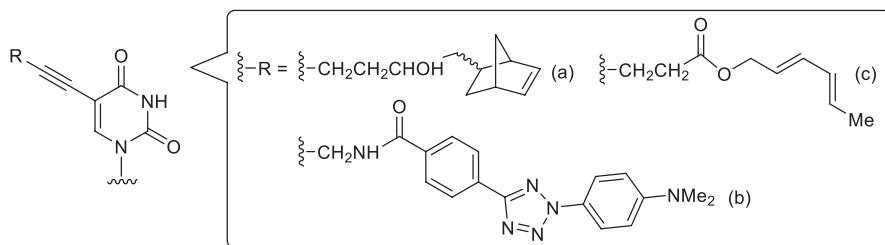
Fig. 6 Structures of nucleobases bearing (**a**) norbornene, (**b**) aryltetrazole, and (**c**) diene moieties

CuAAC reaction is a powerful post-synthetic modification method. A large number of CuAAC reactions between protecting groups- and resin-free oligonucleotides bearing terminal alkyne moieties and functional groups possessing azido groups have been reported to form conjugates through triazole-linkers [3, 4]. On the other hand, CuAAC reaction for synthesis of oligonucleotides containing various triazole-based nucleobases would be a unique approach, and it is applied to explore a nucleobase that specifically recognizes the target site during formation of a nucleic acid complex [70–73].

1,3-Dipolar cycloaddition reactions between oligonucleotides bearing a norbornene moiety linked at the 5-position of uracil and nitrile oxides proceed without any catalyst (Fig. 6a) [74], and the reactions can be applicable either to resin-attached oligonucleotides, or to purified and deprotected oligonucleotides. The use of 1,2,4,5-tetrazines instead of nitrile oxides undergoes inverse-electron-demand Diels-Alder reaction, leading to oligonucleotides possessing functional groups for fluorescence labeling and affinity tagging [75]. Moreover, push-pull-substituted diaryltetrazole attached to the five-position of uracil undergoes photo-mediated copper-free bioorthogonal reactions with maleimides (Fig. 6b) [76]. A uracil analog bearing a diene moiety at the 5-position reacts with maleimides to yield Diels-Alder products with functional tags (Fig. 6c) [77].

Oligonucleotides bearing ketone moieties linked to five-position of uracil can be decorated with diverse aminooxy compounds via oxime formation [78]. This post-synthetic modification by using a 100-fold excess amount of aminooxy compounds in phosphate-buffered saline seems to be complete after 24 h at 37 °C. After polymerase synthesis of DNA using triphosphates of 5-(formylaryl)cytosines, site-specific modifications on the formyl groups can be performed by reductive amination and hydrazone formation [79, 80].

5 Experimental Example: *N,N*-Disubstituted Cytosine Nucleobases

We have developed nucleobases capable of sequence-selective and stable recognition of a pyrimidine-purine interruption within dsDNA by triplex formation. For structural exploration of nucleobases, synthesis of oligonucleotides bearing various
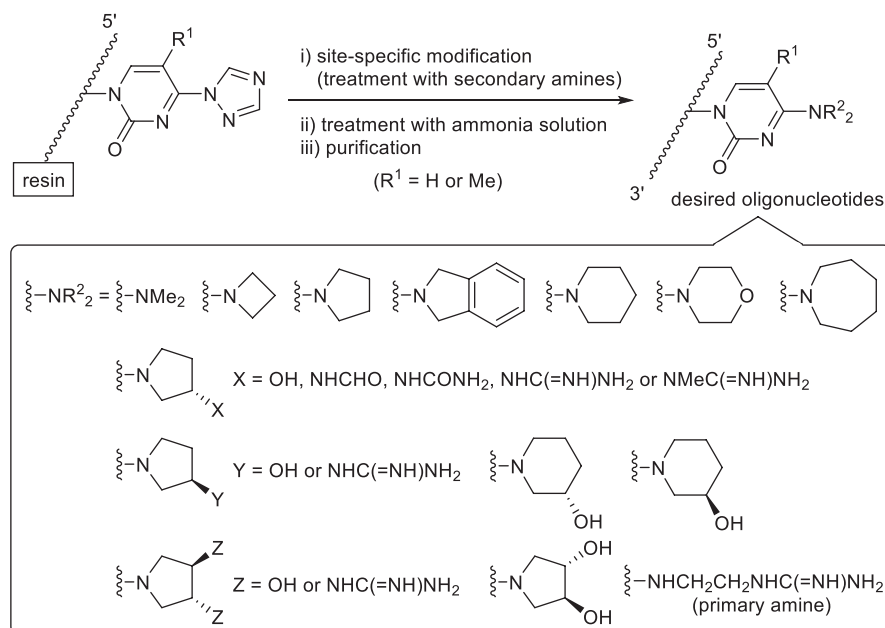
Fig. 7 Site-specific modifications of 4-triazolylated pyrimidin-2-ones, and structures of *N,N*-disubstituted cytosines synthesized

N,N-disubstituted cytosines was successfully achieved by treatment of the corresponding 4-triazolylated pyrimidin-2-ones with secondary amines (Fig. 7) [12, 13]. Experimental procedure, including technical tips, of the site-specific modification is given below.

1. The phosphoramidite of 5′-*O*-dimethoxytritylated nucleoside bearing triazolylated nucleobases is used, and elongation of oligonucleotides consisting of the desired sequence is completed on a 0.2 μmol scale in DMTr-on mode by an automated DNA synthesizer (Gene Design nS-8), using a standard phosphoramidite protocol. The use of phosphoramidites bearing mildly removable protecting groups as other phosphoramidites may be better.
2. Fully protected oligonucleotides attached to the CPG resin are treated with approximately 1 mL of 10–20% aqueous secondary amines solution at room temperature for 2 h. The nucleophilic nitrogen of amines used should be in salt-free form. UV absorbance of the aqueous solution is measured to confirm if sufficient amount of oligonucleotide is cleaved from the resin.
3. If sufficient UV absorbance was observed, after removal of the solution in vacuo, protecting groups of nucleobases and phosphates are removed by a common base treatment [e.g., treatment with 28% ammonia solution (55 °C for 9–10 h for nucleobases with standard protecting groups, and room temperature for 5–6 h for nucleobases with mildly removable protecting groups)]. The solution is removed in vacuo to give the crude 5′-DMTr-oligonucleotide.

4. If the amount is not enough in the step 2 above, treatment of the solution and the resin is conducted as follows. The solution is treated by the same way as step 3. On the other hand, the oligonucleotide is cleaved from the resin, followed by removal of protecting groups of nucleobases and phosphates according to a common base treatment (e.g., treatment with 28% ammonia solution at room temperature for 2 h for cleavage from the resin followed by adequate treatment for deprotection of nucleobases as described in step 3). Finally, both solutions are combined and concentrated in vacuo to give the crude 5′-DMTr-oligonucleotide.

5. The excess amount of amines is removed through Nap™-10 cartridge (GE-Healthcare), a prepacked gel filtration column. This depends on the type of amines used; it can be skipped for low boiling amines.

6. The crude 5′-DMTr-oligonucleotide is roughly purified through Sep-Pack® Plus C18 cartridge (Waters), a prepacked reversed-phase column, to remove shorter oligonucleotides as by-products in oligonucleotide synthesis using an automated DNA synthesizer. All fractions that have been confirmed to include oligonucleotide by UV-absorbance at 260 nm are collected and concentrated in vacuo. The HPLC charts of the crude oligonucleotides obtained after a prepacked reversed-phase column are shown in Fig. 8. Because this purification process includes deprotection of the 5′-DMTr group, protection-free oligonucleotide is produced.

7. The residue obtained in the step 6 is purified by reversed-phase HPLC (Waters XBridge® MS C_{18} 2.5 μm, 10 × 50 mm) using a TEAA solution (0.1 M, pH 7.0)/acetonitrile as an eluent system to obtain the desired oligonucleotide in pure form.

sequence of oligonucleotides synthesized: 5'-TTTTT<u>C</u>T**X**T<u>C</u>T<u>C</u>T<u>C</u>T-3' (<u>C</u> = 2'-deoxy-5-methylcytidine)
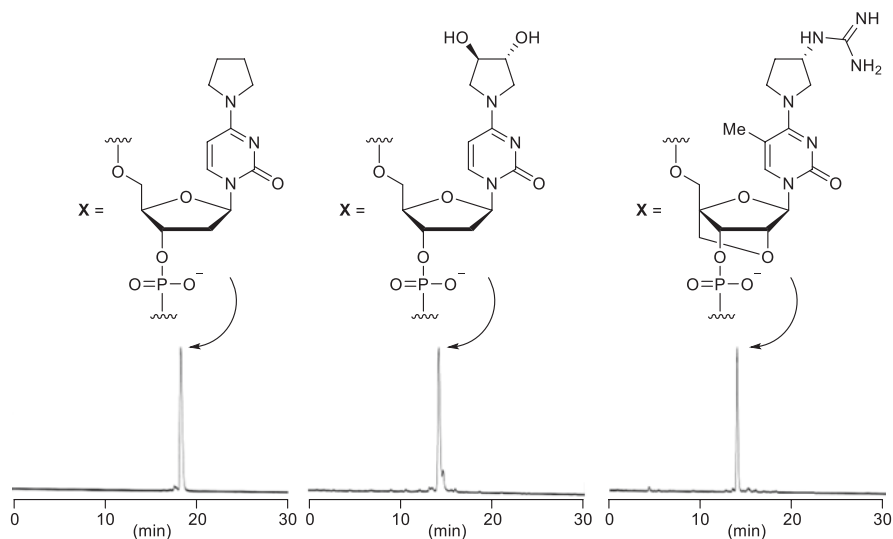
Fig. 8 HPLC charts of representative oligonucleotides containing *N,N*-disubstituted cytosines before HPLC purification (conditions: Waters XBridge® MS C_{18} 2.5 μm, 4.6 × 50 mm; 7–13% MeCN in 0.1 M TEAA buffer, pH 7.0 for 30 min; 1 mL/min of flow rate; 50 °C of column temperature)

6 Summary

For the development of functional oligonucleotides, the rate-limiting step is the synthesis of various derivatives for structural optimization, which is practically difficult because of time constraints. However, site-specific modification of oligonucleotides, as described in this chapter, would allow more efficient exploration of oligonucleotide structure. In future, development of a new class of modifications will contribute to finding greater numbers of functional oligonucleotides.

References

1. Goodchild J (1990) Conjugations of oligonucleotides and modified oligonucleotides: a review of their synthesis and properties. Bioconjug Chem 1:165–187
2. Verma S, Eckstein F (1998) Modified oligonucleotides: synthesis and strategy for users. Annu Rev Biochem 67:99–134
3. Gramlich PME, Wirges CT, Manetto A, Carell T (2008) Postsynthetic DNA modification through the copper-catalyzed azide-alkyne cycloaddition reaction. Angew Chem Int Ed 47:8350–8358
4. El-Sagheer AH, Brown T (2010) Click chemistry with DNA. Chem Soc Rev 39:1388–1405
5. Shaughnessy KH (2015) Palladium-catalyzed modification of unprotected nucleosides, nucleotides, and oligonucleotides. Molecules 20:9419–9454
6. Sung WL (1981) Synthesis of 4-triazolopyrimidinone nucleotide and its application in synthesis of 5-methylcytosine-containing oligodeoxyribonucleotides. Nucleic Acids Res 9:6139–6151
7. Sung WL (1982) Synthesis of 4-(1,2,4-triazol-1-yl)pyrimidin-2(1H)-one ribonucleotide and its application in synthesis of oligoribonucleotides. J Org Chem 47:3623–3628
8. Webb TR, Matteucci MD (1986) Sequence-specific cross-linking of deoxyoligonucleotides via hybridization-triggered alkylation. J Am Chem Soc 108:2764–2765
9. Webb TR, Matteucci MD (1986) Hybridization triggered cross-linking of deoxyoligonucleotides. Nucleic Acids Res 14:7661–7674
10. Shigdel UK, Zhang J, He C (2008) Diazirine-based DNA photo-cross-linking probes for the study of protein-DNA interaction. Angew Chem Int Ed 47:90–93
11. Semenyuk A, Darian E, Liu J, Majumdar A, Cuenoud B, Miller PS, MacKerell AD Jr, Seidman MM (2010) Targeting of an interrupted polypurine:polypyrimidine sequence in mammalian cells by a triplex-forming oligonucleotide containing a novel base analogue. Biochemistry 49:7867–7878
12. Hari Y, Akabane M, Hatanaka Y, Nakahara M, Obika S (2011) A 4-[(3R,4R)-dihydroxypyrrolidino]pyrimidin-2-one nucleobase for a CG base pair in triplex DNA. Chem Commun 47:4424–4426
13. Hari Y, Akabane M, Obika S (2013) 2′,4′-BNA bearing a chiral guanidinopyrrolidine-containing nucleobase with potent ability to recognize the CG base pair in a parallel-motif DNA triplex. Chem Commun 49:7421–7423
14. Fernandez-Forner D, Palom Y, Ikuta S, Pedroso E, Eritja R (1990) Synthesis and characterization of oligodeoxynucleotides containing the mutagenic base analogue 4-O-ethylthymine. Nucleic Acids Res 18:5729–5734
15. Xu Y-Z, Zheng Q, Swann PF (1992) Synthesis of DNA containing modified bases by postsynthetic substitution. Synthesis of oligomers containing 4-substituted thymine: O^4-Alkylthymine, 5-methylcytosine, N^4-(dimethylamino)-5-methylcytosine, and 4-thiothymine. J Org Chem 57:3839–3845

16. Xu Y-Z, Swann PF (1992) Chromatographic separation of oligodeoxynucleotides with identical length: application to purification of oligomers containing a modified base. Anal Biochem 204:185–189

17. Robles J, Grandas A, Pedroso E (2001) Synthesis of modified oligonucleotides containing 4-guanidino-2-pyrimidinone nucleobases. Tetrahedron 57:179–194

18. Allerson CR, Chen SL, Verdine GL (1997) A chemical method for site-specific modification of RNA: the convertible nucleoside approach. J Am Chem Soc 119:7423–7433

19. Komatsu Y, Kumagai I, Otsuka E (1999) Investigation of the recognition of an important uridine in an internal loop of a hairpin ribozyme prepared using post-synthetically modified oligonucleotides. Nucleic Acids Res 27:4314–4323

20. Aviñó A, García RG, Eritja R (2004) Synthesis of oligonucleotides containing 4-thiouridine using the convertible nucleoside approach and the 1-(2-fluorophenyl)-4-methoxypiperidin-4-yl group. Nucleos Nucleot Nucleic Acids 23:1767–1777

21. Schulhof JC, Molko D, Teoule R (1987) Facile removal of new base protecting groups useful in oligonucleotide synthesis. Tetrahedron Lett 28:51–54

22. MacMillan AM, Verdine GL (1990) Synthesis of functionally tethered oligodeoxynucleotides by the convertible nucleoside approach. J Org Chem 55:5931–5933

23. MacMillan AM, Verdine GL (1991) Engineering tethered DNA molecules by the convetible nucleoside approach. Tetrahedron 47:2603–2616

24. MacMillan AM, Chen L, Verdine GL (1992) Synthesis of an oligonucleotide suicide substrate for DNA methyltransferases. J Org Chem 57:2989–2991

25. Coleman RS, Siedlecki JM (1992) Synthesis of a 4-thio-2′-deoxyuridine-containing oligonucleotide. Development of the thiocarbonyl group as a linker element. J Am Chem Soc 114:9229–9230

26. Coleman RS, Kesicki EA (1994) Synthesis and postsynthetic modification of oligonucleotides containing 4-thio-2′-deoxyuridine (ds⁴U). J Am Chem Soc 116:11636–11642

27. Rublack N, Nguyen H, Appel B, Springstubbe D, Strohbach D, Müller S (2011) Synthesis of specifically modified oligonucleotides for application in structural and functional analysis of RNA. J Nucleic Acids 2011:1–18

28. Connolly BA, Newman PC (1989) Synthesis and properties of oligonucleotides containing 4-thiothymidine, 5-methyl-2-pyrimidinone-1-β-D-(2′-deoxyribose) and 2-thiothymidine. Nucleic Acids Res 17:4957–4974

29. Draper DE (1984) Attachment of reporter groups to specific, selected cytidine residues in RNA using a bisulfite-catalyzed transamination reaction. Nucleic Acids Res 12:989–1002

30. Miller PS, Cushman CD (1992) Selective modification of cytosines in oligodeoxyribonucleotides. Bioconjug Chem 3:74–79

31. Huang C-Y, Cushman CD, Miller PS (1993) Triplex formation by an oligonucleotide containing N^4-(3-acetamidopropyl)cytosine. J Org Chem 58:5048–5049

32. Okamura H, Tanigushi Y, Sasaki S (2013) N-(Guanidinoethyl)-2′-deoxy-5-methylisocytidine exhibits selective recognition of a CG interrupting site for the formation of anti-parallel triplexes. Org Biomol Chem 11:3918–3924

33. Maier MA, Barber-Peoc'h I, Manoharan M (2002) Postsynthetic guanidinylation of primary amino groups in the minor and major grooves of oligonucleotides. Tetrahedron Lett 43:7613–7616

34. Akabane-Nakata M, Obika S, Hari Y (2014) Synthesis of oligonucleotides containing N,N-disubstituted 3-deazacytosine nucleobases by post-elongation modification and their triplex-forming ability with double-stranded DNA. Org Biomol Chem 12:9011–9015

35. Kim SJ, Stone MP, Harris CM, Harris TM (1992) A postoligomerization synthesis of oligodeoxynucleotides containing polycyclic aromatic hydrocarbon adducts at the N^6 position of deoxyadenosine. J Am Chem Soc 114:5480–5481

36. Harris CM, Zhou L, Strand EA, Harris TM (1991) New strategy for the synthesis of oligodeoxynucleotides bearing adducts at exocyclic amino sites of purine nucleosides. J Am Chem Soc 113:4328–4329

37. Wang H, Kozekov ID, Kozekova A, Tamura P, Marnett LJ, Harris TM, Rizzo CJ (2006) Site-specific synthesis of oligonucleotides containing malondialdehyde adducts of deoxy-guanosine and deoxyadenosine via a post-synthetic modification strategy. Chem Res Toxicol 19:1467–1474

38. Kierzek E, Kierzek R (2003) The synthesis of oligoribonucleotides containing N^6-alkyladeno-sines and 2-methylthio-N^6-alkyladenosines via post-synthetic modification of precursor oligo-mers. Nucleic Acids Res 31:4461–4471

39. Gao H, Fathi R, Gaffney BL, Goswami B, Kung P-P, Rhee Y, Jin R, Jones RA (1992) 6-O-(Pentafluorophenyl)-2'-deoxyguanosine: a versatile synthon for nucleoside and oligo-nucleotide synthesis. J Org Chem 57:6954–6959

40. Xu Y-Z, Zheng Q, Swann PF (1992) Synthesis and duplex stability of oligodeoxynucleotides containing 6-mercaptopurine. Tetrahedron Lett 33:5837–5840

41. Xu Y-Z, Zheng Q, Swann PF (1992) Synthesis by post-synthetic substitution of oligo-mers containing guanine modified at the 6-position with S-, N-, O-derivatives. Tetrahedron 48:1729–1740

42. Xu Y-Z (1996) Post-synthetic introduction of labile functionalities onto purine residues via 6-methylthiopurines in oligodeoxyribonucleotides. Tetrahedron 52:10737–10750

43. Ferentz AE, Verdine GL (1991) Disulfide cross-linked oligonucleotides. J Am Chem Soc 113:4000–4002

44. Erlanson DA, Chen L, Verdine GL (1993) DNA methylation through a locally unpaired inter-mediate. J Am Chem Soc 115:12583–12584

45. Schmid N, Behr J-P (1995) Recognition of DNA sequences by strand replacement with polyamino-oligonucleotides. Tetrahedron Lett 36:1447–1450

46. Ono A, Haginoya N, Kiyokawa M, Minakawa N, Matsuda A (1994) Nucleosides and nucleo-tides. 127. A novel and convenient post-synthetic modification method for the synthesis of oligodeoxyribonucleotides carrying amino linkers at the 5-position of 2'-deoxyuridine. Bioorg Med Chem Lett 4:361–366

47. Haginoya N, Ono A, Nomura Y, Ueno Y, Matsuda A (1997) Nucleosides and nucleotides. 160. Oligodeoxyribonucleotides containing 5-(N-aminoalkyl)carbamoyl-2'-deoxyuridines by a new postsynthetic modification method and their thermal stability and nuclease-resistance properties. Bioconjug Chem 8:271–280

48. Ueno Y, Ogawa A, Nakagawa A, Matsuda A (1996) Nucleosides and nucleotides. 162. Facile synthesis of 5',5'-linked oligodeoxyribonucleotides with the potential for triple-helix forma-tion. Bioorg Med Chem Lett 6:2817–2822

49. Nomura Y, Ueno Y, Matsuda A (1997) Site-specific introduction of functional groups into phosphodiester oligodeoxynucleotides and their thermal stability and nuclease-resistance properties. Nucleic Acids Res 25:2784–2791

50. Ono A, Dan A, Matsuda A (1993) Nucleosides and nucleotides. 121. Synthesis of oligonucle-otides carrying linker groups at the 1'-position of sugar residues. Bioconjug Chem 4:499–508

51. Nomura Y, Haginoya N, Ueno Y, Matsuda A (1996) Nucleosides and nucleotides. 161. Incorporation of 5-(N-aminoalkyl)carbamoyl-2'-deoxycytidines into oligodeoxyribonucleo-tides by a convenient post-synthetic modification method. Bioorg Med Chem Lett 6:2811–2816

52. Lietard J, Leumann CJ (2012) Synthesis, pairing, and cellular uptake properties of C(6')-functionalized tricycle-DNA. J Org Chem 77:4566–4577

53. Hari Y, Osawa T, Obika S (2012) Synthesis and duplex-forming ability of oligonucleotides containing 4'-carboxythymidine analogs. Org Biomol Chem 10:9639–9649

54. Schlegel MK, Hütter J, Eriksson M, Lepenies B, Seeberger PH (2011) Defined presentation of carbohydrates on a duplex DNA scaffold. Chembiochem 12:2791–2800

55. Kahl JD, Greenberg MM (1999) Introducing structural diversity in oligonucleotides via pho-tolabile, convertible C5-substituted nucleotides. J Am Chem Soc 121:597–604

56. Beilstein AE, Grinstaff MW (2000) On-column derivatization of oligonucleotides with fer-rocene. Chem Commun:509–510

57. Khan SI, Grinstaff MW (1999) Palladium(0)-catalyzed modification of oligonucleotides during automated solid-phase synthesis. J Am Chem Soc 121:4704–4705
58. Rist M, Amann N, Wagenknecht H-A (2003) Preparation of 1-ethylnylpyrene-modified DNA via Sonogashira-type solid-phase couplings and characterization of the fluorescence properties for electron-transfer studies. Eur J Org Chem 2003:2498–2504
59. Mayer E, Valis L, Wagner C, Rist M, Amann N, Wagenknecht H-A (2004) 1-Ethylnylpyrene as a tunable and versatile molecular beacon for DNA. Chembiochem 5:865–868
60. Kottysch T, Ahlborn C, Brotzel F, Richert C (2004) Stabilizing or destabilizing oligodeoxynucleotide duplexes containing single 2′-deoxyuridine residues with 5-alkynyl substitutents. Chem Eur J 10:4017–4028
61. Baumhof P, Griesang N, Bächle M, Richert C (2006) Synthesis of oligonucleotides with 3′-terminal 5-(3-acylamidopropargyl)-3′-amino-2′,3′-dideoxyuridine residues and their reactivity in single-nucleotide steps of chemical replication. J Org Chem 71:1060–1067
62. Filichev V, Pedersen EB (2005) Stable and selective formation of Hoogsteen-type triplexes and duplexes using twisted intercalating nucleic acids (TINA) prepared via postsynthetic Sonogashira solid-phase coupling reactions. J Am Chem Soc 127:14849–14858
63. Beyer C, Wagenknecht (2010) In situ azide formation and "click" reaction of nile red with DNA as an alternative postsynthetic route. Chem Commun 46:2230–2231
64. Wicke L, Engels JW (2012) Postsynthetic on column RNA labeling via Stille coupling. Bioconjug Chem 23:627–642
65. Cahová H, Jäschke A (2013) Nucleoside-based diarylethene photoswitches and their facile incorporation into photoswitchable DNA. Angew Chem Int Ed 52:3186–3190
66. Lercher L, McGouran JF, Kessler BM, Schofield CJ, Davis BG (2013) DNA modification under mild conditions by Suzuki-Miyaura cross-coupling for the generation of functional probes. Angew Chem Int Ed 52:10553–10558
67. Jeong HS, Hayashi G, Okamoto A (2015) Diazirine photocrosslinking recruits activated FTO demethylase complexes for specific N^6-methyladenosine recognition. ACS Chem Biol 10:1450–1455
68. Omumi A, Beach DG, Baker M, Gabryelski W, Manderville RA (2011) Postsynthetic guanine arylation of DNA by Suzuki-Miyaura cross-coupling. J Am Chem Soc 133:42–50
69. Minakawa N, Ono Y, Matsuda A (2003) A versatile modification of on-column oligodeoxynucleotides using a copper-catalyzed oxidative acetylenic coupling reaction. J Am Chem Soc 125:11545–11552
70. Nakahara M, Kuboyama T, Izawa A, Hari Y, Imanishi T, Obika S (2009) Synthesis and base-pairing properties of C-nucleotides having 1-substituted 1H-1,2,3-triazoles. Bioorg Med Chem Lett 19:3316–3319
71. Hari Y, Nakahara M, Pang J, Akabane M, Kuboyama T, Obika S (2011) Synthesis and triplex-forming ability of oligonucleotides bearing 1-substituted 1H-1,2,3-triazole nucleobases. Bioorg Med Chem 19:1162–1166
72. Hari Y, Nakahara M, Obika S (2013) Triplex-forming ability of oligonucleotides containing 1-aryl-1,2,3-triazole nucleobases linked via a two atom-length spacer. Bioorg Med Chem 21:5583–5588
73. Hari Y, Nakahara M, Ijitsu S, Obika S (2014) The ability of 1-aryltriazole-containing nucleobases to recognize a TA base pair in triplex DNA. Heterocycles 88:377–386
74. Gutsmiedl K, Wirges CT, Ehmke V, Carell T (2009) Copper-free "click" modification of DNA via nitrile oxide-norbornene 1,3-dipolar cycloaddition. Org Lett 11:2405–2408
75. Schoch J, Wiessler M, Jäschke A (2010) Post-synthetic modification of DNA by inverse-electron-demand Diels-Alder reaction. J Am Chem Soc 132:8846–8847
76. Arndt S, Wagenknecht H-A (2014) "Photoclick" postsynthetic modification of DNA. Angew Chem Int Ed 53:14580–14582
77. Borsenberger V, Howorka S (2009) Diene-modified nucleotides for the Diels-Alder-mediated functional tagging of DNA. Nucleic Acids Res 37:1477–1485

78. Dey S, Sheppard TL (2001) *Ketone*-DNA: a versatile postsynthetic DNA decoration platform. Org Lett 3:3983–3986
79. Raindlová V, Pohl R, Šanda M, Hocek M (2010) Direct polymerase synthesis of reactive aldehyde-functionalized DNA and its conjugation and staining with hydrazines. Angew Chem Int Ed 49:1064–1066
80. Raindlová V, Pohl R, Hocek M (2012) Synthesis of aldehyde-linked nucleotides and DNA and their bioconjugations with lysine and peptides through reductive amination. Chem Eur J 18:4080–4087

Four-Hydrogen-Bonding Base Pairs in Oligonucleotides: Design, Synthesis, and Properties

Noriko Saito-Tarashima, Akira Matsuda, and Noriaki Minakawa

Abstract Oligodeoxynucleotides (ODNs) having four-hydrogen-bonding (H-bonding) unnatural base pairs have been developed. These examples of nucleobase modification have been designed and prepared to address the fundamental question: why did Watson–Crick base pairs come to contain two or three H-bonds during the evolution of life? As the first generation of four-H-bonding base pairs, imidazo[5′,4′:4,5]pyrido[2,3-*d*]pyrimidine (**Im**) was selected as an aglycon to append a fourth H-bonding site to nucleobases. The stability of **Im:Im** pairs in duplexes depends on the mode of incorporation. Conversely, the second generation of four-H-bonding base pairs comprising **Im** and 1,8-naphthyridine (**Na**) *C*-nucleosides, formed duplexes with drastically enhanced thermal stability (especially $\mathbf{ImN^N{:}NaO^O}$ pair), independent of the modification pattern. In addition, the $\mathbf{ImN^N{:}NaO^O}$ pair was replicated with the highest efficiency and selectivity among the series of **Im:Na** pairs using in vitro replication systems owing to the synergistic effect of favorable thermal and thermodynamic contributions from base pairing and specific H-bonding geometries. $\mathbf{ImO^N{:}NaN^O}$ and $\mathbf{ImN^N{:}NaO^O}$ pairs are transcribed under the optimized concentrations of UTP and **rNaTP** in in vitro transcription catalyzed by T7 RNA polymerase.

Keywords Hydrogen-bonding · Unnatural base pair · Imidazo[5′4′:4,5] pyrido[2,3-*d*]pyrimidine · 1,8-naphthyridine · Base pairing · Thermodynamics · Enzymatic recognition

N. Saito-Tarashima · N. Minakawa (✉)
Faculty of Pharmaceutical Science, Tokushima University, Tokushima, Japan
e-mail: minakawa@tokushima-u.ac.jp

A. Matsuda
Center for Research and Education on Drug Discovery, Faculty of Pharmaceutical Sciences, Hokkaido University, Sapporo, Japan

1 Introduction

DNA generally forms a right-handed B-form helical structure that is maintained by several factors. The specific formation of hydrogen bonds (H-bonds) between Watson–Crick (WC) base pairs comprising adenine (A) and thymine (T) with two H-bonds, and guanine (G) and cytosine (C) with three H-bonds is the most fundamental interaction, and it plays a critical role in the duplex stability and the rigorous conservation and transmission of genetic information. Stacking of aromatic structures and shape complementarity based on the combination of purine and pyrimidine rings are also important factors.

As only four nucleobases were selected for A:T and G:C pairs during the evolution of life, these two base pairs should be ideal genetic polymers. However, with surprising foresight, in 1962 Alexander Rich proposed the possibility of extra artificial base pairs, i.e., isoguanine (isoG, 6-amino-2-oxopurine) and isocytosine (isoC, 2-amino-4-oxopyrimidine), as fifth and sixth DNA nucleobases [50]. If the extra base pair functions selectively in replication, transcription, and translation, it could potentially allow expansion of the genetic code, exploration of synthetic biology, and the creation of new genetic systems. In 1989, Benner et al. reported the chemical synthesis of isoG and isoC nucleosides and their 5′-triphosphates, and examined their polymerase reactions with the goal of expanding "the genetic alphabet" [20, 57, 58]. They also designed other unnatural base pairs with different H-bond donor and acceptor geometries [48, 62, 63]. Although these analogs were less selective and efficient in in vitro replication and transcription than WC base pairs, the alteration of H-bonding geometries in base pairs is one of the most promising strategies for developing new base-pair analogs [2, 16, 42].

More recently, several researchers have explored the creation of unnatural base pairs that exhibit highly selective and effective base-pairing complementarity in polymerase reactions. Kool et al. have explored the possibility of non-hydrogen-bonded unnatural base-pair analogs. They created a base pair comprising 4-methylbenzimidazole (**Z**) and 2,4-difluorotoluene (**F**) as a steric isostere of the A:T pair and investigated the contribution of H-bonding to base pairing in replication [11, 43]. **Z** and **F** were equally replaced with A and T, respectively, in in vitro replication studies, suggesting the importance of shape complementarity and stacking interactions in addition to H-bonding in base pairing [25, 27]. The research groups of Romesberg [37] and Hirao [17] independently designed original non-hydrogen-bonded unnatural base-pair analogs, and several of them have been replicated with a specificity and efficiency equivalent to those exhibited by natural WC base pairs [31, 36, 61].

In contrast, we initiated our unnatural base-pair studies to address the fundamental question: why did WC base pairs come to contain two or three H-bonds during the evolution of life? To answer this, we have explored four-H-bonding base pairs. Prior to our studies, Matteucci et al. have reported the synthesis of the tricyclic cytosine analog 9-(2-aminoethoxy)phenoxazine, which they termed the "G-clamp" [10, 34]. This heterocyclic modification provided a rigid scaffold for interaction

with the Hoogsteen face of a complementary natural G base via four H-bonds. The incorporation a single G:G-clamp pair in a decameric oligodeoxynucleotide (ODN) sequence was found to increase the melting temperature (T_m) of the DNA duplex by 18 °C. This dramatic improvement in the thermal stability of the duplex was presumably caused by formation of a fourth H-bond with the O6 position in the G base. The stability might also be improved by the enhanced stacking ability arising from the expanded aromatic face of the G-clamp. Additionally, incorporation of a G:G-clamp pair at the 3′-end of an ODN duplex efficiently protected it against nuclease digestion by 3′-exonucleases [35]. Although the G-clamp forms a complementary base pair with a natural G base, these results indicate that the design and synthesis of four-H-bonding base pairs, that function orthogonally to WC base pairs is an attractive research strategy not only for understanding the significance of H-bonding in base pairing and the functional modification of nucleosides and nucleotides.

For the first generation in our four-H-bonding unnatural base-pair studies, we designed a series of imidazo[5′,4′:4,5]pyrido[2,3-d]pyrimidine (**Im**) nucleosides designated as **ImO^N**, **ImN^O**, **ImN^N**, and **ImO^O**. As depicted in Fig. 1a, these tricyclic nucleosides have the potential to form the complementary base pairs **ImO^N:ImN^O** and **ImN^N:ImO^O**, with four H-bonds between them. For the second generation, unnatural base pairs comprising **Im** and the complementary 1,8-naphthyridine (**Na**) C-nucleosides designated **NaO^N**, **NaN^O**, **NaN^N**, and **NaO^O** were also created (Fig. 1b). Herein, we describe the design, synthesis, and properties of the four-H-bonding **Im:Im** and **Im:Na** base pairs. Recently, we focus on in vitro replication and transcription reactions involving **Im:Na** base pairs. The expansion of the central dogma with an augmented genetic alphabet featuring the **Im:Na** pair is also reviewed.
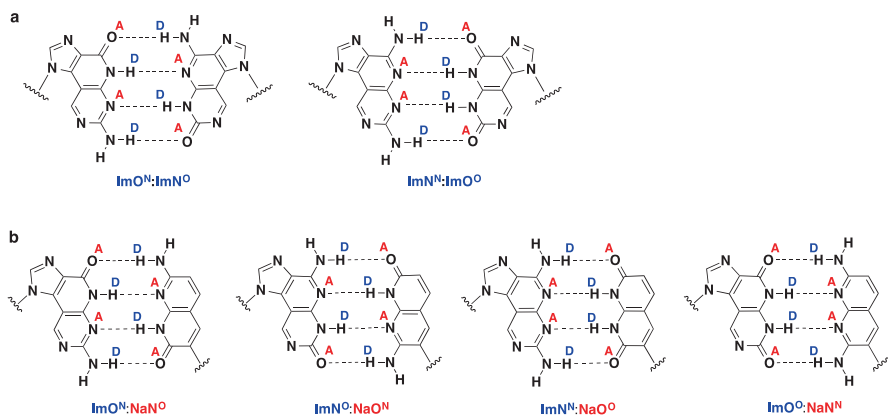
Fig. 1 Four-H-bonding unnatural base pairs. (**a**) A series of **Im:Im** base pairs and (**b**) a series of **Im:Na** base pairs

2 Designing Four-H-Bonding DNA Base Pairs

2.1 Size-Expanded Im:Im Base Pairs

For the first generation of the four-H-bonding base pairs, an **Im** skeleton was selected as an aglycon to append the fourth H-bonding site into nucleobases (Fig. 1a) [40]. The tricyclic **Im** heterocycle possessing 4-oxo (**O**) and 7-amino (**N**) groups in its nucleobase moiety, abbreviated as **ImO^N**, and its geometrical isomer **ImN^O** (i.e., the 4-amino and 7-oxo isomer) could form a complementary **ImO^N:ImN^O** pair with a specific arrangement of the proton donor (D) and acceptor (A) [ADAD:DADA]. Similarly, the **ImN^N:ImO^O** pair with a DAAD:ADDA H-bonding pattern was also prepared. The desired nucleosides were prepared using a Stille coupling reaction between a 5-iodoimidazole nucleoside and an appropriate 5-stannylpyrimidine derivative as the key reaction, followed by intramolecular cyclization.

Prior to prepare ODNs with the resulting nucleosides, the H-bonding characteristics of the tricyclic nucleosides were investigated. Thus, ^{1}H NMR signals of the silylated **ImO^N** nucleoside at -60 °C suggested that formation of a homo-dimer in an anti-parallel direction via four-H-bonding occurs in CDCl$_3$. Similarly, an equimolar mixture of the silylated **ImO^N** and **ImO^N** showed not only signals for each homo-dimer but also those of a hetero-dimer, indicating that the tricyclic **Im** nucleosides will form the desired four-H-bonding base pairs when they are incorporated into ODNs.

Thus, two sets of complementary ODNs of 17 nt length (ODN I:ODN II and ODN III:ODN IV) were prepared to assess the H-bonding abilities of the tricyclic nucleosides in these duplexes, where **ImO^N**, **ImN^O**, **ImN^N**, or **ImO^O** units were incorporated in the X and Y positions of each ODN (Table 1). The thermal stabilities of these duplexes were measured by ultraviolet melting experiments in a 10 mM sodium cacodylate buffer (pH 7.0) containing 100 mM NaCl, and ΔTm values were calculated by reference to the Tm value of a native duplex with an A:T pair at the X:Y position.

Contrary to our initial expectations, the ODN I:ODN II duplexs containing **ImO^N:ImN^O** and **ImN^N:ImO^O**, which feature H-bonds between the two tricycles, were less stable than those with the natural A:T pair, even though this base pair has only two H-bonds ($\Delta T_m = -4.5$ to -0.9 °C). When three pairs of the tricyclic nucleosides were consecutively incorporated into the central positions of the ODN III:ODN IV duplexes, their thermal stabilities were significantly increased ($\Delta T_m = +6.6$ to $+23.5$ °C). The stabilizing ability of the **ImN^N:ImO^O** pair ($\Delta T_m = +10.1$ and $+6.6$ °C) was much lower than that of the **ImO^N:ImN^O** pair ($\Delta T_m = +23.3$ and $+23.5$ °C), despite both pairs being able to form four H-bonds (Fig. 1a), indicating that base pairs form between **ImN^N** and **tImO^O**, which is a tautomeric isoform of **ImO^O**, containing three H-bonds. This suggestion will be verified in the next section (see Fig. 3).

Considering that the stabilizing ability of the **Im:Im** pair having a specific H-bonding geometry is higher than that of a G:C pair with three H-bonds ($\Delta T_m = +1.4$ to $+1.8$ °C per pair), stacking interactions arising from the expanded aromatic sur-

Table 1 Hybridization abilities of a series of **Im:Im** pairs

| **ODN I** 5'-GCACCGAA**X**AAACCACG-3' **ODN II** 3'-CGTGGCTT**Y**TTTGGTGC-5'				**ODN III** 5'-GCACCGA**XXX**AACCACG-3' **ODN IV** 3'-CGTGGCT**YYY**TTGGTGC-5'			
X	Y	T_m (°C)	ΔT_m (°C)	X	Y	T_m (°C)	ΔT_m (°C)
ImO^N	ImO^N	56.9	−3.6	ImO^N	ImO^N	65.8	+5.3
	$\mathbf{ImN^O}$	**58.4**	**−2.1**		$\mathbf{ImN^O}$	**83.8**	**+23.3**
	ImN^N	55.4	−5.1		ImN^N	41.5	−19.0
	ImO^O	53.3	−7.2		ImO^O	57.5	−3.0
ImN^O	$\mathbf{ImO^N}$	**59.6**	**−0.9**	ImN^O	$\mathbf{ImO^N}$	**84.0**	**+23.5**
	ImN^O	57.2	−3.3		ImN^O	70.0	+9.5
	ImN^N	55.1	−5.4		ImN^N	46.3	−14.2
	ImO^O	54.0	−6.6		ImO^O	56.0	−4.5
ImN^N	ImO^N	56.1	−4.4	ImN^N	ImO^N	57.1	−8.8
	ImN^O	54.5	−6.0		ImN^O	49.4	−11.1
	ImN^N	54.5	−6.0		ImN^N	55.7	−4.8
	$\mathbf{ImO^O}$	**56.3**	**−4.2**		$\mathbf{ImO^O}$	**70.6**	**+10.1**
ImO^O	ImO^N	54.0	−6.2	ImO^O	ImO^N	62.3	+1.8
	ImN^O	54.3	−6.2		ImN^O	58.3	−2.2
	$\mathbf{ImN^N}$	**56.0**	**−4.5**		$\mathbf{ImN^N}$	**67.1**	**+6.6**
	ImO^O	54.3	−6.2		ImO^O	53.5	−7.0
G	C	61.9	+1.4	G	C	65.8	+5.3
A	**T**	**60.5**	**−**	**A**	**T**	**60.5**	**−**
G	C	53.8	−6.7	G	C	47.2	−13.3
A	T	52.4	−8.1	A	T	43.1	−17.4

All measurements were carried out using 3 μM solutions of ODN in 10 mM sodium cacodylate (pH 7.0) containing 100 mM NaCl. ΔT_m values were obtained by subtracting data for T_m possessing X:Y = A:T from each duplex. Complementary pairs are represented in bold

face of the tricyclic **Im** base undoubtedly contribute to their thermal stabilities [12]. The remaining question to be considered is why the introduction of one **Im:Im** pair thermally destabilizes the duplexes, whereas consecutive three-pair incorporation, especially that of the **ImO^N:ImN^O** pair, significantly stabilizes the duplexes. Consequently, we further explored the sequence dependency of the stabilization ability of the **Im:Im** pair using duplexes containing the G:**ImN^N** pair, which is an alternative to the **Im:Im** pair. Thus, using T_m of the native ODN duplex as a control (68.3 °C), the sequence-dependent variation was explored by substituting the G:C pair with the G:**ImN^N** pair at different positions (cODN:ODNs V–X). The ODN sequences and their T_m values are summarized in Table 2. The duplexes became less thermally stable as the number of isolated incorporations of the G:**ImN^N** pair increased (ODNs V–VIII). Conversely, the duplexes containing consecutive G:**ImN^N** pairs (ODNs IX and X) exhibited enhanced stabilities compared with that of the control duplex. The duplex of ODN IX with cODN exhibited much higher stability ($Tm = 72.8$ °C) than that of ODN VII ($Tm = 63.0$ °C), indicating that consecutive introduction of the tricyclic base pairs leads to an enhancement of thermal stability in the duplex. The hypothetical duplex structures are illustrated in Fig. 2.

Table 2 Thermal stabilities of duplexes containing G:ImN^N pairs in different modification patterns

cODN	3'-CGTGGCTGGGTTGGTGC-5'	T_m (°C)
ODN V	5'-GCACCGAC**WC**AACCACG-3'	67.2
ODN VI	5'-GCACCGA**WCW**AACCACG-3'	64.3
ODN VII	5'-GCA**WC**GAC**WC**AAC**WC**ACG-3'	63.0
ODN VIII	5'-G**WC**AC**WC**GA**WC**CAA**WC**A**W**G-3'	55.7
ODN IX	5'-GCACCGA**WWW**AACCACG-3'	72.8
ODN X	5'-G**WC**A**WW**GA**WWW**AA**WW**A**W**G-3'	75.7
	5'-G**CACC**GA**CCC**AA**CC**ACG-3'	68.3

All measurements were carried out using 3 μM solutions of the duplex comprising ODN and the complementary sequence (cODN) in 10 mM sodium cacodylate (pH 7.0) containing 100 mM NaCl. **W** = ImN^N
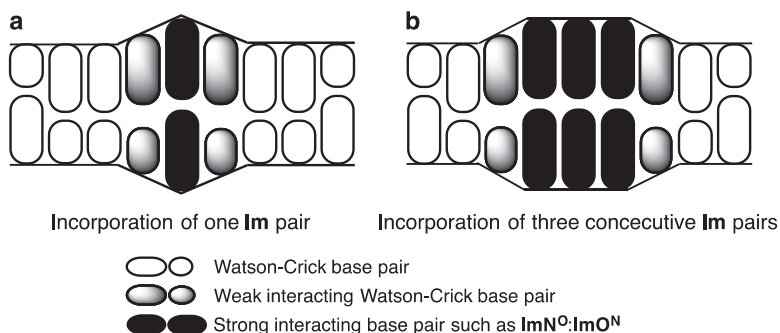
Fig. 2 Hypothetical duplex structures with tricyclic **Im:Im** pairs

The **Im:Im** and G:**ImN^N** pairs would increase the width of the helix around the position where they are introduced, although they form stable H-bonds in the duplex. It is known that the average intra-strand C1′–C1′ distance in a canonical WC base pair is 10.5 (±0.2) Å, whereas the distances in purine(anti)–purine(anti) base pairs are typically much longer. The intra-strand C1′–C1′ distance at **Im:Im** (and G:**ImN^N**) is similar to that of G(anti)–A(anti) mismatched pairs, which is estimated to be 12.5 Å [49]. Accordingly, conformational destabilization of the WC base pairs adjacent to the tricyclic nucleoside pair occurs in the duplex when one **Im:Im** pair is incorporated (Fig. 2a). However, when tricyclic nucleosides are consecutively incorporated, the duplex is thermally stabilized to a greater extent because the stabilization arising from the four H-bonds and strong stacking interactions between adjacent **Im** bases outweigh the conformational destabilization around the boundary of the **Im:Im** pairs. (Fig. 2b).

2.2   Design of Im:Na Base Pairs with Comparable Shape Complementarity to That of WC Base Pairs

The non-canonical four H-bonds and expanded aromatic surface of the **ImN^O:ImO^N** pair significantly stabilize a duplex when it is incorporated consecutively. However, the **Im:Im** pair does not have satisfactory shape complementarity, because it behaves like a purine:purine mismatched base pair. To create a third four-H-bonding base pair with comparable shape complementarity to that of WC base pairs, we designed a series of **Na** C-nucleosides, which have oxo and/or amino groups in the nucleobase moiety and designated them **NaO^N**, **NaN^O**, **NaO^O**, and **NaN^N** [14, 29] (Fig. 1b). The possible **Im:Na** pairs **ImO^N:NaN^O**, **ImN^O:NaO^N**, **ImN^N:NaO^O**, and **ImO^O:NaN^N** have comparable shape complementarity to that of the purine:pyrimidine base pair. The desired **Na** C-nucleosides were prepared by the diastereoselective Heck reaction of an **Na** derivative as an aglycon with a glycal. After being converted into phosphoramidite units, complementary ODN duplexes were prepared to investigate the base-pairing properties of **Im:Na** pairs (Table 3).

As expected, all the **Im:Na** pairs enhanced the thermal stabilities of their duplexes owing to their shape complementarity. When a single **Im**:**Na** pair was incorporated into ODN I:ODN II, where the **Im:Im** base pair thermally destabilized the duplexes, the **ImO^N:NaN^O**, **ImN^O:NaO^N**, and **ImO^O:NaN^N** pairs stabilized the duplexes relative to the duplex containing the A:T pair (ΔT_m = +7.8 °C, +7.5 °C, and +7.9 °C per pair, respectively). The **ImN^N:NaO^O** pair stabilized the duplex by

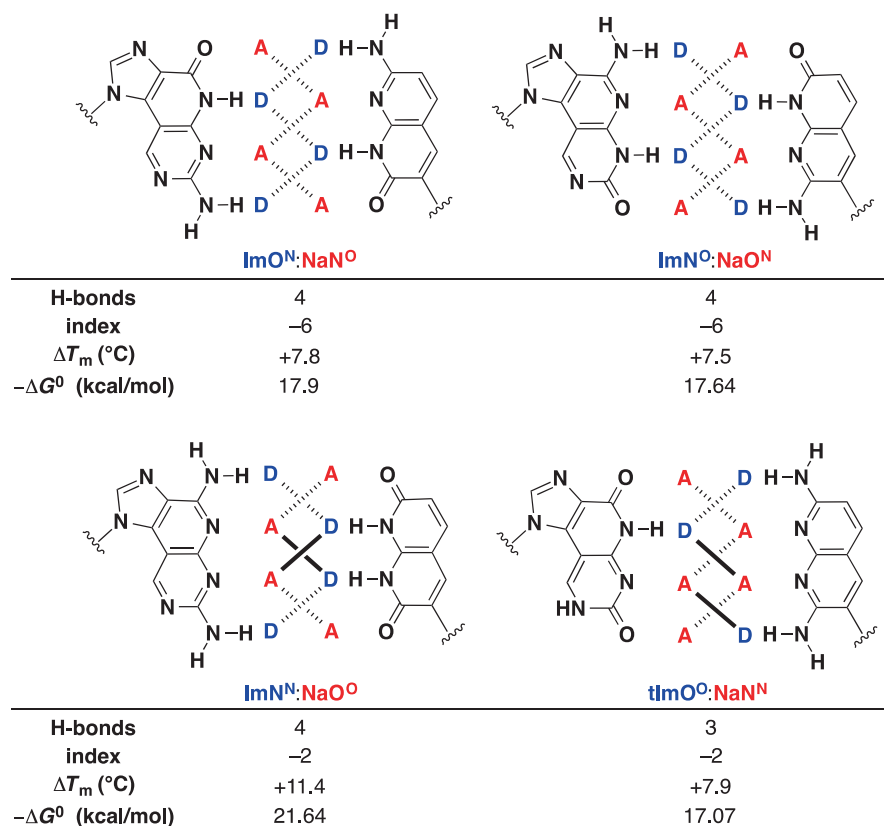**Table 3** Hybridization abilities of a series of **Im:Na** pairs

ODN I 5'-GCACCGAA**X**AAACCACG-3' ODN II 3'-CGTGGCTT**Y**TTTGGTGC-5'				ODN III 5'-GCACCGA**XXX**AACCACG-3' ODN IV 3'-CGTGGCT**YYY**TTGGTGC-5'				ODN XI 5'-GC**X**CCGAA**X**AAACC**X**CG-3' ODN XII 3'-CG**Y**GGCTT**Y**TTTGG**Y**GC-5'			
X	Y	T_m (°C)	ΔT_m (°C)	X	Y	T_m (°C)	ΔT_m (°C)	X	Y	T_m (°C)	ΔT_m (°C)
ImO^N	NaO^N	50.4	+1.8	ImO^N	NaO^N	64.6	+16.0	ImO^N	NaO^N	65.8	+17.2
	NaN^O	**56.4**	**+7.8**		**NaN^O**	**79.0**	**+30.2**		**NaN^O**	**81.4**	**+32.8**
	NaN^N	50.9	+2.3		NaN^N	64.1	+15.5		NaN^N	68.0	+19.4
	NaO^O	53.1	+4.5		NaO^O	70.7	+22.1		NaO^O	72.7	+24.1
ImN^O	NaO^N	56.1	+7.5	ImN^O	NaO^N	80.1	+31.5	ImN^O	NaO^N	79.6	+31.0
	NaN^O	53.3	+4.7		NaN^O	67.2	+18.6		NaN^O	66.7	+18.1
	NaN^N	50.4	+1.8		NaN^N	62.8	+14.2		NaN^N	64.7	+16.1
	NaO^O	54.6	+6.0		NaO^O	76.8	+28.2		NaO^O	70.5	+21.9
ImN^N	NaO^N	48.6	0	ImN^N	NaO^N	55.5	+6.9	ImN^N	NaO^N	58.3	+9.7
	NaN^O	51.5	+2.9		NaN^O	59.1	+10.5		NaN^O	61.7	+13.1
	NaN^N	53.4	+4.8		NaN^N	70.0	+21.4		NaN^N	70.7	+22.1
	NaO^O	**60.0**	**+11.4**		**NaO^O**	**88.9**	**+40.3**		**NaO^O**	**88.0**	**+39.4**
ImO^O	NaO^N	49.3	+0.7	ImO^O	NaO^N	56.5	+7.9	ImO^O	NaO^N	57.5	+8.9
	NaN^O	51.0	+2.4		NaN^O	61.6	+13.0		NaN^O	58.8	+10.2
	NaN^N	**56.5**	**+7.9**		**NaN^N**	**81.3**	**+32.7**		**NaN^N**	**80.5**	**+31.9**
	NaO^O	51.8	+3.2		NaO^O	69.7	+21.1		NaO^O	65.8	+17.2
G	C	49.9	+1.3	G	C	55.2	+6.6	G	C	56.7	+8.1
A	**T**	**48.6**	**−**	**A**	**T**	**48.6**	**−**	**A**	**T**	**60.5**	**−**

All measurements were carried out using 3 μM solutions of ODN in 10 mM sodium cacodylate (pH 7.0) containing 100 mM NaCl. ΔTm values were obtained by subtracting data for Tm possessing X:Y = A:T from each duplex. Complementary pairs are represented in bold

+11.4 °C, which was the highest among the four **Im:Na** pairs, and this tendency was emphasized by the results for ODN III:ODN IV and ODN XI:ODN XII. Both duplexes containing three **ImN^N:NaO^O** pairs were stabilized by ca. +40 °C, which were a dramatic improvement. From these results, it can be concluded that the newly designed **Im:Na** base-pairing motifs, especially that in **ImN^N:NaO^O**, thermally stabilize the duplexes by more than +10 °C per pair compared with an A:T pair with two H-bonds and by more than +8 °C per pair compared with a G:C pair with three H-bonds, presumably owing to the synergistic effect of the four H-bonds, the enhanced stacking interactions, and the shape complementarity of the **Im:Na** pairs, irrespective of where they are incorporated in the duplex.

Why dose the **ImN^N:NaO^O** pair show the highest stabilization ability relative to the other three **Im:Na** pairs despite possessing the same four H-bonds? As one explanation, a secondary interaction that has an important role in stabilizing hydrogen-bonded complexes may be considered. Jorgensen and Pranata reported that a 9-methylguanine:1-methylcytosine pair is much more thermodynamically stable than a 1-methyluracil:2,6-diaminopyridine pair, despite both pairs forming three H-bonds [23]. They explained that this is due to a secondary interaction arising from the geometry of H-bonds, and the validity of their hypothesis was well demonstrated and evaluated for many complexes possessing a variety of H-bonding patterns [1, 7, 44]. Our results can also be understood in view of their hypothesis. The **ImO^N:NaN^O** pair has an ADAD:DADA H-bonding pattern considered to have six repulsive (−6) secondary interactions (dotted lines, with the overall strength of the secondary interactions being represented as "index" = –6) arising from D–D and A–A repulsion, with four primary H-bonds (Fig. 3). Similarly, the **ImN^O:NaO^N** pair with a specific H-bonding geometry [DADA:ADAD] presents the same index value, and this estimation is supported by the T_m values for the **ImO^N:NaN^O** and **ImN^O:NaO^N** pairs (ΔT_m = +7.8 °C versus +7.5 °C, respectively). Conversely, the **ImN^N:NaO^O** pair presents four repulsive (−4) and two attractive (+2) secondary interactions (bold lines) because of its DAAD:ADDA H-bonding pattern, indicating that the overall strength of its H-bonding interactions can be estimated from the four primary H-bonds and the index value of −2, thus conferring more thermal stability than the **ImO^N:NaN^O** and **ImN^O:NaO^N** pairs having alternating H-bonding patterns (ΔT_m = +11.4 °C versus +7.8 and +7.5 °C, respectively). For the **ImO^O:NaN^N** pair, the overall strength of the interaction can be estimated from the four H-bonds and the index of −2 for the secondary interactions, much like those of the **ImN^N:NaO^O** pair, if it has an ADDA:DAAD H-bonding pattern, as illustrated in Fig. 1b. However, the thermal stability conferred by this pair (+7.9 °C) was rather low compared with that conferred by the **ImN^N:NaO^O** pair (Table 3).

As described in the previous section, we suggested that **ImO^O** would exist as a tautomeric form, represented as a **tImO^O** form, possessing an ADAA H-bonding pattern. This being the case, the base pair between **tImO^O** and **NaN^N** should have four repulsive (−4) and two attractive (+2) secondary interactions (Fig. 3). Thus, the overall strength of interactions in the **tImO^O:NaN^N** pair can be estimated from three H-bonds and the index of −2 for the secondary interactions. Because the overall interaction factors of the **tImO^O:NaN^N** pair are similar to those of the **ImO^N:NaN^O**

H-bonds	4	4
index	−6	−6
ΔT_m (°C)	+7.8	+7.5
−ΔG^0 (kcal/mol)	17.9	17.64

H-bonds	4	3
index	−2	−2
ΔT_m (°C)	+11.4	+7.9
−ΔG^0 (kcal/mol)	21.64	17.07

Fig. 3 Thermal and thermodynamic stabilities of a series of **Im:Na** base pairs based on the factor of secondary interactions. Dotted lines represent repulsive secondary interactions, and bold lines represent attractive secondary interactions. Index values represent the sum of secondary interactions; thus, index indicates the overall strength of the secondary interactions

and **ImN^O:NaO^N** pairs, i.e., four H-bonds and an index of −6, their ΔT_m values are almost the same (ΔT_m = +7.9, +7.8, and +7.5 °C, respectively). Thus, the **ImN^N:NaO^O** pair, through a favorable contribution to the enthalpy of formation of the duplex, is the most thermodynamically stable. The −ΔG^0 data also support these conclusions.

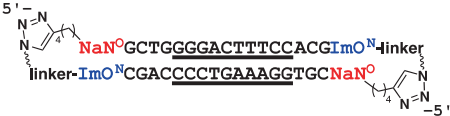# 3   Creation of a Thermally Stabilized Decoy Molecule with Im:Na Pairs

Im:Na base pairs, which confer high thermal (+7.5 to +11.4 °C per pair relative to an A:T pair) and thermodynamic stabilities to complementary ODNs, were applied in a decoy strategy to examine whether the four-H-bonding base pairs could improve nucleic acid functionality.

Decoy DNAs generally comprise short dsODNs encoding the binding sequence for regulatory transcription proteins. These decoys compete with the target sequence in a promoter enhancer and are used to regulate transcription reactions in eukaryotic systems [39]. However, the use of decoy DNAs presents several drawbacks. For examples, short dsODNs have relatively low thermal stability under physiological conditions. Additionally, they are easily degraded by nucleases in biological fluids. Thus, the incorporation of chemical modifications into the decoy ODNs is often used to confer nuclease resistance and thermal stability for their therapeutic use. The most common strategy is the use of phosphorothioate-modified ODNs, which are highly resistant to nuclease digestion [3]. However, their thermal stability is reduced relative to that of the native decoy molecule because of the stereochemistry created at the phosphorus center [54]. Alternatively, to append thermal stability as well as nuclease resistance, the incorporation of an artificial nucleotide at the termini of decoy molecules, e.g., by peptide nucleic acids (PNAs) [51] and bridged nucleic acids/locked nucleic acids (BNAs/LNAs) [5] has also been investigated, and the resulting decoy DNAs showed higher affinity to target proteins and improved stability relative to the native decoy molecules. It is therefore worth investigating the function of decoy DNAs with unnatural **Im:Na** base pairs at their sticky ends [15].

The decoy DNAs prepared, which encode the binding sequence for NF-κB, a transcriptional factor that is important in many signal transduction pathways in the immune system, containing one or two **ImO^N:NaN^O** pairs on their 3′- and 5′-ends, are listed in Table 4 along with their properties. The abilities of the modified decoys were evaluated using a competitive binding assay. The assay was carried out in an appropriate buffer solution containing the NF-κB p50 homo-dimer and the ^{32}P-radiolabeled decoy under increasing concentrations of the non-labeled duplex, and the IC$_{50}$ value was estimated using electrophoretic mobility shift assays. **NF1** with an **ImO^N:NaN^O** pairs at both ends exhibited a T_m value of 60.6 °C, which is +5.1 °C higher than that of native **NF3**, with a slight improvement in inhibition efficacy (IC$_{50}$ for **NF1** = 20.1 μM) relative to native **NF3** (IC$_{50}$ = 22.5 μM). When the **ImO^N:NaN^O** pairs were consecutively incorporated, the resulting duplex **NF2** was stabilized by +20.6 °C (stabilizing effect was calculated to be +5.1 °C per pair) arising from the synergic effect of four H-bonds, shape complementarity, and stacking interactions with the adjacent nucleobases. Hence, **NF2** inhibited NF-κB binding to the target site more strongly than **NF1** and native **NF3** (IC$_{50}$ for **NF2** = 10.9 μM). Thus, the decoy DNA **NF2**, which has at least two consecutive unnatural **ImO^N:NaN^O** pairs at the sticky ends, acts as a strong competitor to the natural NF-κB binding duplex owing to its thermal stability.

Another strategy to overcome the aforementioned drawbacks of decoy DNAs is to use dumbbell-shaped dsDNAs, which exhibit high thermal stability and exonuclease resistance as the dsDNAs have no terminal nucleotide residues [4, 28]. Copper-catalyzed azide-alkyne cycloaddition (CuAAC) is a promising technique for preparing cross-linked dsODNs [21, 45]. Consequently, we combined the **ImO^N:NaN^O** pair and the CuAAC reaction for decoy design, and the resulting dumbbell-shaped decoy DNA **NF4** exhibited high thermal stability and affinity to the NF-κB protein [13].

Table 4 Sequences and properties of decoy DNAs containing $ImO^N:NaN^O$ pairs at the termini

	duplex	Tm (°C)^a	ΔTm (°C)^a	IC$_{50}$ (nM)
NF1	5'–ImO^NGCTG<u>GGGACTTTCC</u>ACGImO^N–3' 3'–NaN^OCGAC<u>CCCTGAAAGG</u>TGCNaN^O–5'	60.6	+5.1	20.1±13.3
NF2	5'–ImO^NImO^NCTG<u>GGGACTTTCC</u>ACImO^NImO^N–3' 3'–NaN^ONaN^OGAC<u>CCCTGAAAGG</u>TGNaN^ONaN^O–5'	76.1	+20.6	10.9±4.8
NF3 **(Native)**	5'–CGCTG<u>GGGACTTTCC</u>ACGG–3' 3'–GCGAC<u>CCCTGAAAGG</u>TGCC–5'	55.5	–	22.5±4.7

NF4^b	

Underlined sequences are the binding site for NF-κB
^{a}*Tm* measurement was carried out using 3 μM solutions of dsODN in 10 mM sodium cacodylate (pH 7.0) containing 1 mM NaCl
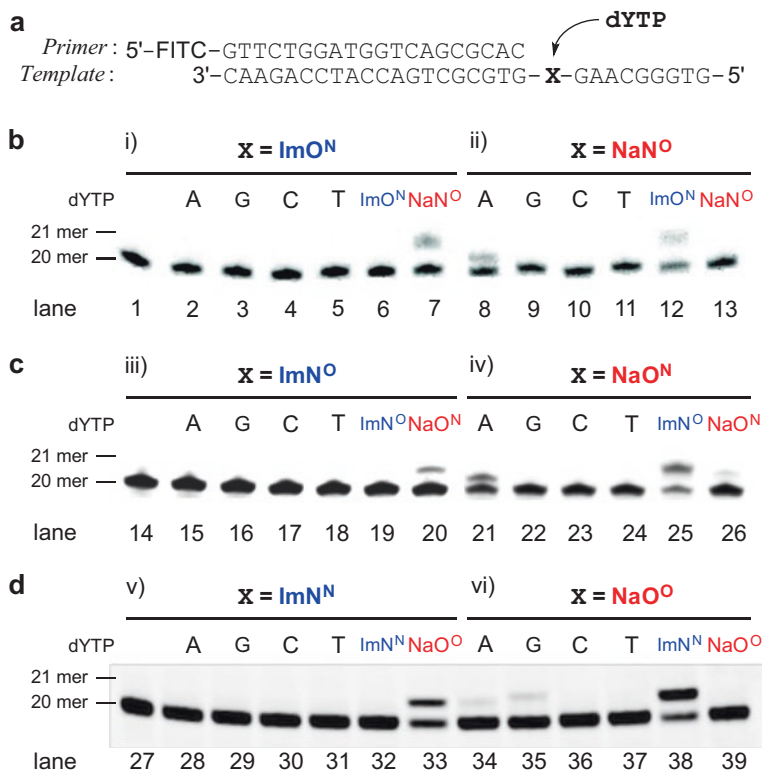^{b}Because of the differences in experimental conditions, the characteristics of **NF4** are not presented in this table, although it showed a drastic improvement in thermal stability and IC$_{50}$. Details appear in our previous report [13]

4   Polymerase Reactions Involving the Im:Na Pair

As described in the Introduction, expansion of the genetic alphabet is also an important application of unnatural base pairs. As is well known, four kinds of WC nucleobase, i.e., A, G, C, and T, act as the letters for genetic information on DNA. If an unnatural base pair comprising fifth and sixth DNA letters that functions well in replication, transcription, and translation systems can be created, the genetic information could be expanded by increased DNA letter classes. One of the most important factors to consider when expanding the genetic alphabet is that the unnatural base pairs created should form a selective base pair and function in accordance with the central dogma, i.e., undergoing enzymatic replication and transcription in the same way as WC base pairs do. Thus, we have evaluated the base-pairing efficiency and specificity of a series of **Im:Na** pairs using in vitro polymerase reactions.

4.1   Enzymatic Replication of Im:Na Pairs by DNA Polymerases

To investigate the selectivity and efficiency of **Im:Na** pairs in in vitro replication systems, we first examined single-nucleotide insertion involving four-H-bonding **Im:Na** pairs, i.e., $ImO^N:NaN^O$, $ImN^O:NaO^N$, and $ImN^N:NaO^O$ pairs, using exonuclease-deficient Klenow fragment (KF) [41, 59], which is a typical DNA polymerase used to assess the replication ability of unnatural base-pair analogs [30] (Fig. 4). As shown in Fig. 4b, in the examination of the $ImO^N:NaN^O$ pair, 2′-deoxy

a

Primer : 5'–FITC–GTTCTGGATGGTCAGCGCAC

dYTP

Template : 3'–CAAGACCTACCAGTCGCGTG–**X**–GAACGGGTG–5'

b

c

d

Fig. 4 Single-nucleotide insertions using KF. (**a**) Sequences of the template and the primer involving an **ImO^N:NaN^O** pair (**b**), an **ImN^O:NaO^N** pair (**c**), and an **ImN^N:NaO^O** pair (**d**). Assay conditions were 0.8 μM of annealed primer–template duplex and 100 μM (i), 2 μM (ii), 100 μM (iii), or 50 μM (iv) dYTPs, or 0.4 μM of annealed primer–template duplex and 20 μM (v) or 2 μM (vi) dYTPs. After being incubated at 37 °C, an aliquot of the reaction was analyzed using 20% poly-acrylamide gel electrophoresis

NaN^O nucleoside 5'-triphosphate (**NaN^{O}TP**) was incorporated selectively as a complementary 5'-triphosphate against **ImO^N** in the template to afford a 21-mer sequence (lane 7), whereas natural dNTPs and **ImO^{N}TP** itself were not incorporated at all (lanes 2–6). Conversely, when **NaN^O** was located at the X position in the template, not only **ImO^{N}TP** (lane 12) but also dATP (lane 8) were incorporated to some extent under the same conditions. Similarly, the enzymatic behaviors of the **ImN^O:NaO^N** (Fig. 4c) and **ImN^N:NaO^O** (Fig. 4d) pairs showed the same tendency as that of the **ImO^N:NaN^O** pair (Fig. 4b), although their incorporation efficiencies appeared to be different.

To evaluate the selectivity and efficiency of these single-nucleotide insertion experiments quantitatively, kinetic parameters including the Michaelis constant (K_m), the maximum rate of enzyme reaction (V_{max}), and the incorporation efficiency (V_{max}/K_m) of each 5'-triphosphate at various concentrations, were determined

Table 5 Steady-state kinetic parameters for insertion of single nucleotides into a template-primer duplex

Entry	Template (X)	Nucleoside triphosphate (dYTP)	K_m (μM)	V_{max} (min⁻¹)	V_{max}/K_m (%·min⁻¹·M⁻¹)
1[a]	ImO^N	dATP	19 (10)[b]	0.43 (0.033)	2.3×10^4
2[a]		dGTP	34 (2.6)	0.18 (0.0071)	5.3×10^3
3[a]		dCTP	51 (13)	0.44 (0.044)	8.6×10^3
4[a]		TTP	54 (18)	0.28 (0.034)	5.1×10^3
5[a]		ImO^{N}TP	n.d.[c]	n.d.[c]	n.d.[c]
6[a]		NaN^{O}TP	2.6 (0.49)	22 (0.96)	8.5×10^6
7[a]	NaN^O	dATP	0.69 (0.22)	20 (3.4)	2.9×10^7
8[a]		dGTP	17 (1.8)	9.4 (1.5)	5.5×10^5
9[a]		dCTP	25 (5.5)	0.12 (0.010)	4.8×10^3
10[a]		TTP	19 (0.14)	0.11 (0.015)	5.8×10^3
11[a]		ImO^{N}TP	0.83 (0.23)	21 (5.3)	2.5×10^7
12[a]		NaN^{O}TP	14 (3.8)	0.32 (0.019)	2.3×10^4
13[a]	ImN^O	dATP	120 (6.4)	0.65 (0.047)	5.4×10^3
14[a]		dGTP	43 (10)	0.095 (0.0070)	2.2×10^3
15[a]		dCTP	n.d.	n.d.	n.d.
16[a]		TTP	16 (4.6)	0.12 (0.019)	7.5×10^3
17[a]		ImN^{O}TP	n.d.[c]	n.d.[c]	n.d.[c]
18[a]		NaO^{N}TP	57 (4.1)	13 (1.5)	2.3×10^5
19[a]	NaO^N	dATP	25 (3.1)	16 (2.1)	6.4×10^5
20[a]		dGTP	33 (7.7)	0.15 (0.027)	4.5×10^3
21[a]		dCTP	71 (31)	0.25 (0.051)	3.5×10^3
22[a]		TTP	20 (2.5)	0.13 (0.012)	6.5×10^3
23[a]		ImN^{O}TP	8.3 (2.5)	27 (4.7)	3.6×10^6
24[a]		NaO^{N}TP	29 (2.9)	2.4 (0.56)	8.3×10^4
25[d]	ImN^N	dATP	27 (1.1)	0.13 (0.48)	4.8×10^3
26[d]		dGTP	56 (2.9)	0.11 (0.037)	2.0×10^3
27[d]		dCTP	160 (13)	0.060 (0.018)	3.8×10^2
28[d]		TTP	140 (23)	0.082 (0.023)	5.6×10^2
29[d]		ImN^{N}TP	190 (39)	0.053 (0.0061)	2.7×10^2
30[d]		NaO^{O}TP	1.1 (0.29)	31 (2.7)	2.8×10^7
31[d]	NaO^O	dATP	4.1 (0.85)	18 (1.6)	4.4×10^6
32[d]		dGTP	3.5 (0.62)	24 (1.2)	6.8×10^6
33[d]		dCTP	140 (35)	0.41 (0.091)	2.9×10^3
34[d]		TTP	130 (14)	0.43 (0.083)	3.3×10^3
35[d]		ImN^{N}TP	0.56 (0.089)	48 (5.3)	8.6×10^7
36[d]		NaO^{O}TP	29 (2.8)	0.12 (0.019)	4.1×10^3
37	A	TTP	0.30 (0.051)	27 (3.2)	9.0×10^7
38	T	dATP	0.43 (0.010)	26 (1.4)	6.0×10^7

[a]These parameters are reproduced from our previous report [41]
[b]Standard deviations are given in parentheses
[c]Not determined
[d]From our previous report [59]

(Table 5). KF incorporated **NaN^{O}TP** preferentially against **ImO^N** in the template with an efficiency 10^2–10^3 times higher than those of dNTPs ($V_{max}/K_m = 8.5 \times 10^6$ versus 5.1×10^3 to 2.3×10^4%min⁻¹M⁻¹). Although the efficiency of **ImO^{N}TP** incorporation against **NaN^O** in the template was slightly higher than that of **NaN^{O}TP** against **ImO^N** ($V_{max}/K_m = 2.5 \times 10^7$ versus 8.5×10^6%min⁻¹M⁻¹), incorporation of

dATP competed with the same efficiency ($V_{max}/K_m = 2.9 \times 10^7$ versus $2.5 \times 10^7\%\text{min}^{-1}\text{M}^{-1}$) as observed in Fig. 4b. For the **ImN^O:NaO^N** pair, **ImN^{O}TP** or **NaO^{N}TP** was incorporated selectively against **NaO^N** or **ImN^O** in the templates, respectively, although the efficiencies were ca. 10 times lower than those for the **ImO^N:NaO^O** pair ($V_{max}/K_m = 8.5 \times 10^6$ versus 2.3×10^5 and 2.5×10^7 versus $3.6 \times 10^6\%\text{min}^{-1}\text{M}^{-1}$, respectively). However, the **ImN^N:NaO^O** pair exhibited the best specificity and efficiency of all the **Im:Na** pairs. Thus, when **ImN^N** was present in the template, KF selectively incorporated **NaO^{O}TP** ($V_{max}/K_m = 2.8 \times 10^7\%\text{min}^{-1}\text{M}^{-1}$) with an efficiency 10^4–10^5 times higher than those for the natural dNTPs ($V_{max}/K_m = 2.7 \times 10^2$ to $4.8 \times 10^3\%\text{min}^{-1}\text{M}^{-1}$). When **NaO^O** was in the template, the kinetic parameters indicated that the efficiency of **ImN^{N}TP** incorporation against **NaO^O** ($V_{max}/K_m = 8.6 \times 10^7\%\text{min}^{-1}\text{M}^{-1}$) is at least ten times more effective than natural dATP and dGTP incorporation ($V_{max}/K_m = 4.4 \times 10^6$ and $6.8 \times 10^6\%\text{min}^{-1}\text{M}^{-1}$, respectively). In addition, it is noteworthy that the incorporation efficiencies of the **ImN^N:NaO^O** pair ($V_{max}/K_m = 2.8 \times 10^7$ and $8.6 \times 10^7\%\text{min}^{-1}\text{M}^{-1}$) are almost the same as those of the natural A:T pair ($V_{max}/K_m = 6.0 \times 10^7$ and $9.0 \times 10^7\%\text{min}^{-1}\text{M}^{-1}$).

From the viewpoint of incorporation efficiency, the reason that the **ImN^O:NaO^N** pair is less effective in in vitro replication reactions is the fact that the **NaO^N** base lacks a proton acceptor corresponding to the O2 of the natural pyrimidine base (Fig. 1), which is considered to form key interactions between a DNA polymerase and the template DNA [8, 26, 32, 33]. Conversely, value of V_{max}/K_m for the **ImO^N:NaN^O** and **ImN^N:NaO^O** pairs are better than that for the **ImN^O:NaO^N** pair because both the **ImO^N** (**ImN^N**) and **NaN^O** (**NaO^O**) bases have proton acceptors at positions corresponding to the N3 of a purine and the O2 of a pyrimidine, respectively. Additionally, the **ImN^N:NaO^O** pair shows the highest incorporation efficiencies of the three **Im:Na** pairs owing to its thermal stability. With respect to specificity, misincorporation of dATP against **NaN^O** in the template can occur owing to the possible formation of an A:**NaN^O** pair with two H-bonds in the **ImO^N:NaN^O** base pairing (Fig. 5a). Conversely, misincorporations of dATP and/or dGTP against **ImN^N** in the template are controlled by the H-bonding geometries of the **ImN^N:NaO^O** pair. Thus, formation of both A:NaO^O and G:NaO^O should be negligible because of the NH proton repulsion between the 6-amino group of A and N8 of **NaO^O**, and N1 of G and N1 of **NaO^O**, respectively (Fig. 5b).

We next attempted the polymerase chain reaction (PCR) involving the **ImN^N:NaO^O** pair [59]. In a repeated replication system, such as PCR, unnatural bases should form a complementary base pair selectively when either base is located in the template because replicated DNA fragments also act as templates for further replication. If the nucleoside 5′-triphosphate (dYTP) is incorporated against X in the template with a selectivity of 99.0% (with the remaining 1% due to misincorporation of dNTPs) in PCR catalyzed by a certain DNA polymerase, then 86% of the unnatural X:Y pairs would remain at the original positions in the amplified DNAs after 15 PCR cycles ($0.99^{15} \approx 0.86$). Because mutations in the base sequence in replicated DNA fragments are accumulated during PCR cycles, specific recognition of unnatural base pairs by DNA polymerase is essential for accurate amplification. According to the method reported by Hirao et al. [61], PCR involving **ImN^N:NaO^O** was examined under various dNTP conditions (Fig. 6a).
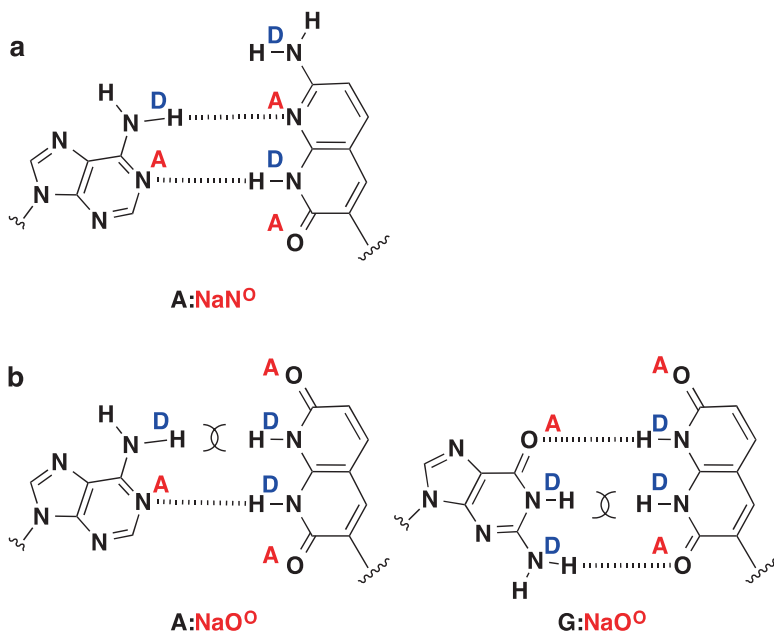
Fig. 5 Structures of possible four-H-bonding mismatched base pairs with natural purine bases

When Taq DNA polymerase, which is a standard thermophilic DNA polymerase for routine PCR, was used, a 75 base-pair (bp) amplicon in the presence of **ImN^{N}TP** and **NaO^{O}TP** along with all four kinds of dNTPs was successfully obtained (Fig. 6b, lane 4). However, similar PCR products were observed under conditions lacking **ImN^{N}TP** (lane 3), indicating that inaccurate amplification occurs when *Taq* DNA polymerase was used. Thus, **NaO^{O}TP** is preferentially incorporated against **ImN^N** in the template to afford DNA fragments containing the **ImN^N:NaO^O** pair in the first cycle of PCR as expected. However, misincorporation of dATP and/or dGTP against **NaO^O** in the resulting DNA fragment occurs during the second cycle of PCR and in further cycles, because complementary **ImN^{N}TP** is absent under these conditions. Accordingly, we screened suitable thermophilic DNA polymerases and typical results are shown in Fig. 6c–e. Exonuclease-deficient Deep Vent (Deep Vent exo⁻) DNA polymerase gave the 75 bp amplicon in both the presence and absence of **NaO^{O}TP** (Fig. 6c). Conversely, the same polymerase with 3′→5′ exonuclease activity (Deep Vent exo⁺) preferentially afforded the PCR product under these conditions in the presence of all the different 5′-triphosphates (Fig. 6d), suggesting that the proofreading activity identifies mismatched base pairs with a WC base and corrects them to the **ImN^N:NaO^O** pair. It has been reported that this proofreading activity of DNA polymerases improves the accuracy of incorporating unnatural base pair analogs [17–19], and the benefits of this activity are apparent in our case.

To further evaluate the accuracy of this PCR amplification, we sequenced the resulting PCR product after 15 cycles. When the PCR products obtained by 3′→5′
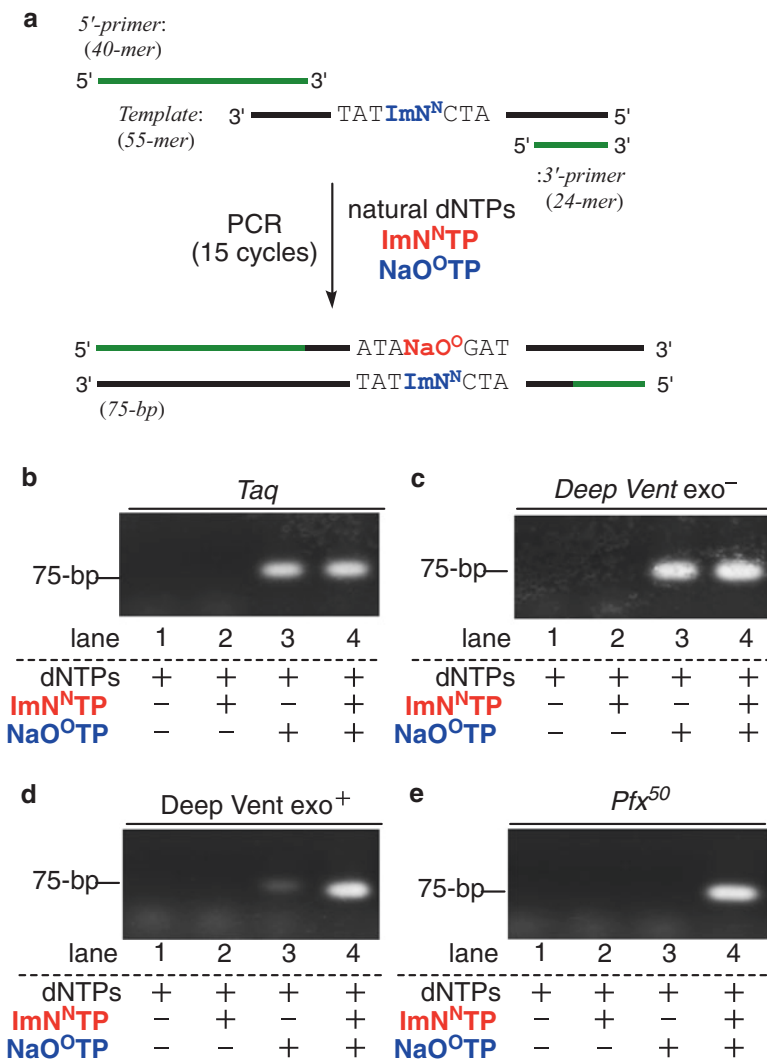
Fig. 6 Fifteen cycles of PCR involving an **ImN^N:NaO^O** pair. (**a**) Schematics of template and primers, and the resulting amplicon. Gel electrophoresis of PCR products obtained using Taq DNA polymerase (**b**), Deep Vent exo⁻ DNA polymerase (**c**), Deep Vent exo⁺ DNA polymerase (**d**), and *Pfx^{50}* DNA polymerase (**e**) under different dNTP conditions

exonuclease-proficient DNA polymerases were analyzed, the resulting read-through peaks terminated at the unnatural base site because there was no appropriate 5′-triphosphate in the standard sequencing reaction. The total mutation rates of the **ImN^N:NaO^O** pair in the PCR product using *Pfx^{50}* DNA polymerase after 15 cycles were estimated to be ca. 6% by comparing the read-through peak heights in the sequencing with a control DNA template (fidelity ≈ 0.995 per doubling) according
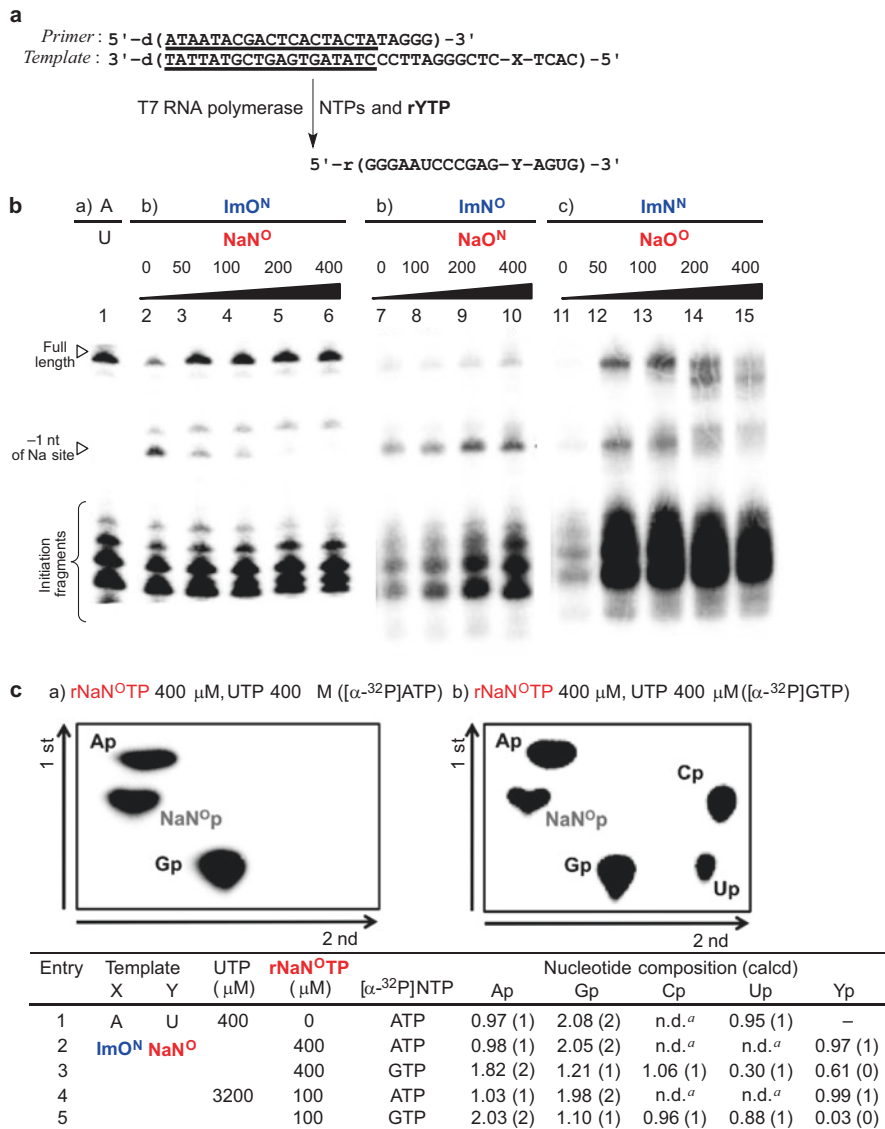
to methods reported by the groups of Benner [38] and Hirao [61]. Although the replication fidelity of the **ImN^N:NaO^O** pair is slightly inferior to those of other unnatural base-pair analogs [6, 17, 22, 38, 61–63], it is strongly indicated that the **ImN^N:NaO^O** pair acts as an orthogonal base pair for WC base pairs during PCR amplification. As is well known, WC base pairs consist of A:T with two H-bonds and G:C with three H-bonds. Thus, it is worth noting that accurate in vitro replication of the unnatural **ImN^N:NaO^O** pair with four H-bonds is achieved similarly to that of WC base pairs.

4.2   Transcription System with an Alternative Genetic Set Im:Na Pair

Since the "central dogma" requires that unnatural base pairs should not only replicate in DNA, but also transcribe to RNA with accuracy, efficiency, and selectivity, we next studied the in vitro transcription of an alternative genetic set **Im:Na** pair [46].

We first prepared a series of Na *C*-ribonucleoside 5′-triphosphates (**rNaTP**) from the corresponding 2′-deoxynucleosides. In the case of transcription catalyzed by T7 RNA polymerase, which would be useful for in vitro systems, RNA production can be terminated within the first 10 nt from the initiation point (termed the initiation phase) because of instability in the quadripartite complex formed by the DNA template, the transcribed RNA, and the rNTPs with the enzyme [9, 55, 56, 64]. Thus, the complementary **Im** base should be located more than 11 nt from the starting point of the transcription. We first examined the reactions with template DNA bearing **ImO^N** at the X position and four kinds of natural rNTPs as well as **rNaN^{O}TP** under various concentrations (Fig. 7). Full-length RNA products were obtained along with abortive products (termed initiation fragments) in the presence of **rNaN^{O}TP** (lanes 3–6), similarly to in the natural control (lane 1), and the amount of initiation fragments in the presence of **rNaN^{O}TP** was much higher than that in its absence (lane 2), suggesting that **rNaN^{O}TP** was preferentially incorporated against **ImO^N** in the template (Fig. 7b).

To validate the accuracy of the sequence transcribed to RNA, 2D TLC experiments [53] were performed. The transcripts obtained using [α-^{32}P]ATP were digested with RNase T$_2$, which cleaves phosphodiester linkages between the 3′-phosphate and the 5′-hydroxy group. On the 2D TLC, 5′-neiboring 3′-^{32}P-monophosphates of A in the transcribed RNA were observed (Fig. 7c), indicating that the nucleotide compositions of the full-length products including **rNaN^O** were accurate (entry 2). However, when [α-^{32}P]GTP was used in the transcription reaction, the amount of uridine 3′-^{32}P-monophosphate was decreased (0.30; calculated to be 1.0) on increasing the amount of **rNaN^O** 3′-^{32}P-monophosphate (0.61; calculated to be 0.00) (entry 3), indicating that some mismatched A:**NaN^O** pairs might be formed during the transcription reaction. Therefore, the concentrations of UTP and **rNaN^{O}TP** were adjusted to prevent inaccurate transcription. We succeeded in minimizing the mismatched formation of the A:**NaN^O** pair to 3% when 3.2 mM UTP and 100 μM

a

Primer : `5'-d(ATAATACGACTCACTACTATAGGG)-3'`
Template : `3'-d(TATTATGCTGAGTGATATCCCTTAGGGCTC-X-TCAC)-5'`

T7 RNA polymerase | NTPs and **rYTP**

`5'-r(GGGAAUCCCGAG-Y-AGUG)-3'`

b

c   a) rNaNOTP 400 μM, UTP 400 M ([α-³²P]ATP) b) rNaNOTP 400 μM, UTP 400 μM ([α-³²P]GTP)

Entry	Template		UTP	rNaNOTP	[α-³²P]NTP	Nucleotide composition (calcd)				
	X	Y	(μM)	(μM)		Ap	Gp	Cp	Up	Yp
1	A	U	400	0	ATP	0.97 (1)	2.08 (2)	n.d.ᵃ	0.95 (1)	–
2	ImON	NaNO		400	ATP	0.98 (1)	2.05 (2)	n.d.ᵃ	n.d.ᵃ	0.97 (1)
3				400	GTP	1.82 (2)	1.21 (1)	1.06 (1)	0.30 (1)	0.61 (0)
4				3200	100	ATP	1.03 (1)	1.98 (2)	n.d.ᵃ	n.d.ᵃ	0.99 (1)
5				100	GTP	2.03 (2)	1.10 (1)	0.96 (1)	0.88 (1)	0.03 (0)

Fig. 7 In vitro transcription involving an **Im:Na** pair using T7 RNA polymerase. (**a**) Sequence of the 35 mer DNA template containing **Im** and the 17-mer transcription product containing **rNa**. (**b**) Gel electrophoresis of transcription products formed using the DNA template with a series of **Im**s at the X position and **rNaTP**. (**c**) 2D TLC experiment using [α-³²P]A/GTP for the full-length transcription product formed with **rNaNOTP** and UTP, and their nucleotide compositions. ᵃn.d. not detected

rNaN^{O}TP along with 400 μM of other kinds of NTPs were used, and the MALDI-TOF mass spectrum of the full-length product confirms this (entries 4 and 5). In the transcription reaction with a DNA template having an **ImN^O** pair, however, **rNa-O^{N}TP** was slightly incorporated into the RNA transcript, even when high concentrations of triphosphates were used (Fig. 7b). The major transcription product appeared to be terminated just one base before the **rNaO^{N}TP** incorporation site. It is not clear whether similar interactions between DNA polymerases and dNTPs occur. However, the atomic-level structures of T7 RNA polymerase complexes indicate the presence of an imidazole ring from the histidine residue at position 784 (His784), which forms a catalytic platform, and is close to the O2 atom of a pyrimidine base in the minor groove [3, 24, 60, 65]. Thus, the in vitro transcription involving the **ImN^O:NaO^N** pair is insufficient because of the weakened interaction between His784 and the amino group on the **rNaO^N** base. In vitro transcription reactions involving several unnatural base pairs, i.e., isoG:isoC [57, 58], s:y [19, 47], Ds:Pa [18], and 5SICS:NaM [52], have been reported, and all the 5′-triphosphates used, such as isoGTP, sTP, yTP, DsTP, PaTP, 5SICSTP, and NaMTP have a H-bond acceptor in the minor groove. For the **ImN^N:NaO^O** pair, full-length transcripts were also obtained, similarly to the **ImN^N:NaO^O** pair, whereas aborted RNA products were produced as the concentration of **rNaO^{O}TP** increased (Fig. 7c). The result of 2D TLC revealed that the full-length product has the expected nucleotide composition when either [α-^{32}P]ATP or [α-^{32}P]GTP is used, although higher concentrations of **rNaO^{O}TP** afford inaccurate transcripts. These results indicate that the four-H-bonding **Im:Na** base pair functions as an orthogonal third base pair, which can be transcribed from a DNA duplex to a corresponding RNA, with appropriate H-bonding geometry between base pairs and 5′-triphosphate concentrations.

5   Conclusion and Perspective

During the last decade, we have developed a series of four-H-bonding unnatural base pairs. In the case of our first-generation **Im:Im** base pair, the single incorporation of **ImO^N:ImN^O** or **ImN^N:ImO^O** destabilized the DNA duplexes, whereas three consecutive incorporations, especially of **ImO^N:ImN^O**, markedly stabilized the duplexes (Table 1). Because the **Im:Im** base pair does not exhibit shape complementarity like the purine:purine pair, the stabilization efficacy of the **Im**:**Im** pair depends on the mode of incorporation (Table 2 and Fig. 2). To satisfy shape complementarity, we developed a series of **Na** *C*-nucleosides as a second generation of unnatural nucleosides having a fourth H-bonding site in nucleobases. The base pairs between **Im** and **Na** with four H-bonds significantly stabilized the DNA duplexes by the synergistic effect of the non-canonical four H-bonds, enhanced stacking interactions arising from the expanded aromatic surfaces, and a similar shape complementarity as that seen in WC base pairs (Table 3). Additionally, careful investigation revealed that secondary interactions arising from H-bonding geometries between base pairs play an important role in the stability of the duplexes. Among the possible

four-H-bonding **Im:Na** pairs (Fig. 3), factors of secondary interaction in **ImO^N:NaN^O** and **ImN^O:NaO^N** pairs, which have alternating H-bonding patterns DADA:ADAD and DADA:ADAD, respectively, are estimated to have an index value of −6. Conversely, the **ImN^N:NaO^O** pair having DAAD:ADDA H-bonding geometry showed superior secondary interactions (index = −2) than the **ImO^N:NaN^O** and the **ImN^O:NaO^N** pairs. As a result, **ImN^N:NaO^O** pair conferred the highest thermal stabilities.

The H-bonding geometries of **ImN^N:NaO^O** pair promoted enzymatic recognition by DNA polymerases. In in vitro replication studies using single nucleotide insertion reactions, KF incorporated either **ImN^{N}TP** or **NaO^{O}TP** against **NaO^O** or **ImN^N** in the templates with the highest efficiency and selectivity among the three **Im:Na** pairs examined (Fig. 4 and Table 5). With respect to efficiency, because **ImO^N:NaN^O** and **ImN^N:NaO^O** pairs possess two proton acceptors corresponding to the N3 of a purine and the O2 of a pyrimidine, which are considered to form key interactions with DNA polymerases, these two **Im:Na** pairs were well replicated. Incorporation efficiencies were also enhanced by the favorable contribution to enthalpy of base-pair formation in the **ImN^N:NaO^O** pair. For selectivity in base pairing, the specific DAAD:ADDA H-bonding geometry of the **ImN^N:NaO^O** pair eliminated unfavorable mismatched base-pair formations between **NaO^O** and WC purine bases (Fig. 5b). Moreover, accurate PCR amplification involving the **ImN^N:NaO^O** pair was achieved using DNA polymerases possessing 3′→5′ exonuclease activity (99.5% per doubling) (Fig. 6). In vitro transcription reactions cauterized by T7 RNA polymerase involving **Im:Na** base pairs, which is another requirement to demonstrate conformity with the central dogma, were also examined. The **ImO^N:NaN^O** and **ImN^N:NaO^O** pairs in ODNs were well transcribed with high fidelity under optimized concentrations of UTP and **rNaTP** (Fig. 7).

These results indicate that not only the number but also the geometry of H-bonds between base pairs are critical factors for polymerase recognition as well as thermal stability. Further development of **Im**:**Na** base pairs possessing DDDD:AAAA and AADD:DDAA H-bonding patterns is ongoing in our research group and will be publish in due course.

References

1. Beijer FH, Sijbesma RP, Kooijman H et al (1998) Strong dimerization of ureidopyrimidones via quadruple hydrogen bonding. J Am Chem Soc 120:6761–6769
2. Benner SA (2004) Understanding nucleic acids using synthetic chemistry. Acc Chem Res 37:784–797

3. Bielinska A, Shivdasani RA, Zhang LQ et al (1990) Regulation of gene expression with double-stranded phosphorothioate oligonucleotides. Science 250:997–1000

4. Clusel C, Ugarte E, Enjolras N et al (1993) Ex vivo regulation of specific gene expression by nanomolar concentration of double-stranded dumbbell oligonucleotides. Nucleic Acids Res 21:3405–3411

5. Crinelli R, Bianchi M, Gentilini L et al (2002) Design and characterization of decoy oligonucleotides containing locked nucleic acids. Nucleic Acids Res 30:2435–2443

6. Dhami K, Malyshev DA, Ordoukhanian P et al (2014) Systematic exploration of a class of hydrophobic unnatural base pairs yields multiple new candidates for the expansion of the genetic alphabet. Nucleic Acids Res 42:10235–10244

7. Djurdjevic S, Leigh DA, McNab H et al (2007) Extremely strong and readily accessible AAA-DDD triple hydrogen bond complexes. J Am Chem Soc 129:476–477

8. Doublie S, Tabor S, Long AM et al (1998) Crystal structure of a bacteriophage T7 DNA replication complex at 2.2Å resolution. Nature 391:251–258

9. Durniak KJ, Bailey S, Steitz TA (2008) The structure of a transcribing T7 RNA polymerase in transition from initiation to elongation. Science 322:553–557

10. Flanagan WM, Wolf JJ, Olson P et al (1999) A cytosine analog that confers enhanced potency to antisense oligonucleotides. Proc Natl Acad Sci U S A 96:3513–3518

11. Guckian KM, Krugh TR, Kool ET (1998) Solution structure of a DNA duplex containing a replicable difluorotoluene-adenine pair. Nat Struct Biol 5:954–959

12. Guckian KM, Schweitzer BA, Ren RX et al (1996) Experimental measurement of aromatic stacking affinities in the context of duplex DNA. J Am Chem Soc 118:8182–8183

13. Higuchi Y, Furukawa K, Miyazawa T et al (2014) Development of a new dumbbell-shaped decoy DNA using a combination of the unnatural base pair ImO^N:NaN^O and a CuAAC reaction. Bioconjug Chem 25:1360–1369

14. Hikishima S, Minakawa N, Kuramoto K et al (2005) Synthesis of 1,8-naphthyridine C-nucleosides and their base-pairing properties in oligodeoxynucleotides: thermally stable nap hthyridine:imidazopyridopyrimidine base-pairing motifs. Angew Chem Int Ed 44:596–598

15. Hikishima S, Minakawa N, Kuramoto K et al (2006) Synthesis and characterization of oligodeoxynucleotides containing naphthyridine:imidazopyridopyrimidine base pairs at their sticky ends. Application as thermally stabilized decoy molecules. ChemBiochem 7:1970–1975

16. Hirao I, Harada Y, Kimoto M et al (2004) A two-unnatural-base-pair system toward the expansion of the genetic code. J Am Chem Soc 126:13298–13305

17. Hirao I, Kimoto M (2012) Unnatural base pair systems toward the expansion of the genetic alphabet in the central dogma. Proc Jpn Acad Ser B 88:345–367

18. Hirao I, Kimoto M, Mitsui T et al (2006) An unnatural hydrophobic base pair system: site-specific incorporation of nucleotide analogs into DNA and RNA. Nat Methods 3:729–735

19. Hirao I, Ohtsuki T, Fujiwara T et al (2002) An unnatural base pair for incorporating amino acid analogs into proteins. Nat Biotechnol 20:177–182

20. Horlacher J, Hottiger M, Podust VN et al (1995) Recognition by viral and cellular DNA polymerases of nucleosides bearing bases with nonstandard hydrogen bonding patterns. Proc Natl Acad Sci U S A 92:6329–6333

21. Ichikawa S, Ueno H, Sunadome T et al (2013) Tris(azidoethyl)amine hydrochloride; a versatile reagent for synthesis of functionalized dumbbell oligodeoxynucleotides. Org Lett 15:694–697

22. Johnson SC, Sherrill CB, Marshall DJ et al (2004) A third base pair for the polymerase chain reaction: inserting isoC and isoG. Nucleic Acids Res 32:1937–1941

23. Jorgensen WL, Pranata J (1990) Importance of secondary interactions in triply hydrogen bonded complexes:guanine-cytosine vs uracil-2,6-diaminopyridine. J Am Chem Soc 112:2008–2010

24. Kennedy WP, Momand JR, Yin YW (2007) Mechanism for de novo RNA synthesis and initiating nucleotide specificity by T7 RNA polymerase. J Mol Biol 370:256–268

25. Khakshoor O, Wheeler SE, Houk KN et al (2012) Measurement and theory of hydrogen bonding contribution to isosteric DNA base pairs. J Am Chem Soc 134:3154–3163

26. Kiefer JR, Mao C, Braman JC et al (1998) Visualizing DNA replication in a catalytically active Bacillus DNA polymerase crystal. Nature 391:304–307

27. Kool ET, Sintim HO (2006) The difluorotoluene debate–a decade later. Chem Commun:3665–3675
28. Kunugiza Y, Tomita T, Tomita N et al (2006) Inhibitory effect of ribbon-type NF-kappaB decoy oligodeoxynucleotides on osteoclast induction and activity in vitro and in vivo. Arthritis Res Ther 8:R103
29. Kuramoto K, Tarashima N, Hirama Y et al (2011) New imidazopyridopyrimidine:naphthyridine base-pairing motif, ImN^N:NaO^O, consisting of a DAAD:ADDA hydrogen bonding pattern, markedly stabilize DNA duplexes. Chem Commun 47:10818–10820
30. Lee I, Berdis AJ (2010) Non-natural nucleotides as probes for the mechanism and fidelity of DNA polymerases. Biochim Biophys Acta 1804:1064–1080
31. Li L, Degardin M, Lavergne T et al (2014) Natural-like replication of an unnatural base pair for the expansion of the genetic alphabet and biotechnology applications. J Am Chem Soc 136:826–829
32. Li Y, Korolev S, Waksman G (1998) Crystal structures of open and closed forms of binary and ternary complexes of the large fragment of Thermus aquaticus DNA polymerase I: structural basis for nucleotide incorporation. EMBO J 17:7514–7525
33. Li Y, Waksman G (2001) Crystal structures of a ddATP-, ddTTP-, ddCTP, and ddGTP-trapped ternary complex of Klentaq1: insights into nucleotide incorporation and selectivity. Protein Sci 10:1225–1233
34. Lin KY, Matteucci MD (1998) A cytosine analogue capable of clamp-like binding to a guanine in helical nucleic acids. J Am Chem Soc 120:8531–8532
35. Maier MA, Leeds JM, Balow G et al (2002) Nuclease resistance of oligonucleotides containing the tricyclic cytosine analogues phenoxazine and 9-(2-aminoethoxy)-phenoxazine ("G-clamp") and origins of their nuclease resistance properties. Biochemistry 41:1323–1327
36. Malyshev DA, Dhami K, Lavergne T et al (2014) A semi-synthetic organism with an expanded genetic alphabet. Nature 509:385–388
37. Malyshev DA, Romesberg FE (2015) The expanded genetic alphabet. Angew Chem Int Ed 54:11930–11944
38. Malyshev DA, Seo YJ, Ordoukhanian P et al (2009) PCR with an expanded genetic alphabet. J Am Chem Soc 131:14620–14621
39. Mann MJ, Dzau VJ (2000) Therapeutic applications of transcription factor decoy oligonucleotides. J Clin Invest 106:1071–1075
40. Minakawa N, Kojima N, Hikishima S et al (2003) New base pairing motifs. The synthesis and thermal stability of oligodeoxynucleotides containing imidazopyridopyrimidine nucleosides with the ability to form four hydrogen bonds. J Am Chem Soc 125:9970–9982
41. Minakawa N, Ogata S, Takahashi M et al (2009) Selective recognition of unnatural imidazo pyridopyrimidine:naphthyridine base pairs consisting of four hydrogen bonds by the klenow fragment. J Am Chem Soc 131:1644–1645
42. Mitsui T, Kimoto M, Harada Y et al (2005) An efficient unnatural base pair for a base-pair-expanded transcription system. J Am Chem Soc 127:8652–8658
43. Morales JC, Kool ET (1998) Efficient replication between non-hydrogen-bonded nucleoside shape analogs. Nat Struct Biol 5:950–954
44. Murray TJ, Zimmerman SC (1992) New triply hydrogen bonded complexes with highly variable stabilities. J Am Chem Soc 114:4010–4011
45. Nakane M, Ichikawa S, Matsuda A (2008) Triazole-linked dumbbell oligodeoxynucleotides with NF-kappaB binding ability as potential decoy molecules. J Org Chem 73:1842–1851
46. Nomura Y, Kashiwagi S, Sato K et al (2014) Selective transcription of an unnatural naphthyridine:imidazopyridopyrimidine base pair containing four hydrogen bonds with T7 RNA polymerase. Angew Chem Int Ed 53:12844–12848
47. Ohtsuki T, Kimoto M, Ishikawa M et al (2001) Unnatural base pairs for specific transcription. Proc Natl Acad Sci U S A 98:4922–4925
48. Piccirilli JA, Benner SA, Krauch T et al (1990) Enzymatic incorporation of a new base pair into DNA and RNA extends the genetic alphabet. Nature 343:33–37

49. Prive GG, Heinemann U, Chandrasegaran S et al (1987) Helix geometry, hydration, and G.A mismatch in a B-DNA decamer. Science 238:498–504
50. Rich A (1962) On the problems of evolution and biochemical information transfer. Horizons in Biochemistry (Kasha, M, Pullman, B), Academic, New York: 103–126
51. Romanelli A, Pedone C, Saviano M et al (2001) Molecular interactions with nuclear factor kappaB (NF-kappaB) transcription factors of a PNA-DNA chimera mimicking NF-kappaB binding sites. Eur J Biochem 268:6066–6075
52. Seo YJ, Matsuda S, Romesberg FE (2009) Transcription of an expanded genetic alphabet. J Am Chem Soc 131:5046–5047
53. Silberklang M, Prochiantz A, Haenni AL et al (1977) Studies on the sequence of the 3′-terminal region of turnip-yellow-mosaic-virus RNA. Eur J Biochem 72:465–478
54. Stec WJ, Grajkowski A, Kobylanska A et al (1995) Diastereomers of nucleoside 3′-O-(2-thio-1,3,2-oxathia(selena)phospholanes)–building-blocks for stereocontrolled synthesis of oligo(nucleoside phosphorothioate)s. J Am Chem Soc 117:12019–12029
55. Steitz TA (2004) The structural basis of the transition from initiation to elongation phases of transcription, as well as translocation and strand separation, by T7 RNA polymerase. Curr Opin Struct Biol 14:4–9
56. Steitz TA (2009) The structural changes of T7 RNA polymerase from transcription initiation to elongation. Curr Opin Struct Biol 19:683–690
57. Switzer C, Moroney SE, Benner SA (1989) Enzymatic incorporation of a new base pair into DNA and RNA. J Am Chem Soc 111:8322–8323
58. Switzer CY, Moroney SE, Benner SA (1993) Enzymic recognition of the base pair between isocytidine and isoguanosine. Biochemistry 32:10489–10496
59. Tarashima N, Komatsu Y, Furukawa K et al (2015) Faithful PCR amplification of an unnatural base-pair analogue with four hydrogen bonds. Chem Eur J 21:10688–10695
60. Temiakov D, Patlan V, Anikin M et al (2004) Structural basis for substrate selection by T7 RNA polymerase. Cell 116:381–391
61. Yamashige R, Kimoto M, Takezawa Y et al (2012) Highly specific unnatural base pair systems as a third base pair for PCR amplification. Nucleic Acids Res 40:2793–2806
62. Yang Z, Chen F, Alvarado JB, Benner SA (2011) Amplification, mutation, and sequencing of a six-letter synthetic genetic system. J Am Chem Soc 133:15105–15112
63. Yang Z, Sismour AM, Sheng P et al (2007) Enzymatic incorporation of a third nucleobase pair. Nucleic Acids Res 35:4238–4249
64. Yin YW, Steitz TA (2002) Structural basis for the transition from initiation to elongation transcription in T7 RNA polymerase. Science 298:1387–1395
65. Yin YW, Steitz TA (2004) The structural mechanism of translocation and helicase activity in T7 RNA polymerase. Cell 116:393–404

Photo-Cross-Linkable Artificial Nucleic Acid: Synthesis and Properties of 3-Cyanovinylcarbazole-Modified Nucleic Acids and Its Photo-Induced Gene-Silencing Activity in Cells

Takashi Sakamoto and Kenzo Fujimoto

Abstract The inter-strand photo-cross-linking reaction between nucleic acid strands has wide potential for regulating gene expression specifically and spatio-temporally due to its sequence specificity and high photo irradiation operability. Therefore, photo-cross-linkable artificial nucleic acids are required to be specific and effective drugs without adverse effects and also be good tools for investigating gene functions in cells.

As one of the most reactive photo-cross-linkable artificial nucleic acids, in this review, 3-cyanovinylcarbazole modified oligodeoxyribonucleotides that can photo-crosslink with their complementary nucleic acid within a few seconds of photoir-radiation are examined. The details of the synthetic method, properties and the applications for regulating gene expression in cells are discussed.

Keywords Inter-strand photo-cross-linking · Nucleic acids · Photoirradiation · 3-cyanovinylcarbazole · Gene expression · Antisense oligonucleotides

1 Introduction

Inter-strand photo-cross-linking of nucleic acids is one of the most useful technologies for regulating nucleic acid functions, such as transcription and replication of the genome, gene silencing activity of microRNAs, and translational activity of mRNAs. The sequence specific and thermally irreversible covalent bond formation between the nucleic acid strand and artificial photo-cross-linkable oligonucelotide caused by the photo-cross-linking reaction enables us to regulate sequence-specifically and spatiotemporally the target nucleic acid function.

T. Sakamoto · K. Fujimoto (✉)
School of Materials Science, Japan Advanced Institute of Science and Technology, Nomi, Ishikawa, Japan
e-mail: kenzo@jaist.ac.jp

As the pioneering works in this field, in the late 1980s, Miller and co-workers reported psoralen-modified oligonucleotide (Fig. 1, left) as the first photo-cross-linkable synthetic oligonucleotide [1, 15, 24]. They introduced trioxalen, a natural DNA photo-cross-linker that can be obtained from plants, at the 5′ end of synthetic oligodeoxyribonucleotides (ODN(s)), and clearly demonstrated that the ODNs cross-linked with single-stranded DNA and double-stranded DNA [14] under UVA (365 nm) irradiation. The findings led to the study on photoresponsive synthetic oligonucleotides. In the late 2000s, advanced-type ODNs having psoralen-modified adenosine were reported by Murakami and co-workers (Fig. 1, center) [11, 13]. Due to the restricted and favorable position of psoralen moiety in double-stranded nucleic acid consisting of the ODN and the complementary nucleic acid, these ODNs have higher photoreactivity compared to 5′ psoralen-modified ODNs. The psoralen-modified ODNs can photo-cross-link with not only single-stranded DNA, but also with single-stranded RNA and double-stranded DNA. The wide photoreactivity toward nucleic acid strands enables us to photoregulate various nucleic acid functions, such as transcription, [2, 7, 8, 18, 19, 29, 31] translation [3, 16] and microRNA activity [17].

In our group, as the next generation of photo-cross-linkers, 3-cyanovinylcarbazole-modified oligonucleotides (Fig. 2) have been developed [26, 30]. Since it has extremely high photoreactivity compared to other artificial photo-cross-linkable ODNs, the 3-cyanovinylcarbazole-modified ODNs can photo-cross-link with complementary DNA or RNA within a few seconds of UVA irradiation. Currently, the 3-cyanovinylcarbazole-modified photo-cross-linkable ODNs are applied to various fields of scientific study, such as the construction of DNA-based
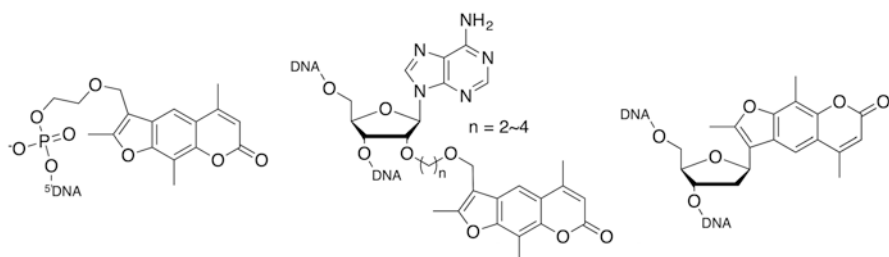
Fig. 1 Psoralen-modified photo-cross-linkable oligonucleotides
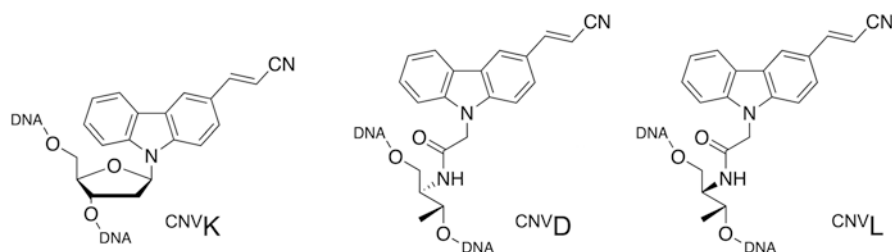
Fig. 2 3-cyanovinylcarbazole-modified photo-cross-linkable oligonucleotides

nanomaterials [23], SELEX-based aptamer selection [21], site-specific nucleic acid editing [4, 5], and gene regulation in cells [25].

In this chapter, the synthetic methods and properties of the 3-cyanovinylcarbazole-modified ODNs, and the applications for gene silencing are described.

2   Synthesis of 3-Cyanovinylcarbazole-Based Photo-Cross-Linker

Currently, 3-cyanovinylcarbazole-modified ODN is the most reactive photo-cross-linkable ODN in the world. However, at this time, the reagents for the modification of ODNs are not commercially available. Therefore, in this section, a practical method to synthesize the 3-cyanovinylcarbazole-modified ODNs is described.

The phosphoramidite monomer of ^{CNV}K can be obtained by multi-step organic synthesis as shown in Scheme 1 from commercially available carbazole (**1**) as a starting material. At first, the electron rich C3 carbon of carbazole is iodized by a general electrophilic halogenation procedure using $NaIO_4$ as a catalyst. In this reaction, 3,6-diiodocarbazole by-product is sometimes generated because the electron density of C6 carbon of the target product, e.g. 3-iodocarbazole (**2**), is larger than that of the starting material. To obtain the target within a high yield, the homogeneity and the molar equivalent of all the reagents should be carefully checked before starting the reaction. 3-Cyanovinylcarbazole (**3**) can be obtained easily by the
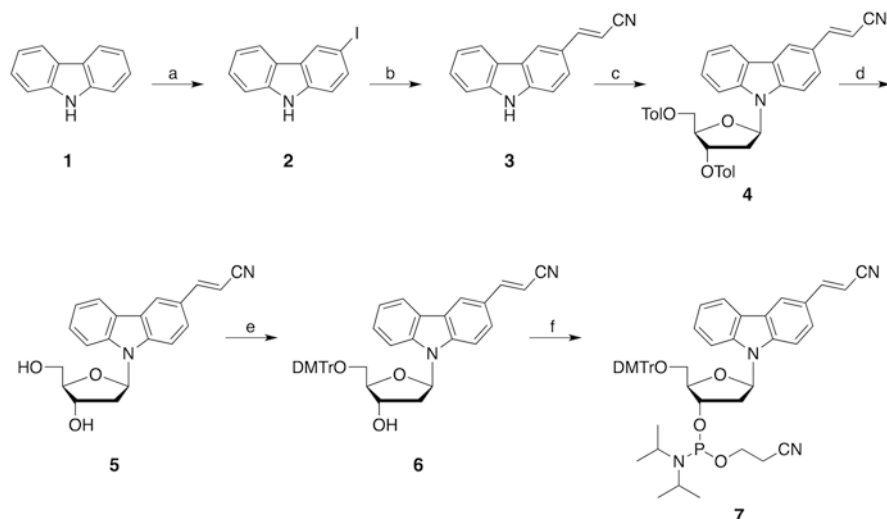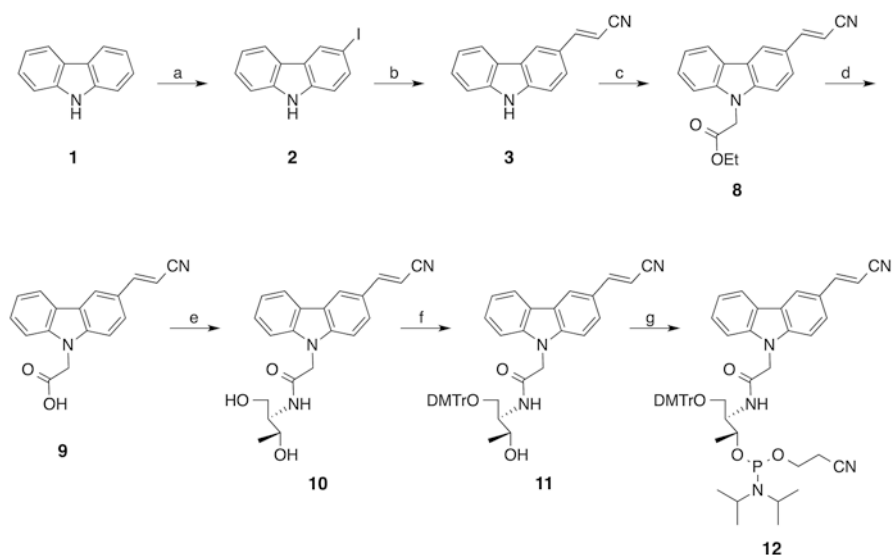

Scheme 1 Synthesis of the phosphoramidite monomer of ^{CNV}K. a) I_2, $NaIO_4$, H_2SO_4, EtOH; b) acrylonitrile, Pd(OAc)$_2$, tributylamine, DMF-H$_2$O;c) KOH, TDA-1, chlorosugar, MeCN; d) MeONa, MeOH, CHCl$_3$; e) DMTr-Cl, DMAP, Pyridine; g) (iPr$_2$N)$_2$POCE, Benzylthio-1H-tetrazole, MeCN

Mizoroki-Heck reaction [10, 20] using acrylonitrile and Pd(OAc)$_2$ as a vinyl donor and palladium catalyst, respectively. In this reaction, a microwave synthesizer can be used for quick and high-yield preparation of the target compound. By adopting this equipment, the reaction is finished within 10 min. To couple 3-cyanovinylcarbazole (**3**) and the deoxyribose ring, 1-chloro-2-deoxy-3,5-di-O-p-toluoyl-D-ribofuranose (chlorosugar) can be used as a commercially-available reagent. The chlorosugar can also be obtained by the literature method [9]. Briefly, the methoxy substitution of 1 OH of 2-deoxy-D-ribofuranose is performed with methanol solution of acetyl chloride, the toluoyl protection of 5 and 3 OH groups of 1′-methoxy-2′-deoxy-D-ribofuranose is carried out using p-toluoyl chloride, and then the chlorination of 1 carbon of 1-methoxy-2-deoxy-3,5-di-O-p-toluoyl-D-ribofuranose is performed with HCl generated from acetyl chloride. According to this procedure, chlorosugar can be obtained as white precipitate generated in the reaction mixture; therefore, we can obtain chlorosugar just by using a simple filtration procedure.

After the deprotection of the p-toluoyl group at 5′ and 3′ OH groups of protected 3-cyanovinylcarbazole-1′-β-deoxyriboside using sodium methoxide, 3-cyanovinylcarbazole-1′-β-deoxyriboside (**5**, ^{CNV}K) can be obtained in good yield. Phosphoramidite monomer of ^{CNV}K can be obtained by 5′ OH DMTr protection and 3′ OH phosphoramidite modification with general procedures, respectively.

The phosphoramidite monomer of ^{CNV}D can be obtained by a multi-step organic synthesis (Scheme 2) from commercially available carbazole (**1**). After the synthesis of 3-cyanovinylcarbazole (**3**) using the same procedures of ^{CNV}K synthesis, an acetic acid derivative of 3-cyanovinylcarbazole, 3-cyanovinylcarbazol-9-yl-acetic

Scheme 2 Synthesis of the phosphoramidite monomer of ^{CNV}D. a) I$_2$, NaIO$_4$, H$_2$SO$_4$, EtOH; b) acrylonitrile, Pd(OAc)$_2$, tributylamine, DMF-H$_2$O; c) K$_2$CO$_3$, BrCH$_2$CO$_2$Et; d) HCl; e) D-threoninol, WSC, HOBt, DMF; f) DMTr-Cl, DMAP, Pyridine; g) (iPr$_2$N)$_2$POCE, Benzylthio-1H-tetrazole, MeCN

acid (**5**), can be obtained easily by the coupling with ethyl bromoacetate, and hydrolysis of the ethyl ester. *N*-(3-cyanovinylcarbazol-9-yl-acetyl) D-threoninol (**10**, ^{CNV}D) can be obtained by a simple condensation reaction with carbodiimide. Phosphoramidite monomer of ^{CNV}D can be obtained by DMTr protection of primary alcohol and phosphoramidite modification of secondary alcohol with general procedures, respectively. ^{CNV}L can also be obtained with the same synthetic procedures using L-threoninol instead of D-threoninol in the case of ^{CNV}D.

2.1 Synthetic Procedures of ^{CNV}K and Its Phosphoramidite Monomer

2.1.1 3-Iodocarbazole (2)

To a solution of carbazole (8.0 g, 47 mmol), iodine (6.0 g, 24 mmol) and $NaIO_4$ (2.5 g, 12 mmol) in EtOH (400 mL) was added a solution of H_2SO_4 (5 mL) in EtOH (200 mL), and stirred at 65 °C for 1 h. After neutralization with NaOH, solvent was evaporated, redissolved in CH_3Cl (700 mL) and washed with H_2O and brine. The organic layer was condensed and recrystallized twice to give **2** as a white solid (4.9 g, 17 mmol, 36%).

2.1.2 3-Cyanovinylcarbazole (3)

To a suspension of **2** (1.5 g, 5.12 mmol) in 20% DMF/H_2O (2.8 mL) in a pressure-resistant glass tube, palladium acetate (115 mg, 0.51 mmol), tributylamine (1.22 mL, 5.12 mmol) and acrylonitrile (0.84 mL, 12.8 mmol) were added, and microwave irradiated (60 W, 160 °C) by a microwave synthesizer (DISCOVER, CEM) for 10 min. The reaction was monitored by TLC (hexane/AcOEt, 4:1), which showed the absence of the starting material. After the reaction mixture was evaporated, the residue was chromatographed on a silica gel using hexane/AcOEt (3:1, v/v) as eluent to give **3** (0.85 g, 76%) as a white powder.

2.1.3 3-Cyanovinylcarbazole-9-yl-1′-β-deoxyriboside-3′,5′-di-(P-toluoyl) ester (4)

To a solution of potassium hydroxide (2.29 g, 40.9 mmol) and tris[2-(2-methoxyethoxy)ethyl]amine (90.0 mg, 0.28 mmol) in CH_3CN (360 mL), **3** (3.02 g, 13.9 mmol) was added and then stirred at room temperature for 30 min. To this reaction mixture chlorosugar (6.09 g, 14.3 mmol) was added and then stirred at room temperature for 60 min. The reaction was monitored by TLC (hexane/AcOEt, 4:1), which showed the absence of the starting material. After the reaction mixture was evaporated, the residue was chromatographed on a silica gel using $CHCl_3$ as eluent to give **4** (7.89 g, 99%) as a yellow powder.

2.1.4 3-Cyanovinylcarbazole-9-yl-1′-β-deoxyriboside (5)

To a solution of **4** (7.89 g, 13.8 mmol) in MeOH (400 mL) was added 0.5 M metha-nolic MeONa (83.0 mL, 41.5 mmol) and CHCl$_3$ (50 mL) and then stirred at room temperature for 1 h. The reaction was monitored by TLC (CHCl$_3$/MeOH, 9:1), which showed the absence of starting material. After the reaction mixture was evap-orated, the residue was chromatographed on a silica gel using CHCl$_3$/MeOH (9:1, v/v) as eluent to give **5** (2.93 g, 63%) as a white powder.

2.1.5 5′-O-(4,4′-Dimethoxytrityl)-3-cyanovinylcarbazole-9-yl-1′-β -deoxyriboside (6)

To a solution of **5** (2.83 g, 8.47 mmol) in pyridine (12 mL) was added a solution of 4,4′-dimethoxytrityl chloride (3.45 g, 10.2 mmol) and 4-(dimethylamino)pyridine (0.21 g, 1.70 mmol) in pyridine (24 mL) on an ice bath and then stirred at room temperature for 23 h. After the reaction mixture was evaporated, the residue was chromatographed on a silica gel using CHCl$_3$/MeOH (99:1, v/v) as the eluent to give **6** (4.20 g, 78%) as yellow foam.

2.1.6 5′-O-(4,4′-Dimethoxytrityl)-3-cyanovinylcarbazole-9-yl-1′-β -deoxyriboside-3′-O-(cyanoethoxy-*N,N*-diisopropylamino) phosphoramidite (7)

6 (0.32 g, 0.50 mmol) in a rubber sealed bottle was dissolved in CH$_3$CN (1 mL) and co-evaporated three times in vacuo. A solution of 2-cyanoethyl *N,N,N′,N′*-tetraisopropylphosphoramidite (160 μL, 0.50 mmol) in CH$_3$CN (2.2 mL) and 0.45 M *1H*-tetrazole in CH$_3$CN (1.18 mL, 0.50 mmol) were added and then stirred at room temperature for 2 h. The reaction mixture was diluted with AcOEt (15 mL) and washed with a saturated aqueous solution of NaHCO$_3$, and water. The organic layer was collected, dried over anhydrous magnesium sulfate, filtered, and evapo-rated in vaccuo to give the crude product of **7** (0.42 g, quant.) and was used as the automated DNA synthesizer without further purification.

2.2 Synthetic Procedures of ^{CNV}D and Its Phosphoramidite Monomer

2.2.1 Ethyl 3-cyanovinylcarbazol-9-yl-acetate (8)

3-Cyanovinylcarbazole (**3**) (1.1 g, 5 mmol) and NaH (60% oil suspension, 0.24 g, 6 mmol) were dissolved in dry DMF (20 mL) and stirred for 1 h at room tempera-ture under N$_2$ atmosphere. Ethyl bromoacetate (1.1 mL, 9.9 mmol) was added

drop-wisely over 30 min. The reaction mixture was diluted with water (300 mL) and extracted with chloroform and then dried over sodium sulfate. After removal of the solvent, the residue was subjected to silica gel column chromatography (0–1% MeOH/CHCl$_3$) to yield **4** as white solid (1.4 g, 4.6 mmol, 92%).

2.2.2 3-Cyanovinylcarbazol-9-yl-acetic Acid (9)

4 (1.4 g, 4.6 mmol) and NaOH (0.18 g, 23 mmol) were dissolved in THF/MeOH/H$_2$O (3:2:1, 30 mL) and stirred for 2 h at ambient temperature. After the addition of 1 N HCl (250 mL), the reaction mixture was extracted with EtOAc (300 mL) and washed with 1 N HCl. The organic layer was dried over MgSO$_4$ and evaporated to yield **5** as white solid (1.2 g, 4.4 mmol, 96%).

2.2.3 *N*-(3-Cyanovinylcarbazol-9-yl-acetyl)-D-threoninol (10, ^{CNV}D)

5 (1.3 g, 4.5 mmol) and D-threoninol (0.47 g, 4.5 mmol) were added to dry DMF (20 mL) containing 1-ethyl-3-(3-dimethylaminopropyl)carbodiimide hydrochloride (EDC; 0.86 g, 4.5 mmol) and 1-hydroxybenzotriazole (HOBt; 0.69 g, 4.5 mmol), and stirred for 5 h at ambient temperature. Sat. NaCl aq. soln. was added and the obtained precipitate was collected and dried under vacuo to yield **6** as white solid (1.5 g, 4.1 mmol, 91%).

2.2.4 *N*-(3-Cyanovinylcarbazol-9-yl-acetyl)-1′-*O*-(4,4′-dimethoxytrityl)-D-threoninol (11)

A solution of **6** (0.40 g, 1.1 mmol), 4,4′-dimethoxytritylchloride (0.41 g, 1.2 mmol) and 4-dimethyl- aminopyridine (DMAP; 30 mg, 0.25 mmol) in dry pyridine (2 mL) were stirred at ambient temperature for 20 h. The reaction mixture was diluted with CHCl$_3$, washed with H$_2$O and the organic layer was dried over NaSO$_4$. After the removal of the solvent, residue was subjected to silica gel column chromatography (CHCl$_3$ with 0.2% TEA) to yield **7** (0.63 g, 86%).

2.2.5 *N*-(3-Cyanovinylcarbazol-9-yl-acetyl)-1′-*O*-(4,4′-dimethoxytrityl)-D-threoninol 3′-*O*-(Cyanoethoxy-*N,N*-diisopropylamino) phosphoramidite (12)

The residual trivial amount of water in **7** was removed by azeotropic distillation with dry acetonitrile (twice). Then, **7** (0.38 g, 0.57 mmol) was dissolved with 0.25 M solution of 5-benzylthio-*1H*-tetrazole in dry MeCN (2.3 mL, 0.57 mmol) and a solution of 2-cyanoethyl *N,N,N′,N′*-tetraisopropylphosphoramidite (0.18 mL, 0.57 mmol) in dry acetonitrile (5 mL) was added and stirred under N$_2$ atmosphere

for 2 h. The crude mixture was dissolved in ethyl acetate. The solution containing **8** was washed with water, sat. NaHCO$_3$ aq. soln. and brine. The organic layer was dried over MgSO$_4$, and then filtered and the ethyl acetate was removed. The yellow foam (0.48 g, 0.55 mmol, 96%) was obtained and immediately used for DNA synthesis without further purification.

2.3   Synthesis of the Oligonucleotide Having ^{CNV}K or ^{CNV}D

ODNs having ^{CNV}K or ^{CNV}D can be obtained by the conventional cyano-ethylphosphoramidite chemistry using phosphoramidite monomer of ^{CNV}K or ^{CNV}D. If the automated DNA synthesizer has the extra phosphoramidite ports, ODNs having ^{CNV}K or ^{CNV}D can be synthesized easily by an automated DNA synthesizer. Due to the high stability of 3-cyanovinylcarbazole in cleavage and deprotection conditions, the general conditions (28% ammonium hydroxide, 55 °C, 8 h) are applicable. Crude ODN solution can be purified by reversed-phase HPLC in the same manner as general ODN purification.

2.4   Further Modification of ^{CNV}K- or ^{CNV}D-Modified ODNs

As the OH group on the 5′ and 3′ termini of the ^{CNV}K- or ^{CNV}D-modified ODNs is free for further modification, the general phosphoramidite-based modification method using 5′ or 3′ modifiers, such as FAM, biotin, amino, thiol, on the automated DNA synthesis is available. In the case of fluorescence labeling of the ODNs, a fluorophore whose stability is sufficiently high during the photo-cross-linking reaction, should be selected. In our cases, the Cy3 and Cy5 label is frequently used as the photo-stable fluorophore. To the best of our knowledge, fluorescein is not suitable for the fluorescent label of ^{CNV}K or ^{CNV}D-modified ODNs because of its lower photostability under UV irradiation.

3   Inter-Strand Photo-Cross-Linking Using ODNs Having ^{CNV}K or ^{CNV}D

In this section, the properties of the photo-cross-linking reaction of ^{CNV}K and ^{CNV}D, which currently are the most highly reactive photo-cross-linkers in the world, are described. Basic findings described here will enable the advanced application of the photo-cross-linking reaction of these photo-cross-linkable ODNs having ^{CNV}K or ^{CNV}D.

3.1 Properties of the Inter-Strand Photo-Cross-Linking Reaction of ᶜᴺⱽK and ᶜᴺⱽD in Nucleic Acid Double Strands

The inter-strand photo-cross-linking reaction of ᶜᴺⱽK and ᶜᴺⱽD occurs between the vinyl group of 3-cyanovinylcarbazole moiety and the C5-C6 double bond of the pyrimidine base situated at the –1 position of ᶜᴺⱽK or ᶜᴺⱽD in the complementary DNA or RNA strand with 366 nm UV irradiation (Fig. 3). Since the 312 nm irradiation under the denaturing condition causes reverse photoreaction and photo-splitting, the stability of the hybrid can be regulated freely by UV irradiation. As shown in Fig. 4, the local sequence around ᶜᴺⱽK or ᶜᴺⱽD largely affects the yield of the photo-cross-linking reaction. This indicates that the local duplex structure is important for the photo-cross-linking reaction. These reactions, photo-cross-linking and photo-splitting, can be monitored quantitatively by HPLC or denaturing PAGE analysis as the change in the retention time or mobility, respectively.
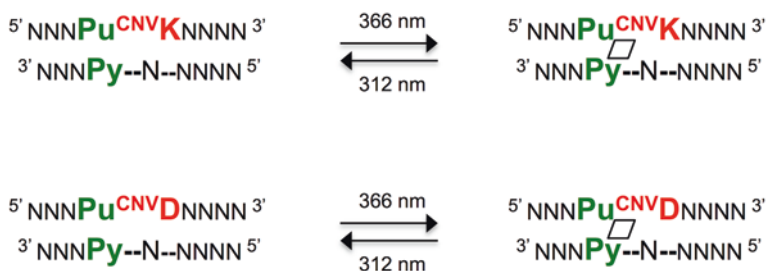

Fig. 3 Schematic drawing of the photo-cross-linking and photo-splitting reaction of 3-cyanovinylcarbazole-modified ODNs
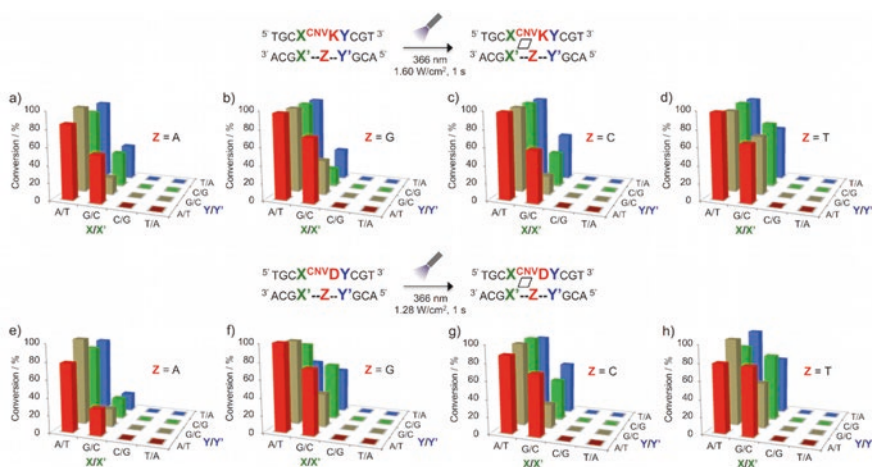

Fig. 4 Sequence dependency of the photo-cross-linking yields of ᶜᴺⱽK- or ᶜᴺⱽD-modified ODNs

^{CNV}K, which was first reported in 2008 [30], has great photoreactivity in the inter-strand photo-cross-linking reaction in the DNA double-strand. The reaction is finished within a few seconds of 366 nm irradiation using UV-LED. Although the pyrimidine bases, T and C, in the complementary strand can be cross-linked with ^{CNV}K, the reactivity depends on the bases, and the reactivity toward C is 27-fold lower than that toward T. This large difference of the photoreactivity dependent on the target pyrimidine base sometimes restricts the design of the ODN sequence for the photoreaction. In 2014, ^{CNV}D, which has a more flexible skeleton compared to ^{CNV}K, was developed [26] as the improved version of ^{CNV}K. The photoreactivity of ^{CNV}D is ca. 1.8-fold (toward T) and eightfold (toward C) greater than that of ^{CNV}K. In the case of ^{CNV}D, since the difference of the photoreactivity between T and C is closer than that of ^{CNV}K, the freedom for designing the sequences for the photo-cross-linking reaction is increased.

3.2 Light Source

For the photoreaction of ^{CNV}K and ^{CNV}D, a high-power UV-LED and a general trans-illuminator can be used depending on the experimental requirements. As the irradiation spotlight of UV-LED is small, ca. 100 mm² at maximum, this light source is not suitable for the simultaneous irradiation of one lot of samples. If the experiment requires simultaneous irradiation of the samples, the transilluminator is suitable because the area that can be uniformly irradiated is larger, ca. 40,000 mm², than that of UV-LED. In the case of the use of the transilluminator, the photoreaction proceeds more slowly compared to the case of UV-LED because of its lower irradiation energy compared to UV-LED.

3.3 Structural Insight of the DNA Duplex Including ^{CNV}K

As shown in Fig. 5, it was demonstrated that only the trans isomer of ^{CNV}K can react with the pyrimidine base on the complementary strand, and that reaction gives the photoadduct that was formed from the trans isomer of ^{CNV}K [6]. As the rate of the photo-isomerization of the cyanovinyl group is higher than that of the [2+2] photo-cycloaddition reaction, the rate determining step of the photo-cross-linking is the [2+2] photocycloaddition reaction. According to the structure of the photoadduct, the duplex structures consisting of ^{CNV}K-modified ODN and its complementary ODN before and after the photo-cross-linking reaction can be estimated by energy minimization calculation. As shown in Fig. 6, the structure of the duplex after the photo-cross-linking is slightly bent compared to that of before the photo-cross-linking. From the distance between the carbon atoms on certain nucleoside units, the major axis of the duplex is bent ca. 20° by the photo-cross-linking reaction. The degree of bend is comparable to the result that measured the bend in the ^{CNV}K photo-cross-linked DNA tile array [28].
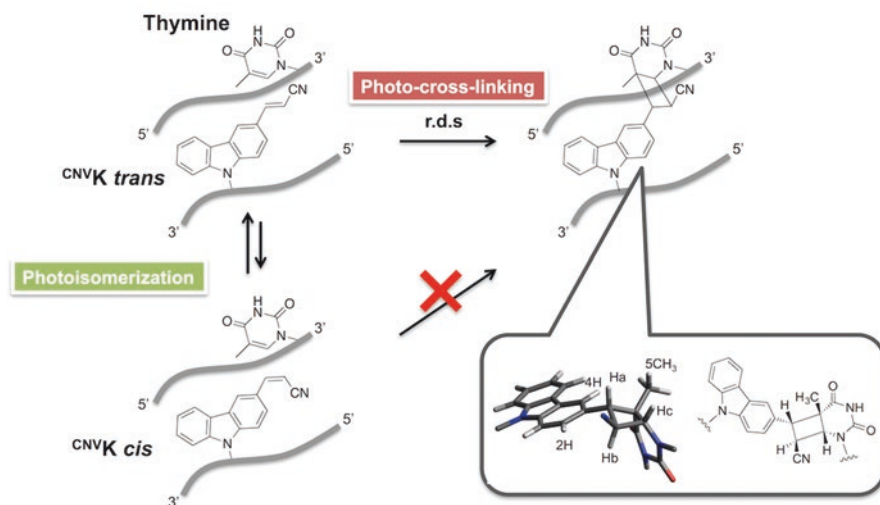
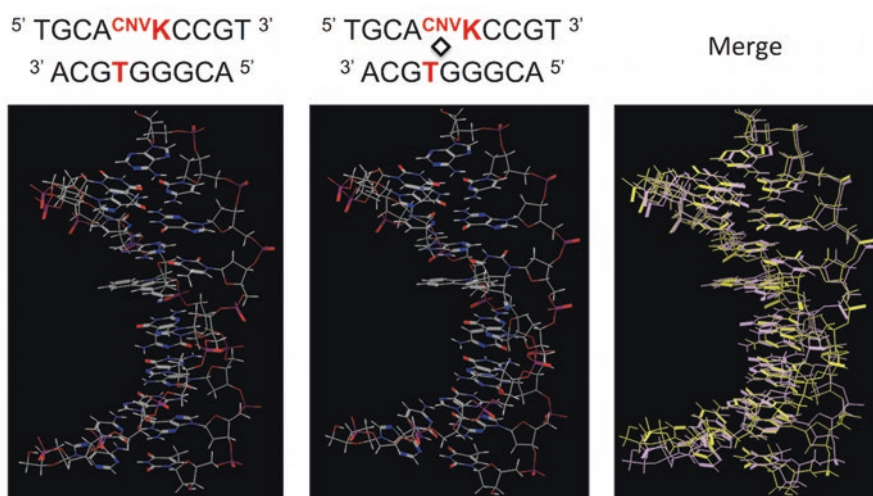**Fig. 5** Photo-cross-linking reaction of ^{CNV}K in DNA duplex

Fig. 6 Predicted energy minimized structure of the duplexes containing ^{CNV}K before and after the photo-cross-linking

4 Gene-Silencing Using ^{CNV}K Modified Antisense ODNs

Because of its ultra-fast photo-cross-linking properties, photo-cross-linkable ODNs having ^{CNV}K or ^{CNV}D might be applicable as the photoresponsive antisense ODNs for specific gene regulation through the photo-cross-linking with target mRNA. The ultra-fast photoresponse might enable us to regulate spatiotemporally the gene

expression in cells without intense photo-damage to the cells and to investigate the function of the gene of interest at various places and timings in cells. There are some reports about the photo-cross-linkable antisense ODNs using psoralen as a photo-cross-linker [12, 22]; however, the lower photoreactivity of psoralen requires long-time UV irradiation that increases photo-cytotoxicity toward living cells. In this section, the practical design, experimental procedures and how to use ^{CNV}K-modified antisense ODNs for gene silencing in the cells are described.

4.1 Design of the Photoreactive Antisense ODNs Having ^{CNV}K

Similar to the general design method of antisense ODNs, the selectivity of the duplex formation with target mRNA and the stability of the hetero-duplex is crucial to obtain the effective sequence. As in the case of ^{CNV}K-modified ODNs, hybrid stability before the photo-cross-linking is lower than that of the unmodified duplex because the 3-cyanovinylcarbazole cannot pair with any canonical bases in the RNA strand, and the position of ^{CNV}K in the antisense ODNs is important to obtain the effective sequence. ^{CNV}K should be possessed at the termini of the antisense sequence to the greatest extent possible. In our cases, highly specific photoresponsive antisense ODNs for K-ras point-mutated mRNA [27], vascular endothelial growth factor mRNA [27], and for enhanced green fluorescent protein mRNA [25] were successfully obtained. These antisense ODNs can photo-cross-link completely with their target mRNA by 1 s of 366 nm irradiation in aqueous buffer solution.

4.2 Evaluation of the Photo-Cross-Linking Reaction with mRNA

In the antisense strategy for gene silencing, the binding between antisense ODNs and target mRNA is crucial for obtaining an effective silencing effect. To evaluate quantitatively the photo-cross-linking efficiency of the ^{CNV}K-modified ODNs and target mRNA, the quantification of the reverse-transcription inhibition is effective. As the reverse-transcription reaction is stopped around the position of the photo-cross-linked hetero-duplex caused by the photoreaction of ^{CNV}K, full-length cDNA derived from the reverse-transcription is decreased with the photo-cross-linking reaction (Fig. 7). Therefore, the photo-cross-linking efficiency of the photo-reactive antisense ODNs can be evaluated quantitatively by the decrease in the amount of full-length cDNA, which can be easily quantified by a real-time PCR method with an appropriate primer set.
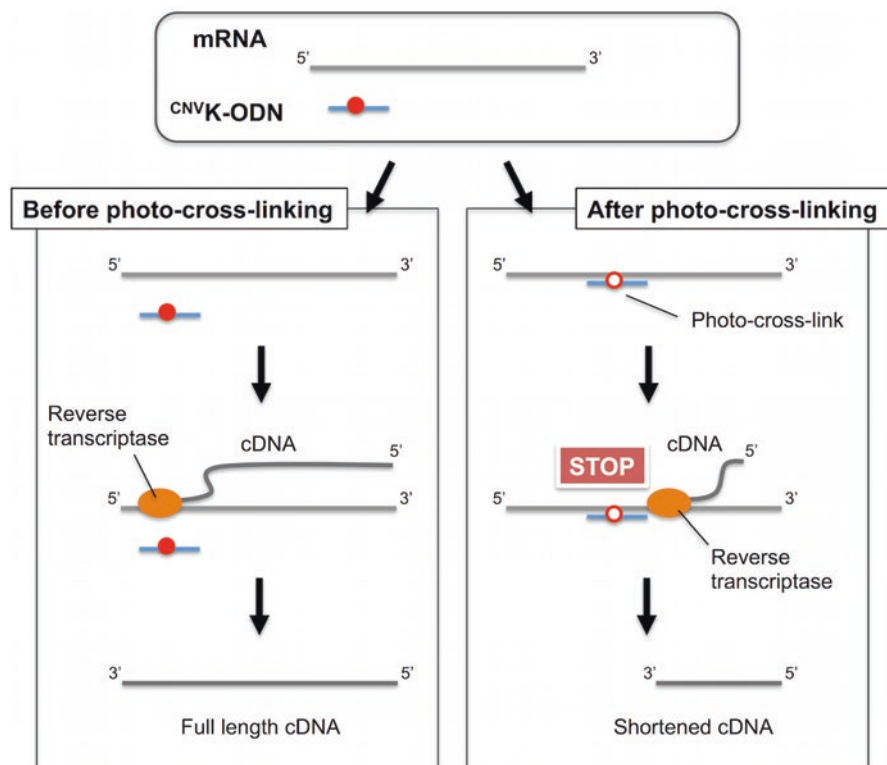
Fig. 7 Schematic drawing of the quantitative evaluation of the photo-cross-linking reaction between the ^{CNV}K-modified antisense ODNs and target mRNAs

4.3 Photo-Induced Gene Silencing in Cells

Relying on the ultra-fast photo-cross-linking manner of the 3-cyanovinylcarbazole-modified photo-cross-linkable antisense ODNs, cellular mRNA might be photo-cross-linked and the gene expression might be down regulated with a few seconds of 366 nm irradiation toward antisense-treated cells. In our study, various photo-cross-linkable antisense ODNs having ^{CNV}K were designed for silencing the GFP gene in constitutively GFP expression cells (GFP–HeLa) [25]. Since a 60% decrease of target mRNA and 40% decrease of GFP protein were observed by 10 s irradiation of 366 nm UV-LED in the case of the most effective antisense ODN (Fig. 8), the applicability of the ^{CNV}K-based photo-cross-linkable ODNs was demonstrated. In particular, multiple-irradiation increases the gene-silencing effect of the antisense ODN, and the effect was comparable to that of siRNA, suggesting that further development of this strategy might provide more sophisticated and effective gene regulation tools that can regulate genes of interest in a spatiotemporal manner.

Fig. 8 Antisense effect of
photo-cross-linkable
antisense ODN having
^{CNV}K toward GFP
expression
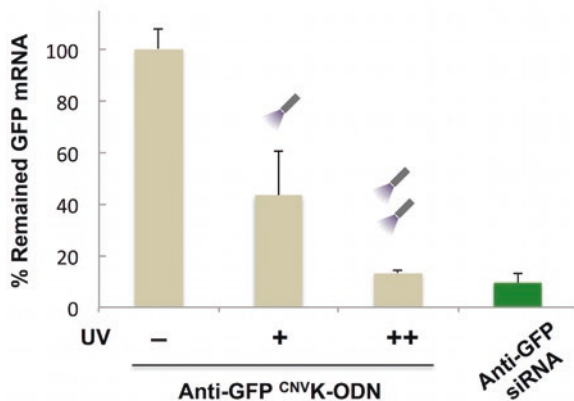
5   Summary

We described a practical method to synthesize and use photo-cross-linkable ODNs having ^{CNV}K and ^{CNV}D, which currently are the most highly reactive photo-cross-linkable ODNs in the world, toward gene silencing in the cells. We hope that further applications based on our photo-cross-linking technique will be developed by chemists, biologists and also medical researchers.

References

1. Bhan P, Miller PS (1990) Photo-cross-linking of psoralen-derivatized oligonucleoside methylphosphonates to single-stranded DNA. Bioconjug Chem 1(1):82–88
2. Cassidy RA, Kondo NS, Miller PS (2000) Triplex formation by psoralen-conjugated chimeric oligonucleoside methylphosphonates. Biochemistry 39(29):8683–8691
3. Chang EH, Miller PS, Cushman C, Devadas K, Pirollo KF, Ts'o PO, Yu ZP (1991) Antisense inhibition of ras p21 expression that is sensitive to a point mutation. Biochemistry 30(34):8283–8286
4. Fujimoto K, Konishi-Hiratsuka K, Sakamoto T, Yoshimura Y (2010) Site-specific cytosine to uracil transition by using reversible DNA photo-crosslinking. Chembiochem 11(12):1661–1664
5. Fujimoto K, Konishi-Hiratsuka K, Sakamoto T, Yoshimura Y (2010) Site-specific photochemical RNA editing. Chem Commun 46(40):7545–7547
6. Fujimoto K, Yamada A, Yoshimura Y, Tsukaguchi T, Sakamoto T (2013) Details of the ultrafast DNA photo-cross-linking reaction of 3-cyanovinylcarbazole nucleoside: cis-trans isomeric effect and the application for SNP-based genotyping. J Am Chem Soc 135(43):16161–16167
7. Giovannangéli C, Thuong NT, Hélène C (1992) Oligodeoxynucleotide-directed photo-induced cross-linking of HIV proviral DNA via triple-helix formation. Nucleic Acids Res 20(16):4275–4281
8. Grigoriev M, Praseuth D, Guieysse AL, Robin P, Thuong NT, Hélène C, Harel-Bellan A (1993) Inhibition of gene expression by triple helix-directed DNA cross-linking at specific sites. Proc Natl Acad Sci U S A 90(8):3501–3505

9. Hall LM, Gerowska M, Brown T (2012) A highly fluorescent DNA toolkit: synthesis and properties of oligonucleotides containing new Cy3, Cy5 and Cy3B monomers. Nucleic Acids Res 40(14):e108

10. Heck RF, Nolley JP (1972) Palladium-catalyzed vinylic hydrogen substitution reactions with aryl, benzyl, and styryl halides. J Org Chem 37(14):2320–2322

11. Higuchi M, Kobori A, Yamayoshi A, Murakami A (2009) Synthesis of antisense oligonucleotides containing 2′-O-psoralenylmethoxyalkyl adenosine for photodynamic regulation of point mutations in RNA. Bioorg Med Chem 17(2):475–483

12. Higuchi M, Yamayoshi A, Kato K, Kobori A, Wake N, Murakami A (2010) Specific regulation of point-mutated K-ras-immortalized cell proliferation by a photodynamic antisense strategy. Oligonucleotides 20(1):37–44

13. Higuchi M, Yamayoshi A, Yamaguchi T, Iwase R, Yamaoka T, Kobori A, Murakami A (2007) Selective photo-cross-linking of 2′-O-psoralen-conjugated oligonucleotide with RNAs having point mutations. Nucleosides Nucleotides Nucleic Acids 26(3):277–290

14. Lee BL, Blake KR, Miller PS (1988) Interaction of psoralen-derivatized oligodeoxyribonucleoside methylphosphonates with synthetic DNA containing a promoter for T7 RNA polymerase. Nucleic Acids Res 16(22):10681–11097

15. Lee BL, Murakami A, Blake KR, Lin SB, Miller PS (1988) Interaction of psoralen-derivatized oligodeoxyribonucleoside methylphosphonates with single-stranded DNA. Biochemistry 27(9):3197–3203

16. Lin M, Hultquist KL, Oh DH, Bauer EA, Hoeffler WK (1995) Inhibition of collagenase type I expression by psoralen antisense oligonucleotides in dermal fibroblasts. FASEB J 9(13):1371–1377

17. Matsuyama Y, Yamayoshi A, Kobori A, Murakami A (2014) Functional regulation of RNA-induced silencing complex by photoreactive oligonucleotides. Bioorg Med Chem 22(3):1003–1007

18. Miller PS, Bi G, Kipp SA, Fok V, DeLong RK (1996) Triplex formation by a psoralen-conjugated oligodeoxyribonucleotide containing the base analog 8-oxo-adenine. Nucleic Acids Res 24(4):730–736

19. Miller PS, Kipp SA, McGill C (1999) A psoralen-conjugated triplex-forming oligodeoxyribonucleotide containing alternating methylphosphonate-phosphodiester linkages: synthesis and interactions with DNA. Bioconjug Chem 10(4):572–577

20. Mizoroki T, Mori K, Ozaki A (1971) Arylation of olefin with aryl iodide catalyzed by palladium. Bull Chem Soc J 44(2):581

21. Mochizuki Y, Suzuki T, Fujimoto K, Nemoto N (2015) A versatile puromycin-linker using [CNV]K for high-throughput in vitro selection by cDNA display. J Biotechnol 212(20):174–180

22. Murakami A, Yamayoshi A, Iwase R, Nishida J, Yamaoka T, Wake N (2001) Photodynamic antisense regulation of human cervical carcinoma cell growth using psoralen-conjugated oligo(nucleoside phosphorothioate). Eur J Pharm Sci 13(1):25–34

23. Nakamura S, Fujimoto K (2014) Creation of DNA array structure equipped with heat resistance by ultrafast photocrosslinking. J Chem Tech Biotech 89(7):1086–1090

24. Pieles U, Englisch U (1989) Psoralen covalently linked to oligodeoxyribonucleotides: synthesis, sequence specific recognition of DNA and photo-cross-linking to pyrimidine residues of DNA. Nucleic Acids Res 17(1):285–299

25. Sakamoto T, Shigeno A, Ohtaki Y, Fujimoto K (2014) Photo-regulation of constitutive gene expression in living cells by using ultrafast photo-cross-linking oligonucleotides. Biomater Sci 2:1154–1157

26. Sakamoto T, Tanaka Y, Fujimoto K (2015) DNA photo-cross-linking using 3-cyanovinylcarbazole modified oligonucleotide with threoninol linker. Org Lett 17(4):936–939

27. Shigeno A, Sakamoto T, Yoshimura Y, Fujimoto K (2012) Quick regulation of mRNA functions by a few seconds of photoirradiation. Org Biomol Chem 10(38):7820–7825

28. Tagawa M, Shohda K, Fujimoto K, Suyama A (2011) Stabilization of DNA nanostructures by photo-cross-linking. Soft Matter 7:10931–10934

29. Takasugi M, Guendouz A, Chassignol M, Decout JL, Lhomme J, Thuong NT, Hélène C (1991) Sequence-specific photo-induced cross-linking of the two strands of double-helical DNA by a psoralen covalently linked to a triple helix-forming oligonucleotide. Proc Natl Acad Sci U S A 88(13):5602–5606
30. Yoshimura Y, Fujimoto K (2008) Ultrafast reversible photo-cross-linking reaction: toward in situ DNA manipulation. Org Lett 10(15):3227–3230
31. Wang G, Glazer PM (1995) Altered repair of targeted psoralen photoadducts in the context of an oligonucleotide-mediated triple helix. J Biol Chem 270(38):22595–22601

Effects of 2′-*O*-Modifications on RNA Duplex Stability

Yoshiaki Masaki, Akihiro Ohkubo, Kohji Seio, and Mitsuo Sekine

Abstract Modifications of RNA have been widely studied. Despite the long history of studies on 2′-hydroxyl modifications, they are still attracting attention because of their facile synthetic accessibility and large influence on the biological and physical properties of RNA duplexes. This chapter focuses on the effects of chemical modifications on RNA duplex stability. The effects of the 2′-hydroxyl modifications on preorganization of the RNA backbone and hydration around the 2′-site are briefly described. Our recent studies on the development of methods for estimating the hybridization ability of synthetic 2′-*O*-modified RNAs using molecular dynamic simulations will be reviewed.

Keywords Chemically modified RNA · 2′-*O*-modification · Deformability · Molecular dynamic simulations

1   Introduction

Chemical modifications on the 2′-hydroxyl group of RNA duplexes can modulate their structural, functional, and biological properties. For example, chemical and biological stabilities can be greatly improved by certain chemical modifications on the 2′-hydroxyl group. In addition, attachment of functional groups, such as reactive moieties and fluorescent dyes to the 2′-oxygen, gives additional functions [47, 48]. Chemical modifications can also be used to avoid off-target effects and immune responses [12, 36, 37]. Among these properties conferred by chemical modifications, enhancement of RNA duplex stability is one of the most important, especially for biological applications. It is known that oligonucleotide-mRNA duplex stability is a key factor for antisense activity [23, 43]. In small interfering RNAs, the duplex

Y. Masaki (✉) · A. Ohkubo · K. Seio
Department of Life Science and Technology, Tokyo Institute of Technology,
Midoriku, Yokohama, Japan
e-mail: ymasaki@bio.titech.ac.jp

M. Sekine
Tokyo Institute of Technology, Yokohama, Kanagawa, Japan

stability of their seed regions plays an important role in their off-target effects [42]. Thus, it is always necessary to pay an attention to the effect of chemical modifications on RNA duplex stability.

One of the most common methods to predict RNA duplex stability is based on the use of the nearest-neighbor parameters [15, 16, 38, 45]. The nearest-neighbor parameters are a set of experimentally determined enthalpy and entropy parameters for thermodynamic stabilities of base-pair steps. RNA duplex stability can be estimated well by analyzing the nearest-neighbor parameters over all the base-pair steps. Although the nearest-neighbor parameters of several typical chemical modifications [15, 16] have already been established, determination of new nearest-neighbor parameters for other chemical modifications and their combinations would be time consuming and impractical. In addition, this method cannot be used for designing novel modifications. Thus, a facile computational method for estimating RNA duplex stability is eagerly anticipated for the design of new RNA modifications.

In this chapter, the effect of chemical modifications will be briefly outlined. Furthermore, our studies on computational evaluations of the effects of chemical modifications on RNA duplex stability will be described.

2 Effects of Modifications on RNA Duplex Stability

2.1 Preorganization of RNA

The stabilizing effect of 2′-*O*-modifications is often explained by its ability to pre-organize RNA prior to complex formation. An excellent review on the concept of preorganization has been published by Kool [17]. Briefly, preorganization can be described as the result of the reduction of entropy loss upon complex formation. If the conformation of single RNA strands in the unbound state is more flexible than that in the complex state, duplex formation results in entropy loss. This entropy loss can be suppressed if the monomer conformation is rigidified to an appropriate structure prior to complex formation.

Preorganization could be used to explain the stabilizing effect of 2′-*O*-methyl modifications especially on pyrimidine residues [14]. The ribose moiety is intrinsically flexible, but introduction of a 2′-*O*-methyl substituent into uridine causes repulsion with the 2-carbonyl group of the uracil base. To minimize this steric repulsion, 2′-*O*-methyluridine derivatives preferentially exist in the C3′-*endo* conformation. This conformation is the canonical sugar puckering in A-type RNA duplexes. Thus, the entropy loss upon duplex formation would be reduced. The electronegativity of 2′-*O*-modified groups also plays an important role in the regulation of sugar puckering [11]. The preference for the C3′-*endo* conformation is well correlated with the electronegativity of 2′-*O*-substituents and could be explained by the gauche effect between O4′ and the 2′-*O*-substituent. Thus, one can assume that substituents having stronger electronegativities than the hydroxyl group would be able to preorganize nucleotides to its preferred conformation.

A prominent example of a modification that fixes the sugar pucker in a C3′-*endo* conformation is the so-called bridged nucleic acid (BNA) or locked nucleic acid

(LNA). BNA/LNA was independently developed by Imanishi [24] and Wengel [18]. This modification has a methylene bridge between 4′-*C* and 2′-*O* of the ribose ring, which physically induces the *C3′-endo* conformation.

2.2 Hydration Effect

RNA duplexes have wide and shallow minor grooves, but ordered hydration patterns can be observed owing to the presence of the 2′-hydroxyl group. These hydrated water molecules could form an additional interstrand-pairing network involving the 2′-hydroxyl groups and nucleobases. It is known that the increased stability of RNA duplexes relative to DNA duplexes is enthalpy-driven [8]. In fact, the comparison of the nearest-neighbor parameters of RNA [9] and DNA [39] implied that RNA duplexes are more enthalpically stable than DNA duplexes. Interestingly, osmotic stress experiments, which could estimate the number of water molecules released upon melting of duplexes, also suggested that RNA duplexes released more water molecules than DNA duplexes [30, 32]. Therefore, it is likely that hydrated water molecules in the minor groove enthalpically stabilize RNA duplexes, although the water molecules captured by RNA duplexes are more entropically unfavorable than those captured by DNA duplexes.

Since 2′-*O*-modified groups would extrude to the shallow minor groove of RNA duplexes, hydrophobic modifications would disturb the hydration pattern and destabilize RNA duplexes. However, this is not always the case. Osmotic stress experiments revealed that 2′-*O*-methyl RNA duplexes released less water molecules than unmodified RNA duplexes [32]. This observation agrees well with the results of molecular dynamic (MD) simulations, which, more importantly, suggested that hydrated water molecules in 2′-*O*-methyl RNA duplexes have longer residence time than those in unmodified RNA duplexes possibly because of the formation of a clathrate-like water structure [1, 7].

Replacement of the 2′-hydroxyl group of RNA with a 2-methoxyethyl (MOE) group results in interesting changes in hydration [6, 40]. Since the MOE group has an additional hydrogen acceptor atom (OC′), it can make a stable hydration structure with a surrounding water molecule using the three oxygen atoms, O2′, O3′, and OC′ (Fig. 1). Moreover, one or two additional water molecules can build a hydrogen-bonding network with the captured water molecule and the nearby phosphate back-

Fig. 1 Plausible hydration structures involving the 2′-*O*-MOE group
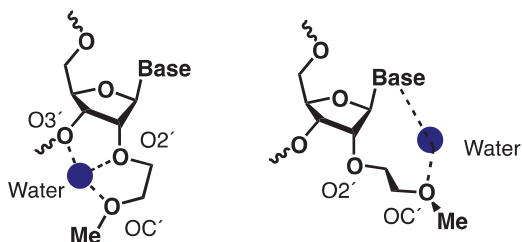
bone. In addition, hydrated water molecules can also make another hydration network between OC′ and the nucleobase (Fig. 1). The formation of these hydration structures may explain why MOE substituted RNA duplexes are more enthalpically stable than unmodified RNA duplexes [40].

2.3   Electrostatic Effect

Electrostatic repulsion between anionic phosphate backbones is one of the most important determinants of duplex stability and largely depends on the ionic strength of a buffer solution [27]. Thus, one should not ignore the salt concentration in the buffer solution. Cationic modification is a reasonable way to reduce electrostatic repulsion upon duplex formation. One such method uses 2′-*O*-guanidiniumethyl (GE) as a cationic substituent [29]. When GEs were dispersedly introduced into duplexes, their melting temperatures increased approximately 3.2 °C per modification. However, the consecutive arrangement of GEs in the RNA sequence induced the destabilization of duplexes rather than stabilization, which may be explained by cationic repulsion among the GE moieties. To avoid such cationic repulsion, longer linkers between the cationic moiety and the nucleoside monomer unit were developed. For example, 2′-*O*-[2-[2-(*N*,*N*-dimethylamino)ethoxy]ethyl] (DMAEOE) could stabilize duplexes even if DMAEOEs were arranged in a consecutive manner in duplexes [31]. 2′-*O*-Aminopropyl (AP) is one of the most well-known cationic modifiers and remarkably improves nuclease resistance. Interestingly, it was reported, based on extensive kinetic studies, that AP modified oligonucleotides significantly improved the k_{on} rate of duplex formation [33].

On the other hand, anionic modifications could destabilize RNA duplexes. In fact, 2′-*O*-phosphorylated oligonucleotides, which are intermediate structures of the pre-tRNA splicing process, significantly destabilized duplexes [41]. Surprisingly, anionic modifications do not always destabilize RNA duplex structures. For example, 2′-*O*-carboxylethyl RNAs could stabilize duplexes to an extent similar to 2′-*O*-methyl RNAs [46]. This anionic modification would induce electrostatic repulsion with the anionic phosphate backbone, but such an effect may be compensated for by the stabilization resulting from hydration networks in the minor groove.

2.4   Effect of Substituent Size

Lesnik et al. evaluated the effect of the size of 2′-*O*-alkyl modifications on the stability of partially modified duplexes [20]. They systematically changed the alkyl chain length from C1 to C8. As a result, the smaller modifications showed better improvements on duplex stability than the longer modifications. They also found that 2′-*O*-propyl modification is the alkyl chain length 'break-even' point that does not alter duplex stability. They discussed that larger modifications may cause local distortions in the helical structure, which resulted in reduced stacking interactions

and/or destabilized hydration structures in the minor groove. We previously evaluated the effect of the size of 2′-O-aryl modifications on duplex stability [25, 35]. Incorporation of a single 2′-O-phenyl, 2′-O-(1-naphtyl), or 2′-O-(2-naphtyl) substituent into RNA strands destabilized duplex stability. On the contrary, incorporation of five consecutive 2′-O-(2-naphtyl) nucleoside units into RNA strands resulted in the stabilization of duplex formation with their complementary 2′-O-methyl RNAs. The CD experiments and MD simulations suggested that the stacking interactions among the 2-naphtyl moieties play a role in this stabilization.

3   Computational Approach to Design Novel Modifications

As discussed in the previous section, the multiple effects induced by 2′-O-modifications controlled the stability of RNA duplexes. We envisioned that the development of computational approaches that can be used to estimate the effect of 2′-O-modifications would facilitate the design of novel 2′-O-modifications. To develop such a computational approach, we compared a series of structural parameters derived from MD simulations of duplexes with experimentally determined melting temperatures.

First, we synthesized various kinds of fully 2′-O-modified U_{14} and A_{14} oligomers and determined the melting temperatures of their duplexes with the complementary RNA 14mers under the same conditions (Fig. 2). 2′-O-Methyl modifications on the uridine strand of $(U_{OH})_{14}/(A_{OH})_{14}$ increased the duplex melting temperature from 24 to 36 °C. In contrast, 2′-O-methyl modifications on the adenosine strand of $(U_{OH})_{14}/$ $(A_{OH})_{14}$ did not change its melting temperature (24 °C), which agrees well with previous results [4]. Similarly, 2′-O-cyanoethyl modifications on the uridine strand of $(U_{OH})_{14}/(A_{OH})_{14}$ increased the melting temperature to 43 °C, whereas those on the adenosine strand showed only a marginal effect (27 °C, 0.2 °C/modification).
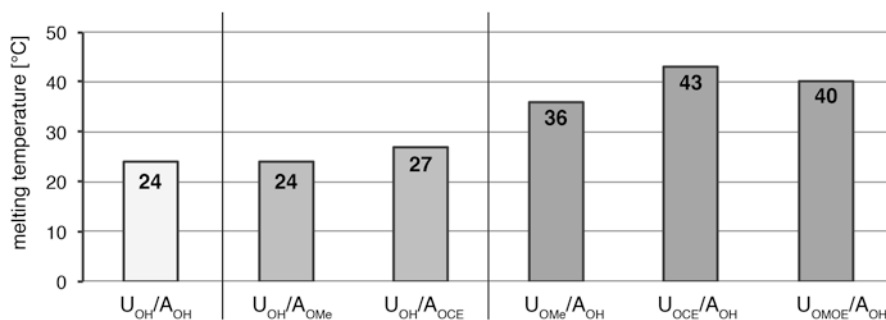

Fig. 2 Melting temperatures of chemically modified and unmodified RNA duplexes. The sequence of the unmodified RNA duplex is $(U)_{14}/(A)_{14}$. The conditions are 10 mM sodium phosphate buffer (pH 7.0), 0.1 M NaCl, 0.1 mM EDTA, and 2 μM duplex. OMe, OCE, and OMOE stand for 2′-O-methyl, 2′-O-cyanoethyl, and 2′-O-methoxyethyl modifications, respectively

2′-*O*-Methoxyethyl modifications on the uridine strand of $(U_{OH})_{14}/(A_{OH})_{14}$ increased the melting temperature to 40 °C.

The hydrogen bonding energies of base pairs obtained by *ab initio* calculations have conventionally been utilized for designing novel chemical modifications. However, *ab initio* calculations would be difficult to apply to 2′-*O*-modifications because most of them do not form direct interactions with residues on the complementary strands. Instead, we assumed that MD simulations could be used to account for indirect interactions such as those mediated by water molecules.

We thus performed a series of MD simulations of RNA duplexes containing 2′-*O*-modified groups. We used the AMBER software package [2, 3, 5, 13, 28, 44] for the MD simulations. Initially, we thought that sugar puckering would be a useful indicator for estimating the effect of modifications of duplex stability, because the stabilizing effect of 2′-*O*-modification is often explained by the rigidification of sugar puckering, as described in the previous section. The rigidity of sugar puckering can be visualized by plotting the fluctuations in the pseudorotation angles during MD simulations. The histograms of the pseudorotation angles of $(U_{OR})_{14}/(A_{OH})_{14}$ and $(U_{OH})_{14}/(A_{OR})_{14}$, where R is H, Me, CE, or MOE, are shown in Fig. 3.

To compare these histograms, we performed stiffness analysis, which is a method used to estimate an apparent force constant from each distribution of fluctuation [10, 19, 26]. In the simple case, the force constant can be derived from the identical form of the normal distribution function (Eq. 1) and Einstein's formula of a harmonic oscillator (Eq. 2).
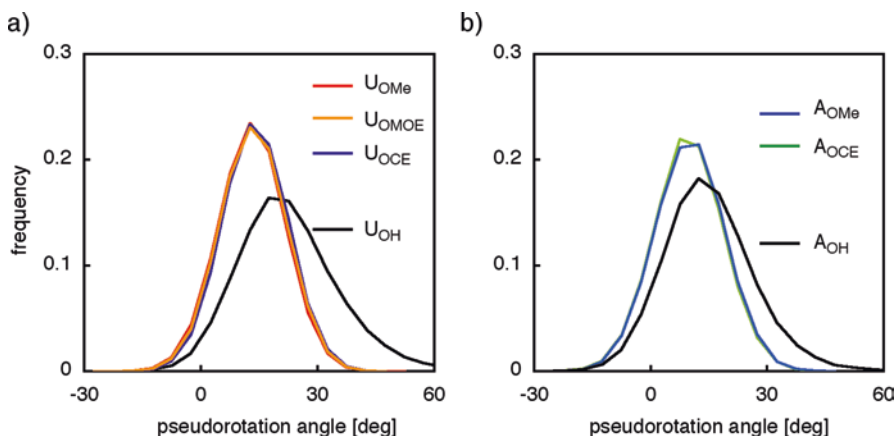
Fig. 3 Histograms of the thermodynamic behavior of the central base pair sets of $(U_{OR})_{14}/(A_{OH})_{14}$ and $(U_{OH})_{14}/(A_{OR})_{14}$, where R is H, Me, CE, or MOE. (**a**) Histograms of the pseudorotation angles of U_{OR} in the two central U_{OR}-A_{OH} base pairs of $(U_{OR})_{14}/(A_{OH})_{14}$. (**b**) Histograms of the pseudorotation angles of A_{OR} in the two central U_{OH}-A_{OR} base pairs of $(U_{OH})_{14}/(A_{OR})_{14}$

$$P(x) = Nexp\left(-\frac{(x-\mu)^2}{2\sigma^2}\right) \qquad (1)$$

$$P(x) = Nexp\left(-\frac{f(x-\mu)^2}{2} \cdot \frac{1}{k_BT}\right) \qquad (2)$$

where x is any structural parameter, μ is the mean value of x, σ is the standard deviation, f is the force constant, N is the normalization constant, k_B is Boltzmann's constant, and T is the absolute temperature. In the case of sugar puckering, force constants f can be calculated from the standard deviations of sugar puckering (Eq. 3). These calculated force constants represent the deformability of sugar puckering.

$$f = \frac{k_BT}{\sigma^2} \qquad (3)$$

In the case of the uridine residues, the calculated force constants for the sugar puckering of U_{OH}, U_{OMe}, U_{OMOE}, and U_{OCE} were 3.5, 8.5, 8.6, and 8.5 cal·mol^{-1}·deg^{-2}, respectively. Larger force constants mean less fluctuated structures. Thus, the 2′-O-methyluridine residues in U_{OMe}/A_{OH} fluctuated less than the unmodified uridine residues in U_{OH}/A_{OH}. The force constants for 2′-O-cyanoethyluridine in U_{OCE}/A_{OH} and 2′-O-methoxyethyluridine in U_{OMOE}/A_{OH} were almost identical to that of 2′-O-methyluridine in U_{OMe}/A_{OH}. In the case of the adenosine residues, the force constants for the sugar puckering of A_{OH}, A_{OMe}, and A_{OCE} were 4.4, 7.7, and 7.6 cal·mol^{-1}·deg^{-2}, respectively. Similarly, the force constant for 2′-O-cyanoethyladenosine in U_{OCE}/A_{OH} was almost identical value to that of 2′-O-methyluridine in U_{OMe}/A_{OH}. These results are in agreement with those from NMR sugar puckering analysis, which revealed that the sugar puckering modes of 2′-O-methyluridine and 2′-O-cyanoethyluridine are almost identical [34]. However, the UV melting analysis indicated that 2′-O-cyanoethyl modifications on the uridine strand (U_{OCE}/A_{OH}, melting temperature = 43 °C) could stabilize duplex structures more than 2′-O-methyl modifications (U_{OMe}/A_{OH}, melting temperature = 36 °C). These results indicated that sugar puckering is not a good indicator for estimating the effect of modifications on duplex stability.

In our search for more accurate indicators, we next looked into the deformation of base pair steps, which we speculated would more directly reflect the thermal melting of duplexes. The deformation of base-pair steps can be represented by local helical parameters, such as shift, slide, rise, tilt, roll, and twist. These parameters have been used for evaluating the bending of DNA in protein-DNA complexes and the heterogeneity of DNA structures. Helical deformability of base-pair steps could be estimated by calculating the stiffness matrix $\boldsymbol{F}$, which represents the force constants for the helical parameters (translational movements, such as rise, shift, and

slide, and rotational parameters such as twist, roll, and tilt) under harmonic function and normal distribution approximation [19, 26]. The F can be calculated by inversion of the covariance matrix C of helical parameters, as shown in Eq. 4.

$$F = k_B T C^{-1} \qquad (4)$$

The diagonal elements represent the force constants for the helical parameters and non-diagonal elements represent the coupling terms. The helical parameters can be calculated using the X3DNA software package [21, 22].

The relationship between the calculated force constants and experimentally determined melting temperatures is shown in Fig. 4. Interestingly, every force constant showed a positive correlation with the corresponding melting temperature. For example, f_{rise}, which is the force constant for the rise parameter, had a correlation coefficient of 0.97 with the corresponding melting temperature. Similarly, f_{shift}, f_{slide}, f_{twist}, f_{roll}, and f_{tilt} had correlation coefficients of 0.94, 0.74, 0.89, 0.89, and 0.86, respectively, with the corresponding melting temperature. These results suggested that rigid structures could be expected to have higher melting temperatures.

To derive a better index for estimating the effect of chemical modifications on duplex stability, we calculated the force constants for translational movement, F_{trans}, which is the product of f_{rise}, f_{shift}, and f_{slide}, rotational movement, F_{rot}, which is the product of f_{twist}, f_{roll}, and f_{tilt}, and their product deformability F_{prod}, which is the product of F_{trans} and F_{rot}, and compared them with the melting temperatures. Interestingly, every calculated value showed strong correlation with the corresponding melting
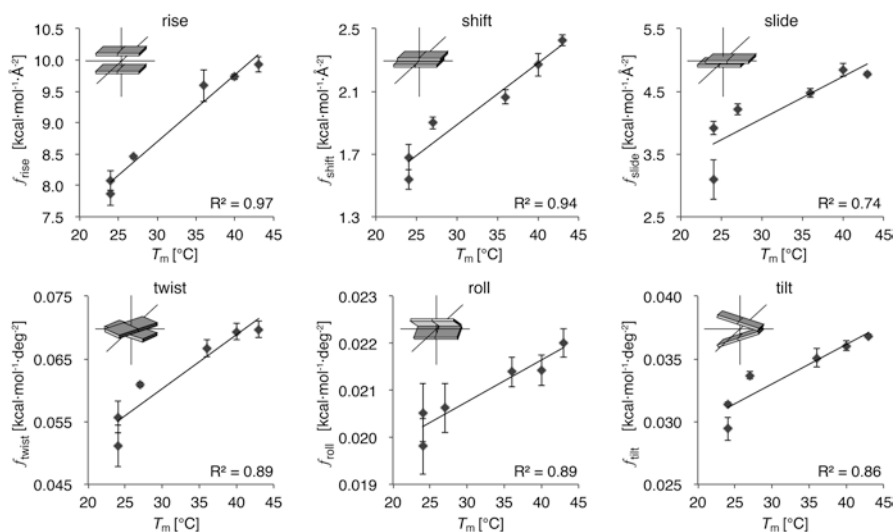
Fig. 4 Relationship between the calculated force constants for the helical parameters and the experimentally determined melting temperatures. The force constant for the rise parameter is denoted by f_{rise}. Similarly, the force constants for the shift, slide, twist, roll, and tilt parameters are denoted by f_{shift}, f_{slide}, f_{twist}, f_{roll}, and f_{tilt}, respectively
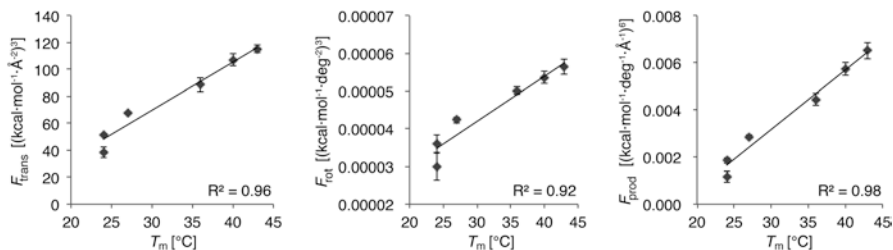
Fig. 5 Relationship between the calculated deformabilities, F_{trans}, F_{rot}, and F_{prod}, and melting temperatures

temperature (Fig. 5). The correlation coefficients of F_{trans}, F_{rot}, and F_{prod} with the corresponding melting temperatures were 0.96, 0.92, and 0.98, respectively. Because of the smaller deviation and higher correlation coefficient of F_{prod} compared with those of F_{trans} and F_{rot}, we concluded that F_{prod} is the appropriate index for estimating the effect of modifications on RNA duplex stability.

$$F_{trans} = f_{rise} \cdot f_{shift} \cdot f_{slide} \tag{5}$$

$$F_{rot} = f_{twist} \cdot f_{roll} \cdot f_{tilt} \tag{6}$$

$$F_{prod} = F_{trans} \cdot F_{rot} \tag{7}$$

4   Discussion

Modulation of RNA duplex stability is an important consideration for the clinical application of chemically modified RNAs. The effect of chemical modifications of the 2′-hydroxyl group on RNA stability is often explained by the ability of such modifications to preorganize RNA to its preferred conformation prior to complex formation. In addition, other effects of chemical modifications, such as those on hydration, play also an important role. Because of their multiple effects, it is difficult to judge whether the chemical modifications would have a positive effect on RNA stability before their actual synthesis.

We have developed a computational tool to estimate the effect of chemical modifications on RNA duplex stability. In this chapter, we described that the deformability is a good indicator for estimating RNA duplex stability. Although deformability is well correlated with melting temperatures, the contribution of physicochemical properties, such as sugar puckering and hydration, to deformability has not been clear. However, some plausible relationships between the physicochemical properties and deformability could be hypothesized. In the case of the 2′-*O*-methyl modification on the uridine residue, the steric repulsion between the 2-carbonyl group of uridine and the 2′-*O*-methyl group rigidified the sugar puckering. In contrast, this

type of steric repulsion was lacking in 2′-*O*-methyladenosine. These differences in the rigidity of sugar puckering might reflect the larger F_{prod} value of duplexes containing 2′-*O*-methyladenosine compared with those containing 2′-*O*-methyluridine. In addition, it was reported that the 2′-*O*-methyl group could suppress the exchange rate of hydrated water molecules [1]. These stabilized water molecules could remain unmoved for a long time, which may reduce the fluctuation of the base pair-steps.

The reason why the calculated force constants and melting temperatures showed a linear relationship is unclear. However, if we assumed that helix-coil transition starts at the temperature where the fluctuations reach a certain value regardless of the chemical modifications, standard deviations σ^2 will be expected to remain constant at a certain temperature (Eq. 3). In such a case, the force constants and the temperatures will have a linear relationship. Thus, our results suggest that the helix-coil transition starts at the temperature where the fluctuations reach a certain value and that that value is irrespective of the presence of chemical modifications.

This method cannot be used for modifications that induce multiple local minima structures. Since this method approximates distributions of fluctuations as a single normal distribution, multiple local minima structures would lead to exaggeratedly small force constants. Thus, it is necessary to check the distribution of the local helical parameters before applying deformability analysis.

Although there are some limitations, it is clear that the deformability of base-pair step enables us to estimate the relative duplex stability of chemically modified RNAs. This method will be useful for designing novel chemical modifications.

5 Conclusion

Chemical modification is a powerful tool to modulate the functional, structural, and biological properties of RNAs. In this chapter, we focused on its effect on RNA duplex stability. The preorganization of RNA, hydration and electrostatic effects, and the effect of substituent size on RNA duplex stability were briefly outlined. Then, our efforts to estimate the effect of chemical modifications on RNA duplex stability were described. We believe that the development of computational methods to estimate duplex stability would be of great importance in the development of novel chemically modified RNAs.

References

1. Auffinger P, Westhof E (2001) Hydrophobic groups stabilize the hydration shell of 2′-*O*-methylated RNA duplexes. Angew Chem Int Ed 40(24):4648–4650
2. Bayly CI, Cieplak P, Cornell W, Kollman PA (1993) A well-behaved electrostatic potential based method using charge restraints for deriving atomic charges: the RESP model. J Phys Chem 97(40):10269–10280

3. Berendsen HJC, Postma JPM, van Gunsteren WF, Dinola A, Haak JR (1984) Molecular-dynamics with coupling to an external bath. J Chem Phys 81(8):3684–3690

4. Bobst AM, Rottman F, Cerutti PA (1969) Effect of the methylation of the 2′-hydroxyl groups in polyadenylic acid on its structure in weakly acidic and neutral solutions and on its capability to form ordered complexes with polyuridylic acid. J Mol Biol 46(2):221–234

5. Cornell WD, Cieplak P, Bayly CI, Gould IR, Merz KM, Ferguson DM, Spellmeyer DC, Fox T, Caldwell JW, Kollman PA (1995) A second generation force field for the simulation of proteins, nucleic acids, and organic molecules. J Am Chem Soc 117(19):5179–5197

6. Egli M, Minasov G, Tereshko V, Pallan PS, Teplova M, Inamati GB, Lesnik EA, Owens SR, Ross BS, Prakash TP, Manoharan M (2005) Probing the influence of stereoelectronic effects on the biophysical properties of oligonucleotides: comprehensive analysis of the RNA affinity, nuclease resistance, and crystal structure of ten 2′-*O*-ribonucleic acid modifications. Biochemistry 44(25):9045–9057

7. Egli M, Pallan PS (2010) Crystallographic studies of chemically modified nucleic acids: a backward glance. Chem Biodivers 7(1):60–89

8. Egli M, Portmann S, Usman N (1996) RNA hydration: a detailed look. Biochemistry 35(26):8489–8494

9. Freier SM, Kierzek R, Jaeger JA, Sugimoto N, Caruthers MH, Neilson T, Turner DH (1986) Improved free-energy parameters for predictions of RNA duplex stability. Proc Natl Acad Sci U S A 83(24):9373–9377

10. Go M, Go N (1976) Fluctuations of an α-helix. Biopolymers 15(6):1119–1127

11. Guschlbauer W, Jankowski K (1980) Nucleoside conformation is determined by the electronegativity of the sugar substituent. Nucleic Acids Res 8(6):1421–1433

12. Jackson AL, Burchard J, Leake D, Reynolds A, Schelter J, Guo J, Johnson JM, Lim L, Karpilow J, Nichols K, Marshall W, Khvorova A, Linsley PS (2006) Position-specific chemical modification of siRNAs reduces "off-target" transcript silencing. RNA 12(7):1197–1205

13. Joung IS, Cheatham TE 3rd (2008) Determination of alkali and halide monovalent ion parameters for use in explicitly solvated biomolecular simulations. J Phys Chem B 112(30):9020–9041

14. Kawai G, Yamamoto Y, Kamimura T, Masegi T, Sekine M, Hata T, Iimori T, Watanabe T, Miyazawa T, Yokoyama S (1992) Conformational rigidity of specific pyrimidine residues in tRNA arises from posttranscriptional modifications that enhance steric interaction between the base and the 2′-hydroxyl group. Biochemistry 31(4):1040–1046

15. Kierzek E, Mathews DH, Ciesielska A, Turner DH, Kierzek R (2006) Nearest neighbor parameters for Watson–Crick complementary heteroduplexes formed between 2′-*O*-methyl RNA and RNA oligonucleotides. Nucleic Acids Res 34(13):3609–3614

16. Kierzek E, Pasternak A, Pasternak K, Gdaniec Z, Yildirim I, Turner DH, Kierzek R (2009) Contributions of stacking, preorganization, and hydrogen bonding to the thermodynamic stability of duplexes between RNA and 2′-*O*-methyl RNA with locked nucleic acids. Biochemistry 48(20):4377–4387

17. Kool ET (1997) Preorganization of DNA: design principles for improving nucleic acid recognition by synthetic oligonucleotides. Chem Rev 97(5):1473–1488

18. Koshkin AA, Singh SK, Nielsen P, Rajwanshi VK, Kumar R, Meldgaard M, Olsen CE, Wengel J (1998) LNA (locked nucleic acids): synthesis of the adenine, cytosine, guanine, 5-methylcytosine, thymine and uracil bicyclonucleoside monomers, oligomerisation, and unprecedented nucleic acid recognition. Tetrahedron 54(14):3607–3630

19. Lankas F, Sponer J, Langowski J, Cheatham TE 3rd (2003) DNA basepair step deformability inferred from molecular dynamics simulations. Biophys J 85(5):2872–2883

20. Lesnik EA, Guinosso CJ, Kawasaki AM, Sasmor H, Zounes M, Cummins LL, Ecker DJ, Cook PD, Freier SM (1993) Oligodeoxynucleotides containing 2′-*O*-modified adenosine: synthesis and effects on stability of DNA:RNA duplexes. Biochemistry 32(30):7832–7838

21. Lu XJ, Olson WK (2003) 3DNA: a software package for the analysis, rebuilding and visualization of three-dimensional nucleic acid structures. Nucleic Acids Res 31(17):5108–5121

22. Lu XJ, Olson WK (2008) 3DNA: a versatile, integrated software system for the analysis, rebuilding and visualization of three-dimensional nucleic-acid structures. Nat Protoc 3(7):1213–1227
23. Matveeva OV, Mathews DH, Tsodikov AD, Shabalina SA, Gesteland RF, Atkins JF, Freier SM (2003) Thermodynamic criteria for high hit rate antisense oligonucleotide design. Nucleic Acids Res 31(17):4989–4994
24. Obika S, Nanbu D, Hari Y, Morio K-I, In Y, Ishida T, Imanishi T (1997) Synthesis of 2′-O,4′-C-methyleneuridine and -cytidine. Novel bicyclic nucleosides having a fixed C3′-endo sugar puckering. Tetrahedron Lett 38(50):8735–8738
25. Oeda Y, Iijima Y, Taguchi H, Ohkubo A, Seio K, Sekine M (2009) Microwave-assisted synthesis of 2′-O-aryluridine derivatives. Org Lett 11(24):5582–5585
26. Olson WK, Gorin AA, Lu XJ, Hock LM, Zhurkin VB (1998) DNA sequence-dependent deformability deduced from protein–DNA crystal complexes. Proc Natl Acad Sci U S A 95(19):11163–11168
27. Owczarzy R, You Y, Moreira BG, Manthey JA, Huang L, Behlke MA, Walder JA (2004) Effects of sodium ions on DNA duplex oligomers: improved predictions of melting temperatures. Biochemistry 43(12):3537–3554
28. Perez A, Marchan I, Svozil D, Sponer J, Cheatham TE 3rd, Laughton CA, Orozco M (2007) Refinement of the AMBER force field for nucleic acids: improving the description of α/γ conformers. Biophys J 92(11):3817–3829
29. Prakash TP, Puschl A, Lesnik E, Mohan V, Tereshko V, Egli M, Manoharan M (2004) 2′-O-[2-(guanidinium)ethyl]-modified oligonucleotides: stabilizing effect on duplex and triplex structures. Org Lett 6(12):1971–1974
30. Pramanik S, Nagatoishi S, Saxena S, Bhattacharyya J, Sugimoto N (2011) Conformational flexibility influences degree of hydration of nucleic acid hybrids. J Phys Chem B 115(47):13862–13872
31. Prhavc M, Prakash TP, Minasov G, Cook PD, Egli M, Manoharan M (2003) 2′-O-[2-[2-(N,N-dimethylamino)ethoxy]ethyl] modified oligonucleotides: symbiosis of charge interaction factors and stereoelectronic effects. Org Lett 5(12):2017–2020
32. Rozners E, Moulder J (2004) Hydration of short DNA, RNA and 2′-OMe oligonucleotides determined by osmotic stressing. Nucleic Acids Res 32(1):248–254
33. Sabahi A, Guidry J, Inamati GB, Manoharan M, Wittung-Stafshede P (2001) Hybridization of 2′-ribose modified mixed-sequence oligonucleotides: thermodynamic and kinetic studies. Nucleic Acids Res 29(10):2163–2170
34. Saneyoshi H, Seio K, Sekine M (2005) A general method for the synthesis of 2′-O-cyanoethylated oligoribonucleotides having promising hybridization affinity for DNA and RNA and enhanced nuclease resistance. J Org Chem 70(25):10453–10460
35. Sekine M, Oeda Y, Iijima Y, Taguchi H, Ohkubo A, Seio K (2011) Synthesis and hybridization properties of 2′-O-methylated oligoribonucleotides incorporating 2′-O-naphthyluridines. Org Biomol Chem 9(1):210–218
36. Shukla S, Sumaria CS, Pradeepkumar PI (2010) Exploring chemical modifications for siRNA therapeutics: a structural and functional outlook. ChemMedChem 5(3):328–349
37. Sioud M (2006) Innate sensing of self and non-self RNAs by toll-like receptors. Trends Mol Med 12(4):167–176
38. Sugimoto N, Nakano S, Katoh M, Matsumura A, Nakamuta H, Ohmichi T, Yoneyama M, Sasaki M (1995) Thermodynamic parameters to predict stability of RNA/DNA hybrid duplexes. Biochemistry 34(35):11211–11216
39. Sugimoto N, Nakano S, Yoneyama M, Honda K (1996) Improved thermodynamic pand helix initiation factor to pedict stability of DNA duplexes. Nucleic Acids Res 24(22):4501–4505
40. Teplova M, Minasov G, Tereshko V, Inamati GB, Cook PD, Manoharan M, Egli M (1999) Crystal structure and improved antisense properties of 2′-O-(2-methoxyethyl)-RNA. Nat Struct Biol 6(6):535–539

41. Tsuruoka H, Shohda K, Wada T, Sekine M (2000) Synthesis and conformational properties of oligonucleotides incorporating 2′-*O*-phosphorylated ribonucleotides as structural motifs of pre-tRNA splicing intermediates. J Org Chem 65(22):7479–7494

42. Ui-Tei K, Naito Y, Nishi K, Juni A, Saigo K (2008) Thermodynamic stability and Watson–Crick base pairing in the seed duplex are major determinants of the efficiency of the siRNA-based off-target effect. Nucleic Acids Res 36(22):7100–7109

43. Walton SP, Stephanopoulos GN, Yarmush ML, Roth CM (2002) Thermodynamic and kinetic characterization of antisense oligodeoxynucleotide binding to a structured mRNA. Biophys J 82(1):366–377

44. Wang J, Wolf RM, Caldwell JW, Kollman PA, Case DA (2004) Development and testing of a general amber force field. J Comput Chem 25(9):1157–1174

45. Xia T, SantaLucia J Jr, Burkard ME, Kierzek R, Schroeder SJ, Jiao X, Cox C, Turner DH (1998) Thermodynamic parameters for an expanded nearest-neighbor model for formation of RNA duplexes with Watson–Crick base pairs. Biochemistry 37(42):14719–14735

46. Yamada T, Masaki Y, Okaniwa N, Kanamori T, Ohkubo A, Tsunoda H, Seio K, Sekine M (2014) Synthesis and properties of oligonucleotides modified with 2′-*O*-(2-carboxyethyl) nucleotides and their carbamoyl derivatives. Org Biomol Chem 12(33):6457–6464

47. Yamana K, Iwase R, Furutani S, Tsuchida H, Zako H, Yamaoka T, Murakami A (1999) 2′-pyrene modified oligonucleotide provides a highly sensitive fluorescent probe of RNA. Nucleic Acids Res 27(11):2387–2392

48. Zatsepin TS, Gait MJ, Oretskaya TS (2004) 2′-functionalized nucleic acids as structural tools in molecular biology. IUBMB Life 56(4):209–214

2′,4′-Bridged Nucleic Acids Containing Plural Heteroatoms in the Bridge Moiety

Yoshiyuki Hari and Satoshi Obika

Abstract Bridge modifications between the 2′- and 4′-positions of a nucleoside have attracted much attention for improving properties of nucleic acid drugs, and many classes of 2′,4′-bridged nucleic acids have been developed to date. Evaluation of oligonucleotides containing 2′,4′-bridged nucleic acids suggests that, in addition to the bridge size, the number, type, and position of atoms composing the bridge unit affect (i) the binding affinity to target nucleic acid, (ii) resistance against nuclease degradation, and other factors. The addition of plural heteroatoms is an attractive bridge modification because interaction of the heteroatom with water can affect the properties of the oligonucleotides. In this chapter, focusing on 2′,4′-bridged nucleic acids containing plural heteroatoms in the bridge moiety, we mainly describe the design concept and synthesis. In addition, properties of 2′,4′-bridged nucleic acids are briefly explained.

Keywords 2′,4′-Bridged nucleic acid · Modified oligonucleotide · Oligonucleotide synthesis · Duplex-forming ability · Nuclease resistance

1 Introduction

The sugar moiety in nucleic acids predominantly adopts either a C3′-*endo* or C2′-*endo* conformation, which can be observed in A-type duplexes like RNA-RNA duplexes and in B-type duplexes like DNA-DNA duplexes, respectively. Thus, oligonucleotides including modified nucleosides that preferentially exist in the C3′-*endo* conformation are entropically advantageous in forming duplexes with single-stranded RNA (ssRNA).

Y. Hari (✉)
Faculty of Pharmaceutical Sciences, Tokushima Bunri University, Tokushima, Japan
e-mail: hari@ph.bunri-u.ac.jp

S. Obika
Osaka University, Suita, Osaka, Japan
e-mail: obika@phs.osaka-u.ac.jp
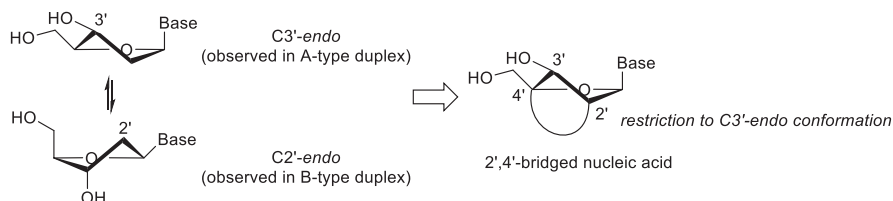
**Fig. 1** Conformational equilibrium of the sugar conformation and its restriction to C3′-*endo* by 2′,4′-bridge modification

Bridge modification between the 2′- and 4′-positions of a nucleoside is a powerful and attractive strategy that forces the sugar conformation to be C3′-*endo* (Fig. 1). Since 2′,4′-BNA (LNA) with a methylene bridge between 2′-oxygen and 4′-carbon atoms, independently reported by Wengel's group [1, 2] and our group [3, 4], dramatically improved properties of oligonucleotides like hybridization ability with ssRNA and nuclease resistance [5–11], various 2′,4′-bridged nucleic acids with different bridge structures have been developed [12–17]. For instance, 2′,4′-bridged nucleic acids, such as ENA [18, 19], with a different bridge size from 2′,4′-BNA (LNA) [18–21], and 2′,4′-bridged nucleic acids with other atoms in place of the 2′-oxygen in 2′,4′-BNA (LNA) have been implemented [22–26]. Moreover, introduction of substituents like a methyl group into the bridge and composite modifications have also been attempted [27–39]. Examples of 2′, 4′-bridged nucleic acids are summarized in Fig. 2. On the other hand, a heteroatom in the bridge can interact with water molecules around the nucleic acid complexes, forming a stable hydrogen bond network, which may contribute to the improved stabilization of the formed nucleic acid complexes and resistance against nuclease degradation. Recently, 2′, 4′-bridged nucleic acids containing plural heteroatoms in the bridge moieties have been developed. This chapter mainly summarizes the design concept and the synthesis of 2′, 4′-bridged nucleic acids (BNAs) containing plural heteroatoms.

2 Five-Membered Bridged Nucleic Acids

Amido-bridged nucleic acids (AmNAs: AmNA[NR]) were previously designed by our group (Fig. 3) [40]. Since the C-N (amide) bond is generally shorter than a C-O bond in the bridge of 2′, 4′-BNA (LNA), AmNAs are expected to adopt a more rigid structure in comparison to 2′, 4′-BNA (LNA). Moreover, increased hydrophilicity by the amide bridge could contribute to stabilization of nucleic acid complexes by the advantageous construction of a water network.
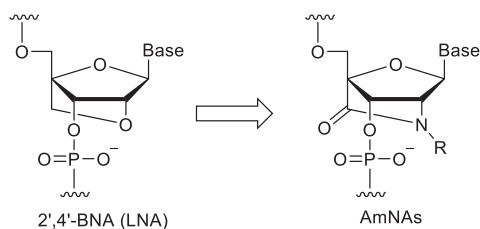
The synthesis of nucleoside **1** with an amide bridge was achieved via intramolecular condensation between the 2′-amino group and the 4′-carboxylic acid in **2**, prepared by reduction of the azide group in **3**, as shown in Scheme 1. AmNAs **4a–f**
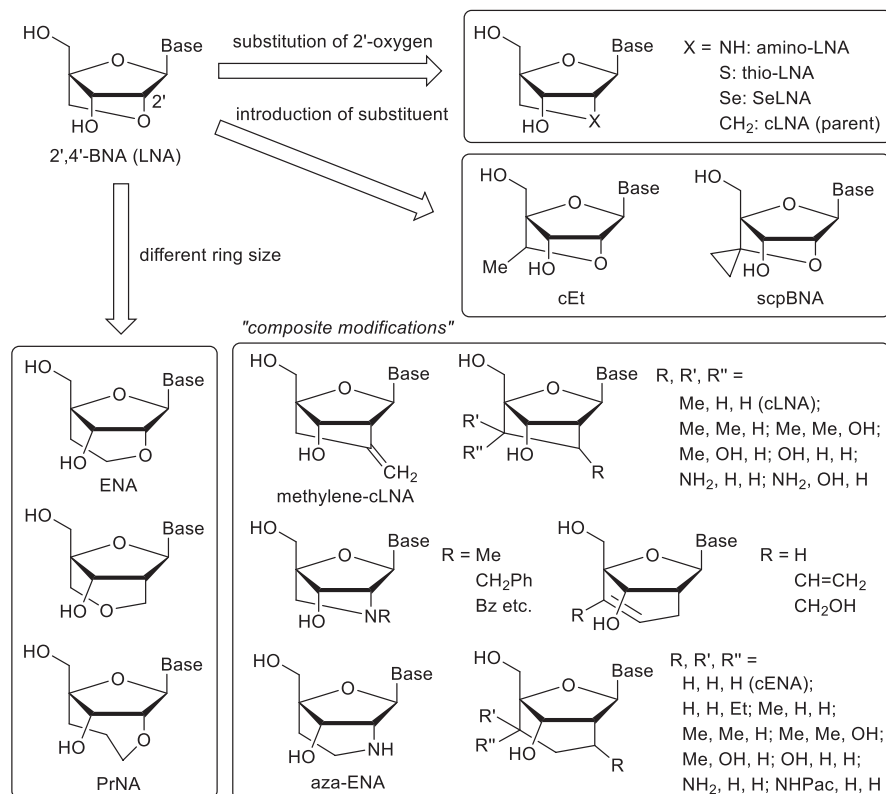
**Fig. 2** Structures of 2′,4′-BNA (LNA) monomer and its analogues

Fig. 3 Structure of AmNAs

2′,4′-BNA (LNA)

AmNAs

bearing various substituents on the nitrogen of the amide unit could be prepared by alkylation of compound **1** and the results are summarized in Table 1 [41]. Concerning the synthesis of AmNAs-modified oligonucleotides, thymidine phosphoramidites of AmNAs were successfully coupled using 5-[3,5-bis(trifluoromethyl)phenyl]-1*H*-tetrazole (Activator 42®) as an activator at extended coupling time (16 min). For AmNA[NH] and AmNA[NMe] phosphoramidites, 5 min of coupling time in the presence of 1*H*-tetrazole as an activator was sufficient [40]. Removal of all protecting groups on oligonucleotides and cleavage from a resin was carried out by 0.05 M
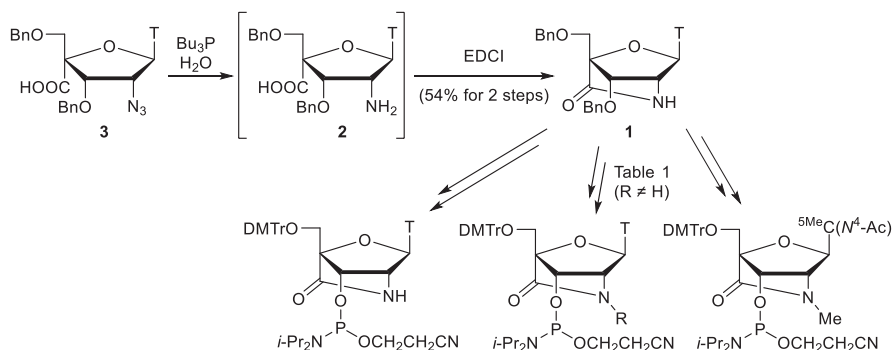
Scheme 1 Synthesis of AmNA[NR] phosphoramidites

Table 1 N-alkylation of **1** for synthesis of various AmNA[NR] analogues **4a–f**
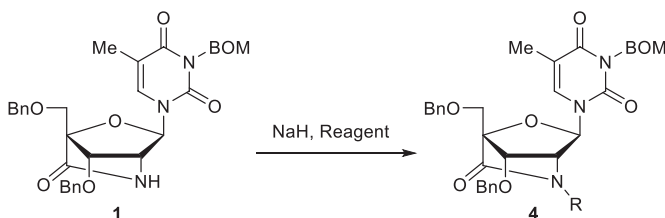
R	Reagent	Isolated yield
Me	MeI	86% (**4a**)
Et	EtBr	Quant. (**4b**)
n-Pr	*n*-PrBr	76% (**4c**)
i-Pr	*i*-PrI	Quant. (**4e**)
Bn	BnBr	Quant. (**4d**)
Phenethyl	PhCH$_2$CH$_2$Br	43% (**4f**)

K$_2$CO$_3$ in MeOH at room temperature for 1.5 h for AmNA[NH]-modified oligonucleotides, and by a concentrated ammonia solution at room temperature for 1 h for other AmNA-modified oligonucleotides. Most types of AmNA modifications had high binding affinity to single-stranded RNA (ssRNA) targets, comparable to the affinity of LNA modifications. Moreover, it was found that *N*-substituted AmNAs enhanced hepatic tropism of the oligonucleotides.

Seth's group considered constrained methoxyethyl nucleic acid (cMOE) by combining the structural elements of MOE [42, 43] and 2′,4′-BNA (LNA) (Fig. 4) [34]. Synthesis of *R*-cMOE and *S*-cMOE uridine monomers was achieved via bridge construction shown in Scheme 2. Mesylation of the hydroxyl group in **5** (1:1 inseparable diastereo-mixture) followed by acetolysis of actonide gave **6**. After introduction of the uracil nucleobase, the ring-closure reaction with K$_2$CO$_3$ in MeOH resulted in
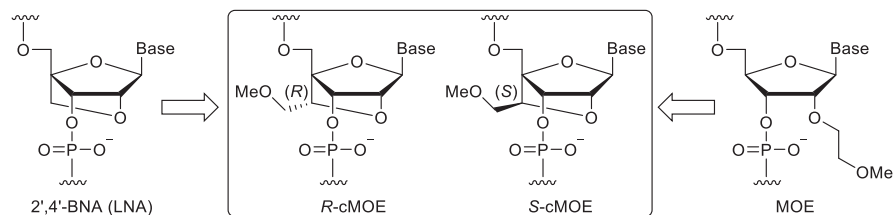
**Fig. 4** Structures of *R*-cMOE and *S*-cMOE
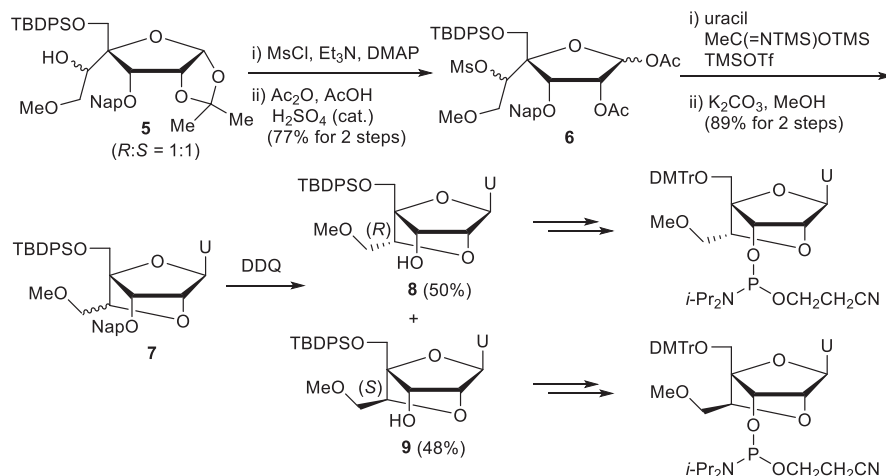
Scheme 2 Synthesis of *R*-cMOE and *S*-cMOE phosphoramidites

the cMOE structure (**7**). Then, removal of the 2-naphthylmethyl group (Nap) by DDQ treatment enabled isolation of *R*-cMOE and *S*-cMOE nucleosides **8** and **9** by silica gel column chromatographic separation. In the synthesis of cMOE-modified oligonucleotides, introduction of the uridine phosphoramidites with cMOE modifications could be conducted at a coupling time of 5 min. Oligonucleotides modified by *R*-cMOE or *S*-cMOE showed high hybridization ability and base-discrimination ability with complementary ssRNA, similarly to LNA. Moreover, oligonucleotides containing *R*-cMOE or *S*-cMOE residues produced less hepatotoxicity compared to LNA [44].

N-Methoxyamino-BNA was designed by Prakash's group (Fig. 5) [45]. The bridge moiety in **10** was successfully constructed by methoxyamine treatment of the uridine analogue **11** in the presence of DMF and *i*-Pr₂NEt as shown in Scheme 3. This strategy of bridge construction is unique and powerful because two bonds, C2′-N and C6′-N, are formed in one step. Uridine and cytidine phosphoramidites of *N*-methoxyamino-BNA were synthesized. Introduction of the *N*-methoxyamino-BNA unit into an oligonucleotide was achieved using 4,5-dicyanoimidazole as an activator at a coupling time of 10 min. *N*-Methoxyamino-BNA modification highly

Fig. 5 Structure of
N-methoxyamino-BNA
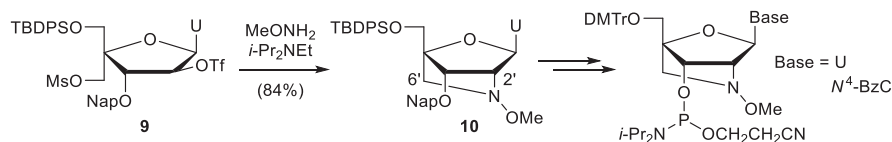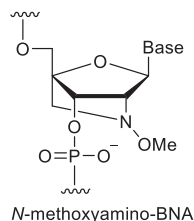

N-methoxyamino-BNA

**Scheme 3** Synthesis of *N*-methoxyamino-BNA phosphoramidite

stabilized the duplex formed with ssRNA to the same degree as LNA modification. In animal studies, an oligonucleotide with *N*-methoxyamino-BNA modifications reduced PTEN mRNA expression in a dose-dependent manner, and, unlike the LNA-modified oligonucleotide, showed normal toxicity parameters.

Carba-LNA analogues shown in Fig. 6 were designed by Chattopadhyaya's group [26]. Radical cyclization of **11** produced **12** and **13** (Scheme 4). The coupling of modified phosphoramidites **14** and **15** was performed for a prolonged time (10 min comparing 25 s for natural ones) using 5-ETT. While the coupling efficiency of **14** was satisfactory (60–80% yield), **15** showed a low coupling efficiency of 20%, likely due to steric hindrance of the 7′-trifluoroacetamide group with the *R*-configuration against the 3′-phosphoramidite moiety. Concerning the duplex-forming ability with ssRNA, oligonucleotides including 7′*S*-analogues were superior to those including 7′*R*-ones. This might also be caused by steric repulsion between the 7′*R*-amino group and the 3′-phosphate.

6′-Mercapto-thioBNA can be conjugated with various functional molecules at the 6′-position (Fig. 7) [46]. Bridge construction of 6′-mercapto-thioBNA was achieved by a unique strategy shown in Scheme 5. Photo-irradiation of disulfide-type BNA **16** [47], caused generation of a dithiyl radical followed by a 1,2-H-shift [48, 49] to produce 6′-mercapto-thioBNA **17** as a sole diastereoisomer. Benzoyl protection of the 6′-mercapto group yielded **18**, which was converted into the phosphoramidite **19** for oligonucleotide synthesis. The concentration of the phosphoramidite of 6′-mercapto-thioBNA was 0.1 M, and the coupling time was 20 min, while the concentration and coupling time were 0.067 M and 90 s, respectively, for unmodified phosphoramidites. Activator 42® was used as a coupling activator, and the coupling yields were estimated to be over 95% based on trityl monitoring. After full elongation of oligonucleotides on an automated DNA synthesizer, alkaline treatment in the presence of 2,2′-dithiodipyridine gave oligonucleotides including
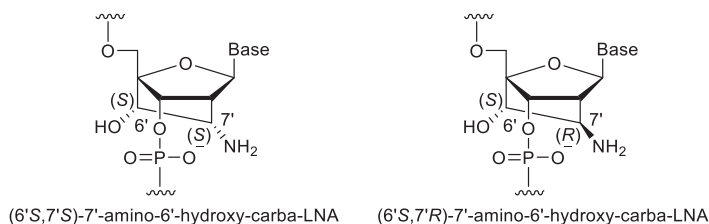
Fig. 6 Structures of 7′-amino-6′-hydroxy-carba-LNAs

Scheme 4 Synthesis of 7′-amino-6′-hydroxy-carba-LNA phosphoramidites
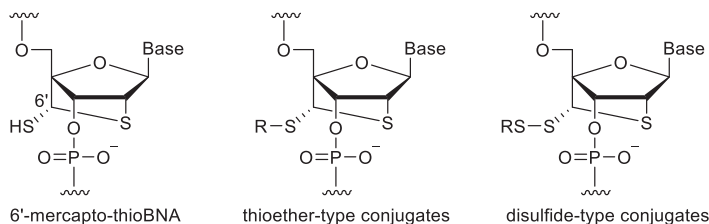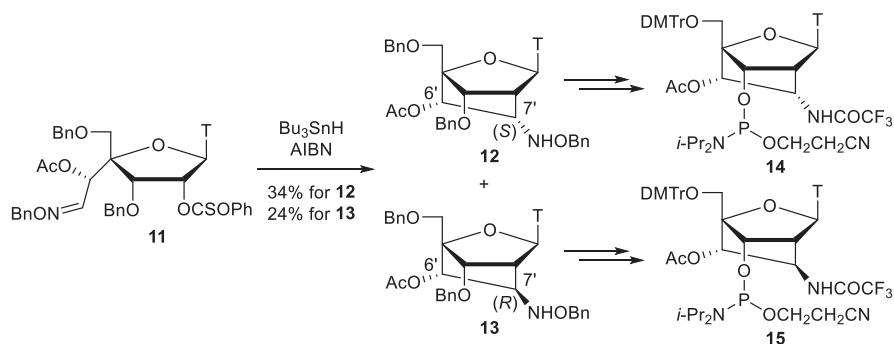
**Fig. 7** Structures of 6′-mercapto-thioBNA and the conjugates

the thiol protected by a pyridinesulfenyl group. By reactions occurring after removal of the pyridinesulfenyl group or disulfide exchange reactions, conjugations of various molecules can be achieved.

Guanidine bridged nucleic acid (GuNA) was designed by our group (Fig. 8) [50]. Since a guanidino group possessing positive charge can counteract the negative charge of the phosphate backbone in an oligonucleotide, introduction of guanidine unit into the bridge structure can improve hybridization ability with ssRNA and cellular permeability.
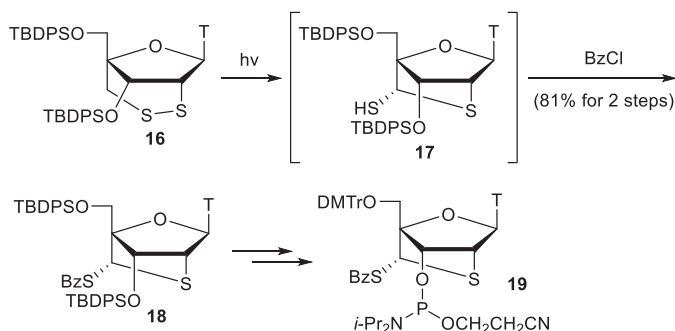
Scheme 5 Synthesis of 6′-mercapto-thioBNA phosphoramidite

Fig. 8 Structure of GuNA
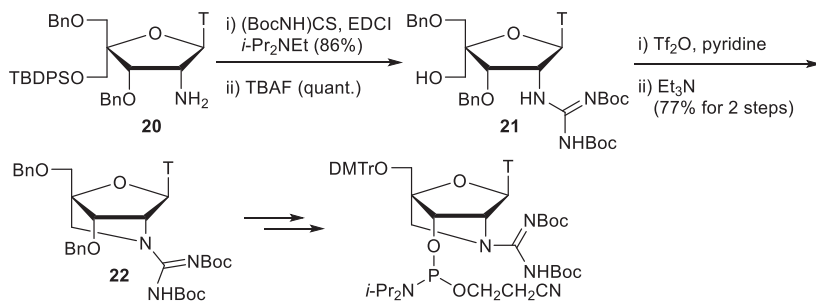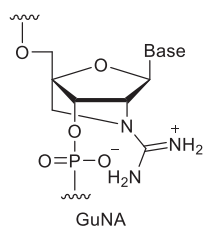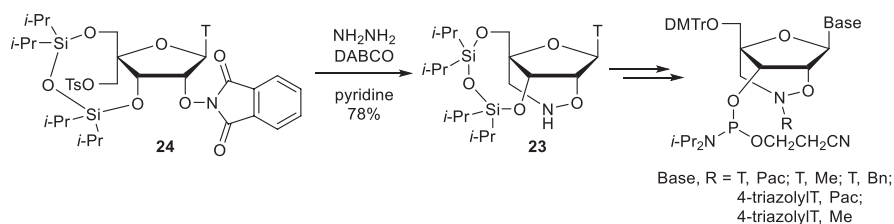

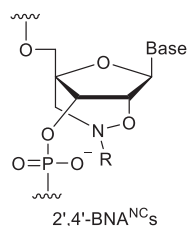**Scheme 6** Synthesis of GuNA phosphoramidite

The synthesis of the thymidine phosphoramidite of GuNA, including the process of bridge construction, is shown in Scheme 6. Condensation of **20** with Boc-protected thiourea and treatment with TBAF yielded **21**. The protected GuNA thymidine monomer **22** could be constructed by triflation of the resulting alcohol followed by mild base treatment. For oligonucleotide synthesis, coupling of the

GuNA phosphoramidite was performed using 1*H*-tetrazole as an activator for 20 min while the coupling time for natural phosphoramidites was 32 s. Deprotection of Boc groups of guanidine moieties was achieved by 75% trifluoroacetic acid. However, because the conditions were harsh to the oligonucleotides, the use of alternate protecting groups would be desirable. GuNA-modified oligonucleotides formed more stable duplexes with ssRNA and ssDNA than LNA-modified oligonucleotides did. Stabilization of duplexes with ssDNA is a unique property that is not seen in previous bridged nucleic acids. GuNA-modified oligonucleotides also had high base-discrimination ability during duplex formation of duplexes and good resistance against 3′-exonuclease.

3 Six-Membered Bridged Nucleic Acids

2′,4′-BNA[NC] possesses a unique N-O bond in the bridge, and introducing various functional groups and/or molecules on the nitrogen atom is possible (Fig. 9) [51–53]. The bridge structure (**23**) was constructed by nucleophilic attack on the 6′-carbon atom by the aminoxy group at the 2′-position of **24** (Scheme 7). Regarding protecting groups at the 3′- and 5′-positions, benzyl groups instead of the cyclic disiloxane group of **23** could not be used because deprotection of benzyl groups without decomposition of an N-O bond in the bridge was unsuccessful [52]. Finally, phosphoramidites of 2′,4′-BNA[NC][NPac], 2′,4′-BNA[NC][NMe] and 2′,4′-BNA[NC][NBn]


**Fig. 9** Structure of 2′,4′-BNA[NC]s

Scheme 7 Synthesis of 2′,4′-BNA[NC][NR] phosphoramidites

were prepared. The phosphoramidites were successfully coupled for a prolonged coupling time (5–6 min) using 1*H*-terazole or Activator 42®, and the coupling efficiency was over 95% on the trityl monitor. 2′,4′-BNA^NC^[NPac] modification was converted into 2′,4′-BNA^NC^[NH] by ammonia treatment after oligonucleotide synthesis. All types of 2′,4′-BNA^NC^-modified oligonucleotides formed highly stable duplexes with ssRNA, and had excellent nuclease resistance. In particular, 2′,4′-BNA^NC^[NMe]-modified oligonucleotides were very promising for antisense application [51, 52, 54–56]. Among 2′,4′-BNA^NC^ derivatives, 2′,4′-BNA^NC^[NH] modification was effective for targeting double-stranded DNA by triplex formation [51, 53, 57].

N-Methylaminoxy-BNA was designed as the N-O inverse analogue of 2′,4′-BNA^NC^[NMe] (Fig. 10) [45]. The bridge (**25**) was constructed by nucleophilic substitution on the 2′-carbon atom by the methylaminoxymethyl group at the 4′-position of **26**, which was prepared by reducing **27** using NaBH₃CN (Scheme 8). Finally, *N*-methylaminoxy-BNA phosphoramidites with thymine and *N*⁴-benzoylcytosine as nucleobases were prepared. During oligonucleotide synthesis, coupling of the *N*-methylaminoxy-BNA unit successfully proceeded under the same conditions (activator: 4,5-dicyanoimidazole; coupling time: 10 min) as *N*-methoxyamino-BNA mentioned above. It was shown that *N*-methylaminoxy-BNA
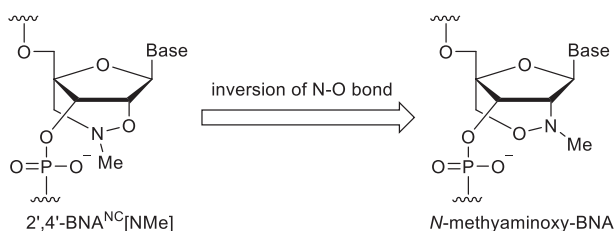
**Fig. 10** Structure of *N*-methylaminoxy-BNA
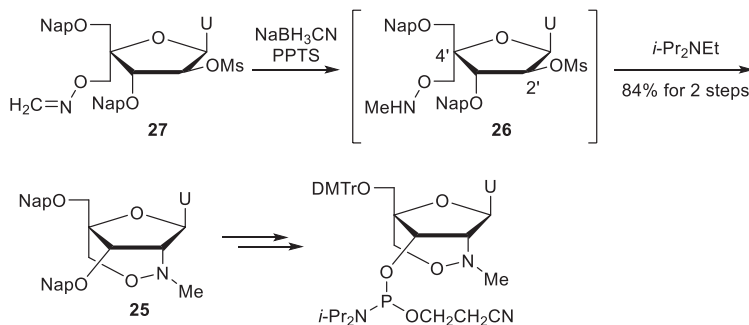
**Scheme 8** Synthesis of *N*-methylaminoxy-BNA phosphoramidite

was a useful modification for oligonucleotide-based drug discovery applications like antisense oligonucleotides.

Installing a carbonyl group in the bridge of 2′,4′-BNA^{NC} is expected to further restrict the sugar conformation, and to improve the properties of modified oligonucleotides. Thus, hydroxamate-bridged nucleic acid (HxNA) was designed by our group (Fig. 11) [58]. The hydroxamate bridges, NH and NMe, were constructed by condensation between oxyamino groups at the 2′-position and carboxyl groups at the 4′-position. Example of NMe analogue is shown in Scheme 9. After reducing **28**, intramolecular condensation of **29** using EDCI and HOBt yielded **30**. Although the HxNA[NMe] phosphoramidite was synthesized by a common procedure, it was difficult to obtain the HxNA[NH] phosphoramidite because of the lability of the NH analogue **31** under basic conditions. For oligonucleotide synthesis, Activator 42® was used as an activator and the coupling time of HxNA[NMe] phosphoramidite was prolonged to 30–40 min. For base treatment after oligonucleotide synthesis, 50 mM methanolic K$_2$CO$_3$ yielded the desired oligonucleotides though ammonolytic cleavage of the bridge upon treatment with ammonia solution. Stabilization of duplexes with ssRNA by HxNA[NMe] modification was almost as effective as that by the same six-membered analog, ENA. However, compared to 2′,4′-BNA^{NC}[NMe],
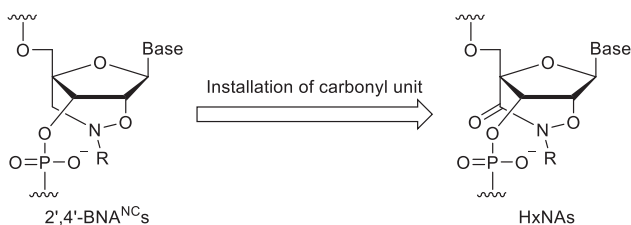
Fig. 11 Structure of HxNAs
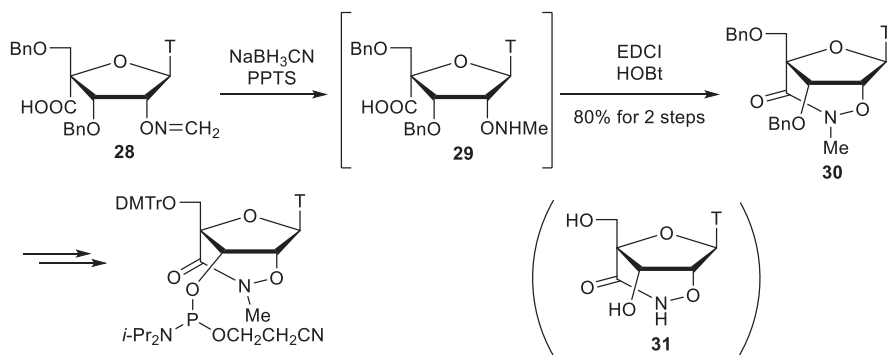
Scheme 9 Synthesis of HxNA[NMe] phosphoramidite

the stabilization ability was reduced. The nuclease resistance of HxNA[NMe] was a little higher than the resistance of LNA, which resulted in production of the ring-opened analogue of HxNA[NMe] possessing high stability against nuclease.

6-AmNA is the one-carbon enlarged analogue of AmNA (Fig. 12) [59]. The synthesis of NH and NMe derivatives of 6-AmNA from one-carbon elongated derivative at the 6′-position was performed by a similar route as AmNA. The amide bridge (**31**) can be constructed not only by condensation between the amino group and the carboxyl group in **32** but also by intramolecular Staudinger ligation of **33** as shown in Scheme 10. The introduction of 6-AmNA phosphoramidite into an oligonucleotide was successfully achieved upon prolonged coupling time. The amide bridges, NH and NMe, were stable under ammonia solution at room temperature for 1.5 h or under methanolic K_2CO_3 at room temperature for 2 h. The stabilizing ability of the duplexes with ssRNA seemed to be AmNA[NH] ≈ AmNA[NMe] > 6-AmNA[NH] > 6-AmNA[NMe] ≈ HxNA. Nuclease resistance of 6-AmNA[NH] and 6-AmNA[NMe] was similar to that of AmNA[NH] and AmNA[NMe] with the smaller five-membered bridges.

Sulfonamide-bridged nucleic acids (SuNAs) were expected to have high nuclease resistance because of the bulkiness of the sulfonamide moiety (Fig. 13) [60, 61]. Moreover, the effect of the sulfonamide bridge on hybridization ability was also interesting. The bridge was formed by nucleophilic substitution of an aminosulfonylmethyl group at the 4′-position to the 2′-carbon atom with a leaving group (Scheme 11). Concerning the SuNA[NH] analogue, ring-closure using *N*-(2-naphthyl)methyl compound **34a** constructed the bridge structure in **35a**. The NMe
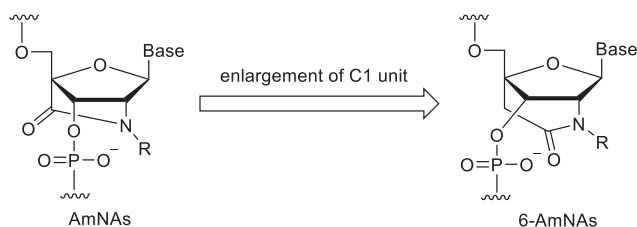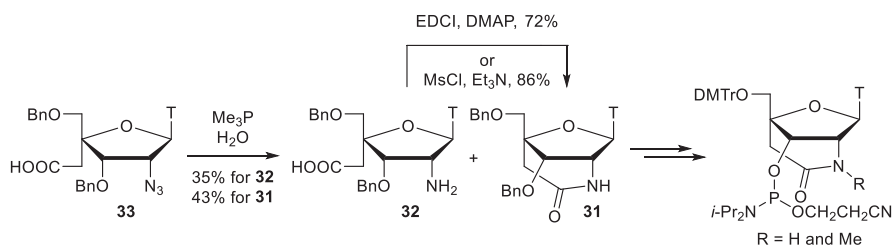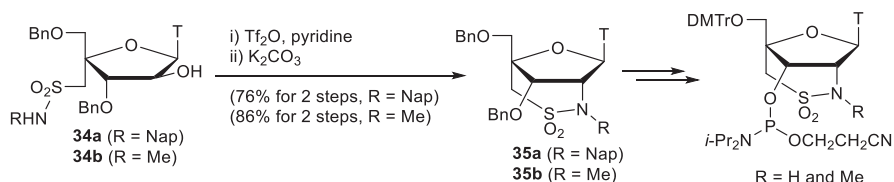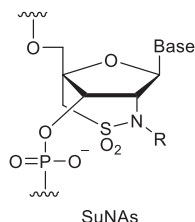

Fig. 12 Structure of 6-AmNAs

**Scheme 10** Synthesis of 6-AmNA[NH] and 6-AmNA[NMe] phosphoramidites

Fig. 13 Structure of SuNAs

Scheme 11 Synthesis of SuNA[NH] and SuNA[NMe] phosphoramidites

analogue **35b** was prepared from *N*-methyl compound **34b**. Concerning oligonucleotide synthesis, the sulfonamide of SuNA[NH] was usable in a NH-free form. Both SuNA[NH] and SuNA[NMe] were successfully coupled at a prolonged coupling time (32 s to 16 min) using 5-ETT as an activator. It was found that SuNA[NMe] rather than SuNA[NH] had significantly high duplex-forming ability with ssRNA. SuNA[NMe] also showed high nuclease resistance, comparable to 2′,4′-BNA^COC with a larger seven-membered bridge. This would imply that the bulkiness of the bridge was increased by installing a sulfonamide unit in the bridge. In addition, X-ray structures of duplexes including SuNAs clarified the difference in hydration patterns between SuNA[NH] and SuNA[NMe] [61].

Nielsen's group considered (6′*S*,7′*S*)-6′,7′-dihydroxy-2′,4′-bridged nucleic acid as a carbacyclic ENA analogue (Fig. 14) [33]. The synthetic route of the phosphoramidite is shown in Scheme 12. Construction of the bridge (**36**) including two hydroxy groups was achieved by ring-closing metathesis of **37** followed by diastereoselective dihydroxylation of **38**. The coupling of modified deoxyuridine phosphoramidite for oligonucleotide synthesis required a prolonged time (30 min) using pyridine hydrochloride [62] instead of 1*H*-tetrazole as an activator. The modified oligonucleotides showed significantly increased stability of duplexes with ssRNA, compared to the natural oligonucleotide.

2′-*N*-Guanidino,4′-*C*-ethylene-bridged nucleic acid (GENA), a one-carbon enlarged analogue of GuNA, was reported by Varghese's group (Fig. 15) [63]. The synthesis was achieved by guanylation of the 2′-amino group in the thymidine analogue of 2′-*N*,4′-*C*-ethylene-bridged nucleic acid (azaENA) [28]. A 2-cyanoethoxycarbonyl (CEOC) group was used as a nitrogen-protecting group in the guanidine moiety. The removal of the CEOC group in GENA after oligonucle-

Fig. 14 Structure of
(6′S,7′S)-6′,7′-dihydroxy-
2′,4′-bridged nucleic acid

6',7'-dihydroxy-2',4'-bridged nucleic acid
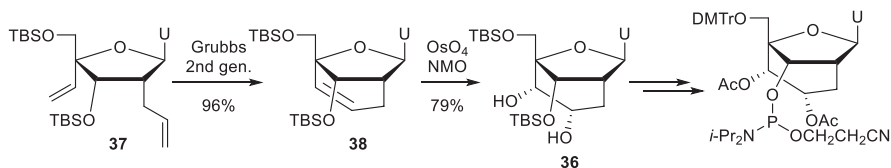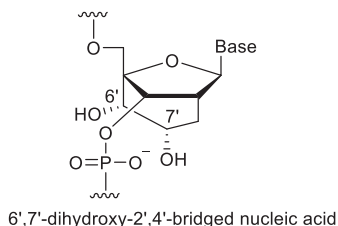
Scheme 12 Synthesis of the phosphoramidite of 6′,7′-dihydroxy-2′,4′-bridged nucleic acid

Fig. 15 Structure of
GENA

GENA
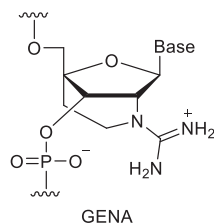
otide synthesis was carried out by treatment with 50% aqueous piperidine. The modified oligonucleotides showed high triplex-forming ability with double-stranded DNA and excellent stability against nuclease.

4 Seven-Membered Bridged Nucleic Acids

2′,4′-BNA^COC possesses an acetal unit in the bridge (Fig. 16) [64]. Therefore, restriction of sugar conformational flexibility is expected by the anomeric effect. Bridge structures (**39**) were constructed by methylenation between the 2′-OH and the 6′-OH in **40** (Table 2) [64, 65]. In the case of the adenosine analogues **39c** and **39d**, both benzoyl and benzyloxymethyl groups, not only a common benzoyl group, as the protecting group at the N^6-position were required to construct the bridge. For the synthesis of 2′,4′-BNA^COC-modified oligonucleotides, the coupling of 2′,4′-BNA^COC phosphoramidites required 45 min using 1H-terazole as an activator and the efficiency was estimated to be approximately 80% by the trityl monitor. The use of 4,5-dicyanoimidazole or 5-ethylthio-1H-tetrazole achieved a coupling efficiency of

Fig. 16 Structure of 2′,4′-BNA^{COC}
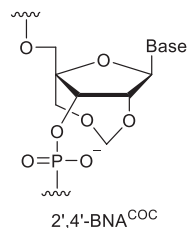
2′,4′-BNA^{COC}

Table 2 Methylenation of **40** for synthesis of 2′,4′-BNA^{COC} analogues **39a–e** bearing natural nucleobases

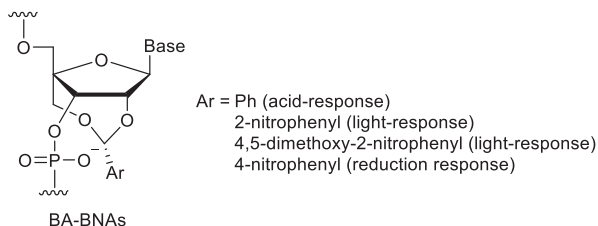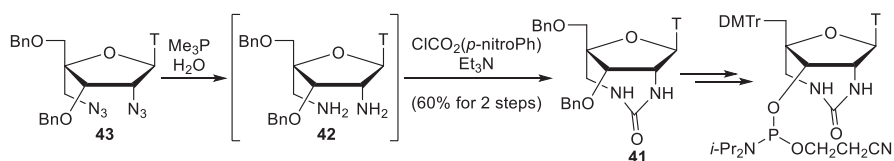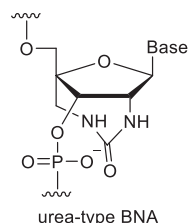| Base	Conditions	Isolated yield
T	$(CHO)_n$, p-TsOH•H_2O, $(CH_2Cl)_2$, reflux	81% (**39a**)
N^4-Bz-5-methylC	$(CHO)_n$, p-TsOH•H_2O, $(CH_2Cl)_2$, 60 °C	70% (**39b**)
N^6-BzA	NBS, DMSO, 60 °C	Trace (**39c**)
N^6-Bz(N^6-BOM)A	NBS, DMSO, 60 °C	74% (**39d**)
N^2-isobutyryl(O^6-Ph$_2$NCO)G	NBS, DMSO, 60 °C	45% (**39e**)

over 95% with a coupling time of 20 min. 2′, 4′-BNA^{COC} modifications stabilized the duplex formed with ssRNA, while PrNA, possessing a C-C-C linkage instead of the C-O-C linkage seen in 2′,4′-BNA^{COC}, led to the slight destabilization of the duplex with ssRNA. This indicates the importance of the second oxygen atom in the bridge of 2′,4′-BNA^{COC}. Moreover, 2′,4′-BNA^{COC} showed high resistance against nuclease because the bulky seven-membered bridge structure prevented nuclease access.

Benzylidene acetal-type bridged nucleic acids (BA-BNAs) were also considered (Fig. 17) [66, 67]. Cleavage of the bridges in BA-BNAs by external stimuli such as acid, light and reducing reagents is possible, and the properties can be changed. Thymidine analogues of BA-BNAs have been synthesized, and the bridge structures in BA-BNAs were constructed in a similar way as 2′,4′-BNA^{COC}, namely, acetalization of benzaldehyde analogues by the 2′-OH and 6′-OH of sugar moieties. Acetalization proceeded in a diastereoselecive manner [68]. Introduction of BA-BNA phosphoramidites into oligonucleotides on an automated DNA synthesizer required a prolonged coupling time from 1.5 to 40 min using 5-ETT, and the coupling efficiency was over 95%.

Urea containing two N-H bonds and a carbonyl group can work not only as a hydrogen donor but also as a hydrogen acceptor, and is considered to be effective in forming a rigid hydrogen bond network. Thus, urea-bridged nucleic acid (urea-type

Fig. 17 Structures of
BA-BNAs

Ar = Ph (acid-response)
     2-nitrophenyl (light-response)
     4,5-dimethoxy-2-nitrophenyl (light-response)
     4-nitrophenyl (reduction response)

BA-BNAs

Fig. 18 Structure of
urea-type BNA

urea-type BNA

Scheme 13 Synthesis of the urea-type BNA phosphoramidite

BNA) was designed (Fig. 18) [69]. The urea bridge in **41** was constructed by a ring-closure reaction of the bis-amino compound **42**, prepared from **43**, with *p*-nitrophenyl chloroformate (Scheme 13). Like BA-BNAs, the coupling of a urea-type BNA phosphoramidite for 40 min in the presence of 5-ETT was necessary for synthesizing urea-type BNA-modified oligonucleotides. Consequently, the duplex-forming ability and nuclease resistance of urea-type BNA were comparable to those of 2′,4′-BNA^{COC}.

2′-*O*,4′-*C*-Ethyleneoxy bridged nucleic acid (EoNA) is the first 2′,4′-bridged nucleic acid possessing an additional heteroatom on the 4′-carbon atom (Fig. 19) [70]. The additional oxygen in the bridge is expected to act as a proton acceptor for forming a water network, and to restrict sugar conformational flexibility by the anomeric effect. Nucleophilic attack by the 2′-OH in **44** constructed the bridge structure to give **45** (Scheme 14). Consequently, it should be noted that the synthetic process of 5-methyluridine phosphoramidite with EoNA modification is short; 12 steps from 5-methyluridine. For oligonucleotide synthesis, when EoNA phosphoramidite was coupled with the oligonucleotide on the resin for a prolonged coupling time (20 min) using Activator 42®, the efficiency was estimated to be 90–95% by trityl monitoring. If oligonucleotides with consecutive EoNA modifications are synthe-

Fig. 19 Structure of EoNA
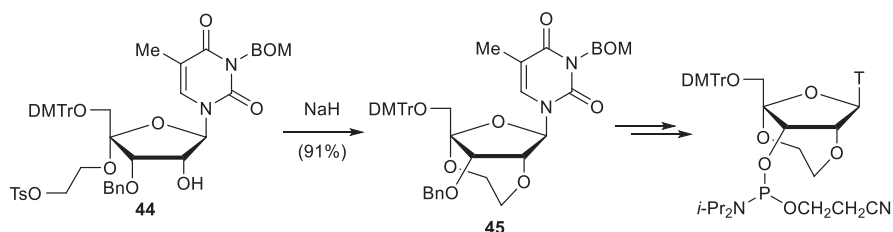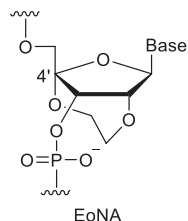
Scheme 14 Synthesis of EoNA phosphoramidite

sized, double-coupling cycles together with a coupling time of 20 min were required. It was found that EoNA modifications of oligonucleotides significantly stabilized duplexes with ssRNA and triplexes with double-stranded DNA compared to 2′,′-BNA^{COC} with the same seven-membered ring. Moreover, EoNA showed excellent nuclease resistance.

5 Summary

As described in this chapter, many 2′,4′-bridged nucleic acids containing plural heteroatoms in the bridge moieties have been developed. However, the complete effects of these bridges are still unclear. Continuous studies on synthesis and evaluation of new 2′,4′-bridged nucleic acids can be expected to contribute to deepening our understanding, and will produce nucleic acid analogues with improved performance.

References

1. Singh SK, Koshkin AA, Wengel J, Nielsen P (1998) LNA (locked nucleic acids): synthesis and high-affinity nucleic acid recognition. Chem Commun: 455–456
2. Koshkin AA, Singh SK, Nielsen P, Rajwanshi VK, Kumar R, Meldgaard M, Olsen CE, Wengel J (1998) LNA (locked nucleic acids): synthesis of the adenine, cytosine, guanine, 5-methylcytosine, thymine and uracil bicyclonucleoside monomers, oligomerisation, and unprecedented nucleic acid recognition. Tetrahedron 54:3607–3630

3. Obika S, Nanbu D, Hari Y, Morio K, In Y, Ishida T, Imanishi T (1997) Synthesis of 2′-*O*,4′-*C*-methyleneuridine and – cytidine. Novel bicyclic nucleosides having a fixed C$_{3'}$-*endo* sugar puckering. Tetrahedron Lett 38:8735–8738

4. Obika S, Nanbu D, Hari Y, Ando J, Morio K, Doi T, Imanishi T (1998) Stability and structural features of the duplexes containing nucleoside analogues with a fixed N-type conformation, 2′-*O*,4′-*C*-methyleneribonucleosides. Tetrahedron Lett 39:5401–5404

5. Petersen M, Wengel J (2003) LNA: a versatile tool for therapeutics and genomics. Trends Biotech 21:74–81

6. Koch T (2003) Locked nucleic acids: a family of high affinity nucleic acid probes. J Phys Condens Matter 15:S1861–S1871

7. Vester B, Wengel J (2004) LNA (locked nucleic acid): high-affinity targeting of complementary RNA and DNA. Biochemistry 43:13233–13241

8. Jepsen JS, Sørensen MD, Wengel J (2004) Locked nucleic acid: a potent nucleic acid analog in therapeutics and biotechnology. Oligonucleotides 14:130–146

9. Kaur H, Babu R, Maiti S (2007) Perspectives on chemistry and therapeutic applications of locked nucleic acid (LNA). Chem Rev 107:4672–4697

10. Veedu RN, Wengel J (2009) Locked nucleic acid as a novel class of therapeutic agents. RNA Biol 6:321–323

11. Campbell MA, Wengel J (2011) Locked *vs.* unlocked nucleic acids (LNA *vs.* UNA): contrasting structures work towards common therapeutic goals. Chem Soc Rev 40:5680–5689

12. Zhou C, Chattopadhyaya J (2009) The synthesis of therapeutic locked nucleos(t)ides. Curr Opin Drug Discov Dev 12:876–898

13. Rahman SMA, Imanishi T, Obika S (2009) Synthesis of several types of bridged nucleic acids. Chem Lett 38:512–517

14. Obika S, Rahman SMA, Fujisaka A, Kawada Y, Baba T, Imanishi T (2010) Bridged nucleic acids: development, synthesis and properties. Heterocycles 81:1347–1392

15. Yamamoto T, Nakatani M, Narukawa K, Obika S (2011) Antisense drug discovery and development. Fut Med Chem 3:339–365

16. Zhou C, Chattopadhyaya J (2012) Intramolecular free-radical cyclization reactions on pentose sugars for the synthesis of carba-LNA and carba-ENA and the application of their modified oligonucleotides as potential RNA targeted therapeutics. Chem Rev 112:3808–3832

17. Astakhova IK, Wengel J (2014) Scaffolding along nucleic acid duplexes using 2′-amino-locked nucleic acids. Acc Chem Res 47:1768–1777

18. Morita K, Hasegawa C, Kaneko M, Tsutsumi S, Sone J, Ishikawa T, Imanishi T, Koizumi M (2002) 2′-*O*,4′-*C*-Ethylene-bridged nucleic acids (ENA): high-nuclease-resistant and thermodynamically stable oligonucleotides for antisense drug. Bioorg Med Chem Lett 12:73–76

19. Morita K, Takagi M, Hasegawa C, Kaneko M, Tsutsumi S, Sone J, Ishikawa T, Imanishi T, Koizumi M (2003) Synthesis and properties of 2′-*O*,4′-*C*-ethylene-bridged nucleic acids (ENA) as effective antisense oligonucleotides. Bioorg Med Chem 11:2211–2226

20. Wang G, Gunic E, Girardet J-L, Stoisavljevic V (1999) Conformationally locked nucleosides. Synthesis and hybridization properties of oligodeoxynucleotides containing 2′,4′-*C*-bridged 2′-deoxynucleosides. Bioorg Med Chem Lett 9:1147–1150

21. Wang G, Girardet J-L, Gunic E (1999) Conformationally locked nucleosides. Synthesis and stereochemical assignments of 2′-*C*,4′-*C*-bridged bicyclonucleosides. Tetrahedron 55:7707–7724

22. Singh SK, Kumar R, Wengel J (1998) Synthesis of novel bicycle[2.2.1] ribonucleosides: 2′-amino- and 2′-thio-LNA monomeric nucleosides. J Org Chem 63:6078–6079

23. Singh SK, Kumar R, Wengel J (1998) Synthesis of 2′-amino-LNA: a novel conformationally restricted high-affinity oligonucleotide analogue with a handle. J Org Chem 63:10035–10039

24. Kumar R, Singh SK, Koshkin AA, Rajwanshi VK, Meldgaard M, Wengel J (1998) The first analogues of LNA (locked nucleic acids): phosphorothioate-LNA and 2′-thio-LNA. Bioorg Med Chem Lett 8:2219–2222

25. Morihiro K, Kodama T, Kentefu, Moai Y, Veedu RN, Obika S (2013) Selenomethylene locked nucleic acid enables reversible hybridization in response to redox changes. Angew Chem Int Ed 52:5074–5078

26. Xu J, Liu Y, Dupouy C, Chattopadhyaya J (2009) Synthesis of conformationally locked carba-LNAs through intramolecular free-radical addition to C=N. Electrostatic and steric implication of the carba-LNA substituents in the modified oligos for nuclease and thermodynamic stabilities. J Org Chem 74:6534–6554

27. Sørensen MD, Petersen M, Wengel J (2003) Functionalized LNA (locked nucleic acid): high-affinity hybridization of oligonucleotides containing N-acylated and N-alkylated 2′-amino-LNA monomers. Chem Commun: 2130–2131

28. Varghese OP, Barman J, Pathmasiri W, Plashkevych O, Honcharenko D, Chattopadhyaya J (2006) Conformationally constrained 2′-N,4′-C-ethylene-bridged thymidine (aza-ENA-T): Synthesis, structure, physical, and biochemical studies of aza-ENA-T-modified oligonucleotides. J Am Chem Soc 128:15173–15187

29. Albæk N, Petersen M, Nielsen P (2006) Analogues of a locked nucleic acid with three-carbon 2′,4′-linkages: synthesis by ring-closing metathesis and influence on nucleic acid duplex stability and structure. J Org Chem 71:7731–7740

30. Srivastava P, Barman J, Pathmasiri W, Plashkevych O, Wenska M, Chattopadhyaya J (2007) Five- and six-membered conformationally locked 2′,4′-carbocyclic ribo-thymidines: synthesis, structure, and biochemical studies. J Am Chem Soc 129:8362–8379

31. Zhou C, Liu Y, Andaloussi M, Badgujar N, Plashkevych O, Chattopadhyaya J (2009) Fine tuning of electrostatics around the internucleotidic phosphate through incorporation of modified 2′,4′-carbocyclic-LNAs and – ENAs leads to significant modulation of antisense properties. J Org Chem 74:118–134

32. Zhou C, Plashkevych O, Chattopadhyaya J (2009) Double sugar and phosphate backbone-constrained nucleotides: synthesis, structure, stability, and their incorporation into oligodeoxynucleotides. J Org Chem 74:3248–3265

33. Kumar S, Hansen MH, Albæk N, Steffansen SI, Petersen M, Nielsen P (2009) Synthesis of functionalized carbocyclic locked nucleic acid analogues by ring-closing diene and enyne metathesis and their influence on nucleic acid stability and structure. J Org Chem 74:6756–6769

34. Seth PP, Vasquez G, Allerson CA, Berdeja A, Gaus H, Kinberger GA, Prakash TP, Migawa MT, Bhat B, Swayze EE (2010) Synthesis and biophysical evaluation of 2′,4′-constrained 2′O-methoxyethyl and 2′,4′-constrained 2′O-ethyl nucleic acid analogues. J Org Chem 75:1569–1581

35. Liu Y, Xu J, Karimiahmadabadi M, Zhou C, Chattopadhyaya J (2010) Synthesis of 2′,4′-propylene-bridged (carba-ENA) thymidine and its analogues: the engineering of electrostatic and steric effects at the bottom of the minor groove for nucleobase and thermodynamic stabilities and elicitation of RNase H. J Org Chem 75:7112–7128

36. Johannsen MW, Crispino L, Wamberg MC, Kalra N, Wengel J (2011) Amino acids attached to 2′-amino-LNA: synthesis and excellent duplex stability. Org Biomol Chem 9:243–252

37. Seth PP, Allerson CA, Berdeja A, Siwkowski A, Pallan PS, Gaus H, Prakash TP, Watt AT, Egli M, Swayze EE (2010) An exocyclic methylene group acts as a bioisostere of the 2′-oxygen atom in LNA. J Am Chem Soc 132:14942–14950

38. Upadhayaya RS, Deshpande SG, Li Q, Kardile RA, Sayyed AY, Kshirsagar EK, Salunke RV, Dixit SS, Zhou C, Földesi A, Chattopadhyaya J (2011) Carba-LNA-[5Me]C/A/G/T modified oligos show nucleobase-specific modulation of 3′-exonuclease activity, thermodynamic stability, RNA selectivity, and RNase H elicitation: synthesis and biochemistry. J Org Chem 76:4408–4431

39. Yamaguchi T, Horiba M, Obika S (2015) Synthesis and properties of 2′-O,4′-C-spirocyclopropylene bridged nucleic acid (scpBNA), an analogue of 2′,4′-BNA/LNA bearing a cyclopropane ring. Chem Commun 51:9737–9740

40. Yahara A, Shrestha AR, Yamamoto T, Hari Y, Osawa T, Yamaguchi M, Nishida M, Kodama T, Obika S (2012) Amido-bridged nucleic acids (AmNAs): synthesis, duplex stability, nuclease resistance, and in vitro antisense potency. ChemBioChem 13:2513–2516

41. Yamamoto T, Yahara A, Waki R, Yasuhara H, Wada F, Harada-Shiba M, Obika S (2015) Amido-bridged nucleic acids with small hydrophobic residues enhance hepatic tropism of antisense oligonucleotides in vivo. Org Biomol Chem 13:3757–3765

42. Martin P (1995) Ein neuer zugang zu 2′-O-alkylribonucleosiden und eigenschaften deren oligonucleotide. Helv Chim Acta 78:486–504

43. Baker BF, Lot SS, Condon TP, Cheng-Flournoy S, Lesnik EA, Sasmor HM, Bennett (1997) 2′-O-(2-methoxy)ethyl-modified anti-intercellular adhesion molecule 1(ICAM-1) oligonucleotides selectively increase the ICAM-1 mRNA level and inhibit formation of the ICAM-1 translation initiation complex in human umbilical vein endothelial cells. J Biol Chem 272:11994–12000

44. Seth PP, Siwkowski A, Allerson CA, Vasquez G, Lee S, Prakash TP, Wancewicz EV, Witchell D, Swayze EE (2009) Short antisense oligonucleotides with novel 2′-4′ conformationally restricted nucleoside analogues show improved potency without increased toxicity in animals. J Med Chem 52:10–13

45. Prakash TP, Siwkowski A, Allerson CR, Migawa MT, Lee S, Gaus HJ, Black C, Seth PP, Swayze EE, Bhat B (2010) Antisense oligonucleotides containing conformationally constrained 2′,4′-(N-methoxy)aminomethylene and 2′,4′-aminooxymethylene and 2′-O,4′-C-aminomethylene bridged nucleoside analogues show improved potency in animal models. J Med Chem 53:1636–1650

46. Mori K, Kodama T, Baba T, Obika S (2011) Bridged nucleic acid conjugates at 6′-thiol: synthesis, hybridization properties and nuclease resistances. Org Biomol Chem 9:5272–5279

47. Baba T, Kodama T, Mori K, Imanishi T, Obika S (2010) A novel bridged nucleoside bearing a conformationally switchable sugar moiety in response to redox changes. Chem Commun 46:8058–8060

48. Barrón LB, Waterman KC, Filipiak P, Hug GL, Nauser T, Schöneich C (2004) Mechanism and kinetics of photoisomerization of a cyclic disulfide, trans-4,5-dihydroxy-1,2-dithiacyclohexane. J Phys Chem A 108:2247–2255

49. Barrón LB, Waterman KC, Offerdahl TJ, Munson E, Schöneich C (2005) Reactions of aliphatic thiyl radicals in the solid state: photoisomerization of trans-4,5-dihydroxy-1,2-dithiacyclohexane and oxidation of dithiothreitol. J Phys Chem A 109:9241–9248

50. Shrestha AR, Kotobuki Y, Hari Y, Obika S (2014) Guanidine bridged nucleic acid (GuNA): an effect of a cationic bridged nucleic acid on DNA binding affinity. Chem Commun 50:575–577

51. Rahman SMA, Seki S, Obika S, Yoshikawa H, Miyashita K, Imanishi T (2008) Design, synthesis, and properties of 2′,4′-BNA^NC: a bridged nucleic acid analogue. J Am Chem Soc 130:4886–4896

52. Miyashita K, Rahman SMA, Seki S, Obika S, Imanishi T (2007) N-methyl substituted 2′,4′-BNA^NC: a highly nuclease-resistant nucleic acid analogue with high-affinity RNA selective hybridization. Chem Commun: 3765–3767

53. Rahman SMA, Seki S, Obika S, Haitani S, Miyashita K, Imanishi T (2007) Highly stable pyrimidine-motif triplex formation at physiological pH values by a bridged nucleic acid analogue. Angew Chem Int Ed 46:4306–4309

54. Yamamoto T, Yasuhara H, Wada F, Harada-Shiba M, Imanishi T, Obika S (2012) Superior silencing by 2′,4′-BNA^NC-based short antisense oligonucleotides compared to 2′,4′-BNA/LNA-based apolipoprotein B antisense inhibitors. J Nucleic Acids 2012:707323

55. Yamamoto T, Harada-Shiba M, Nakatani M, Wada S, Yasuhara H, Narukawa K, Sasaki K, Shibata M, Torigoe H, Yamaoka T, Imanishi T, Obika S (2012) Cholesterol-lowering action of BNA-based antisense oligonucleotides targeting PCSK9 in atherogenic diet-induced hypercholesterolemic mice. Mol Ther Nucleic Acids 1:e22

56. Kondo J, Nomura Y, Kitahara Y, Obika S, Torigoe H (2016) The crystal structure of 2′,4′-BNA^NC[N-Me]-modified antisense gapmer in complex with the target RNA. Chem Commun 52:2354–2357

57. Torigoe H, Rahman SM, Takuma H, Sato N, Imanishi T, Obika S, Sasaki K (2011) Interrupted 2′-*O*,4′-*C*-aminomethylene bridged nucleic acid modification enhances pyrimidine motif triplex-forming ability and nuclease resistance under physiological condition. Nucleosides Nucleotides Nucleic Acids 30:63–81

58. Shrestha AR, Hari Y, Yahara A, Osawa T, Obika S (2011) Synthesis and properties of a bridged nucleic acid with a perhydro-1,2-oxazin-3-one ring. J Org Chem 76:9891–9899

59. Hari Y, Osawa T, Kotobuki Y, Yahara A, Shrestha AR, Obika S (2013) Synthesis and properties of thymidines with six-membered amide bridge. Bioorg Med Chem 21:4405–4412

60. Mitsuoka Y, Fujimura Y, Waki R, Kugimiya A, Yamamoto T, Hari Y, Obika S (2014) Sulfonamide-bridged nucleic acid: synthesis, high RNA selective hybridization, and high nuclease resistance. Org Lett 16:5640–5643

61. Mitsuoka Y, Aoyama H, Kugimiya A, Fujimura Y, Yamamoto T, Waki R, Wada F, Tahara S, Sawamura M, Noda M, Hari Y, Obika S (2016) Effect of an *N*-substituent in sulfonamide-bridged nucleic acid (SuNA) on hybridization ability and duplex structure. Org Biomol Chem. https://doi.org/10.1039/c6ob01051b

62. Gryaznov SM, Letsinger RL (1992) Selective O-phophitilation with nucleoside phosphoramidite reagents. Nucleic Acids Res 20:1879–1882

63. Barman J, Gurav D, Oommen OP, Varghese OP (2015) 2′-*N*-Guanidino,4′-*C*-ethylene bridged thymidine (GENA-T) modified oligonucleotide exhibits triplex formation with excellent enzymatic stability. RSC Adv 5:12257–12260

64. Hari Y, Obika S, Ohnishi R, Eguchi K, Osaki T, Ohishi H, Imanishi T (2006) Synthesis and properties of 2′-*O*,4′-*C*-methyleneoxymethylene bridged nucleic acid. Bioorg Med Chem 14:1029–1038

65. Mitsuoka Y, Kodama T, Ohnishi R, Hari Y, Imanishi T, Obika S (2009) A bridged nucleic acid, 2′,4′-BNA[COC]: synthesis of fully modified oligonucleotides bearing thymine, 5-methylcytosine, adenine and guanine 2′,4′-BNA[COC] monomers and RNA-selective nucleic-acid recognition. Nucleic Acids Res 37:1225–1238

66. Morihiro K, Kodama T, Nishida M, Imanishi T, Obika S (2009) Synthesis of light-responsive bridged nucleic acid and changes in affinity with complementary ssRNA. ChemBioChem 10:1784–1788

67. Morihiro K, Kodama T, Obika S (2011) Benzylidene acetal type bridged nucleic acids: changes in properties upon cleavage of the bridge triggered by external stimuli. Chem Eur J 17:7918–7926

68. Kasahara Y, Kitadume S, Morihiro K, Kuwahara M, Ozaki H, Sawai H, Imanishi T, Obika S (2010) Effect of 3′-end capping of aptamer with various 2′,4′-bridged nucleotides: enzymatic post-modification toward a practical use of polyclonal aptamers. Bioorg Med Chem Lett 20:1626–1629

69. Nishida M, Baba T, Kodama T, Yahara A, Imanishi T, Obika S (2010) Synthesis, RNA selective hybridization and high nuclease resistance of an oligonucleotide containing novel bridged nucleic acid with cyclic urea structure. Chem Commun 46:5283–5285

70. Hari Y, Morikawa T, Osawa T, Obika S (2013) Synthesis and properties of 2′-*O*, 4′-*C*-ethyleneoxy bridged 5-methyluridine. Org Lett 15:3702–3705

Synthesis and Therapeutic Applications of Oligonucleotides Containing 2′-*O*,4′-*C*-Ethylene- and 3′-*O*,4′-*C*-Propylene-Bridged Nucleotides

Koji Morita and Makoto Koizumi

Abstract Recently, bridged nucleic acids have come to be more utilized as one of the promising components of therapeutic oligonucleotides. Oligonucleotides containing 2′-*O*,4′-*C*-ethylene-bridged nucleic acid (ENA) have been synthesized as functional oligonucleotides to further optimize the 2′-*O*,4′-*C*-methylene-linkage of bridged nucleic acids (2′,4′-BNA) or locked nucleic acids (LNA). Oligonucleotides containing ENA residues show three notable properties: (i) a high affinity to complementary single-stranded RNA to form duplexes, (ii) a triplex formation with double-stranded DNA, and (iii) a dramatically high resistance compared to 2′,4′-BNA/LNA against exonucleases and endonucleases. On the basis of these properties, ENA-modified oligonucleotides are currently being developed as therapeutics of genetic disorders such as Duchenne muscular dystrophy (DMD). On the other hand, a modified nucleotide containing 3′-*O*,4′-*C*-propylene linkage can be incorporated into the third position of 2′,5′-oligoadenylate (2-5A) to maintain biological activities with nuclease resistance. This modified 2-5A with 3′-*O*,4′-*C*-propylene adenosine could be useful for novel anti-cancer and anti-viral reagents as an RNase L activator.

Keywords 2′-*O*,4′-*C*-ethylene-bridged nucleic acid · 3′-*O*,4′-*C*-propylene-bridged nucleic acid · Locked nucleic acids · Antisense · Triplex-forming oligonucleotides · Exon skipping · Duchenne muscular dystrophy · 2′,5′-oligoadenylate and RNase L

K. Morita · M. Koizumi (✉)
Modality Research Laboratories, Daiichi Sankyo Co., Ltd., Tokyo, Japan
e-mail: koizumi.makoto.h7@daiichisankyo.co.jp

1 Introduction

Applications of antisense oligonucleotides (AONs) and small interfering RNA (siRNA) as research tools for gene validation have been increasing [7]. Moreover, they have the potential of being new modality therapeutics for treatment of cancer, inflammation and genetic diseases. As first generation AONs, phosphorothioate oligodeoxynucleotides (PS ODNs) with nuclease resistance, which are substituted non-bridged oxygens of phosphodiester bonds with sulfur atoms, have been used. PS ODNs are able to be recognized by RNase H when PS ODNs form duplexes with mRNA. However, PS ODNs have some drawbacks, such as reduced affinity to RNA (ΔT_m per modification = $ca.$ −1 °C), inhibition of the blood clotting cascade, immunoactivation, and severe hypotension in vivo.

In order to improve on these drawbacks, numerous oligonucleotide modifications for second and third generation AONs have been reported [5, 7]. As the most potent and promising oligonucleotides, there are oligonucleotides containing nucleotides that are bridged by alkylene linkers such as methylene and ethylene between the 2′-oxygen and 4′-carbon, named as 2′,4′-BNA/LNA [6, 13] and ENA [9, 10], respectively. Synthesis and properties of ENA oligonucleotides for gene modulation as antisense oligonucleotides, exon skipping, triplex-forming oligonucleotides and small interfering RNAs are described below.

As a naturally occurring oligonucleotide, 2′,5′-oligoadenylate 5′-triphosphate (2-5A) is known as an activator of RNase L, which cleaves messenger and ribosomal RNA, resulting in inhibition of protein production in mammalian cells. 2-5A and RNase L play an important role in the 2-5A system that is an interferon-regulated RNA degradation pathway with antiviral, growth-inhibitory, and apoptotic activities in cells [15]. Because natural 2-5A is rapidly degraded by phosphatases and nucleases, it is unstable in cells. When we designed 2-5A analogues containing 3′-O,4′-C-bridged adenosine, they showed RNase L activity with nuclease stability, which would be feasible as novel anti-cancer and anti-viral reagents [11].

1.1 Structural Properties of 2′-**O**,4′-**C**-Ethylene-Bridged Nucleic Acids (ENA) and 2′-**O**,4′-**C**-Propylene-Bridged Nucleic Acids (PrNA) Residues

A nucleoside that is bridged by a methylene linker between the 2′-oxygen and 4′-carbon to form a five-membered ring, has been named as 2′,4′-BNA/LNA. On the other hand, an ethylene-bridge in ENA and a propylene-bridge in 2′-O,4′-C-propylene-bridged nucleic acids (PrNA) forms six- and seven -membered rings, respectively (Fig. 1). Syntheses of ENA and PrNA phosphoramidites for oligonucleotide synthesis are described in the papers cited [9, 10].

Sugar puckering of ENA and PrNA residues were shown to be conformationally restricted to the N-conformation and C3′-$endo$ conformation in the same way as
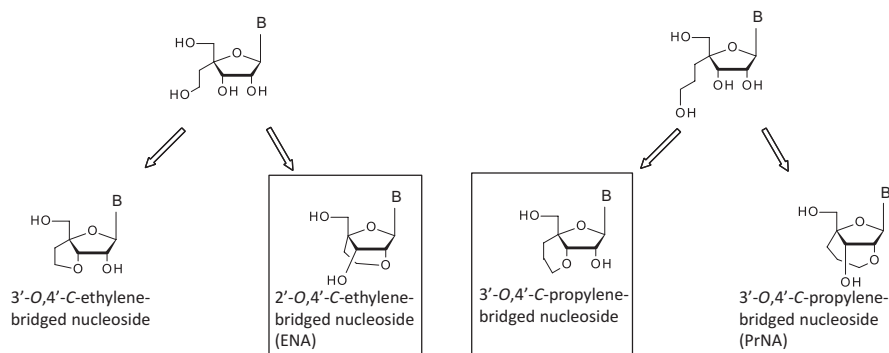
Fig. 1 Structures of 2′-*O*,4′-*C*-alkylene- and 3′-*O*,4′-*C*-alkylene-bridged nucleosides

2′,4′-BNA/LNA from the results of ^{1}H-NMR [10]. Furthermore, X-ray crystal structure analysis of ENA revealed that pseudorotation phase angle *P* values corresponded to typical C3′-*endo* conformations. The differences appeared clearly in the torsion angle δ of C5′-C4′-C3′-O3′, with the mean δ angles of 2′-*O*,4′-*C*-ethylene nucleosides and 2′-*O*,4′-*C*-methylene nucleosides being 77° and 66°, respectively [10]. The mean δ angle of 2′-*O*,4′-*C*-ethylene nucleoside was approximately 11° larger than that of the 2′-*O*,4′-*C*-methylene nucleosides. From the view of overall oligonucleotide structure, this difference in each nucleoside unit might make a large difference in influencing the duplex formations with complementary DNA/RNA and triplex formations with double-stranded DNA.

1.2 Properties of Oligonucleotides Containing ENA and PrNA Residues

Properties of oligonucleotides containing ENA and PrNA residues are summarized in Fig. 2. High affinity towards single-stranded RNA/DNA or double-stranded DNA under physiological pH is one of the important factors for creating biological molecules, such as antisense and antigene molecules. When the melting temperatures of duplexes of oligonucleotides containing ENA residues with complementary DNA or RNA were measured, the ΔT_m values of the duplexes of the oligonucleotides containing ENA residues with complementary RNA or DNA were increased by ca. +5.5°C per modification or + 2.2°C per modification, respectively, which is the similar case for duplexes containing 2′,4′-BNA/LNA [9, 10]. On the other hand, a large decrease in the T_m values of the duplexes of oligonucleotides containing PrNA residues with complementary DNA was observed (−2.0°C per modification), even with complementary RNA (−0.5°C per modification).

Oligopyrimidine nucleotides known as triplex-forming oligonucleotides (TFOs) can bind to the major groove of double-stranded DNA (dsDNA) in parallel with the
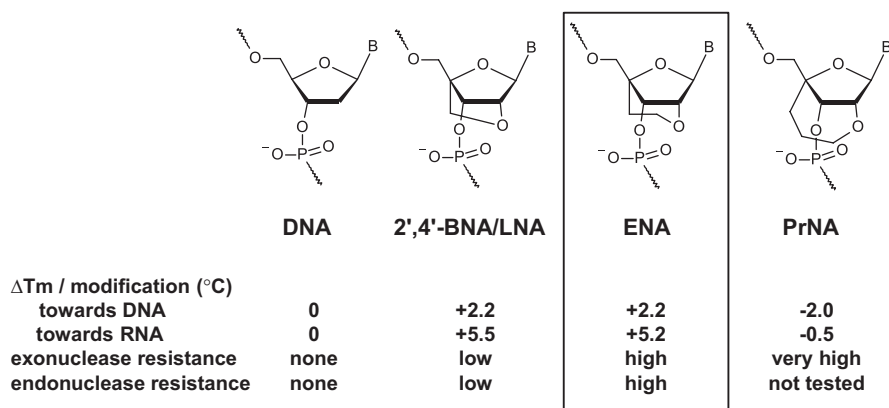
Fig. 2 Properties of oligonucleotides containing DNA, 2′, 4′-BNA/LNA, ENA or PrNA residues

Table 1 Summary of triplex formation of DNA duplex with natural TFO or modified TFO containing 5-methylcytosine from the data of references [4, 14]

Modified nucleotides	Modification pattern	Triplex formation	
		pH 6.6	pH 7.2
DNA	–	No	No
2′,4′-BNA/LNA	Partial	Yes	Yes
	Full	No	No
ENA	Partial	Yes	Yes
	Full	Yes	Yes

purine strand of dsDNA to form complexes, which are known as triplexes. The adenine of an A:T base pair in dsDNA can form hydrogen bonds with thymine in oligopyrimidine nucleotides as the third strand in a Hoogsteen fashion. On the other hand, the guanine of a G:C base pair of dsDNA needs the *N*-3 protonated cytosine or 5-methylcytosine under an acidic condition to make stable triplexes. When oligopyrimidine nucleotides that were partially modified with ENA residues as TFO were used, we determined from the data of the UV melting analysis, gel shift assay, CD spectral analysis and restriction enzyme inhibition that they could form a triplex with dsDNA at a physiological pH (Table 1, [4, 14]). Moreover, the oligonucleotide fully modified with ENA was found to be favorable in forming the triplex at a physiological pH, although no triplex was formed with fully modified 2′,4′-BNA/LNA.

Another factor that required caution in the design of AONs and TFOs is that oligonucleotides containing modified nucleosides were stable against nucleases. When stability of oligonucleotides containing 2′,4′-BNA/LNA, ENA or PrNA residues were compared, oligonucleotides containing ENA residues were much more stable than those containing 2′,4′-BNA/LNA against both exonucleases and endonucleases (Table 1, [9, 10]). Moreover, an oligonucleotide containing a PrNA resi-

due was the most stable of all the tested compounds in the paper, maybe due to the blockage of the phosphorodiester bond at the 3′-side of the nucleoside by the propylene-bridge of PrNA [10]. Dual-modification of the ENA residue and phosphorothioate bond indicated a stability identical to the modification with PrNA. Continuous modification with ENA residues increased stability against exonucleases. Indeed, an oligonucleotide modified with some ENA residues at both the 3′- and 5′-ends and phosphorothioated DNA in the center was completely stable under a condition of almost 100% of rat plasma [11]. These results encouraged us to incorporate ENA residues into oligonucleotides to create nuclease-resistant AONs and TFOs.

1.3 Therapeutic Applications of Oligonucleotides Containing ENA Residues

Currently, potential ENA oligonucleotides for treatment of Duchenne muscular dystrophy (DMD) have been found [17, 20]. One of such oligonucleotides induces exon 45 skipping in the pre-mRNA splicing reaction of a mutated dystrophin gene (one with an exon 44 deletion) to create a dystrophin protein that is incomplete but functional [18]. A clinical trial of the ENA oligonucleotide on a group of DMD patients for whom it is anticipated to prove effective was begun in early 2016 in Japan (ClinicalTrials.gov Identifier: NCT02667483).

1.4 The Development of Novel 2-5A Analogs Containing 3′-O,4′-C-Alkylene-Bridged Nucleosides as a Therapeutic Reagent

Nucleosides that are bridged by an ethylene or propylene linker between 3′-oxygen and 4′-carbon form five- or six-membered rings as shown in Fig. 1. As we previously reported in the literature [12], the novel 2-5A analog **1** (Fig. 3) was found to be the most potent RNase L agonist with RNase L activity as high as unmodified 2-5A and a high resistance to enzymatic degradation. In designing 2-5A analog **1**, the 3′-O,4′-C-propylene adenosine was the key unit for stabilizing 2-5A structure against nuclease degradation while retaining the same RNase L agonistic activity as unmodified 2-5A. In the following chapter, we describe the details of the synthesis of the 3′-O,4′-C-propylene adenosine unit and 2-5A analog **1.** And also we report the cell activity of **1,** which demonstrates that **1** can work as a potent RNase L agonist in cells without any transfection assistance.
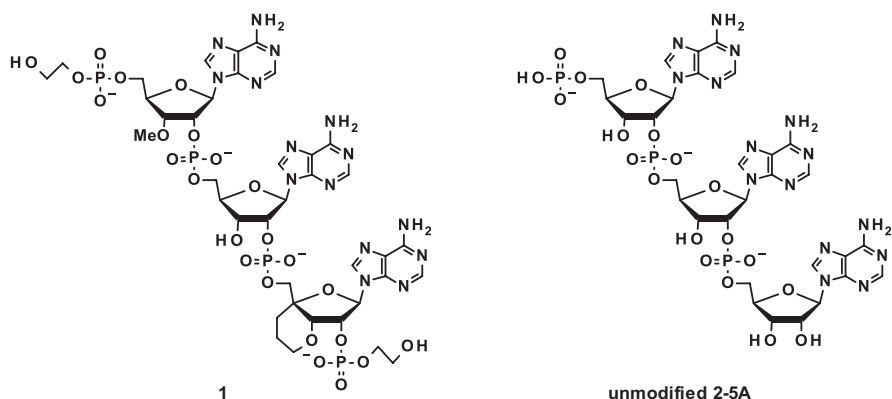
Fig. 3 Structure of novel 2-5A analog **1** and unmodified 2-5A
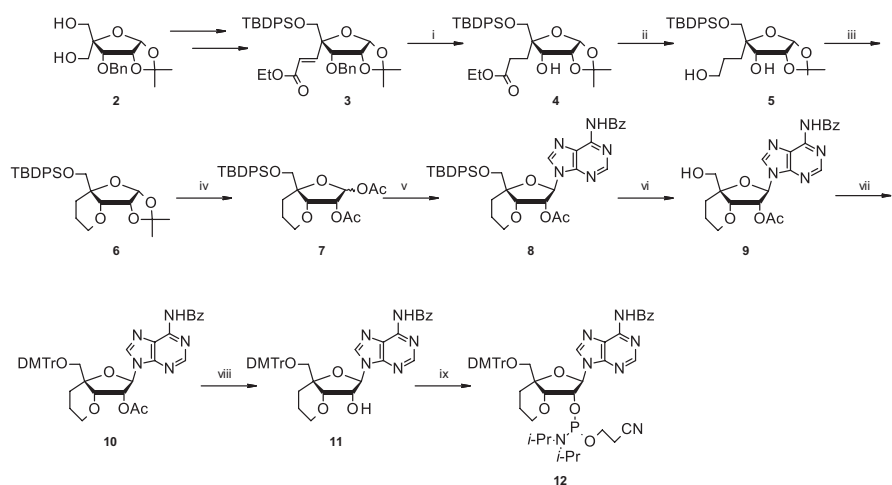
Scheme 1 (i) Pd(OH)$_2$, H$_2$ (4 MPa), AcOEt, 71%; (ii) L-selectride, THF, 90%; (iii) TsCl, Et$_3$N, CH$_2$Cl$_2$ then LHMDS, THF, 83%; (iv) Ac$_2$O, H$_2$SO$_4$, AcOH, 91%; (v) silylated *N*-benzoyladenine, TMSOTf, toluene, reflux, 81%; vi) TBAF, THF, 90%; (vii) DMTrOTf, pyridine, CH$_2$Cl$_2$, 92%; (viii) 1 M NaOH, pyridine–H$_2$O, 71%; (ix) ((*i*Pr)$_2$N)$_2$P(OC$_2$H$_4$CN), *N,N*-diisopropylammonium tetrazolide, CH$_2$Cl$_2$, 98%

1.5 Synthesis of 3'-**O**,4'-**C**-Propylene Adenosine as the Potent Modified Unit for 2-5A Analog

3'-*O*,4'-*C*-propylene adenosine, the original modified adenosine unit for **1**, was synthesized according to Scheme 1. Swern oxidation and chain extension by Horner–Wadsworth–Emmons olefination of 4-*C*-hydroxymethyl pentofuranose derivative **2** furnished the (*E*)-enoate **3** as reported previously [10]. Pd(OH)$_2$-catalyzed reduction afforded both olefin hydrogenation and debenzylation of **3**, and

the following reduction using L-selectride led to 4-hydroxypropyl furanose derivative **5**. Tosylation of **5** followed by base treatment afforded 3-*O*,4-*C*-propylene furanose **6**. After acetolysis of **6**, the compound **7** was coupled with silylated *N*-benzoyl adenine to afford fully protected 3′-*O*,4′-*C*-propylene adenosine **8**. By the exchange of 5′-protecting group to DMTr and subsequent 3′-phosphitylation, the 3′-*O*,4′-*C*-propylene adenosine phosphoramidite **12** was synthesized as a 2-5A analog synthesis unit.

1.6 Synthesis of 2-5A Analog 1 Using DNA/RNA Autosynthesizer

2-5A analog **1** was synthesized by solid-phase phosphoramidite chemistry using an automated DNA/RNA synthesizer (Scheme 2). Controlled pore glass (CPG) solid support bearing hydroxyethyl group **13** was prepared according to the literature [3]. To the CPG, the sequential coupling of the 3′-*O*,4′-*C*-propylene adenosine phosphoramidite **12,** adenosine phosphoramidite **14** (ChemGenes Corporation), 3′-*O*-methyl adenosine phosphoramidite **15** (ChemGenes Corporation) and 2-(4,4′-Dimethoxytrityloxy) ethyl-1-phosphoramidite **16** [8] was performed according to standard synthesis cycles except for an elongation of the coupling time (15 min). Each coupling step was followed by oxidation and detritylation with the normal conditions used in a DNA/RNA synthesizer. After synthesis in the DMTr-on mode in the DNA/RNA synthesizer, the CPG with the attached fully protected 2-5A
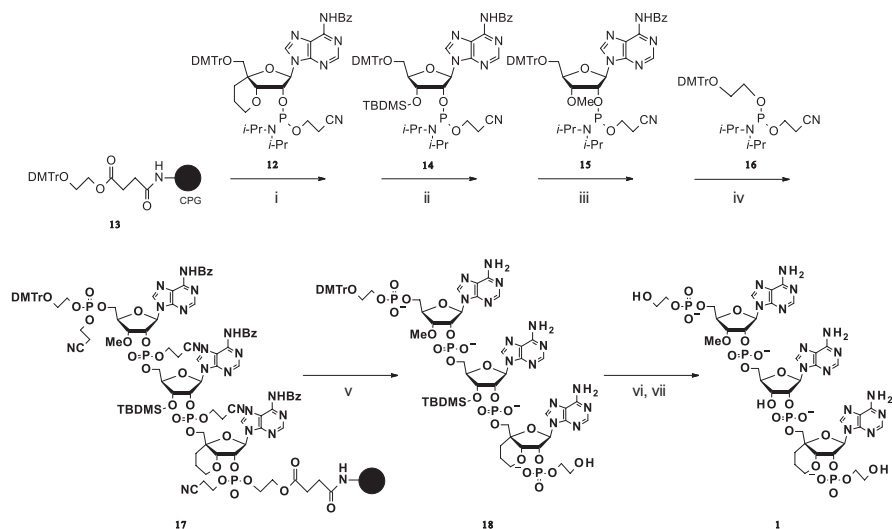

Scheme 2 (i) to (iv) *a*. Trichloroacetic acid, CH_2Cl_2, 85 s; *b*. phosphoramidite, tetrazole, CH_3CN, 15 min; *c*. acetic anhydride, 1-methylimidazole, pyridine, THF, 15 s; *d*. I_2, H_2O, THF, 15 s; (v) aq.ammonia, EtOH (4:1 v/v), 60°C; vi) 80% CH_3COOH; vii) aq.HCl (pH 2), 30°C

analog **17** was treated with concentrated aqueous ammonia and EtOH (4:1 v/v) solution at 60°C for 5 h to cleave 2-5A from CPGs and to deprotect the cyanoethyl and benzoyl group. The DMTr-on compound **18** was purified by reverse phase HPLC (RP HPLC). Then the DMTr group was removed by the treatment of 80% acetic acid for 30 min at room temperature. The pH of the solution was then set to pH 2 by adding 2 N HCl and the solution was incubated at 30 °C for 5 h to remove the 2′-*O*-TBDMS group and give fully de-protected **1**. The final product **1** was further purified by RP HPLC. The purity of **1** was confirmed as 99% by RP HPLC. The molecular weight was confirmed by negative-ion FAB ([M-H]$^-$ = 1226).

1.7   *In* Vitro *Activity of 2-5A Analog 1 in Cancer Cells*

We examined intracellular activity of 2-5A analog **1** in a cell assay. At first, we evaluated the cytotoxicity of **1** and unmodified 2-5A in human lung cancer carcinoma cell line A549 without using any transfection reagents. As the result, **1** showed a cytotoxicity in A549 cells in a dose-dependent manner while unmodified 2-5A did not show any cytotoxicity even at a high dose of 60 μM (Fig. 4A). On the other hand, the cytotoxicity of **1** was not observed in human liver cancer carcinoma cell line HepG2, which is deprived of RNase L expression (Fig. 4B, [19]). Next, we examined the RNA degradation activity caused by RNase L activation inside cells. Native 2-5A and phosphorothioated 2-5A are reported to show rRNA degradation via RNase L activation in cases where they have been efficiently delivered inside of cells by using transfection reagents. The rRNA degradation pattern in A549 cells caused by **1** treatment was well-similar to the pattern already reported (Fig. 5, [16]). In HepG2 cells lacking RNase L expression, rRNA degradation was not observed by the treatment of **1**. These results indicated that the 2-5A analog 1 was taken into cells without being decomposed by nuclease and phosphatase in the serum-containing medium and it exhibited the cytotoxicity against RNase L-positive
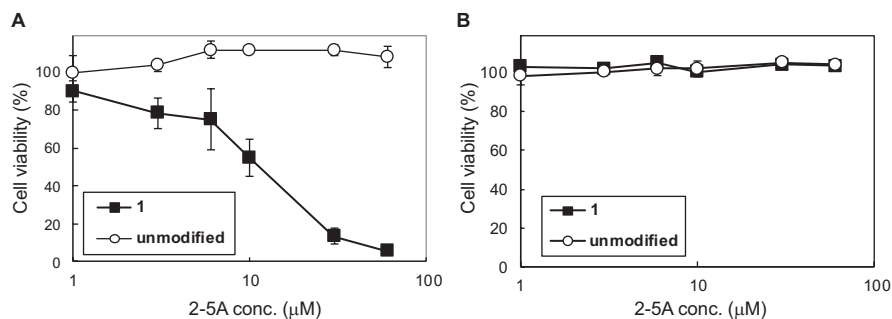
Fig. 4 The cytotoxicity of 2-5A analog **1** in cancer cells (**a**: A549 cells, **b**: HepG2 cells) 2-5A analog **1** and unmodified 2-5A was added into cell medium at 1, 3, 6, 10, 30 and 60 μM. In 72 h, ATP amount in the well was measured as the number of viable cells
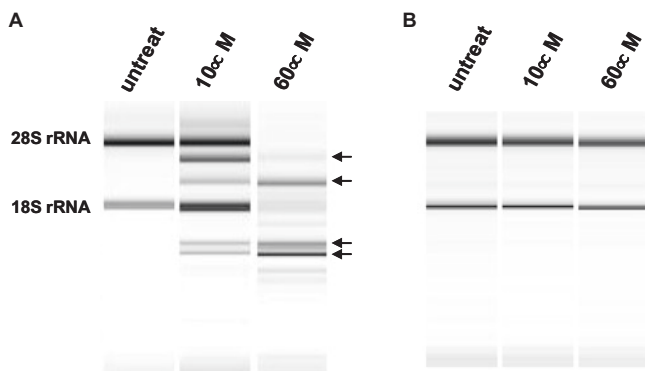
Fig. 5 Intracellular rRNA degradation pattern of (**a**) A549 cells and (**b**) HepG2 cells induced by RNase L activated by **1**. **1** was added into cell medium at 10 or 60 μM. In 24 h, total RNA was extracted from cells and analyzed by gel electrophoresis

cancer cells by activating RNase L, while unmodified 2-5A was subject to degradation and did not work. It is anticipated that **1** would be a good tool for investigating the biological function of RNase L in the 2-5A system and the therapeutic drug for 2-5A system's relevant diseases such as viral infections, cancer and chronic fatigue syndrome [1, 2]. In *vivo* activity of **1** is under investigation.

References

1. Bisbal C, Silverman RH (2007) Diverse functions of RNase L and implications in pathology. Biochimie 89:789–798
2. Chakrabarti A, Jha BK, Silverman RH (2011) New insights into the role of RNase L in innate immunity. J.Interferon Cytokine Res 31:49–57
3. Koizumi M, Koga R, Hotoda H et al (1997) Biologically active oligodeoxyribonucleotides–IX. Synthesis and anti-HIV-1 activity of hexadeoxyribonucleotides, TGGGAG, bearing 3′- and 5′-end-modification. Bioorg Med Chem 5:2235–2243
4. Koizumi M, Morita K, Daigo M et al (2003) Triplex formation with 2′-*O*,4′-*C*-ethylene-bridged nucleic acids (ENA) having C3′-endo conformation at physiological pH. Nucleic Acids Res 31:3267–3273
5. Koizumi M (2007) True antisense oligonucleotides with modified nucleotides restricted in the N-conformation. Curr Top Med Chem 7:661–665
6. Koshkin AA, Singh SK, Nielsen P et al (1998) LNA (locked nucleic acids): synthesis of the adenine, cytosine, guanine, 5-methylcytosine, thymine and uracil bicyclonucleoside monomers, oligomerisation, and unprecedented nucleic acid recognition. Tetrahedron 54:3607
7. Kurreck J (2003) Antisense technologies. Improvement through novel chemical modifications. Eur J Biochem 270:1628–1644
8. Lin P, Ganesan A (1998) Solid-phase synthesis of peptidomimetic oligomers with a phosphodiester backbone. Bioorg Med Chem Lett 8:511–514
9. Morita K, Hasegawa C, Kaneko M et al (2002) 2′-O,4′-C-ethylene-bridged nucleic acids (ENA): highly nuclease-resistant and thermodynamically stable oligonucleotides for antisense drug. Bioorg Med Chem Lett 12:73–76

10. Morita K, Takagi M, Hasegawa C et al (2003) Synthesis and properties of 2′-*O*,4′-*C*-ethylene-bridged nucleic acids (ENA) as effective antisense oligonucleotides. Bioorg Med Chem 11:2211–2226
11. Morita K, Yamate K, Kurakata S et al (2006) Inhibition of VEGF mRNA by 2′-O,4′-C-ethylene-bridged nucleic acids (ENA) antisense oligonucleotides and their influence on off-target gene expressions. Nucleosides Nucleotides Nucleic Acids 25:503–521
12. Morita K, Kaneko M, Obika S et al (2007) Biologically stable 2-5A analogues containing 3′-*O*,4′-*C*-bridged adenosine as potent RNase L agonists. ChemMedChem 2:1703–1707
13. Obika S, Nanbu D, Hari Y et al (1997) Synthesis of 2′-*O*,4′-*C*-methyleneuridine and -cytidine. Novel bicyclic nucleosides having a fixed C3′-endo sugar puckering. Tetrahedron Lett 38:8735–8738
14. Obika S, Uneda T, Sugimoto T et al (2001) 2′-*O*,4′-*C*-Methylene bridged nucleic acid (2′,4′-BNA): synthesis and triplex-forming properties. Bioorg Med Chem 9:1001–1011
15. Player MR, Torrence PF (1998) The 2-5A system: modulation of viral and cellular processes through acceleration of RNA degradation. Pharmacol Ther 78:55–113
16. Rusch L, Zhou A, Silverman RH (2000) Caspase-dependent apoptosis by 2′, 5′-oligoadenylate activation of RNase L is enhanced by IFN-beta. J Interf Cytokine Res 20:1091–1100
17. Surono A, Van Khanh T, Takeshima Y et al (2004) Chimeric RNA/ethylene-bridged nucleic acids promote dystrophin expression in myocytes of duchenne muscular dystrophy by inducing skipping of the nonsense mutation-encoding exon. Hum Gene Ther 15:749–757
18. Takagi M, Yagi M, Ishibashi K et al (2004) Design of 2′-*O*-Me RNA/ENA chimera oligonucleotides to induce exon skipping in dystrophin pre-mRNA. Nucleic Acids Symp Ser 48:297–298
19. Tnani M, Bayard BA (1998) Lack of 2′,5′-oligoadenylate-dependent RNase expression in the human hepatoma cell line HepG2. Biochim Biophys Acta 1402:139–150
20. Yagi M, Takeshima Y, Surono A et al (2004) Chimeric RNA and 2′-O, 4′-C-ethylene-bridged nucleic acids have stronger activity than phosphorothioate oligodeoxynucleotides in induction of exon 19 skipping in dystrophin mRNA. Oligonucleotides 14:33–40

RNA Bioisosteres: Chemistry and Properties of 4′-thioRNA and 4′-selenoRNA

Check for updates

Noriaki Minakawa, Noriko Saito-Tarashima, and Akira Matsuda

Abstract The design and synthesis of nucleic acid-based therapeutics is one of the most promising approaches to drug development and disease therapy. In order to develop agents with improved nuclease resistance and hybridization ability, a large number of chemically modified oligonucleotides (ONs), especially RNA analogs, have been designed and prepared. However, this has led to ONs with overly complex structures, resulting in a lack of biocompatibility with natural RNA. With this in mind, 4′-thioRNA, which has a sulfur atom in place of the furanose ring oxygen, was proposed as a natural RNA bioisostere. The building blocks for 4′-thioRNA, i.e., 4′-thioribonucleosides, were prepared stereoselectively via the Pummerer reaction between a silylated nucleobase and the corresponding sulfoxide, which was obtained from a 4-thiosugar. The resulting 4′-thioRNA exhibited sufficient hybridization ability and nuclease resistance, as well as biocompatibility with natural RNA, and was used effectively as a chemically modified siRNA and for isolation of 4′-thioRNA aptamers. Current progress in the development of a new RNA bioisostere 4′-selenoRNA, which contains a selenium atom, is also described.

Keywords RNA bioisostere · RNA analog · 4′-thioRNA · 4′-selenoRNA · RNA interference · SiRNA · RNA aptamer

N. Minakawa (✉) · N. Saito-Tarashima
Graduate School of Pharmaceutical Science, Tokushima University, Tokushima, Japan
e-mail: minakawa@tokushima-u.ac.jp

A. Matsuda
Center for Research and Education on Drug Discovery, Faculty of Pharmaceutical Sciences, Hokkaido University, Sapporo, Japan

1 Introduction

The development of nucleic acid-based therapeutics, such as antisense [20], short-interfering RNA (siRNA) [23], anti-microRNA (anti-miRNA) [6], and aptamers identified by systematic evolution of ligands by exponential enrichment (SELEX) [15] is one of the most promising approaches to drug development. Therefore, the design and synthesis of chemically modified oligonucleotides (ONs), especially RNA analogs, is a highly active area of research. Since the instability of natural RNA comes from the presence of the 2′-hydroxyl group in its structure, substitution or protection of the 2′-hydroxyl group is considered an effective strategy for the development of stable RNA analogs. 2′-FluoroRNA and 2′-O-methylRNA are typical RNA analogs and have been thoroughly investigated in the development of nucleic acid-based therapeutics [24, 47]. Furthermore, locked nucleic acid/bridged nucleic acid (LNA/BNA) is also regarded as one of the most promising RNA analogs [10, 42]. Because of the favorable properties (i.e., high hybridization ability and nuclease resistance) and biological activities of these RNA analogs, much attention has been paid to the development and evaluation of further RNA analogs based on 2′-O-methylRNA and LNA/BNA. For example, a variety of alkyl groups have been introduced at the 2′-hydroxyl group to give 2′-O-alkylated RNAs, and their properties and potentials as therapeutic agents have been examined [21, 33]. The development of LNA/BNA related analogs has also been intensely investigated [29, 43]. Such modifications generally provide enhanced hybridization ability and nuclease resistance, and thus, some of these have been clinically applied as antisense drugs and aptamers [28, 41]. However, these modifications lead to complicated structures that lack biocompatibility with natural RNA, which restricts the scope of application of the resulting RNA analogs as nucleic acid-based therapeutics.

Consequently, we have attempted to develop an RNA analog that exhibits biocompatibility with natural RNA, as well as hybridization ability and nuclease resistance. In medicinal chemistry, substitution of a certain atom in a molecule with another atom belonging to same group in the periodic table is a well-known strategy for the development of new agents that show similar biocompatibilities to those of the parent molecules. Accordingly, we have focused on 4′-thioRNA, which has a sulfur atom in place of the furanose ring oxygen. More than two decades ago, Imbach and coworkers first reported the synthesis of 4′-thioRNAs consisting of 4′-thiouridine [1], and 4′-thiouridine, -cytidine, and -adenosine [22]. Investigation of their properties revealed that 4′-thioRNAs form more thermally stable duplexes with their complementary natural RNAs than the corresponding natural RNAs, and that they hybridize more tightly to natural RNA than to natural DNA. Moreover, the 4′-thioRNAs showed high resistance to both exonucleases and endonucleases. However, despite the favorable properties of 4′-thioRNAs, no further investigation of these molecules has been reported owing to the difficulty in efficiently synthesizing the 4′-thioribonucleoside units. Consequently, we started this project with the development of a practical stereoselective synthesis of 4′-thioribonucleoside units, and then reevaluated the properties of 4′-thioRNA with an aim toward developing a new generation of artificial RNA analogs.

Fig. 1 Structures of
4′-thioRNA and
4′-selenoRNA
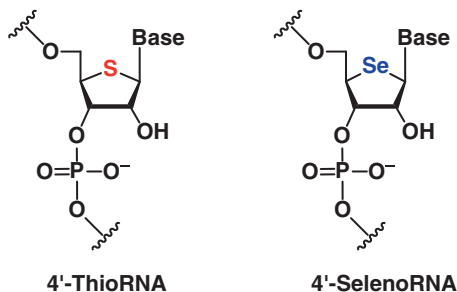
In this chapter, we present our research on the development of the RNA bioisostere 4′-thioRNA, and its properties and biological applications. In addition, the current progress in the development of the new RNA bioisostere 4′-selenoRNA, which contains a selenium atom in place of the furanose ring oxygen, is also described (Fig. 1).

2   Chemistry and Properties of 4′-thioRNA

2.1   *Stereoselective Synthesis of 4'-thioribonucleosides*

In 1964, 4′-thioadenosine was synthesized as the first example of this class of compound [34]. Although further examples were reported [2], research in this area declined due to unfavorable results in the biological evaluation of 4′-thionucleoside units and difficulties in devising an efficient preparation of 4′-thioribonucleosides. In general, the desired 4′-thioribonucleosides had been synthesized by classical thioglycosidation of the corresponding 4-thiosugars and nucleobases. However, unlike in the normal glycosidation between a ribofuranose derivative and a nucleobase, the stereocontrol in this thioglycosidation was unsatisfactory, even with the assistance of the neighboring *C*-2 acetoxy group. To better understand the differences between furanose and thiofuranose derivatives, computational studies on oxo- and thiocarbonium intermediates were performed [27]. As a result, it was suggested that the net atom charges at the α-position are quite different in furanose and thiofuranose derivatives, implying that thiocarbonium intermediates are less susceptible to neighboring group effects than oxocarbonium intermediates. Based on these theoretical considerations, we developed an alternative synthetic method based on the Pummerer reaction between a nucleobase and a sulfoxide derived from a 4-thiosugar [26].

As shown in Scheme 1, the best result was obtained when (*R*)-sulfoxide **1** having a 2,4-dimethoxybenzoyl (DMBz) group on its 2-position was subjected to the Pummerer reaction in the presence of silylated uracil or N4-acetylcytosine to give the respective 4′-thiouridine and 4′-thiocytidine derivatives **2** and **3** stereoselectively. Unlike in reactions with pyrimidine bases, the formation of regioisomers,
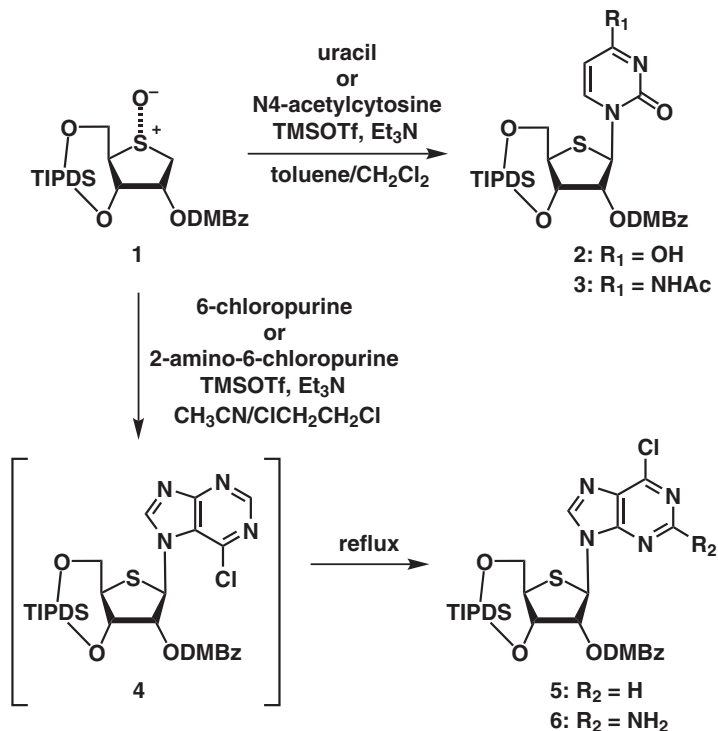
Scheme 1 Synthesis of 4′-thioribonucleoside derivatives

i.e., N7 and N9 isomers, must be considered for reactions with purine bases. When the Pummerer reaction of **1** in the presence of silylated 6-chloropurine was performed at room temperature, the N7-6-chloropurine derivative **4**, which is a kinetically controlled product, was obtained in moderate yield along with a trace amount of the desired N9-6-chloropurine derivative **5**. In order to improve the formation of **5**, the reaction conditions were investigated and optimized. As a result, the desired **5** was obtained in 65% yield upon treatment of **1** with silylated 6-chloropurine in a mixture of acetonitrile and dichloroethane under reflux. In a similar manner, the Pummerer reaction of **1** with silylated 2-amino-6-chloropurine afforded the desired N9 isomer **6** in 56% yield. The products **2**, **3**, **5**, and **6** were all converted into the corresponding phosphoramidite units for 4′-thioRNA synthesis.

2.2 Synthesis and Properties of 4'-thioRNA

Using the phosphoramidite units prepared above, fully modified 4′-thioRNAs containing four kinds of 4′-thioribonucleoside units were prepared according to the standard RNA synthesis techniques. Prior to the ON synthesis, it was thought that

oxidation of the 4′-sulfur atoms in the growing ON into the corresponding sulfoxides via oxidation with I_2 could be a possible problem under standard ON synthesis conditions. However, this was not observed, and the desired ONs were prepared in good yields [8]. It is noteworthy that this is in marked contrast with the 4′-selenoRNA synthesis described in Sect. 4.2.

Using the fully modified 4′-thioRNAs (**SRNA1** and **SRNA2**) prepared, thermal and thermodynamic stabilities of a series of duplexes were evaluated using UV melting and differential scanning calorimetry (DSC) measurements in a buffer of 10 mM Na cacodylate (pH 7.0) containing 10 mM NaCl (Table 1). The duplexes consisting of natural RNA and DNA, namely **RNA1:RNA2** and **RNA1:DNA1**, had T_m values of 55.8 °C and 40.2 °C, respectively. When **RNA1** was changed to **SRNA1**, the corresponding T_m values changed depending on the complementary sequences. Thus, the duplex of **SRNA1:RNA2** showed a higher T_m value than that of **RNA1:RNA2** (63.4 °C vs. 55.8 °C), while the duplex of **SRNA1:DNA1** had a lower T_m value than that of **RNA1:DNA1** (28.4 °C vs. 40.2 °C). Furthermore, a drastic enhancement in thermal stability was observed for the **SRNA1:SRNA2** duplex (T_m = 89.6 °C). The overall order of thermal stability for the duplexes examined was **SRNA1:SRNA2** >> **SRNA1:RNA2** > **RNA1:RNA2** > **RNA1:DNA1** > **SRNA1:DNA1**. As described in the introduction, 2′-fluoroRNA, 2′-O-methylRNA, and LNA/BNA have been developed as RNA analogs. Although these RNA analogs exhibit excellent hybridization with complementary RNAs, their duplex formation with complementary DNAs is also thermally stabilized [45]. However, unlike these RNA analogs, the 4′-thioRNAs presented here exhibited a significant preference for RNA over DNA as a complementary partner in duplex formation. In addition, the particularly high thermal stability of the 4′-thioRNA:4′-thioRNA duplex should be noted.

The thermodynamic parameters obtained by DSC measurements are also shown in Table 1. In the case of duplex formation with RNA (**RNA1:RNA2** vs. **SRNA1:RNA2**), the effect of substitution of **SRNA1** increased the stability of the duplex. This substitution provided a more favorable enthalpy of formation but less favorable entropy of formation, with the net result being an increase in the stability

Table 1 Thermal and thermodynamic stabilities of 4′-thioRNA

| Duplex | UV melting | DSC | | |
	T_m (°C)	$\Delta H°$ (kcal mol^{-1})	$\Delta S°$ (cal mol^{-1} K^{-1})	$\Delta G°$ (37 °C) (kcal mol^{-1})
RNA1:RNA2	55.8	−85.2	−263.2	−3.58
SRNA1:RNA2	63.4	−100.8	−299.4	−7.90
SRNA1:SRNA2	89.6	−126.9	−350.8	−18.1
RNA1:DNA1	40.2	−87.8	−279.5	−0.98
SRNA1:DNA1	28.4	−61.7	−200.8	3.31

Thermal and thermodynamic stabilities of a series of duplexes were evaluated in a buffer of 10 mM Na cacodylate (pH 7.0) containing 10 mM NaCl. The sequence of a series of RNA1 is 5′-AGUCCGAAUUCACGU-3′ and a series of RNA2 is 5′-ACGUGAAUUCGGACU-3′. The sequence of DNA1 is 5′-ACGTGAATTCGGACT-3′

of the duplex. Therefore, this increase in stability is the result of the more favorable enthalpic contribution. The same general result was also observed for formation of the **SRNA1**:**SRNA2** duplex. However, in the case of duplex formation with DNA (**RNA1**:**DNA1** vs. **SRNA1**:**DNA1**), the same substitution gave rise to an unfavorable contribution to the enthalpy of formation, while affecting the entropy in a favorable manner. The net result of this substitution was a decrease in the stability of the duplex. This reduction in stability is the result of the more unfavorable enthalpic contribution. Although the enthalpic and entropic contributions were opposite for RNA and DNA, the factor dominating the stability of duplexes containing 4′-thioRNA was enthalpic in character.

Since the structure of 2′-fluoroRNA lacks the 2′-hydroxy groups, this RNA analog is resistant against ribonuclease (RNase) digestion [30]. However, 2′-fluoroRNA is degraded as rapidly as natural DNA in calf serum, probably as a result of 3′-exonuclease activity [18]. 2′-*O*-MethylRNA is also highly resistant to RNase digestion owing to methylation of the 2′-hydroxy groups. Furthermore, 2′-*O*-methylRNA shows higher stabilities to snake venom phosphodiesterase (SVPD; a typical 3′-exonuclease) and S1 nuclease (a typical endonuclease) compared to those of natural DNA [4]. The preliminary results reported by Imbach and coworkers also indicated that 4′-thioRNA is highly resistant against not only 3′-exonuclease, but also endonuclease, despite possessing a 2′-hydroxy group in its structure. However, no comprehensive comparison of their nuclease stabilities has been reported. Accordingly, a comprehensive comparison of the nuclease stabilities of single-stranded **SRNA1** along with 2′-fluoroRNA (**FRNA1**), 2′-*O*-MeRNA (**MeRNA1**), and natural **RNA1** and **DNA1** was performed, and the results are summarized in Table 2.

A series of RNA analogs labeled at the 5′-end with ^{32}P were incubated in appropriate buffers with S1 nuclease, SVPD, and human plasma. Each reaction was then analyzed using polyacrylamide gel electrophoresis (PAGE) under denaturing conditions, and the half-lives ($t_{1/2}s$) were estimated based on the full-length RNA contents at each time interval. In the presence of S1 nuclease, **RNA1** and **DNA1** were both rapidly cleaved to give $t_{1/2}$ values of <1 min. To our surprise, **FRNA1** was also immediately cleaved, while **MeRNA1** was completely stable ($t_{1/2} > 24$ h) under the same conditions. The **SRNA1** showed moderate stability with a $t_{1/2}$ of 76.8 min,

Table 2 Comparison of the nuclease stabilities of different RNA analogs

ON	S1 nuclease $t_{1/2}$	SVPD $t_{1/2}$	50% human plasma $t_{1/2}$	Degradation pattern
RNA1	25.4 s	6.0 min	<10 s	Endo
DNA1	7.4 s	3.1 min	46.8 min	Exo
FRNA1	1.1 min	5.8 min	53.2 min	Exo
MeRNA1	>24 h	5.3 min	187 min	Exo
SRNA1	76.8 min	54.4 min	65.7 min	Endo
MeSRNA1	>24 h	79.2 min	1631 min	Exo

Each sample labled with ^{32}P at the 5′-end was treated with S1 nuclease, SVPD and 50% human plasma, and the reaction was analyzed by electrophoresis on 20% PAGE. The sequence of ON1 is 5′-AGUCCGAAUUCACGU-3′

which was much higher than that of **FRNA1**. Thus, the rank order of S1 nuclease resistance was **MeRNA1** >> **SRNA1** > **FRNA1** > **RNA1** > **DNA1**. For the stability against SVPD, both natural sequences (**RNA1** and **DNA1**) and the 2′-modified RNA analogs (**MeRNA1** and **FRNA1**) were cleaved to give $t_{1/2}$ values of <10 min, while **SRNA1** was more stable ($t_{1/2}$ = 54.4 min). Thus, the rank order of SVPD resistance was **SRNA1** > **MeRNA1**, **FRNA1**, **RNA1,** and **DNA1**, implying that 2′-modification has no effect upon 3′-exonuclease resistance, while 4′-modofication affords 3′-exonuclease resistance. To evaluate the overall stability of the RNA analogs, they were incubated in 50% human plasma. Under these conditions, **RNA1** was rapidly cleaved ($t_{1/2}$ < 10 sec), while **DNA1** was much more stable ($t_{1/2}$ = 46.8 min). **SRNA1** was relatively stable, and was slightly more stable than **FRNA1** ($t_{1/2}$ = 65.7 min vs. 53.2 min). Among these sequences, **MeRNA1** was the most stable ($t_{1/2}$ = 187 min), with the rank order of stability in human plasma being **MeRNA1** > **SRNA1** > **FRNA1** > **DNA1** >> **RNA1**. Since human plasma contains multiple nucleases, the predominant nuclease activity for degradation was estimated based on the PAGE results. The results indicated that **SRNA1** was digested by endonuclease activity such as RNase, much like **RNA1**, because of the existence of the 2′-hydroxy groups. However, both **MeRNA1** and **FRNA1** afforded fragments corresponding to n-1 and n-2 (where n = full length), and thus their degradations occurred by exonuclease activity.

The higher stability in human plasma of 4′-thioRNA, despite possessing 2′-hydroxyl groups in its structure, is worth noting. Furthermore, the highest stability of 4′-thioRNA against SVPD is also an attractive feature. These results prompted us to develop a new 4′-thioRNA analog imbued with further nuclease stability. Thus, a hybrid chemical modification based on a combination of those in 4′-thioRNA and 2′-*O*-MeRNA was performed, resulting in 2′-*O*-methyl-4′-thioRNA (**MeSRNA1**). As expected, **MeSRNA1** showed a synergistic improvement against not only endonuclease ($t_{1/2}$ > 24 h), but also exonuclease ($t_{1/2}$ = 79.2 min), and was thus extremely stable in human plasma ($t_{1/2}$ = 1631 min). Details of the chemistry, properties, and biological applications of hybrid-type modified RNAs are reviewed elsewhere [35–38].

3   Biological Applications of 4′-thioRNA

As described above, 4′-thioRNA exhibited sufficient hybridization ability and nuclease resistance, which are the minimum requirements in the development of artificial RNA analogs. In addition, this RNA analog was expected to show biocompatibility with natural RNA, as its structure bears a minimum of chemical modification. Accordingly, utilization of 4′-thioRNA to induce RNA interference (RNAi) triggered by siRNA was thought to be an ideal strategy for its potential therapeutic application. Furthermore, isolation of 4′-thioRNA aptamers, which would be thermally and biologically stable than natural RNA aptamers, by SELEX was also thought to be a viable strategy, because the corresponding nucleoside

5′-triphosphates have to be recognized by RNA polymerases effectively. Consequently, the biological applications of 4′-thioRNA as a chemically modified siRNA and as an aptamer-isolation agent were investigated, and are described in this section.

3.1   Application of 4′-thioRNA for Chemically Modified siRNA

In order to induce RNAi, siRNA must be recognized by proteins composed of RNA-induced silencing complex (RISC). Accordingly, excessive chemical modification of siRNA can lead to loss of RNAi activity, even if the resultant siRNA shows stability in biological fluid. Thus, chemical modification of siRNA with 4′-thioRNA is thought to be one of the best approaches to the development of a potent modified siRNA [7, 9]. With this in mind, the modification pattern–RNAi activity relationship of siRNAs modified with 4′-thioRNA was investigated by targeting *photinus* luciferase genes in cultured mammalian NIH/3T3 cells [5]. The siRNA sequences and their RNAi activity at 25 nM are summarized in Table 3. The RNAi activities of the siRNAs **siR2** and **siR3**, which were partially modified with 4′-thioRNA at sense strand (upper strand), almost equaled that of natural siRNA (**siR1**). RNAi activity was still observed even when all the residues in the sense strand were modified (**siR4**). Conversely, the activity was dramatically affected by the modification at the antisense strand (lower strand) (**siR5**–**siR7**). To identify the position most sensitive to chemical modification for RNAi activity, siRNAs consecutively modified with 4′-thioRNA at the 5′-end, 3′-end, both ends, and in the central position (**siR8**–**siR14**) were also tested. All of the modified siRNAs on their sense strand (**siR8**–**siR11**) were almost equal to natural siRNA (**siR1**) in RNAi activity. However, RNAi activity was reduced to some degree compared with that of **siR1** when the 5′- or 3′-end of the antisense strand was modified (**siR12** and **siR13**). The RNAi activity of **siR14**, modified on the central position of the antisense strand, was fairly lower than those of **siR12** and **siR13**, although the number of modification is nearly equal.

Although the siRNAs modified with 4′-thioRNA did not exhibit improved activity relative to that of **siR1**, modification with 4′-thioRNA was well tolerated in terms of RNAi activity compared to modification with 2′-*O*-MeRNA, at least, in a certain type of modification. In addition, the modified siRNAs (**siR3** and **siR11**) showed higher RNAi activity than **siR1** after 5 days, implying that modification with 4′-thioRNA appended long-term RNAi activity owing to nuclease resistance. These results prompted us to optimize the best modification pattern with 4′-thioRNA in terms of RNAi activity. The RNAi activities of siRNAs modified on both strands are summarized in Table 4. As the number of modifications decreased from six to four to two, the RNAi activity improved (**siR15**–**siR20**). Thus, when the 5′-end of the antisense strand was modified (i.e., together with modification on the 3′-end of the sense strand), modification with two residues was tolerated (**siR17**), while modification with four residues at the 3′-end of the antisense strand (**siR19**) was

Table 3 Sequences and RNAi activities of siRNAs modified with 4′-thioRNA

Name	Sequnece	RNAi activity (%)
Scramble	5'-GCGCGCUUUGUAGGAUUCGTT-3' 3'-TTCGCGCGAAACAUCCUAAGC-5'	0
siR1	5'-CGUACGCGGAAUACUUCGATT-3' 3'-TTGCAUGCGCCUUAUGAAGCU-5'	95.4
siR2	5'-CGUACGCGGAAUACUUCGATT-3' 3'-TTGCAUGCGCCUUAUGAAGCU-5'	93.6
siR3	5'-CGUACGCGGAAUACUUCGATT-3' 3'-TTGCAUGCGCCUUAUGAAGCU-5'	92.9
siR4	5'-CGUACGCGGAAUACUUCGATT-3' 3'-TTGCAUGCGCCUUAUGAAGCU-5'	60.3
siR5	5'-CGUACGCGGAAUACUUCGATT-3' 3'-TTGCAUGCGCCUUAUGAAGCU-5'	68.5
siR6	5'-CGUACGCGGAAUACUUCGATT-3' 3'-TTGCAUGCGCCUUAUGAAGCU-5'	27.3
siR7	5'-CGUACGCGGAAUACUUCGATT-3' 3'-TTGCAUGCGCCUUAUGAAGCU-5'	16.6
siR8	5'-CGUACGCGGAAUACUUCGATT-3' 3'-TTGCAUGCGCCUUAUGAAGCU-5'	94.0
siR9	5'-CGUACGCGGAAUACUUCGATT-3' 3'-TTGCAUGCGCCUUAUGAAGCU-5'	93.3
siR10	5'-CGUACGCGGAAUACUUCGATT-3' 3'-TTGCAUGCGCCUUAUGAAGCU-5'	87.4
siR11	5'-CGUACGCGGAAUACUUCGATT-3' 3'-TTGCAUGCGCCUUAUGAAGCU-5'	91.5
siR12	5'-CGUACGCGGAAUACUUCGATT-3' 3'-TTGCAUGCGCCUUAUGAAGCU-5'	70.9
siR13	5'-CGUACGCGGAAUACUUCGATT-3' 3'-TTGCAUGCGCCUUAUGAAGCU-5'	72.2
siR14	5'-CGUACGCGGAAUACUUCGATT-3' 3'-TTGCAUGCGCCUUAUGAAGCU-5'	36.5

RNAi activity after 24 h was quantified by the dual luciferase assay, and is presented as the inhibition efficiency of target gene when NIH/3T3 cells were treated with 25 nM of siRNA. Modifications with 4′-thioRNA are indicated in red

tolerated. In order to find effective siRNAs containing as many modified units as possible, further examination was carried out with different highly modified siRNAs. As can be seen in the results of **siR21–siR26**, a boundary to RNAi activity exists between the six and four residues for modification of both ends of the sense strand (**siR23** and **siR26** vs. other siRNAs). When the sense strand of a sequence had four consecutive modifications on both ends, and either four consecutive modifications on the 3′-end or two consecutive modifications on each end of the antisense strand such as **siR24** and **siR25**, this modification pattern was well-tolerated for RNAi activity. As a result, these two siRNAs were highly modified with 4′-thioRNA without significant loss of RNAi activity.

Table 4 Optimization of siRNA modification with 4′-thioRNA

Name	Sequnece	RNAi activity (%)
siR1	5'-CGUACGCGGAAUACUUCGATT-3' 3'-TTGCAUGCGCCUUAUGAAGCU-5'	95.4
siR15	5'-CGUACGCGGAAUACUUCGATT-3' 3'-TTGCAUGCGCCUUAUGAAGCU-5'	10.9
siR16	5'-CGUACGCGGAAUACUUCGATT-3' 3'-TTGCAUGCGCCUUAUGAAGCU-5'	35.1
siR17	5'-CGUACGCGGAAUACUUCGATT-3' 3'-TTGCAUGCGCCUUAUGAAGCU-5'	91.2
siR18	5'-CGUACGCGGAAUACUUCGATT-3' 3'-TTGCAUGCGCCUUAUGAAGCU-5'	47.8
siR19	5'-CGUACGCGGAAUACUUCGATT-3' 3'-TTGCAUGCGCCUUAUGAAGCU-5'	86.1
siR20	5'-CGUACGCGGAAUACUUCGATT-3' 3'-TTGCAUGCGCCUUAUGAAGCU-5'	91.3
siR21	5'-CGUACGCGGAAUACUUCGATT-3' 3'-TTGCAUGCGCCUUAUGAAGCU-5'	92.1
siR22	5'-CGUACGCGGAAUACUUCGATT-3' 3'-TTGCAUGCGCCUUAUGAAGCU-5'	92.0
siR23	5'-CGUACGCGGAAUACUUCGATT-3' 3'-TTGCAUGCGCCUUAUGAAGCU-5'	74.2
siR24	5'-CGUACGCGGAAUACUUCGATT-3' 3'-TTGCAUGCGCCUUAUGAAGCU-5'	88.1
siR25	5'-CGUACGCGGAAUACUUCGATT-3' 3'-TTGCAUGCGCCUUAUGAAGCU-5'	87.7
siR26	5'-CGUACGCGGAAUACUUCGATT-3' 3'-TTGCAUGCGCCUUAUGAAGCU-5'	26.6
siR27	5'-AAACAUGCAGAAAAUGCUGTT-3' 3'-TTUUUGUACGUCUUUUACGAC-5'	41.7
siR28	5'-AAACAUGCAGAAAAUGCUGTT-3' 3'-TTUUUGUACGUCUUUUACGAC-5'	91.0
siR29	5'-AAACAUGCAGAAAAUGCUGTT-3' 3'-TTUUUGUACGUCUUUUACGAC-5'	86.3

RNAi activity after 24 h was quantified by the dual luciferase assay, and is presented as the inhibition efficiency of target gene when NIH/3 T3 cells were treated with 25 nM of siRNA. Modifications with 4′-thioRNA are indicated in red

In order to examine the generality of the optimized modification pattern described above, siRNAs with 4′-thioRNA targeting *renilla* luciferase genes were prepared and evaluated their RNAi acvity in cultured mammalian NIH/3T3 cells. Unlike when targeting *photinus* luciferase genes, the RNAi activity of natural siRNA (**siR27**) was moderate. To our delight, the RNAi activities of **siR28** and **siR29**, which had same modification pattern with **siR24** and **siR25**, were much higher than that of **siR27**. As described above, we have succeeded in developing the novel RNA analog 2′-*O*-methyl-4′-thioRNA, and have been investigating to use this RNA analog toward chemically modified siRNA. The optimized modification pattern

obtained from the aforementioned investigation was also applicable to the project of siRNA modified with 2′-*O*-methyl-4′-thioRNA [37].

## 3.2 Application to Isolation of 4'-thioRNA Aptamers

RNA aptamers have been obtained for a variety of target molecules using SELEX [31], which is an innovative technology used to isolate functional RNA molecules. Since the resulting aptamers, like antibodies, show a potent and selective binding affinity for the target molecule, they are expected to become not only useful biological tools, but also diagnostic and therapeutic agents [15]. However, since SELEX requires a transcription step by T7 RNA polymerase in the presence of nucleoside 5′-triphosphates (NTPs), few of the modified nucleoside 5′-triphosphates are only good candidates for SELEX. Thus far, 2′-amino- and 2′-fluoropyrimidine nucleoside 5′-triphosphates (NH_2UTP and NH_2CTP, and FUTP and FCTP) are frequently used as modified 5′-triphosphates to isolate modified RNA aptamers [32]. Consequently, we were prompted to prepare 4′-thiopyrimidine nucleoside 5′-triphosphates (SUTP and SCTP) and investigate whether the 5′-triphosphates are applicable to the SELEX strategy (Fig. 2) [17].

Prior to the isolation of 4′-thioRNA aptamers, transcription by T7 RNA polymerase in the presence of SUTP and SCTP was examined. For comparison, transcriptions in the presence of NH_2UTP and NH_2CTP, and FUTP and FCTP were also examined under the same conditions. Thus, using a DNA template to form a 30 mer RNA sequence, the transcription by T7 RNA polymerase was performed at 37 °C in the presence of ATP, GTP, and modified pyrimidine nucleoside 5′-triphosphates (0.4 mM each), and the transcription products at various time points were detected by PAGE analysis. As can be seen in Fig. 3, a significant amount of the complete transcription product, a 30 mer 4′-thioRNA, was observed under the conditions in which UTP and CTP were replaced by SUTP and SCTP, and the efficiency was estimated to be 90% relative to that using the natural NTPs (lanes 3–6 vs. lanes 7–10). In contrast, the transcription efficiencies decreased when NH_2UTP and NH_2CTP (estimated to be 54%), and FUTP and FCTP (estimated to be 10%) were used (lanes 11–14 and 15–18). The DuraScribe™ T7 RNA polymerase, a mutant

**Fig. 2** Structures of SUTP and SCTP

SUTP: R = OH
SCTP: R = NH$_2$
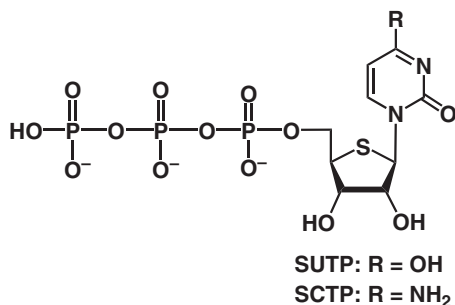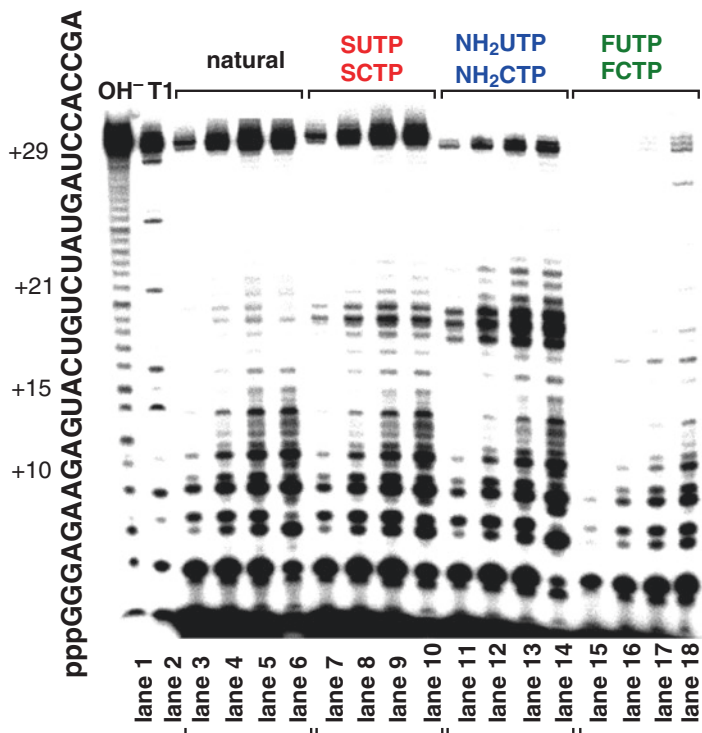
Fig. 3 PAGE analysis of in vitro transcription by T7 RNApolymerase using 47 mer dsDNA. (see Kato et al. [17])

polymerase used for effective incorporation of FUTP and FCTP, was also examined. The relative efficiency increased to ca. 20% giving a 30 mer 2′-fluoroRNA. In contrast, the incorporation of SUTP and SCTP using this mutant polymerase was ineffective and the relative efficiency decreased to less than 10%.

Moving toward the end-goal of this project, selection of 4′-thioRNA aptamers using SUTP and SCTP was examined. Human α-thrombin was chosen as the target protein for SELEX because both the RNA and the DNA aptamers have been isolated, and their structures and functions have been thoroughly investigated. Using single-stranded DNA templates comprising 30 nucleotides in randomized positions, the selection was carried out for ten rounds. As a result, a 23 mer of the stem-bulge-loop structure CI-2-23 and a similar stem-bulge-loop structure CII-1-37 were predicted using the Zuker RNA *mfold* computer algorithm. After being prepared the predicted sequences as 4′-thioRNA (Fig. 4), the binding assay of CI-2-23 and CII-1-37 with α-thrombin was examined along with RNA-24 [19], which had previously been selected as the high affinity RNA aptamer and DNA aptamer DNA-G4 [3] for comparison. The aptamer possessing the highest binding affinity was CII-1-37, whose K_d value was estimated as 4.7 nM, while that of CI-2-23 was lower. Since the K_d value of RNA-24 was estimated to be 85 nM, we have succeeded in

Fig. 4 The secondary structures of 4′-thioRNA aptamers. Modifications with 4′-thioRNA are indicated in red

CI-2-23

CII-1-37
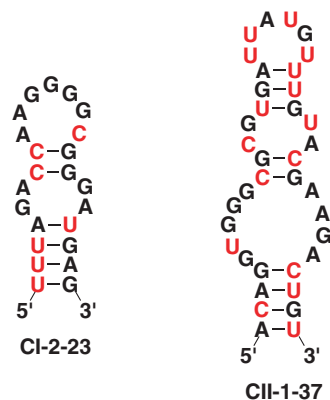
isolating a high affinity 4′-thioRNA aptamer to human α-thrombin using SUTP and SCTP. In addition, we have also succeeded in developing a SELEX protocol to isolate fully modified 4′-thioRNA aptamers via transcription in the presence of four kinds of 4′-thionucleoside 5′-triphosphates (i.e., SUTP, SCTP, SATP, and SGTP) together with the natural GTP and ATP at the appropriate concentrations [25].

The results described in this section suggested that 4′-thioRNA, as well as its components 4′-thionucleoside 5′-triphosphates (SNTPs), showed good biocompatibility with natural RNA and NTPs, and were versatile for the development of nucleic acid-based therapeutics. These successful results prompted us to develop 4′-selenoRNA as a next generation of RNA bioisostere. In the next section, the current progress in the development of 4′-selenoRNA is described.

4 Chemistry for the Synthesis of 4′-selenoRNA

4.1 *Practical Synthesis of 4′-selenoribonucleosides*

There is high expectation for the potential uses of 4′-selenoribonucleoside as a nucleoside antimetabolite and as a building block for 4′-selenoRNA. Thus, our research group and others have expended considerable research effort into developing a practical synthesis of 4′-selenoribonucleosides [11, 14, 16]. Since selenium belongs to the same group as sulfur in the periodic table, a Pummerer-like reaction was expected to proceed between the silylated nucleobase and the selenoxide sugar. However, the yields of this coupling reaction reported by every group were rather low compared to those of the Pummerer reaction between silylated nucleobases and the sulfoxide sugar. For example, the Pummerer-like reaction between silylated uracil and selenoxide **8** via **7** afforded the 4′-selenouridine derivative **9** in only 36% yield. In addition, the reproducibility of this reaction was poor. Since these unfavorable results were found to arise from the instability of the selenoxide **8**, an

alternative method for the Pummerer-like reaction using hypervalent iodine, which does not require isolation of the unstable selenoxide intermediate, was developed [39]. Thus, the desired **9**, which is also transformable into a 4′-selenocytidine derivative, was obtained in 64% yield when **7** was treated with iodosylbenzene, trimethylsilyl trifluoromethanesulfonate (TMSOTf), 2,6-lutidine, and the silylated uracil in dichloroethane at 50 °C (Scheme 2A). However, unlike in the reaction with uracil, the Pummerer-like reaction of **7** with purine bases, such as 6-chloropurine and 2-amino-6-chloropurine, did not proceed well. In the case of the reaction with 6-chloropurine, the Pummerer-like reaction proceeded in moderate yield (>40%) to give the N7-6-chloropurine derivative. However, isomerization to the desired
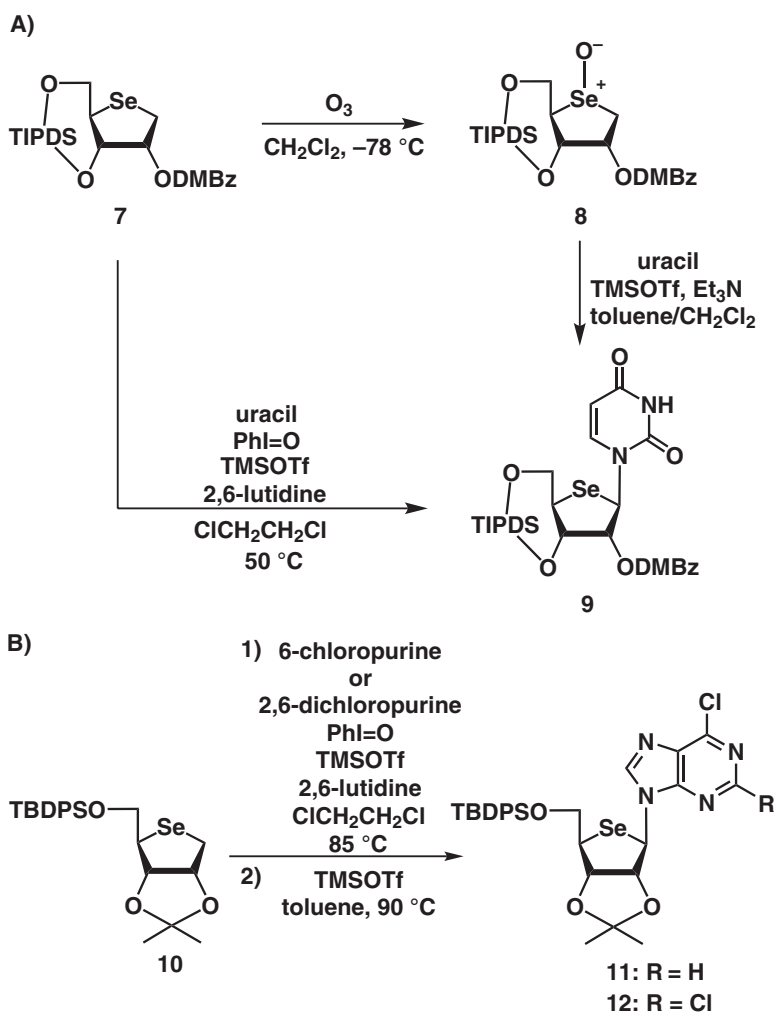
Scheme 2 Synthesis of 4′-selenoribonucleoside derivatives

N9-6-chloropurine isomer was undetectable. Furthermore, only a trace amount of the N7-2-amino-6-chloropurine derivative was obtained in the reaction with 2-amino-6-chloropurine. This problem was solved when the 'armed' 4-selenosugar **10** [14, 46] bearing an electron-donating group at the 2-position was used instead of **7**, which bears an electron-withdrawing group at the 2-position (Scheme 2B). Thus, a solution of silylated 6-chloropurine was added to a mixture of **10** and iodosylbenzene in dichloroethane, and 2,6-lutidine was added to the reaction mixture. The resulting mixture was subsequently heated at 85 °C to afford the desired N9-6-chloropurine derivative **11** in 39% yield, along with the N7-6-chloropurine derivative in 31% yield. Differ from previous case, the separated N7-6-chloropurine derivative was isomerized to the desired N9 isomer **11** in 53% yield upon treatment with TMSOTf in toluene at 90 °C, and thus we succeeded in obtaining **11** in 55% yield from **10** in two steps. Although the reaction of **10** with 2-amino-6-chloropurine under the same conditions was still insufficient, the coupling reaction followed by isomerization proceeded smoothly to give the desired N9 isomer **12** in 62% yield, when 2,6-dichloropurine, which is transformable into a guanine skeleton, was used [13].

4.2 Synthetic Study of 4′-selenoRNA

Two research groups, including ours, independently reported the synthesis of 4′-selenoRNA [12, 44]. However, both groups only succeeded in incorporating one 4′-selenoribonucleoside unit into an ON with very low yield under the standard phosphoramidite conditions. Furthermore, a certain strand-break during the ON synthesis has been suggested, although no obvious answers has been given. Since no such problems were encountered in the 4′-thioRNA synthesis, we carefully investigated the problems associated with ON synthesis using 4′-selenonucleosides [40]. In order to simplify the reaction conditions, the 2′-OMe-4′-selenoU phosphoramidite unit **13** and the corresponding CPG resin **14** were prepared, and the stability of the 2′-OMe-4′-selenoU unit was examined prior to the ON synthesis (Fig. 5). The CPG resin **14** was subjected to standard phosphoramidite conditions (3% TCA in CH_2Cl_2, 110 s; 0.45 M 1*H*-tetrazole in CH_3CN, 10 min; Ac_2O in THF/pyridine and 1-methylimidazole in THF, 18 s; and 0.02 M I_2 in THF/H_2O/pyridine, 40 s) without coupling to another phosphoramidite unit. After subjecting **14** to these conditions six times, the resin was treated with ammonium hydroxide. Then, an aliquot of the reaction solution was analyzed by using HPLC. Only the peak corresponding to 2′-OMe-4′-selenoU was observed, meaning that the nucleoside unit is stable. These results strongly suggest that the problems encountered in ON synthesis with 4′-selenoribonucleosides are due to a strand-break during the formation of a phosphite (III) and/or phosphate (V) linkage in the growing ON.
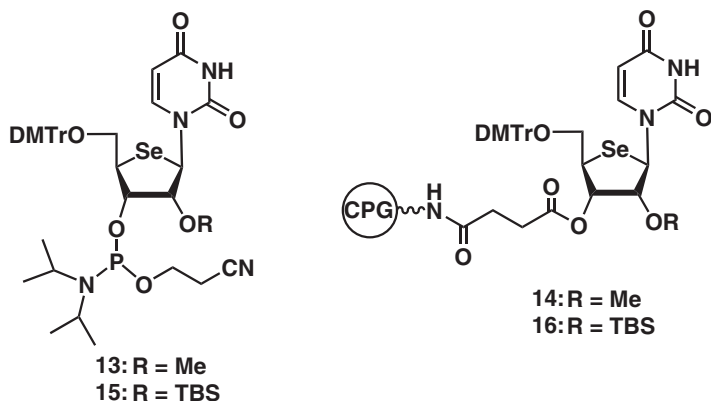
Fig. 5 Structures of building blocks of 4′-selenoRNA

To identify the conditions that induce this strand-break, manual ON synthesis using **13** and **14** was performed in a reservoir tube, but not using a DNA/RNA synthesizer. Starting with the CPG resin **14** in the reservoir tube, the resin was first treated with 3% TCA in CH_2Cl_2. Then, phosphoramidite **13** (0.2 M in CH_3CN) and the coupling reagent (0.45 M 1*H*-tetrazole in CH_3CN) were added to the reservoir tube, and the mixture was allowed to stand for 1 h. After the capping procedure, the CPG resin was treated with 0.02 M I_2 in $THF/H_2O/$pyridine to give the CPG resin-supported dimer. Repeating these procedures once and twice more afforded a CPG resin-supported trimer and tetramer, respectively. After treatment with ammonium hydroxide, the resulting solutions were analyzed by using HPLC. Insufficient yields of the dimer, trimer, and tetramer consisting of 2′-OMe-4′-selenoU units (DMTrO-<u>UU</u>-OH, DMTrO-<u>UUU</u>-OH, and DMTrO-<u>UUUU</u>-OH, respectively, where <u>U</u> = 2′-OMe-4′-selenoU) relative to those consisting of 2′-OMe-U units were indicated. In addition, their HPLC profiles were rather complicated. Multiple peaks were observed at faster elution times than the desired sequence when the coupling reactions were repeated. Among the multiple peaks, a common peak observed in every HPLC profile was isolated, and its structure was analyzed by high-resolution mass spectrometry and ^{1}H NMR spectroscopy. To our surprise, the byproduct did not contain a DMTr group and a phosphorus atom, and its structure was deternined as the C_2-symmetric homo-dimer **17**. In addition, it was found that the formation of **17** occurred during the I_2 oxidation step, and a proposed mechanism for its formation is illustrated in Fig. 6. With these results in hand, the first synthesis of a fully modified 4′-seleoRNA with phosphoramidite unit **15** and CPG resin **16** using alternative oxidation conditions was investigated. As a result, the desired 4′-selenoRNA consisting of 4′-selenoU (12 mer) was successfully prepared via the modified phosphoramidite conditions (3% TCA in CH_2Cl_2, 40 s; 0.25 M 5-benzylthio-1*H*-tetrazole in CH_3CN, 60 s; Ac_2O in THF/pyridine and 1-methylimidazole in THF, 60 s; and 1.0 M *tert*-butyl hydroperoxide in toluene, 50 s).
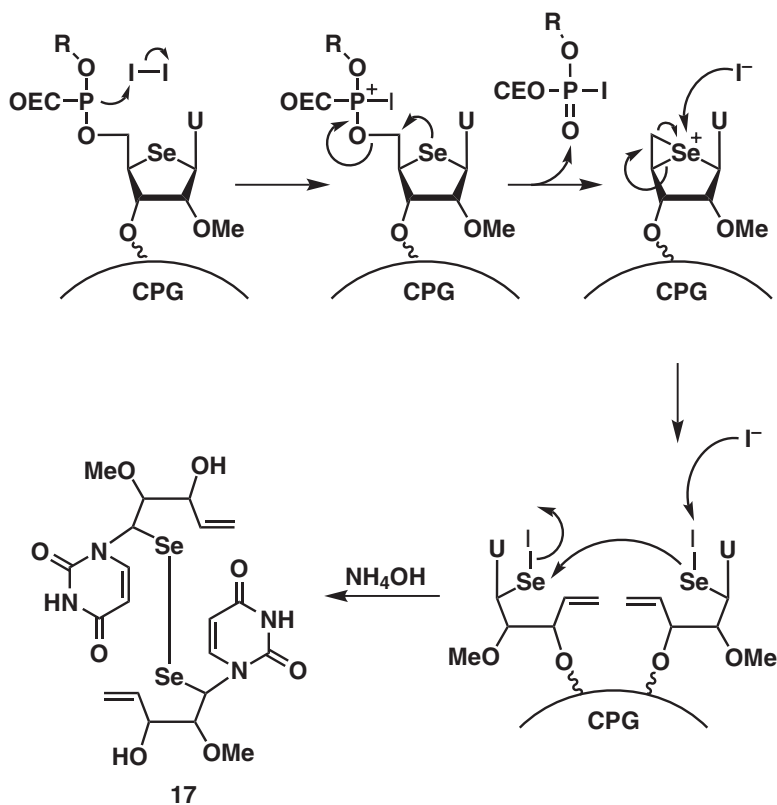
Fig. 6 Proposed mechanism for byproduct **17** formation

5   Conclusion and Perspective

4′-ThioRNA was envisioned as an RNA bioisostere for utilization in a variety of nucleic acid-based therapeutics. Its 4′-thioribonucleoside building blocks were synthesized stereoselectively via the Pummerer reaction between the silylated nucleobase and the corresponding sulfoxide obtained from the 4-thiosugar. Using the resulting building blocks, 4′-thioRNAs were prepared, and their properties and applications were investigated. The resulting 4′-thioRNA showed sufficient hybridization ability and nuclease resistance compared with those of other typical chemically modified RNA analogs. Furthermore, the 4′-thioRNA exhibited biocompatibility with natural RNA as expected, and was used to prepare chemically modified siRNA and for the isolation of 4′-thioRNA aptamers. These successful results prompted us to develop a new RNA bioisostere, 4′-selenoRNA, which contains a selenium atom. The synthesis of its 4′-selenoribonucleoside building blocks was achieved via a Pummerer-like reaction between the silylated nucleobase and the appropriate 4-selenosugar using hypervalent iodine, and the phosphoramidite

conditions for 4′-selenoRNA synthesis were also optimized. A comprehensive comparison of 4′-selenoRNA with 4′-thioRNA and other RNA analogs in terms of their properties and biological applications will be summarized elsewhere as a review article.

References

1. Bellon L, Barascut JL, Maury G et al (1993) 4-Thio-oligo-β-D-ribonucleotides: synthesis of β -4′-thio-oligouridylates, nuclease resistance, base pairing properties, and interaction with HIV-1 reverse transcriptase. Nucleic Acids Res 21:1587–1593
2. Bobek M, Bloch A, Parthasarathy R et al (1975) Synthesis and biological activity of 5-fluoro-4′-thiouridine and some related nucleosides. J Med Chem 18:784–787
3. Bock LC, Griffin LC, Latham JA et al (1992) Selection of single-stranded DNA molecules that bind and inhibit human thrombin. Nature 355:564–566
4. Cummins LL, Owens SR, Risen LM et al (1995) Characterization of fully 2′-modified oligoribonucleotide hetero- and homoduplex hybridization and nuclease sensitivity. Nucleic Acids Res 23:2019–2024
5. Elbashir SM, Harborth J, Lendeckel W et al (2001) Duplexes of 21-nucleotide RNAs mediate RNA interference in cultured mammalian cells. Nature 411:494–498
6. Esau CC (2008) Inhibition of microRNA with antisense oligonucleotides. Methods 44:55–60
7. Hoshika S, Minakawa N, Kamiya H et al (2005) RNA interference induced by siRNAs modified with 4′-thioribonucleosides in cultured mammalian cells. FEBS Lett 579:3115–3118
8. Hoshika S, Minakawa N, Matsuda A (2004) Synthesis and physical and physiological properties of 4′-thioRNA: application to post-modification of RNA aptamer toward NF-κB. Nucleic Acids Res 32:3815–3825
9. Hoshika S, Minakawa N, Shionoya A et al (2007) Study of modification pattern–RNAi activity relationships by using siRNAs modified with 4′-thioribonucleosides. ChemBiochem 8:2133–2138
10. Imanishi T, Obika S (2002) BNAs: novel nucleic acid analogs with a bridged sugar moiety. Chem Commun 0:1653–1659
11. Inagaki Y, Minakawa N, Matsuda A (2007) Synthesis of 4′-selenoribo nucleosides. Nucleic Acids Symp Ser 51:139–140
12. Inagaki Y, Minakawa N, Matsuda A (2008) Synthesis and properties of oligonucleotides containing 4′-selenoribonucleosides. Nucleic Acids Symp Ser 52:329–330
13. Ishii K, Saito-Tarashima N, Ota M et al (2016) Practical synthesis of 4′-selenopurine nucleosides by combining chlorinated purines and 'armed' 4-selenosugar. Tetrahedron 72:6589–6594
14. Jayakanthan K, Johnston BD, Pinto BM (2008) Stereoselective synthesis of 4′-selenonucleosides using the Pummerer glycosylation reaction. Carbohydr Res 343:1790–1800
15. Jayasena SD (1999) Aptamers: an emerging class of molecules that rival antibodies in diagnostics. Clin Chem 45:1628–1650
16. Jeong LS, Tosh DK, Kim HO et al (2008) First synthesis of 4′-selenonucleosides showing unusual Southern conformation. Org Lett 10:209–212
17. Kato Y, Minakawa N, Komatsu Y et al (2005) New NTP analogs: the synthesis of 4′-thioUTP and 4′-thioCTP and their utility for SELEX. Nucleic Acids Res 33:2942–2951

18. Kawasaki AM, Casper MD, Freier SM et al (1993) Uniformly modified 2′-deoxy-2′-fluoro-phosphorothioate oligonucleotides as nuclease-resistant antisense compounds with high affinity and specificity for RNA targets. J Med Chem 36:831–841
19. Kubik MF, Stephens AW, Schneider D et al (1994) High-affinity RNA ligands to human α-thrombin. Nucleic Acids Res 22:2619–2626
20. Kurreck J (2003) Antisense technologies. Improvement through novel chemical modifications. Eur J Biochem 270:1628–1644
21. Lesnik EA, Guinosso CJ, Kawasaki AM et al (1993) Oligodeoxynucleotides containing 2′-O-modified adenosine: synthesis and effects on stability of DNA:RNA duplexes. Biochemistry 32:7832–7838
22. Leydier C, Bellon L, Barascut J-L et al (1995) 4′-thio-RNA: synthesis of mixed base 4′-thiooligoribonucleotides, nuclease resistance, and base pairing properties with complementary single and double strand. Antisense Res Develop 5:167–174
23. Manoharan M (2004) RNA interference and chemically modified small interfering RNAs. Curr Opin Chem Biol 8:570–579
24. Manoharan M, Akinc A, Pandey RK, Antisense Research and Development (2011) Unique gene-silencing and structural properties of 2′-fluoro-modified siRNAs. Angew Chem Int Ed 50:2284–2288
25. Minakawa N, Sanji M, Kato Y et al (2008) Investigations toward the selection of fully-modified 4′-thioRNA aptamers: optimization of in vitro transcription steps in the presence of 4′-thioNTPs. Bioorg Med Chem 16:9450–9456
26. Naka T, Minakawa N, Abe H et al (2000) The stereoselective synthesis of 4′-β-thioribonucleosides via the Pummerer reaction. J Am Chem Soc 122:7233–7243
27. Naka T, Nishizono N, Minakawa N et al (1999) Nucleosides and nucleotides. 189. Investigation of the stereoselective coupling of thymine with meso-thiolane-3,4-diol-1-oxide derivatives via the pummerer reaction. Tetrahedron Lett 40:6297–6300
28. Ng EW, Shima DT, Calias P et al (2006) Pegaptanib, a targeted anti-VEGF aptamer for ocular vascular disease. Nat Rev Drug Discov 5:123–132
29. Obika S, Rahman SMA, Fujisaka A et al (2010) Bridged nucleic acids: development, synthesis and properties. Heterocycles 81:1347–1392
30. Ono T, Scalf M, Smith LM (1997) 2′-Fluoro modified nucleic acids: polymerase-directed synthesis, properties and stability to analysis by matrix-assisted laser desorption/ionization mass spectrometry. Nucleic Acids Res 25:4581–4588
31. Osborne SE, Ellington AD (1997) Nucleic acid selection and the challenge of combinatorial chemistry. Chem Rev 97:349–370
32. Pagratis NC, Bell C, Chang Y-F et al (1997) Potent 2′-amino-, and 2′-fluoro-2′- deoxyribonucleotide RNA inhibitors of keratinocyte growth factor. Nat Biotech 15:68–73
33. Prakash TP (2011) An overview of sugar-modified oligonucleotides for antisense therapeutics. Chem Biodivers 8:1616–1641
34. Reist EJ, Gueffroy DE, Goodman L (1964) Synthesis of 4-thio- D- and -L-ribofuranose and the corresponding adenine nucleosides. J Am Chem Soc 86:5658–5663
35. Saito Y, Hashimoto Y, Arai M et al (2014) Chemistry, properties, and in vitro and in vivo applications of 2′-O-methoxyethyl-4′-thioRNA, a novel hybrid type of chemically modified RNA. ChemBiochem 15:2535–2540
36. Takahashi M, Minakawa N, Matsuda A (2009) Synthesis and characterization of 2′-modified-4′-thioRNA: a comprehensive comparison of nuclease stability. Nucleic Acids Res 37:1353–1362
37. Takahashi M, Nagai C, Hatakeyama H et al (2012) Intracellular stability of 2′-OMe-4′-thioribonucleoside modified siRNA leads to long-term RNAi effect. Nucleic Acids Res 40:5787–5793
38. Takahashi M, Yamada N, Hatakeyama H et al (2013) In vitro optimization of 2′-OMe-4′-thioribonucleoside-modified anti-microRNA oligonucleotides and its targeting delivery to mouse liver using a liposomal nanoparticle. Nucleic Acids Res 41:10659–10667
39. Taniike H, Inagaki Y, Matsuda A et al (2011) Practical synthesis of 4′-selenopyrimidine nucleosides using hypervalent iodine. Tetrahedron 67:7977–7982

40. Tarashima N, Hayashi K, Terasaki M et al (2014) First synthesis of fully modified 4′-sele-noRNA and 2′-OMe-4′-selenoRNA based on the mechanistic considerations of an unexpected strand break. Org Lett 16:4710–4713
41. Thomas GS, Cromwell WC, Ali S et al (2013) Mipomersen, an apolipoprotein B synthesis inhibitor, reduces atherogenic lipoproteins in patients with severe hypercholesterolemia at high cardiovascular risk: a randomized, double-blind, placebo-controlled trial. J Am Coll Cardiol 62:2178–2184
42. Wahlestedt C, Salmi P, Good L et al (2000) Potent and nontoxic antisense oligonucleotides containing locked nucleic acids. Proc Natl Acad Sci U S A 97:5633–5638
43. Wan WB, Seth PP (2016) The medicinal chemistry of therapeutic oligonucleotides. J Med Chem 59:9645–9667
44. Watts JK, Johnston BD, Jayakanthan K et al (2008) Synthesis and biophysical characterization of oligonucleotides containing a 4′-selenonucleotide. J Am Chem Soc 130:8578–8579
45. Wengel J, Petersen M, Nielsen KE et al (2001) LNA (locked nucleic acid) and the diastereo-isomeric α-L-LNA: conformational tuning and high-affinity recognition of DNA/RNA targets. Nucleosides Nucleotides Nucleic Acids 20:389–396
46. Yu J, Kim JH, Lee HW et al (2013) New RNA purine building blocks, 4′-selenopurine nucleo-sides: first synthesis and unusual mixture of sugar puckerings. Chem Eur J 19:5528–5532
47. Zimmermann TS, Lee AC, Akinc A et al (2006) RNAi-mediated gene silencing in non-human primates. Nature 441:111–114

Development of Triplex Forming Oligonucleotide Including Artificial Nucleoside Analogues for the Antigene Strategy

Yosuke Taniguchi and Shigeki Sasaki

Abstract The sequence-specific triplex formation against duplex DNA offers a potential basis for genome targeting technology, such as diagnostics, regulation of gene expression and sequencing technologies. In an antiparallel triplex DNA, a purine-rich triplex forming oligonucleotide (TFO) consisting of a dG, dA or T forms two reverse Hoogsteen hydrogen bonds with a GC, AT or AT base pair of the duplex DNA, respectively, with a high selectivity in a sequence specific manner. However, there is no natural nucleoside which can recognize the inverted CG and TA base pair of the duplex DNA. Therefore, the development of recognition molecules for the CG and TA inversion sites with a high stability and selectivity has been demanded for the triplex forming technology. In this chapter, we describe the design and synthesis of W-shaped nucleoside analogues (WNA-βT) and pseudo-dC derivatives (^{Me}AP-ΨdC) for selective recognition of the TA and CG base pair, respectively, to expand the triplex-forming sequence.

Keywords Antiparallel triplex DNA · Antigene · Inhibition of gene expression · Anti-proliferative effect · Artificial nucleoside analogues · Inversion site

1 Introduction

The formation of a stable triplex DNA is powerful tool to inhibit or activate the gene expression at the transcription steps for the development of gene targeting technology including diagnostics, regulation of gene expression and sequencing technologies [1–4]. In general, triplex forming oligonucleotides (TFOs) can form hydrogen bonds to the homopurine strand from the major groove of the duplex DNA. This is classified into two types according to the base composition and binding-direction of TFO against the duplex DNA. A purine-motif is characterized by the purine-rich TFO binding anti-parallel orientation to the homopurine strand of a duplex DNA via two reverse Hoogsteen hydrogen bonds (Fig. 1a, G-GC, A-AT or T-AT triplets) and
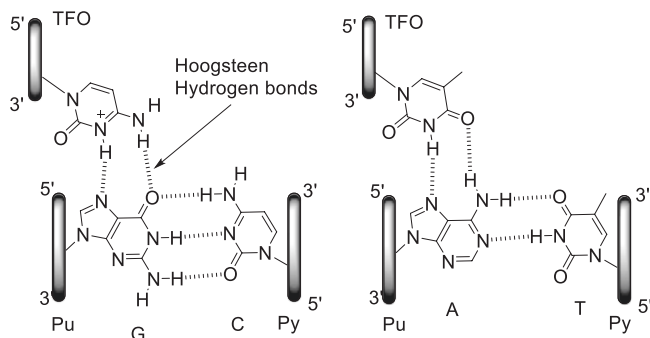
Y. Taniguchi · S. Sasaki (✉)

Graduate School of Pharmaceutical Sciences, Kyushu University, Fukuoka, Japan
e-mail: taniguch@phar.kyushu-u.ac.jp; sasaki@phar.kyushu-u.ac.jp
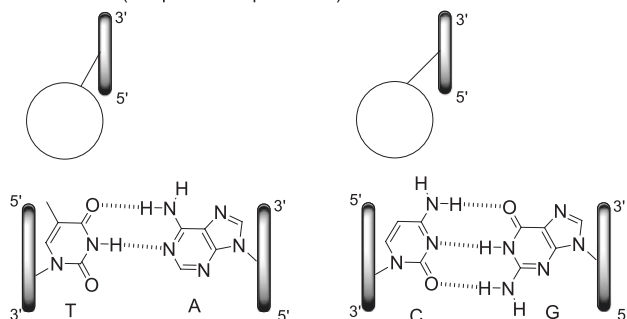
(A) Antiparallel Triplex DNA
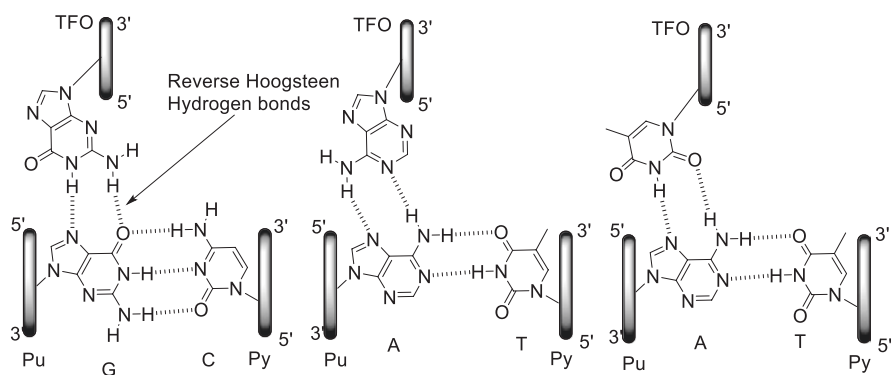
(B) Parallel Triplex DNA

(C) Inversion sites (Antiparallel Triplex DNA)

Fig. 1 Structures of base triplets (**a**) antiparallel triplet, (**b**) parallel triplex and (**c**) inversion sites in antiparallel triplex DNA
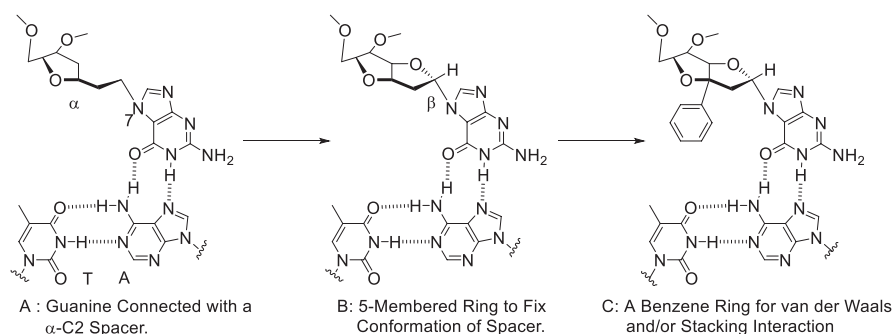
a pyridimidine-rich motif by the pyrimidine-rich TFO binding parallel orientation via two Hoogsteen hydrogen bonds (Fig. 1b, C+-GC and T-AT triplets) [5–8]. However, there is no natural nucleoside that can form stable hydrogen bonds with the inverted CG and TA base pairs (Fig. 1c). Therefore, the presence of these sites

in the homopurine strand in the target duplex DNA disturbed the stable triplex DNA formation and their versatile application.

A wide variety of nucleosides has been designed for the inversion site recognition in both cases of the parallel type [9–13] and anti-parallel type triplex formations [14–16], however, a fundamental solution has not been achieved in the terms of low selectivity, insufficient affinity and, particularly, the limited base pair recognition ability to a certain sequence context; the base pair recognition by a non-natural nucleoside is significantly influenced by the nearest neighboring bases.

2 Design of W-shaped Nucleoside Analogues (WNAs) for TA Inversion Site

The basic concept for the design of the new nucleoside analogue is schematically illustrated in Fig. 2 using WNA-7βG (guanine attached to sugar part at seven-position of nucleobase with β-configuration.) as an example [17]. An ethylene spacer with C1′ stereochemistry was designed to connect a nucleobase unit for hydrogen bonds to a distant purine base (Fig. 2a). Conformation of a nucleobase unit might become restricted by construction of a bicyclic ring (Fig. 2b). Finally, we considered that a benzene ring at the C1′ position might occupy a space where a base unit of a natural nucleoside is located and provide stacking and/or van der Waals interactions (Fig. 2c). As a benzene ring, a five-membered ring and a nucleobase seem to be aligned in a W-shape; we called the new molecule the W-shaped nucleoside analogue (WNA) with the number and α or β to represent the alkylation position of the nucleobase and the stereochemistry of its glycosidic bond, respectively.

A : Guanine Connected with a
    α-C2 Spacer.

B: 5-Membered Ring to Fix
   Conformation of Spacer.

C: A Benzene Ring for van der Waals
   and/or Stacking Interaction

Fig. 2 Design of a bicyclic structure having a base and a benzene ring (**a**) Guanine connected with a α-C2 spacer. (**b**) 5-Membered ring to fix conformation of spacer. (c) A benzene ring for van der Waals and/or stacking interaction

## 2.1 Synthesis of Oligonucleotides Including WNAs (WNA-βT)

The WNA derivatives were synthesized with D-ribose (Scheme 1). The intermediate having a benzene ring at the 1-position (2) was prepared by a multistep synthesis [6, 18]. Allylation at the 1-position gave 3 in the ratio of α:β = 7:6 for the stereochemistry of the allyl group, which was used for the following reaction without separation. Subsequently, oxidative cleavage of the vinyl group and subsequent deprotection spontaneously provided the corresponding bicyclo[3.3.0]octane derivative, then the formed hydroxyl groups were acetylated to afford the key intermediate 4. The cyclic compound 4 was easily separated from the noncyclic compound which was derived from 3 with a undesired α-allyl stereochemistry. N-Glycosidation to 4 with the corresponding base derivatives was done under different conditions to produce a mixture of α and β-isomers (5), which were separated by flash chromatography. Compound 5 was converted to the corresponding amidite derivative (6) and incorporated into the TFOs (7–10) and antigene TFO (11) by an automated DNA synthesizer. The structure and purity of the obtained TFO were confirmed by MALDI-TOF MASS measurements.

TFO (8): 5' AGGGAGGAGG**Z**GGGAAGG 3'
calc. 5874.28, found 5875.76
TFO (9): 5' AGGGAGGAGA**Z**AGGAAGG 3'
calc. 5842.30, found 5841.49
TFO (10): 5' AGGGAGGAGA**Z**GGGAAGG 3'
calc. 5858.29, found 5857.72
Antigene TFO (11):
5' GGUUGUUGGUGGGUG**Z**GUUGUG-amino 3'
calc. 7055.93, found 7054.34
Z = WNA-βT, amino: propyl amine.

TFO (7)
MALDI-TOF MS (m/z)
calc. 5858.29
found 5857.91
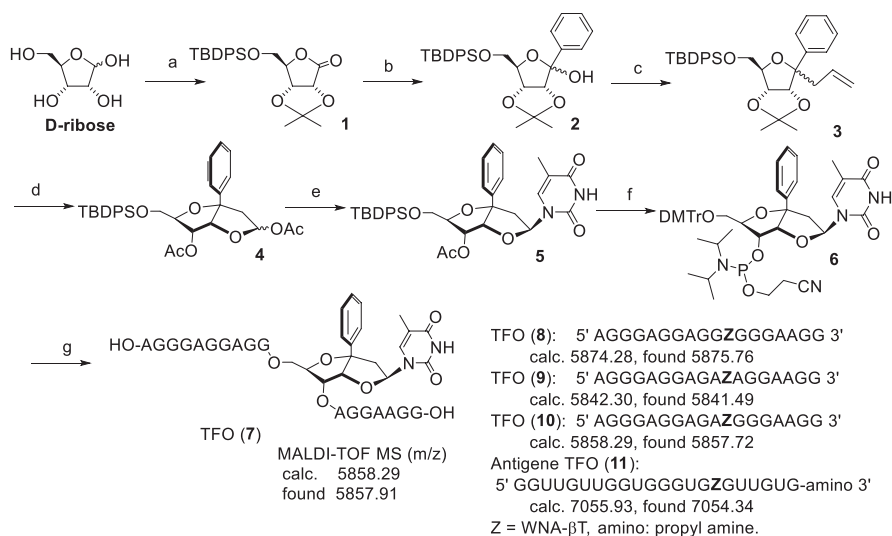
Scheme 1 (a) (1) acetone, H$^+$, (2) TBDPSCl, TEA, DMAP, CH$_2$Cl$_2$, (3) PCC, CH$_2$Cl$_2$, 64% for three steps. (b) PhLi, THF, 82%, (c) allyltrimethylsilane, ZnBr$_2$, CH$_3$NO$_2$, (α:β = 7:6), (d) (1) OsO$_4$, NaIO$_4$, pyridine, (2) 5% H$_2$SO$_4$, THF, (3) Ac$_2$O, pyridine, 41% for four steps. (e) HMDS, TMSCl, SnCl$_4$, CH$_3$CN, thymine, 42% (WNA-βT) and 37% (WNA-αT), (f) (1) 1.0 M TBAF (2) 0.2 M NaOH aq., (3) DMTrCl, pyridine, (4) 2-cyanoethyl-N,N-diisopropylchlorophosphoramidite, DIPEA, CH$_2$Cl$_2$, 54% for four steps. (g) TFO was synthesized by DNA Synthesizer, and then purified by HPLC

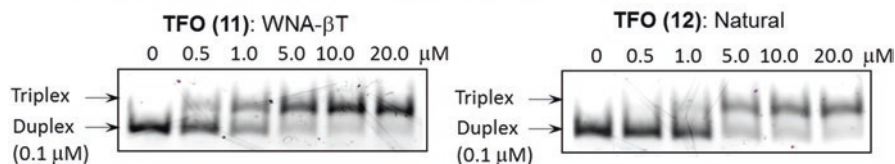## 2.2 Evaluation of Triplex Formation

Triplexes were formed by incubating the TFO, the ^{32}P-labeled TFO as a tracer and the duplex for 12 h at 22 °C in a buffer containing 20 mM Tris-HCl, 5 mM MgCl$_2$, 2.5 mM spermidine and 10% sucrose at pH 7.5. The formed triplex was evaluated by a gel shift assay with 15% non-denatured polyacrylamide gel at 10 °C and the equilibrium association constant was obtained by the quantification of the bands intensity (Fig. 3). The TFO (**7**) with WNA-βT yielded almost complete formation of a triplex with a TA interrupting site at a 10 nM duplex concentration (TFO/duplex = 1:1), whereas the other duplexes needed much higher concentrations for the triplex formation (Fig. 3). Interestingly, the triplex with the WNA-βT/TA combination showed a higher stability (K_s value is 0.300×10^9 M^{-1}) than the natural type triplexes (K_s values (10^9 M^{-1}): 0.086 for G/GC, 0.074 for A/AT.). However, subsequent studies showed that the triplex forming ability of TFO containing WNA-βT is dependent on the neighboring bases. In the case of WNA-βT, the TFO sequences, 3′-AZA-5′ and 3′-GZA-5′, could not recognize the TA inversion site [19, 20]. All synthesized TFOs containing WNA analogues were evaluated by a gel-shift assay. Among the wide variety types of the WNA analogues, WNA-βT has a good ability to form the stable and selective triplex DNA in spite of the sequence dependency [21–27]. Therefore, to investigate the ability of the triplex formation of amino-modified TFOs containing WNA-βT with the survivin gene sequence, the gel-shift assay was performed using the antigene TFOs (Z = WNA-βT (**11**) and Z = T (**12**)) and FAM-labeled target duplexes as the model sequence [28]. It was reported that the TFOs modified with 3′ phosphopropyl amine prevented the nuclease digestion and enhanced the bioavailability [29, 30]. This result suggested that the TFO (**11**)
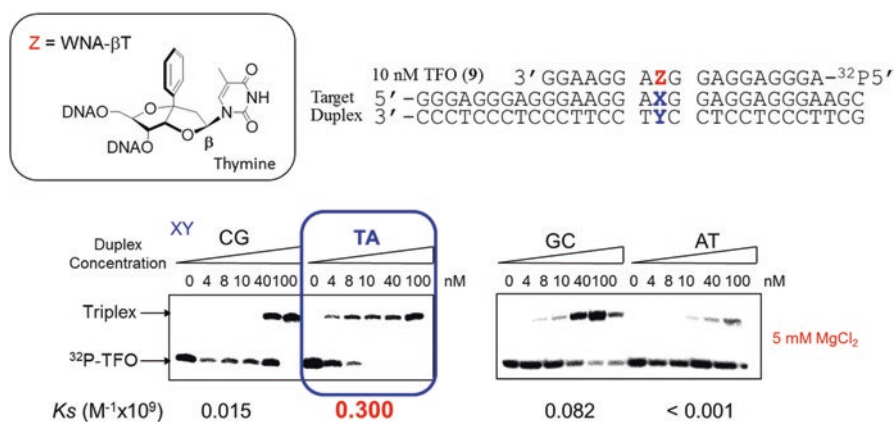
Fig. 3 Gel results of the triplex formation of TFO containing WNA-βT. Triplex formation was done for 12 h at 22 °C in the buffer containing 20 mM Tris-HCl, 5 mM MgCl$_2$, 2.5 mM spermidine and 10% sucrose at pH 7.5. Electrophoresis was done at 10 °C with 15% non-denatured polyacrylamide gel. 10 nM TFO (18 mer) containing the ^{32}P-labeled one as the tracer was used. The concentration of the target duplex (30 bp) was increased. K_s = [triplex]/([TFO][duplex])

survivin gene

5′ FAM-CACTG CCTTCTTCCTCCCTC**A**CTTCTC ACCTG-3′
3′ -GTGAC GGAAGAAGGAGGGAG**T**GAAGAG TGGAC-FAM 5′

TFO (11): WNA-βT 5′ GGUUGUUGGUGGGUGβ**T**GUUGUG-amino 3′ βT = WNA-βT
**TFO (12): Natural** 5′ GGUUGUUGGUGGGUG**T**GUUGUG-amino 3′

Fig. 4 The triplex formations of the TFOs were evaluated by a gel-shift assay. Triplex formation was done for 12 h at 37 °C in the buffer containing 20 mM Tris-HCl, 5 mM MgCl$_2$, 2.5 mM spermidine and 10% sucrose at pH 7.5. Electrophoresis was done at 10 °C with 10% non-denatured polyacrylamide gel. 5′-FAM labeled 100 nM target duplex (32 bp). The concentration of the survivin TFOs (22 nt) increased from 0 to 20.0 mM

with WNA-βT showed a triplex formation to the survivin target at around 0.5 μM, whereas the natural-type TFO (**12**) displayed a lower triplex-forming ability under the same conditions (Fig. 4, the K_s values of TFO (**11**) and TFO (**12**) were 0.65×10^6 and 0.28×10^6 M^{-1}, respectively).

2.3 Antiploriferative Effect and Inhibition of Gene Expression Product for A549 Cells

The survivin gene products are an important regulator of cell proliferation and over-expressed in a variety of tumors [31]. To evaluate the biological activity of the anti-gene TFO (**11** and **12**), their inhibitory abilities for cell growth were measured [32]. The antigene TFO was transfected into A549 cells incubated for 72 h using Oligofectamine™ (invitrogen), and the cell viability was then evaluated by a cell titer assay. The obtained cell viabilities are summarized in Fig. 5. TFO (**11**) with WNA-βT inhibited the cell growth by about 50% at a concentration of 1.25 μM (Fig. 5, red bar), whereas the natural TFO (**12**) induced about a 30% growth inhibition (Fig. 5, blue bar). In addition, the scrambled sequence of TFO (5′ UUGTGUGGGUGGUGGUGUGUU-amino 3′) did not have a significant effect on the A549 cell growth at any concentration (Fig. 5, green bar). We speculate that the antigene TFOs with WNA-βT are able to exist in cells and form a stable triplex DNA with the target site, resulting in a significant antiproliferative effect. The antigene effect was determined by quantification of the amount of survivin protein in the A549 cells (Fig. 6). The sample that underwent incubation for 48 h, which had the highest caspase activity (data not shown), was used for the Western blot
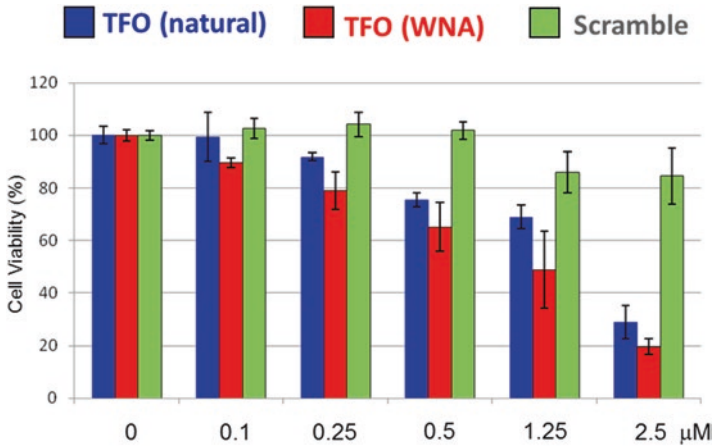
Fig. 5 Antiproliferative effect of antigene TFOs. The A549 cell was treated with the complex of TFOs and Oligofectamine™, and PLUS reagent in the DMEM medium containing 10% FBS was incubated for 72 h under 5% CO_2 at 37 °C. The cell proliferation was checked by Cell-Titer 96® (PROMEGA) (n = 3)

Fig. 6 Western blot analysis of survivin protein. The A549 cell was treated with the complex of TFOs (0 μM (gray bar) and 0.5 μM (red bar and blue bar) of TFO (**11**) having WNA-βT or TFO (**12**) having T) and OligofectamineTM and PLUS Reagent in DMEM medium containing 10%FBS and incubated for 48 h under 5% CO_2 at 37 °C. (n = 3)
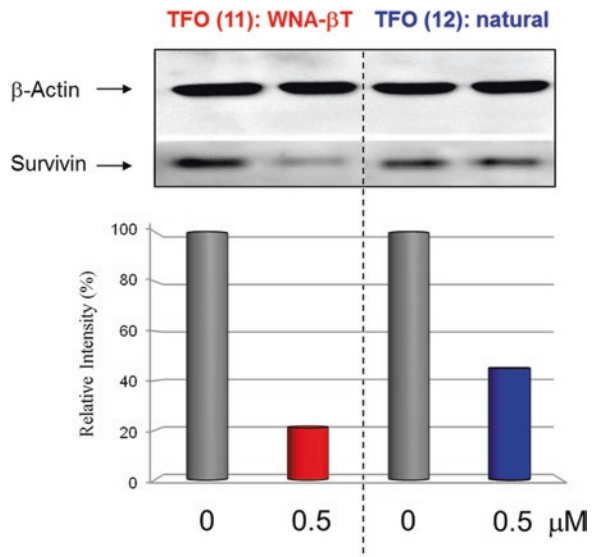
analysis. The intensity of the survivin protein was normalized by the corresponding β-actin. TFO (**12**) suppressed the generation of the survivin gene product by about 50% (Fig. 6, red bar). On the other hand, the result of TFO (**11**) showed a more effective suppression of the production of the survivin protein by about 80% (Fig. 6,

blue bar). These results indicated that TFO, which has a high ability for triplex formation, is able to significantly inhibit the gene expression.

3 Design of Pseudo-dC Derivatives (^{Me}AP-ΨdC) for CG Inversion Site

We have developed artificial nucleosides including WNA analogues, which are significantly influenced by the nearest neighboring bases. We suspected that such a sequence dependency might be overcome by the design based on the canonical T/CG base triplet [33, 34]. Previously, isocytidine (isodC) derivatives were designed for the selective CG base pair recognition in the antiparallel triplex DNA [35]. Indeed, of the various designed isocytidine derivatives, AP-isodC was shown to possess the ability to recognize the CG base pair with a moderate selectivity and generality [36]. Based on the validity of the design concept of AP-isodC, we find the novel pseudo-dC (ΨdC) derivatives, which possess a comparable affinity toward the CG inversion site with the canonical base triplet, and notably, without being influenced by the neighboring bases [37]. The design of the ΨdC derivative is shown in Fig. 7. The validity of the design concept for AP-isodC has been proven in that the triplex DNA containing a CG inversion site can be selectively stabilized with its use. However, the stabilization effect with AP-isodC was not satisfactory, which was thought to be due to the high flexibility of the aminopyridinylmethyl group. In order to restrict the conformational mobility of the aminopyridine unit, it was designed to directly attach to the isodC skeleton. We anticipated that such a rigid and planar nucleobase should place the hydrogen bonding groups within close proximity to the guanine base of the CG base pair as well as to enhance the stacking interactions with the adjacent bases. Considering the chemical instability of the isodC derivative, the design was further
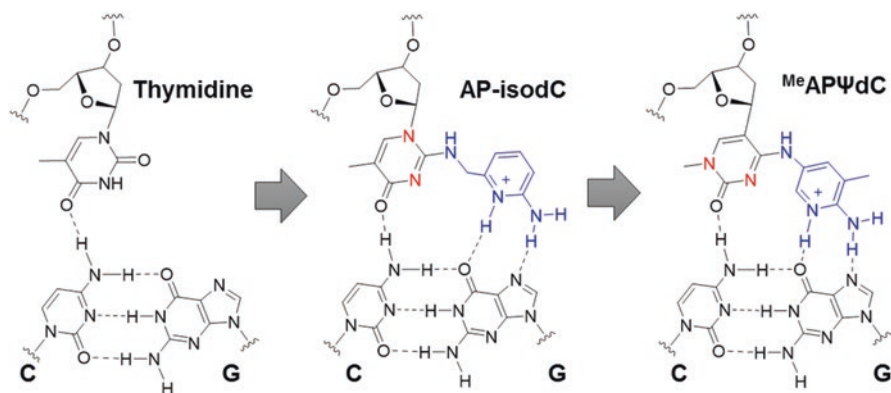

Fig. 7 Molecular design of ΨdC derivative, and the schematic structure of T/CG triplet (left), AP-isodC/CG triplet (center), ^{Me}AP-ΨdC/CG triplet (right)

optimized by replacing the isodC structure with 1-methyl-pseudocytidine, a C-nucleoside analogue of isodC, which is known for its high chemical stability [38]. Thus, an 2-amino-3-methylpyridine (^{Me}AP-ΨdC) was introduced as a guanine recognition unit, which has been used for the guanine recognition through the hydrogen bond formation on the Hoogsteen face of the guanine base [39].

3.1 Synthesis of Oligonucleotides Including ΨdC Derivatives (^{Me}AP-ΨdC)

The synthesis of the phosphoramidite compound of the ^{Me}AP-ΨdC is shown in Scheme 2. Pseudothymidine (**13**) was treated with 4,4′-dimethoxytrityl chloride followed by TBSCl to provide the hydroxyl-protected nucleoside **14**. Compound **14**
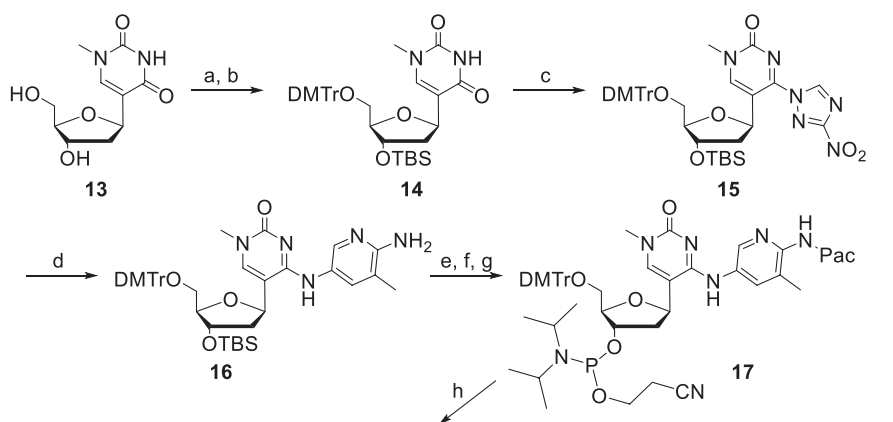
TFO (**18**): 5' AGGGAGGAGA**Z'**GGGAAGG 3'
      calc. 5845.07, found 5845.86
TFO (**20**): 5' AGGGAGGAGG**Z'**AGGAAGG 3'
      calc. 5845.07, found 5845.36

TFO (**19**): 5' AGGGAGGAGG**Z'**GGGAAGG 3'
      calc. 5861.06, found 5861.45
TFO (**21**): 5' AGGGAGGAGA**Z'**AGGAAGG 3'
      calc. 5829.08, found 5828.81

Antigene TFO (**22**):
 5' GGAAAGG**Z'**G**Z'Z'**GGGG**Z'**GGGAGAGGAG 3'
      calc. 8716.64, found 8716.69

Antigene ^{am}TFO (**23**):
 5' GGAAAGG**Z'**G**Z'Z'**GGGG**Z'**GGGAGAGGAG-amino 3'
      calc. 8853.66, found 8853.58

Z' = ^{Me}AP-ΨdC, amino: propyl amine.

Scheme 2 Synthesis of phosphoramidite compound of ^{Me}AP-ΨdC. Reagents and conditions: (**a**) DMTrCl, pyridine, 84% (**b**) TBSCl, imidazole, DMF, 95% (**c**) 3-nitro-1,2,4-triazole, diphenyl chlorophosphate, TEA, CH₃CN, 0 °C, 96% (**d**) aromatic amines, DBU, CH₃CN, 80 °C, 70%, (**e**) phenoxyacetic anhydride, pyridine (**f**) 3HF-TEA, THF (**g**) 2-cyanoethyl-*N,N*-diisopropylchlorophosphoramidite, DIPEA, CH₂Cl₂, 0 °C, 64% in three steps. (**h**) TFO was synthesized by DNA Synthesizer, and then purified by HPLC

was subsequently nitrotriazolated to provide compound **15**. Compound **15** was subjected to a substitution reaction with an aromatic amine in the presence of DBU to establish the corresponding pseudocytidine structure **16**. Compound **16** was then treated with phenoxyacetic anhydride to protect the amine groups followed by desilylation and phosphitylation to provide the corresponding phosphoramidite compound **17**, which was incorporated into the TFOs (**18–23**) using the automated DNA synthesizer. The synthesized TFOs were removed from the resin by heating in ammonium hydroxide at 55 °C and purified using reverse-phase HPLC. The DMTr group was deprotected in an aqueous AcOH solution. The structural integrity of each TFO was confirmed by MALDI-TOF MS measurements.

3.2 Evaluation of Triplex Formation

The triplex forming ability of the synthesized TFOs (**18–21**) was investigated by electrophoretic mobility shift assays using the FAM-labeled target duplexes, and the association constants (K_s) were obtained by the intensity of these bands. To compare the K_s values of all the triplexes under the same conditions, the triplex-forming experiments were performed in the buffer containing 20 mM Tris-HCl and 20 mM MgCl$_2$ at pH 7.5 and 37 °C. The results are summarized in Table 1. TFOs incorporating T at position Z formed a stable triplex against the duplex DNAs with the AT target base pair regardless of the flanking bases. T also showed a moderate affinity

Table 1 The association constants of each TFO in four different sequence contexts

TFO 3′-GGAAGG NZ′ N′ GAGGAGGGA-5′					
Duplex 5′-GAGGGAAGG NX N′ GAGGAGGGAAGC					
DNA 3′-CTCCCTTCC MY M′ CTCCTCCCTTCG-FAM	-				
		K_s (10^6 M^{-1}) for XY			
3′ NZ′N′5′	Z′	GC	CG	AT	TA
3′ GZ′A5′	T	5.0 ± 0.8	11.2 ± 0.4	**31.2 ± 1.6**	4.1 ± 0.9
	^{Me}AP-ΨdC	1.8 ± 0.5	**32.6 ± 0.5**	n.d.	n.d.
3′ GZ′ G5′	T	5.2 ± 1.3	6.2 ± 0.2	**10.9 ± 0.2**	4.7 ± 0.4
	^{Me}AP-ΨdC	5.3 ± 0.4	**16.6 ± 0.5**	0.8 ± 0.1	2.6 ± 0.5
3′ AZ′ G5′	T	2.5 ± 0.2	4.2 ± 0.3	**20.8 ± 1.6**	**2.3 ± 0.2**
	^{Me}AP-ΨdC	1.8 ± 0.6	**19.4 ± 1.8**	n.d.	0.2 ± 0.1
3′ AZ′ A5′	T	n.d.	1.4 ± 0.3	**41.8 ± 1.5**	n.d.
	^{Me}AP-ΨdC	0.2 ± 0.1	**20.8 ± 0.9**	n.d.	n.d.

Conditions: FAM-labeled duplex DNA (24 bp; 100 nM) was incubated with increasing concentrations of TFO (18 mer; 0~1000 nM) in the buffer containing 20 mM Tris-HCl and 20 mM MgCl$_2$ at pH 7.5 and 37 °C. Electrophoresis was performed with 10% non-denatured polyacrylamide gel. K_s (10^6 M^{-1}) = [Triplex]/([TFO][Duplex])
*n.d.* not detected
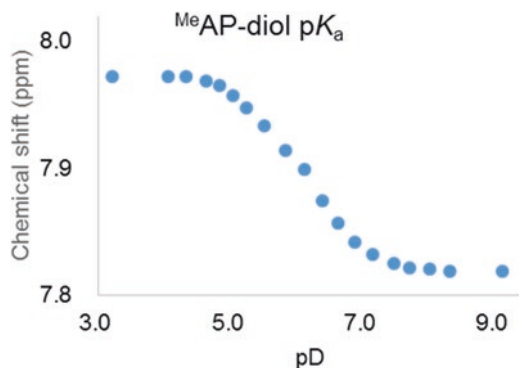
Fig. 8 Determination of pK_a value of ^{Me}AP-ΨdC by NMR titration assay. ^{Me}AP-ΨdC was dissolved in 0.1 M Na$_2$HPO$_4$ in D$_2$O (pD 9.1, 400 μl), and titrated with 0.5 M citric acid in D$_2$O. The NMR spectra were collected at the each point of the titration. The chemical shift of 6-H of the pyridine ring was plotted versus the pD value

toward the CG base pair as previously reported, however, the stability of the T/CG triplet is significantly influenced by the adjacent bases. On the other hand, ^{Me}AP-ΨdC showed a selective CG base pair recognition regardless of the sequence context, and notably, with an affinity comparable to the canonical T/AT base triplet. These results indicated that the selective recognition of the CG base pair by the ^{Me}AP-ΨdC is attributable to the specific interaction of the 2-aminopyridine ring with the CG base pair. The pK_a values of ^{Me}AP-ΨdC were determined to be 6.3 (Fig. 8). Accordingly, we speculated that the 2-aminopyridine unit is protonated and interacts with the guanine base by hydrogen bonding as depicted in Fig. 7.

3.3 Speculation of the Recognition Model of ^{Me}AP-ΨdC/CG Triplet

The possible formation of hydrogen bonds was checked by MD calculations of the triplex DNAs containing ^{Me}AP-ΨdC in a protonated form and the CG base pair on the counterpart. In the triplex DNA containing ^{Me}AP-ΨdC, the most stable structure was obtained by the protonated form; ^{Me}AP-ΨdC was shown to form a nearly coplanar base triplet with the CG base pair via the hydrogen bonds (Fig. 9). The molecular modeling also suggested that the dihedral angle between the pseudocytosine ring and the 2-aminopyridine ring is not strictly fixed but is partially flexible, being located at the appropriate position to interact with the guanine base. Such a partial mobility might allow the 2-aminopyridine ΨdC to adjust its conformation for interaction with a CG base pair in the different flanking base context.
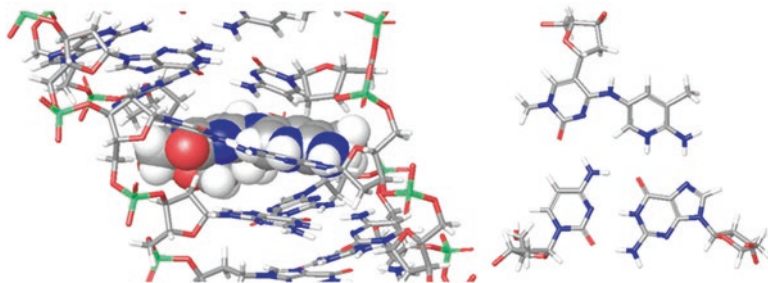
Fig. 9 The MD calculation of the triplex DNAs containing the ^{Me}AP-ΨdC and the CG base pair as its counterpart. The MD calculation was done using an OPLS_2005 force field in GB/SA solvation model of water. The minimization was performed using the PRCG method to obtain structures optimized to within a gradient (0.05 kJ/mol Å), simulation temperature (300 K), time step (1.5 fs) and simulation time (1.0 ns). During the MD simulations, hydrogen vibrations were removed using SHAKE bond constraints, allowing a longer time step of 2 fs

3.4 Inhibition of Transcription of the hTERT Gene in HeLa Cells

The highly general recognition ability of the ^{Me}AP-ΨdC for a CG pair was further demonstrated by the triplex formation against the promoter sequence of the hTERT gene, of which up-regulation is known to be associated with human carcinogenesis [40, 41]. Importantly, the triplex-forming site in the target duplex DNA contains four CG inversion sites with two of them consecutive (Fig. 10). The ^{Me}AP-ΨdC or thymidine was incorporated into the positions corresponding to each of the four CG base pairs in TFO-Z' (**22**) or TFO-T (**24**). The triplex formation was performed using the FAM-labelled target duplex DNA in the buffer containing 20 mM Tris-HCl, 2.5 mM MgCl$_2$ and 2.5 mM spermidine at pH 7.5 and 37 °C, and the triplex was observed as the low mobility bands by the gel shift assay. TFO (**22**) formed a stable triplex with the target duplex even at its low concentration (Fig. 10). It should be noted that ^{Me}AP-ΨdC is useful for the formation of the stable triplex even in the presence of multiple and consecutive CG base pairs. On the other hand, the natural type TFO (**24**) did not form a stable triplex as shown by the duplex bands at the high concentrations (Fig. 10). This is due to the low stability of the T-CG triplets.

The stable triplex formation against the hTERT promoter sequence indicates the potential to inhibit transcription of the hTERT gene. Thus, TFO-T and TFO-Z' were tested for the transcription inhibition of the endogenous hTERT gene in cultured human cancer cells. In order to prevent the digestion of the TFOs by exonuclease, which is known as the dominant nuclease species inside the cells, the TFOs were modified with the aminopropyl group at their 3′ end (^{am}TFO-Z' (**23**) and ^{am}TFO-T (**25**)). We revealed that the triplex forming ability of the aminopropyl- modified TFOs were compared to the non-modified oligonucleotides to confirm that the aminopropyl modification has no significant influence on their binding affinity. When treated with Exonuclease I, the nuclease resistance of the aminopropyl-modified
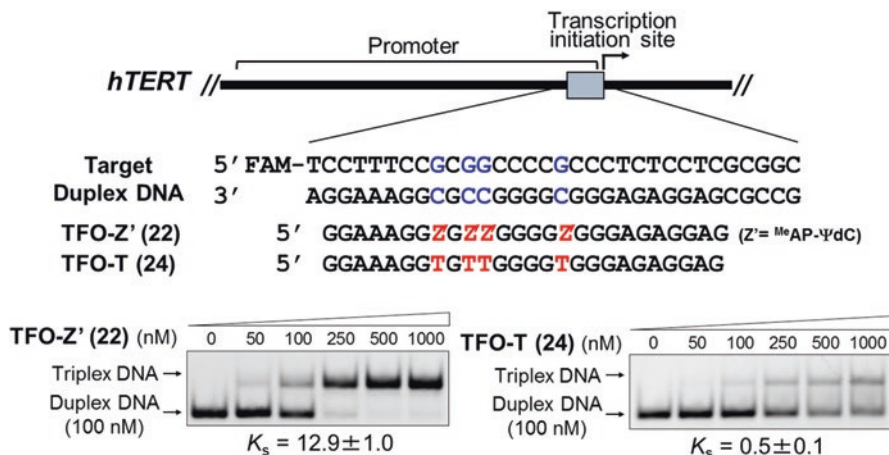
Fig. 10 The hTERT promoter sequence containing four CG inversion sites and the sequences of the corresponding TFOs (TFO-Z′ (**22**) and TFO-T (**24**)). FAM-labeled target duplex DNA (32 bp; 100 nM) was incubated with increasing concentrations of each TFO (26 mer; 0–1000 nM) in the buffer containing 20 mM Tris-HCl, 2.5 mM MgCl$_2$ and 2.5 mM spermidine at pH 7.5 and 37 °C. Electrophoresis was performed with 10% non-denatured polyacrylamide gel at 4 °C. K_s (10^6 M^{-1}) = [Triplex]/([TFO][Duplex])

TFOs was enhanced, whereas the non-modified ones were immediately digested (Fig. 11a). However, these TFOs have no S1 endonuclease resistance. Notably, the higher nuclease resistance was observed for the ^{am}TFO-Z' (**23**) compared to ^{am}TFO-T (**25**), the incorporation of the artificial nucleosides might prevent an access of Exonuclease I to the oligonucleotides. Furthermore, we tested the triplex forming ability and the stability of the amino-modified TFOs in the presence of Hela cell nuclear extracts to assess whether the TFOs can compete with the DNA binding proteins to bind to the target duplex DNA. The gel shift assays clearly indicated that ^{am}TFO-Z' (**23**) is capable of forming a triplex against the target duplex DNA even in the presence of nuclear proteins (Fig. 11b). Finally, ^{am}TFO-Z' (**23**) and ^{am}TFO-T (**25**) were transfected to Hela cells using the X-tremeGENE HP Transfection Reagent (Sigma-Aldrich) in serum-free optiMEM [42]. In the meantime, the cellular uptake of TFO was confirmed by the fluorescence spectroscopic measurements using the FITC-labeled TFO (Fig. 12a). After 24 h, the total RNA was extracted, and the relative expression levels of the hTERT mRNA were quantified by real-time RT-PCR (Fig. 12b). Compared to the ^{am}TFO-T (**25**), ^{am}TFO-Z' (**23**) containing ^{Me}AP-ΨdC effectively suppressed the hTERT expression. As the results are in good agreement with the triplex forming ability of each TFO, we concluded that the inhibition of the hTERT transcription is attributable to the binding of ^{am}TFO-Z' (**23**) to
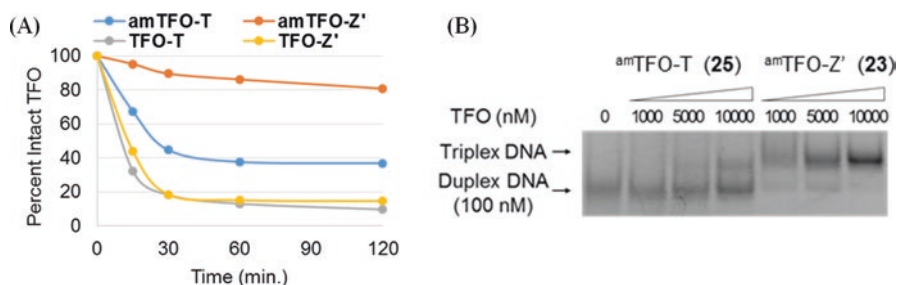
Fig. 11 The property of aminopropyl modified TFOs. (**a**) Nuclease digestion of the TFOs with Exonuclease I. Each TFO was treated with Exonuclease I (0.5 U) in a buffer containing 20 mM Tris-HCl (pH 7.5), 2.5 mM MgCl$_2$ and 2.5 mM spermidine at 37 °C for 0–120 min. The digestion was analyzed by 15% denatured polyacrylamide gel containing 8 M urea, and the gel was stained with SYBR Gold Nucleic Acid Gel Stain according to the manufacture's protocol. The amount of the intact TFO was measured by quantification of the corresponding fluorescence using luminoimage analyzer. (**b**) Triplex formation of the aminopropyl-modified TFOs in the presence of the Hela cell nuclear extract. FAM-labeled duplex DNA (100 nM) was incubated with 5% Hela nuclear extracts for 30 min at 37 °C in the buffer. Subsequently, increasing concentrations of the TFO (0–10,000 nM) were added, and the solution was incubated for an additional 1 h at 37 °C. Each solution was analyzed by gel electrophoresis and detected by LAS-4000
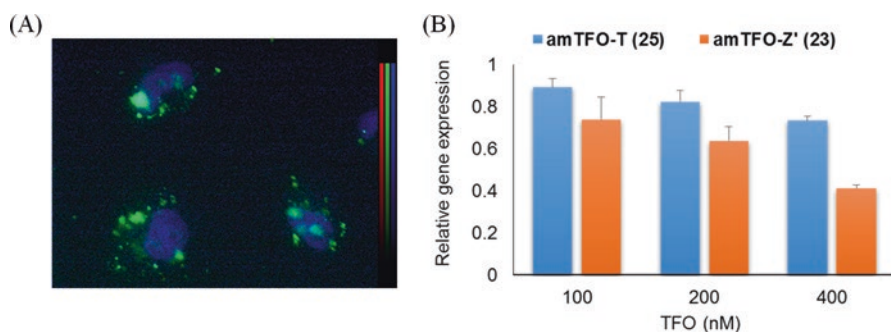
Fig. 12 (**a**) Confirmation of the endogenous uptake of TFO by fluorescence microscopy. The green represents the FITC-labeled ^{am}TFO-Z′ containing ^{Me}AP-ΨdC and blue indicating nucleus stained with Hoechst 33,258. (**b**) Intracellular inhibition of hTERT gene expression using ^{am}TFO-Z′ (**23**) and ^{am}TFO-T (**25**). The relative gene expression levels were obtained by normalizing the amount of hTERT mRNA with GAPDH mRNA. The standard deviations were calculated from three independent experiments

the target hTERT promoter sequence. No significant transcription inhibition was observed after 48 h, because a part of the TFOs were hydrolyzed by nucleases. Attempts for duration of the antigene inhibition are now ongoing with TFOs constructed of modified nucleosides with resistance to the endo- and exonucleases.

4   Conclusion and Perspectives

This chapter highlights the development of artificial nucleoside analogues which can form the stable triplex DNA including TA and CG inversion sites and the application of them for the antigene methods. The triplex forming oligonucleotides including WNA-βT and [Me]AP-ΨdC recognize the duplex DNA containing the TA and CG base pair, respectively. Notably, [Me]AP-ΨdC stabilizes the CG base pair that continuously exists. The antigene TFOs with WNA-βT are able to inhibit the generation of the survivin protein in the A549 cells, on the other hand, the antigene TFOs with [Me]AP-ΨdC are able to inhibit the generation of hTERT mRNA. In any case, these artificial nucleoside analogues have a good potential to develop the genome targeting tool in any region of the duplex DNA with TFOs, and they will become great therapeutic oligonucleotides.

References

1. Thuong NT, Helene C (1993) Sequence-specific recognition and modification of double-helical DNA by oligonucleotides. Angew Chem Int Ed 32:666–690
2. Chan PP, Glazer PM (1997) Triplex DNA: fundamentals, advances, and potential applications for gene therapy. J Mol Med 75:267–282
3. Buchini S, Leumann CJ (2003) Recent improvements in antigene technology. Curr Opin Chem Biol 7:717–726
4. Jain A, Wang G, Vasquez KM (2008) DNA triple helices: biological consequences and therapeutic potential. Biochimie 90:1117–1130
5. Moser HE, Dervan PB (1987) Sequence-specific cleavage of double helical DNA by triple helix formation. Sicence 238:645–650
6. Rajagopal P, Feigon L (1989) NMR studies of triple-strand formation from the homopurine-homopyrimidine deoxyribonucleotides d(GA)$_4$ and d(TC)$_4$. Biochemistry 28:7859–7870
7. Beal PA, Dervan PB (1991) Second structural motif for recognition of DNA by oligonucleotide-directed triple-helix formation. Science 251:1360–1363
8. Beal PA, Dervan PB (1992) The influence of single base triplet changes on the stability of a pur.pur.pyr triple helix determined by affinity cleaving. Nucleic Acids Res 20:2773–2776
9. Huang CY, Miller PS (1996) Triplex formation by oligonucleotides containing novel deoxycytidine derivatives. Nucleic Acids Res 24:2606–2613
10. Rusling DA, Powers VEC, Ranasinghe RT, Wang Y, Osborne SD, Brown T, Fox KR (2005) Four base recognition by triplex-forming oligonucleotides at physiological pH. Nucleic Acids Res 33:3025–3032
11. Semenyuk A, Darian E, Liu J, Majumdar A, Cuenoud B, Miller PS, MacKerell AD, Seidman MM (2010) Targeting of an interrupted polypurine:polypyrimidine sequence in mammalian cells by a triplex-forming oligonucleotide containing a novel base analogue. Biochemistry 49:7867–7878
12. Hari Y, Akabane M, Obika S (2013) 2′,4′-BNA bearing a chiral guanidinopyrrolidine containing nucleobase with potent ability to recognize the CG base pair in a parallel-motif DNA triplex. Chem Commun 49:7421–7423
13. Ohkubo A, Yamada K, Ito Y, Yoshimura K, Miyauchi K, Kanamori T, Masaki Y, Seio K, Yuasa H, Sekine M (2015) Synthesis and triplex-forming properties of oligonucleotides capable of recognizing corresponding DNA duplexes containing four base pairs. Nucleic Acids Res 43:5675–5686

14. Stilz HU, Dervan PB (1993) Specific recognition of CG base pairs by 2-deoxynebularine within the purine-purine-pyrimidine triple-helix motif. Biochemistry 32:2177–2185

15. Parel SP, Leumann CJ (2001) Triple-helix formation in the antiparallel binding motif of oligo-deoxynucleotides containing N^9- and N^7-2-aminopurine deoxynucleosides. Nucleic Acids Res 29:2260–2267

16. Kolganova NA, Shchyolkina AK, Chudinov AV, Zasedatelev AS, Florentiev VL, Timofeev EN (2012) Targeting duplex DNA with chimeric α,β-triplex-forming oligonucleotides. Nucleic Acids Res 40:8175–8185

17. Sasaki S, Yamauchi H, Nagatsugi F, Takahashi R, Taniguchi Y, Maeda M (2001) W-shape nucleic acid (WNA) for selective formation of nonnatural anti-parallel triplex including a TA interrupting site. Tetrahedron Lett 42(39):6915–6918

18. Sasaki S, Taniguchi Y, Takahashi R, Senko Y, Kodama K, Nagatsugi F, Maeda M (2003) Selective formation of stable triplexes including a TA or a CG interrupting site with new bicy-clic nucleoside analogues (WNA). J Am Chem Soc 126:516–528

19. Taniguchi Y, Nakamura A, Senko Y, Kodama K, Nagatsugi F, Sasaki S (2005) Expansion of tri-plex recognition codes by the use of novel bicyclic nucleoside derivatives (WNA). Nucleosides Nucleotides Nucleic Acids 24:823–827

20. Taniguchi Y, Nakamura A, Senko Y, Nagatsugi F, Sasaki S (2006) Effects of halogenated WNA derivatives on sequence dependency for expansion of recognition sequences in non-natural-type triplexes. J Org Chem 71:2115–2122

21. Nasr T, Taniguchi Y, Sasaki S (2007) Synthesis of 1′-phenyl substituted nucleoside analogs. Heterocycles 71:2659–2668

22. Taniguchi Y, Togo M, Aoki E, Uchida Y, Sasaki S (2008) Synthesis of p-amino-WNA deriva-tives to enhance the stability of the anti-parallel triplex. Tetrahedron 64:7164–7170

23. Taniguchi Y, Uchida Y, Takaki T, Aoki E, Sasaki S (2009) Recognition of the CG interrupt-ing site by W-shaped nucleoside analogs (WNA) having the pyrozole ring in an anti-parallel triplex DNA. Bioorg Med Chem 17:6803–6810

24. Aoki E, Taniguchi Y, Wada Y, Sasaki S (2012) Efficient DNA strand displacement by a W-shaped nucleoside analogue (WNA-βT) containing an ortho-methyl-substituted phenyl ring. Chembiochem 13:1152–1160

25. Nasr T, Taniguchi Y, Takaki T, Okamura H, Sasaki S (2012) Properties of oligonucleotide with phenyl-substituted carbocyclic nucleoside analogues for the formation of duplex and triplex DNA. Nucleosides Nucleotides Nucleic Acids 31:8441–8460

26. Taniguchi Y, Okamura H, Fujino N, Sasaki S (2013) Synthesis of 1′-phenyl-2-OMe ribose analogues connecting the thymine base at the 1′ position through a flexible linker for the for-mation of a stable anti-parallele triplex DNA. Tetrahedron 69:600–606

27. Taniguchi Y, Tomizaki A, Matsueda N, Okamura H, Sasaki S (2015) Enhancement of TFO tri-plex formation by conjugation with pyrene via click chemistry. Chem Pharm Bull 63:920–926

28. Shen C, Buck A, Polat B, Schmid-Kotsas A, Matuschek C, Gross H-J, Bachem M, Reske SN (2003) Triplex-forming oligodeoxynucleotides targeting survivin inhibit proliferation and induce apoptosis of human lung carcinoma cells. Cancer Gene Ther 10:403–410

29. Zendegui JG, Vasquez KM, Tinsley JH, Kessler DJ, Hogan ME (1992) In vivo stability and kinetics of absorption and disposition of 3′ phosphopropyl amine oligonucleotides. Nucleic Acids Res 20:307–314

30. Gamper HB, Reed MW, Cox T, Virosco JS, Adams AD, Gall AA, Scholler JK, Meyer RB (1993) Facile preparation of nuclease resistant 3′ modified oligodeoxynucleotides. Nucleic Acids Res 21:145–150

31. Shin S, Sung B-J, Cho Y-S, Kim H-J, Ha N-C, Hwang J-I, Chung C-W, Jung Y-K, Oh B-H (2001) An anti-apoptotic protein human survivin is a direct inhibitor of caspase-3 and -7. Biochemistry 40:1117–1123

32. Taniguchi Y, Sasaki S (2012) An efficient antigene activity and antiproliferative effect by tar-geting the Bcl-2 or survivin gene with triplex forming oligonucleotides containing a W-shaped nucleoside analogue (WNA-βT). Org Biomol Chem 10:8336–8341

33. Dittrich K, Gu J, Tinder R, Hogan M, Gao X (1994) T·C·G triplet in an antiparallel purine·purine·pyrimidine DNA triplex conformational studies by NMR. Biochemistry 33:4111–4120
34. Durland RH, Rao TS, Revankar GR, Tinsley JH, Myrick MA, Seth DM, Rayford J, Singh P, Jayaraman K (1994) Binding of T and T analogs to CG base pairs in antiparallel triplexes. Nucleic Acids Res 22:3233–3240
35. Okamura H, Taniguchi Y, Sasaki S (2013) N-(Guanidinoethyl)-2′-deoxy-5-methylisocytidine exhibits selective recognition of a CG interrupting site for the formation of anti-parallel triplexes. Org Biomol Chem 11:3918–3924
36. Okamura H, Taniguchi Y, Sasaki S (2014) An isocytidine derivative with a 2-amino-6-methylpyridine unit for selective recognition of the CG interrupting site in an antiparallel triplex DNA. Chembiochem 15:2374–2378
37. Okamura H, Taniguchi Y, Sasaki S (2016) Aminopyridinyl-pseudodeoxycytidine derivatives selectively stabilize antiparallel triplex DNA with multiple CG inversion sites. Angew Chem Int Ed. 55:12445-12449
38. Kim H-J, Leal NA, Benner SA (2009) 2′-deoxy-1-methylpseudocytidine, a stable analog of 2′-deoxy-5-methylisocytidine. Bioorg Med Chem 17:3728–3232
39. Hildbrand S, Blaser A, Parel SP, Leumann CJ (1997) 5-substituted 2-aminopyridine C-nucleosides as protonated cytidine equivalents: increasing efficiency and selectivity in DNA triple-helix formation. J Am Chem Soc 119:5499–5511
40. Ito H, Kyo S, Kanaya T, Takakura M, Inoue M, Namiki M (1998) Expression of human telomerase subunits and correlation with telomerase activity in urothelial cancer. Clin Cancer Res 4:1603–1608
41. Takakura M, Kyo S, Kanaya T, Hirano H, Takeda J, Yutsudo M, Inoue M (1999) Cloning of human telomerase catalytic subunit (hTERT) gene promoter and identification of proximal core promoter sequences essential for transcriptional activation in immortalized and cancer cells. Cancer Res 59:551–557
42. Govan JM, Uprety R, Hemphill J, Lively MO, Deiters A (2012) Regulation of transcription through light-activation and light-deactivation of triplex-forming oligonucleotides in mammalian cells. ACS Chem Biol 7:1247–1256

Chemical Synthesis of Boranophosphate Deoxy-ribonucleotides

Yohei Nukaga and Takeshi Wada

Abstract Boranophosphate deoxyribonucleotides, in which a non-bridging oxygen atom of each phosphodiester internucleotidic linkage is replaced by a BH_3 group, are useful as therapeutic agents owing to affinity for complementary RNA, nuclease resistance, RNase H activity, efficient cellular uptake, and potency for gene suppression. Over past two decades, chemists have tried to develop an efficient method for the chemical synthesis of boranophosphate deoxyribonucleotides. In this review, recent studies on the synthesis of boranophosphate deoxyribonucleotides are focused.

Keywords Boranophosphate DNA · Stereodefined boranophosphate DNA · Solid-phase synthesis · Stereocontrolled synthesis · *H*-phosphonate approach · Phosphoramidite approach · Boranophosphotriester approach · *H*-boranophosphonate approach · Oxazaphospholidine approach

1 Introduction

Chemically modified oligonucleotides have lately gained significant attention as therapeutic agents to silence target mRNAs sequence-specifically, *i.e.*, antisense DNAs [1], small interfering RNAs (siRNAs) [2], anti-miRs [3], and DNA/RNA heteroduplex oligonucleotides [4]. Among the many types of modifications, phosphorothioate deoxyribonucleotides (PS-DNAs), in which a non-bridging oxygen atom of each phosphodiester internucleotidic linkage is replaced by a sulfur atom, have been used the most commonly for therapeutic oligonucleotides under clinical trials and recently Mipomersen (Kynamro®), which is used to treat homozygous familial hypercholesterolemia (HoFH), approved for marketing [5]. PS-DNAs have moderate affinity for complementary RNA, nuclease resistance, potency for gene suppression, and favorable pharmacokinetic properties [6]. However, PS-DNAs

Y. Nukaga · T. Wada (✉)
Department of Medicinal and Life Science, Faculty of Pharmaceutical Sciences, Tokyo University of Science, Noda, Chiba, Japan
e-mail: twada@rs.tus.ac.jp

have some drawbacks such as lower affinity for complementary RNA than unmodified counterparts and cytotoxicity effect at the high concentration [7]. On the other hand, boranophosphate deoxyribonucleotides (PB-DNAs), in which a non-bridging oxygen atom of each phosphodiester internucleotidic linkage is substituted by a BH_3 group, have recently attracted much attention as next-generation therapeutic agents owing to higher stability to nuclease [8] and the potential for lower cytotoxicity [9] than PS-DNAs, RNase H activity [10], efficient cellular uptake [11], and high potency for gene suppression [9, 11]. Furthermore, PB-DNAs have been expected as target-specific ^{10}B carriers for boron neutron capture therapy (BNCT) [12]. Over past two decades, chemists have tried to develop a method for the efficient synthesis of PB-DNAs. In Sects. 2, 3, 4, and 5, recent studies on the chemical synthesis of PB-DNAs by the *H*-phosphonate approach, the phosphoramidite approach, the boranophosphotriester approach, and the *H*-boranophosphonate approach are reviewed. On the other hand, one of the most important properties of PB-DNAs is the charity of the phosphorus atoms. PB-DNAs have two diastereomers in each internucleotidic linkage. Their properties are dependent on the configurations of the phosphorus atoms [13–15]. For the reason, the stereocontrolled chemical synthesis of PB-DNAs has been challenged during the past years. In Sect. 6, the synthesis of *P*-stereodefined PB-DNAs by the oxazaphospholidine approach which our group has recently developed is summarized.

2 Synthesis of Boranophosphate DNA by the Phosphoramidite Approach

In 1990, Shaw et al. achieved the first chemical synthesis of PB-DNAs. As shown in Fig. 1, the synthesis was performed by the conventional phosphoramidite approach [16]. The procedure started from the condensation, which was the reaction of a free 5′-OH thymidine nucleoside with 5′-*O*-dimethoxytrithyl (DMTr) thymidine phosphoramidite in the presence of 1*H*-tetrazole. The resultant phosphite triester was converted to the dinucleoside boranophosphate methyl ester and simultaneously removed the 5′-*O*-DMTr group by boronation with $BH_3 \cdot Me_2S$. After was treated with concentrated NH_3, thymidine boranophosphate dimer was successfully obtained.

However, Shaw's method is limited to sequences with only thymidine nucleoside because undesirable reductions occurred at the *N*-acyl protecting groups on the nucleobases A, G, and C by the borane reagent [17]. As shown in Fig. 2, the *N*-acyl groups were reduced into the corresponding *N*-alkyl groups which could not be removed by treatment with concentrated NH_3. For a reason, this method could not be applicable to the synthesis of PB-DNAs with mixed sequences.

To solve this problem, in 2006, Caruthers et al. developed a new strategy for the synthesis of PB-DNAs with mixed sequences as shown in Fig. 3 [18]. Caruthers's method used benzhydroxybis(trimethylsilyloxy)silyl (BzH) as a protecting group of
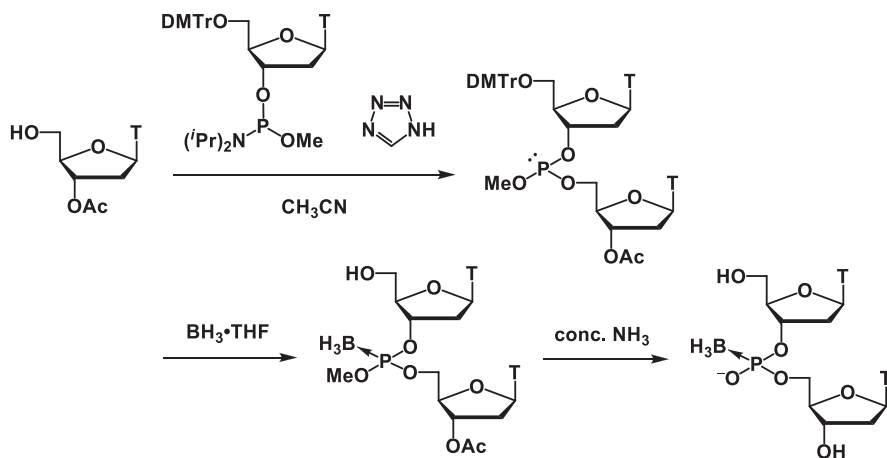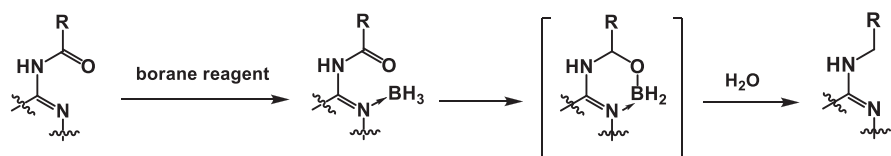
Fig. 1 Synthesis of PB-DNA by the phosphoramidite approach

R = methyl, isopropyl or phenyl

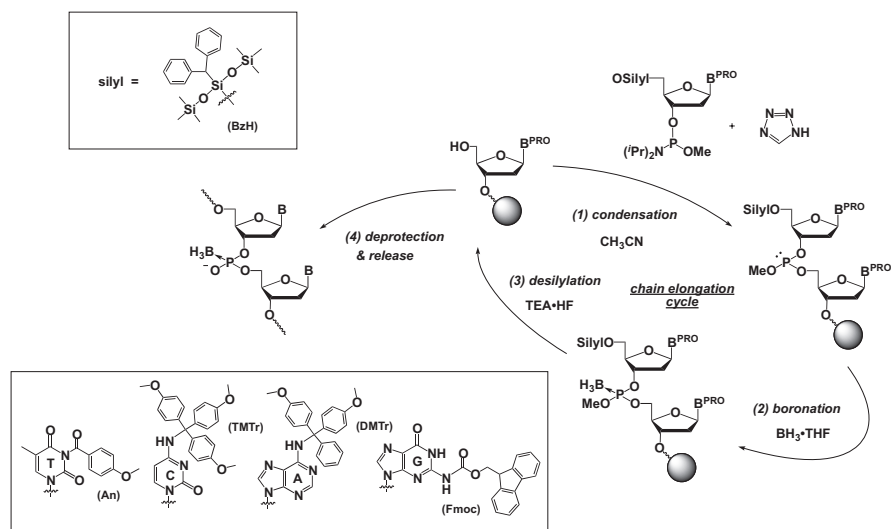**Fig. 2** Proposed mechanism for the reduction of *the N*-acyl protecting group on the nucleobase

Fig. 3 Solid-phase synthesis of PB-DNA using the 5′-*O*-silyl group

the 5′-OH, which is substituted for the conventional DMTr group. These silyl ester could be compatible with the synthesis of PB-DNAs and removed by treatment with $Et_3N \cdot HF$ before the next chain elongation cycle. For the purpose of suppression of the nucleoside N-acyl group reduction, the nucleobases A, C, and G were protected with 6-N-DMTr, 4-N-trimethoxytrityl (TMTr), 2-N-9-fluorenylmethoxycarbonyl (Fmoc), respectively. Also, Thymidine was protected with N^3-anisoyl (An) for elimination of the possible reduction by a borane reagent.

After the chain elongation following to the procedure shown in Fig. 3, protecting groups of the resultant oligomers attached to the support are removed. Initially, DMTr and TMTr groups were eliminated from adenosine and cytidine by using 80% AcOH. Next, the resulting molecules were treated with a dithiolate to remove the methyl protection in internucleotidic linkages. Finally, concentrated NH_3 removed Fmoc and An from guanosine and thymidine, respectively and cleaved the fully-deprotected oligomers from solid support. As a result, $d(T^bC^bT^bT^bA^bC^bT^bG^bA^bT)$ 10mer was very efficiently obtained in 99% coupling yield and 88% isolated yield.

However, Caruthers's method has a drawback that a customized automatic synthesizer is essential to handle basic fluoride solutions which are required for removal of the 5′-O-silyl protection. To overcome this limitation, in 2013, Caruthers et al. have developed a new strategy using N-silyl protected 5′-O-DMTr nucleoside phosphoramidites matched with the conventional phosphoramidite method [19]. Surprisingly, silyl protecting group di-*tert*-butylisobutylsilyl (BIBS) on the nucleobases A, G, and C was quiet stable toward the 0.5% TFA in the detritylation step and applicable to the phosphramidite approach. The chain elongation is shown in Fig. 4. In this process, trimethylphosphite borane (TMPB) was used as an efficient DMTr⁺
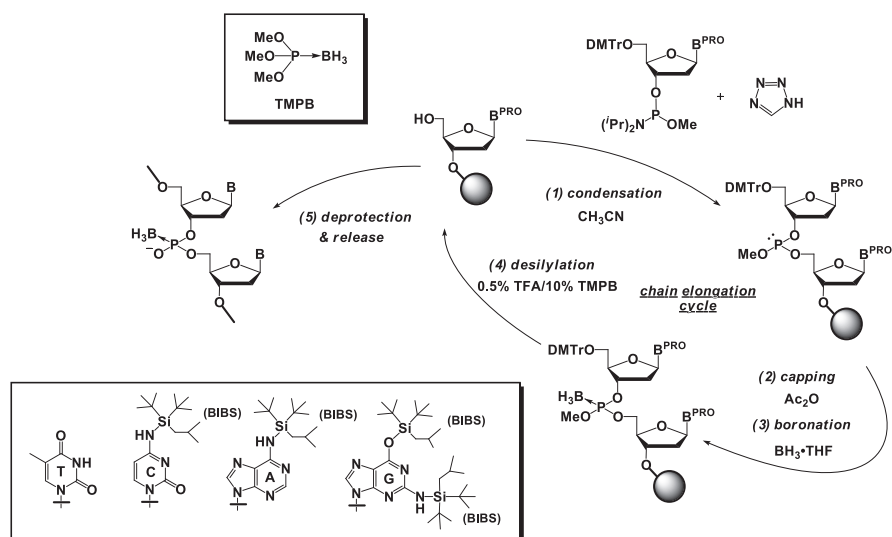

Fig. 4 Solid-phase synthesis of PB-DNA using the 5′-O-DMTr group

scavenger. After this cycle was repeated, the methyl protection in internucleotidic linkages was eliminated on solid support. Subsequently, BIBS groups were desilylated by fluoride treatment. After fully-deprotection of protecting groups, release of the resultant oligomer was accomplished by treatment with concentrated NH_3. The results showed that d(C^{b}A^{b}G^{b}T^{b}G^{b}A^{b}C^{b}C^{b}G^{b}C^{b}A^{b}T^{b}C^{b}G^{b}G^{b}A^{b}C^{b}A^{b}G^b-C^{b}A^{b}G^{b}C^{b}T) 24-mer was very efficiently synthesized. Also, d(C^{p}A^{p}G^{p}T^{b}G^{p}A^{p}C^{p}C^b-G^{p}C^{p}A^{p}T^{b}C^{p}G^{p}G^{p}A^{b}C^{p}A^{p}G^{p}C^{b}A^{p}G^{p}C^{p}T) 14-mer having phosphate and boranophosphate linkages was successfully synthesized by combining the oxidization and boronation. To our knowledge, the 24-mer is the longest length reported to have been synthesized to date.

3 Synthesis of Boranophosphate DNA by the *H*-phosphonate Approach

As shown in Fig. 5, *H*-phosphonate, in which a non-bridging oxygen atom of each phosphodiester internucleotidic linkage is replaced by a hydrogen atom, is convertible to a variety of *P*-modified oligonucleotides (e.g., phosphorothioate, phosphoroamidate, and alkyl phosphonate). The *H*-phosphonate has been prepared as a useful intermediate for the synthesis of *P*-modified oligonucleotides.

In 1997, Matteucci et al. firstly reported the synthesis of PB-DNAs by the *H*-phosphonate approach [20]. Shortly after this report, Shaw et al. and Caruthers et al. independently synthesized counterparts using a similar method [8, 21]. The synthetic procedure is shown in Fig. 6. 5′-*O*-DMTr thymidine *H*-phosphonate was condensed with a free 5′-OH thymidine nucleoside in the presence of a condensing reagent. The resultant molecule was treated with deblock solution for the removal of the 5′-*O*-DMTr group. After this cycle was repeated, *H*-phosphonate intermediates P(V) were converted into silyloxyl phosphite intermediates P(III) by sliylation with a silylating reagent. Subsequently, the silyloxyl phosphite was exchanged into
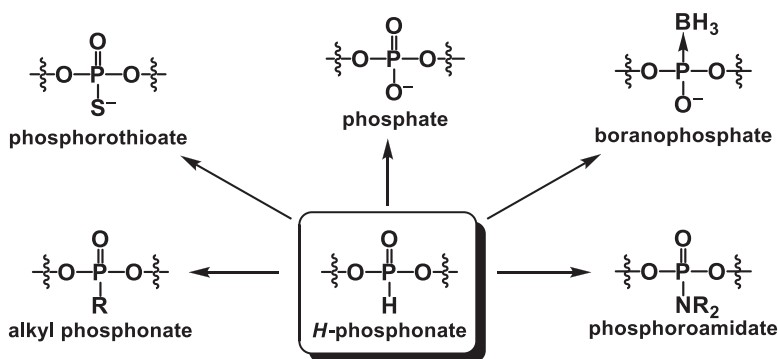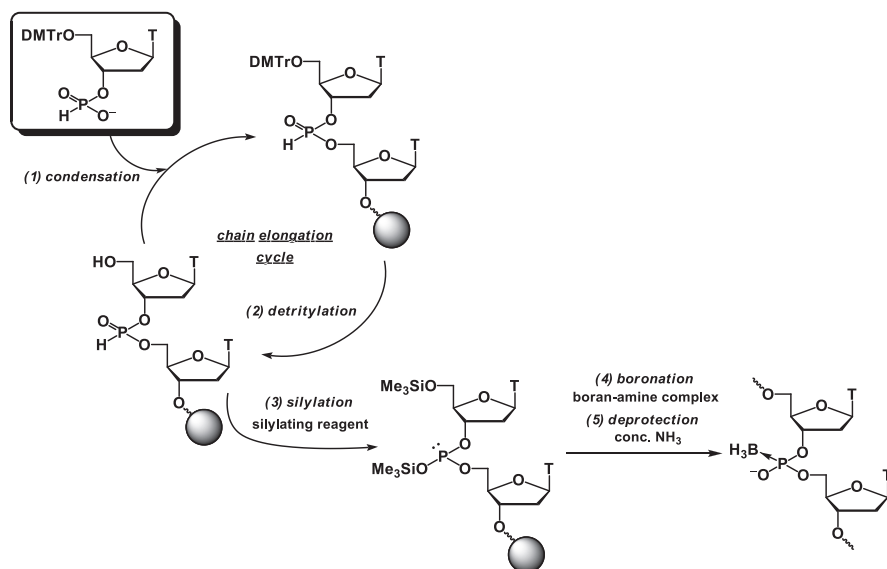

Fig. 5 Conversion of *H*-phosphonate to *P*-modified oligonucleotides

Fig. 6 Solid-phase synthesis of PB-DNA by the *H*-phosphonate approach

boranophosphate triester by using a borane reagent. Finally, the deprotection of the silyl group along with the cleavage of the linker was carried out to afford the desired oligomer. Using the *H*-phosphonate method, PB-DNAs with only thymidine nucleoside up to 15-mer were synthesized in good yields.

However, as described in Sect. 2, because of undesirable reductions that occur at the *N*-protecting groups during the boronation step, this method could not be applicable to the preparation of PB-DNAs with mixed sequences.

In 2001, Shaw et al. successfully overcome this problem by using the *N*-unprotected *H*-phosphonate method [22]. The *N*-unprotected strategy was developed by Wada et al. for the efficient synthesis of native phosphate DNAs *via* the *H*-phosphonate intermediates [23]. The chain elongation cycle was performed completely without protecting groups, which was expected that PB-DNAs with mixed sequences could be synthesized without undesirable reductions by a borane reagent.

First, Shaw et al. prepared d(G^{b}A^{b}C^{b}T) 4-mer with mixed sequences following the procedure in Fig. 7. 5′-*O*-DMTr *N*-unprotected nucleoside *H*-phosphonate was allowed to react with the free 5′-OH nucleoside in the presence of 2-(benzotriazol-1-yloxy)-1,1-dimethyl-2-pyrrolidin-1-yl-1,3,2-diazaphospholidinium hexafluorophosphate (BOMP) as a condensing reagent. After the chain elongation, the resultant *H*-phosphonate intermediates were converted into PB-DNAs by boronation following to silylation and then the linker was cleaved by concentrated NH$_3$ to afford the desired oligomer. Consequently, d(G^{a}A^{b}C^{b}T) 4-mer was efficiently obtained in 48% isolated yield. However, the synthesis of the longer d(T^{b}C^{b}A^{b}A^{b}C^{b}G^{b}T^{b}T^{b}G^{b}A) 10-mer was less efficiency. The lower yield might be due to the relatively instability of internucleotide *H*-phosphonate linkages during the chain elongation cycle. Therefore, so far, *N*-unprotected *H*-phosphonate method has been limited to the synthesis of the length sequence of up to ten bases.
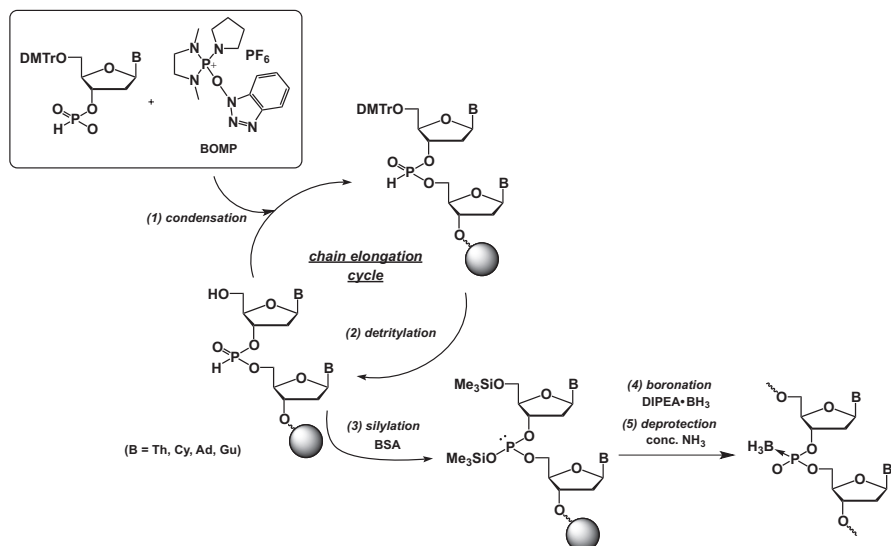
Fig. 7 Solid-phase synthesis of PB-DNA by the *N*-unprotected *H*-phosphonate approach

4 Synthesis of Boranophosphate DNA by the Boranophospho-Triester Approach

Recently, our group has developed the boranophosphotriester method as a new strategy for the synthesis of PB-DNAs [24–26]. In this method, 5′-*O*-DMTr nucleoside boranophosphates, which were prospectively incorporated P→BH₃ coordination linkages into molecules, were used as monomers to introduce a BH₃ group into an internucleotidic linkage. Consequently, side reactions by a borane reagent in the conventional methods for the synthesis of PB-DNAs could be completely avoided.

Ahead of the solid-phase synthesis of PB-DNAs, 5′-*O*-DMTr nucleoside boranophosphate monomers with full base protection were synthesized in 51–81% yields by using boranophosphorylating reagent. Appropriate protecting groups were introduced at the N^3 of thymidine and 6-*O* of 2-*N*-phenyacetyl guanosine to avoid side reactions of boranophosphate monomer or boranophosphorylating reagent with the nucleobase. Following to the procedure in Fig. 8, the monomer was condensed with a free 5′-OH nucleoside in the presence of 1,3-dimethyl-2-(3-nitro-1,2,4-triazol-1-yl)-2-pyrrolidin-1-yl-1,3,2-diazapholidinium hexafluorophosphate (MNTP) as condensing reagent. Consequently, the detritylation reaction was carried out in the presence of Et₃SiH as the DMTr⁺ scavenger. After the procedure was repeated, the cyanoethyl group of boranophosphate triester intermediates was removed by treatment with DBU. Later, PB-DNA on solid support was deprotected and cleaved by treatment with methanolic ammonia solution. HPLC analysis of the crude mixtures showed that the desired PB-DNA 2-mers were obtained in 90–96% coupling yields. By using this method, d(CᵇAᵇGᵇTᵇCᵇAᵇGᵇTᵇCᵇAᵇGᵇT) 12-mer was synthesized in 16% isolated yield.
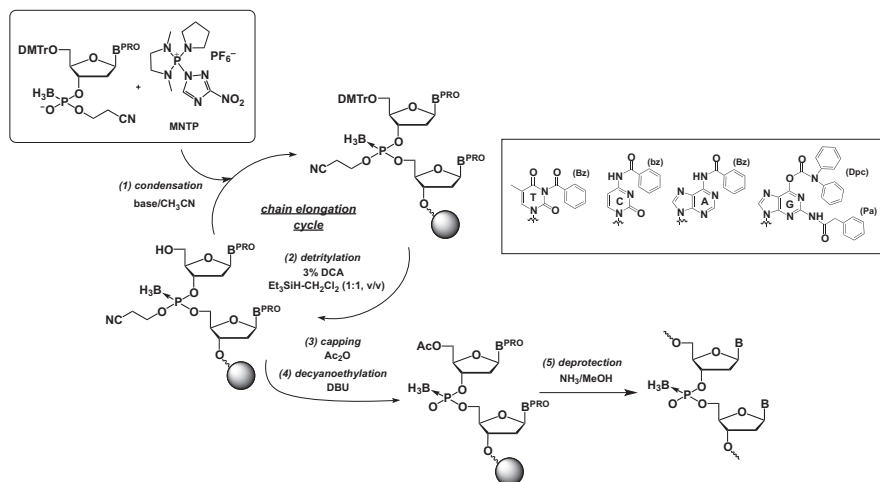
Fig. 8 Solid-phase synthesis of PB-DNA by the boranophosphotriester approach
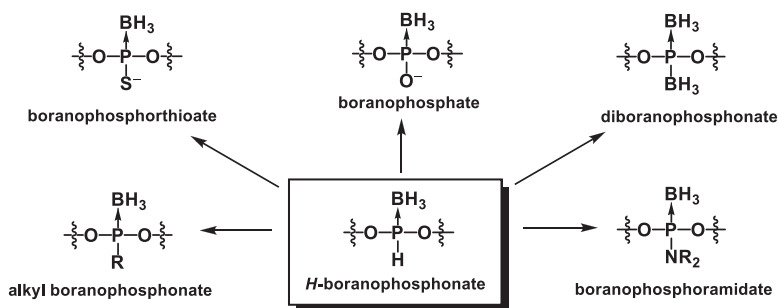

Fig. 9 Conversion of *H*-boranophosphonate to *P*-modified oligonucleotides

5 Synthesis of Boranophosphate DNA by the *H*-boranophospho-nate Approach

Further, our group has developed *H*-boranophosphate oligonucleotides as a key intermediate for the synthesis of PB-DNAs [27, 28]. As shown in Fig. 9, the *H*-boranophoshate oligonucleotide, which has a P→BH₃ and a P-H group into internucleotidic linkages, is used as a versatile procedure to various *P*-modified oligonucleotides (e.g., boranophosphate, boranophosphorothioate, and boranophosphoramidite). The *P*-modified oligonucleotides are prepared by the reaction of various electrophiles with the phosphonium anion generated *via* the activation of the P-H function by bases.

The synthetic procedure of the *H*-boranophosphonate method is described in Fig. 10. First, fully-protected *H*-boranophosphate monomers were obtained in 60–95% yields by the reaction of a free 3′-OH nucleoside with *H*-boranophosphorylating reagent. The monomers were condensed with the 5′-OH of nucleosides or oligonu-
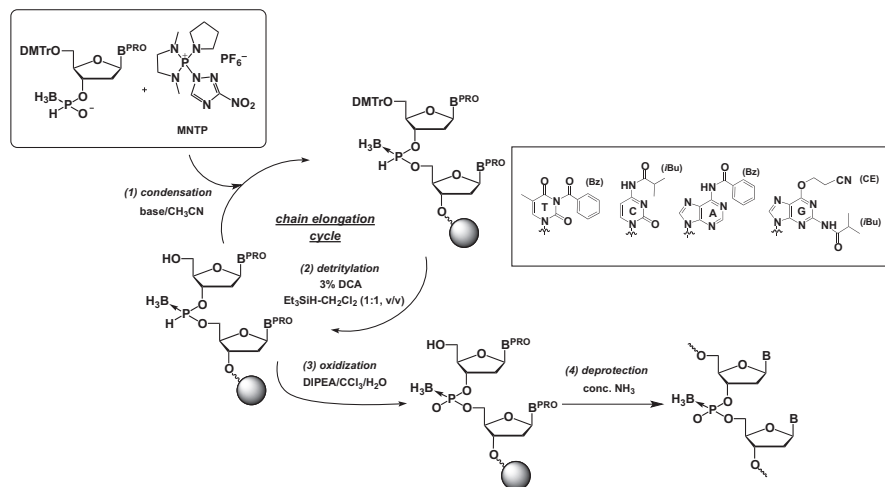
Fig. 10 Solid-phase synthesis of PB-DNA by the *H*-boranophosphonate approach

cleotides on solid-phase synthesis in the presence of MNTP, and the 5′-end was eliminated by 3% DCA containing Et₃SiH as a DMTr⁺ scavenger.

The resultant *H*-boranophoshate diester intermediates were oxidized *via P*-chlorination with CCl₄ and subsequent hydrolysis by H₂O in the presence of DIPEA. After deprotection and cleavage, RP-HPLC analysis showed that PB-DNA 2-mers were synthesized in 95–97% yields, and the coupling efficiency of *H*-boranophosphonate monomers was greater than that of boranophosphotriester monomers. According to the procedure described in Fig. 10, d(GᵇCᵇAᵇTᵇTᵇTᵇGᵇGᵇTᵇAᵇTᵇTᵇC) 12-mer was synthesized in 44% isolated yield. Subsequently, d(GᵇCᵇAᵇTᴸᵇTᴸᵇGᵇGᵇTᴸᵇAᵇTᴸᵇTᴸᵇC) 12-mer, which was replaced all the thymidine 3′-boranophosphate moiety with LNA thymidine 3′-boranophosphate, was also obtained in 7% isolated yield.

6 Stereocontrolled Synthesis of Boranophosphate DNA by the Oxazaphospholidine Approach

The disadvantage of the methods described in Sects. 2, 3, 4, and 5 is that the oligonucleotides are synthesized in a nonstereocontrolled manner and subsequent prepared as diastereomixtures of the *R*p and *S*p isomers. For examples, PB-DNAs containing a diastereopure boranophosphate linkage have been prepared by chromatographic separation [13]. However, this method is not applicable to the preparation of PB-DNAs with multiple *P*-stereodefined boranophosphate linkages. Diastereopure dimer building blocks can be used to incorporate multiple stereodefined boranophosphate linkages into ORNs. However, this method cannot produce PB-DNAs having consecutive stereodefined boranophsohate linkages. The
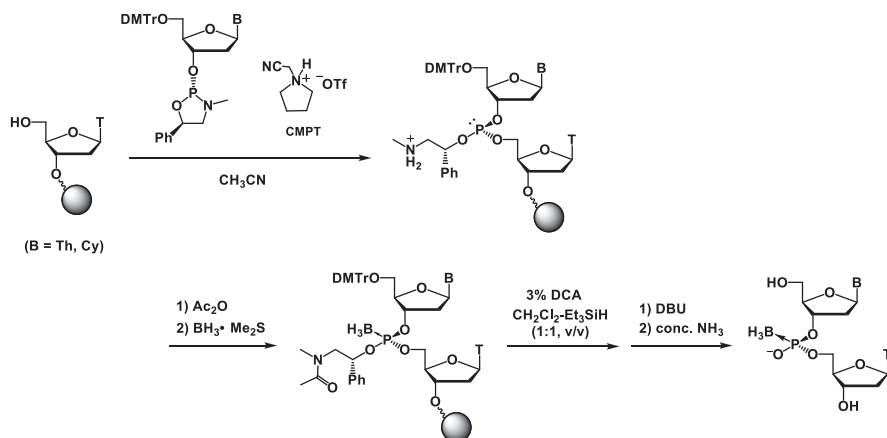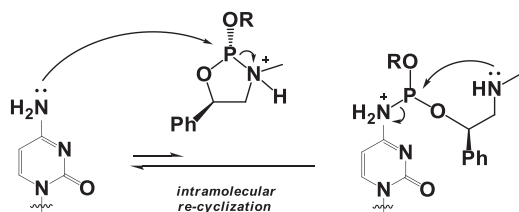
Fig. 11 Stereocontrolled synthesis of PB-DNA by the *N*-unprotected oxazaphospholidine approach

enzymatic synthesis can incorporate only (*S*p)-boranophosphate linkages into oligonucleotides due to the substrate recognition specificity of the enzymes [29]. For these reasons, the stereocontrolled chemical synthesis of PB-DNAs has been studied over the past few decades.

Our group have recently developed the oxazaphospholidine method for synthesizing stereocontrolled PS-DNAs using nucleoside 3′-*O*-oxazaphospholidine derivatives as monomers and less-nucleophilic acid activator [30–32]. This method allows us to stereoselectively synthesize phosphite triester intermediates. The resultant phosphites were converted to the corresponding *P*-stereodefined boranophosphates [33].

As shown in Fig. 11, this method is applied to the stereocontrolled synthesis of dithymidine boranophoshate. The oxazaphospholidine monomers were stereoselectivity synthesized from enantiopure 1,2-aminoalcohol as chiral auxiliaries. The monomer was condensed with a free 5′-OH nucleoside on solid support in the presence of *N*-(cyanomethyl)pyrrolidinium triflate (CMPT) as an acidic activator. The resultant phosphite triester intermediates were boronated with $BH_3 \cdot Me_2S$ and then 5′-*O*-DMTr group was removed by treatment with 3% DCA in the presence of Et_3SiH. After acetylation of 5′-OH, the dimer was treated with DBU to remove chiral auxiliary proceeded with retention of the *P*-configuration. Finally, the dimer was released from solid support by treatment with concentrated NH_3. As a result, the (*R*p)- and (*S*p)-dithymidine boranophosphates were synthesized with good yields (92–94%) and diastereoselectivities (dr 98:2 to 99:1).

Also, our group has found out that oxazaphospholidine monomers selectively reacted with 5′-OH groups without any adducts with the nucleobase amino groups [34]. The unique chemoselectivity of the oxazaphospholidine monomers could be explained by the intramolecular re-cyclization of the oxazaphospholidine ring, which would be much faster than the intermolecular nucleobase phosphitylation as shown in Fig. 12. Through use of this chemoselectivity, (*R*p)-d(C^bT) 2-mer was synthesized

Fig. 12 Proposed mechanism of intermolecular nucleophilic attack of the amino group of nucleobase to oxazaphospholidine monomer, and the intramolecular re-cyclization
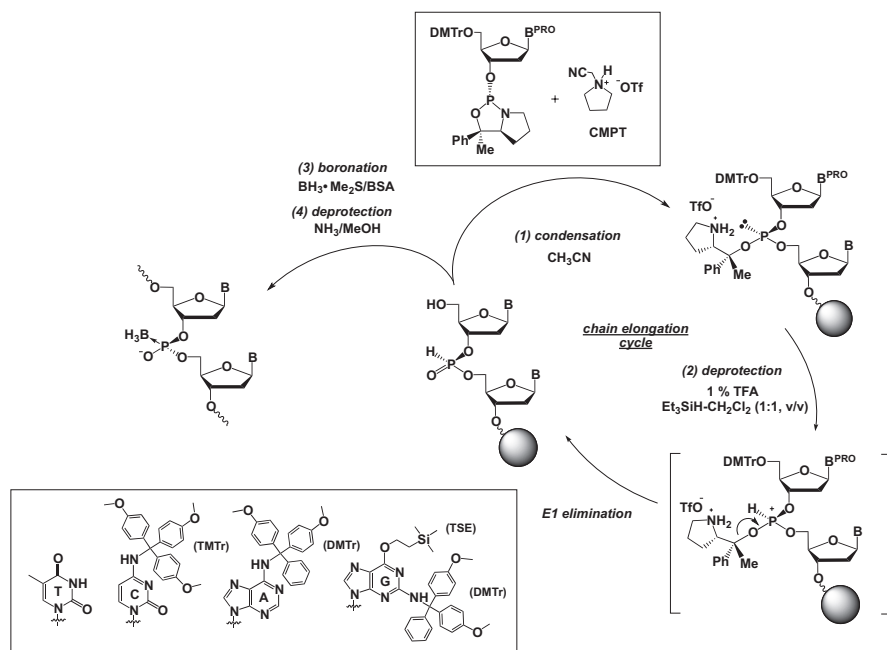
Fig. 13 Stereocontrolled synthesis of PB-DNA by the oxazaphospholidine approach

by using a N^4-unprotecting cytidine monomer. The result showed that the desired 2-mer was obtained in 86% yield without any base modifications. However, a significant loss of diastereoselectivity was observed (dr 76:24). Although the mechanism is not still clarified, the cause of this low diastereoselectivity might be epimerization of monomers by the intramolecular re-cyclization of the oxazaphospholidine ring. Therefore, so far, N-unprotected oxazaphospholidine method has been limited to the stereocontrolled synthesis of the length sequence of up to two bases.

After that, our group developed a new method for the stereocontrolled synthesis of PB-DNAs *via* diastereopure *H*-phosphonate intermediates [35, 36]. As shown in Fig. 13, the bicyclic oxazaphospholidine ring, which was given more excellent diastereoselectivity than monocyclic counterparts, was adopted as chiral auxiliaries.

The nucleobases A, C, and G were protected with 6-*N*-DMTr, 4-*N*-TMTr, 2-*N*-DMTr-6-*O*-TSE, respectively. Since base protection is unnecessary for the chemoselectivity as shown in Fig. 15, we employed acid-labile base protecting groups which would be removed in the deblocking step. As you noticed, the resultant unmodified bases induce no irreversible side reactions by a borane reagent as described in Sect. 2. The monomer was condensed with the 5′-OH of nucleosides or oligonucleotides on solid-phase synthesis in the presence of CMPT. The resultant phosphite triester intermediates were converted into the corresponding *H*-phosphonate diester intermediates by an E1 elimination of the chiral auxiliaries with retention of the *P*-configuration. After chain elongation, *P*-stereodefined PB-DNAs were synthesized by silylation and then boronation of *H*-phosphonate intermediates. The side reaction on silylated thymidine base reported in previous study could be suppressed by using DMF or DMAc as a solvent. The RP-HPLC analysis showed that the (*R*p)- and (*S*p)-dinucleoside boranophosphates were synthesized in modest to good yields (84–95%) and excellent diastereoselectivities (dr >99:1), respectively. In application of this method on the synthesis of oligonucleotides, we obtained (*R*p)- and (*S*p)-d(T^{b}T^{b}T^{b}T^{b}T^{b}T^{b}T^{b}T^{b}T^{b}T^{b}T^{b}T) 12-mers in 13–19% isolated yields. Also, we achieved the synthesis of (*R*p)- and (*S*p)-d(C^{b}A^{b}G^{b}T) 4-mers with mixed sequences in 54–73% isolated yields. To our knowledge, this is a first report of the stereocontrolled synthesis of PB-DNAs with four nucleobases.

7 Summary and Perspectives

In the current study, the chemical synthesis of PB-DNAs with the moderate nucleoside length of 20-mer demanded in biological and medicinal study achieved with sufficient coupling efficiency and then the desired counterparts could be obtained as pure products. The expanded availability of PB-DNAs should promote their use in therapeutic studies and would be clarified the ability as nucleic acid therapeutics. In addition, the chemists devoted much effort to the development of the efficient method of the synthesis of stereopure PB-DNAs. Now, the availability of stereopure PB-DNAs with mixed sequences limited to the nucleoside length of 4-mer. We expect that the longer stereopure PB-DNAs is synthesized by the development of the more efficient approach and the different of pharmacokinetics and pharmacodynamics properties between diastereomers is clarified in detail.

References

 1. Bennett CF, Swayze EE (2010) RNA targeting therapeutics: molecular mechanisms of antisense oligonucleotides as a therapeutic platform. Annu Rev Pharmacol Toxicol 50:259–293
 2. Shukla S, Sumaria CS, Pradeepkumar PI (2010) Exploring chemical modifications for siRNA therapeutics: a structural and functional outlook. ChemMedChem 5:328–349

3. Seto AG (2010) The road toward microRNA therapeutics. Int J Biochem Cell Biol 42:1298–1305

4. Nishina K, Piao W, Yoshida-Tanaka K et al (2015) DNA/RNA heteroduplex oligonucleotide for highly efficient gene silencing. Nat Commun 6:7969

5. Sharma VK, Sharma RK, Singh SK (2014) Antisense oligonucleotides: modifications and clinical trials. Med Chem Commun 5:1454–1471

6. Guga P, Koziołkiewicz M (2011) Phosphorothioate nucleotides and oligonucleotides – recent progress in synthesis and application. Chem Biodivers 8:1642–1681

7. Dirin M, Winkler J (2013) Influence of diverse chemical modifications on the ADME characteristics and toxicology of antisense oligonucleotides. Expert Opin Biol Ther 13:875–888

8. Sergueev DS, Shaw BR (1998) *H*-phosphonate approach for solid-phase synthesis of oligodeoxyribonucleoside boranophosphates and their characterization. J Am Chem Soc 120:9417–9427

9. Hall AH, Wan J, Shaughnessy EE et al (2004) RNA interference using boranophosphate siRNAs: structure–activity relationships. Nucleic Acids Res 32:5991–6000

10. Rait VK, Shaw BR (1999) Boranophosphates support the RNase H cleavage of polyribonucleotides. Antisense Nucleic Acid Drug Dev 9:53–60

11. Olesiak M, Krivenko A, Krishna H et al (2011) Synthesis and biological activity of borane phosphonate DNA. Phosphorus Sulfur Silicon Relat Elem 186:921–932

12. Li P, Sergueeva ZA, Dobrikov M et al (2007) Nucleoside and oligonucleoside boranophosphates: chemistry and properties. Chem Rev 107:4746-–4796

13. Chen Y-Q, Qu F-C, Zhang Y-B (1995) Diuridine 3′,5′-boranophosphate: preparation and properties. Tetrahedron Lett 36:745–748

14. Wang JX, Sergueev DS, Shaw BR (2005) The effect of a single boranophosphate substitution with defined configuration on the thermal stability and conformation of a DNA duplex. Nucleosides Nucleotides Nucleic Acids 24:951–955

15. Johnson CN, Spring AM, Sergueev D et al (2011) Structural basis of the RNase H1 activity on stereo regular borano phosphonate DNA/RNA hybrids. Biochemistry 50:3903–3912

16. Sood A, Shaw BR, Spielvogel BF (1990) Boron-containing nucleic acids. 2. Synthesis of oligodeoxynucleoside boranophosphates. J Am Chem Soc 112:9000–9001

17. Sergueeva ZA, Sergueev DS, Shaw BR (2001) Borane-amine complexes – versatile reagents in the chemistry of nucleic acids and their analogs. Nucleosides Nucleotides Nucleic Acids 20:941–945

18. McCuen HB, Noé MS, Sierzchala AB et al (2006) Synthesis of mixed sequence borane phosphonate DNA. J Am Chem Soc 128:8138–8139

19. Roy S, Olesiak M, Shang S et al (2013) Silver nanoassemblies constructed from boranephosphonate DNA. J Am Chem Soc 135:6234–6241

20. Zhang JC, Terhorst T, Matteucci MD (1997) Synthesis and hybridization study of a boranophosphate-linked oligothymidine deoxynucleotide. Tetrahedron Lett 38:4957–4960

21. Higson AP, Sierzchala A, Brummel H et al (1998) Synthesis of an oligothymidylate containing boranophosphate linkages. Tetrahedron Lett 39:3899–3902

22. Sergueev DS, Sergueeva ZA, Shaw BR (2001) Synthesis of oligonucleoside boranophosphates via an *H*-phosphonate method without nucleobase protection. Nucleosides Nucleotides Nucleic Acids 20:789–795

23. Wada T, Sato Y, Honda F et al (1997) Chemical synthesis of oligodeoxyribonucleotides using *N*-unprotected *H*-phosphonate monomers and carbonium and phosphonium condensing reagents: *O*-selective phosphonylation and condensation. J Am Chem Soc 119:12710–12721

24. Wada T, Shimizu M, Oka N et al (2002) A new boranophosphorylation reaction for the synthesis of deoxyribonucleoside boranophosphates. Tetrahedron Lett 43:4137–4140

25. Shimizu M, Wada T, Oka N et al (2004) A novel method for the synthesis of dinucleoside boranophosphates by a boranophosphotriester method. J Org Chem 69:5261–5268

26. Shimizu M, Saigo K, Wada T (2006) Solid-phase synthesis of oligodeoxyribonucleoside boranophosphates by the boranophosphotriester method. J Org Chem 71:4262–4269

27. Higashida R, Oka N, Kawanaka T et al (2009) Nucleoside *H*-boranophosphonates: a new class of boron-containing nucleotide analogues. Chem Commun:2466–2468
28. Uehara S, Hiura S, Higashida R et al (2014) Solid-phase synthesis of *P*-boronated oligonucleotides by the *H*-boranophosphonate method. J Org Chem 79:3465–3472
29. Li H, Porter K, Huang FQ et al (1995) Boron-containing oligodeoxyribonucleotide 14mer duplexes: enzymatic synthesis and melting studies. Nucleic Acids Res 23:4495–4501
30. Oka N, Wada T, Saigo K (2002) Diastereocontrolled synthesis of dinucleoside phosphorothioates using a novel class of activators, dialkyl(cyanomethyl)ammonium tetrafluoroborates. J Am Chem Soc 124:4962–4963
31. Oka N, Wada T, Saigo K (2003) An oxazaphospholidine approach for the stereocontrolled synthesis of oligonucleoside phosphorothioates. J Am Chem Soc 125:8307–8317
32. Oka N, Yamamoto M, Sato T et al (2008) Solid-phase synthesis of stereoregular oligodeoxyribonucleoside phosphorothioates using bicyclic oxazaphospholidine derivatives as monomer units. J Am Chem Soc 130:16031–16037
33. Wada T, Maizuru Y, Shimizu M et al (2006) Stereoselective synthesis of dinucleoside boranophosphates by an oxazaphospholidine method. Bioorg Med Chem Lett 16:3111–3114
34. Oka N, Maizuru Y, Shimizu M et al (2010) Solid-phase synthesis of oligodeoxyribonucleotides without base protection utilizing *O*-selective reaction of oxazaphospholidine derivatives. Nucleosides Nucleotides Nucleic Acids 29:144–154
35. Iwamoto N, Oka N, Sato T et al (2009) Stereocontrolled solid-phase synthesis of oligonucleoside *H*-phosphonates by an oxazaphospholidine approach. Angew Chem Int Ed 48:496–499
36. Iwamoto N, Oka N, Wada T (2012) Stereocontrolled synthesis of oligodeoxyribonucleoside boranophosphates by an oxazaphospholidine approach using acid-labile *N*-protecting groups. Tetrahedron Lett 53:4361–4364